TILL GEOCHEMISTRY AND LITHOGEOCHEMICAL EXPLORATION FOR A CONCEALED KIMBERLITE, NORTHWEST TERRITORIES, CANADA

by

Andrew Wickham

B.Sc., Colorado State University, 2016

A THESIS SUBMITTED IN PARTIAL FULFILLMENT
OF THE REQUIREMENTS FOR THE DEGREE OF

MASTER OF SCIENCE

in

THE FACULTY OF GRADUATE AND POSTDOCTORAL STUDIES
(Geological Sciences)

The University of British Columbia
(Vancouver)

April 2022

© Andrew Wickham, 2022

The following individuals certify that they have read, and recommend to the Faculty of Graduate and Post-doctoral Studies for acceptance, the thesis entitled:

Till geochemistry and lithogeochemical exploration for a concealed kimberlite, Northwest Territories, Canada

submitted by **Andrew Wickham** in partial fulfillment of the requirements for the degree of **Master of Science** in **Geological Sciences**.

Examining Committee:

Dr. Maya Kopylova, Department of Earth, Ocean and Atmospheric Sciences, UBC
Supervisor

Dr. Kenneth Hickey, Department of Earth, Ocean and Atmospheric Sciences, UBC
Supervisory Committee Member

Dr. Craig Hart, Department of Earth, Ocean and Atmospheric Sciences, UBC
Supervisory Committee Member

Dr. Mitch D'Arcy, Department of Earth, Ocean and Atmospheric Sciences, UBC
Additional Examiner

Abstract

Research at the Kelvin kimberlite, NWT, is helping to define surface exploration practices and is testing new host rock lithogeochemical exploration tools that will result in reduced costs and improved discovery success. In regions where recent glaciation has buried kimberlites under glacial sediments, surface geochemical detection methods are best interpreted when coupled with a comprehension of the landscape formation processes. The glacial, post-glacial, and cryoturbation processes that have affected the landscape have, in turn, affected the dispersal of geochemical signatures in the till that can be detected and exploited by detailed surface mapping, sampling, and geochemical analysis.

The Kelvin kimberlite is an inclined pipe that subcrops from metaturbidite country-rock beneath a lake. No indicator mineral train has been detected at Kelvin by traditional indicator mineral methods. Relative uniformity of surficial material (<6m thick till blanket) allows for extensive B-horizon soil sampling above the kimberlite, up-ice, and up to 1 km down-ice. Four acid and aqua regia ICP-MS results of the -180 µm fraction indicate the presence of subtle pathfinder element trains originating from the kimberlite subcrop location and extending for >1km down-ice. Dry sonic sieving and four acid digestion results provide interpretations of geochemical partitioning and the ideal size fraction for geochemical sampling. Trace elements demonstrate systematically elevated concentrations in the fine and very fine silt fractions; however, background is higher and anomalous-to-background contrast is not enhanced compared to bulk -180 µm ratios. Elevated pathfinder concentrations in the fine to very fine sand fraction are attributed to fine kimberlite indicator minerals and their fragments, and display the best anomalous-to-background contrast.

Additional research aims to detect mineralogical and metasomatic alteration signatures in the country-rock surrounding the Kelvin kimberlite in an attempted to develop exploration vectors. Hyperspectral scanning of drill core shows that the emplacement of the kimberlite did not produce pervasive mineralogical alteration of the surrounding country-rock. Evidence of alteration is limited to breccias and is vein-controlled, only extending a few meters from pipe contacts. Hyperspectral imaging and partial- and whole-rock lithogeochemical results do not detect evidence of pervasive alteration and preclude the identification of mineralogical or geochemical exploration vectors.

Lay Summary

The goal of this research is to develop new ways of detecting mineral deposits (particularly diamond deposits) in regions that have recently experienced glaciation, in areas like northern Canada. During these recent glaciations, sediment was deposited on top of these diamond deposits (kimberlites) effectively concealing them from surface detection. Results from this researched analyzed the geochemistry of the sediment surrounding a well-documented kimberlite and was successful in developing new methods that can be employed by exploration geologists to more time- and cost-effectively explore for kimberlite deposits in these types of landscapes. These methods, however, are dependent on the history of glacial movement, the sediment and soil material sampled, and the specific chemical analyses performed on the samples. This research also analyzed the composition of the rocks surrounding the kimberlite using drill core in an attempt to detect a zone of chemically and mineralogically altered rock surrounding the deposit.

Preface

The author and late supervisor, Dr. Peter Winterburn, are responsible for the development of the project and research objectives. The research was developed to further expand upon the research presented in the thesis by Erika Cayer, and was developed in collaboration with Barrett Elliott of the Northwest Territories Geological Survey (NTGS). Dr. Maya Kopylova is credited with fulfilling the role of supervisor in the absence of Dr. Peter Winterburn. Committee members, Dr. Ken Hickey and Dr. Craig Hart, are credited with their valuable input to the design of the project during committee meetings and reviews to the manuscript. The field sampling plan was developed by the author in conjunction with Dr. Peter Winterburn and Bianca Iulianella Phillips and her Master's research program. The author is responsible for interpreting the data and writing the manuscript in its entirety.

Soil samples were analyzed by ALS Minerals (ALS) in North Vancouver by four acid, aqua regia, lithium-borate fusion digestion and ICP-MS analyses, Leco carbon, Pb-isotope analyses, and sequential extractions. Sieving of till samples was performed by the author at the EGI laboratory at the MDRU using the *Gilson GilSonic Ultrasiever GA-8*. The UBC EOAS X-ray diffraction laboratory was used for X-ray diffraction analysis. Soil hydrocarbon analyses were submitted to Activision Laboratories (ActLabs) in Ancaster, Ontario for analysis and interpretation. Hyperspectral imaging of the drill core was performed by Corescan at their laboratory in Denver, Colorado.

Table of Contents

Abstract . . . . . **iii**

Lay Summary . . . . . **iv**

Preface . . . . . **v**

Table of Contents . . . . . **vi**

List of Tables . . . . . **xi**

List of Figures . . . . . **xii**

Glossary . . . . . **xv**

Acknowledgments . . . . . **xix**

1 Introduction **1**

1.1 Project Rational 1

1.2 Objectives 1

1.3 Thesis Structure 2

1.4 Research Site 2

1.5 Geologic Overview 2

1.5.1 Slave Geologic Province 2

1.5.1.1 Slave Surface at Time of Emplacement 6

1.5.2 Glacial History of Kelvin-Faraday Corridor 6

1.5.3 Local Geology 7

1.5.4 Geology of the Kelvin Kimberlite 7

1.5.4.1 Emplacement Process 13

1.5.4.2 Discovery at the Kelvin-Faraday Corridor 14

2 Surficial Geochemistry **17**

2.1 Introduction 17

2.1.1 Kimberlite Exploration in Covered Terranes . . . 18
2.1.2 Mechanisms of Element Migration . . . 19
2.1.3 Soil Chemistry . . . 20
2.1.4 Inorganic Soil Geochemical Analyses . . . 21
2.1.5 Geochemical Partitioning in Size Fractions . . . 24
2.1.6 Pb Isotope Systematics . . . 25
2.1.7 Soil Hydrocarbons . . . 26
2.2 Surface Materials . . . 27
2.2.1 Surface Materials . . . 27
2.2.2 Soil Classification . . . 30
2.2.3 Discussion . . . 33
2.3 Methodologies . . . 33
2.3.1 Soil Sampling . . . 34
2.3.2 Soil Physicochemical Properties . . . 34
2.3.3 Chemical Analyses . . . 35
2.3.4 Sequential Extraction . . . 35
2.3.5 Soil Size Fraction . . . 35
2.3.6 Pb Isotopes . . . 35
2.3.7 Soil Hydrocarbons . . . 35
2.4 Results . . . 36
2.4.1 Physicochemical Properties . . . 36
2.4.1.1 Discussion . . . 40
2.4.2 Soil Geochemistry . . . 40
2.4.2.1 4-Acid ICP-MS . . . 40
2.4.2.2 Aqua Regia ICP-MS . . . 46
2.4.2.3 Organic Carbon . . . 51
2.4.2.4 Discussion . . . 51
2.4.3 Sequential Extraction . . . 52
2.4.3.1 Discussion . . . 54
2.4.4 Soil Size Fraction . . . 55
2.4.4.1 Discussion . . . 56
2.4.5 Pb Isotopes . . . 59
2.4.5.1 Discussion . . . 61
2.4.6 Spatiotemporal Geochemical Hydrocarbons . . . 62
2.4.6.1 Discussion . . . 63
2.5 Discussion . . . 64
2.5.1 Surficial Geochemical Anomalies . . . 64
2.5.1.1 Mechanical Chemical Dispersion . . . 64
2.5.1.2 Vertical Chemical Dispersion . . . 66

2.5.2 Landscape Evolution Model . . . 66
2.5.3 Exploration Implications . . . 67
2.5.3.1 Sampling Procedure . . . 68
2.5.3.2 Analytical Procedure . . . 68
2.5.3.3 Data Interpretation . . . 69
2.6 Conclusions . . . 70

3 Bedrock Mineralogy and Lithogeochemistry . . . 72
3.1 Introduction . . . 72
3.1.1 Kimberlite - Country-Rock Alteration . . . 73
3.1.2 Country-rock Alteration at the Kelvin Kimberlite . . . 74
3.2 Methodologies . . . 77
3.2.1 X-Ray Diffraction . . . 77
3.2.2 Hyperspectral . . . 77
3.2.3 Lithogeochemistry . . . 77
3.3 Results . . . 78
3.3.1 X-Ray Diffraction . . . 79
3.3.2 Petrography . . . 79
3.3.2.1 Discussion . . . 85
3.3.3 Hyperspectral . . . 85
3.3.3.1 General Observations . . . 85
3.3.3.2 Sericite/White Mica Composition . . . 87
3.3.3.3 Chlorite Composition . . . 89
3.3.3.4 Kaolinite Crystallinity . . . 91
3.3.3.5 Chlorite - Dark Mica Relationship: Ternary Image . . . 91
3.3.3.6 Discussion . . . 93
3.3.4 Lithogeochemistry . . . 95
3.3.4.1 Lithium Borate Fusion ICP-MS . . . 95
3.3.4.2 Weak Aqua Regia ICP-MS . . . 97
3.3.4.3 Discussion . . . 99
3.4 Discussion and Conclusions . . . 101

4 Conclusions . . . 104
4.1 Conclusions and Exploration Implications . . . 104
4.1.1 Surficial Geochemistry . . . 104
4.1.2 Lithogeochemical Exploration . . . 105
4.2 Recommendations for Further Research . . . 105
4.2.1 Surficial Geochemistry . . . 105
4.2.2 Lithogeochemical Exploration . . . 105
Bibliography . . . 107

Appendices **118**

A Methodologies **119**
A.1 Soil Sampling 119
A.2 Physicochemical Measurements 121
A.3 Sieving 122
A.4 Geochemical Analyses - ALS Minerals 123
A.4.1 ME-MS41L - Aqua Regia ICP-MS 123
A.4.2 ME-MS61L - Four Acid ICP-MS 123
A.4.3 C-IR06a - Organic Carbon 123
A.4.4 PbIS-RAT61 - Pb Isotope Ratios by Four Acid ICP-MS 123
A.4.5 ME-MS41W - Modified Weak Aqua Regia ICP-MS 124
A.4.6 ME-MS03-07 - Sequential Extraction 124
A.4.7 MS41W-PbIS - Pb Isotope by Modified Weak Aqua Regia ICP-MS 124
A.4.8 ME-MS81d - Lithium Borate Fusion ICP 124
A.4.9 C-IR07 - Total Carbon 125
A.5 Spatiotemporal Geochemical Hydrocarbons (SGH) 125

B QA/QC **126**
B.1 Slurry QAQC 127
B.2 Till Four Acid ICP-MS QAQC 129
B.3 Till Aqua Regia ICP-MS QAQC 140
B.4 Till Pb Isotope Q-ICP-MS QAQC 152
B.5 Till Size Fraction Four Acid ICP-MS QAQC 154

C ActLabs SGH Interpretation Report **160**

D Raw Data **187**
D.1 Soil Sample Locations and Sample ID Numbers 187
D.2 Soil Profile Field Measurements 189
D.3 Soil Slurry Physicochemical Results 208
D.4 Till Four Acid ICP-MS Results 214
D.5 Till Aqua Regia ICP-MS Results 245
D.6 Till Pb Isotope Ratios Q-ICP-MS Results 276
D.7 Till Sequential Extraction Results 278
D.8 Till Size Fraction Four Acid ICP-MS Results 284
D.9 Till Size Fraction Sieving Mass Measurements 291
D.10 Drill Core Fusion ICP-MS and Whole Rock ICP-AES Results 293
D.11 Drill Core Aqua Regia ICP-MS Results 306
D.12 Drill Core Pb Isotope Ratio Q-ICP-MS Results 322
D.13 Country Rock Thin Section Descriptions 324

D.14 Kelvin Kimberlite Thin Section Descriptions (SRK Consulting) 335

List of Tables

Table 2.1 Kimberlite Mineralogy, Formulae, and Elemental Substitutions 18
Table 2.2 Summary of Sequential Extraction Methods 23
Table 2.3 Soil Analyses 34
Table 2.4 Four Acid ICP-MS Pathfinder Element Response Ratios 42
Table 2.5 Aqua Regia ICP-MS Pathfinder Element Response Ratios 51
Table 2.6 Samples Selected for Sequential Extraction, Size Fraction, and Pb Isotope Analyses . . . 53
Table 2.7 Analytical Reproducibility of Soil Pb Isotope Ratios 60

Table 3.1 Drill Hole Collar and Survey Table 79

List of Figures

Figure 1.1 Slave Province Regional Bedrock Geology Map 3
Figure 1.2 Regional Bedrock Geology 8
Figure 1.3 Study Area Bedrock Geology 9
Figure 1.4 Kelvin Internal Geology 10
Figure 1.5 Exploration at Kennady North 15
Figure 1.6 NTGS KIDD Database Indicator Minerals 16

Figure 2.1 Pathfinder Element Concentrations Average Kimberlite and Slave Country Rock Spider Diagram 20
Figure 2.2 Conceptual Frost Boil Diagram 21
Figure 2.3 Grain Size of Kimberlite Minerals and Size Fractions Analyzed in Exploration 25
Figure 2.4 Regional Surface Materials and Glacial Landforms 28
Figure 2.5 Surface Materials Map 29
Figure 2.6 Aerial Imagery of Study Area 30
Figure 2.7 Surface Materials Images 31
Figure 2.8 Vegetation Images 32
Figure 2.9 Soil Profiles 32
Figure 2.10 pH and TDS Drift Test 36
Figure 2.11 Slurry pH and TDS Field and Lab Duplicate Mean Percent Differences 37
Figure 2.12 Slurry Eh, pH, and Moisture Measurements Over Kimberlite 38
Figure 2.13 Pourbaix Eh - pH Diagram for Ca and pH - IDH Plot 38
Figure 2.14 H^+ and Inverse Difference Hydrogen Map and Probability Plots 39
Figure 2.15 Organic Carbon and Soil Moisture Map, and C_{org} - Moisture Plot 39
Figure 2.16 Peltier Weathering Plot and Feldspar Control Diagram 41
Figure 2.17 Four Acid ICP-MS Pathfinder Element Maps: Cr, Mg, Mn, Ni 43
Figure 2.18 Four Acid ICP-MS Pathfinder Element Maps: Fe, Ca, La, Ce 44
Figure 2.19 Four Acid ICP-MS Pathfinder Element Maps: Nb, Ta, Ti, Ba 45
Figure 2.20 Four Acid ICP-MS Ba-Cr-Fe-Mg-Mn-Nb-Ni-Ta-Ti Normalized Pathfinder Map 46
Figure 2.21 Th/U Map and XY Plot 47
Figure 2.22 Four Acid Nb/Zr Map and Box Plot of Average Kimberlite and Slave Values 47

Figure 2.23 Average Field Duplicate MPD for Aqua Regia and Four Acid Elements 48
Figure 2.24 Aqua Regia ICP-MS Pathfinder Element Maps: Cr, Mg, Fe, Ni 49
Figure 2.25 Aqua Regia ICP-MS Pathfinder Element Maps: Ba, Ca, Sr, Ti 50
Figure 2.26 Plots of Organic Carbon to Aqua Regia Mg, Ni, and Sr 51
Figure 2.27 Recovery Percent of Aqua Regia Digestions Relative to Four Acid ICP-MS 52
Figure 2.28 Map of Samples Selected for Sequential Extraction, Size Fraction, and Pb Isotope Analyses 53
Figure 2.29 Sequential Extraction Pathfinder Element Bar Charts 54
Figure 2.30 Size Fraction Reconstituted Sum vs Bulk -180 µm Concentrations 55
Figure 2.31 Size Fraction Pathfinder Element Concentrations 57
Figure 2.32 Lab Duplicate Mean Percent Difference of Pathfinder Elements for Size Fractions 58
Figure 2.33 Size Fraction A-CN-K Ternary Plot 59
Figure 2.34 Sub-Fraction Pathfinder Element Concentrations and Response Ratios 60
Figure 2.35 Bivariate Till Pb Isotope Plots 61
Figure 2.36 ActLabs SGH Pathfinder Class Map of Survey Area 63
Figure 2.37 ActLabs SGH Pathfinder Class Map of Grid 64
Figure 2.38 SGH Pathfinder Class Values Plotted versus Soil Slurry Eh 65
Figure 2.39 Idealized Palimpsest Models 65
Figure 2.40 Box Plots of Four Acid and Aqua Regia Cr, Fe, Mg, Nb and Ni Values for Frost Boils vs. Soils 66
Figure 2.41 Surface Landscape Evolution Diagram 67
Figure 2.42 Central Slave Map with NTGS TILL Database and SE Slave Country Rock Locations . 69

Figure 3.1 3D Fault and Joint Interpretation at Kelvin 75
Figure 3.2 Hyperspectral Hydration Values from Kelvin Drill Core 76
Figure 3.3 Mineral Class Map Schematic Diagram 78
Figure 3.4 Drill Hole Locations 80
Figure 3.5 XRD Pattern of Greywacke Metaturbidite 81
Figure 3.6 Metaturbidite country-rock Core Images and Photomicrographs 82
Figure 3.7 KDI-HQ14-024b and KDI-HQ14-016b Core Photos and Photomicrograph 84
Figure 3.8 Biotite, Chlorite, Sericite, and Kaolinite Example Spectra 86
Figure 3.9 Biotite - Chlorite Pixels XY Plot; Chlorite Percentage - 2250 nm Feature XY Plot 87
Figure 3.10 Mineral Class Maps Overview for all Drill Holes 88
Figure 3.10 Mineral Class Maps Overview for all Drill Holes Continued 89
Figure 3.11 Drill Hole Sericite Pixel Count and White Mica 2200 nm Feature 90
Figure 3.12 Drill Hole Chlorite Pixel Count and 2250 nm Feature 90
Figure 3.13 Drill Hole Kaolinite Pixel Count and Crystallinity 91
Figure 3.14 Dark Mica/Biotite - Chlorite Ternary Image Corebox View for All Drill Holes 92
Figure 3.15 Dark Mica/Biotite - Chlorite Ternary Images 93

Figure 3.16 Distance from Kelvin versus Aspectral Slope, Chlorite 2250 nm Shift, Sericite Pixels, Sericite 2200 nm Shift, Kaolinite Pixels, and Kaolinite Crystallinity 94
Figure 3.17 Down Hole Sericite Crystallinity Logs 96
Figure 3.18 Nb:TiO_2 Lithium Borate Fusion Conservative Element Biplot 96
Figure 3.19 Downhole Plots of Al_2O_3/TiO_2, Fe_2O_3/TiO_2, MgO/TiO_2, and LOI (%) 97
Figure 3.20 Downhole Plots of SiO_2/TiO_2, K_2O/TiO_2, Na_2O/TiO_2, and CaO/TiO_2 98
Figure 3.21 Chloritization Intensity: Titanium Recovery Ratio Biplot 98
Figure 3.22 Downhole Plots of C (%), Mg/Zr, Mn/Zr, and Fe/Zr 99
Figure 3.23 Downhole Plots of Rb/Zr, Cs/Zr, and Sr/Zr 100
Figure 3.24 Mg/Zr - C and Sr/Zr - C Weak Aqua Regia Biplots 101

Figure A.1 B Horizon Sampling Procedure Images 121

Figure D.1 B Horizon Sample Locations and ID 188

Glossary

AA ammonium acetate

AGI Amplified Geochemical Imaging

C-HA-HC cold hydroxylamine hydrochloride

CEC cation exchange capacity

CIW Chemical Index of Weathering

CRM certified reference material

CSBC Central Slave Basement Complex

CSCG Central Slave Cover Group

CV coefficient of variance

DCEI DeBeers Canada Exploration Inc

DIW deionized water

EOAS Department of Earth, Ocean and Atmospheric Sciences

EM electromagnetic

GKJV Gahcho Kué Joint Venture

GPR ground penetrating radar

GSC Geological Survey of Canada

H-HA-HC hot hydroxylamine hydrochloride

HK hypabyssal kimberlite

ICP-AES inductively coupled plasma atomic emission spectrometry

ICP-MS inductively coupled plasma mass spectrometry

IDH inverse difference hydrogen

KDI Kennady Diamonds Inc

KIDD Kimberlite Indicator and Diamond Database

KFC Kelvin-Faraday Corridor

KIM kimberlite indicator mineral

KPK Kimberley-type pyroclastic kimberlite

LGM last glacial maximum

LOI loss on ignition

MC-ICP-MS multi-collector inductively coupled plasma mass spectrometry

MID M'Clintock Ice Divide

MPD Mean percent difference

MPDI Mountain Province Diamonds Inc

MPM Mountain Province Mining Inc

NaP sodium pyrophosphate

NTGS Northwest Territories Geological Survey

ORP oxidation reduction potential

PER Pearce element ratio

Q-ICP-MS quadruple inductively coupled plasma mass spectrometry

RC reverse circulation

REE rare earth element

RSD relative standard deviation

SGH Spatio-temporal Geochemical Hydrocarbon

SWIR short wavelength infrared

TDS total dissolved solids

TDS_A acidified total dissolved solids

TIMS thermal ionization mass spectrometry

UBC University of British Columbia

VNIR visible near infrared

XRD X-ray diffraction

Acknowledgments

I offer my appreciation to the faculty, staff, and students at EOAS and the MDRU for supporting me in every step of my graduate research experience. My sincerest gratitude is extended to Dr. Peter Winterburn who is credited with envisioning this research and the many other innovative projects conducted during his time at the MDRU. Dr. Maya Kopylova is thanked for stepping in to fill the supervisory roll and providing encouragement and support. I am also thankful to my committee members, Dr. Ken Hickey and Dr. Craig Hart, for providing revisions and continued support.

Fellow students and all alumni of the Exploration Geochemistry Initiative (EGI) and the MDRU are thanked for their guidance and for always being available for scientific discussions, notably Bianca Iulianella Phillips, Ryan Shaw, and Pearce Luck.

This study would not have been possible without the significant financial contributions from Bureau Veritas and NSERC, and I extend gratitude to the Society of Economic Geologists for granting a fellowship award. Barrett Elliott from the Northwest Territories Geological Survey is thanked for sharing his expertise in diamond exploration and helping facilitate the research. Mountain Province Diamonds (formerly Kennady Diamonds) is thanked for permitting access to the Kelvin kimberlite site and for providing field support and drill core samples. Finally, Corescan is also thanked for providing hyperspectral imaging services and support.

Chapter 1

Introduction

1.1 Project Rational

The exploration challenges faced in detecting mineral deposits through transported cover are inherently different than those of outcropping or regolith terranes. Thus, the historical practices employed by explorers are not always applicable in areas of exotic cover. Therefore, the demand for indirect methods of detection through cover is a developing field of research to unlock the vast areas of Canada that are covered in recent glacial material and, as a result, are under-explored.

In an effort to reduce risk during kimberlite exploration and increase the efficiency of target evaluation and prioritization before and during drilling, this research aims to evaluate the effectiveness of detection methods on the surface and in host rock. Constraining the mechanisms by which geochemical anomalies may or may not form will yield new and refined exploration tools for Canadian geologists when exploring on the surface and when evaluating drill core.

1.2 Objectives

The objectives of this research are to:

1. Constrain factors controlling surface geochemical anomaly generation as a function of landscape evolution and geology.
2. Develop surface sampling techniques that will detect the presence of a kimberlite concealed under till and bedrock in the subarctic environment.
3. Identify and quantify alteration in the host rock surrounding the kimberlite to generate mineralogical and geochemical exploration vectors.

1.3 Thesis Structure

This thesis composes two research subjects: surficial till geochemistry; and country rock drill core geochemistry and mineralogy. The deposit geology and setting are included in Chapter 1 (*1: Introduction*). The two research subjects are separated into comprehensive chapters *2: Surficial Geochemistry* and *3: Bedrock Mineralogy and Geochemistry*, respectively, that both include the following:

- Introduction: including the rationale and background information;
- Methodologies: methodologies of the employed analyses;
- Results: including results and discussion of geochemistry and/or mineralogy;
- Discussion: integrating results with anomaly formation models, and presenting exploration implications;
- Conclusions: summarizing the key findings of the research.

The final chapter (*4: Conclusions*) includes a reiteration of the conclusions of each research subject addressing the research objectives and includes recommendations for future research.

1.4 Research Site

The Kelvin kimberlite site was selected based on criteria of till cover uniformity, access to site, minimal anthropogenic influences, and accessible third party information including regional surficial and bedrock geology data, and NI 43-101 technical reports with resource estimates. The target also presents the opportunity to evaluate the geochemical responses of a target with a unique morphology and distinct absence of a traditional kimberlite indicator mineral (KIM) train.

1.5 Geologic Overview

1.5.1 Slave Geologic Province

The Slave geologic province encompasses the exposed portion of the Slave craton, an Archean craton that comprises part of the Canadian Shield. The formation of the craton occurred within the Sclavia supercraton, and therefore its crustal development during the Archean and early Paleoproterozoic must be considered within the context of the broad tectonic system that was the Sclavia supercraton. The breakup of Sclavia ca. 2.2 Ga (Bleeker, 2003) and the subsequent amalgamation with other cratons ca. 2.0 - 1.8 Ga (Hoffman, 1988) resulted in the Slave be observe today, and it's context within Laurentia.

The Slave province is regionally divided into the western and eastern terranes based on basement composition and variation in Neoarchean supracrustal successions. The Central Slave Basement Complex (CSBC) represents Mesoarchean sialic basement that underlies the western Slave(Figure 1.1; Baragar and McGlynn, 1976; Bleeker et al., 1999, 2000; Henderson, 1970; McGlynn and Henderson, 1970). The

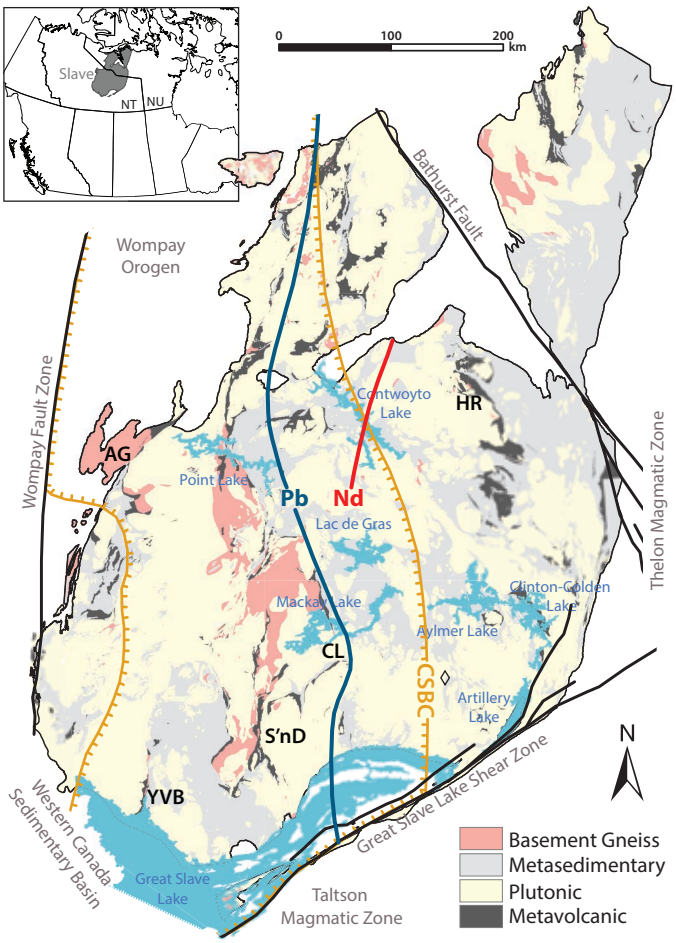

Figure 1.1: Regional geologic map of the Slave province after Bleeker (2003). Pb isotope boundary from Thorpe et al. (1992); Nd isotope boundary after Davis and Hegner (1992); inferred eastern and western extent of CSBC from Bleeker et al. (1999) and Bleeker et al. (2000). Yellowknife Volcanic Belt (YVB), Step'nduck Complex (S'nD), Camsell Lake greenstone belt (CL), Acasta Gneiss Complex (AG), and Hackett River greenstone belt (HR) are noted. Kelvin study area is noted by diamond south of Aylmer Lake.

CSBC is predominantly >2.8 Ga dioritic to tonalitic gneisses of the south central Slave, with localized regions of >3.5 Ga tonalitic to gabbroic gneisses in the Acasta River region along the western margin (Bleeker et al., 1999; Bowring et al., 1989; Sircombe et al., 2001). The eastern extent of the CSBC is generally poorly defined but extends as far east as the Step'nduck Complex and the Camsell Lake greenstone belt before terminating between MacKay and Clinton - Colden Lakes (Figure 1.1; Bleeker et al., 1999). Although little is known about the basement complex of the eastern Slave (Bleeker et al., 1999), Pb and Nd isotopic studies have identified regional boundaries within the basement, suggesting a Neoarchean suture zone between more juvenile <2.7 Ga basement to the east and the >3.0 Ga CSBC to the west (Davis et al., 1996; Davis and Hegner, 1992; Thorpe et al., 1992).

In the western Slave province, the CSBC is unconformably overlain by the Central Slave Cover Group (CSCG): a ca. 2.85 Ga continuous quartzite and banded iron-formation sequence (Bleeker et al., 2004). Parauthocthonous sequences of ca. 2.73 - 2.70 Ga tholeiitic mafic volcanics are unconformably overlain

by ca. 2.70 - 2.66 Ga calc-alkaline felsic volcanics that grade into overlying thick turbidite sequences of mudstones and greywackes (Isachsen et al., 1991). Tholeiitic mafic volcanics exclusive to the western Slave are presumably mantle plume or rift related; whereas province-wide calc-alkaline volcanism (and associated minor plutonism) evolved in a continent-arc collisional event ca 2.64 Ga (Kusky, 1989; Van Breemen et al., 1992) and represent the earliest stratigraphic connection between the eastern and western Slave (Bleeker, 2001). Multiple large sedimentary basins formed in the eastern and western Slave from 2.66 - 2.63 Ga depositing the Burwash Formation east of the Yellowknife volcanic belt, the Aylmer – MacKay domain east of the Courageous – MacKay belt, and the Beechey Lake Group of the Hackett River belt (Padgham and Fyson, 1991). Stratigraphically younger turbidites are intercalated with underlying calc-alkaline volcanic rocks and indicate locally contemporaneous volcanism and sedimentation in a volcanically and tectonically active terrane.

Regional horizontal shortening across the province related to distal tectonic process outside of the preserved cratonic margins began ca. 2.64 Ga, resulting in three regional crustal deformation events (D1, D2, D3) and two major plutonic events. The D1 event locally overlapped with sedimentation, formed NE-SW trending fold belt, and predates the onset of magmatism of diorite to granodiorite composition (Davis and Bleeker, 1999; Davis et al., 2003). Regional medium-pressure granulite metamorphic aureoles are often centered around post-D1 plutons (Davis and Bleeker, 1999). Northwest dipping subduction along a paleomargin of the Slave is suggested to have resulted in the arc-related plutonism (Davis et al., 2003).

Compression continued and shifted to east-west shortening producing regionally synchronous deformation (D2), plutonism, and metamorphism. *Two-mica* (biotite + muscovite) granites and K-feldspar megacrystic granodiorite-granites across the province are characteristic of the ca. 2.61 - 2.585 Ga syn-D2 plutonism (Van Breemen et al., 1992). High temperature-low pressure metamorphic aureoles around plutons produced regional metamorphic zones characterized by biotite-cordierite-andalusite-sillimanite (Cairns, 2003; Van Breemen et al., 1992). In the central and northeastern province, metamorphism peaked at 2.61 - 2.595 Ga, whereas retrograde voluminous K-feldspar megacrystic granitoid emplacement and migmatite formation occurred until 2.58 Ga (Van Breemen et al., 1992). Davis et al. (2003) employed a post-collisional lithospheric detachment model to explain the mantle-enriched crustal melts; whereas Percival and Pysklywec (2007) argued eclogitization of mafic lower crust caused lithospheric inversion and upward heat transfer sufficient for crustal melting. Other proposed models include post-collisional upper crustal extension resulting in decompressional mantle melting and assimilation with the lower crust upon ascension (Kusky, 1993). Post-peak metamorphism D3 deformation consists of supracrustal folding, crenulation, and sinistral strike-slip fault zones; however, is not related to plutonism and its timing is poorly constrained (Davis and Bleeker, 1999).

The late-Neoarchean *bloom* of K-feldspar megacrystic granites transferred fluids and heat-producing elements from the deep crust to the near-surface, ultimately allowing for cooling and stiffening of the lower crust for stabilization and cratonization (Bleeker, 2002). Davis et al. (2003) proposed a model of craton stabilization arguing against the presence of stable lithosphere under the western and central Slave prior to late-Neoarchean tectonism, resulting in Neoarchean diamond formation. However, the sequence of stabilization of the craton is debated. Most recently, Helmstaedt (2009) suggests that the presence of Mesoarchean peri-

dotitic and Paleoproterozoic eclogitic diamonds, and the notable absence of Neoarchean diamonds, support the formation of Mesoarchean lithospheric roots under the western and central Slave, and its preservation through Neoarchean tectonism and Paleoproterozoic underplating associated with the Wopmay orogen.

Paleoproterozoic rifting separated the Slave craton from Sclavia at 2.2 Ga, and subsequent collision between the Slave, Hearne, Superior, Rae, Nain, and Wyoming Archean cratons ca. 2.0 - 1.8 Ga formed the majority of Laurentia. The Slave province now is bound to the east by the Rae craton and the 2.02 - 1.91 Ga Taltson-Thelon orogen and the resulting Great Slave Lake shear zone to the south. Collision along the western Slave margin with the Hottah and Great Bear magmatic arcs produced the Wopmay orogen at 1.95 - 1.84 Ga (Hoffman, 1988).

Multiple stages of Proterozoic diabase dyke swarms related to the initiation of the breakup of Sclavia and Paleoproterozoic rifting crosscut the Slave province. Within the southeast Slave surrounding the study area, three dyke populations are identified (Figure 1.2) based on orientation (Stubley, 2005), geochronology (LeCheminant et al., 1996), magnetism, and geochemistry (Wilkinson et al., 2001). The earliest dyke swarm is the 050° trending Malley swarm of 2.23 Ga age; followed by the 1.27 Ga 340° trending Mackenzie swarm (LeCheminant et al., 1996). The Fletcher swarm trends at 080° and is presumably associated with the 080° trending 2.21 Ga MacKay swarm to the north (Cairns, 2003; LeCheminant et al., 1996). Minor undifferentiated swarms in the area are interpreted as the eastern extent of the 022° trending 2023 - 2030 Ma Lac de Gras swarm. Three kilometers to the southwest of the study area lies the 050° Hearne swarm of 2038 Ma (Pehrsson et al., 1993).

The Malley and MacKay swarms were laterally sourced from rifting and initial breakup of Sclavia along the south and east margins of the Slave province ca. 2.2 Ga (Bleeker, 2003; LeCheminant et al., 1996). The Hearne swarm was emplaced immediately before the collisional Thelon Tectonic Zone from 2.01 to 1.91 Ga and the Great Slave Lake shear zone from 1.98 to 1.92 Ga (LeCheminant et al., 1996). The Lac de Gras swarm, although temporally associated with the Hearne swarm, is related to rifting along the western Slave province and the emplacement of the Booth River intrusive suite in the Kilohigok basin. After the formation of Laurentia, mantle upwelling at 1.27 Ga and rifting north of the present Slave craton (current Beaufort Sea) locally thinned parts of the Slave lithosphere and emplaced the Mackenzie swarm (LeCheminant et al., 1996).

The series of diabase dyke swarms record a larger Archean craton that underwent repeated rifting, collision, and mantle pluming during the Proterozoic. Despite repeated dyke swarm emplacement, thermal weakening and thinning of the lithosphere was localized around mantle plume sources and still allowed for preservation of the stable craton and resulting kimberlite potential (LeCheminant et al., 1996).

The cool, stable lithospheric root of the Slave is favorable for the preservation of diamonds and formation and ascent of kimberlite magmas. Four temporal distributions of kimberlites occur in the Slave: (1) a Siluro-Ordovician magmatism focused in the southwest Slave; (2) a Cambrian magmatism in the southeast Slave; (3) a Cretaceous and Eocene magmatism in the central Slave; (4) and the northern Slave consisting of multiple magmatic episodes during the Jurassic, Permian, and Eocambrian (Heaman et al., 2004). The

Slave province is considered a Type 3 province as it contains multiple kimberlite fields of different ages (e.g. Southern Africa and the Yakutian Province, Eastern Siberia; Mitchell, 1986; Pell, 1997).

1.5.1.1 Slave Surface at Time of Emplacement

Due to repeated erosional events and recent glaciation, the Slave province is largely devoid of Phanerozoic cover. Thermochronometry and kimberlite emplacement depths and xenoliths record repetitive sedimentation, erosion, and uplift across the Slave province (Ault et al., 2013). Phanerozoic sediments associated with the Western Canada Sedimentary Basin to the southwest extended across the Slave. However, at the time of emplacement of the Kelvin, Faraday, and Gahcho Kué kimberlites in the early Cambrian, the craton is believed to have lacked substantial sedimentary cover due to the lack of sedimentary xenoliths in the Gahcho Kué kimberlites (Hetman et al., 2004). Small black volcanic xenoliths in the Gahcho Kué pipes indicates the area may have been roofed by thin volcanic cover. Thick sequences of marine sediments emplaced in the Devonian were significantly eroded by the late Jurassic period, recorded by the Cross and Jericho kimberlites. Subsequent deposition of Cretaceous marine sediments at sea level were eroded, followed by deposition of Eocene terrestrial sediments. In the last $\sim$100 My, the Slave craton has been uplifted $>$300 m to its current elevation and repeated Quaternary glaciation has since eroded most remnants of Phanerozoic geology.

1.5.2 Glacial History of Kelvin-Faraday Corridor

The last glacial maximum (LGM) produced the majority of the glacial features in northern Canada, and little geologic evidence is preserved of the ice mechanics prior to the LGM. The LGM of the Laurentide ice sheet during the Late Wisconsin glaciation likely consisted of three sectors; one of which, the Keewatin sector, was centered over northwestern Canada. The Walmsley Lake area is believed to have been ice-free ca. 9,000 ka with most of the Keewatin sector disappearing by 8 ka (Dyke and Prest, 1987b).

Regional surficial geology mapping by the Geological Survey of Canada (GSC) (1:125,000 scale; Kerr et al., 2014), the Northwest Territories Geological Survey (NTGS) (1:50,000 scale; Knight, 2017), and Mountain Province Mining Inc (MPM) (1:57,000 scale; Hardy et al., 1997) record ice flow indicators (striations, grooves, and roche moutonnees) evidencing an early west-southwest flow ($\sim$250°), overprinted by a westward flow at 268° - 272°, followed by a later northwest flow (Figure 2.4). Ice direction indicators within three kilometers of the study area vary from 265° to 302° and most commonly trend 270°.

Dyke and Prest (1987b) suggest the southwest flow observed north of Aylmer Lake is instead youngest and records evidence of an ice dome east of the Great Slave Lake that was the center of multiple radiating regional ice divides, including the north-south M'Clintock Ice Divide (MID). With the onset of deglaciation and retreat along the western margin of the Keewatin sector, the MID migrated east resulting in complex flow histories north and northwest of the Great Slave Lake (Dyke and Prest, 1987a,b). Kerr et al. (2014) and Sharpe et al. (2017) suggest glacial history is more simple in the east arm of the Great Slave Lake defined by sustained westward flow in the Fletcher and Walmsley Lake areas preceded by a southwest flow only evidenced in the erosional record. Despite the lack of consensus on the paleoflow reconstruction, the

westward flow is responsible for most of the dispersion as ribbon-shaped KIM trains from the nearby Doyle, Faradays, Hearne, 5034, CL-25, and Snap Lake kimberlites trend west (Figure 1.6; Hardy et al., 1997; Kaiser, 2003; McClenaghan, 2005).

1.5.3 Local Geology

The Kelvin kimberlite lies under Kelvin Lake, eight kilometers northeast of Kennady Lake, 12 kilometers west of Walmsley Lake, and eight kilometers southwest of Fletcher Lake (Figure 1.2). The Walmsley Lake area lies in the eastern Slave province where calc-alkaline volcanics and metaturbidite sequences overlie juvenile basement rocks. Exposure of volcanic rocks is minor in the Walmsley Lake area; rather, it is dominated by overlying metaturbidites that are correlated across the basement suture zone with the Burwash Formation of the Yellowknife Domain (Bleeker, 2001).

By volume, volcanic rocks comprise $<10\%$ of the supracrustal rocks in the Walmsley Lake area, whereas turbidite sequences comprise $>90\%$ (Maclachlan et al., 2002). The volcanic rocks mainly occur in two volcanic belts: Aylmer Lake volcanic belt $\sim$60 km northeast of Kennady Lake, and the Cook Lake volcanic belt $\sim$35 km southeast. These belts are composed of intercalated mafic to intermediate pillows, and intermediate to felsic flows and volcaniclastics that grade upward into turbidites (Maclachlan et al., 2002; Renaud et al., 2002). Turbidites, host rocks to the Kelvin and Faraday kimberlites, are composed of psammitic greywackes and semipelitic mudstones. Metamorphic grade in the Walmsley Lake area increases to the south and west, transitioning from cordierite to sillimanite grade. The first appearance of anatectic melts appear between the Kelvin and Faraday kimberlites increasing towards the west and south. Migmatites related to peak metamorphism are more common in pelitic units, form foliation-parallel lenses, and range from haplogranitic to tonalitic composition. The paragneisses contain the upper-sillimanite metamorphic assemblage quartz-plagioclase-biotite-muscovite-garnet-sillimanite-cordierite with the addition of andalusite-tourmaline-apatite in more semipelitic rocks (Cairns, 2003).

North of Fletcher Lake, granitoids are dominated by syn- to post-kinematic *two-mica* granites forming elliptical bodies with steep granite-metaturbidite contacts. East of the Kelvin-Faraday Corridor (KFC), surrounding Walmsley Lake, lies a pre- to syn-kinematic, sheet-like, biotite$\pm$hornblende granodiorite pluton showing parallel contacts to metaturbidite layers and foliation (Maclachlan et al., 2002). West of the KFC, granitoids are dominated by pre- to syn-kinematic granodiorites (Cairns, 2003,) which have been subdivided based on magnetism (Figure 1.3; Vivian and Nowicki, 2017). Minor gabbros and diabase dykes are mapped to the east of the study area.

1.5.4 Geology of the Kelvin Kimberlite

The Kelvin kimberlite lies within the KFC, a 210° trending, three-kilometer long grouping of three kimberlite pipes and associated dykes of similar structural orientation (Vivian and Nowicki, 2017). The Kelvin, Faraday 2, and Faraday 1-3 kimberlites make up the cluster (Bezzola et al., 2018). The KFC lies within a larger NE-SW structural trend encompassing the nearby Gahcho Kué kimberlite cluster and Doyle Sheet. The Kelvin-Faraday kimberlites were emplaced into the metaturbiditic greywacke-mudstone sequences, al-

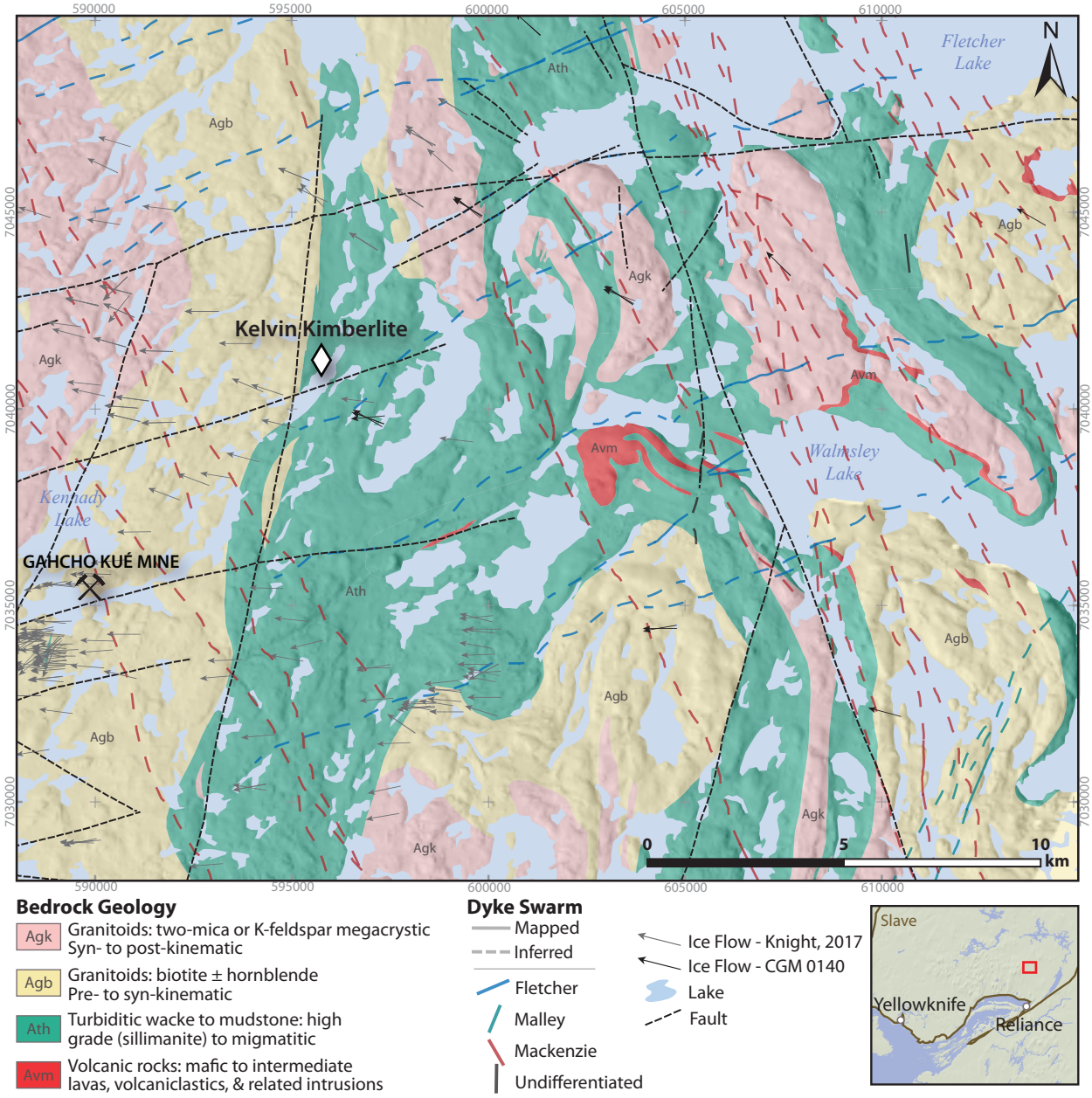

Figure 1.2: Bedrock geology west of Walmsley Lake area after Stubley (2005) and Stubley (2015). Dyke swarms after Stubley (2005); dykes inferred from high-resolution aeromagnetics and topographic expression.

though is believed to contact granitoid rocks at depth outside the defined areas of the pipe due to the presence of locally derived granitoid xenoliths within some kimberlite phases (Barnett et al., 2018).

The Kelvin kimberlite encompasses a chonolith pipe and an associated sheet dyke. The pipe body is an irregular, inclined, L-shaped pipe with two limbs referred to as the North and South Limbs. The pipe subcrops from bedrock with a surface expression of 0.08 ha, and plunges into metaturbidite bedrock towards the northwest at approximately 15° before turning north and plunging at 20° along the upper contact of the pipe. The body has been extensively drilled and defined with a strike length of 700m, although is still open

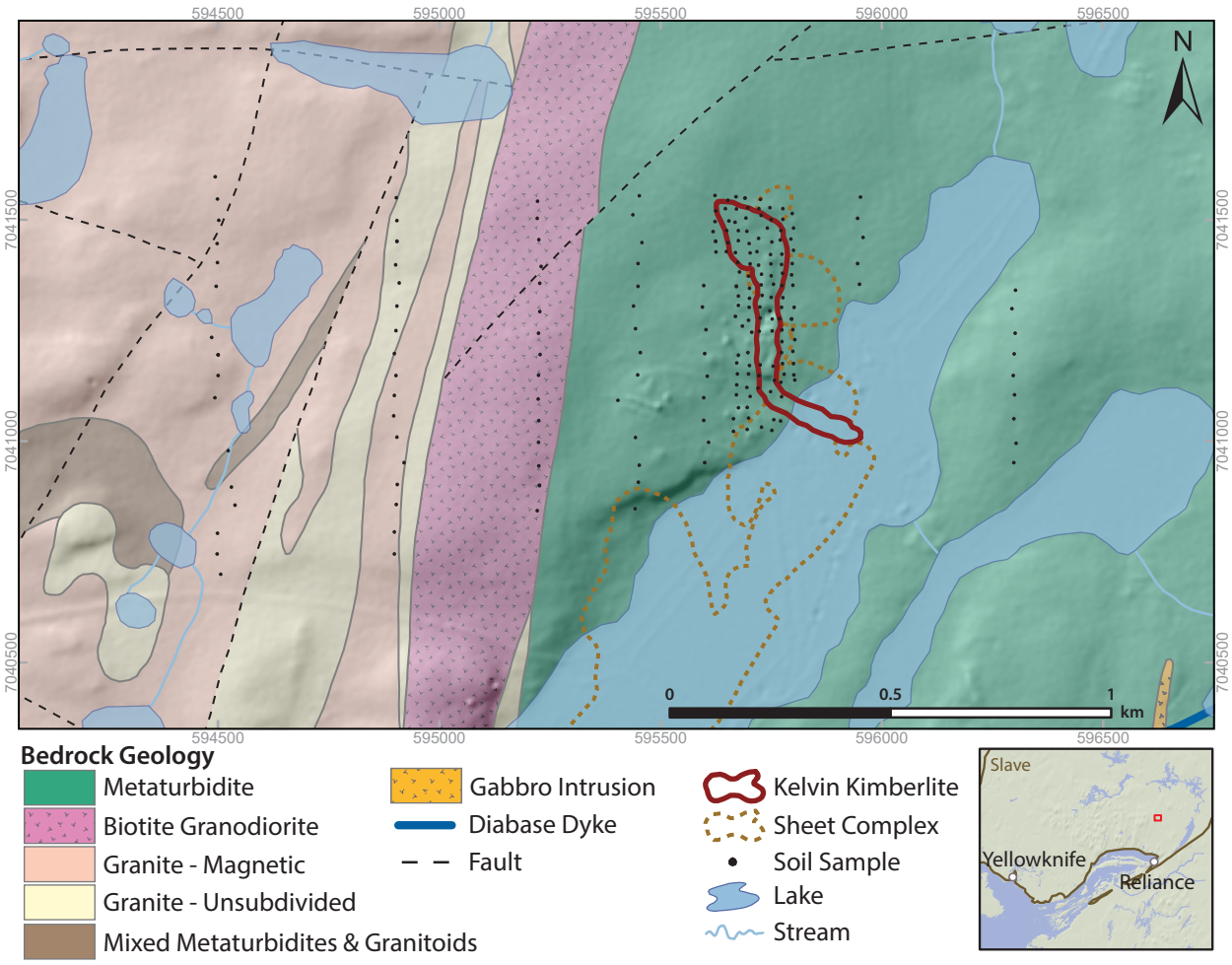

Figure 1.3: Bedrock geology of the Kelvin study area after Vivian and Nowicki (2017) and Stubley (2015)

at depth to the north. The South Limb of the pipe is 30m wide and 60m thick; as the pipe continues north it flairs up to 70m wide and 200m thick, then plunges steeper into bedrock (Vivian and Nowicki, 2017). Indicated resource of Kelvin is 8.5 million tonnes at a grade of 1.6 carats per tonne (Vivian et al., 2019). Rb-Sr dating of groundmass phlogopite yield emplacement ages of 531 $\pm$ 8 Ma and 546 $\pm$ 8 Ma (Bezzola et al., 2018).

From extensive drilling and bulk sampling, seven kimberlite phases have been identified at the Kelvin kimberlite exhibiting internal layering sub-parallel to plunge. The phases are distinguished by sharp contacts, textural variations, groundmass mineralogy, indicator mineral abundance, country rock xenolith assemblage, and diamond value and grade. Select phases contain subphases largely based on varying country rock xenolith abundance, often showing gradational contacts from 10cm to 5m thick. The descriptions and classifications follow terminology from Scott Smith et al. (2013). Kelvin is dominated by Kimberly-type pyroclastic kimberlite (KPK) facies with lesser infill of hypabyssal (HK) and members exhibiting transitional textures. Of the 3.49 Mm^3 of the defined pipe, KIMB3 constitutes 68% by volume, KIMB2 constitutes 24%, and the remaining 8% made up from the minor phases KIMB1, KIMB4, KIMB7, and large country rock

xenoliths (Bezzola et al., 2018). Description of these phases follow the most recent classifications according to Scott Smith et al. (2013).

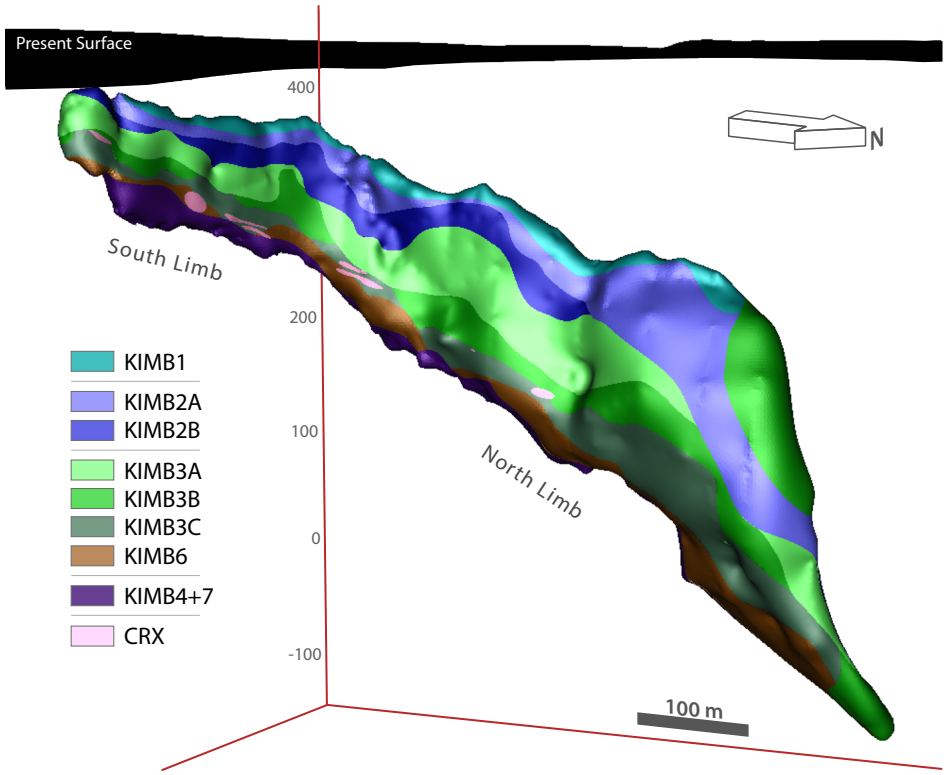

Figure 1.4: Geology of Kelvin pipe phases and subphases after Bezzola et al. (2018). Sheet dykes not shown.

KIMB1

KIMB1 is volcaniclastic kimberlite limited to the upper contact of the pipe. It is a moderately altered, massive, green phase containing 31% country rock xenolith and xenocryst dilution which are moderately to strongly altered to serpentine and hematite. Olivine macrocrysts (on average 1 - 4 mm, and up to 4 - 8 mm) constitute 12% of the phase, whereas subhedral to euhedral olivine phenocrysts constitute an additional 18%, although all olivine has been pseudomorphed by serpentine and chlorite. KIMB1 is clast supported with a serpentine and microlitic phlogopite matrix. Melt-bearing pyroclasts are common in the phase as complete to incomplete <0.5 mm thick melt selvages on either country rock xenoliths/xenocrysts or olivine. Mantle xenoliths are rare in KIMB1, and kimberlite indicator minerals (peridotitic garnet and chrome diopside) abundance is low. KIMB1 is classified as fine to medium-grained olivine macrocryst-poor, country rock xenolith-rich Kimberley-type pyroclastic phlogopite kimberlite.

KIMB2

KIMB2 is the second most common phase by volume in Kelvin pipe and contains two subphases based on textural variability. KIMB2 is dark green to black, contains 14 - 19% strongly altered country rock xenoliths and xenocrysts, rare mantle xenoliths, and low kimberlite indicator mineral counts of peridotitic garnet, ilmenite, and chrome diopside. KIMB2 is texturally variable between coherent and volcaniclas-

tic; therefore, volcaniclastic to transitional textures are classified as KIMB2A and coherent to transitional textures are classified as KIMB2B. Olivine macrocrysts and phenocrysts are partially to completely pseudomorphed by serpentine and chlorite; coarser-grained (4 - 8 mm) and occasionally fresh olivine is more commonly observed in KIMB2B. KIMB2A contains more country rock xenoliths and xenocrysts, although those of KIMB2B exhibit more intense digestion occasionally indistinguishable from matrix. White halos of clinopyroxene around completely serpentinized country rock xenoliths is a unique characteristic of KIMB2B. The matrix of KIMB2 contains phlogopite, spinel, perovskite, carbonate (groundmass and veined) and clinopyroxene exclusive to KIMB2B. On average, the matrix of KIMB2B is coarser-grained and more crystalline compared to KIMB2A, as commonly observed in hypabyssal kimberlites. Olivine-cored, melt-bearing pyroclasts with thin melt selvages are exclusive to KIMB2A: a diagnostic feature of pyroclastic textures. KIMB2A is classified as fine to medium-grained olivine macrocryst-rich, country rock xenolith-poor Kimberley-type pyroclastic to transitional textured phlogopite kimberlite; whereas KIMB2B is termed medium to coarse-grained olivine macrocryst-rich, country rock xenolith-poor hypabyssal to transitional textured phlogopite kimberlite.

KIMB3

The dominant phase at Kelvin is KIMB3, which is variably green-brown to blue-green volcaniclastic kimberlite with highly variable country rock dilution (and consequently diamond grade) resulting in gradational contacts between five subphases (KIMB3A/KIMB5, KIMB3B, KIMB3C, KIMB6) that extend subhorizontally along the strike length of the pipe. Spatially, KIMB6 lies below KIMB3 subphases, and above KIMB4 and KIMB7. Initially, KIMB5 was classified as a separate phase (Vivian and Nowicki, 2017), but has since been determined to be an altered product of KIMB3A. KIMB3A/KIMB5 contains <40% country rock dilution, KIMB3B 40 - 60% dilution, KIMB3C and KIMB6 >60% dilution. In cross section, country rock xenolith abundance increases from top to bottom of the phase, and degree of alteration of xenoliths exhibits the inverse. Olivine macrocryst and phenocryst abundance is variable between subphases, although consistently completely pseudomorphed by serpentine. The mineralogy of the matrix is typified by serpentine, phlogopite microlites, and ultra-fine (<0.125 mm) crystal and lithic fragments. Melt-bearing pyroclasts are common throughout the phase, either cored by country rock xenoliths/xenocrysts or olivine with complete to incomplete <0.5 mm thick melt selvages with a groundmass comprised of phlogopite, spinel, and perovskite. Kimberlite indicator minerals (peridotitic garnet and rare chrome diopside) abundance is low and mantle xenoliths are rare in KIMB3. The KIMB3 phase is classified as fine to medium-grained olivine macrocryst-poor, country rock xenolith-rich to xenolith-dominated Kimberley-type pyroclastic phlogopite kimberlite.

KIMB4

KIMB4 lies along the base of the pipe in close association with KIMB7. The phase is green-brown, massive, homogenous, coherent kimberlite with 17% country rock xenoliths that are commonly completely replaced by serpentine and hematite. Olivine macrocrysts and phenocrysts are completely pseudomorphed by serpentine. The homogenous, crystalline groundmass consists of phlogopite, spinel, perovskite, and

localized clinopyroxene around digested country rock xenoliths. Mantle xenoliths are rare in KIMB4, and the rare kimberlite indicator minerals of only peridotitic garnet have been identified. KIMB4 is classified as fine to coarse-grained olivine macrocryst-rich, country rock xenolith-rich hypabyssal phlogopite kimberlite.

KIMB7

KIMB7 is complexly interwoven with KIMB4 along the base of the Kelvin pipe and commonly modeled together as one geologic unit. The rock is green-brown, massive, homogenous, volcaniclastic kimberlite with 25% country rock xenoliths that have been moderately to strongly altered to serpentine. 31% of KIMB7 is olivine macrocrysts and phenocrysts which have been completely pseudomorphed by serpentine. KIMB7 is matrix supported by serpentine, phlogopite microlites, and ultra-fine crystal and lithic fragments. Melt-bearing pyroclasts are common throughout the phase often cored by country rock xenoliths/xenocrysts or olivine and contain selvages on average $<$4 mm thick, although $>$2 cm selvages are characteristic of KIMB7. Mantle xenoliths are rare in KIMB7, and kimberlite indicator minerals (peridotitic garnet) abundance is low. KIMB7 is termed fine to medium-grained olivine macrocryst-poor, country rock xenolith-rich Kimberley-type pyroclastic phlogopite kimberlite.

KIMB8

KIMB8 is a dark green-black, layered, coherent kimberlite sheet occurring outside of the north end of the Kelvin pipe. The matrix mineralogy consists of phlogopite, spinel, carbonate, and perovskite. The phase contains little to no country rock dilution, and 51% olivine macrocrysts and phenocrysts showing variable degrees of deuteric replacement by serpentine. Magmaclasts, pyroclasts, and mantle xenoliths are all absent from KIMB8, and only kelyphitized peridotitic garnets have been identified in extremely rare abundance. KIMB8 is classified as fine to coarse-grained olivine macrocryst-rich, very country rock xenolith-poor hypabyssal phlogopite-carbonate kimberlite.

KDYKE-EXT

KDYKE-EXT is a 0.5 - 2m thick hypabyssal sheet complex surrounding the Kelvin pipe oriented along the same shallow dip. The phase contains 12% country rock xenoliths that are strongly digested. The dark-green to black, crystalline matrix is composed of phlogopite, carbonate, spinel, perovskite, and monticellite. Uniformly distributed flow-aligned olivine macrocrysts and phenocrysts are completely pseudomorphed by serpentine and hematite. Mantle xenoliths and kimberlite indicator minerals are extremely rare in KDYKE-EXT. The phase has been classified as fine to coarse-grained olivine macrocryst-rich, country rock-xenolith-poor hypabyssal phlogopite-carbonate$\pm$monticellite kimberlite.

BRECCIAS

Two phases of country rock breccia are identified at the Kelvin kimberlite. The first is a clast supported flow breccia with a matrix of serpentine and ash-sized fragments. Subrounded country rock fragments exhibit thin melt selvage, faint layering, and clast alignment suggestive of an abrasive flow environment along the contacts of the chonolith and country rock where this breccia is found (Barnett et al., 2018).

The second breccia phase is dominantly found along the upper hangingwall contact of the Kelvin kimberlite and thickest at the bend between the North and South Limbs (Bezzola et al., 2018). Little to no breccia is found along the sides or base of the Kelvin pipe. This high-energy, explosive jig-saw breccia contains angular clasts of variable geometries and size. The presence of preserved fragile clast geometries and shattered crystals indicates the breccia is unevolved and has avoided post-formational clast transportation or reworking.

1.5.4.1 Emplacement Process

Recent research at the Kelvin-Faraday complex has suggested two end-member emplacement models for the chonoliths. The key factor between the two proposed models is the connection of the kimberlites to surface volcanic systems that breached the paleosurface, or lack thereof. Both proposed models term the Kelvin and Faraday pipes as chonoliths, referring to tabular intrusive bodies implying formation processes based on internal and external geometries. The formation of mafic-ultramafic chonolith intrusions requires long-lived channelized magma and fluid flow, and space creation by assimilation and physical or thermomechanical erosion and removal of country rock (Barnes et al., 2016). The depth of emplacement of the Kelvin and Faraday kimberlites has not yet been determined (Barnett et al., 2018).

Both proposed models recognize the importance of the spatial and temporal relationship between the shallow dipping sheet dykes and pipes. The sheets at Kelvin (KIMB8 and KDYKE-EXT) are believed to show segmented geometries (similar to dykes observed at Snap Lake Mine, Weddeslton Mine, Koidu Mine, Helam Mine, Star Mine) rather than geologic continuity across the study area. The geometries of these segmented dykes suggest σ_1 at the time of emplacement was parallel to the NW trend and plunge of the elongate dykes (Barnett et al., 2018). At the Kelvin and Faraday kimberlites, hypabyssal dykes are orientated sub-parallel to the base of the chonoliths and interfingered with pyroclastic units (e.g. KIMB4 and KIMB7) suggesting magma flow within the dykes temporally overlapped with pyroclastic pipe formation (Barnett et al., 2018).

In the subterranean emplacement model, the formation of the KFC chonoliths is characterized as repetitive kimberlite magma intrusions parallel to σ_1 stress orientation. Brecciation of the country rock would occur by explosive expansion of water from kimberlite fluids reaching the supercritical P-T point (22 MPa, 373°C), and by contraction and cooling of repetitive kimberlite magma pulses. Jig-saw breccias and Kimberley-type pyroclastic kimberlite textures are a result of the explosive iterative intrusive processes of magma and fluids. With intrusive bodies that do not involve surface breaching or dilation (roof-lifting), making space to accommodate magma volumes must be considered (Paterson and Fowler, 1993). Barnett et al. (2018) suggest that the small nature of kimberlite magmas require small volumes in country rock, and the high volatile and fluid content of kimberlite magmas allows for the creation of space if they escape the limits of the chonolith. The escape of volatiles and fluids through country rock fractures is supported by the subtle hydration halos recently identified in the country rocks surround the Kelvin, Faraday, and other kimberlites (Tappert and Tappert, 2018).

Barnett et al. (2018) alternatively present a model where the kimberlite systems at the KFC breached the

paleo-surface. This model relies heavily on the orientation of the dyke sheets, and the linkage zones between them. The four chonoliths at the KFC are located and formed at rock bridges between dyke sheets. Over time, linkage zones between sheets expanded by magmatic fluid brecciation, channelized magma and fluid flow, physical abrasion, and thermomechanical spalling of wall rock. Fine-grained flow breccias along pipe contacts exhibit evidence of abrasion by partially crystallized magma containing xenoliths flowing through the chonoliths. The connection to a volcanic system at surface allows the flux of large volumes of magma and xenoliths through the chonoliths over time. The internal stratification of kimberlite phases within the chonoliths and the presence of granitic xenoliths (presumably from a deeper bedrock source) support magma flux through the chonoliths.

The Kelvin pipe and dykes are unweathered; no weathered kimberlite has been documented (Bezzola et al., 2018; Vivian and Nowicki, 2017). Preglacially weathered material was likely removed by repetitive erosional and glacial events. In situ postglacial chemical and physical weathering limited to the subcrop area is likely minor, if any.

1.5.4.2 Discovery at the Kelvin-Faraday Corridor

Exploration at the Kennady Lake properties began with gold and base metal exploration within the volcanic and sedimentary sequences before staking of the properties for diamond exploration in 1992 in a joint venture between Inukshuk Capital Corp. and MPM. Exploration efforts were conducted by Canamera Geological Ltd. under Mountain Province Diamonds Inc (MPDI) from 1992 to 1996. Canamera performed kimberlite indicator mineral glacial drift sampling, an airborne electromagnetic (EM) survey, bedrock and surficial mapping, airborne and ground geophysical surveys, and follow-up sediment sampling leading to the discovery of the 5034 kimberlite in 1995 (Johnson et al., 2010). The Gahcho Kué Joint Venture (GKJV) project between MPDI and DeBeers Canada Exploration Inc (DCEI) began in 1997 where exploration efforts were focused around Kennady Lake and the 5034 body. Low-level magnetics, five-frequency EM surveys, and follow-up sediment sampling discovered the Tesla, Tuzo, and Hearne kimberlites of the Gahcho Kué cluster (Johnson et al., 2010).

EM surveys at 40 m line spacing and 20 m station spacing were flown around the Gahcho Kué cluster and to its north. Multiple subsequent ground gravity surveys and glacial sediment sampling campaigns were undertaken. Kelvin was initially drilled during the 2000 campaign and revisited in 2003 by geophysics (magnetics and gravity) and additional drilling of the pipe and sheet. Exploration efforts ceased in 2003 as the GKJV focused efforts on mine development at the Gahcho Kué cluster (Vivian and Wyllie, 2012). In late 2011, MPDI flew 3860 line kilometers of Fugro Heli-Falcon airborne gravimetrics identifying over 70 additional targets in the Kennady North properties (Figure 1.5) (Vivian and Nowicki, 2017). 100% ownership of the Kennady Lake project outside of the Gahcho Kué cluster was transferred to Mountain Province and subsequently their subsidiary company Kennady Diamonds Inc (KDI) in 2012 (Figure 1.5). KDI's work on the property has been to expand their land claims, explore the remaining property, and define the resources at the Kelvin-Faraday cluster. Since 2012, targets have been tested by ground magnetics, bathymetric, Horizontal Loop EM, OhmMapper Capacitively Coupled Resistivity, and gravity surveys (Figure 1.5). In April

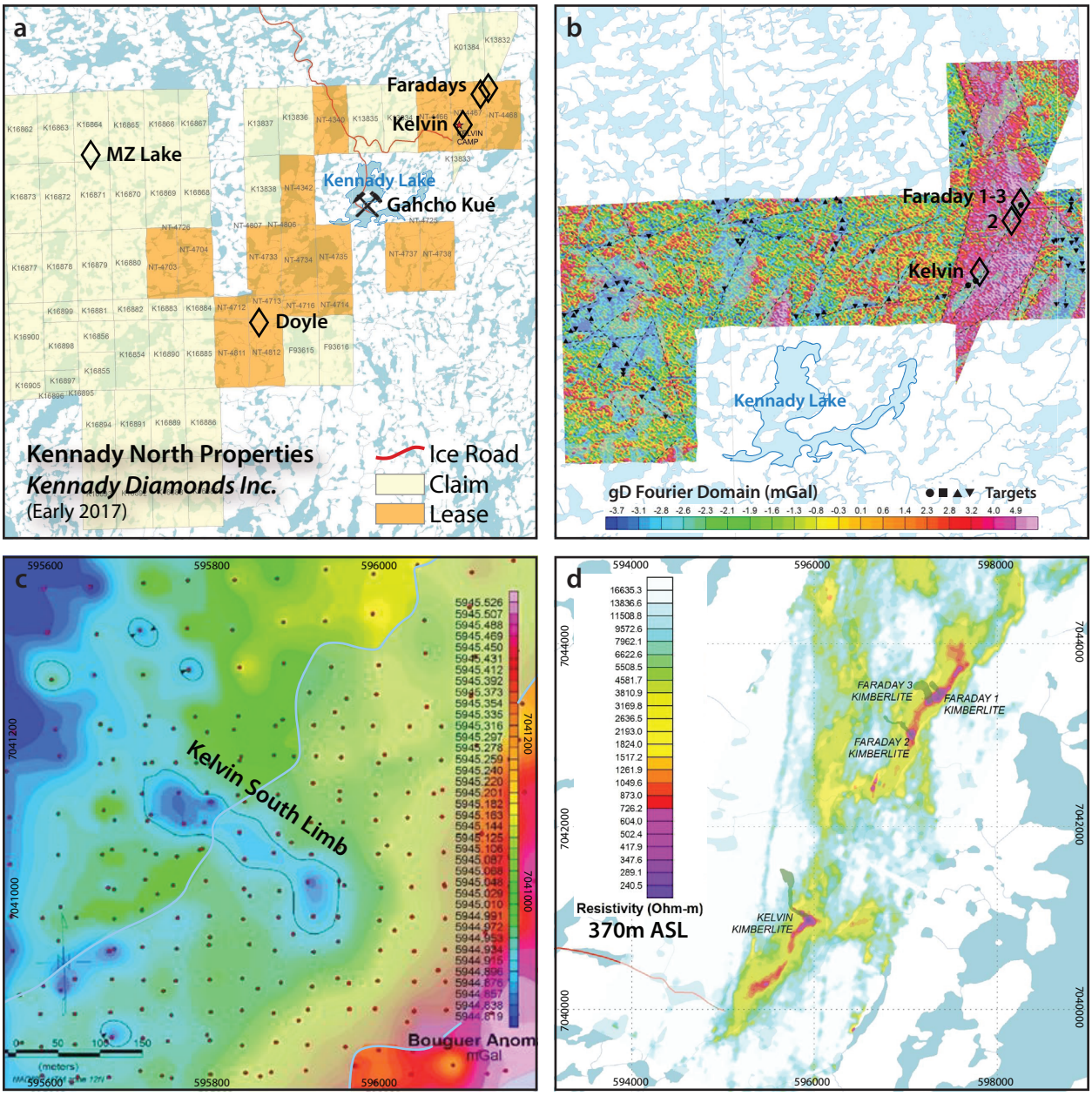

Figure 1.5: (a) Claims map of Kennady Diamond's Kennady North properties and known kimberlites and sheets. (b) 2011 Fugro HeliFalcon Airborne Gravity Gradiometry (AGG) identified 70 geophysical ranked targets. (c) Gridded 2013 Bouguer ground gravity survey over Kelvin Lake with first order trend removed. Identifies gravity low of Kelvin southern lobe extending to the northwest, and weakly detects sheet trending to southwest. (d) Slice at 370 m asl of 129 line kilometers of 2016 OhmMapper© Capacitively Coupled Resistivity survey at 20 - 40 m spacing. The use of the shallow penetrating survey (<70 m depth) is possible due to the inclined nature of the Kelvin and Faraday kimberlites and sheets. All figures after Vivian and Nowicki (2017).

2018, KDI and their mineral properties were acquired by MPDI.

KIM data from the NTGS Kimberlite Indicator and Diamond Database (KIDD) database (Figure 1.6) and 2014 reverse circulation (RC) till sampling west of Kennady Lake by KDI (Vivian and Nowicki, 2017) identify trains sourcing from the Faradays, Hearne, 5034, Doyle, and MZ kimberlites. However, no KIM train sourcing from the Kelvin kimberlite has been identified.

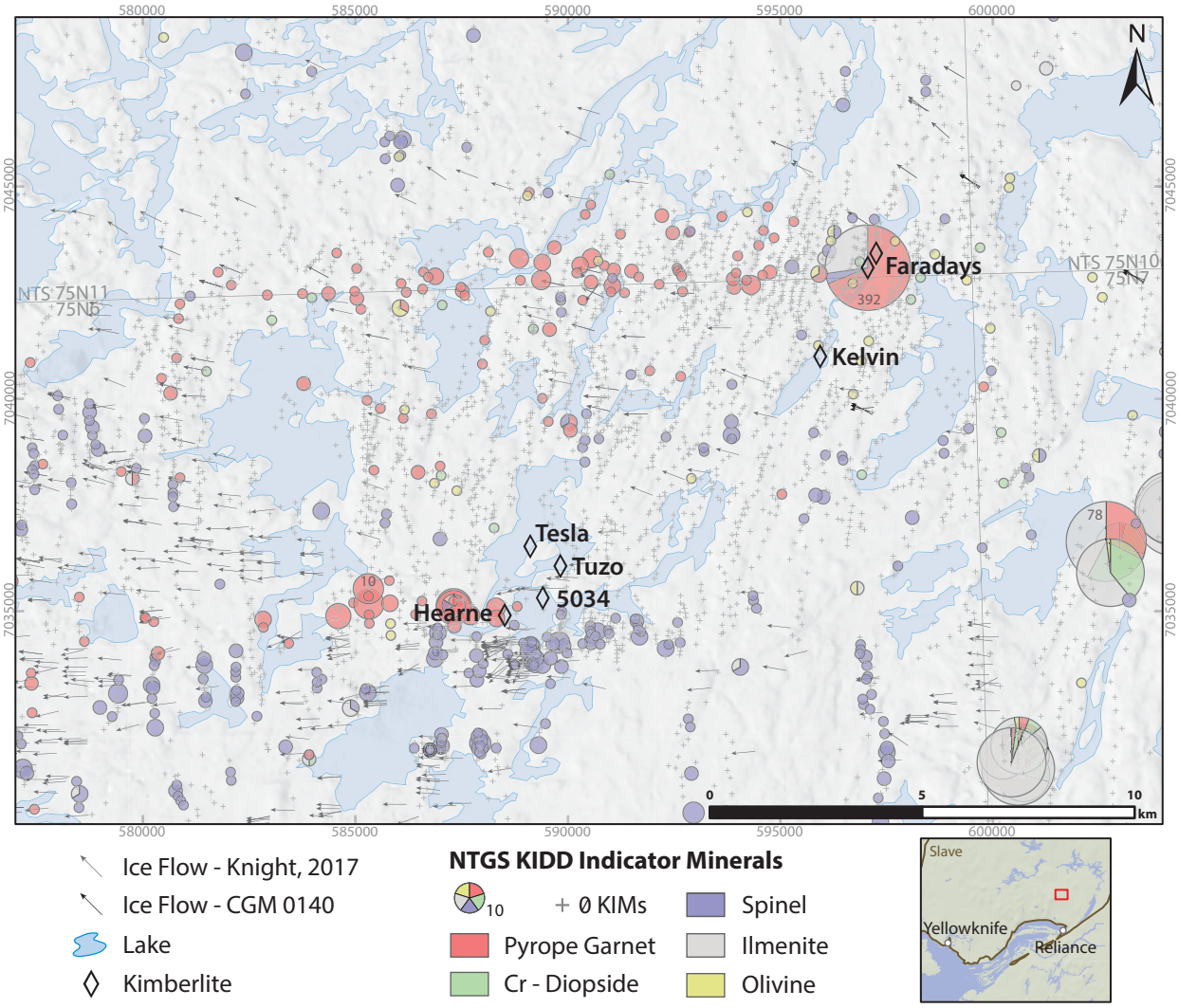

Figure 1.6: NTGS KIDD database of kimberlite indicator mineral surveys. Discernible KIM trains are sourcing from the Faradays, Hearne, and 5034 kimberlites; whereas noticeably absent from Kelvin, Tesla, and Tuzo. Precise locations of some samples have proven to be inaccurate and the database contains errors.

Chapter 2

Surficial Geochemistry

To test the application of soil geochemistry in detecting kimberlites through cover, B horizon soil samples were collected across the 2 km^2 study area above the Kelvin kimberlite. Samples were analyzed by a series of physicochemical, inorganic, organic, and hydrocarbon commercial analyses. Sequential extraction, Pb isotope, and size fraction analyses were conducted on select samples. Results and discussions from all analyses are presented in this chapter, prefaced by a technical background review and rationale.

2.1 Introduction

Kimberlites are continental ultrabasic alkaline rocks composed of varying degrees of mantle xenoliths, asthenosphere-derived magmas, and crustal xenoliths. Diamonds are contained in the mantle xenolith component including suites of websterite pyroxenite, eclogite, MARID (mica-amphibole-rutile-ilmenite-diopside nodules), and lherzolite, harzburgite, and metasomatized peridotite. Fragmentation of mantle xenoliths results in xenocrysts which make up the majority of megacryst and macrocryst textures observed in kimberlites. Additional populations of megacrysts and macrocrysts may crystallize from kimberlite magma in the upper mantle or may be unrelated to kimberlite; these include Mg-ilmenite, Cr-poor pyrope, Cr-poor diopside, enstatite, phlogopite, olivine, and zircon (Mitchell, 1995). Primary minerals crystallizing from kimberlite magma during emplacement include subhedral to euhedral phenocrysts, microphenocrysts, groundmass, and mesostasis textures composed of olivine, spinel, ilmenite, perovskite, monticellite, apatite, phlogopite, carbonate, serpentine, and chlorite. During ascent and emplacement of kimberlite magmas, crustal xenoliths of host rock are incorporated into the kimberlite in various quantities depending on emplacement textures and depth.

Kimberlitic magmas form from low degrees of partial melting in the mantle. The resultant ultrabasic, potassic melts become enriched in volatiles and incompatible elements. They contain low SiO_2 and Al_2O_3 contents (25% - 30% and <5%, respectively) and low Na_2O/K_2O ratios (Mitchell, 1986). Volatile content of CO_2 and H_2O commonly exceed 10%, consequently facilitating their rapid ascent and emplacement. Kimberlites are geochemically unique in that they display transition metal signatures of ultramafic rocks and

the incompatible and rare earth element (REE) signatures of alkaline rocks. Ultramafic signatures (largely the first-series transitional elements) are preserved in kimberlites as their rapid ascent and absence of magma chambers precludes fractional crystallization at depth. Olivine and spinel macrocrysts and phenocrysts largely host these first-series transitional elements including Sc, V, Cr, Co, Ni, Cu, and Zn (Mitchell, 1986).

Due to low degrees of partial melting, kimberlite magmas are elevated in incompatible elements including Rb, Ba, Sr, Zr, Hf, Nb, Ta, U, and Th. Incompatible and REE are partitioned into groundmass minerals in the later stages of crystallization. Phlogopite is the dominant host of Ba and Rb, while Sr is hosted in apatite, carbonate, perovskite, and diopside. Zr and Hf, which are strongly correlated, are hosted in perovskite and zircon, although zircon content in kimberlites is extremely rare. Perovskite and ilmenite are the principle hosts of Nb and Ta, although Ta is preferentially partitioned into ilmenite (Mitchell, 1986). Perovskite and apatite are the dominant hosts of U, Th, and REE. In general, kimberlites are significantly elevated in LREE and exhibit La/Yb values significantly greater than most ultramfic rocks. Major and trace element concentrations of kimberlites are influenced by contamination by mantle and crustal xenoliths and post-emplacement weathering. Despite inherent variability in global kimberlite compositions, kimberlites are easily geochemically distinguishable from most crustal country rocks.

Mineral	Formula	Common Substitutions
Olivine	$(Mg, Fe)_2SiO_4$	Mn, Ni, Co
Pyrope	$Mg_3Al_2(SiO_4)_3$	Fe, Mn, Ca, Co, Ti, Al, Cr,
Cr-diopside	$MgCaSi_2O_6$	Fe, V, Cr, Mn, Zn, Al, Ti, Na, K, Sr
Ilmenite	$FeTiO_3$	Nb, Ta, Mn, Mg, Co, Ni, Cr, V, Ta, Zr, Hf
Phlogopite	$KMg_3(AlSi_3O_{10})(OH)_2$	Ba, Rb, Sr, Mn, Cr, Na, Ti, Ni, Zn, Ca, Li, F, Cl
Spinel (Chromite)	$FeCr_2O_4$	Mg, Mn, Zn, Al, Ti
Perovskite	$CaTiO_3$	Th, U, Fe, Nb, Ta, REE, Zr, Hf, Sr
Apatite	$Ca_5(PO_4)_3(Cl, F, OH)$	REE, Sr, U, Th
Monticellite	$CaMgSiO_4$	Ti, Al, Ni, Fe, Mn, Zn
Calcite	$CaCO_3$	Sr, Mg, Fe, Mn, REE
Serpentine	$A_3 (Si_2O_5)(OH)_4$	A = Mg, Fe, Ni, Mn, Al, Zn
Chlorite	$A_{5\text{-}6}D_4(O, OH)_{18}$	A = Al, Fe, Li, Mg, Mn, Ni; D = Al, Fe, Si

Table 2.1: Common mineralogy of Group I kimberlites, formulae, and common trace element substitutions.

2.1.1 Kimberlite Exploration in Covered Terranes

Drift prospecting, the method of detecting mechanically dispersed mineralogical or geochemical evidence in glacial sediment and vectoring towards the mineral deposit source, is the most commonly used exploration practice in glaciated terranes. Drift prospecting requires knowledge of the bedrock geology, glacial history, post-glacial history, and surficial materials. Kimberlite drift prospecting hinges on the unique mineralogy and geochemistry of kimberlites that commonly contrasts against other bedrock sources. Till provides the simplest transport history for sampling, although some exploration programs employ glaciofluvial, glaciolacustrine, and stream sediment sampling representing various transport histories more suitable for regional to reconnaissance scale interpretation (McClenaghan and Kjarsgaard, 2007). Basal till repre-

sents primary material derived directly from glacial erosion of bedrock with a relatively simple transport history dictated by glacial flow history. Tracing mineralogical and geochemical signatures in the till to the source (i.e. kimberlite) requires detailed knowledge of flow histories, ice bed conditions, till stratigraphy, and bedrock topography (Kelley et al., 2019). Ultimately, exploration geologists are tasked with modeling dispersal plumes in glacial sediments from their surface expression.

KIM sampling from till or stream sediments is widely used across Canada and the most common methodology applied in kimberlite exploration. Many indicator minerals are, to a degree, physically and chemically resistant to pre-glacial weathering, glacial comminution, and post-glacial weathering and occur as sand-sized grains in glacial sediment. Indicator minerals include mantle xenocrysts of olivine, enstatite, Cr-diopside, Cr-pyrope, Cr-spinel, eclogitic garnet, and omphacitic pyroxene; megacrystic low-Cr Ti-pyrope, Mg-ilmenite, Cr-diopside, phlogopite, zircon, and olivine; and primary phenocrystic olivine and spinel (McClenaghan and Kjarsgaard, 2007). Till sampling guidelines from the GSC require 20 - 30 kg of unweathered till and focus on recovering coarser sand-sized (0.25 - 2.0 mm) indicators (Spirito et al., 2011). Mantle-derived xenocryst indicators can be subsequently analyzed to geochemically evaluate diamond potential and mantle composition, while transport distance can be interpreted from grain morphologies and textures (McCandless, 1990; McCandless and Nash, 1996; McClenaghan, 2005).

Till matrix geochemistry has been applied in drift exploration to many deposit types and its application is increasing with reducing costs and improving detection limits of commercial analytical methods. The mafic and alkaline geochemical signatures of kimberlites distinguish them from most Slave province country rocks; pathfinder elements expected to be significantly elevated in anomalous till include Mg, Ni, Cr, Co, Nb, Ta, Ti, Ba, K, Rb, Sr, P, and LREE (Figure 2.1). Strong digestions (four acid and lithium borate fusion) are recommended for kimberlite exploration in order to digest resistant kimberlite silicate and oxide minerals that resist chemical weathering (Table 2.1 McClenaghan and Kjarsgaard, 2007). Selective leaches target mobile geochemical signatures that migrate vertically from the deposit through overburden (Hamilton, 2007b; McClenaghan et al., 2006; Sader et al., 2009). Soil hydrocarbon responses above kimberlites have been tested, however, the application of sequential leach and soil hydrocarbons have largely been limited to academic research and case studies (Cayer, 2017; Hamilton, 2007b; Sader et al., 2009). Complementary geophysical exploration methods ubiquitously used in kimberlite exploration include magnetics, resistivity, gravity, EM, seismic refraction surveys, and ground penetrating radar (GPR), which all require interpretation based on bedrock geology, overburden thickness, and kimberlite facies and erosion depth (Power and Hildes, 2007).

2.1.2 Mechanisms of Element Migration

Inorganic geochemical surface exploration through cover relies on pathfinder elements migrating via mechanical or labile dispersion from the deposit at depth into the near-surface environment. The mechanisms for physical element dispersion in northern Canada are dominated by glacial erosion, transport, and deposition as till and its derivatives. Post-depositional mechanical processes include soil formation processes, mass wasting, fluvial erosion, and cryoturbation. Kimberlite drift exploration relies on this me-

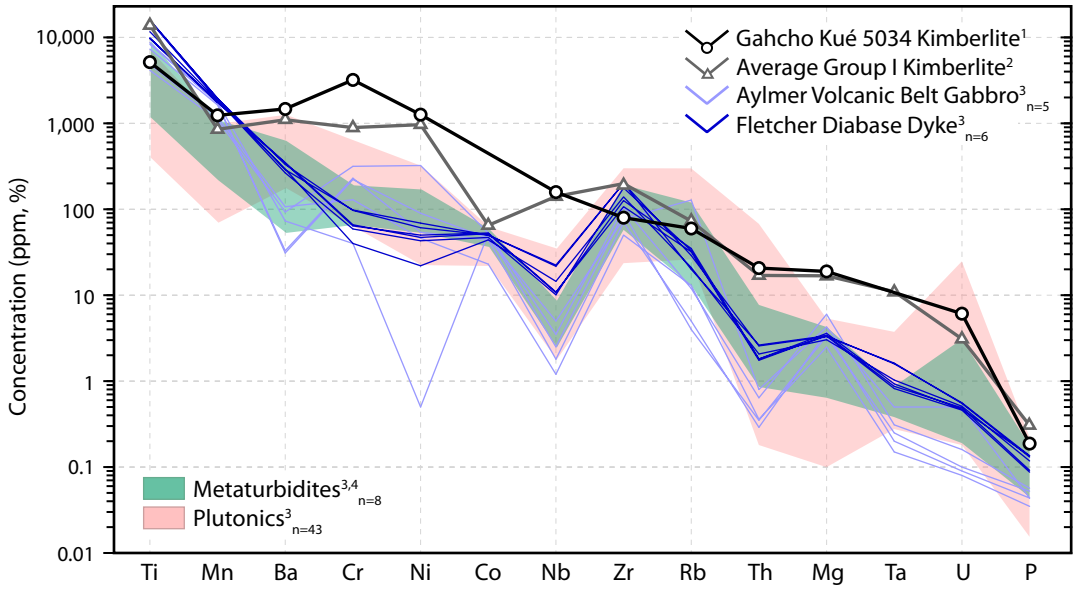

Figure 2.1: Spider diagram showing pathfinder elements concentrations of average Group I kimberlite and Slave country rocks. [1] Caro et al. (2004); [2] Dawson (1967); [3] Cairns et al. (2003); [4] this study.

chanical dispersion of kimberlite material and its preservation within glacial sediments.

Vertical ionic dispersion through overburden may be facilitated by vadose zone diffusion, groundwater flow, capillary rise, electrochemical migration, and vadose zone gaseous transport. Given the short time of soil formation since deglaciation (<10,000 years), electrochemical and groundwater transport are expected to be the dominant processes in the subarctic (Hamilton, 2007b). Selective leaches are commonly used to detect buried mineralization through cover by targeting specific mineral phases that host mobile geochemical signatures that have migrated from depth (McClenaghan et al., 2006). In many case studies, these surveys detect pathfinder elements over the center and peripheries of concealed kimberlite subcrops (Hattori et al., 2009; McClenaghan et al., 2006; Sader et al., 2009; Seneshen et al., 2001). At the Kelvin kimberlite, due to the inclined pipe morphology and small subcrop expression concealed by the lake, selective leach extractions to measure vertical ion-migration processes were not collected. Instead, the research focuses on the mechanical element migration from clastic glacial dispersion and post-depositional reworking.

2.1.3 Soil Chemistry

Soil development is the result of the parent material on which it forms (e.g., till or bedrock) and chemical and physical weathering controlled by climate, topography, organisms, and time. Oxidation and leaching of soluble and mobile elements in the uppermost profile yields elluviated horizons (Ah and Ae horizons) immediately below organic accumulations on the surface (O horizon). Mobile cations leached from the elluviated horizons accumulate in the underlying B horizon, in addition to organic matter, secondary clay minerals, and Fe-Mn-Al oxides and hydroxides (Hall, 1998; Soil Classification Working Group, 1998; Spirito et al., 2011). The cation exchange capacity (CEC) of the zone of illuviation (accumulation) increases due to the formation of these secondary phases, resulting in an accumulation of trace elements and metal

cations.

Collectively, all soil horizons are sampled for various exploration surveys. Biotic processes in the organic-rich mineral horizons (Ah) may allow trace element uptake and the formation of geochemical anomalies (Heberlein, 2010; Rate, 2010). B horizon is the most common sampling medium in the use of partial extractions and in areas of residual cover (Cameron et al., 2004; Mann et al., 2005; McClenaghan et al., 2006). However, in till sampling with the ultimate goal of identifying geochemical or indicator mineral dispersal plumes, C horizon is the standard sampling medium in order to collect the freshest till that most accurately represents bedrock provenance (McClenaghan and Paulen, 2018; McClenaghan et al., 2013; McMartin and McClenaghan, 2001; Spirito et al., 2011). Collection of C horizon material may require augering, trenching, drilling, or be impeded by permafrost in the subarctic (Spirito et al., 2011). Samples were collected from the upper B horizon to provide a consistent medium for tight sample spacing, limit variation across the study area, and exploit illuviated trace element signatures.

Humic material is amorphous, colloidal organic matter synthesized in soils by decomposition of plant and animal material (Tan, 1998). It is broadly classified into two operational terms: humic and fulvic acids. Both humic and fulvic acids have high exchange capacities and form organo-metallic complexes between metal ions and functional groups. Fulvic acid complexes are largely soluble and responsible for metal mobility, whereas less mobile humic acid complexes are responsible for metal scavenging and immobility (Tan, 1998). High organic carbon contents in mineral soils have been shown to control trace metal (Ca, Cd, Mg, Ni, P, Pb, Sr, Zn, Mo) content and organic carbon rich soils should be interpreted separately from organic carbon poor datasets (McClenaghan et al., 2006; Rich, 2016). Careful consideration must be taken in cryosols where cryoturbation in frost boils may produce broken organic horizons at depth due to circulation of surface organics down along the margins (Figure 2.2).

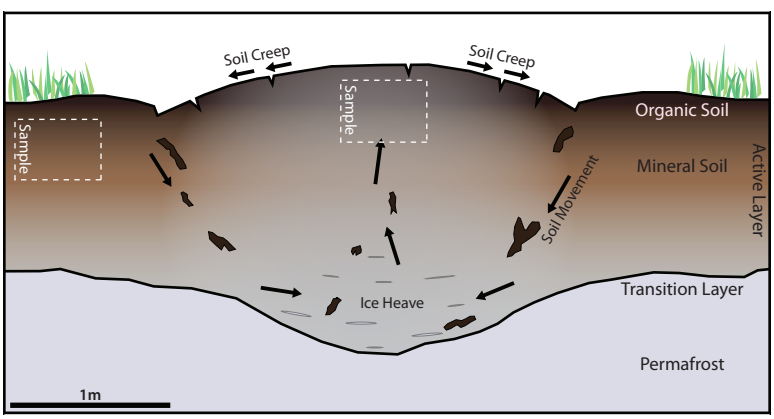

Figure 2.2: Conceptual cross section of frost boil and circulation of broken organic horizons down the margins and up through center. Samples are collected from the center of the frost boil. Modified after Walker et al. (2004).

2.1.4 Inorganic Soil Geochemical Analyses

Four Acid

Four acid digestions (HNO_3:$HClO_4$:HF:HCl) are considered total or near-total digestion methods that accurately determine major, minor, and trace element concentrations. Digested phases include silicates, oxides, sulfides, carbonates, phosphates, borates, and most sulfates (Hall, 1991). Notable refractory (resistant) phases not digested in four acid solution include chromite, spinel, beryl, zircon, tourmaline, magnetite, and baryte (ALS Geochemistry, 2016; Hall, 1991). As a result, REE determinations are not complete and volatilization of Si, As, Sb, and Au occur upon dissolution from HF acid.

Total digestions of till are commonplace in drift exploration to relate till composition to bedrock provenance; four acid or lithium borate fusion are the most commonly used total digestions (McClenaghan and Kjarsgaard, 2007; McClenaghan and Paulen, 2018). In kimberlite exploration, total digestions are recommended to ensure digestion of oxide and silicate mineralogy of kimberlites (reference kimberlite mineralogy table here: Introduction). Consequently, the dissolution of major rock-forming minerals (e.g., quartz and feldspars) may dilute anomalous signals relative to background resulting in lower anomalous to background response ratios. Four acid digestion was completed on all soil samples to ensure digestion of kimberlite indicator mineralogy, to asses standard industry practice, and to follow the recommendation of Cayer (2017) that supports four acid digestion for geochemical clastic kimberlite exploration.

Aqua Regia

Aqua regia (3:1 HCl:HNO_3) is a partial digestion method that targets oxides, sulfides, carbonates, phosphates, sulfates, and associated sorbed elements (Hall, 1991). Partial digestion of micas and clay minerals may occur, however notable resistant minerals include chromite, garnet, ilmenite, olivine, pyroxenes, rutile, zircon. Aqua regia is widely used to target (1) primary minerals commonly associated with mineralization including sulfides and clay minerals; (2) elements migrated from mineralization at depth (exogenic phases); and (3) trace metals redistributed into secondary phases during soil formation (Section 2.1; Cameron et al., 2004). Its application in many regional exploration programs in residually and till-covered terranes allows for comparison between datasets. Aqua regia was applied to all soils to asses its application in kimberlite exploration in transported covered terranes.

Sequential Extraction

Sequential extraction chemistry is employed in exploration to determine residence phases of elements in soils and sediments, particularly secondary phases that may host labile ions. Results quantify elemental concentrations hosted (1) as labile and weakly adsorbed ions; (2) as exchanged cations; (3) bound to carbonates; (4) bound to Mn oxides; (5) bound to Fe oxides; and (6) bound to soluble organic matter (Hall, 1998). When performed sequentially, specific phases are individually extracted reducing unwanted reactions or dissolution of other phases (Hall et al., 1996). Common commercial procedure involves the leach sequence of deionized water (DIW), ammonium acetate (AA), cold hydroxylamine hydrochloride (C-HA-HC), hot hydroxylamine hydrochloride (H-HA-HC), sodium pyrophosphate (NaP), aqua regia, four acid, and possibly lithium borate fusion (Table 2.2). Additional commercially available partial leaches that seek to replace the necessity of sequential extractions by targeting multiple phases include the Enzyme Leach (Activision Laboratories) and MMI (Mobile Metal Ion; Mann et al., 1998). Sequential extraction analyses were completed

on two background and two anomalous samples to quantify the geochemical partitioning in soil phases, therefore establishing the mechanism of anomaly formation.

	Extraction Reagent	Abbreviation	Target Phase	ALS Code
1	Deionized Water @ 60°C	DIW	labile and water soluble salts, weakly sorbed ions	ME-MS03
2	Ammonium Acetate pH 5	AA	Ca-carbonate, exchanged cations	ME-MS04
3	Cold Hydroxalamine Hydrochloride 0.14M @ 25°C	C-HA-HC	amorphous + crystalline Mn oxides	ME-MS05
4	Hot Hydroxalamine Hydrochloride 0.25M @ 60°C	H-HA-HC	amorphous Fe oxides	ME-MS06
5	Na pyro-phosphate (0.1M)	NaP	organic acids	ME-MS07
6	Aqua Regia	AR	sulfides, amorphous + crystalline Fe/Mn oxides, clay minerals	ME-MS41L
7	Four Acid	4A	most silicates	ME-4ACD81

Table 2.2: Table of sequential extractions, reagents, and target phases. See Section A.4 for detailed methodologies.

pH and Oxidation-Reduction Potential

Slurry pH surveys have been shown to detect acid caps formed in the vadose zone above reduced chimneys related to buried sulfide mineralization (Hamilton, 2007b; Smee, 1999). Kimberlites and ultramafic rocks are reducing and alkaline bodies relative to their common country rocks and may form an "alkaline chimney" as well. Low temperature weathering (also referred to as low temperature serpentinization at standard temperature and pressure) of ultramafic minerals (olivine and pyroxene) consumes H^+ increasing pH and releasing Ca^{2+}, Mg^{2+}, and Fe^{2+} cations (Equation 2.1, Equation 2.2). Magnesium is consumed in the production of serpentine whereas the oxidation of Fe^{2+} forming hematite and magnetite reduces the surrounding environment yielding reduced groundwater (Equation 2.3, Equation 2.4; Burt and Hamilton, 2004; McClenaghan et al., 2006; Palandri and Reed, 2004; Sader et al., 2007). Advection and/or convection of alkaline groundwater in contact with the kimberlite, likely facilitated along the brecciated margins, has produced elevated pH conditions above kimberlites (Burt and Hamilton, 2004; McClenaghan et al., 2006). Where advective groundwater movement through overburden is restricted due to permafrost or less permeable clay-bearing cover (i.e. basal till), electrochemical transport will be the dominant mechanism resulting in an acidic cap above mineralization (Hamilton, 2007a). Slurry pH measurements were collected to aid in the interpretation of trace element mobility in the soils. oxidation reduction potential (ORP) measurements were not collected in the field due to time constraints, and only collected on 38 samples upon return to the laboratory at the University of British Columbia (UBC).

$$\text{Olivine Dissolution: } FeMgSiO_4 + 4H^+ \rightarrow Fe^{2+} + Mg^{2+} + H_4SiO_{4(aq)} \tag{2.1}$$

$$\text{Pyroxene Dissolution: } (Ca,Mg)SiO_3 + 2H^+ + H_2O \rightarrow \tfrac{1}{2}Ca^{2+} + \tfrac{1}{2}Mg^{2+} + H_4SiO_{4(aq)} \tag{2.2}$$

$$\text{Serpentine Production: } 3Mg^{2+} + 2H_4SiO_4 + H_2O \rightarrow Mg_3Si_2O_5(OH)_4 + 6H^+ \tag{2.3}$$

$$\text{Oxidation of } Fe^{2+}\text{: } 2Fe(OH)^+ + 2OH^- \rightarrow Fe_2O_3 + H_2O + H_{2(g)} \tag{2.4}$$

2.1.5 Geochemical Partitioning in Size Fractions

During glacial erosion and transport, the comminution of mineral grains to their optimum minimum grain size is termed the *terminal mode* (Dreimanis and Vagners, 1971). The terminal mode of a mineral is controlled by the physical properties of the original grain, including size, hardness, cleavage, and petrographic affiliations within its host rock. Hard minerals lacking cleavage (e.g., quartz, feldspars, garnet, magnetite) are expected to resist comminution and, depending on original grain size, concentrate in the coarse to fine sand fraction of basal till. The softness and cleavage of calcite and dolomite lend their terminal modes in the silt fraction. Micas, phyllosilicates, clay minerals, serpentine, and hematite have terminal modes in the clay fraction due to their softness, cleavage, and predominance to crystallize as fine-grained minerals. Naturally, the predominance of certain minerals in different size fraction will be reflected in the geochemistry. This process is referred to as geochemical size fraction partitioning. The concentration of phyllosilicates in the fine fraction ultimately results in increased CEC and the capture of labile cations. Weathering and formation of secondary Fe-Mn (hydr)oxides and clay minerals in B horizon soils introduce additional cation capturing ability, in addition to organic acids (Section 2.1.3).

The largely bimodal grain size distribution of kimberlite minerals contains megacryst, macrocryst, and phenocryst indicator minerals, as well as groundmass and matrix minerals (Figure 2.3). The <0.063 mm fraction (silt + clay) of till has proven to be the most effective commercially viable size fraction in kimberlite exploration, consistently providing the highest anomalous to background contrast compared to 0.063 - 0.25 mm (very fine to fine sand), 0.25 - 0.5 mm (medium sand), and 0.5 - 2.0 mm (coarse and very coarse sand) fractions (McClenaghan et al., 1999b,c, 2011). The <0.002 mm (<2 µm) is also suggested to reduce both dilution and nugget effects, however, its widespread application is deterred by the preparation cost and large sample volume required (McClenaghan and Paulen, 2018). The clay fraction, as it contains weathering products such as secondary clays, organic compounds, and Fe-Mn (hydr)oxides, hosts the mobile geochemical signature. It is commonly utilized by the GSC for mineralization expected to weather under oxidizing conditions and release labile pathfinder elements in till (i.e. sulfide and carbonate mineralization; Spirito et al., 2011). However, the analysis of the <2 µm fraction is not necessary for weathering resistant kimberlite indicator minerals (Shilts, 1993, 1995).

The texture of a kimberlite may influence which fraction exhibits the strongest anomalous response (McClenaghan and Kjarsgaard, 2001). Till geochemistry studies at the hypabyssal Peddie kimberlite observed the 0.5 - 2 mm fraction displays the best anomalous to background contrast for pathfinder elements due to abundant fresh sand sized olivine phenocrysts and macrocrysts, Mg-ilmenite, apatite, and phlogopite (McClenaghan et al., 1999a). Studies of the pyroclastic C14 and A4 kimberlites indicated the <0.063 mm fraction displayed the best contrast ratio (McClenaghan et al., 1999b,c). Geochemical interrogation of soil size fractions was undertaken at the Kelvin kimberlite in an attempt to assess geochemical partitioning within the soil. The grains size distribution of till, most importantly the clay fraction, can widely vary across the Canadian Shield from 2 - 20% by weight of the <2 mm fraction (Shilts, 1971, 1993). Therefore, the inclusion of size fraction geochemistry of till and soil is imperative in orientation surveys prior to conducting a large scale survey.

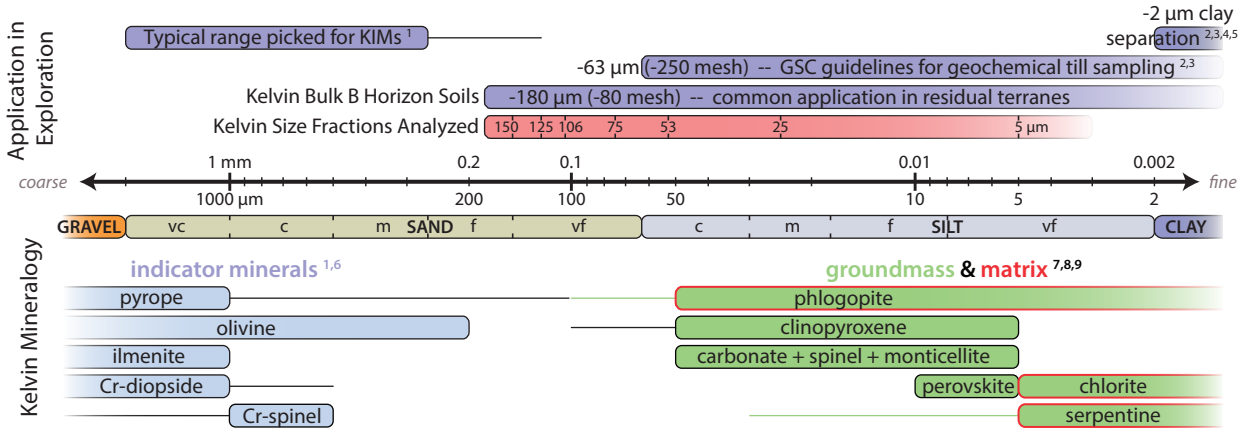

Figure 2.3: Wentworth log-scale grain size classification showing size fractions commonly analyzed in covered and residual terranes. Because indicator minerals, and published information about them, are rare in Kelvin, typical grain sizes are shown from kimberlite literature. Groundmass and matrix mineralogy is from Kelvin literature. Groundmass refers to primary groundmass minerals crystallized from late stage melt, e.g., magmaclasts and selvages. Matrix refers to intermagmaclast matrix and mesostasis products. Kimberlite mineral sizes are based on primary grain size in kimberlites and does not account for glacial comminution. [1] McClenaghan and Kjarsgaard (2007); [2] Spirito et al. (2011); [3] McClenaghan et al. (2013); [4] Noble et al. (2019); [5] Benn et al. (2016); [6] McClenaghan and Kjarsgaard (2001); [7] Mitchell and Scott Smith (2017); [8] Bezzola et al. (2018); [9] Vivian and Nowicki (2017).

2.1.6 Pb Isotope Systematics

Lead has four stable isotopes: one non-radiogenic (^{204}Pb) and three radiogenic isotopes (^{206}Pb, ^{207}Pb, ^{208}Pb) themselves a stable end result of radioactive decay from ^{238}U, ^{235}U, ^{232}Th, respectively. Through geologic time, the abundance of radiogenic Pb has increased through radioactive decay, while non-radiogenic ^{204}Pb has remained the same. The present day Pb isotope values of a mineral deposit reflect the combination of the initial isotopic signature plus radiogenic Pb production since formation, assuming no migration of Th, U or daughter Pb.

Lead isotopes do not fractionate as a result of weathering, mineral crystallization, evaporation, biological activity, or processes that affect light isotopes (S, C, O, H; Gulson, 1986). Due to the similar mass of Pb isotopes, the chemical reactivity of the four isotopes behave similarly. Pb is relatively insoluble and mobility is restricted in average ground and surface water conditions (McLean and Bledsoe, 1992). Effects from aqueous dispersion are minimal in the near-surface, although solubility increases in acidic conditions and as organic complexes (Schwedt, 2001). Pb^{2+} does not behave similarly to U and Th due to its larger ionic radius; and is soluble at moderate to high temperatures of hydrothermal, magmatic, and metamorphic fluids (Tosdal et al., 1999). Uranium and thorium behave similarly as incompatible elements in partial melting and fractional crystallization. Under oxidizing conditions, uranium is mobile as U^{6+} and may be fractionated from thorium.

The application of Pb isotope ratios to mineral exploration has largely been limited to sulfide and U-rich deposit types. Uranium exploration operates under the systematics that uranium ore enriched in ^{238}U/^{206}Pb and ^{235}U/^{207}Pb will become significantly more radiogenic (increased ^{206}/^{204}Pb and ^{207}/^{204}Pb, respectively)

over time strongly contrasting against country rocks (Holk et al., 2003). In glaciated terranes of Canada, the application of Pb isotope ratios has been focused on VMS deposits where the strongly non-radiogenic nature of sulfides (negligible U and Th, and elevated Pb) do not allow ratios to appreciably change over time. This contrasts against radiogenic country rocks that, through radioactive decay, will become more radiogenic with time (Bell and Franklin, 1993; Gulson, 1986; Hussein et al., 2003; Rukhlov and Ferbey, 2015). Selective and partial leaches are recommended in situations when Pb-bearing sulfides are weathered in oxidized till, and scavenging by phyllosilicates and secondary Fe-Mn (hydr)oxides preserve Pb ratios within soil profiles (Simonetti et al., 1996).

Kimberlites exhibit varying and radiogenic Pb isotopic compositions, and trends similar to ocean island basalts and carbonatites (Kramers, 1977; Mitchell, 1986). Pb isotopic values of bulk kimberlite or kimberlite autoliths are only available for Cretaceous southern African (Kramers, 1977; Smith, 1983; Weis and Demaiffe, 1985), Devonian Russian kimberlites (Beard et al., 2000; Maas et al., 2005), and the Cretaceous Nikos kimberlite of Nunavut (Schmidberger et al., 2001).

Lead isotope analysis by single collector inductively coupled plasma mass spectrometry (ICP-MS) is increasingly becoming more commonplace to sacrifice a degree of precision and accuracy for decreased cost and increased throughput. High precision and accuracy analyses of Pb isotopes are traditionally performed by thermal ionization mass spectrometry (TIMS) and multi-collector inductively coupled plasma mass spectrometry (MC-ICP-MS) requiring clean laboratory environments, Pb isolation, and purification. An increase in recent environment and health research has focused on isotopic source and pathway utilizing the cheaper and faster, albeit less precise and accurate, quadruple inductively coupled plasma mass spectrometry (Q-ICP-MS) (Gulson et al., 2018; Rukhlov and Ferbey, 2015). The routine analysis for ^{202}Hg by MC-ICP-MS allows the correction of isobaric interferences on ^{204}Pb by ^{204}Hg; however. this correction is not made in single collector ICP-MS analyses (including those in this research; Gulson et al., 2018; Ridley, 2005). Gulson et al. (2018) and Rukhlov and Ferbey (2015) suggest the diminished accuracy and precision of single collector ICP-MS (i.e. Q-ICP-MS) limits its application to simple cases with mixing of only two end-member components with $>10\%$ isotopic contrast.

2.1.7 Soil Hydrocarbons

Soil hydrocarbons form as a result of microbial activity. Soil hydrocarbon responses are attributed to changes in microbes in variable redox/pH conditions of 'reduced chimneys' above and around buried mineralization (Hamilton, 2007b; Sader et al., 2009; Sutherland, 2018). It has been suggested that vertical migration for soil hydrocarbons from depth via buoyancy and gas entrainment, as in petroleum microseepage (Amplified Geochemical Imaging LLC, 2015), may operate in conjunction with redox gradient hydrocarbon formation to produce surface responses (Noble et al., 2013).

In non-petroleum exploration, hydrocarbon analysis is largely limited to two commercial laboratories: Amplified Geochemical Imaging (AGI) and Activation Laboratories Spatio-temporal Geochemical Hydrocarbon (SGH). AGI involves time-integrated, passive sampling with gas permeable - waterproof collectors and analysis by thermal desorption gas chromatography mass spectrometry (GC-MS)(Amplified Geochem-

ical Imaging LLC, 2015). The SGH method involves a proprietary weak leach to extract surface-bound hydrocarbons from a soil sample prior to analysis by GC-MS (Sutherland, 2018). Recent studies have explored the application of both AGI (Bodnar, 2017; Chouinard, 2018; Noble et al., 2018; Rich, 2016; Sader et al., 2009) and SGH methods (Cayer, 2017; Heberlein, 2010; Noble et al., 2013) to detect mineralization through exotic cover and validate the proprietary techniques. SGH analysis was applied at the Kelvin kimberlite to further explore some of the correlations between individual hydrocarbon compounds and kimberlite pathfinder elements and surface material (Cayer, 2017).

2.2 Surface Materials

2.2.1 Surface Materials

The surficial cover in and around the KFC is dominated by largely continuous and residual till blanket (2 - 5m thick) and till veneer (1 - 2 m thick). Till thickness and depth to bedrock is estimated from drill hole data provided by KDI(Figure 2.5). Till thickness averages 2.8 m, but can be up to 8.4 m as it increases in thickness to the northeast. Field mapping and depth to bedrock measurements largely agree with regional mapping from Kerr et al. (2014) and Hardy et al. (1997), however, local discrepancies have been identified. Accounting for local topographic variations, till in the study area is continuous and conformable as no bedrock exposures were noted in the immediate area. Due to the extensive surface cover and lack of bedrock outcrop, no ice flow indicators were documented.

The dominant surficial material in the KFC is till deposited by basal or lodgement processes with a short travel distance from its bedrock source (Hardy et al., 1997). The dominant surface material is diamicton: poorly sorted sediments containing clay, silt, sand, gravel, and boulder fractions. Regional surface mapping campaigns classify till largely into three regimes based on thickness and surface characteristics: veneer (<2 m thick), blanket (2 - 5 m thick), and hummocky (>5 m thick) (Dredge et al., 1994; Kerr et al., 2014, 2013; Sacco et al., 2018). The till across the study area can broadly be termed a till blanket due to cover thickness, lack of bedrock outcrops, and generally conforming to bedrock topography. The till blanket is largely unworked by secondary glacial processes and is easily distinguishable on the surface as it commonly forms featureless plains with frequent frost boils and low distribution of partially-exposed, subangular boulders (Figure 2.7b, c). Till in the study area exhibits subangular clasts of granite and gneiss; sandy silt matrix characteristic of shield basal till (Sharpe et al., 2013); and has commonly been cryoturbated destroying any primary structures.

The Kelvin kimberlite subcrops in the center of Kelvin Lake capped by <5 m overburden (till and lacustine sediments) and <10 m water. Kelvin Lake currently sits at 410 - 413 m elevation. Evidence of paleo-shorelines (sand beaches, washed bedrock patches) are absent in the field and in aerial imagery (Figure 2.6).

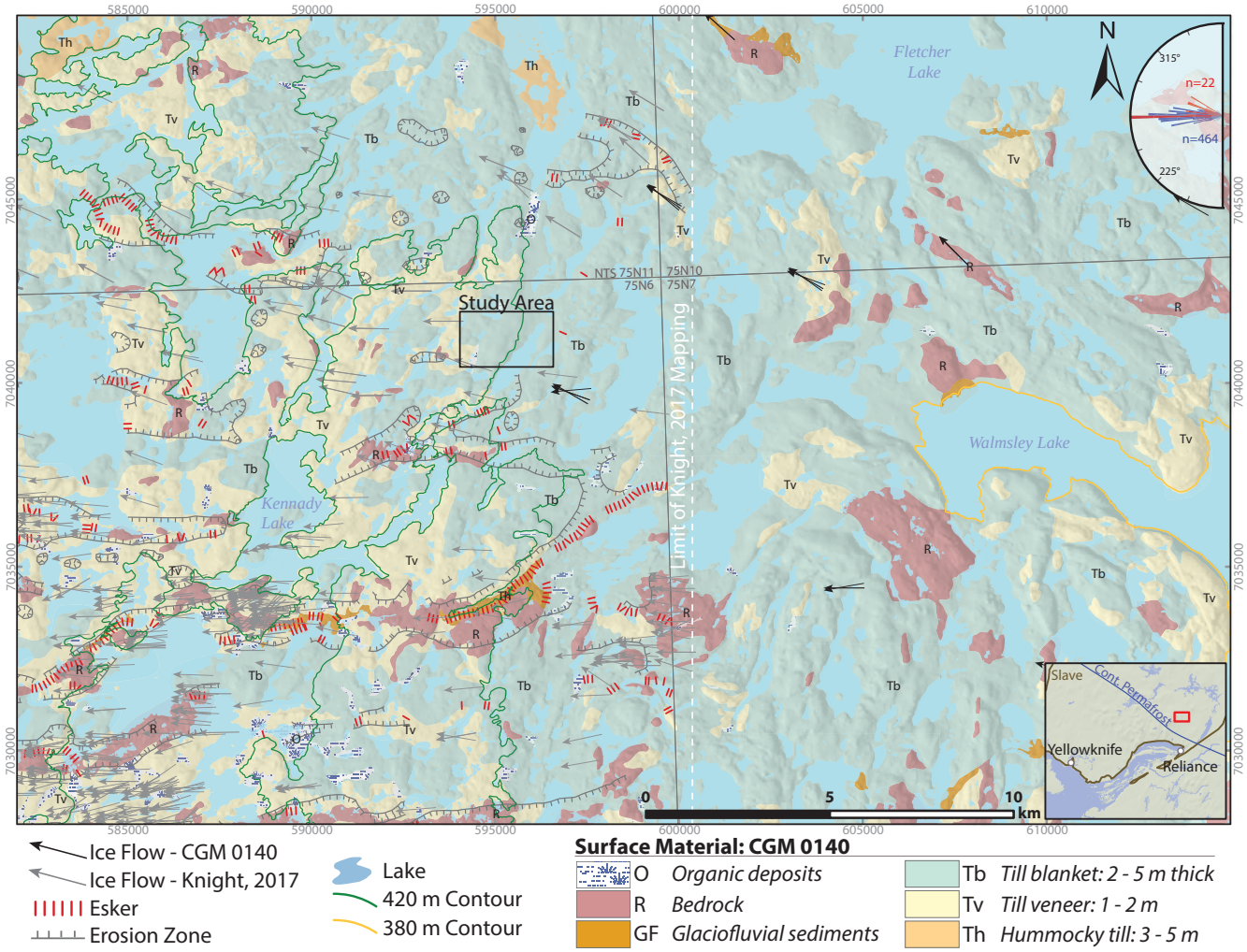

Figure 2.4: Compilation of surficial geology and glacial landform maps. Rose diagram displaying measured ice flow indicators. Blue: all data in map frame. Red: Indicators within three kilometer radius of study area boundary. Esker and erosion zone data after 1:50,000 Surficial Maps (Knight, 2017). Surficial geology after CGM0140 1:125,000 Surficial Geology Maps (Kerr et al., 2014).

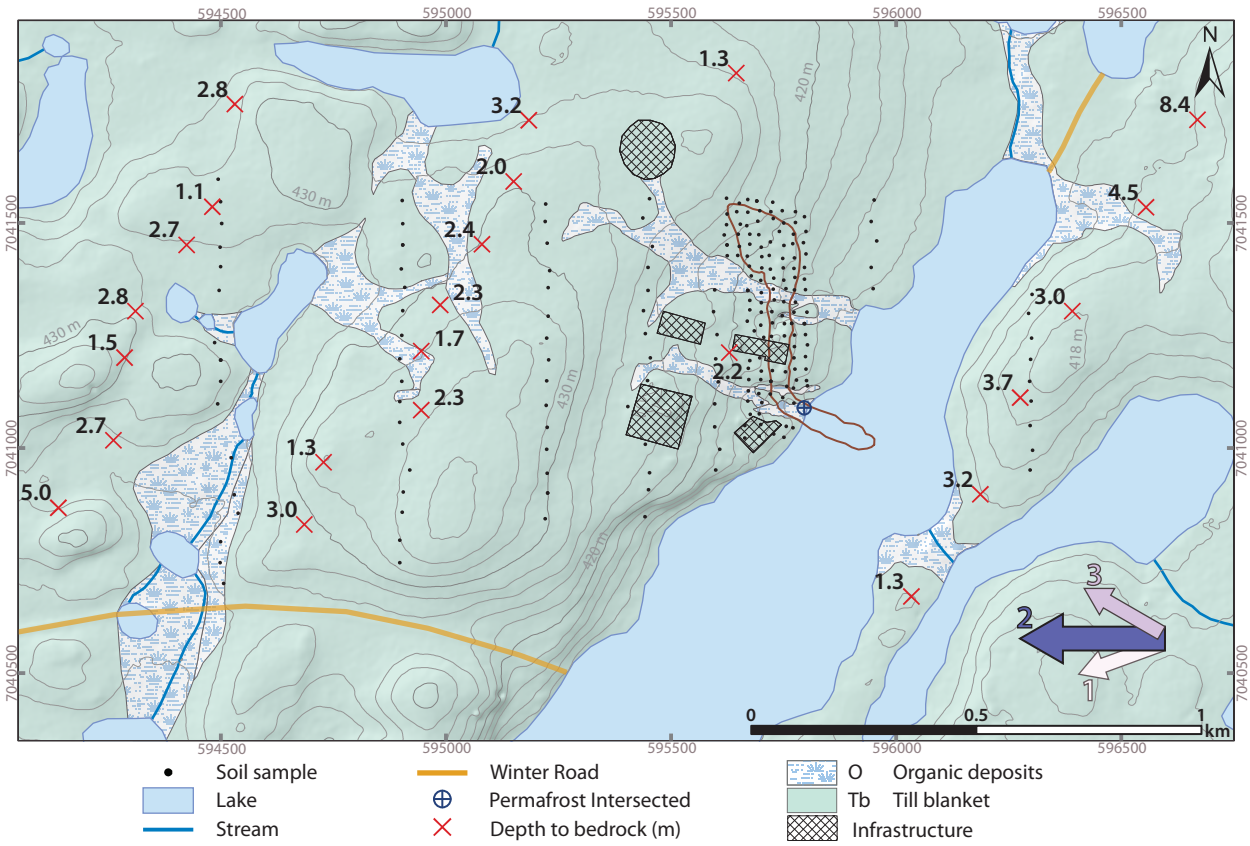

Figure 2.5: Surface materials of the study area including till thickness measurements from drill holes. Large arrows summarizing three ice flow directions through time; sequence of flows are numbered and arrow size illustrates intensity. Ice flow directions from Kerr et al. (2014); Knight (2017).

Partially exposed subangular boulders are common in the basal till across the study area. The concentration, rounding, and exposure of the boulders increases in the center of the study area along the north-south ridge coinciding with areas above 430 m elevation. These small irregular patches show partially to fully exposed surface boulders (<2 m) set in a sandy-silt till matrix surrounded by frost boils (Figure 2.7d).

Bogs occur around lakes and form drainage channels into and between bodies of water. They are distinguishable on the surface by a change in vegetation to thickened shrubs <2 m tall, sedges, and the rare stand of stunted spruce (Figure 2.8c, d) often obscuring any surface boulders or small glacial landforms. Partially decomposed organic material of the Om horizon can be greater than 30 cm thick overlying mineral soil horizons and/or permafrost. Samples in bogs were actively avoided for sampling; however, along the thinner and less active margins of bogs, the occasional presence of frost boils allows the sampling of mineral soil lying below the thick Om horizon.

Patterned frost boils (or mud boils) are most common on, and are a distinguishing feature of, unworked till blankets. Frost boils are up to 3 m in diameter and penetrate down to the transition layer, the uppermost layer of permafrost in contact with the active layer of soils (Bockheim, 2015; Walker et al., 2004). The life span of a single frost boil varies from hundreds to a few thousand years (Dyke and Zoltai, 1980; Mackay,

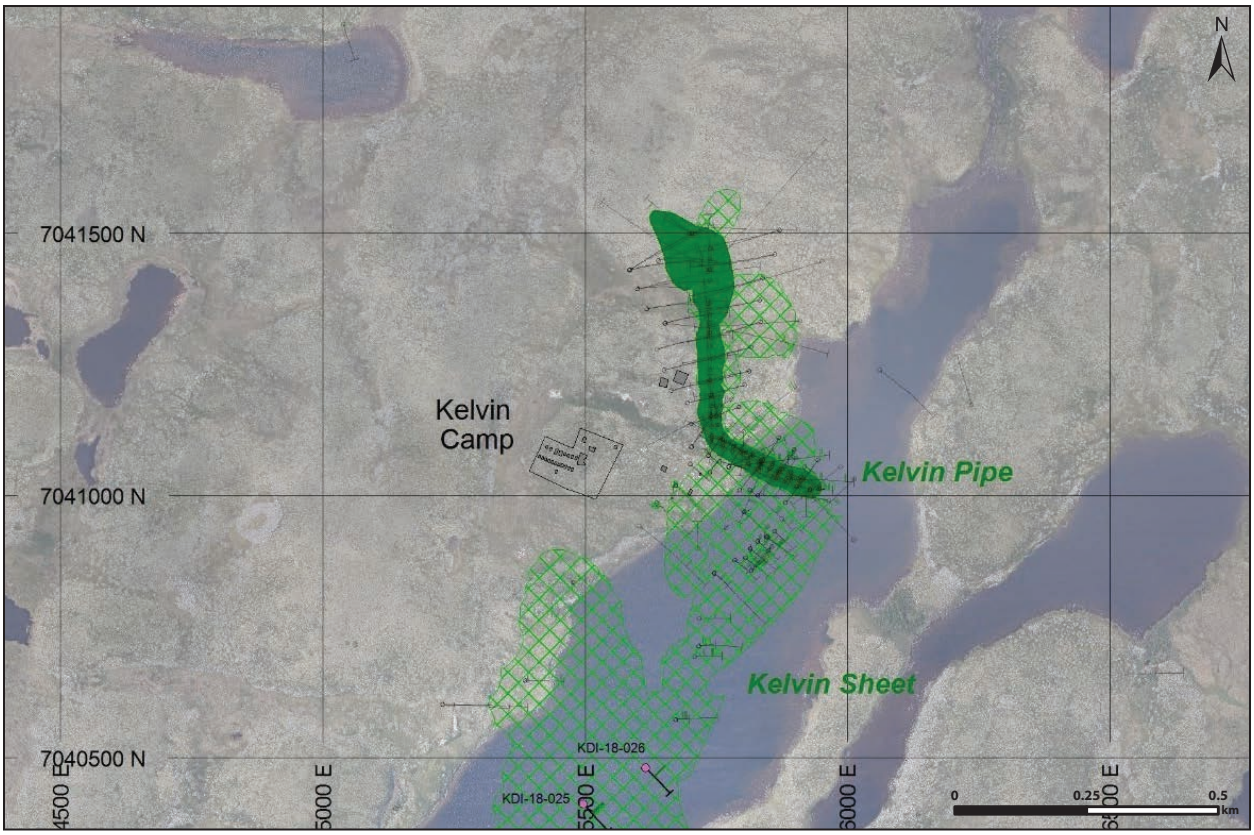

Figure 2.6: Extent of high resolution aerial imagery of study area from Vivian et al. (2019).

1980); relic frost boils occur throughout the study area, often ceasing due to vegetation overgrowth and reclaimed frost boils can be difficult to distinguish in the field. Frost boil formation is typically inhibited by thinner till and proximity to bedrock outcrop (Knight, 2017). Despite this, they are present in areas of reworked till in between patches of exposed surface boulders (Figure 2.7a). Solifluction was not observed in the study area due to the generally low water content of the active layer.

2.2.2 Soil Classification

Assuming a permafrost table of <2 m depth (due to average cover thickness and frost boil abundance) the majority of the soils in the study area fall under the cryosol order. Soils developed on uncryoturbated material are classified as static cryosols: mineral soils with permafrost presumably around 1 m depth. Static crysols are typified by Om, Ah, Ae, Bm, and C horizons (Figure 2.9a). Turbic cryosols are mineral soils that are cryoturbated forming mixed and broken horizons. Due to the seasonal churning of frost boils, soil profiles on active and relic frost boils are poorly developed often consisting of Om, Ah, Bm or BC, and C horizons - notably lacking Ae leached zones (Figure 2.9b). Cryosols in the area may exhibit gleying from seasonal water saturation forming mottled reduced zones and thixotrophic properties (becoming less viscous when agitated), causing quick natural collapse of some sample pits (Figure 2.9c). Soils within bogs are classified as organic cryosols as permafrost was intersected at 32.5 cm depth in one abandoned sample pit. It is therefore assumed that soils in the bogs across the study area are largely organic cryosols, and

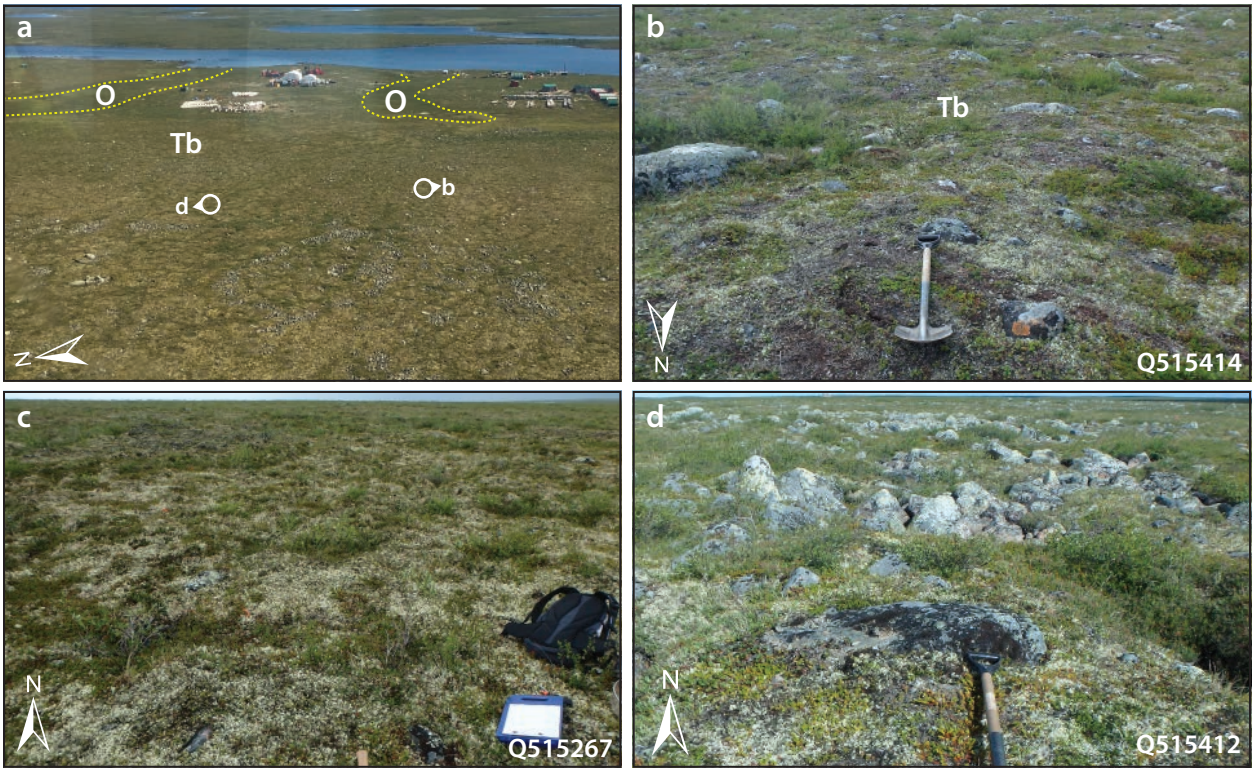

Figure 2.7: (a) Aerial image looking west over weakly reworked till blanket, organic deposits, and infrastructure. Note till blanket (Tb), organic deposits (O), and frost boils in foreground (outlined by vegetation) between irregular patches of <2 m boulders. **(b)** Till blanket with few partially exposed subangular and subrounded surface boulders. **(c)** Till blanket containing low abundance of boulders rarely exposed at surface characterizes the majority of the study area. **(d)** Moderate abundance of partially to fully exposed boulders limited to topographic high in center of study area. Location and orientation of photos marked in (a).

due to the insulating capacity of thick organic horizons have a permafrost table shallower than 1 m depth. Permafrost was not intersected in any other sample pits due to shallow sampling depth and the true depth to permafrost is speculative. The depth of the base of permafrost is unconstrained, however, permafrost extends to a depth of 300 m at Gahcho Kué (De Beers Canada, 2018).

Soils in the subartic are often composed of thin organic horizons generally overlying mineral horizons. Organic horizons contain organic material decomposed to varying degrees, dominated by Of, Om, and/or Oh horizons (in order of increasing decomposition) in high subarctic ecoregions. Mineral horizons contain less than 17% organic carbon; in an ideal profile the A horizon lies beneath the organic soil and is mineral soil with an accumulation of soil organic material (Ah) and/or an elluviated horizon (Ae) (Soil Classification Working Group, 1998). Clay, soil organic matter, iron, and aluminum is leached from the Ae horizon resulting in a bleached coloring. Leached material accumulates in the underlying B horizon. Of the various sub-classifications of the B horizon, water-saturated reduced (gleying: Bg) and oxidized (Bm) horizons are most commonly observed in the study area. Underlying the B horizon is largely unaffected parent material (e.i. unweathered till) (C) that overlies bedrock (R). Soils in the study area are classified by order and great group according to Soil Classification Working Group (1998).

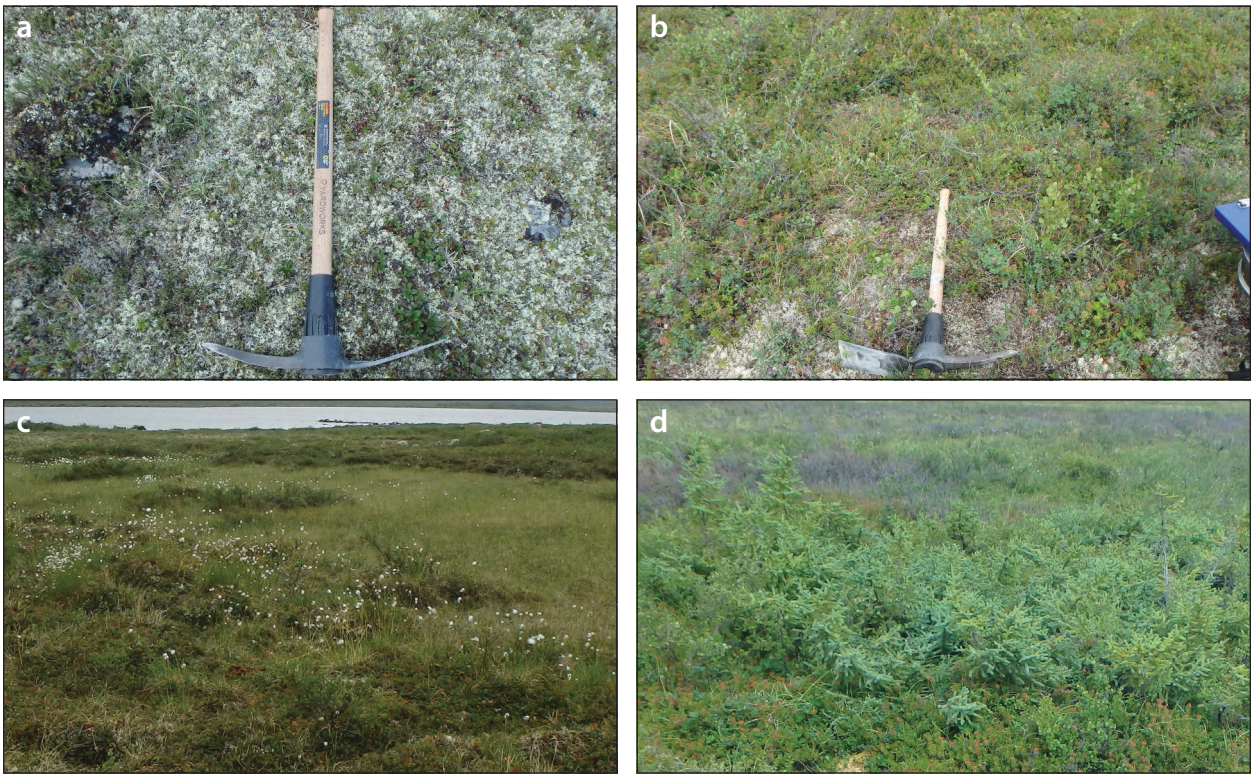

Figure 2.8: Characteristic vegetation of the study area. **(a)** lichen and moss, **(b)** moss and dwarf birch shrubs <1 m tall, **(c)** dwarf shrubs and hummocky sedges in a bog, and **(d)** stand of stunted spruce <2 m tall surrounded by dwarf shrubs in a bog.

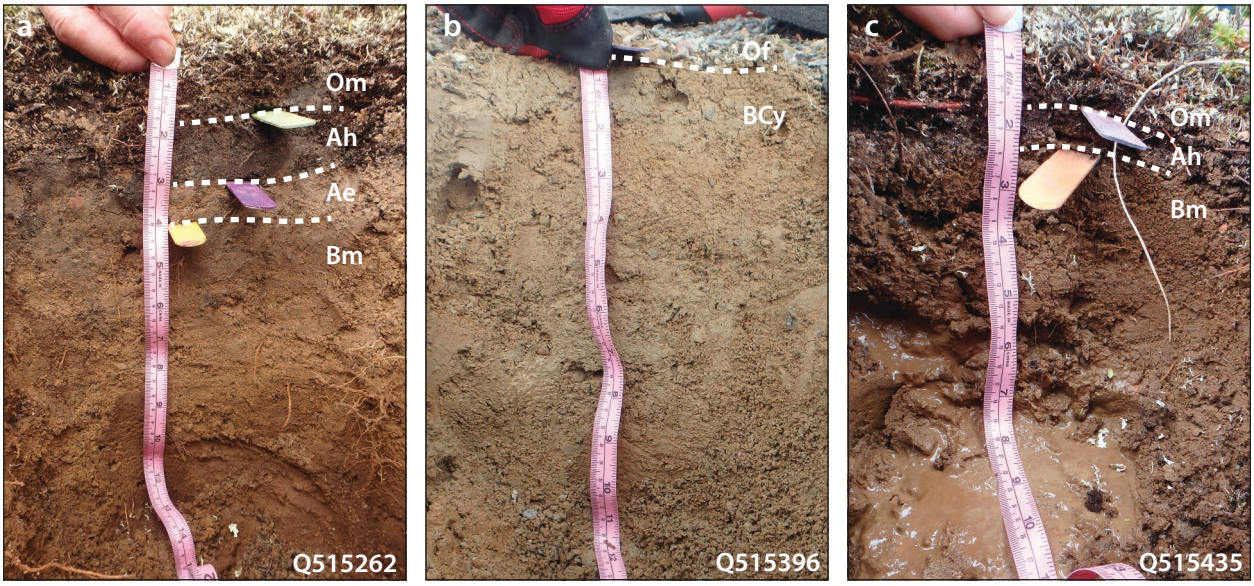

Figure 2.9: **(a)** Representative static cryosol with distinctive Ae and thick Bm horizons. Commonly found in weakly cryoturbated domains of the study area. **(b)** Turbic cryosol of an active frost boil. Very thin gravel surface and Of horizon, and cryoturbated undifferentiated mixture of B and C horizons. Turbic cryosols may contain mottling and subsurface organic patches from material circulation. **(c)** Turbic cryosol exhibiting thixotropic lower horizons due to saturation. Sample pits quickly collapse and field sieving soils is often difficult.

2.2.3 Discussion

Basal till across the KFC is interpreted to have been deposited by the west-flowing glacial ice. This flow overprints landforms created by an earlier west-southwest ice direction. A later north-northwest ice flow is evidenced by rare striae to the east of the study area. Presumably, this late ice flow was topographically controlled and not sustained as most glacial landforms and KIM trains in the KFC trend westward (Figure 1.6). The texture of the diamicton till indicates the majority of the study area is unaffected by glaciofluvial reworking.

Partially exposed subangular boulders are a common feature of till blankets and veneers. The increased abundance of exposed boulders along the central ridge may simply represent a thinner till veneer. Alternatively, boulder concentrations are interpreted as deflational lags where till has been reworked by subglacial meltwater removing matrix material (Sharpe et al., 2013). These small patches (<100 m) of boulders suggest exposure to singular or episodic reworking by channelized subglacial meltwater flow within erosional corridors related to esker complexes (Sharpe et al., 2013). Rounding and distribution of boulders is not consistent with sorted polygonal patterned ground from cryoturbation. Reworking of the till is channelized in a meter to tens-of-meter scale as fresh diamict till and frost boils are observed within a few meters of subrounded boulder exposures (Figure 2.7a). Fresh unworked compact till is commonly observed immediately below boulder lags (Sharpe et al., 2013) and frost boils allow the opportunity to sample this underlying unworked material.

Post-glacial reworking of the landscape is minimal, inhibited by low topography and dry climate. Cryoturbation, in the form of frost boils, formed across the landscape after deglaciation by permafrost-related frost heaving, intensifying in thick fresh till. Seasonal drainage since deglaciation has eroded the till host and formed bogs in areas of seasonal inundation and drainage between lakes and ponds, possibly following areas of more intense channelized meltwater flow; however, these glaciofluvial sediments are now covered by thick organic deposits.

2.3 Methodologies

Soil samples were collected in seven transects (herein referenced as Lines 1-7 from east to west) perpendicular to ice flow at 50 m sample spacing (n = 88), and in a 25×25 m grid over the surface projection of the Kelvin kimberlite (n = 127). Transects extend up to 1.5 km down ice of the known kimberite subcrop (n = 74), and 0.25 km up ice to establish background samples (n = 14). Samples within 10 m of infrastructure or bogs were relocated or abandoned. Soil samples were collected in the field and transported from Camp Kelvin to Yellowknife via fixed wing aircraft. From Yellowknife, samples were shipped directly to ALS Minerals, Vancouver and ActLabs, Ancaster for analysis. Completed chemical analyses are summarized in Table 2.3.

Analysis	Lab	Lab Code	Preparation
Physicochemical: pH, TDS, pH_A, TDS_A	UBC	-	Dry @ 60°C, -180µm sieve (PREP-41)
Aqua Regia ICP-MS	ALS	ME-MS41L	
Four Acid ICP-MS		ME-MS61L	
Organic Carbon by Leco Furnace		C-IR06a	
Sequential Extraction		ME-MS03/4/5/6/7	
Pb Isotope Ratio by Four Acid ICP-MS		PbIS-RAT61	
Spatiotemporal Geochemical Hydrocarbons	ActLabs	SGH	Dry @ 60°C, -250µm seive

Table 2.3: Geochemical analyses employed on soils, including the laboratory codes and preparation procedures.

2.3.1 Soil Sampling

The following procedure was employed for all samples collection across the study area. Sample location, surrounding surface materials and vegetation were recorded before sampling. Sampling pits (30×30 cm) were dug with mattock pick and shovel to an average depth of 30 cm. All horizons were described including classification, thickness, grain size, color, moisture content, clast content and lithology, and were photographed. Clast content, lithology, and rounding was recorded from the +6.3 mm fraction. Soils were sampled from the pit walls using plastic trowels and sieved to -6.3 mm. Sampling targeted the upper 10 cm of the B horizon - allowing for a 1 cm buffer between the sample and overlying horizons. Where B horizon was absent, or mixed with C horizon (BC), samples were collected from the C or BC horizons. One kilogram of sample was packaged and labelled for transport to Vancouver and subsequent multi-element geochemical analysis by ALS Minerals. Detailed procedure can be found in Section A.1. 0.25 kg of B horizon sample - following the same procedure - was collected for SGH analysis by Activation Laboratories (ActLabs, Ancaster, Ontario).

2.3.2 Soil Physicochemical Properties

In situ moisture content of all soil horizons were measured using the ExTech Soil Moisture Meter MO750. Due to time constraints in the study area, the physicochemical properties of the soils were analyzed once the samples were returned to UBC after commercial geochemical analysis by ALS Minerals. Soil slurries using a 1:1 soil to deionized water volume ratio were prepared in the lab and recorded for pH, acidified pH, total dissolved solids (TDS), and acidified TDS. The Oakton Multi-Parameter PTTestr^{TM} 35 Meter was inserted into the slurry and allowed to stabilize for 60 second before recording pH and TDS. For select samples, ORP was recorded with the Oakton ORP Test 10 Meter after 60 seconds of stabilization. An Ag-AgCl electrode standard potential correction (for 3N KCl electrolyte at 25°C) of +209 mV is applied to all ORP measurements to convert to Eh (Langmuir, 1971). Slurries were acidified using an acid dropper bottle and 1 drop of 10% hydrochloric acid, and measured for acidified pH (pH_A) and acidified acidified total dissolved solids (TDS_A). Detailed lab methodologies can be found in Section A.2.

2.3.3 Chemical Analyses

All multi-element geochemical analyses were performed on soil samples by ALS Minerals, North Vancouver. Samples were dried at <60°C and sieved to -180 µm (80 mesh)(ALS Code PREP-41) for analysis of the fine fraction. The following analyses were performed on all 215 sample:

- Aqua Regia ICP-MS (ME-MS41L): 0.5 g aliquot is digested in a 3:1 HCl:HNO_3 mixture and analyzed for trace elements by ICP-MS.
- Four Acid ICP-MS (ME-MS61L): 0.25 g aliquot is sequentially digested with a HNO_3 and $HClO_4$ solution, HF acid, and hot HCl acid prior to trace multi-element analysis by ICP-MS.
- Organic Carbon (C-IR06a): Sample is digested in hot HCl acid and analyzed for organic carbon concentration by direct combustion and infrared absorption by Leco furnace.

2.3.4 Sequential Extraction

Following preliminary interpretations from aqua regia and four acid ICP-MS data, four -180 µm samples were selected for commercial sequential analysis at ALS Minerals. The sequential extraction procedure consists of five leaches in order of DIW (ME-MS03), AA (ME-MS04), C-HA-HC (ME-MS05), H-HA-HC (ME-MS06), followed by NaP (ME-MS07). After each extraction, the final solution is separated from the solids by centrifuging and decanting, the solution pH is measured, and the supernatant is analyzed for major and trace elements by ICP-MS. Results are compared to aqua regia and four acid ICP-MS data analyzed separately.

2.3.5 Soil Size Fraction

Select soils were sieved at UBC after splits were returned from commercial analysis by ALS Minerals. Samples are sieved with the *Gilson GilSonic Ultrasiever GA-8* into incremental size fractions (180-150 µm, 150-125, 125-106, 106-75, 75-53, 53-25, 25-5, and -5). Extraction of -5 µm by *Gilson GilSonic Ultrasiever* was minimal, <0.5% by weight, and were not analyzed. Four soil samples were selected for size fraction investigation: two background and two samples anomalous in kimberlite pathfinder elements(Table 2.6). The size fractions were analyzed by Four Acid ICP-MS (ME-MS61L).

2.3.6 Pb Isotopes

A selection of soils samples (n = 17) were analyzed for lead isotope ratios by high precision isotope Q-ICP-MS following conventional four acid digestion (ME-MS61L) of -180 µm soil. Six ratios are reported: $^{206}Pb/^{204}Pb$, $^{207}Pb/^{204}Pb$, $^{208}Pb/^{204}Pb$, $^{208}Pb/^{206}Pb$, $^{208}Pb/^{207}Pb$, and $^{206}Pb/^{207}Pb$.

2.3.7 Soil Hydrocarbons

Soil samples for SGH analysis were collected in identical fashion as Section 2.3.1, however 0.25 kg of -6.3 mm soil was packaged in a 5×8 inch sample bag. Samples were analyzed by ActLabs, Ancaster: dried at <60°C, sieved to -250 µm (60 mesh), digested with a weak leach, and analyzed by high resolution gas

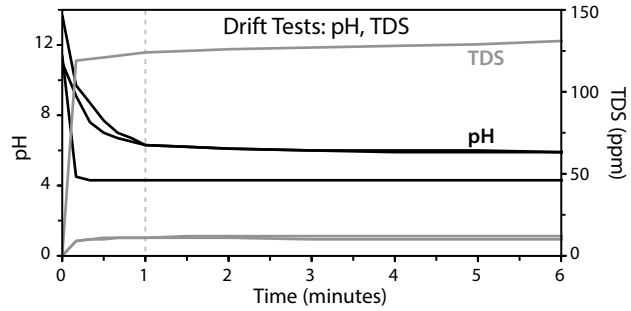

Figure 2.10: pH and TDS drift tests on the *Oakton Multi-Parameter PTTestr^{TM} 35 Meter* on multiple soil samples. Measurements were taken after allowing 1 minute for stabilization.

chromatography mass spectrometry for 162 hydrocarbon compounds in the C_5 - C_{17} carbon range. Results are presented in an interpretation report prepared by ActLabs including pathfinder class maps and confidence ratings (Appendix C). Ratings are predicated on both the strength of a rabbit ear anomaly (i.e. the detection a redox cell), and the SGH signature compared to the kimberlite signature from other SGH case studies.

2.4 Results

2.4.1 Physicochemical Properties

QA-QC

pH, TDS, and ORP probes were calibrated for accuracy twice a day following calibration procedures outlined in Section A.2. Drift tests for slurry pH and TDS probes determined a wait time of 60 seconds for sufficient levelling (Figure 2.10). Nine field duplicate pairs were used to interpret natural variability and field reproducibility, in addition to ten lab duplicates pairs for procedural and precision variation. Mean percent difference (MPD) was used to assess variation between both field and lab duplicates per Equation 2.5, where V_1 is the value of the original sample and V_2 is the duplicate sample. All pH and pH_A field and lab duplicates have MPD below 15% representing high quality data both in laboratory procedures and precision and field reproducibility and minimal natural variability on a few-meter scale (Figure 2.11a & c). Most TDS and TDS_A lab duplicates show <20% MPD and acceptable data quality (Figure 2.11b). TDS and TDS_A indicates there is significant natural variability as many field duplicate pairs have >20% MPD and up to 45% (Figure 2.11d). Generally, acidified pH and TDS values exhibit higher lab duplicate MPD likely due to the acidification process using a conventional dropper bottle to deliver one drop of 10% HCl.

$$MDP\,(\%) = \frac{|V_1 - V_2|}{(\frac{V_1+V_2}{2})} \times 100 \tag{2.5}$$

Results

Slurry pH values exhibit circum-neutral to acidic pH ranging from 3.7 to 6.8 (Figure 2.13). Under acidic conditions, carbonate is not stable in the majority of the soils below a pH of 6.0. Acidic soils are largely

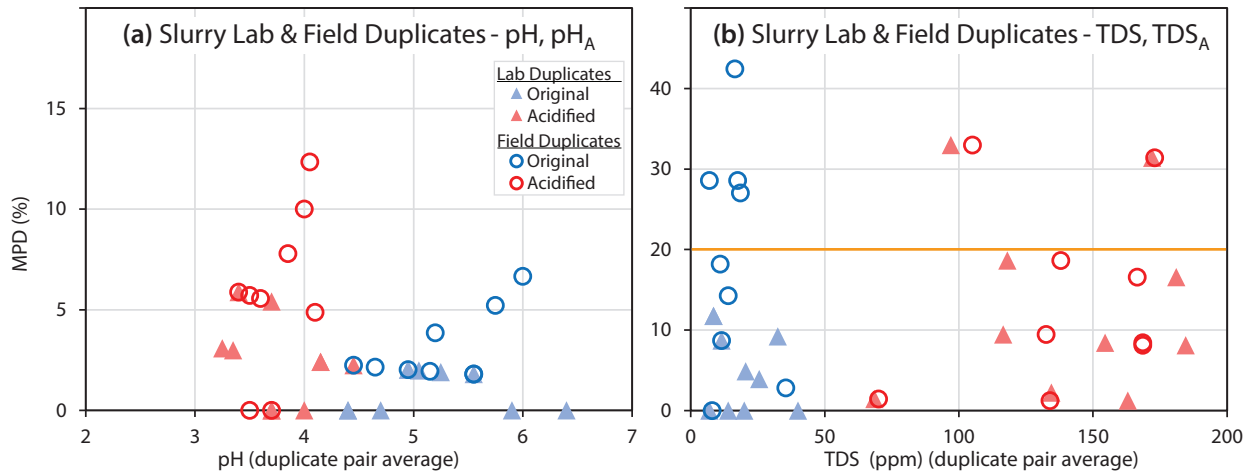

Figure 2.11: (a) MPD of slurry pH and and acidified pH of lab and field duplicates. **(b)** Lab and field duplicate MPD for TDS and acidified TDS measurements. MPD <20% is deemed good quality data.

confined to the north half of the grid above the North Limb of the kimberlite and spatially associated with bogs (Figure 2.14). There is no correlation between observed slurry pH values and the location and depth of the kimberlite.

The buffering capacity of soil slurries is displayed by inverse difference hydrogen (IDH) and calculated as the inverse of the difference in hydrogen concentrations between acidified ($[H^+]_A$) and non-acidified slurries ($[H^+]$; Equation 2.6). Increased IDH values indicate increased buffering capacity of the soil. Apical or 'rabbit-ear' anomalies have been observed above kimberlites where carbonate precipitates at the water table on the margins of reduced columns (Smee, 2009). Although carbonate is not stable in the majority of the soils, pH conditions above 5.5 - 6.0 have noticeably higher IDH values indicative of increased buffering capacity likely in the form of carbonate (Figure 2.13b). Samples with increased IDH or a pH above 6 do not spatially correlate with the location and depth of the kimberlite and do not detect any redox cell that may form around the kimberlite (Figure 2.14).

Two lines of soils above the North Limb were measured for slurry oxidation-redox potential. Measured ORP values (mV) were corrected by +209 mV to yield Eh (mV) values based on the temperature at the time of measurement in the lab. Eh and pH display an inverse relationship (Figure 2.12). Slurry Eh values exhibit suboxic to oxic conditions ranging from 448 to 534 mV. However, trends in the ORP data do not correlate with the depth of the kimberlite.

$$Inverse\ Difference\ Hydrogen\ (IDH) = \frac{1}{[H^+]_A - [H^+]} \tag{2.6}$$

Organic carbon in B horizon soils, measured by Leco furnace (Section 2.3.3), is highest in the southern half of the grid area. Elevated C_{org} is not spatially correlated with bogs and organic deposits (Figure 2.15a) because careful sampling methods were taken to avoid collecting organic-rich horizons. Elevated *in situ* moisture content does not appear to be exclusively located within organic deposits (Figure 2.15a), and is not

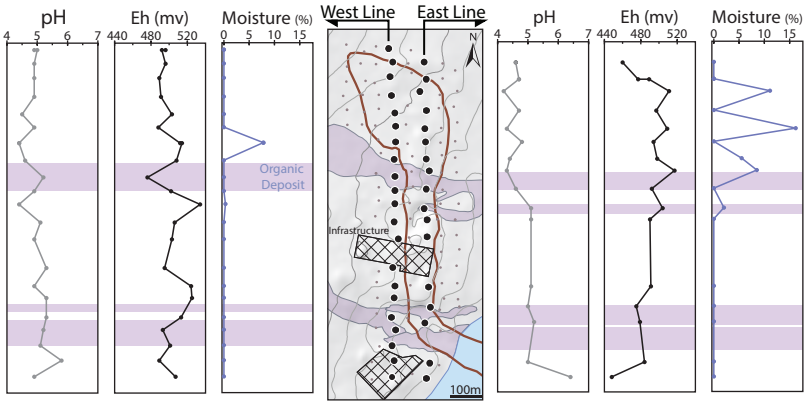

Figure 2.12: Two lines of samples were measured for slurry Eh above the North Limb of the kimberlite. Eh and pH display an inverse relationship. Elevated moisture content correlates with more acidic soil conditions most evident in east line, whereas reducing conditions are caused by organic deposits in the west line.

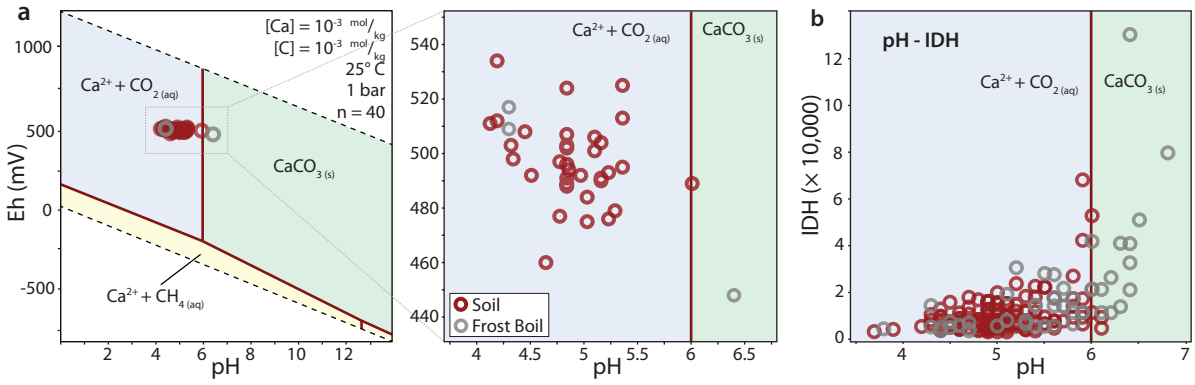

Figure 2.13: Slurry Eh, pH, and IDH values from soils and frost boil samples. **(a)** Pourbaix diagram indicating carbonate is not stable in most soils. Diagram modified from *materialsproject.org*. **(b)** pH - IDH plot showing sharp increase in soil buffering capacity near pH = 5.5 - 6.0 suggesting of carbonate stability at circum-neutral pH conditions.

correlated to increased C_{org} content. This suggests the water-bearing capacity of the soil is also influenced by grain size of the till. Soils with elevated moisture contain elevated dissolved solids (Figure 2.15b). Moisture data should be interpreted with extreme caution; measurement did not prove fully reliable in the field as many visibly wet or saturated soils measured 0% moisture content using the ExTech Soil Moisture Meter MO750.

Samples across the study area were consistently taken of B horizon soils. Frost boils samples, however, were visibly less oxidized and weathered, often sampling the BC or C horizons. Samples from frost boils display less acidic pH conditions (median pH = 5.6) compared to other soils (median pH = 5.0). This difference is attributed to the accumulation of organic carbon and humic and fulvic acids in B horizon soils resulting in more acidic conditions (frost boil median C_{org} = 0.07; soil median C_{org} = 0.1) Despite the more circum-neutral pH conditions and visual distinction between grey frost boil material and brown B horizon soil, frost boils samples are only slightly less chemically weathered than B horizon soils (frost boil median Chemical Index of Weathering = 58.4; soil median Chemical Index of Weathering = 58.8).

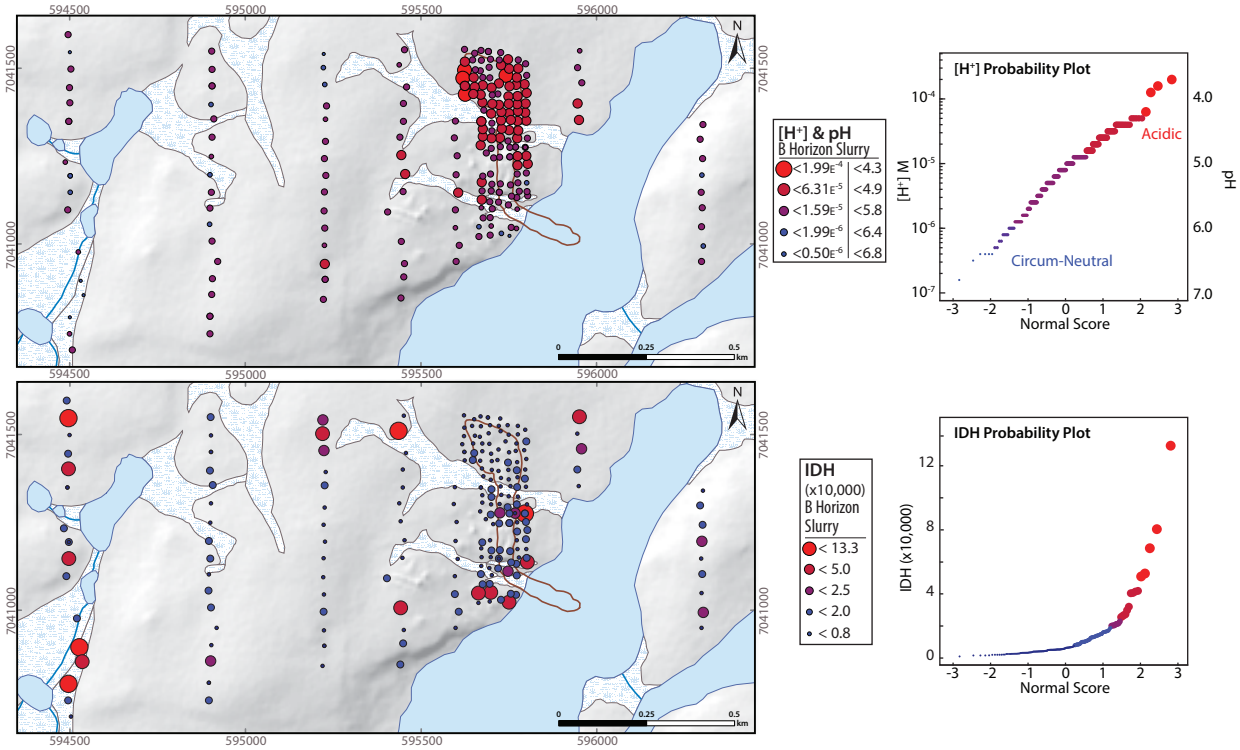

Figure 2.14: Maps of soil slurry [H$^+$] concentration, pH, and inverse difference hydrogen calculated per Equation 2.6. Population breakdowns were delineated based on visual assessment of probability plots.

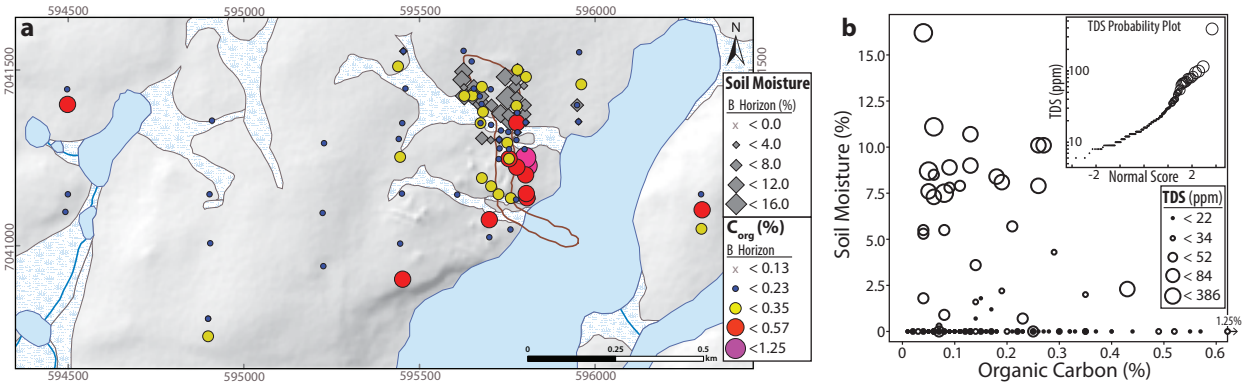

Figure 2.15: **(a)** Map of soil organic carbon content (by Leco furnace) lacks correlation with bogs. Elevated *in situ* moisture values are limited above the North Limb of the kimberlite. Moisture values below 0% and C_{org} below 0.13% are not plotted. **(b)** Moisture - TDS showing positive correlation between *in situ* moisture and total dissolved solids.

2.4.1.1 Discussion

Despite the more circum-neutral conditions of the frost boil samples, the degree of chemical weathering between frost boil and soil samples do not significantly vary. The elluviation and illuviation processes in the two sample materials appear similar, and herein the inorganic geochemistry is interpreted as one dataset. In regions where frost boils are present but chemical weathering may be more intense, the difference of weathering between the two populations may require separate interpretation.

Physicochemical measurements (pH, Eh, IDH) do not directly detect the presence of the kimberlite, but do aid in the interpretation of trace element geochemistry. The low permeability of basal till precludes the formation of alkaline pH responses above the kimberlite from advection of hyper-alkaline groundwater (Hamilton, 2007b; Sader et al., 2009). pH responses above the North Limb of the kimberlite do not detect alkaline groundwaters sourcing from the kimberlite. At Kelvin, Eh and pH responses do not provide evidence for the development of a reduced column through barren country rock and till cover. Granted, the electrochemical transport model described by Hamilton (2007b) is based on steeply dipping mineralized bodies that form apical or rabbit-ear anomalies directly above mineralization subcrop. The potential to generate surface responses from an electrochemical cell at Kelvin is likely complicated due to the pipe's inclined morphology, thick bedrock cover over the North Limb, and small subcrop expression under the lake.

2.4.2 Soil Geochemistry

2.4.2.1 4-Acid ICP-MS

QA-QC

Data quality was assessed using field duplicates and certified reference material (CRM). Accuracy and precision were assessed by analysis of CRM OREAS25a and comparison to certified and indicated values. The acceptability of an element depends on the percentage of samples at or below ten times the lower limit of detection, and percentage of CRM measurements outside $\pm$2SD or $\pm$3SD (standard deviations) of the certified value. For elements with indicative values, $\pm$20% and $\pm$30% are used instead of standard deviation. See detailed QA-QC in Appendix B for CRM plots.

- Elements for which >50% of measured values are at or below the practical detection limit (10 $\times$ the reported lower limit of detection) include Cd, Ge, In, Re, S, Sb, Se, and Te. These elements are discussed no further. Elements with >30% of CRM measurements that outside $\pm$3 standard deviations from the certified value are discussed with extreme caution; these include Ag, Ba, and Li.
- Elements discussed with caution are those where >30% of CRM measurements lie outside $\pm$2SD from the certified value. These elements include Ca, P, W.
- Elements of sufficient accuracy and precision include Al, As, Be, Bi, Ce, Co, Cr, Cs, Cu, Fe, Ga, Hf, K, La, Mg, Mn, Mo, Na, Nb, Ni, Pb, Rb, Sc, Sn, Sr, Ta, Th, Ti, Tl, U, W, Y, Zn, and Zr.

Natural variability and field reproducibility is assessed by MPD (Equation 2.5) from ten field duplicate

pairs (4.4% of dataset). Duplicate sample pits were placed within three meters of the original pit. Elements whose average MPD exceeds 20% have significant natural variability, and those which exceed 30% are deemed non-reproducible. Elements for which >50% of measured values are at or below ten times the reported lower limit of detection are not included in this duplicate quality assessment.

- Non-reproducible elements, of which the average MPD exceeds 30%, include As, Th, and W.
- Elements that display significant natural variability (average MPD >20%) include Bi, Ce, Cu, La, Mo, Ta.
- Reproducible elements that do not display significant natural variability include Ag, Al, Ba, Be, Ca, Co, Cr, Cs, Fe, Ga, Hf, K, Li, Mg, Mn, Na, Nb, Ni, P, Pb, Rb, Sc, Sn, Sr, Ti, Tl, U, V, Y, Zn, and Zr.

Results

Weathering processes show minimal chemical destruction as soils are immature. Weathering is limited to weak mechanical processes due to the climate and annual precipitation at the Kelvin Faraday Corridor (Figure 2.16a). Depletion of alkali elements during chemical weathering is minimal and uniform across all soils as they plot on a well-defined trend near the feldspar control slope (Figure 2.16b).

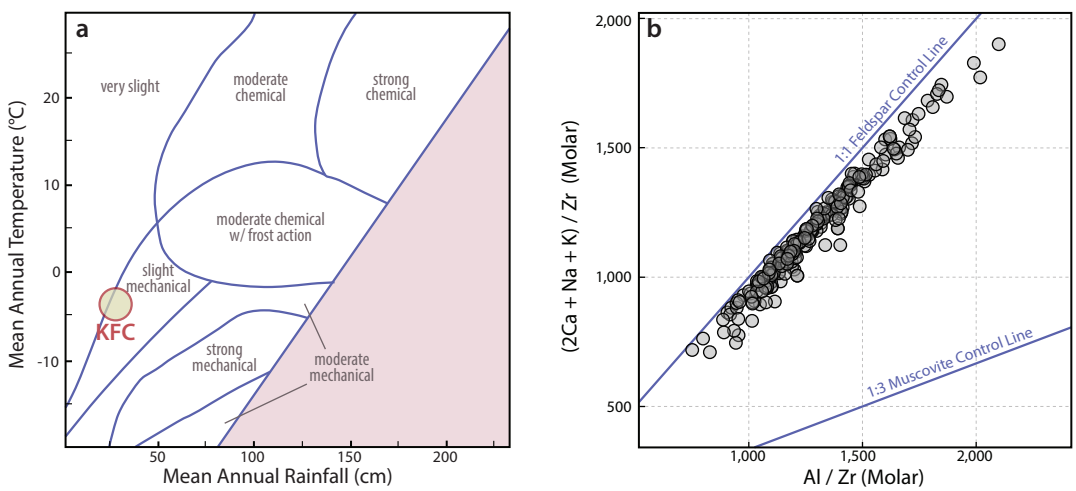

Figure 2.16: (a) Average weathering regime of Kelvin Faraday Corridor. Diagram after Peltier (1950). **(b)** Feldspar Control Diagram (from four acid data) levelled to conservative Zr to describe material transfer with weathering and soil formation process.

Select pathfinder element concentrations that are expected to show positive anomalies are plotted to summarize four acid ICP-MS results (Figure 2.17, Figure 2.18, and Figure 2.19). Populations are manually selected by visual interpretation of probability plots to identify slope breaks. Background values are demarcated by black and blue points, elevated values include yellow points, anomalous points encompass red and pink points. The main spatial distributions of pathfinder elements are summarized as follows:

- Elevated concentrations of pathfinder elements (Ba, Cr, Fe, Mg, Mn, Nb, Ni, Ta, Ti) show trends sub-parallel to the 265° - 270° ice flow direction extending from the west shore of Kelvin Lake. This

multi-element east-west trend is confined to the southern portion of the sample grid, dominated by frost boil samples, and up to 250 m wide. This anomalous Zone 1 extends to the west out of the study area, and its western extent is undefined and appears to intersect the kimberlite subcrop location under Kelvin Lake.

- Another trend (Zone 2) of anomalous concentrations of Ba, Cr, Fe, Mg, Mn, Nb, Ni, Ta, and Ti exists in the sample grid over the surface projection of the Kelvin North Limb. The western and northern extent of the trend is constrained, however, the eastern extent is open where Kelvin lake obstructs soil sampling. The anomalous samples lie northwest of the kimberlite subcrop, down ice flow direction of the latest glaciation. This trend is limited to soil samples - surrounding frost boil samples exhibit background concentrations.

- For Cr, Mn, Nb, Ti, and Ba many up ice values (lines 6 and 7) show concentrations more elevated than background values.

- Zn exhibits anomalous trends similar to other transition metals of similar size and charge (i.e. Mg, Cr, Mn, Fe, Ti).

- Anomalous concentrations of light rare earth elements (La and Ce) do not show trends sub-parallel to ice flows. Elevated concentrations of La and Ce exist in, but are not limited to, the westernmost line 1. This increase in LREE concentrations towards the west may reflect bedrock geology and the contact between eastern metaturbidites and western granitoids in the study area.

- Although Ba analyses of CRM consistently measure 2-3 standard deviations higher than certified values, Ba was evaluated as a pathfinder element. Elevated and anomalous Ba shows similar spatial context to other pathfinder elements. Rb, an additional common substitute for K in micas, exhibits a similar spatial relationship as elevated Ba values.

- Elevated Ca concentrations (>1.26%) are found directly over, but not limited to, the North Limb and are associated with the grid cluster of elevated pathfinder metals. Anomalous concentrations are distributed across the study area without any distinct trends sub-parallel to ice flows or flanking the surface projection of the kimberlite.

	Ba	Cr	Fe %	Mg %	Mn	Nb	Ni	Ta	Ti %
Cutoff Value	580	25.7	1.59	0.46	264	4.60	12.3	0.35	0.21
Average Background	504	20.3	1.19	0.35	196	3.40	9.4	0.25	0.15
Average Anomalous	605	30.2	1.84	0.53	289	5.58	14.7	0.43	0.23
Response Ratio	1.20	1.49	1.55	1.50	1.47	1.64	1.57	1.70	1.56

Table 2.4: Response ratios of anomalous to background values from four acid ICP-MS -180 µm soils. Response ratios calculated from the average background and anomalous populations; the anomalous-background cutoff is determined between blue (background) and yellow (elevated) populations in Figure 2.17, Figure 2.18, and Figure 2.19. Data displayed in ppm unless otherwise noted; response ratios are unitless.

Cr, Mg, Nb, and Ni best define the two dispersal trends; Ta, Ti, Mn, Fe, and Ba adequately identify the trends. Response ratios are highest for Ta, Nb, Ni, Ti, Fe, and Mg. These elements are most enriched

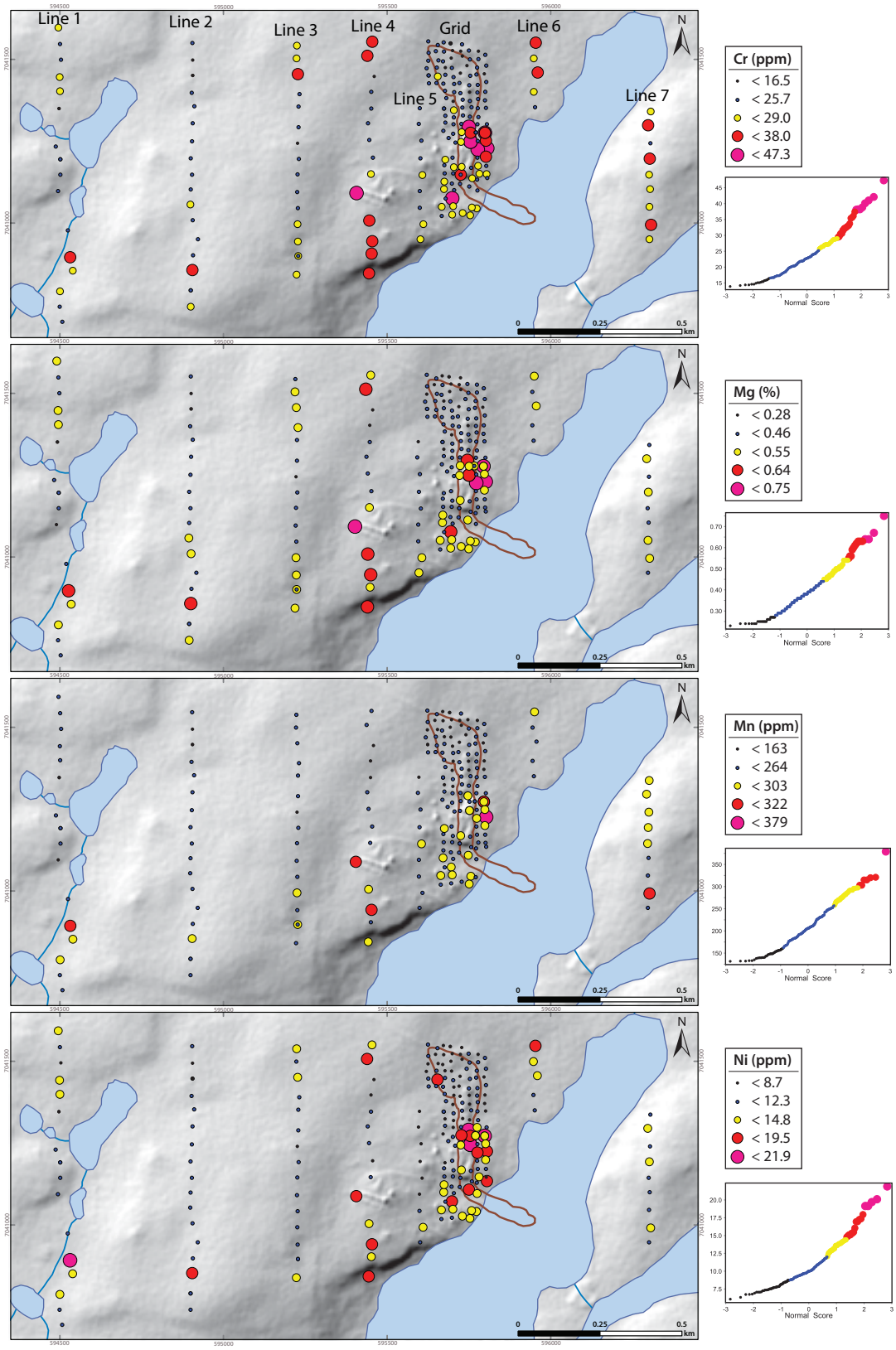

Figure 2.17: Maps of four acid ICP-MS Cr, Mg, Mn, Ni results of -180 µm soils. Background, elevated, and anomalous populations determined according to probability plot trends.

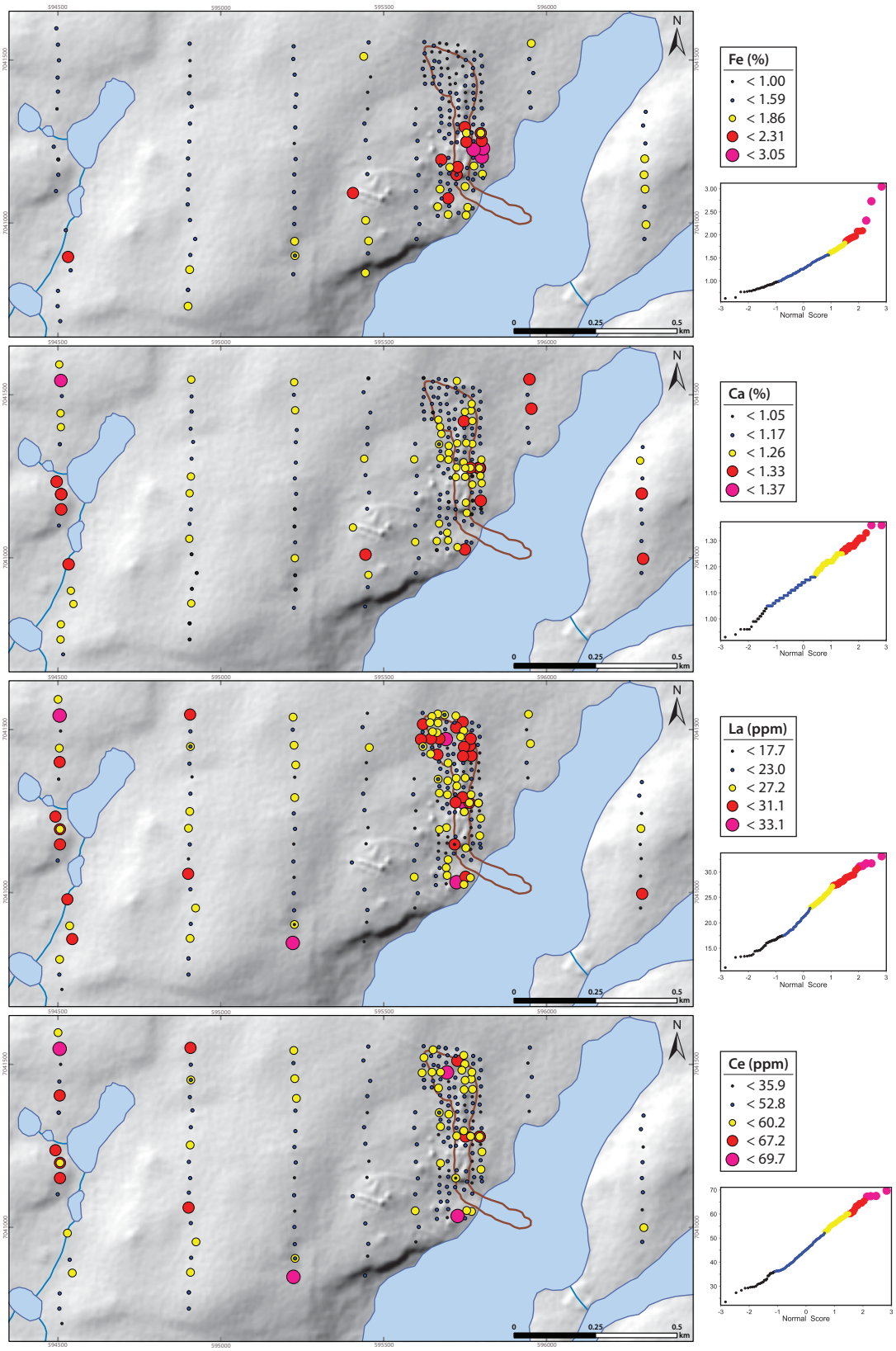

Figure 2.18: Maps of four acid ICP-MS Fe, Ca, La, Ce results of -180 µm soils. Background, elevated, and anomalous populations determined according to probability plot trends.

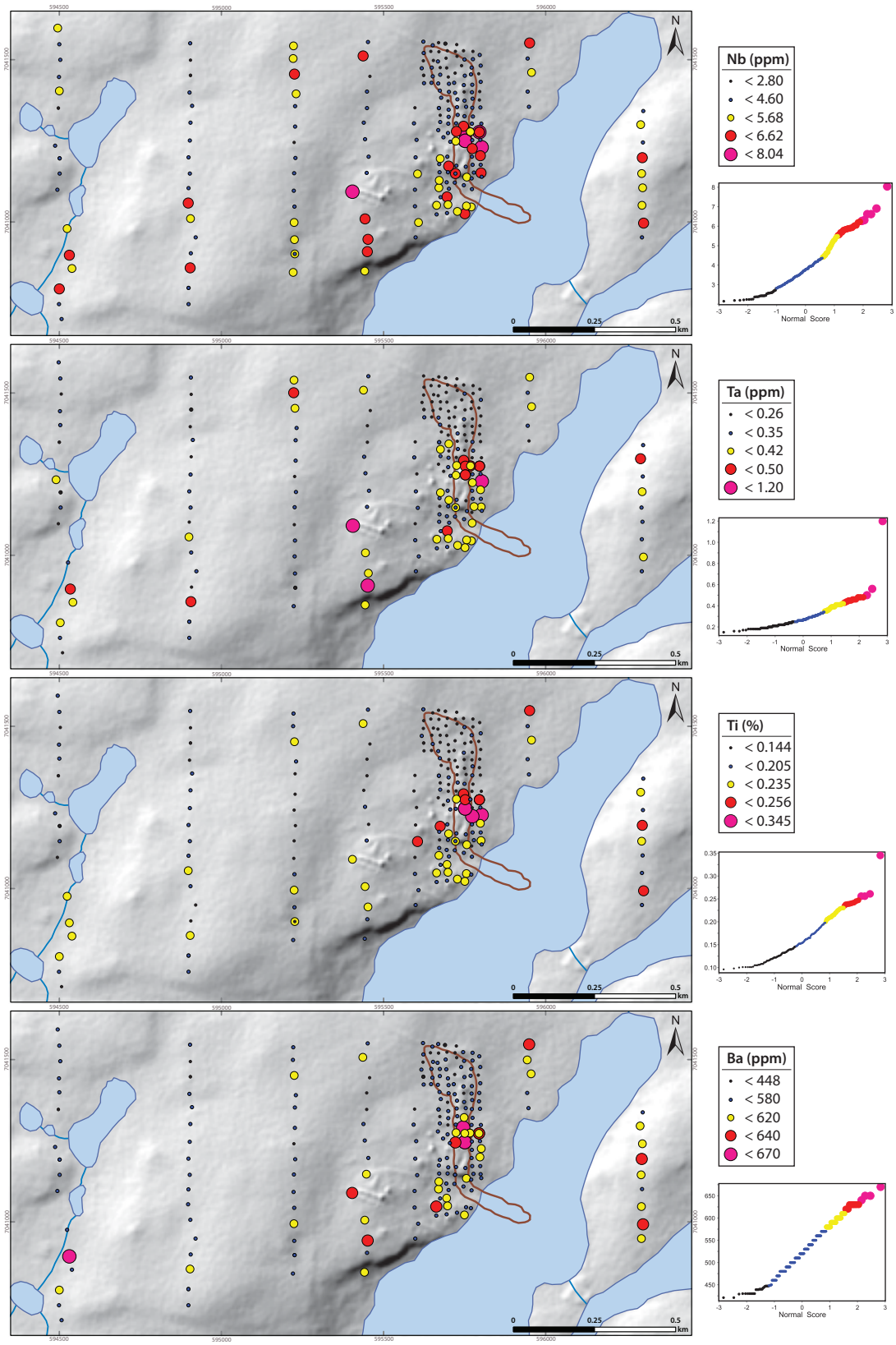

Figure 2.19: Maps of four acid ICP-MS Nb, Ta, Ti, Ba results of -180 µm soils. Background, elevated, and anomalous populations determined according to probability plot trends.

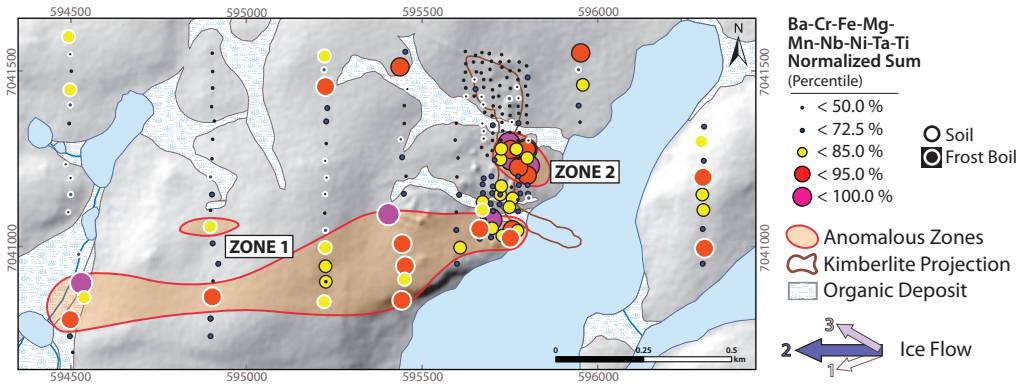

Figure 2.20: Map of Ba, Cr, Fe, Mg, Mn, Nb, Ni, Ta, and Ti averaged after normalization to percentile from four acid -180 µm ICP-MS data. Two zones of alevated pathfinder elements are outlined and herein referred to as Zones 1 and 2. Arrows summarize the three ice flow directions. Flows are chronologically labelled and size of arrow represents intensity. B horizon soils are marked with black borders, frost soil samples are marked with white borders.

in kimberlites relative to Slave metaturbidite and plutonic country rocks (Figure 2.1). Positive pathfinders can be averaged after normalizing to their percentile to display multi-element anomalies. A map of Ba, Cr, Fe, Mg, Mn, Nb, Ni, Ta, and Ti averaged after normalization to percentile effectively displays the multi-element anomalous trends within the study area (Figure 2.20). This normalized value is herein referred to as representing the degree to which a sample is anomalous in four acid extractable kimberlite pathfinder elements.

Immobile element ratios, Th/U and Nb/Zr, may provide additional identification of anomalous responses. The majority of soils exhibit Th/U values between average supracrustal and plutonic rocks (Th/U = 2.8 and 4.3, respectively). Samples with elevated Th/U exhibit values closer to average Group I kimberlites plot in the southern half of the study area correlating with only the east-west dispersal trend (Figure 2.21a). Whole rock Th/U values may strongly vary between kimberlites: the hypabyssal 5034 kimberlite of the Gahcho Kué cluster averages Th/U = 3.4 (Caro et al., 2004) whereas hypabyssal Snap Lake Kimberlite averages Th/U = 11.6 (Agashev et al., 2008). Oxidation and preferential removal of uranium during weathering may elevate Th/U ratios forming false positive anomalies. In more weathered soils, residual Th/U ratios calculated after a robust linear regression to the Chemical Index of Weathering (CIW) may account for oxidative leaching of U. This calculation does not enhance the geochemical responses at Kelvin because oxidative leaching is minimal across the field site due to the brief exposure since deglaciation and weak weathering regime. Average Group I kimberlites exhibit elevated Nb/Zr values compared to Slave supracrustal and plutonic rocks, and elevated Nb/Zr ratios adequately identify both the east-west and northwest dispersion at Kelvin (Figure 2.22).

2.4.2.2 Aqua Regia ICP-MS

QA-QC

Data quality was assessed with field duplicates and CRMs following the same methodology as four acid

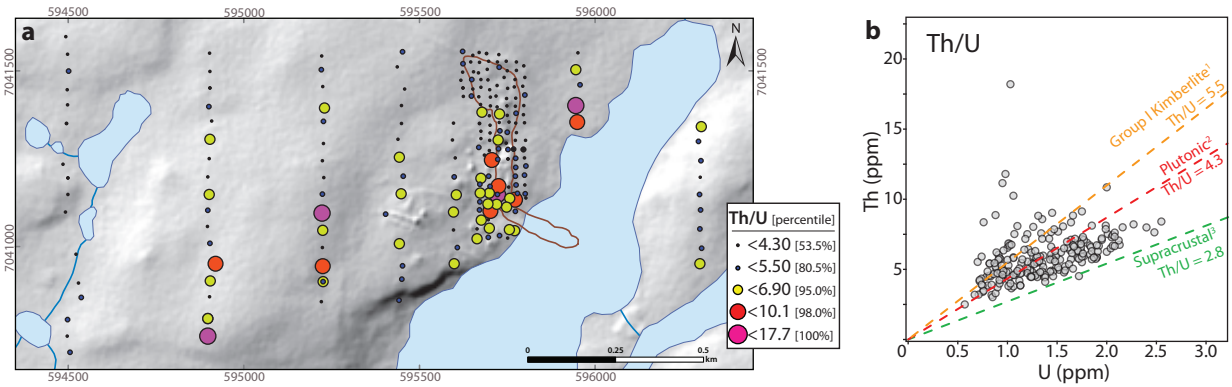

Figure 2.21: **(a)** Map of four acid -180 µm soil Th/U ratios. Elevated values adequately identify only the east-west dispersal plume. **(b)** XY plot of Th and U ratios illustrating the majority of data trend between average ratios for Slave supracrustal and plutonic rocks. Samples with elevated Th/U trend above average Group I kimberlite ratios. [1] Dawson (1967); [2] Cairns et al. (2003); [3] this study and Cairns et al. (2003).

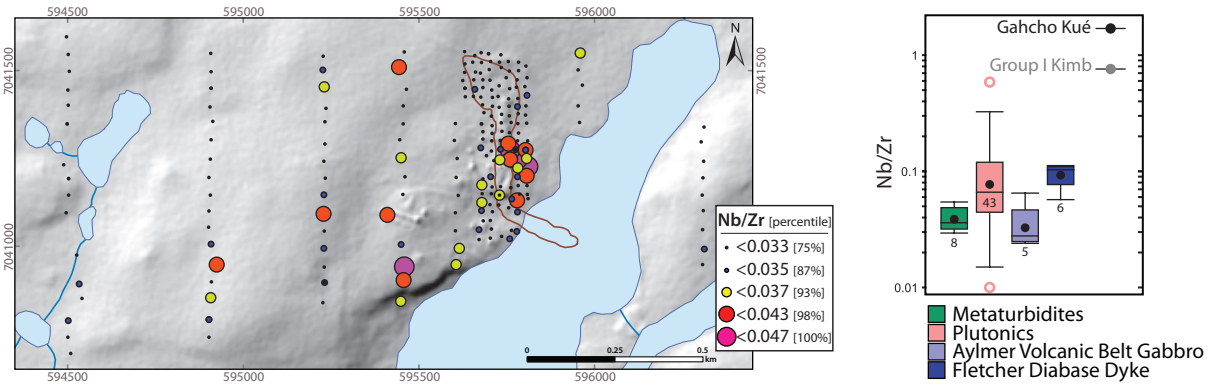

Figure 2.22: Map of four acid -180 µm soil Nb/Zr ratios. Elevated values clearly delineate two dispersal plumes at Kelvin. Tukey box plot shows average kimberlite Nb/Zr values up to an order of magnitude higher than SE Slave province country rocks.

ICP-MS data. See detailed QA-QC in Appendix B for detailed QA-QC.

- Elements for which >50% of measured values fall below the practical lower detection limits include Au, B, Hg, In, K, Na, Pd, Pt, Re, S, Sb, Se, Ta, and Te; these elements are discussed no further. Additionally, elements with 30% or more of CRM measurements outside ±3 standard deviations from the certified value (or ±30% of indicated value) are discussed with extreme caution; these include Ge, Nb, and Ti.

- Elements discussed with caution are those where 30% or more of CRM measurements lie outside ±2SD from the certified value. These elements include Ag, Cd, Hf, and Zr.

- Elements of sufficient accuracy and precision include Al, As, Ba, Be, Bi, Ca, Ce, Co, Cr, Cs, Cu, Fe, Ga, La, Li, Mg, Mn, Mo, Ni, P, Pb, Rb, Sc, Sn, Sr, Th, Tl, U, V, Y, and Zn.

Natural variability and field reproducibility is assessed by MPD (Equation 2.5) of ten field duplicate pairs (4.4% of dataset).

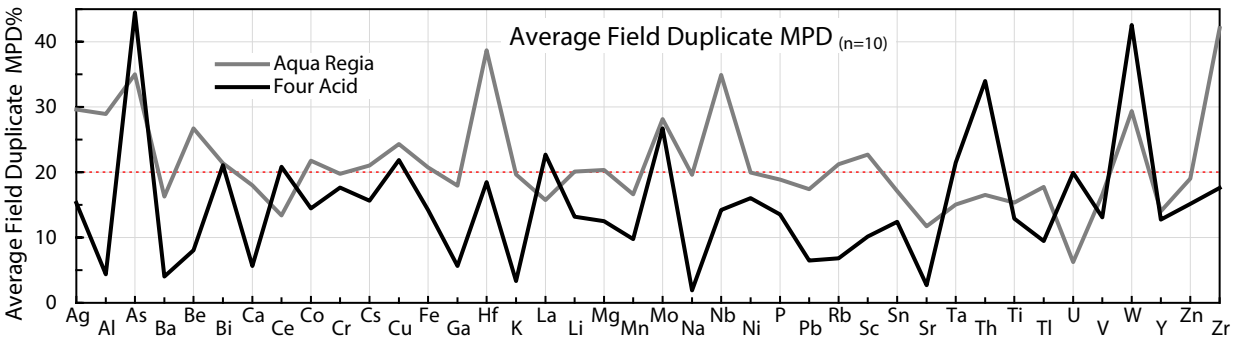

Figure 2.23: Plot of average MPD of ten field duplicate pairs for aqua regia and four acid results. Four acid consistently displays lower MPD for most elements. Elements for which >50% of measured values fall below the practical lower detection limits for either aqua regia or four acid are excluded.

- Non-reproducible elements, of which the average MPD exceeds 30%, include As, Hf, Nb, and Zr.
- Elements that display significant natural variability (average MPD >20%) include Ag, Al, Be, Bi, Cd, Co, Cs, Cu, Fe, Li, Mg, Mo, Rb, Sc, Se, and W.
- Reproducible elements that do not display significant natural variability include Ba, Ca, Ce, Cr, Ga, Ge, K, La, Mn, Na, Ni, P, Pb, Sn, Sr, Ta, Th, Ti, Tl, U, V, Y, and Zn.
- Aqua regia data displays less field reproducibility that four acid data and consistently displays higher MPD for most elements (Figure 2.23).

Results

The application of aqua regia ICP-MS analysis at the Kelvin kimberlite is more limited than four acid results. Field duplicates exhibit significant natural variability, and several elements fall below the practical lower detection limit. Results from aqua regia ICP-MS analysis are summarized in Figure 2.24 and Figure 2.25, and the following observations are made:

- Elevated and anomalous Cr, Mg, Mn, Fe, and Ni concentrations define both the east-west and northwest trends (Zones 1 and 2) identified by four acid data.
- Up-ice samples consistently exhibit background concentrations, except for Ca and Sr.
- Elevated and anomalous values of Ba, Rb, Sr, and Ti define both trends moderately well.
- Aqua regia soluble Ca shows anomalous values within the east-west trend and the northwest trend, and more natural variation across the survey.
- Light rare earth elements, La and Ce, (not shown) display significant noise across the survey without any spatial correlation to other pathfinder elements - similar to four acid data.

Aqua regia results detect pathfinder anomalies down ice of the kimberlite. The locations and patterns of anomalies overlap with those mapped by four acid results and noise across the study area is reduced -

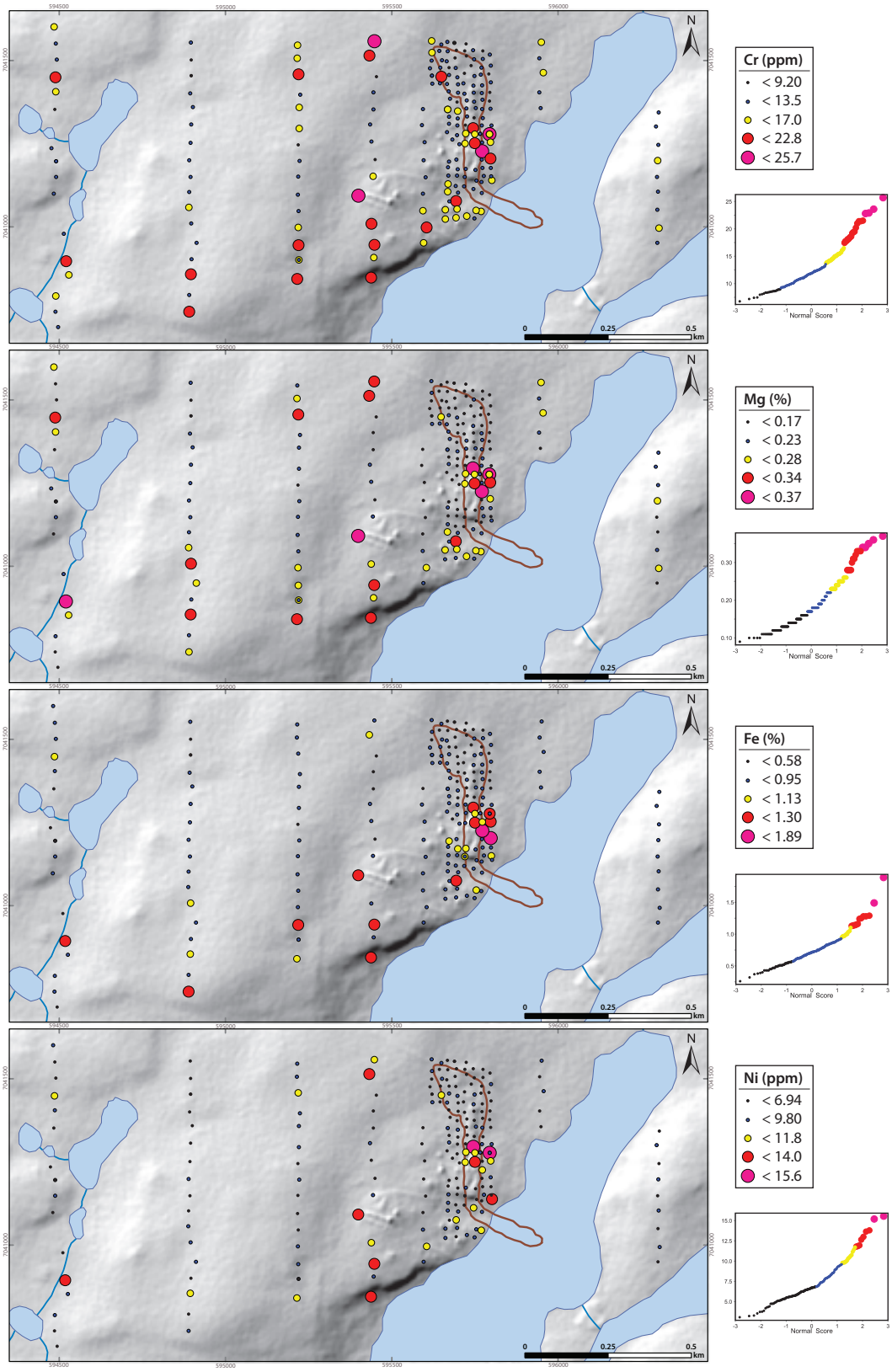

Figure 2.24: Maps of aqua regia ICP-MS Cr, Mg, Fe, Ni results of -180 µm soils. Background, elevated, and anomalous populations determined according to probability plot trends.

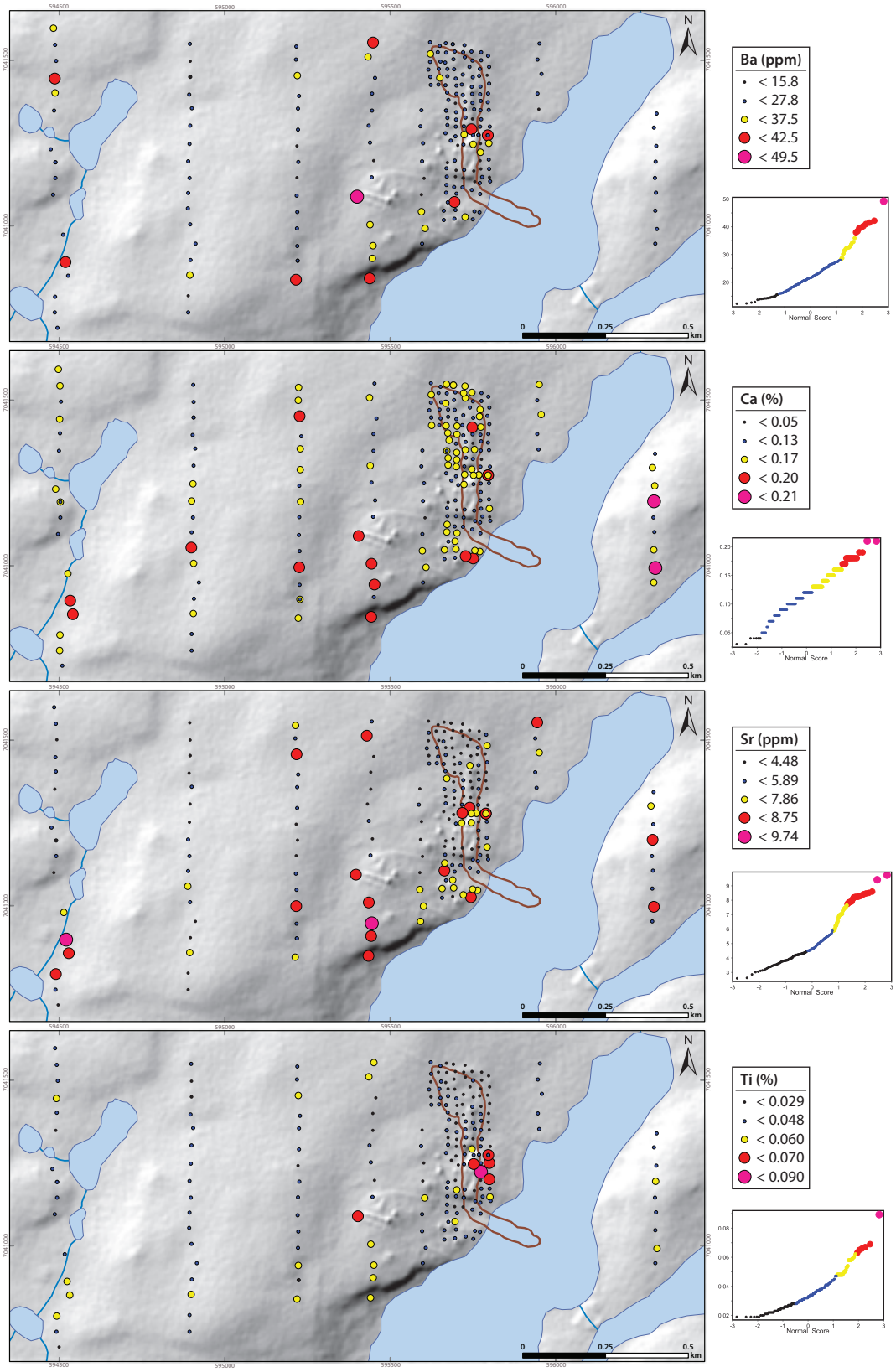

Figure 2.25: Maps of aqua regia ICP-MS Ba, Ca, Sr, Ti results of -180 µm soils. Background, elevated, and anomalous populations determined according to probability plot trends.

	Ba	Ca	Cr	Fe %	Mg %	Ni	Sr	Ti %
Cutoff Value	27.8	0.13	13.5	0.95	0.23	9.80	5.89	0.048
Average Background	20.7	0.097	10.8	0.68	0.16	6.58	4.41	0.032
Average Anomalous	34.2	0.149	16.6	1.14	0.27	11.4	7.37	0.056
Response Ratio	1.65	1.54	1.54	1.68	1.69	1.73	1.67	1.75

Table 2.5: Response ratios of anomalous to background values from aqua regia ICP-MS soil data. Response ratio calculated from the average background and anomalous populations; the cutoff threshold is determined between blue (background) and yellow (elevated) populations in Figure 2.24 and Figure 2.25. Data displayed in ppm unless otherwise noted.

particularly in up-ice samples. Response ratios are higher than four acid (Table 2.5, Table 2.4) presumably because four acid digests more sample substrate, including country rock feldspars and phyllosilicates and their trace elements. Elements that successfully detect the kimberlite include Cr, Mg, Fe, Mn, Ni, Co, Ba, Ca, Sr, Rb, and Nb, Ta, and Ti despite questionable data quality.

2.4.2.3 Organic Carbon

Just over half of organic carbon values lie below the practical limit of detection, and natural variability is high with an average field duplicate MPD of 59%. Therefore organic carbon data is interpreted with significant caution. Careful sampling methods ensured organic carbon content never exceeded 1.25% and values vary little across the study area. There are no correlations or controls on trace element concentrations that would result from complexation with humic and fulvic acids (Figure 2.26).

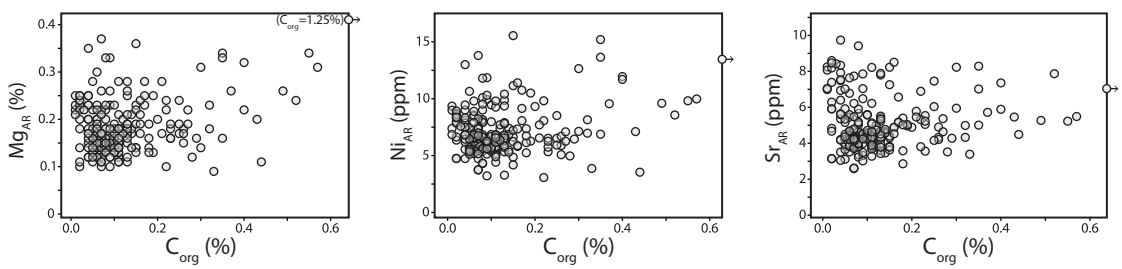

Figure 2.26: Organic carbon by Leco Furnace plotted against aqua regia soluble Mg, Ni, and Sr. No correlation exists between organic carbon and pathfinder element concentrations in soils. One sample lies outside the plotted C_{org} range.

2.4.2.4 Discussion

Geochemical patterns within the survey area trend east-west and appear to be controlled by the dominant second ice direction rather than north-south trending bedrock patterns. Anomalous responses of four acid and aqua regia soluble pathfinder elements are largely limited to the southern half of the survey. In addition to traditional pathfinder elements, immobile element ratios, including Th/U and Nb/Zr, adequately delineate the clastic dispersion at Kelvin. Gabrros and diabse dykes from the Slave exhibit Th/U values similar to metaturbidite and plutonic rocks (Figure 2.21). Th/U ratios should be interpreted as a supplementary pathfinder or used with caution because kimberlite values vary between fields and may not always be elevated compared to country rock, and post-depositional oxidation and removal of uranium may form false

positive anomalies.

Four acid results define the down-ice anomalies; however, several anomalous samples are present up-ice. Noise within the aqua regia dataset is decreased compared to four acid results, and up-ice samples display lower background concentrations. As observed at Kelvin, in situations where KIM trains are not detected and geochemical anomalies are presumably very subtle (if present), the low recovery rate via aqua regia digestion may prove inadequate compared to four acid. Aqua regia is unable to fully digest resistant kimberlite oxide and silicate minerals resulting in insufficient data quality for select elements. Aqua regia insufficiently digests resistant titanium-oxide minerals ilmenite and perovskite - the dominant hosts to Nb, Ta, and Ti in kimberlites resulting in low recovery rates and concentrations that fall below practical detection limits (Figure 2.27). As a result, Ta data is of unacceptable quality and Nb and Ti are interpreted with caution despite vaguely identifying the dispersal patterns at Kelvin. Ba and Rb aqua regia responses are more subtle because of incomplete digestion of kimberlite phlogopite and country rock biotite. Anomalous and elevated aqua regia Ca and Sr identify the dispersion from the kimberlite because of the selective digestion of Sr-rich kimberlite carbonates by aqua regia. However, recovery rates of Ca, Sr, and Nb are low indicating the majority of these elements are hosted in aqua regia resistant phases (Figure 2.27).

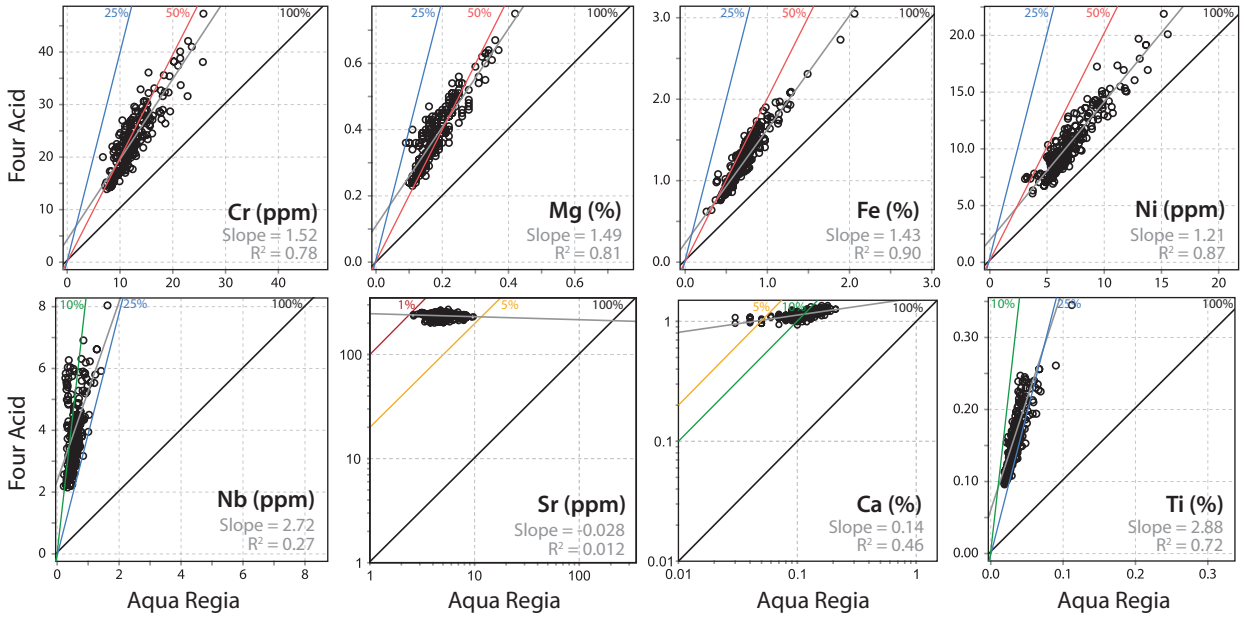

Figure 2.27: Pathfinder concentrations of four acid and aqua regia soil data to show percent recovery by aqua regia relative to four acid digestion and ICP-MS. Colored lines indicate calculated percent recoveries, grey line indicates regression line for B horizon data.

2.4.3 Sequential Extraction

Two samples from anomalous Zones 1 and 2 were selected for sequential extraction analysis, in addition to an up-ice and down-ice background sample (Figure 2.28, Table 2.6). Results from the five sequential extractions were compared to the separate aqua regia and four acid data (Section 2.4.2.1, Section 2.4.2.2).

Concentrations extracted by the weak sequential leaches are considerably low and often fall below

lower limits of detection (Appendix D). Such values were replaced with values half the limit of detection, and the suite of pathfinder elements with acceptable data quality is diminished.

Sample	Sample Type	Ba-Cr-Fe-Mg-Mn-Nb-Ni-Ta-Ti Norm. Percentile Sum (4-Acid)		Sequential Extraction	Size Fraction	Pb Isotopes
Q515255	Soil	97.6%	Anom	×		
Q515469	Soil	69.8%	BG	×	×	
Q515396	Frost Boil	93.8%	Anom	×	×	×
Q515414	Frost Boil	5.1%	BG	×	×	×
Q515300	Soil	96.9%	Anom		×	×
Q515282	Soil	46.2%	BG			×
Q515344	Soil	83.1%	Anom			×
Q515367	Soil	22.5%	BG			×
Q515404	Soil	15.2%	BG			×
Q515419	Frost Boil	79.8%	Anom			×
Q515425	Soil	51.6%	BG			×
Q515431	Frost Boil	79.5%	Anom			×
Q515438	Soil	31.6%	BG			×
Q515449	Soil	4.1%	BG			×
Q515458	Frost Boil	79.3%	Anom			×
Q515463	Soil	60.7%	BG			×
Q515470	Frost Boil	91.7%	Anom			×

Table 2.6: Samples selected for sequential extraction, size fraction, and Pb isotope analyses. See Figure 2.28 for sample locations. Anomalous (Anom), background (BG).

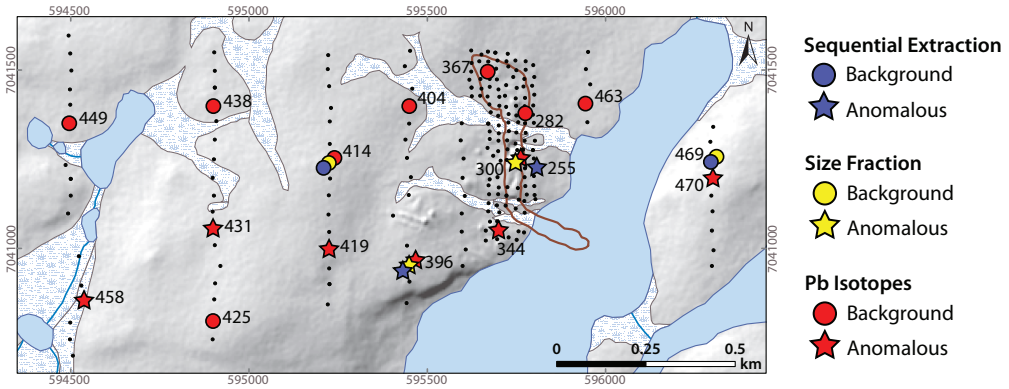

Figure 2.28: Map of samples selected for sequential extraction, size fraction, and Pb isotope analyses. Sample prefix 'Q515' has been removed from labels. See Table 2.6 for sample information.

Aqua regia and four acid digestions extract the majority of pathfinder elements (Cr, Mg, Fe, Ni, Nb, Ti) indicating they largely reside in their primary mineral form as silicates, phyllosilicates, crystalline oxides, and clay minerals (Figure 2.29). Four acid extracts 87% - 93% of Nb indicating most Nb is residing in silicates and oxides in both background and anomalous samples. Small amounts of Nb are hosted in aqua regia soluble phases, as well as with organic acids (Figure 2.29). Ti recoveries display similar patterns as Nb. Aqua regia and four acid steps extract nearly equal Ni concentrations indicating Ni is hosted in silicates, phyllosilicates, crystalline Fe oxides, and clay minerals. The most likely source of aqua regia soluble Ni in anomalous samples is deuteric serpentine that replaced olivine during kimberlite emplacment.

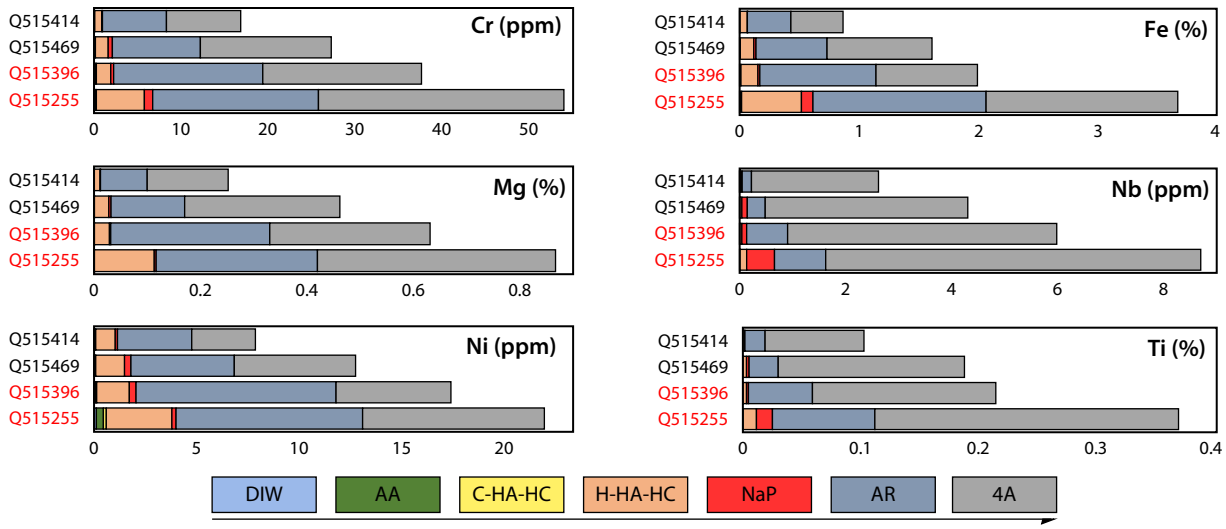

Figure 2.29: Bar chart of sequential extraction results for pathfinder elements. Anomalous samples (Q515255, Q515396) in red; background samples (Q515414, Q515469) in black. See Table 2.2 for extraction abbreviations and targeted phases.

2.4.3.1 Discussion

Sample Q515255 consistently displays slightly elevated Fe, Cr, Mg, and Ni hosted by amorphous Fe oxides recovered by H-HA-HC (Figure 2.29). 16% of total Fe is extracted by H-HA-HC for Q515255 compared to an average of 8% in other samples. Tthis sample is more chemically weathered containing more amorphous Fe oxides present as coatings on mineral grains and thus adsorb elevated trace metal concentrations. The concentrations hosted in amorphous Fe oxides do not account for the difference between anomalous and background bulk samples, and are not a significant factor in generating anomalous (possibly false) geochemical responses in soils at Kelvin.

Sample Q515255 contains 1.25% organic carbon, the highest value in the study area. Sample Q515255 contains elevated concentrations of Nb, Ti, and Mo hosted in NaP extractable organic carbon phases of the soil. Albeit in low concentrations, these results clearly indicate the strong influence organic acid can have, particularly in samples with increased organic content.

In all soils, sources of labile pathfinder elements are very low as extraction by the five weak sequential leaches rarely exceed 15% of the total concentrations. Evidence of labile metal phases is lowest for Nb and Ti - presumably hosted in resistant kimberlite oxides. Overall, pathfinder concentrations present as labile cations or bound to carbonates and Mn oxides extracted by DIW, AA, and C-HA-HC, respectively, do not significantly contribute to bulk chemistry of the soils. Carbonate stability is inhibited by the acidic soil conditions and secondary Mn oxides are a minor phase in the soils based on low Mn concentrations extracted during C-HA-HC leach.

Deionized water is recommended to most accurately represent vertically transported responses by partially extracting the exogenic labile ions introduced to the soil as water soluble ions from exterior sources (e.g., mineralization at depth; Cameron et al., 2004). Anomalous sample Q515255 above the North Limb

of the kimberlite would be most susceptible to vertical element migration from the kimberlite at depth. Anomalous pathfinder elements, including those proven to be labile in acidic to circum-neutral and (sub)oxic groundwater conditions around kimberlites (Ba, Cr, Ni, LREE, Y; Sader et al., 2011), are dominantly hosted in primary minerals extracted by aqua regia and four acid. There is no significant evidence of vertical transported pathfinder signatures in anomalous Zone 2. Instead, sequential extraction results confirm the source of anomalous pathfinder elements in Zones 1 and 2 are clastic, hosted in primary minerals, and there has been little redistribution by soil formation processes.

2.4.4 Soil Size Fraction

QA-QC

Four samples were selected for size fraction analysis: two samples exhibiting background pathfinder concentrations (Q515414 and Q515469) and two anomalous samples exhibiting elevated pathfinder concentrations (Q515300 and Q515396; Table 2.6). Six lab duplicates were used to assess precision and reproducibility.

- All elements display adequate reproducibility excluding Bi, Se, and Th which average MPD >20%.
- Lower detection limits exclude Cd, Ge, In, Mo, Re, S, Sb, Se, and Te from the dataset as well.

Sieve efficiency was assessed by comparing reconstituted calculated concentrations to bulk -180 µm analyses (Section 2.4.2.1). Less than 2.0% of sample mass was lost during sample sieving based on reconstituted mass of the eight fractions (including the -5 µm). The reconstituted sums (calculated as the weight percent multiplied by the element concentration, and summed for all fractions) mostly fall below bulk values, and commonly within 10% of bulk values and rarely exceed 20% error (Figure 2.30 and Appendix B).

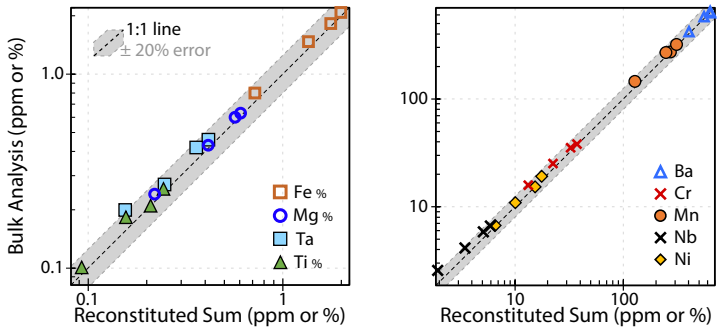

Figure 2.30: Bulk -180 µm pathfinder concentrations plotted against reconstituted sums (calculated as the weight percent multiplied by the element concentration, and summed for all fractions). Nearly all values fall within 10% of bulk values and rarely exceed 20% error. Values in ppm unless otherwise noted at percent. Additional QA-QC in Appendix B.

Results

Dry sieving capabilities resulted in <0.5% weight recovery of material smaller than 5 µm - insufficient

quantity for commercial four acid ICP-MS analysis. Therefore the following results do not accurately represent the clay size fraction (<2 µm) which often requires centrifuging to effectively recover. The 25-5 µm fraction discussed herein likely contains material smaller than 5 µm that failed to be removed by dry sonic sieving.

Geochemical partitioning into the various size fractions is assessed by four acid results. Grain size distribution is dominated by silt and fine silt-sized particles, although anomalous samples are more strongly skewed towards the finer fraction. Concentrations of pathfinder and major elements are lowest in the coarser fractions as resistant quartz and feldspars preferentially occupy the coarser fractions effectively diluting trace element signatures (Shilts, 1995). Pathfinder and major element concentrations are highest in the 25-5 µm fraction. As a result, nearly all size fractions except the 25-5 µm exhibit concentrations below the bulk -180 µm concentration (Figure 2.31). Due to the negatively skewed grain size distributions and elevated concentrations in the finest fractions, trace element chemistry of the soils is dominantly hosted in the 25-5 µm and 53-25 µm fractions.

For all pathfinder elements, anomalous samples are slightly elevated in all size fractions relative to background samples. The anomalous to background contrast is most pronounced in the 150-125 µm and 125-106 µm fractions. Average response ratios, calculated as the ratio of the average anomalous value to the average background value, are used to evaluate each size fractions potential to distinguish anomalous from background values. The 150-125 µm and 125-106 µm fractions exhibit the highest response ratios and are above reconstituted -180 µm ratios (Figure 2.31). Response ratios in the finest fractions are lower than reconstituted -180 µm responses and are not enhanced because background samples are elevated in pathfinder elements as well. Although response ratios are not enhanced, the finest fractions are more homogeneous and provide better analytical reproducibility. Increased MPD for Cr, Fe, Mg, Ni, and Nb in the coarser fractions is a result of nugget effects from sand-sized indicator minerals and their fragments (Figure 2.32).

2.4.4.1 Discussion

Size fraction response ratios reflect the primary indicator mineral grain size and the degree of comminution during glacial clastic transport. Anomalous samples enriched in the 150-125 µm and 125-106 µm fractions are due to sand-sized kimberlite phenocrysts, macrocrysts, and their fragments. Cr-diopside and ilmenite are shown to resist glacial comminution. In contrast, pyrope garnet and olivine more easily break down to silt-sized fractions due to inclusions and abundant decompression fractures associated with kimberlite emplacement (Cummings et al., 2014). Response ratios for Cr, Nb, and Ti in the 150-125 µm and 125-106 µm fraction are elevated compared to other pathfinder elements suggesting these pathfinders are preferentially hosted in minerals resisting comminution (e.g., ilmenite and Cr-diopside).

Enrichment in the silt fraction is attributed to kimberlite groundmass and matrix minerals and minor input from indicator mineral fragments. Microcrystalline and cryptocrystalline groundmass and matrix minerals include phlogopite, clinopyroxene, serpentine, carbonate, monticellite, perovskite, chlorite, and spinel. Barium does not show elevated response ratios in the 150-125 µm and 125-106 µm fractions. Barium is almost exclusively hosted in groundmass and matrix phlogopite which rarely exceeds 100 µm in size and is

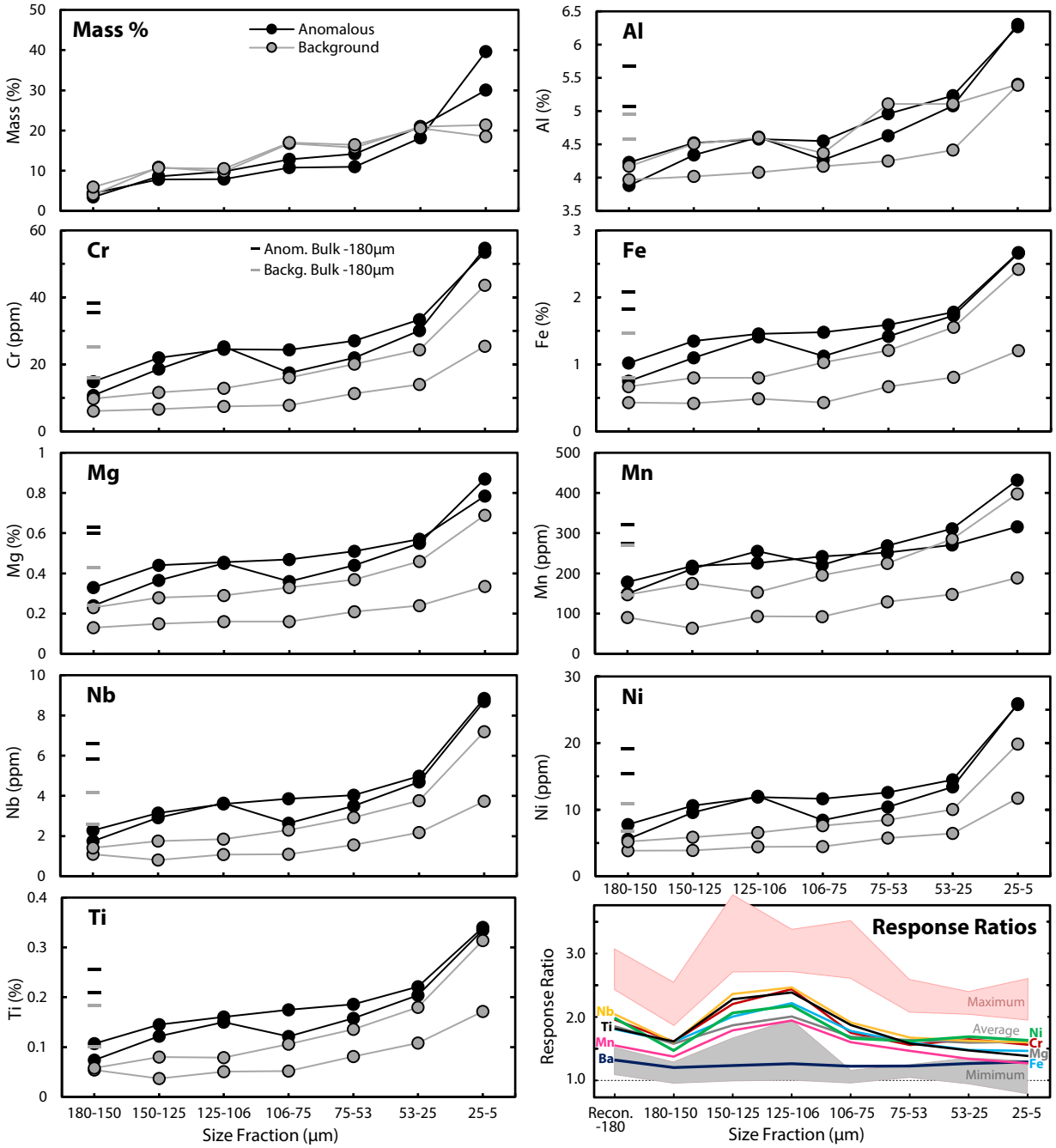

Figure 2.31: Pathfinder element concentration, as determined by four acid ICP-MS analysis, plotted against size fractions. Bulk -180 µm concentrations shown as tick marks. Average response ratios shown as colored lines are calculated as a ratio of the average background and average anomalous values. Maximum ratios are calculated as the ratio between the most elevated anomalous value ratioed to the minimum background value. Minimum response is the ratio of the most elevated background to the minimum anomalous value. All response ratios systematically increase in the 150-125 µm and 125-106 µm fractions for all pathfinder elements. Reconstituted -180 µm ratios are calculated from reconstituted -180 µm sums.

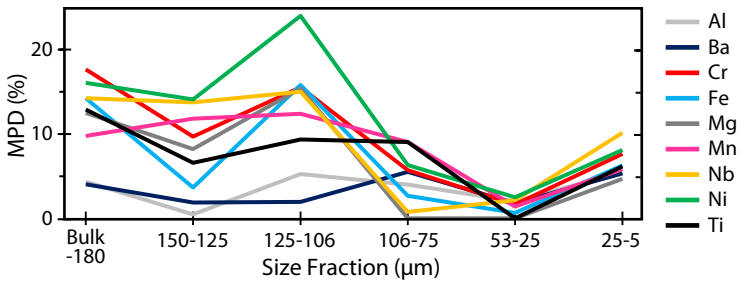

Figure 2.32: Lab duplicate mean percent difference for pathfinder elements from different size fractions. No lab duplicates taken of the 180-150 µm and 75-53 µm fractions.

expected to be easily comminuted during glacial transport on account of its cleavage and softness.

Clay minerals, Fe-Mn (hydr)oxides, organic compounds, and other secondary phases concentrated in the fine silt and clay fractions host and adsorb the mobile geochemical signatures of soil and have the ability to significantly influence the bulk geochemistry because of their large proportion by mass. The degree of weathering of the soils is assessed by CIW, A-CN-K ternary plot (Figure 2.33), and by Pearce Element Ratio Feldspar Control diagram (Figure 2.16). Although all soils across the study area are very immature and not significantly weathered, anomalous samples (Q515300 and Q515396) are more weathered based on alkali-alumina ratios (Figure 2.33). The finest fractions of anomalous samples correlate with higher degrees of weathering, providing a possible explanation for the increased aluminum content and more negatively skewed grain size distribution of anomalous samples by the production of clay-sized secondary minerals. Field observations contradict the calculated degree of chemical weathering. Samples Q515396 and Q515414 are from active, or recently active, frost boils and represent nearly unweathered, grey, C horizon till compared to samples Q515300 and Q515469 that sampled visibly weathered, brown, B horizon till. Despite the difference in weathering indices between anomalous and background, all samples are immature and secondary liberation and adsorption of labile cations by clay minerals and Fe-Mn (hydr)oxides is shown by sequential extraction data to have little effect.

Detection limits, sieving throughput, and cost dictate the practicality of targeted sieving of a specific size interval. Therefore, sub-fractions were calculated by summing the concentrations of finer fractions weighted by percent weight. The finest sub-fractions exhibit the highest pathfinder concentrations. As the upper limit of sieving coarsens, concentrations are diluted with the addition of coarser, more inert, material. As a result, evidence of anomalous responses in the 150-125 µm and 125-106 µm fractions are obscured in sub-fraction plots (Figure 2.34). Anomalous samples are consistently enriched in all sub-fractions. However, the enrichment in anomalous samples is too low to overcome the elevated background concentrations in the finest fractions. This results in a decrease in the anomalous to background response ratios in the finer fractions (Figure 2.34).

Additional research on geochemical partitioning is required to constrain the secondary processes in the fine fraction of the soils at Kelvin. Possible areas of study should include mineral spectrometry of the fine fraction to identify clay and kimberlite matrix mineralogy; or evidence of chemical corrosion on silt sized

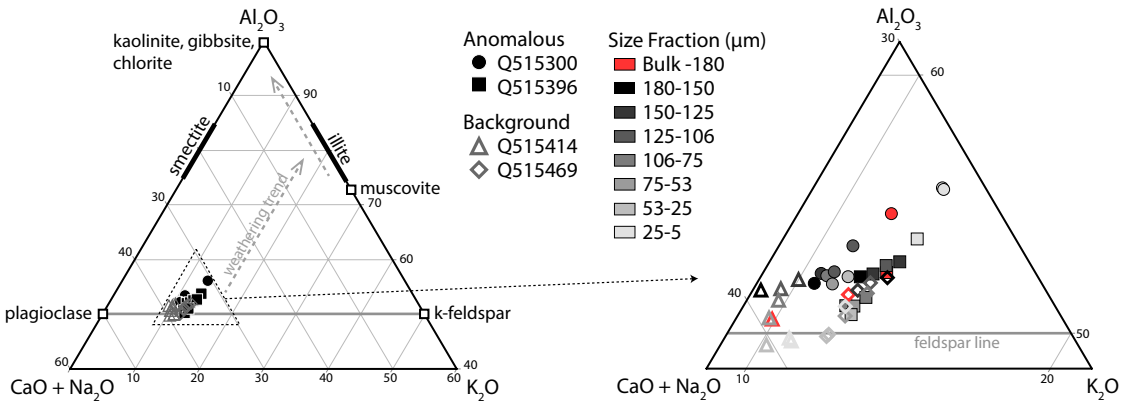

Figure 2.33: A-CN-K ternary plot of soil size fractions based on four acid ICP-MS data. General weathering trends after Nesbitt and Young (1984). Weathering is largely weak to absent as all samples lie close to feldspar line and do not strongly trend towards phyllosilicate and clay minerals. Inset diagram shows bulk -180 µm background samples are less weathered than bulk -180 µm anomalous; and degree of weathering increases in the finest fractions of only anomalous samples. Left diagram is not colored by size fraction as the right diagram is.

indicator minerals with scanning electron microscope (DiLabio, 1995). Analysis of size fractions by partial or selective extractions is also recommended to determine resident phases of pathfinder elements and to attribute signatures to primary clastic or secondary phases. Additionally, sonic sieve efficiency of the clay fraction should be tested and compared to commercial clay extraction by centrifuge. Finally, additional samples from Kelvin should be sieved and analyzed by four acid ICP-MS for spatial interpretation within the study area.

Results show the strong control of the fine fractions and grain-size distribution on bulk geochemistry, and supports the inclusion of grain-size analysis in an orientation survey to recommend possible targeting sieving and limit textural bias. This study shows the 150-125 µm and 125-106 µm fractions are most appropriate for targeting sieving. However, where subtle responses may fall below lower detection limits, finer fractions are suggested. Research should be conducted on more samples to examine the ideal sub-fraction for exploration, however, current results display better anomalous to background contrast in the coarser fractions. Response ratios indicate the -180 µm fraction may be a more suitable size fraction for analysis than the commonly used -63 µm fraction.

2.4.5 Pb Isotopes

QA-QC

In total, 17 samples were selected for Pb isotope analysis: 7 background samples, 8 samples anomalous in kimberlite pathfinder elements, and two lab duplicates (Figure 2.28).

The laboratory QA-QC procedures do not report associated error percentages. Mass bias is monitored and corrected by analyzing NBS SRM981 every five samples. However, the analysis of a pure Pb standard does not truly quantify the precision associated with digestion methods and matrix effects. The lab reports a

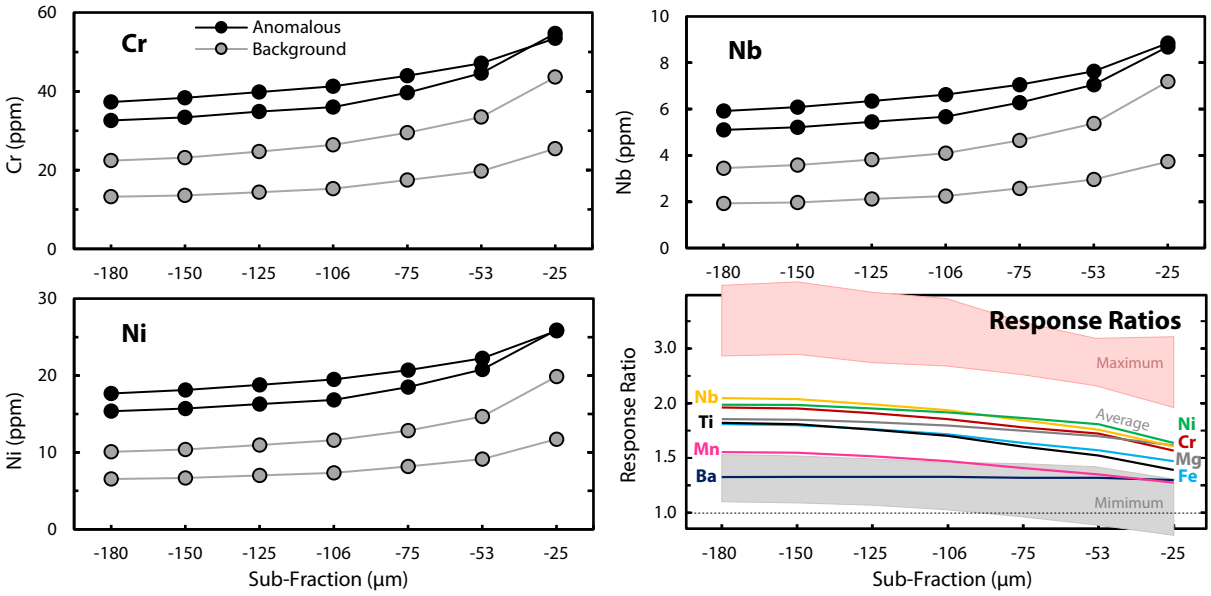

Figure 2.34: Pathfinder element concentrations plotted for all sub-fractions. A similar trend is exhibited for all pathfinder elements including Ba, Fe, Mg, Mn, Ta, and Ti. Highest concentrations occur in the finest fractions and are progressively diluted with coarser fractions. Average response ratios shown as colored lines are calculated as a ratio of the average background and average anomalous values. Maximum ratios are calculated as the ratio between the most elevated anomalous value ratioed to the minimum background value. Minimum response is the ratio of the most elevated background to the minimum anomalous value. Response ratios systematically increase in the coarser fractions for all pathfinder elements.

method precision tolerance of 2%. Internal geologic standards MRGeo08 and SY-4 are also used to monitor accuracy of the analyses.

Precision is monitored by lab duplicates to assess the reproducibility of digestion methods and sample matrix effects. The average MPD of two duplicate pairs (Table 2.7) is displayed as uncertainty bars on bivariate isotope plots.

	$^{206}Pb/^{204}Pb$	$^{207}Pb/^{204}Pb$	$^{208}Pb/^{204}Pb$	$^{208}Pb/^{206}Pb$	$^{208}Pb/^{207}Pb$	$^{206}Pb/^{207}Pb$	$^{207}Pb/^{206}Pb$
Average MPD (%)	0.97	0.45	1.22	1.75	1.70	1.01	1.01

Table 2.7: Analytical reproducibility (%) of Pb isotope ratios based on average MPD from two duplicate pairs.

Results

Limits in detecting ^{204}Pb by Q-ICP-MS precludes using ^{204}Pb in interpreting isotopic ratios. Therefore, ratios of the three radiogenic isotopes are only discussed.

Background soils display isotope ratios overlapping whole-rock four acid Q-ICP-MS isotope ratios of metaturbidite country rock (Figure 2.35). Anomalous samples largely lie outside of the present day metaturbidite field and trend towards present day values of elevated Th/U (κ) growth curves. Available Pb isotope literature on bulk or whole rock kimberlite is limited. Kimberlites exhibit a wide range of anomalously radiogenic present day values which significantly overlap with present day metaturbidite country rock values.

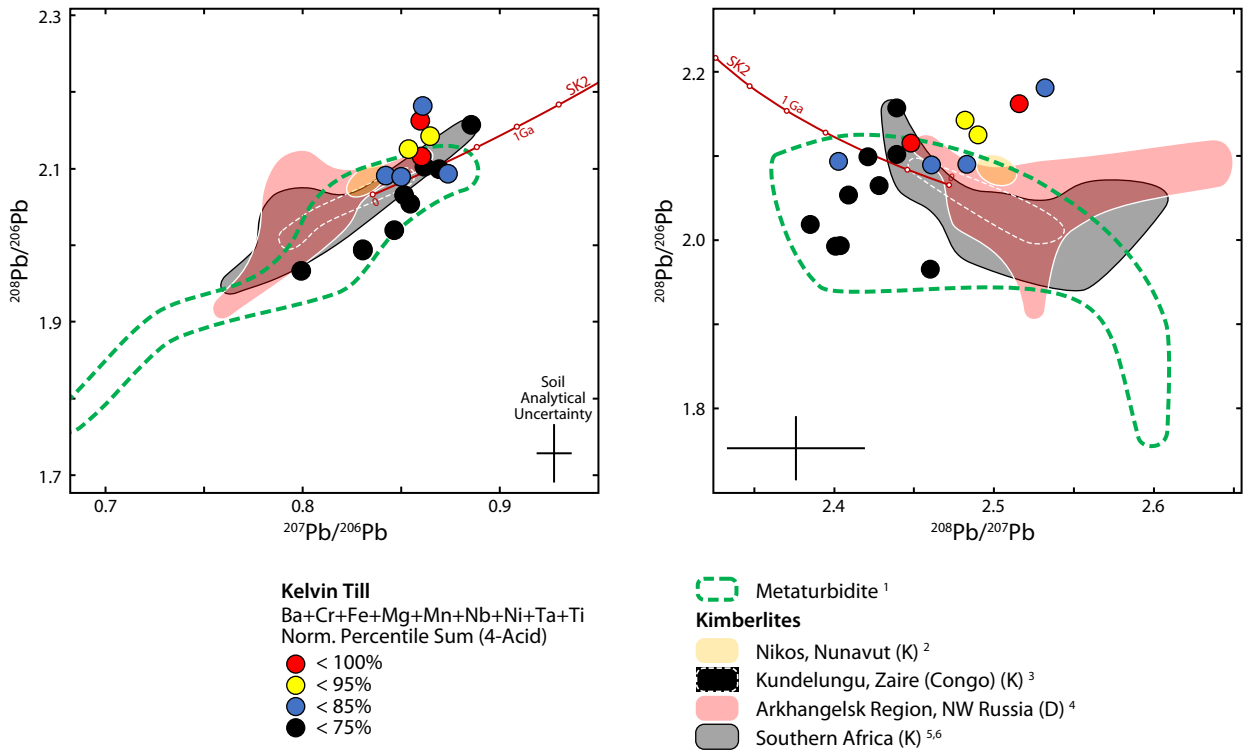

Figure 2.35: Bivariate Pb isotope plots of till and metaturbidite country rock analyzed by four acid Q-ICP-MS. Analytical reproducibility (%) of soil Pb isotope ratios based on average MPD from two duplicate pairs. Present day kimberlite values include kimberlite matrix, groundmass, and autolith samples. Global primary kimberlite values exhibit similar values, and partially overlap present day metaturbidite values. Stacey-Kramers second stage growth curve (SK2) included for reference. [1] this study; [2] Schmidberger et al. (2001); [3] Weis and Demaiffe (1985); [4] Beard et al. (2000); [5] Kramers (1977); [6] Smith (1983).

Lead isotope ratios are preserved through weathering and in soil profiles, allowing their application in residual and till covered terranes (Gulson, 1986; Rukhlov and Ferbey, 2015). Till is derived from the most recent glaciation and post-depositional oxidative weathering and preferential removal of U is presumably limited to the last last ca. 9,000 years. Any radioactive decay since the preferential removal of U is expected to be negligible in the subarctic.

2.4.5.1 Discussion

Pb isotope results do not definitively fingerprint kimberlite isotopic signatures in anomalous till samples. The significant overlap between global kimberlite and metaturbidite present day isotopic values complicates the identification of clastic mixing trends between the two end-member sources. Although kimberlite isotopic values vary due to mantle heterogeneities and varying mixing degrees between multiple mantle magma sources and crustal contamination, there is significant similarity between global kimberlite values. Therefore, Slave kimberlites are assumed to display values within these fields.

Anomalous samples trending away from background and metaturbidite values may represent heterogeneity in the basal till and an additional bedrock source containing elevated Th/U (or κ) values. Whole-

rock Pb isotopic data for Slave granites are not available to confirm these as a source. Additionally, isotopic trends within till data may represent lithologic variation between the sialic basement and calc-alkaline volcanic sediment sources of Slave metaturbidites (Section 1.5.1).

2.4.6 Spatiotemporal Geochemical Hydrocarbons

QA-QC

Data quality was assessed by ActLabs and is included in the appended report (Appendix C). Precision and reproducibility is assessed by 15 lab duplicates. The coefficient of variance (CV), equivalent to the relative standard deviation (RSD), calculated per Equation 2.7 is of very good precision, averaging 11.4%. Seven field duplicate pairs have an average CV of 19.5%, indicating the field reproducibility is acceptable.

$$Coefficient\ of\ Variation\ (\%) = \frac{\sigma}{\mu} \times 100 \ = \ \frac{standard\ deviation}{mean} \times 100 \tag{2.7}$$

Results

Interpretations in the report are made entirely on SGH data and sample locations; no geophysical, geochemical, or geographical data was considered in the interpretations. Although only relative sample coordinates were provided and the exact survey location area was not disclosed, ActLabs correctly hypothesized that the orientation of the survey was to target westward glacial dispersion. Therefore, the report includes interpretations from the entire survey area and separate interpretations of the 25×25 m grid directly over the surface projection of Kelvin.

The confidence of both interpretations are rated by the lab based on the magnitude of the response of the SGH pathfinder class, and the degree of matching between the measured signatures and the expected mineralization SGH fingerprint. The SGH fingerprint for kimberlites includes a group of pathfinder classes developed from SGH case studies over known kimberlites. Although at least three pathfinder classes are used in the interpretation, only one pathfinder class map is included in the report. Pathfinder class values are reported for this map as semi-quantitative parts-per-trillion, specific compounds are not reported. Pathfinder classes are the sum of between four and fourteen chemically similar moderate to heavy hydrocarbon compounds including alkanes, alkenes, thiophenes, aromatic, and polyaromatic compounds grouped using multivariate statistics.

A SGH pathfinder class map of the whole survey area indicates three proposed linear trends of low SGH values that ActLabs interprets as kimberlite mineral pathways (Figure 2.36). The three pathways trend sub-parallel to known ice directions. Two proposed pathways vector up ice to the area of known subcrop. The confidence of this interpretation is rated 4.5 out of 6.0. ActLabs interprets these trends as evidence of kimberlite material transported from the kimberlite(s) and entrained in the till in sufficient quantity to support microbial communities and form hydrocarbon responses.

The sample grid over the surface projection of Kelvin was interpreted separately due to the tighter

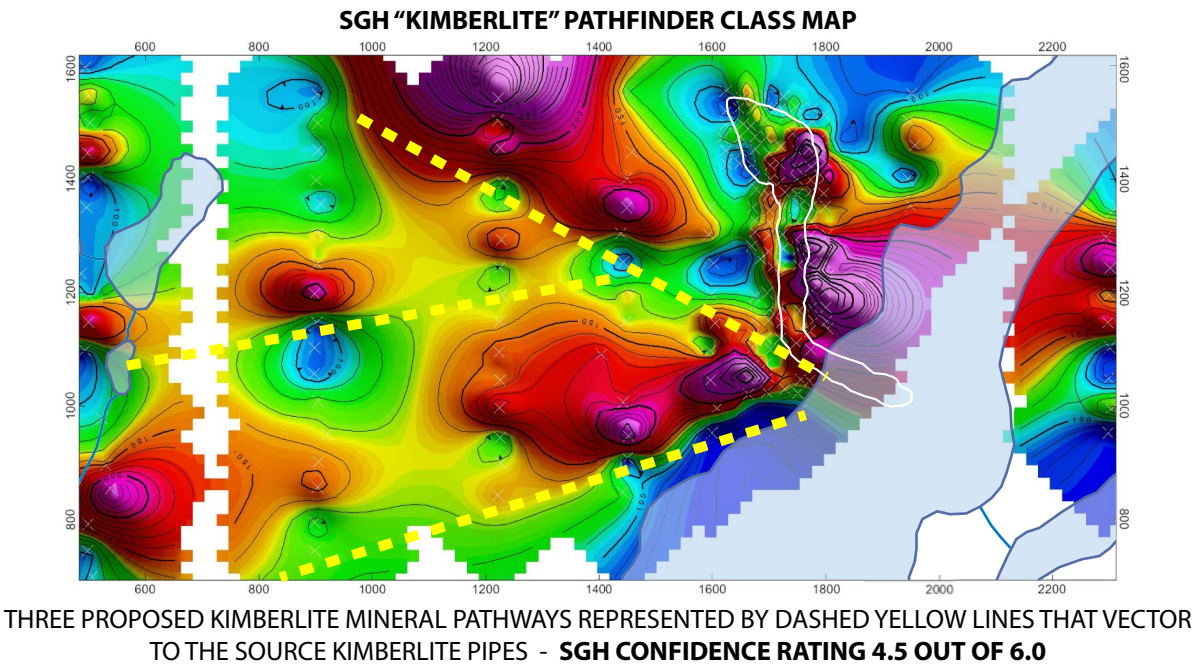

Figure 2.36: ActLabs-produced map of SGH pathfinder class most reliable for detecting kimberlites. Yellow dashed lines represent kimberlite indicator trains interpreted by ActLabs. Lakes and known surface projection of Kelvin is overlain.

sample spacing. Figure 2.37 is plotting the same pathfinder class as Figure 2.36. ActLabs proposes two kimberlite pipes centered over lows flanked by high values. The predicted targets are given a confidence rating of 4.5 out of 6.0 because "there is not sufficient with to [sic] this area to confidently states their location."

2.4.6.1 Discussion

It is proposed that SGH responses are due to changes in autotrophic organism in various redox regimes associated with reduced chimneys (Hamilton, 2007b; Sader et al., 2009; Sutherland, 2018). Predicted kimberlite locations proposed by ActLabs center on troughs of low pathfinder class values flanked by elevated values forming concentric or 'rabbit-ear' anomalies. However, there is no clear evidence correlating SGH values to Eh and changing redox conditions at Kelvin (Figure 2.38).

ActLabs' interpretation of the SGH did not correctly identify the presence of the kimberlite. The two proposed locations coincidentally are above the North Limb of the Kelvin pipe, and appear to be focused over low SGH values not attributable to reducing conditions. Dispersal trains interpreted by ActLabs also focus on low SGH values in the down-ice transects that are flanked by elevated values. ActLabs correctly hypothesized the transects as a means to detect down ice dispersal, and therefore the results and interpretations are not blind. Further discussion of the relationships between SGH pathfinder compounds and (in)organic geochemistry (e.g., Cayer, 2017) is not possible because the hydrocarbon compounds comprising the classes are not reported.

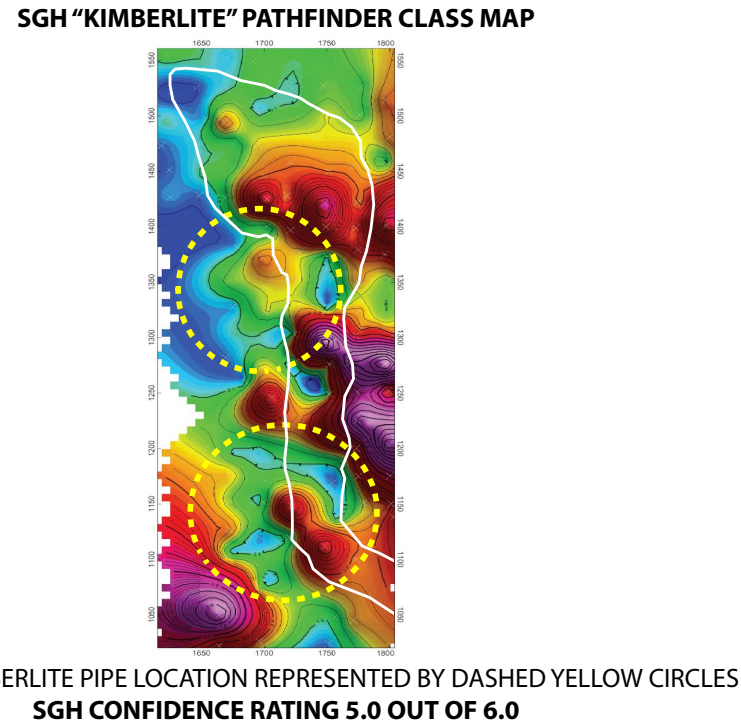

Figure 2.37: ActLabs-produced map of the same SGH pathfinder classes interpreted separately for the 25×25 m grid. Yellow dashed circles represent the surface projections of two kimberlite pipes predicted by ActLabs. Known surface projection of Kelvin is overlain.

2.5 Discussion

2.5.1 Surficial Geochemical Anomalies

2.5.1.1 Mechanical Chemical Dispersion

Till geochemistry results define a thin till composite dispersal pattern. Two assumptions are necessary with a two-stage ice flow model: (1) the late northwest flowing ice was erosional and in contact with *in situ* kimberlite, and therefore should be preserved in the erosional record; and (2) the existing till blanket was reworked and partially re-entrained, to a degree, resembling a fan or palimpsest (Parent et al., 1996). Zone 1 defines the original ribbon-shaped dispersal plume and shows evidence of subsequent reworking by the later northwest flow. Zone 1 is up to 250 m wide north-to-south (perpendicular to dispersion vector) and is significantly wider than the subcrop source (<30 m). The earlier Zone 1 dispersal pattern is better defined than the secondary Zone 2 dispersal, contrary to idealized models of palimpsest patterns which observe protracted younger flows (Figure 2.39; McClenaghan and Paulen, 2018; McClenaghan et al., 2018; Parent et al., 1996; Paulen et al., 2013). The anomalous Zone 2 can be correlated to the late northwest flow assuming the current Kelvin subcrop was the point source.

A single-stage ice flow towards the west that dominates glacial landforms and nearby KIM trains does not explain the anomalous Zone 2 above the North Limb. Sequential leach results indicate the anomalous

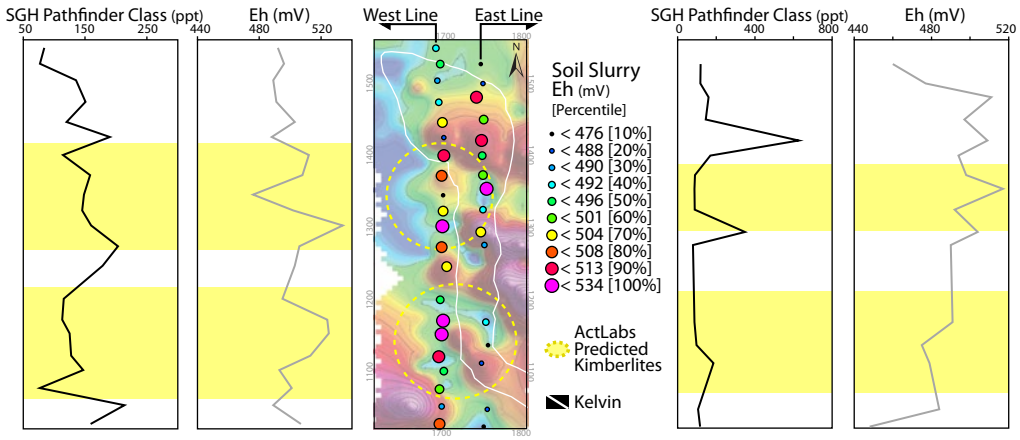

Figure 2.38: SGH pathfinder class values plotted with Eh values measured by soil slurry. Slurry Eh values are overlying SGH pathfinder class map (Figure 2.37). Predicted kimberlites coincide with low SGH values between peaks. Redox conditions do not appear to exert any control on SGH values or areas predicted as kimberlites.

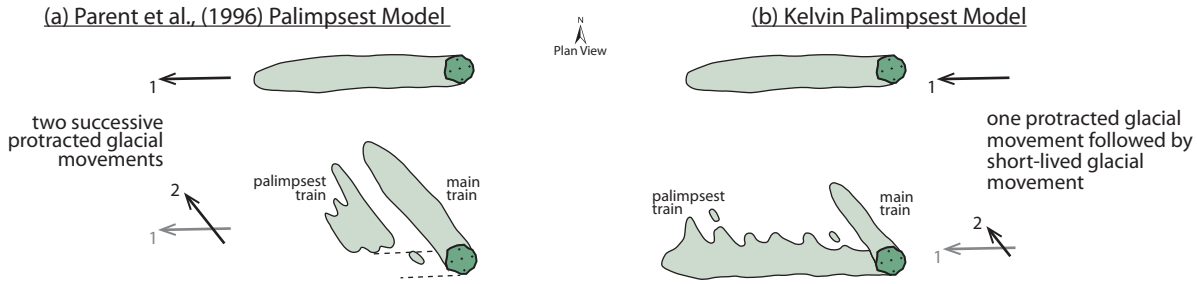

Figure 2.39: **(a)** Idealized palimpsest dispersion model modified from Parent et al. (1996) formed from two successive, oblique, protracted glacial movements. First ribbon-shaped train has been re-entrained by later ice flow forming a palimpsest dispersal train, in addition to forming a new main dispersal train. **(b)** Proposed palimpsest model at Kelvin formed from a protracted glacial movement followed by a short-lived, oblique glacial movement. First ribbon-shaped dispersal train is slightly dispersed by later ice flow, in addition to forming a new, small main train.

phases are resistant minerals of clastic origin, rather than exogenic origin. The lateral extent of this anomalous zone is small. The west and north extents are constrained, whereas the eastern extent is undefined. A possible source west of this anomalous area could be undefined kimberlite dyke that presumably subcrops below the lake north of the pipe subcrop. Thin kimberlite dykes have been shown to produce short, albeit wide, dispersal plumes (e.g., Snap Lake kimberlite dyke; McClenaghan and Kjarsgaard, 2007). The Kelvin dyke presumably subcrops south of the pipe subcrop under the lake, however, sampling transects do not extend far enough south to characterize dispersal patterns from the dyke. However, background values on the southern-most samples of lines 1 and 2 suggest clastic dispersion from the dyke is short (<750 m).

Of the 215 sample locations, active (or recently active) frost boils constitute 53 samples. Soil samples exhibit slightly depleted metal concentrations due to the slightly more acidic pH conditions resulting in increased solubility and mobility of most transition metals (Figure 2.40). A stronger geochemical contrast between these datasets may exist where weathering processes cause significant contrast between fresh and

weathered till. As chemical weathering is weak and soils are immature in the study area, soil and frost boil samples are geochemically comparable and are interpreted together.

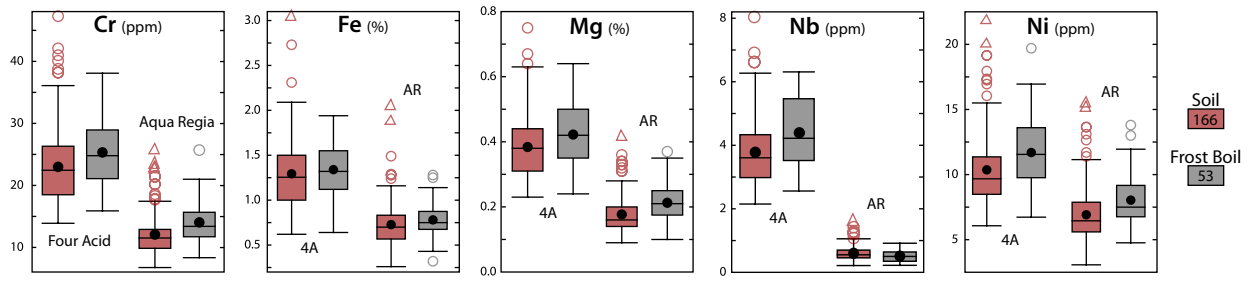

Figure 2.40: Tukey box plots of four acid and aqua regia ICP-MS pathfinder concentrations attributed between soil and active frost boil samples.

As frost boil samples represent material circulated to the surface from depth, they add three-dimensional interpretations into otherwise two dimensional surface responses. The Zone 1 dispersal plume at Kelvin is mostly defined by frost boil samples, whereas the northwest-trending Zone 2 population is mostly defined by B horizon soils (Figure 2.20). Till thickness does not significantly vary across the study area, and results support a two-stage ice flow model where the latest northwest glacial ice flow deposited anomalous Zone 2.

2.5.1.2 Vertical Chemical Dispersion

ORP and pH of the soils do not identify physicochemical evidence of an electrochemical cell above the Kelvin kimberlite. Sequential extraction results show anomalous pathfinder concentrations in Zones 1 and 2 are hosted in primary minerals rather than mobile phases. Although labile Cr, Mg, and Ni is hosted in secondary amorphous Fe oxides which increase with degree of weathering, the overall weathering regime of the study area is weak and redistribution into secondary phases does not have a significant effect on bulk geochemistry. Additionally, ions of exogenic origin measured by deionized water leach are negligible above the kimberlite (Figure 2.29). Results suggest permafrost and thick bedrock cover over the Kelvin North Limb impede groundwater flow and redox gradient vertical transport.

2.5.2 Landscape Evolution Model

Figure 2.41 schematically displays the evolution of the landscape since the LGM. First, west-flowing glacial ice deposited a basal diamict till blanket and largely overprinted landforms of previous west-southwest ice directions while forming a ribbon-shaped dispersal plume. With continued deglaciation, ice flow briefly shifted to the north-northwest evidenced by rare striae to the east of the study area. The formation of the second northwest-trending dispersal plume reworked the existing till blanket and east-west dispersal plume. Presumably, this ice flow was not sustained and topographically controlled as most glacial landforms and KIM trains in the KFC trend westward. After glacial retreat, shallow lakes and bogs formed in topographic lows partially concealing the dispersal plumes. Cryoturbation in the form of frost boils formed across the landscape after deglaciation by permafrost-related frost heaving - intensifying in thick, fresh till. Seasonal drainage since deglaciation may erode the till host and form bogs in areas of seasonal

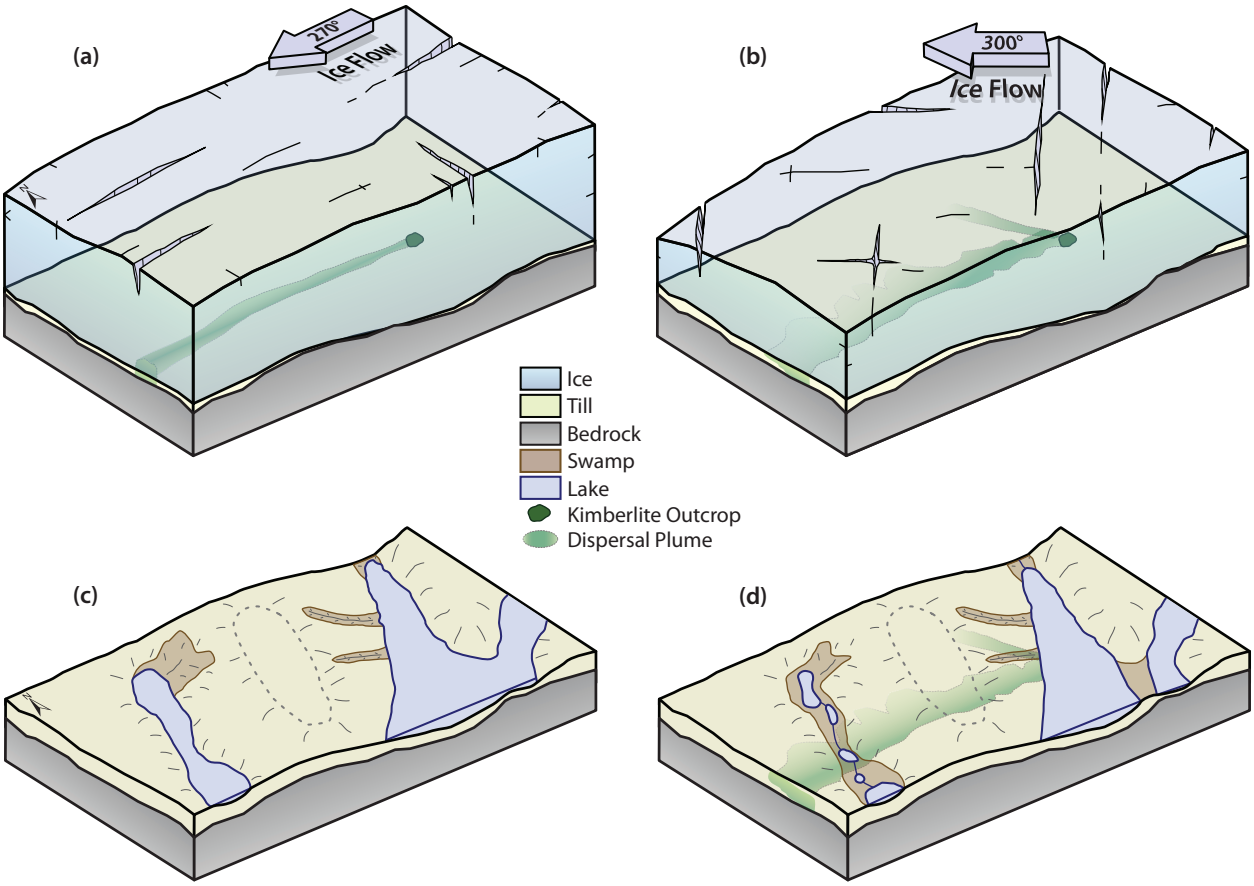

Figure 2.41: **(a)** Sustained ice flow of the Laurentide Ice Sheet during the last glacial maximum towards the west eroding bedrock and entraining kimberlite material into ice and till, depositing it as basal till forming ribbon-shaped dispersal plume. **(b)** Due to warming bed conditions and topographic deflection, ice flow shifts towards the northwest partially eroding bedrock and outcropping kimberlite, depositing basal till, and reshaping first dispersal train into a palimpsest-type pattern. **(c)** After glacial retreat lakes and localized swamps form in areas of drainage into - and between - lakes and ponds. **(d)** Current landscape due to partial lake drainage and bog formation. Surface projection of expected dispersal trains shown.

inundation and drainage between lakes and ponds.

2.5.3 Exploration Implications

This research tests and refines till sampling practices that can be employed to geochemically detect kimberlites through transported cover. The benefit to this method lies in its cost-effective sampling and analytical procedures allowing the method to be applied in large scale programs testing multiple - possibly dozens - of targets. Numerous targets are often identified by airborne geophysical surveys in prospective areas previously delineated by regional KIM sampling. Deposit scale till sampling allows the opportunity to discriminate false positive targets while prioritizing others prior to drilling, and the expenditures associated with implementing a till sampling campaign is a fraction of that required for an exploratory drill hole. Based on research conducted at the Kelvin kimberlite, the following recommendations are made for executing a till sampling survey.

2.5.3.1 Sampling Procedure

Surficial material maps are necessary to design sampling surveys and in interpreting geochemical signatures. A recent increase in published regional surficial material maps, till suitability maps, regional deglaciation literature, and bedrock geology maps by the NTGS has greatly benefited exploration in the north and should be used as a principle resource when designing sampling surveys. Basal till is the ideal sample material as it represents a first derivative of bedrock without significant post-depositional influences. Shallow till samples extracted from the upper portion of the B horizon represents the most convenient geologic samples bypassing the need for exposing fresh C horizon which may require trenching, augering, or be impeded by shallow permafrost. Soil formation processes and weathering imparts inherent complexities to soils, particularly in moderately weathered terranes (Anand et al., 2016; Bodnar, 2017; Cameron et al., 2004; Mann et al., 2005). Sampling the center of frost boils is an acceptable medium and, where chemical weathering is weak, can be directly compared to B horizon soil data. Frost boil samples are often an indication of unworked basal till (Knight, 2017; Sharpe et al., 2013) and provide a third dimension to interpreting and projecting dispersal plume morphologies.

Surveys should be designed to detect clastic dispersion from a point source that can be deduced from geophysical data. It is important to consider the orientation or dip of geophysical anomalies, and where they expect to subcrop from bedrock. Bedrock topography may cause ice flow deflections and preservation of relict till populations preserving early dispersal directions that lack expression on the surface (Kelley et al., 2019). Dispersal plumes in shallow basal till have been shown to reach the surface close to their source. In thick till anomalies may not surface for several hundreds of meters in the down ice direction (McClenaghan and Paulen, 2018). Ribbon-shaped dispersal plumes tend to be as wide as their bedrock source; therefore, effective sampling spacing must be inferred from the geophysical target. Elongate or linear bedrock sources perpendicular to ice flow tend to produce short and wide dispersal patterns (e.g., Snap Lake kimberlite dyke; McClenaghan and Kjarsgaard, 2007).

Relatively small B horizon soil samples are required compared to traditional KIM sampling. One kilogram of material pre-screened in the field to -6.3 mm is sufficient for geochemical analyses and more material may be collected for archival. The upper B horizon should be consistently sampled to minimize intra-survey variation in sample material.

2.5.3.2 Analytical Procedure

Results support the application of strong or complete digestions to extract resistant kimberlite silicates and oxides despite increased noise due to digestion of the till substrate (McClenaghan and Kjarsgaard, 2007). Aqua regia may also be effective; however, where dispersal plumes are subtle partial digestions may result in unacceptable data quality for poorly recovered elements such as Nb, Ta, Ti, and REE. This research validates the -180 µm fraction for complete digestion and analysis. Results at Kelvin prove indicator minerals are geochemically detectable in the sand fraction and may provide important exploration context, therefore coarser fractions should not be discounted. Additional research is necessary before objectively recommending the -180 µm fraction over the -63 µm fraction. The decision is at the discretion of the

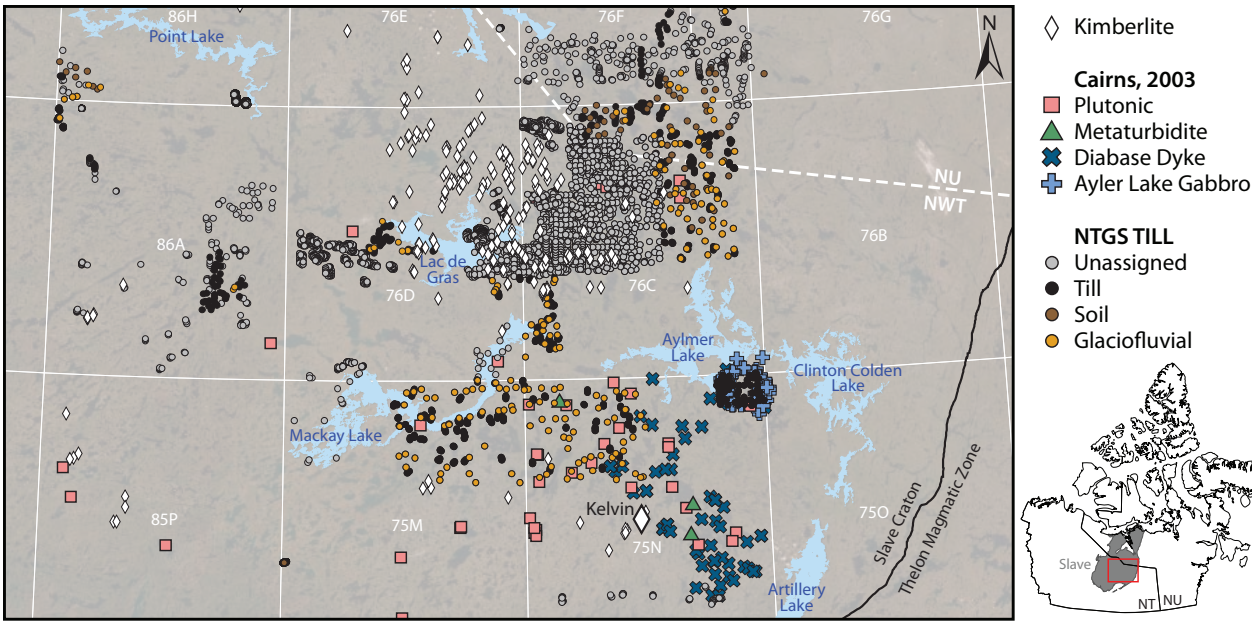

Figure 2.42: Map of publicly available till geochemistry data from NTGS TILL Database in the central Slave province. Cairns et al. (2003) geochemistry dataset shown including plutonic and metaturbidite rocks, Aylmer Lake Volcanic Belt gabbros, and diabase dykes.

exploration geologist. Organic carbon rich samples should be avoided as sequential extraction and C_{org} data demonstrates the metal cation exchange capacities of organic acids. These effects can be mitigated during the sampling process or by analyzing for total organic carbon.

2.5.3.3 Data Interpretation

Multi-element interrogation of the dataset will more effectively distinguish anomalies related to kimberlites from background, natural variation, and false positives. The use of probability plots and/or histograms is recommended to distinguish background and anomalous populations within datasets. Regional background geochemistry can be extracted from publicly available till and soil geochemistry datasets available from the NTGS TILL database. Data density is highest in the Lac de Gras region and sparse in the southeast Slave province near the KFC (Figure 2.42). These sources may prove useful in defining background and up-ice pathfinder concentrations.

Bedrock and surficial features may produce false targets in geophysical datasets including, but not limited to, thick cover in bedrock recessions; conductive or thick lake sediments; alteration or gouge infill at intersections of structures; and small intrusive granites or diabases with possible alteration (Power et al., 2004). In general, hypabyssal kimberlite shows less physical contrast to country rocks generating less concise resistivity, gravity, and seismic responses than diatreme and crater facies (Power and Hildes, 2007). Diabase dykes and volcanic belts (e.g., Aylmer Lake Volcanic Belt) may impart mafic signatures into till, and are distinguishable from kimberlite by their lack of enrichment in incompatible elements. Incompatible elements may be ineffective in granitic terranes and when distinguishing against carbonatites. In such cases, first-series transition metals will highlight the ultramafic signature of kimberlites. An additional potential

application of till geochemistry is correlating matrix geochemistry to indicator mineral counts to pre-screen and prioritize till samples for indicator mineral picking and analyses (McClenaghan et al., 2004).

2.6 Conclusions

A common disadvantage of using B horizon soils in till geochemistry is the distortion of bulk geochemistry by soil processes. However, due to the immature soils, podzolic illuviation has not occurred and soils are directly compared to fresh till from frost boils. The soils are shown to be geochemically similar to fresh till, and therefore retain significant correlation to bedrock provenance. Interpretation of geochemical data should account for metal illuviation in oxidized till, particularly in more chemically weathered terranes. Sampling methods should target basal till minimizing the variation in surficial material so geochemical variance can be better interpreted.

Physicochemical properties of the soil including pH, ORP, C_{org}, and TDS provide insight to the solubility and mobility of metals in the B horizon soils, however, they do not detect reducing or alkaline signatures formed by the inclined kimberlite concealed by bedrock and thin cover. Four acid and aqua regia ICP-MS define a palimpsest dispersal pattern following the most recent ice directions despite the absence of a traditional KIM train detected at Kelvin. Although aqua regia results display less noise in the survey, four acid is preferred in order to digest resistant oxide and silicate kimberlite minerals that have resisted chemical and physical weathering. The pathfinder elements extracted by four acid digestion that effectively detect clastic signatures from the kimberlite include Ba, Cr, Fe, Mg, Mn, Nb, Ni, Ta, Ti, and Zn. Applicable pathfinder elements are expected to vary with changes is country rock and the potential anomaly source. Geochemical evidence of kimberlite indicator minerals are detected in the fine to very fine sand fractions of anomalous samples. The fine silt and clay fractions host the majority of bulk trace element geochemistry and as a result, grain size distribution plays a significant role. Analysis of the -180 µm fraction exhibits the highest anomalous to background contrast and requires further investigation on additional datasets.

Although commercial whole rock/soil Pb isotope analysis by Q-ICP-MS represents a time- and cost-effective supplemental analysis for VMS and uranium exploration, it's application is not recommended for kimberlite exploration because present day isotopic kimberlite signatures do not contrast Slave province country rocks.

Soil hydrocarbon responses by ActLab's SGH method coincide with the location of the kimberlite; however, relationships between hydrocarbons and inorganic geochemistry were not able to be explored. For the first time, SGH interpretations detect dispersal trains that coincide with known ice directions. These results suggest hydrocarbon responses developed around *in situ* kimberlite can be mechanically transported with till, or kimberlite material entrained in till may develop post-depositional hydrocarbon responses.

Interpretation of the spatial distribution of anomalies should account for bedrock topography, till thickness, relationship between ice flows, and post-deposition reworking. Regional surficial datasets should aid in survey design and interpretation.

The presented sampling methods employ the existing protocols used by current drift exploration practices in northern Canada while making use of cost-effective commercial geochemical analyses. The methods are most efficient when testing upwards of dozens of targets delineated by geophysics. Its successful application will distinguish kimberlite anomalies from false positives, thus prioritizing targets for subsequent drilling while eliminating others.

Chapter 3

Bedrock Mineralogy and Lithogeochemistry

Lithogeochemistry and hyperspectral imaging of metaturbidite country-rock core was undertaken at the Kelvin kimberlite to attempt to identify and quantify alteration in the host rock surrounding the kimberlite pipe. KDI and MPDI supplied 72 approximately 20 cm long samples of HQ drill core totalling 13.7 meters from four drill holes surrounding and intersecting the Kelvin kimberlite outside of the sample area. Samples are spaced in approximately 10 m intervals along the length of the core, and include samples adjacent and up to 200 m away from the kimberlite pipe; as well as proximal and up to 75 m from the hypabyssal sheet. Core samples were analyzed by a series of inorganic commercial geochemical analyses and imaged by hyperspectral scanning. Results and discussions are presented in this chapter, prefaced by a technical background review and rationale.

The research presented in this chapter was undertaken to detect geochemical and mineralogical alteration signatures in the country-rock that can be confidently attributed to the emplacement or post-emplacement processes of the Kelvin kimberlite using traditional whole rock analyses available at most commercial laboratories. Although exploring for kimberlites using traditional country-rock alteration vectoring techniques is uncommon, if not absent, barren drill core is a common by-product of drilling campaigns testing targets defined by geophysical surveys. Therefore, identifying and describing country-rock alteration in drill core may aid in detecting the signatures of a nearby missed kimberlite.

3.1 Introduction

Emplacement of Kimberley-type pyroclastic kimberlites involves preconditioning of the country-rock by brecciation, alteration, and net-veining by ascending volatile-rich magmas prior to pipe expansion if the surface is breached (Clement, 1982). Once the surface is breached, brecciated and altered country-rock is commonly excavated as the pipe widens through explosive degassing of magma within several hundred meters of the surface (Hetman, 2008; Sparks et al., 2006). Country-rock brecciation and chemical corrosion due to the preconditioning process can be preserved around kimberlite pipes, particularly around blind intrusions that have failed to breach the paleosurface. After pipe emplacement, cooling volcaniclastic deposits

interact with meteoric water resulting in hydrothermal metamorphism and low temperature kimberlite alteration dominated by serpentinization (Sparks et al., 2006). Of Canadian kimberlites, the varying external and internal geometry of kimberlite bodies depends on emplacement mechanisms, which in turn are controlled by the depth of emplacement, country-rock geology, and sequence of volcanic events.

3.1.1 Kimberlite - Country-Rock Alteration

Few studies document, in detail, the degree of alteration in country-rocks surrounding kimberlites. Of the well documented cases, metasomatic exchanges along the kimberlite margins have been facilitated by the geochemical contrast between kimberlite and silicic country-rocks (e.g. gneiss and granitoid). The spatial relationship to the kimberlite facies (e.g. hypabyssal, pyroclastic) also produced markedly different styles of alteration.

The degree of country-rock alteration appears to be related to the time exposed to an ascending kimberlite magma. Kimberlite dyke ($\sim$1 m thick) propagation speeds have been estimated between $<$4 m/s and 20 m/s (Sparks et al., 2006). At these time scales, significant alteration of the country-rock is expected to be minimal unless there is episodic magma ascent. It has also been proposed that groundwater can be heated by stalled magmas and produce hydrothermal chemical corrosion (Brown et al., 2007). Longer residence times of hypabyssal magmas at the Snap Lake kimberlite produced metasomatic reactions between the kimberlite and granitoid country-rock that appeared more complex than simply assimilating granitoid xenoliths into kimberlite magma in varying degrees. Geochemical gradients between the kimberlite and felsic granitoid country-rock produced meter-scale metasomatic transport of Al from the granitoid to the kimberlite, as well as Mg and Fe flux from the kimberlite into the granitoid country-rock (Fulop et al., 2018). As a result, granitoid feldspars were replaced by serpentine, chlorite, and carbonate while biotite was increasingly chloritized. Due to their increased high-temperature mobility, Ca, K, and Na recorded evidence of more distal metasomatic transport. In both the kimberlite and granitoid, Ca and K were introduced whereas Na was removed resulting in phlogopite, carbonates, sericite, and apatite precipitation as well as feldspar replacement by serpentine and carbonate in granitoid rocks (Fulop et al., 2018).

Chemical alteration of country-rocks have been briefly documented at the Gahcho Kué cluster, and were best developed surrounding hypabyssal units and associated with an enrichment in CO_2, H_2O, MgO, FeO, MnO, CaO, K_2O, and REEs. Quartz leaching resulted in bleached and fractured/pitted granitoid country-rock and was intensified along joint surfaces up to tens of meters from the pipe contacts at the Gahcho Kué cluster (Hetman et al., 2004). Silica leaching of granitic country-rock was also observed surrounding the diatreme facies K2 kimberlite extending laterally up to 50 m from the pipe contacts (Harder et al., 2013).

Country-rock brecciation and fracturing has been documented surrounding several volcaniclastic-dominated kimberlite pipes at the Renard cluster of Québec (Gaudet et al., 2018; Muntener and Gaudet, 2018; Muntener and Scott Smith, 2013). Country-rock breccia (CRB) and cracked/fractured country-rock (CCR) units were observed in gneiss and granitoid country-rocks surrounding the Renard 2, Renard 3, and Renard 65 kimberlites. CRB zones were characterized as marginal, discontinuous zones of clast-supported country-rock fragments in a dominantly kimberlite-derived matrix (up to a total of 5% kimberlite-derived

material). A larger halo of cracked country-rock (CCR) was characterized as <1 mm thick fractures at meter-scale intervals infilled w ith p ulverized c ountry-rock f ragments c emented w ith kimberlite-derived carbonate, serpentine, and rarely olivine grains (Muntener and Gaudet, 2018; Muntener and Scott Smith, 2013). The cracked country-rock halo was believed to represent the remnants of the initial stage of pipe formation along a volcanic feeder and was cross-cut by the later country-rock breccia (CRB) contemporaneous with the emplacement of the first phase of tuffistic kimberlite (Muntener and Scott Smith, 2013).

Smith et al. (2004) documented extensive, pervasive, metasomatism at the Murowa and Sese pipes, Zimbabwe, penetrating up to 100 m into granitoid country-rock. The distal fingerprint was characterized by green staining from chlorite, needles of alkaline amphibole (winchite, riebeckite, arfvedsonite), and pyroxene (aegerine - augite). Proximal alteration was analogous to fenitization associated with carbonatite emplacement. Quartz was leached and/or replaced by carbonate while amphibole and pyroxene replaced biotite resulting in a syenitic composition. Potassium feldspar remained unaltered whereas plagioclase was commonly dusted by Fe-oxides or replaced by sericite. Extensive carbonate and amphibole - pyroxene veins penetrated the country-rock adjacent to the pyroclastic pipes resembling a crackle or mosaic breccia texture. Altered granite country-rock contained elevated Mg, Cr, Ni, CO_2, H_2O, Ca, Mn, Nb, Sr, P, Na_2O/K_2O, and markedly lower SiO_2, Al_2O_3, Ga, and Y (Smith et al., 2004).

Blind kimberlites that have not breached the paleosurface often preserve preconditioning and brecciation of the overlying country-rock observable. Above a blind hypabyssal lobe of the 5034 kimberlite (Gahcho Kué), at least 50 m of overlying country-rock has been altered and disaggregated by the exsolution of volatiles (Hetman et al., 2004). Similar textures were observed at the blind K08 pipe (Venetia kimberlite, South Africa) where country rock was undercut by upward-propogating breccias forming collapse breccia textures. Late stage hypabyssal kimberlite dykes intruded these country-rock breccias and formed meter-wide, serpentine-rich, alteration zones along the dyke contacts (Barnett et al., 2011).

3.1.2 Country-Rock Alteration at the Kelvin Kimberlite

At the Kelvin kimberlite, no evidence of texturally destructive chemical alteration or thermochemical spalling of country-rock has been observed (Barnett et al., 2018). However, it is presumed that these processes likely contributed to the formation of the pipe, particularly its vertical ellipsoidal elongation, and were subsequently excavated during pipe formation. North-south trending, steeply dipping bedding and foliation (Figure 3.1c) possibly contributed to the vertical elongation of Kelvin's North Limb. Jig-saw breccias are particularly well preserved along the upper hanging wall contact of the pipe indicative of explosive fragmentation (Section 1.5.4). With a subterranean blind emplacement model, volatiles released are presumed to leak into country-rock breccias resulting in alteration above the pipe (Barnett et al., 2018).

Cryptic hydration halos in the country-rock surrounding the Kelvin and Faraday kimberlites have been detected by a previous study using short wavelength infrared (SWIR) analysis of drill core. Tappert and Tappert (2018) measured the abundance of adsorbed water which produced reflectance spectra in the 1300 to 2000 nm wavelength. Water molecules are adsorbed to mineral surfaced by weak hydrogen bonds or van de Waals forces. Adsorbed water was distinguished from structurally-bound water and was therefore

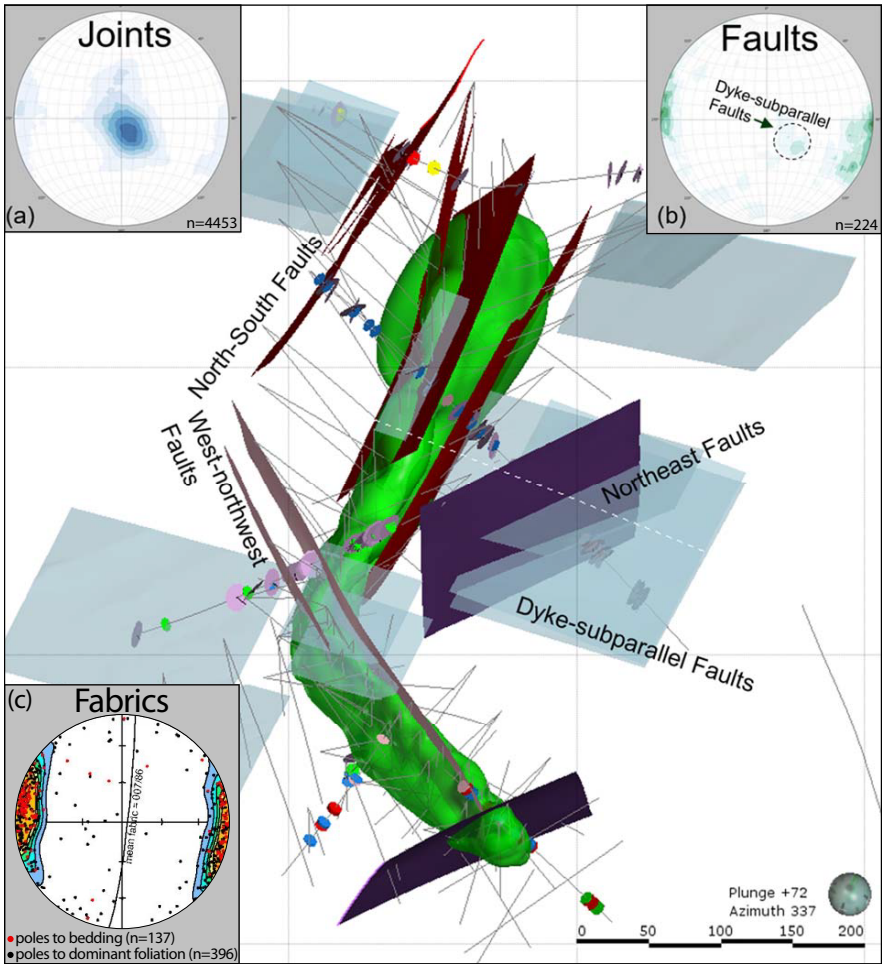

Figure 3.1: Three dimensions interpretation of fault and joint sets around the Kelvin pipe (green) from oriented drill hole intersections. Three fault sets are delineated: 1) north-south to northeast-southwest striking dextral shearing of foliation parallel to sedimentary layering; 2) minor west-northwest faults; and 3) shallow dipping faults and joints subparallel to the hypabyssal dyke system. Fault set 1 and 2 are interpreted to have formed prior to kimberlite emplacement, whereas dyke-subparallel faults and joints are interpreted to be related to inflation from dyke emplacement. From Barnett et al. (2018) electronic supplementary material. Fabrics inset **(c)** shows poles to bedding (red) and dominant foliation (black) from Stubley (2015).

less influenced by mineralogy and the abundance of hydrous minerals (e.g. micas and clay minerals). The development and abundance of these adsorption features appeared to identify cryptic hydration halos and were able to be used to vector towards the kimberlites. The study utilized a portable point (1 $\times$ 1 cm) SWIR spectrometer to analyze continuous drill core at a 30 - 75 cm spacing (Tappert and Tappert, 2018). Hydration halos at the Kelvin and A418 (Diavik) kimberlites were detected up to 65 m away from the kimberlite (Figure 3.2). At several larger Slave kimberlites (Tuzo, Snap Lake), a thin dehydration halo is observed in the country-rocks within 3 meters of kimberlite contacts suggesting a the country-rock was dehydrated by high temperature kimberlite magmas (Tappert and Tappert, 2018). However, a thin dehydration halo was not observed at Kelvin, likely due to the increased sample spacing by (Tappert and Tappert, 2018). The study by Tappert and Tappert (2018) analyzed and detected elevated hydration values in four drill holes

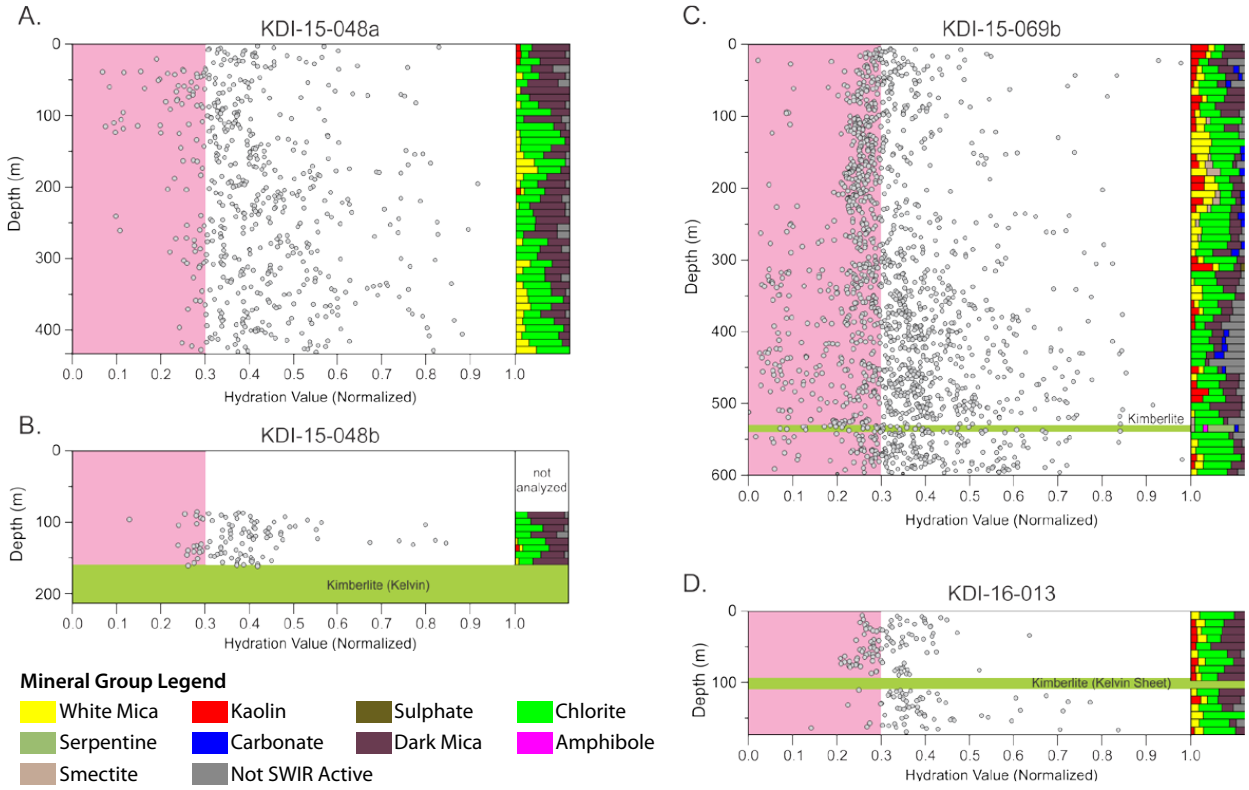

Figure 3.2: Hydration values versus drill core depth from four drill holes surrounding the Kelvin kimberlite. Hydration value calculated by proprietary methods from point hyperspectral analysis by Hyperspectral Intelligence Inc. Higher hydration values indicate increased abundance of adsorbed water; values less than 3.0 represent samples with little to no hydration. Bar diagrams represent qualitative abundance of the dominant mineral from 10 m interval averages. From Tappert and Tappert (2018).

surrounding the Kelvin kimberlite including KDI-15-048a, KDI-15-048b, KDI-15-069b, and KDI-016-013. The research presented in this thesis analysis the same four drill holes.

Novel results from Tappert and Tappert (2018) indicate the geometry of hydration haloes surrounding kimberlites from the Slave province are variable and related to pipe size, pipe shape, and country rock composition. Hydration halos were detected in silicate host rocks and in carbonate rocks, and it was noted that small-scale compositional heterogeneities did not have a large effect on the hydration values. Haloes observed in carbonate host rocks were smaller than those in silicate host rocks, but was primarily attributed to the decreased permeability of the carbonate rocks. They observed extensive hydration directly above the shallowly-dipping Kelvin and Faraday 2 pipes compared to lateral country-rock hydration values. Additionally, hydration halos surrounding kimberlite pipes are better developed compared to hypabyssal dykes presumably because kimberlite derived fluids and volatiles are incorporated into primary hydrous minerals and carbonate, and otherwise devolatilized during pyroclastic emplacement (Tappert and Tappert, 2018). The preservation and detection of hydration values are sensitive to metamorphic history and decreasing pressure or increasing temperature. At ambient pressures, heating to temperatures of 110°C has been shown to remove adsorbed water from mineral surfaces (Ming et al., 2007).

3.2 Methodologies

Quartered HQ core was delivered to ALS Minerals, North Vancouver for geochemical analyses and to Corescan, Denver for hyperspectral scanning. Samples provided by KDI and MPDI constituted 72 HQ core samples from four drill holes spaced approximately every 10 m along the length of the core.

3.2.1 X-Ray Diffraction

A single sample was analyzed by X-ray powder diffractometer at the Electron Microbeam and X-Ray Diffraction Facility (EMXDF) at Department of Earth, Ocean and Atmospheric Sciences (EOAS), UBC using the Bruker D8 Focus (0-20, LynxEye detector).

3.2.2 Hyperspectral

Quartered HQ core was analyzed by hyperspectral imaging by Corescan, Denver. Imaging included core photography at 50 µm resolution and spectral imagery at 500 µm resolution. Using the visible near infrared and short wave infrared ranges of the electromagnetic spectrum, Corescan is able to identify minerals based on diagnostic electronic and vibrational absorption features dictated by the mineral formulae and chemical bonds. Identifiable minerals include clays, sulfates, carbonates, micas, amphiboles, iron oxides, and others. Unaltered silicates (feldspar and anhydrous silica) do not produce diagnostic vibrational absorption features in the SWIR and are indistinguishable by Corescan. These minerals are simply represented as ”Aspectral class”. However, measurable electronic absorption features (generally shorted than 1400 nm wavelength) may provide compositional information of aspectral unaltered silicates. Corescan produces two products to spatially display hyperspectral data: mineral maps and mineral class maps.

Mineral Map Images: Maps are produced to show how well the measured spectrum in each pixel fits compared to a standard library reference spectrum. This ”goodness of fit” is quantified on a scale from a lower match threshold (cold colors) to a perfect match (warmer colors). The threshold for the lower match is set by Corescan and is determined based on the quality of spectra from the project and the expected mineralogy.

Mineral Class Map: A mineral classification map allocates priorities to each mineral (color) and displays higher priority minerals (colors) rather than lower priority minerals. These priorities can be changed to create new class maps prioritizing different minerals over others (Figure 3.3). The most abundant mineral is typically the least prioritized. In addition to prioritizing/stacking minerals, absorption features can be prioritized/stacked instead.

3.2.3 Lithogeochemistry

All multi-element geochemical analyses were performed on core samples by ALS Minerals, North Vancouver. Samples were crushed to 70% less than 2mm, riffle split off 1kg, and pulverized to better than 85% passing 75 microns (ALS Code PREP-31B). The following analyses were performed on all 72 sample:

- Modified Weak Aqua Regia ICP-MS (ME-MS41W): 0.5 g aliquot is digested in a 1:1 $HCl:HNO_3$

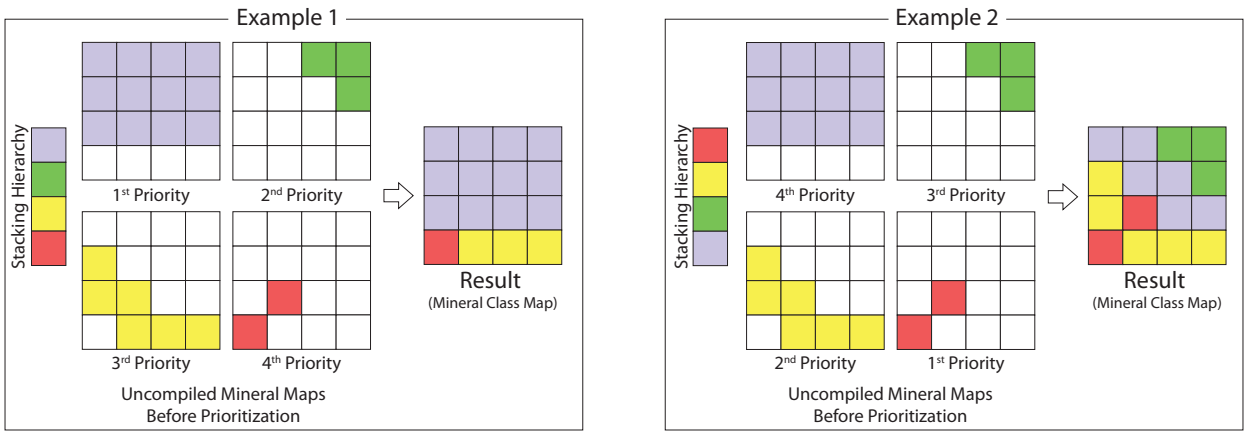

Figure 3.3: Examples of how mineral class maps are created based on different stacking hierarchy and priority of mineral classes. As multiple minerals can be identified in a single 500×500 µpixel, minerals of interest must be prioritized for visual mapping using mineral hierarchies. A mineral class map compiles all mineral maps (every mineral identified in each pixel) by prioritizing minerals for display when multiple minerals are identified in a single pixel. These hierarchies can be changed to create new class maps prioritizing minerals over others. The most abundant mineral is typically the least prioritized (example 2).

mixture and analyzed for trace elements by ICP-MS.

- Pb Isotope Add on to ME-MS41W (MS41W-PbIS): ICP-MS analysis of Pb isotope concentrations added onto weak aqua regia digestion.
- Lithium Borate Fusion ICP-MS (ME-MS81D): 0.100 g aliquot is added to lithium metaborate/lithium tetraborate flux and fused at 1020°C and subsequently digested by a HNO_3, HF and HCl solution prior to trace element and rare earth analysis by ICP-MS, and for major rock forming elements by inductively coupled plasma atomic emission spectrometry (ICP-AES).
- Pb Isotope Ratio Analysis ICP-MS (PbIS-RAT61): 0.5 g aliquot is digested with a HNO_3 and $HClO_4$ solution, HF acid, and hot HCl acid prior to Pb isotope ratio analysis by high precision Q-ICP-MS.
- Total Carbon (C-IR07): Sample is analyzed for total carbon by direct combustion and infrared absorption by Leco furnace.

3.3 Results

Thin sections and core photography of drill holes provided by SRK Consulting on behalf of MPDI provide a nearly vertical representative cross section through the South Limb of the Kelvin pipe and proximal country-rock. Ten thin sections from two diamond drill holes (KDI-HQ14-016b and KDI-HQ14-024b) passing through the Kelvin pipe were provided for petrographic investigation and were coupled with associated photos of core at Camp Kelvin.

Samples from drill holes KDI-15-048a, KDI-15-048b, KDI-15-069b, and KDI-16-013 provide the opportunity to analyze country-rock both proximal and distal to the Kelvin pipe and dyke. Drill hole 15-048b

Drill Core ID	UTM E	UTM N	Elevation	Azimuth	Dip	Length	# of Samples	Sample Interval	Target	Kimberlite Intersection
KDI-15-048a	595737.3	7041431.6	421	41.3	-49.7	433	21	202.5 - 400.8	Kelvin	-
KDI-15-048b	595736.7	7041431.0	421	188	-89.7	317	7	70.7 - 130.0	Kelvin	170.0 - 317.0
KDI-15-069b	595703.1	7041500.3	424	302.8	-81.3	598	28	302.5 - 510.4 542.5 - 591.6	Kelvin	523.6 - 532.8
KDI-16-013	595834.9	7041053.5	413	199	-51	169	16	9.9 - 87.9 110.7 - 168.9	Dyke	96.9 - 103.7
KDI-HQ14-016b	595838.0	7041069.0	412.91	312.8	-88.35	133	1*	37.16	Kelvin	37.25 - 117.90
KDI-HQ14-024b	595779.4	7041085.3	413.9	94.5	-89.66	142	9*	54.14 - 135.57	Kelvin	59.3 - 137.3

* samples include core photography and thin sections

Table 3.1: Data summary of drill hole ID, collar, survey, interval analyzed, and kimberlite intersection.

lies directly above the North Limb, whereas 15-048a dips to the northeast of the North Limb and does not intersect the kimberlite (Figure 3.4). 15-069b passes north of the North Limb, and briefly intersects the deepest modelled part of the pipe. 16-013 passes south of the South Limb and intersects the hypabyssal dyke for <7 m (Table 3.1).

3.3.1 X-Ray Diffraction

X-ray diffraction (XRD) analysis of sample 16-013 GC12 110.7 m indicates the bulk mineralogy representative of the greywacke metaturbidite 7 m from a kimberlite dyke intersection. Major rock forming minerals include quartz, plagioclase (albite), biotite, and clinochlore (Figure 3.5). Accessory amounts of calcite are detected, in addition to the possible presence of phlogopite.

3.3.2 Petrography

Fresh metaturbidite country-rock is dominated by interbedded greywacke and mudstone and metamorphosed to amphibolite facies paragneiss sequences. Metamorphic grade is high in the KFC and migmatites are occasionally observed. Primary sedimentary structures including graded bedding and bed thickness is obscured by extensive deformation and metamorphisms. However, 30 - 150 cm thick greywacke beds are commonly observed grading into overlying 1 - 50 cm thick mudstone units in the area (Cairns et al., 2003). The non-continuous nature of the core precludes the determination of relationships between sedimentary protoliths, however several sharp contacts between coarse-grained greywacke and fine-grained mudstones are observed in core at the contact at the base of psammitic beds and underlying pelitic beds (Figure 3.6a).

Greywacke in core is dark, medium-grained, and dominated by 20 - 50% quartz and 20 - 30% feldspar (plagioclase and K-feldspar). Rough, anastamosing, spaced foliation is defined by biotite (10 - 30%), muscovite (5%), and sillimanite (5 - 15%). Sillimanite occurs as both fibrolite needles and as acicular nodules parallel to foliation replacing <2 cm porphyroblasts of cordierite or andalusite (Figure 3.6d). Petrographically, biotite is variably chloritized up to 75%. Elongate muscovite may display poikilitic textures encom-

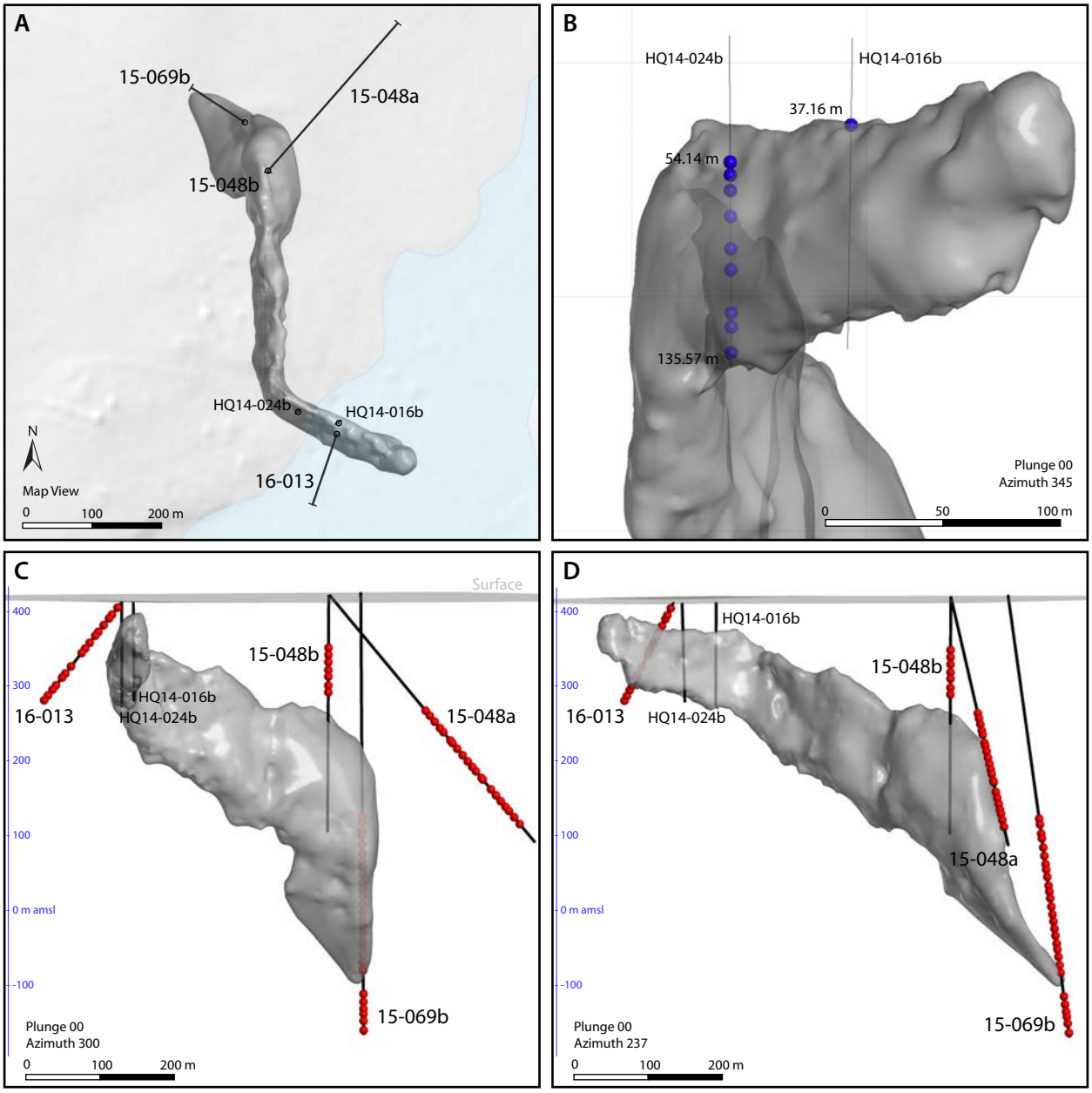

Figure 3.4: **(a)** Map view of collar and hole trace. **(b)** Kelvin pipe model and KDI-HQ14-016b and KDI-HQ14-024b drill holes provided by SRK consulting. Samples locations indicated as blue circles only include observations based on core photography and petrography. **(c,d)** Kelvin pipe model and drill hole traces. Red circles indicate samples analyzed.

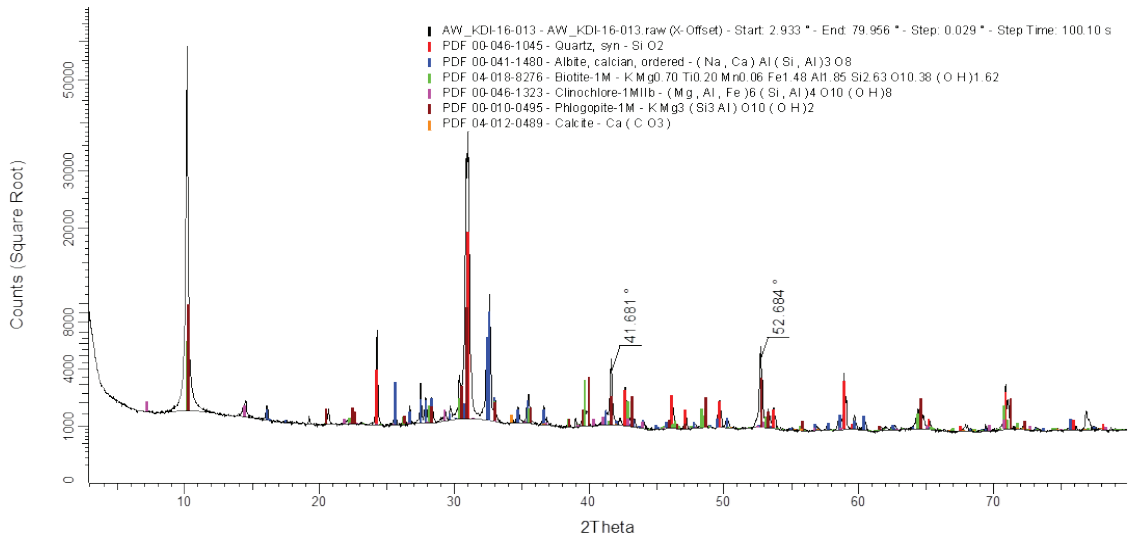

Figure 3.5: XRD pattern from 16-013 GC12 110.7m indicating the bulk mineralogy of a representative greywacke sample.

passing quartz and feldspar chadacrysts.

Mudstone in core is dark, fine grained, and dominated by equant quartz (30 - 50%) and feldspar (20 - 30%). Foliation is defined by evenly spaced euhedral biotite (15%), muscovite (5%), and accessory sillimanite (<5%; Figure 3.6c). Remnant porphyroblasts replaced by fibrous sillimanite are less common in mudstones. Biotite is variably chloritized (50 - 75%) and muscovite exhibits euhedral and poikilitic crystals.

Migmatites in core contain anatectic luecosomes of coarse equant quartz, plagioclase, and orthoclase. Leucosomes are <4 cm thick, lack foliation, and have ragged margins often selvaged by <1 cm thick restite composed of strongly foliated biotite-sillimanite±muscovite±cordierite (Figure 3.6b).

In several thin sections, quartz and plagioclase are variably replaced by sericite, often preserving relict polysynthetic twinning features (Figure 3.6e, f). Sericite alteration is documented up to 57 m away from the Kelvin pipe or dyke. Sericite abundance is discussed further in Section 3.3.3.

Drill holes HQ14-024b and HQ14-016b provide evidence of proximal (<10 m) country-rock alteration around Kelvin's South Limb and kimberlite-country-rock contacts. HQ14-016b shows the hanging wall contact between pyroclastic kimberlite (KIMB1) and country-rock breccia along the spine of the South Limb. In core photos, brecciated country-rock extends 7 m vertically above the pipe (Figure 3.7c). Within KIMB1, country-rock xenolith abundance increases with proximity to the gradational contact at 37.25 m depth.

HQ14-024b shows the contact between hypabyssal KIMB2 and metaturbidite country-rock along the lateral side of the pipe. Coherent hypabyssal kimberlite core transitions to coherent metaturbidite country-rock within two meters, however country-rock breccia extends up to 5 m from the pipe contact (Figure 3.7a). In thin section 54.14, primary Kimberley-type pyroclastic kimberlite textures including olivine macrocrysts,

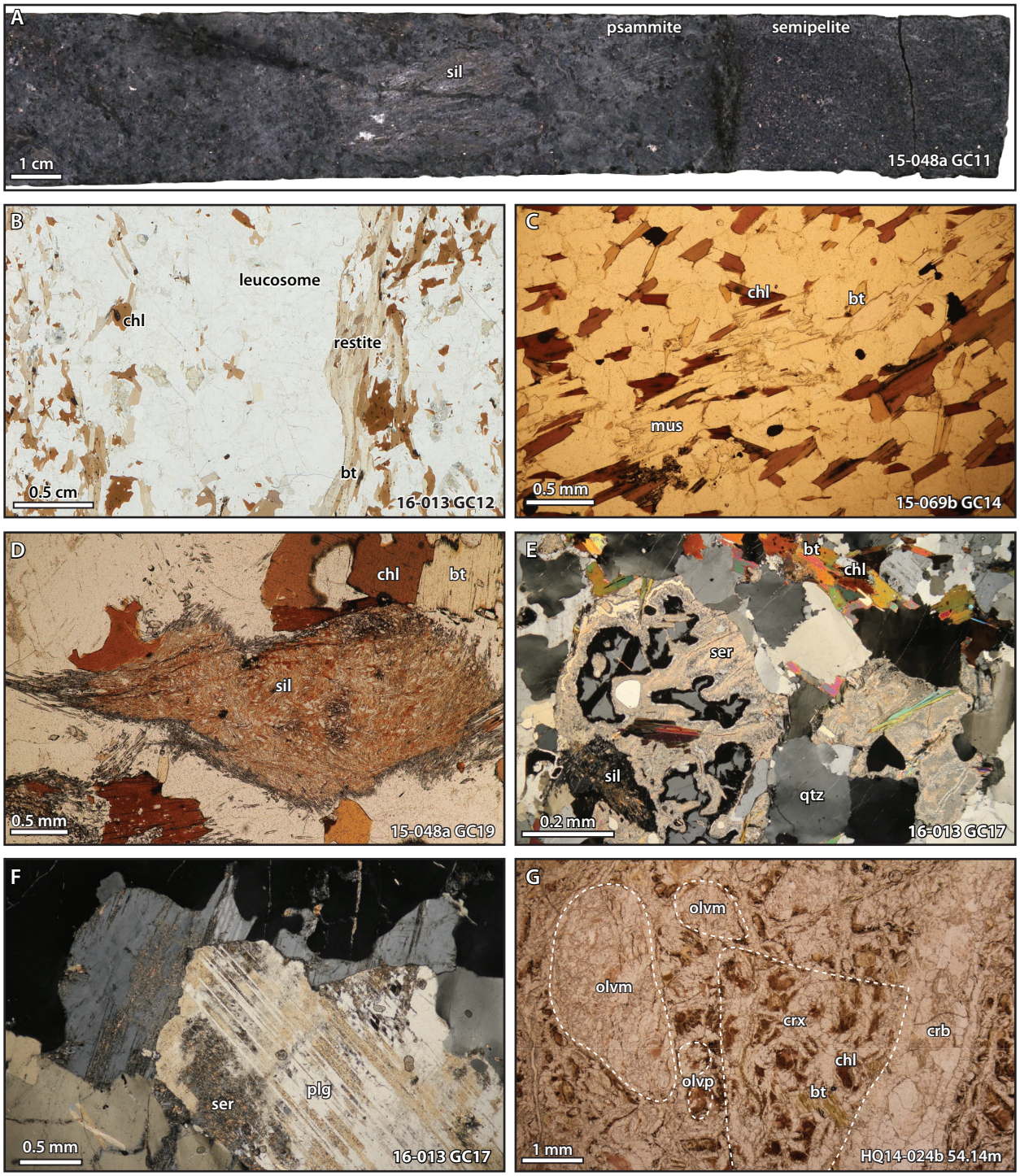

Figure 3.6: **(a)** Core image of contact between base of coarse-grained psammite and semipelite. **(b)** PPL photomicrograph of coarse-grained quartz-feldspar leucosome and biotite-sillimanite restite. **(c)** PPL photomicrograph of mudstone. **(d)** PPL photomicrograph of porphyroblast replaced by fibrous sillimanite in greywacke. **(e)** PPL photomicrograph of sericite (ser) replacing quartz (qtz) in greywacke. **(f)** PPL photomicrograph of sericite repalcing plagioclase (plg) with relic polysynthetic twinning in greywacke. **(g)** PPL photomicrograph of country-rock breccia from HQ14-024b at 54.14 m showing remnant olivine macrocrysts (olvm), phenocrysts (olvp), and country-rock clasts (crx) cross cut by late stage carbonate (crb) veining.

phenocrysts, and thin-skinned melt-bearing magmaclasts are preserved (Figure 3.6g). Country-rock xenoliths are present in thin section as relict patches of biotite and remnant feldspar textures replaced by chlorite. The sample is heavily crosscut by <0.1 - 5 mm thick carbonate veins (70%) with accessory fibrous talc.

Pipe foot wall contacts between KIMB4/7 and visually unaltered and coherent metaturbidite are gradational on a <1 m scale and may contain 0.3 m of unconsolidated altered kimberlite material, however significant country-rock brecciation is absent Figure 3.7b, d). Below the pipe foot wall, HQ14-016b intersects 2.46 m of hypabyssal kimberlite dyke (KDYKE-EXT) with sharp contacts lacking country-rock brecciation or carbonate veining (Figure 3.7d).

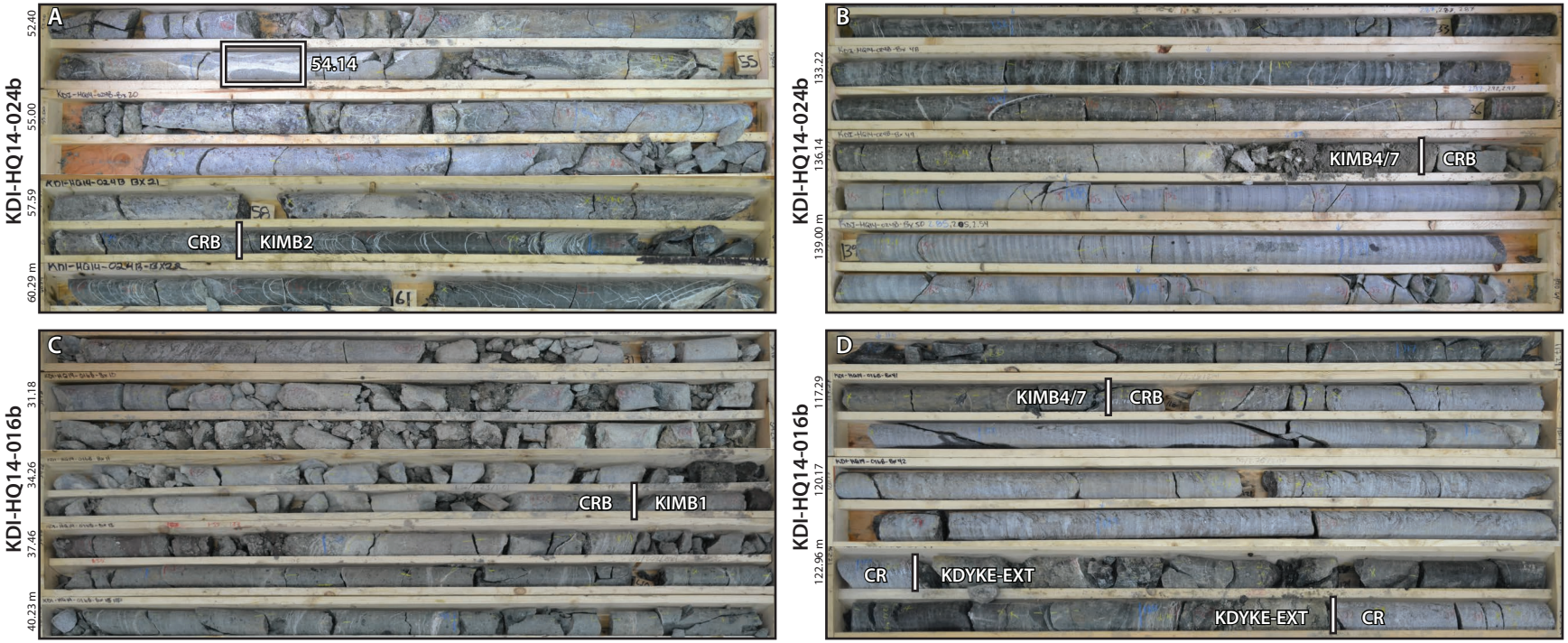

Figure 3.7: **(a)** Core photos of drill hole HQ14-024b showing pipe hanging wall contact between hypabyssal kimberlite (HK) KIMB2 and several meters of country-rock breccia (CRB). **(b)** Core photos of drill hole HQ14-024b showing pipe foot wall contact between HKt KIMB4/7 and minor country-rock breccia (CRB). **(c)** Core photos of drill hole HQ14-016b showing pipe hanging wall contact between Kimberley-type pyroclastic kimberlite (KPK) KIMB1 and minor country-rock breccia (CRB). **(d)** Core photos of drill hole HQ14-016b showing pipe foot wall contact between HKt KIMB4/7 and minor country-rockk breccia (CRB). Hole intersects hypabyssal dyke (KDYKE-EXT) for 2.46 m just below pipe foot wall contact.

3.3.2.1 Discussion

Sericite alteration replacing plagioclase in granitoid rocks surrounding kimberlites has been documented as a result of the metasomatic enrichment of K and depletion of Na in proximal country-rocks (Fulop et al., 2018; Smith et al., 2004). Metaturbidite country-rocks at Kelvin display variable sericitization and replacement of plagioclase up to 57 m from the pipe, however a direct increase in alteration intensity with proximity to the kimberlite is not distinguishable in the data. Sericite abundance will be further explored in Section 3.3.3.

Core photos from the South Limb provided by SRK identify the extent of country-rock brecciation surrounding the pipe. Country-rock breccias are dominantly observed above the upper hanging wall contact of the pipe in contact with Kimberly-type pyroclastic kimberlite units. Little to no country-rock breccia is found along the sides or base of the Kelvin pipe in accordance with observations from Bezzola et al. (2018) and Barnett et al. (2018). Country-rock breccias up to 5 m away from the pipe observed in HQ14-024b preserve remnant olivine phenocrysts overprinted by late-stage carbonate veining and evidence of volatile exsolution (Figure 3.6g). These country-rock breccias are likely attributed to the emplacement of the lateral KPK KIMB1 unit rather than the underlying hypabyssal kimberlite. Metaturbidites in contact with hypabyssal kimberlite units (KIMB2, KIMB4/7, KDYKE-EXT) exhibit little to no brecciation, indicative of its less explosive emplacement process.

3.3.3 Hyperspectral

Minerals identified by SWIR hyperspectral imaging include aspectral (anhydrous silicates), chlorite, dark mica/biotite, kaolinite, sericite, and white micas including muscovite, phengite, and paragonite. Compositional variations in white mica, chlorite, dark mica/biotite, and aspectral minerals were identified, as well as the crystallinity of sericite and kaolinite. Mineral match maps, mineral class maps, and pixels counts are provided by Corescan.

3.3.3.1 General Observations

The aspectral mineral class representing unaltered silicates including feldspars and anhydrous silica, is present in all core samples dominantly as discrete intervals or veins. In greywacke paragneisses, the aspectral class identifies felsic gneissose layering, and specifically identifies coarse grained leucosomes in migmatites. The aspectral slope, calculated as the variation in the slope between the 1050 - 2220 nm wavelength, varies within the core samples. Increased Fe^{2+} content creates broad electronic absorption bands in the visible near infrared (VNIR) resulting in increasingly positive aspectral slopes (Hunt, 1977); more positive slopes are displayed as values <1. Mudstones contain more positive aspectral slopes indicating increased Fe^{2+} content in silicates; alternatively, migmatites have more negative slopes (>1.15) indicating less Fe^{2+} content.

Dark mica/biotite is identified by the OH bond absorption feature at 1385 nm, AlFe-OH feature at 2250 nm, and Mg-OH feature at 2385 nm. Dark mica/biotite is abundant in all samples and is commonly interpreted with chlorite, sericite/white mica, and aspectral classes. In general, due to the dark color of the rocks the reflectance for most spectra are low (Figure 3.8). Additionally, preferential surface area of

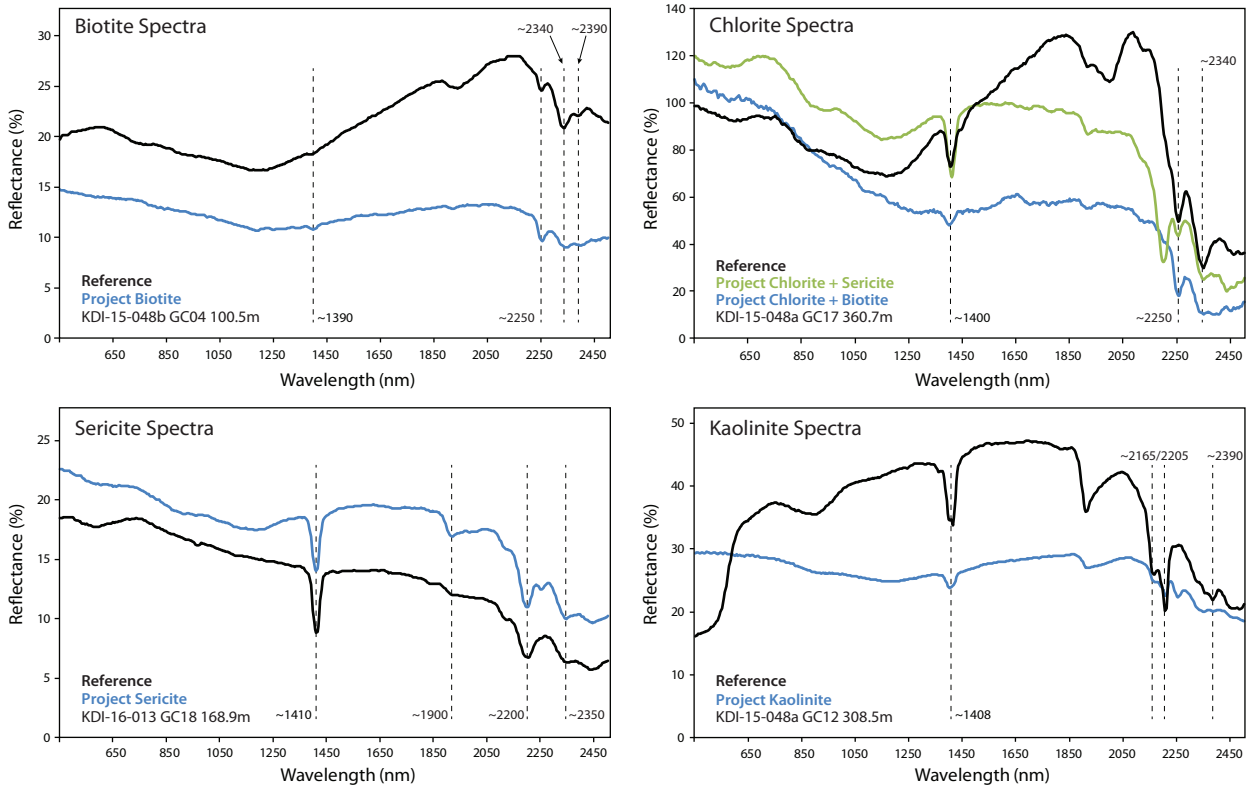

Figure 3.8: Examples of biotite, chlorite, sericite, and kaolinite spectra and notable absorption features compared with reference spectra. Spectra provided by Corescan.

phyllosilicates, particularly biotite, overestimates their abundance.

Chlorite is identified by the characteristic OH bond absorption feature at 1400 nm, AlFe-OH feature at 2250 nm, and the MgFe-OH feature at 2340 nm. Chlorite is often interpreted with dark mica/biotite and sericite/white mica. Chlorite's intimate spatial and spectral relationship with biotite indicates the abundance of chloritized biotite. Mudstones generally contain lower chlorite and chlorite/biotite content and elevated biotite abundance indicating less intense chloritization. Chlorite and biotite pixel counts are strongly inversely related (Figure 3.9a). Increased chloritization results in shorter wavelengths of the 2250 nm feature indicating more Mg-rich chlorite composition trending toward clinochlore composition (Figure 3.9b).

Sericite and white mica are recognized by three absorption features: the OH bond feature at 1400 nm and Al-OH features at 2200 nm and 2350 nm. Sericite/white mica is present in nearly all samples in variably quantities, however, it is notably scarce in mudstones. The sericite/white mica class is often interpreted with dark mica/biotite in strongly foliated gneissose bands. Sericite abundance strongly increases in felsic leucosomes where it is commonly interpreted as a mixture with the aspectral class. The sericite/white mica class displays a consistent paragonitic muscovite composition as the 2200 nm wavelength feature ranges between 2195 nm and 2208 nm. Mudstones display shorter wavelengths of the 2200 nm feature trending towards more paragonitic/muscovitic composition compared to greywackes.

Kaolinite is recognized by the OH bond absorption feature at 1408 nm, 2390 feature, and Al-OH doublet

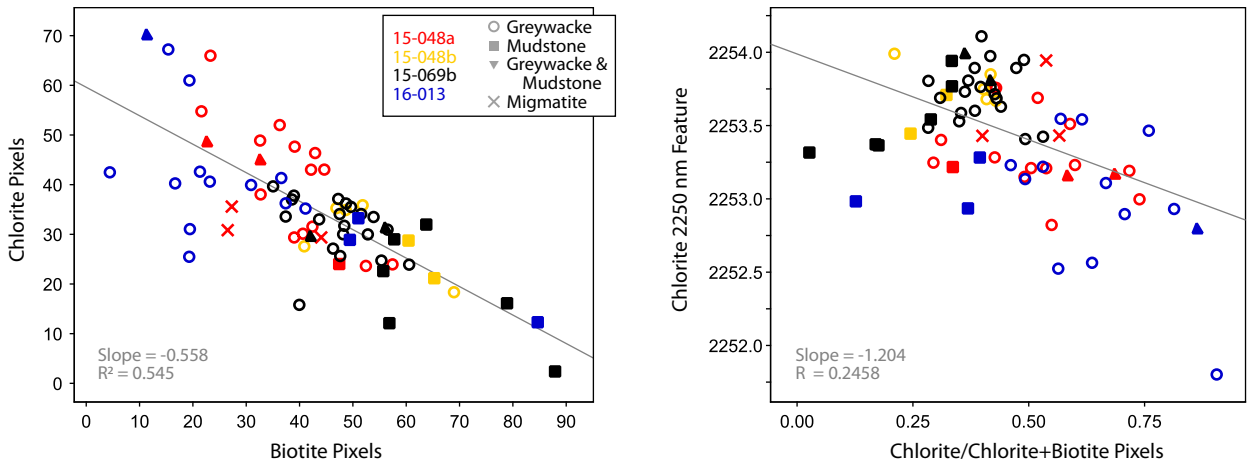

Figure 3.9: Pixel counts are normalized to total pixel count and equivalent to modal percent. **(a)** Chlorite abundance display an inverse relationship to biotite abundance. **(b)** Increasing chloritization broadly correlates to shorter wavelength 2250 nm features.

at 2165 and 2205 nm; the crystallinity is determined by the depth of the doublet feature. Kaolinite is mapped exclusively in greywacke rocks in several samples as discrete veins often mixed with white mica and/or chlorite.

Carbonate minerals are identified by absorption features at 1900 nm and 2335 nm; and compositional changes in Fe, Mg, and Mn are reflected as shifts in the 2335 nm feature. Carbonate was not detected by hyperspectral imaging in any core samples at Kelvin. In hand specimen, several discrete <1 mm thick carbonate veins are identified (16-013 GC07 58.62 m, 16-013 GC10 87.8 m, 16-013 GC17 160.8 m, 15-048a GC19 377.8 m, 15-048b GC06 121 m , 15-069b GC11 400.9 m). These carbonate veins often occupy fresh fracture surface on the ends of core samples and are obscured from overhead hyperspectral imaging.

3.3.3.2 Sericite/White Mica Composition

Shifts in the position of the 2200 nm Al-OH feature are indicative of the composition of white mica. Muscovite and paragonite are identified by shorter wavelength (2190 nm), but are indistinguishable in SWIR (Laukamp, 2011). Phengitic compositions with increased Fe^{2+} and Mg^{2+} substitution for Al^{3+} shift the feature to longer wavelengths (2220 nm). The various rock types display unique white mica compositions; mudstones trend more paragonitic whereas greywackes trend more phengitic. Normalizing the 2200 nm wavelength feature to the median of the rock type reduces lithological variation allowing for down hole comparison.

Drill holes 15-048a and 15-048b do not show any white mica compositional trends correlated with proximity to the pipe. Additionally, 16-013 displays slightly more phengitic compositions compared to other holes. 15-069b shows relatively consistent compositions, however, below the known intersection at 525 m depth two samples show a longer wavelength 2200 nm feature. Below this intersection the geometry of the pipe is unconstrained and the proximity of these samples to the pipe is unknown. These sample with more phengitic white mica compositions may represent country-rock metasomatized by kimberlite fluids.

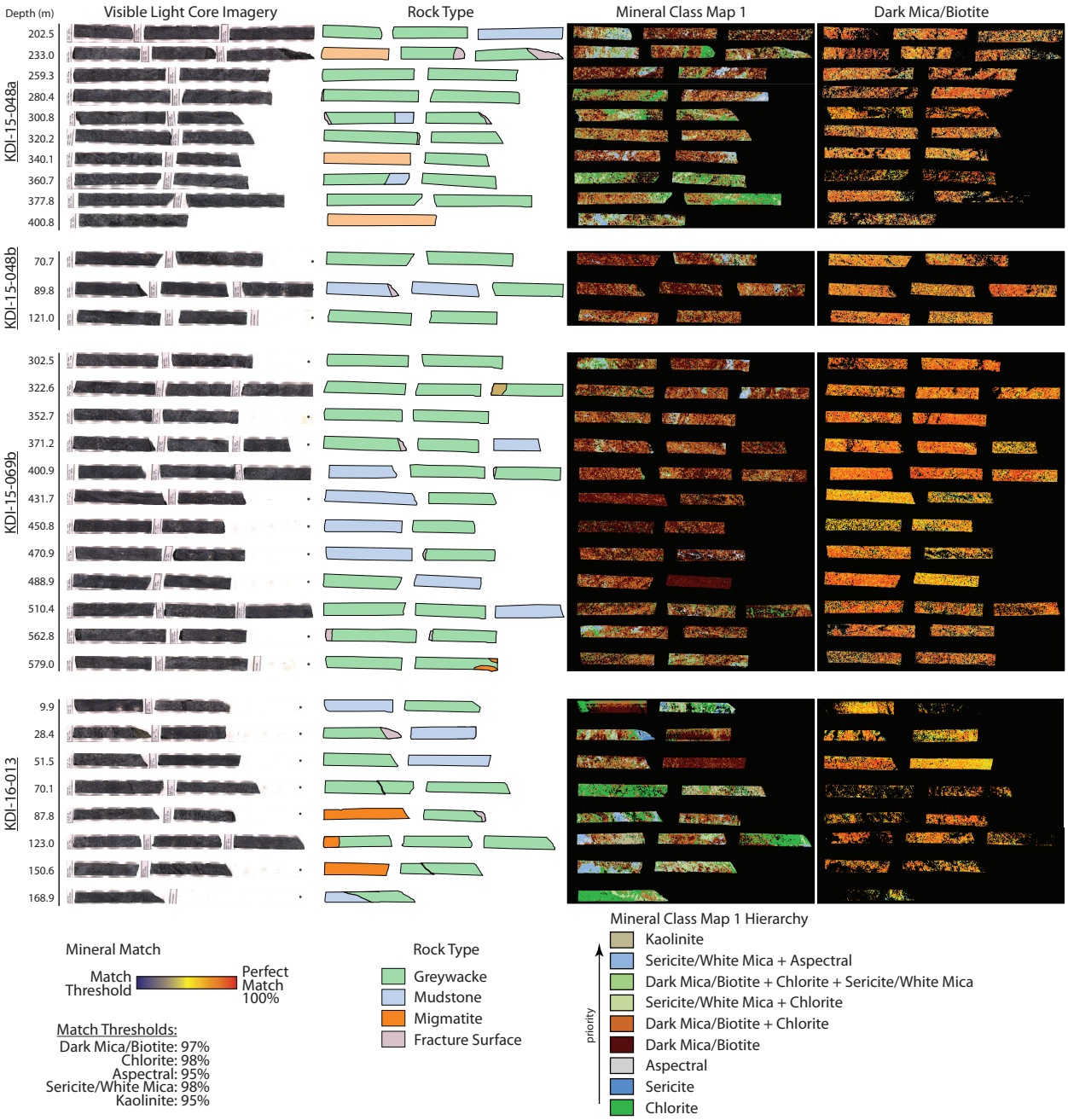

Figure 3.10: Profile through drill holes analyzed by hyperspectral imaging showing general patterns of mineral distribution using visible light core photography, rock type, mineral match maps, and Mineral Class Map. Mineral match maps include dark mica/biotite, chlorite, aspectral, sericite/white mica, and kaolinite. Mineral match maps display the quality of the measured spectrum compared to reference spectrum. The match threshold (identified by a Corescan technician) represents the lowest acceptable value returned from a comparison and is displayed in cooler colors. Warmer colors represent a more perfect match. Mineral Class Map 1 displays obvious mineral trends according to the hierarchy selected by a Corescan technician (shown in legend).

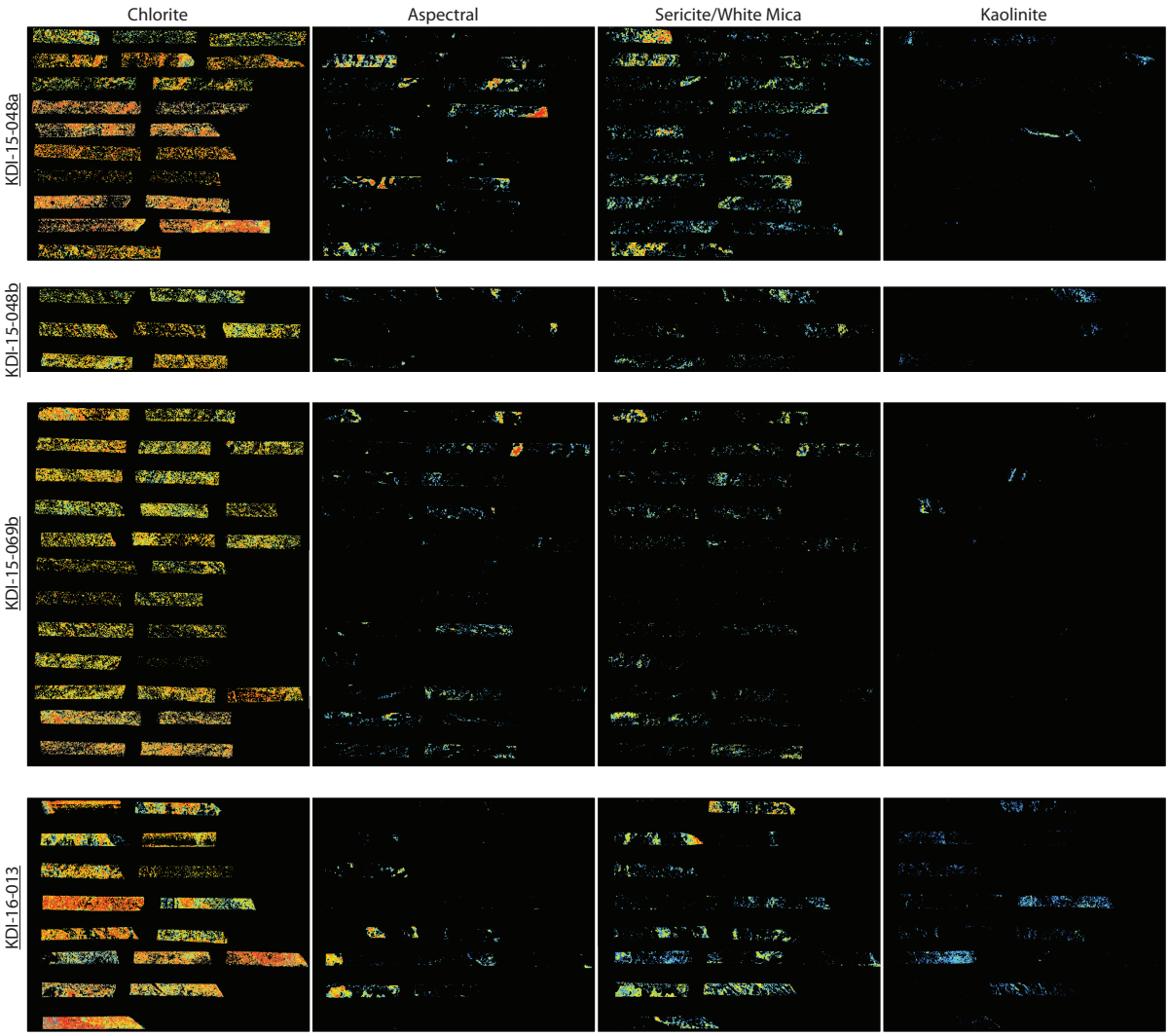

Figure 3.10: Continued. Profile through drill holes analyzed by hyperspectral imaging showing general patterns of mineral distribution using visible light core photography, rock type, mineral match maps, and Mineral Class Map. Mineral class match maps include dark mica/biotite, chlorite, aspectral minerals, sericite/white mica, and kaolinite. Mineral hierarchy for Mineral Class Map 1 shown in legend.

3.3.3.3 Chlorite Composition

Compositional shifts in chlorite between clinochlore and chamosite endmembers shift the 2250 feature from 2248 to 2261 nm, respectively (Laukamp, 2011). Additionally, the 2350 nm feature become more prominent with compositional changes in the Mg# (Mg/Mg+Fe^{2+}) (Laukamp, 2011). Chlorite composition is relatively uniform in all samples. Most 2250 nm features shift between 2252.5 nm and 2254 nm indicating an intermediate Fe-Mg composition. There are no apparent shifts in chlorite composition related to proximity to the kimberlite pipe or dyke. However, 15-048b shows a subtle increase in chlorite abundance with depth and proximity to the hanging wall contact of the North Limb (Figure 3.12).

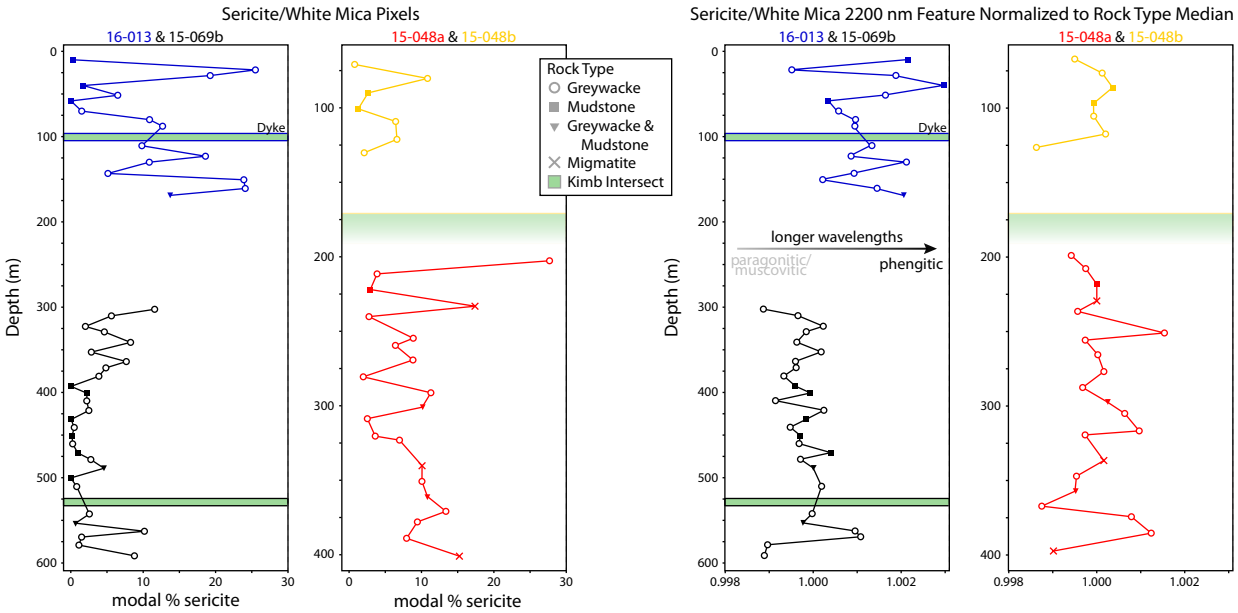

Figure 3.11: Downhole plots showing sericite pixel counts and wavelength of the white mica 2200 nm absorption feature. Sericite pixel counts are normalized to total pixels and is equivalent to sericite modal percent. The 2200 nm feature wavelength is normalized to the median wavelength per rock type. More phengitic white mica composition shifts the Al-OH feature to longer wavelengths. Drill hole 15-048a does not intersect kimberlite.

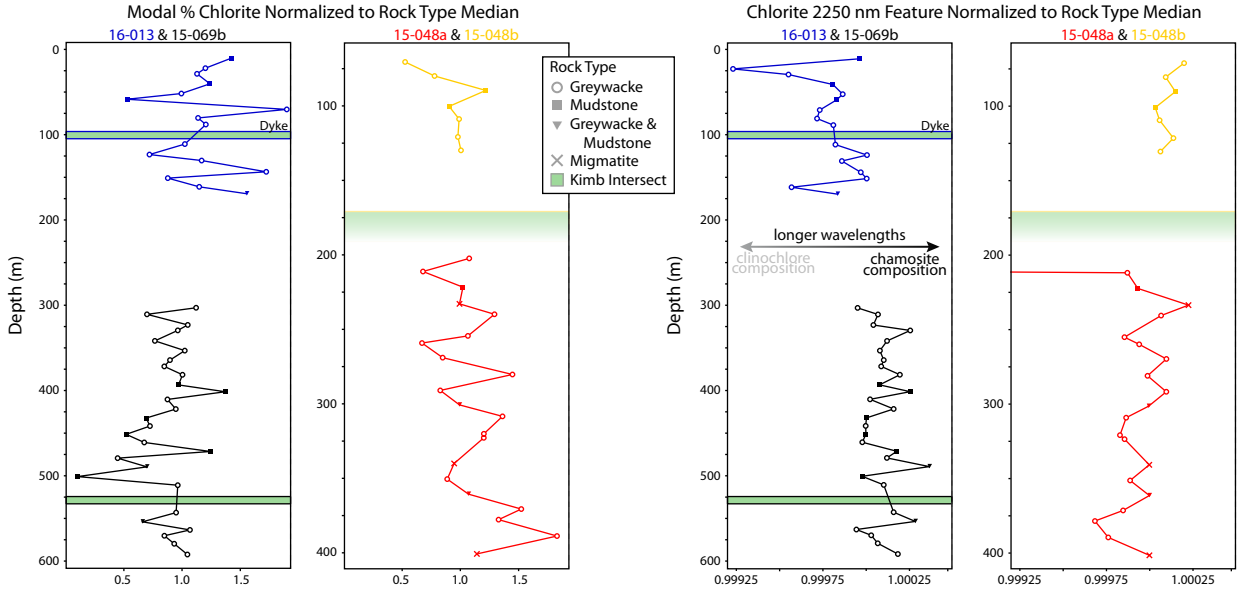

Figure 3.12: Downhole plots showing chlorite pixel counts and wavelength of the 2250 nm absorption feature. Chlorite modal percentages are normalized to rock type median to minimize lithological variation in chlorite abundance. The 2250 nm feature wavelength is normalized to the median wavelength per rock type. Shorter wavelengths indicate Mg-rich clinochlore composition; longer wavelengths indicate increased Mg-Fe-Al substitution trending towards chamosite end member composition. Drill hole 15-048a does not intersect kimberlite.

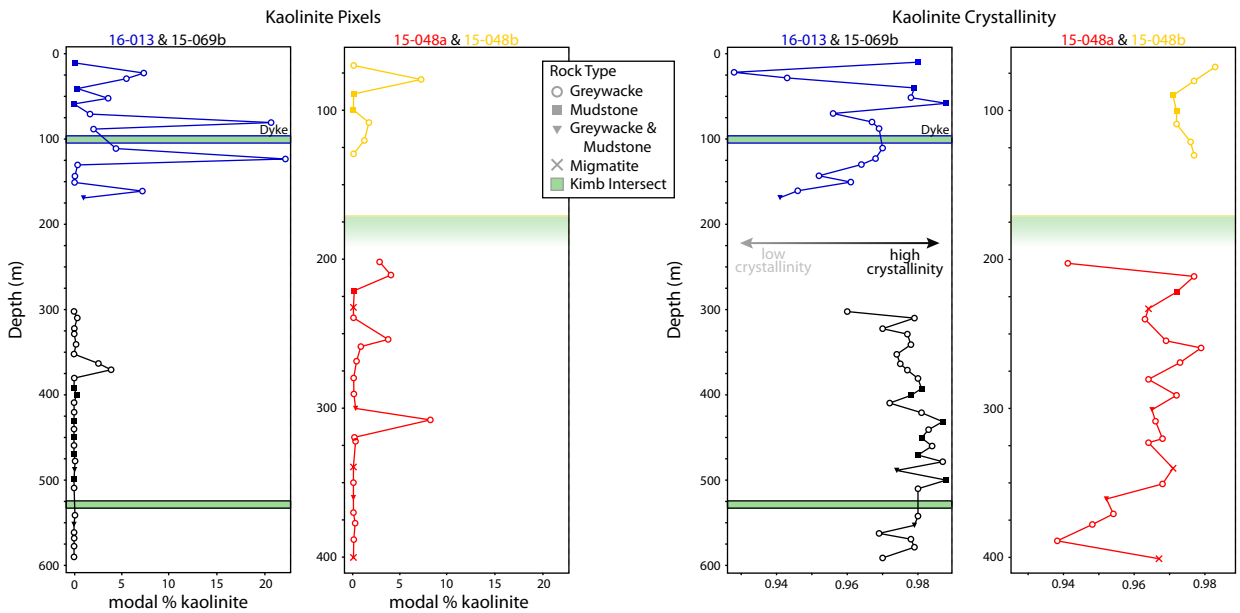

Figure 3.13: Downhole plots showing kaolinite pixel counts and crystallinity. Kaolinite pixel counts are normalized to total pixels and is equivalent to kaolinite modal percent. Kaolinite crystallinity based on the development of the 2165/2205 nm doublet absorption feature. Drill hole 15-048a does not intersect kimberlite.

3.3.3.4 Kaolinite Crystallinity

Kaolinite is not common in metaturbidite country-rock, however, it is more abundant in greywackes compared to mudstones. Mineral maps show kaolinite is present as both discrete veins cross cutting gneissose banding and on fracture surfaces (15-048a GC12 308.5m). Kaolinite is also associated with white mica and chlorite defining gneissose layering (16-013 GC17 160.8 m). Both habits of kaolinite exhibit moderately high crystallinity indices. Kaolinite crystallinity is calculated by Corescan as the ratio of the reflectance at 2184 nm to 2164 nm. Obvious trends in the pixel count and crystallinity of kaolinite are absent, however 16-013 displays anomalously elevated kaolinite pixel counts up to 20 m above and below the hypabyssal dyke (Figure 3.13). Crystallinity values in these samples above and below the dyke intersection show a trend of increasing crystallinity with proximity to the intersection, however, there is significant background variation within the drill holes.

3.3.3.5 Chlorite - Dark Mica Relationship: Ternary Image

Three spectral features are shared by chlorite and dark mica/biotite: 2250, 2350, and 2390 nm. The depth of these three features are displayed in a RBG ternary image map provided by Corescan (Figure 3.14). Color variations in the maps highlight compositional and mineralogical variations and could possibly be due to increased chloritization of biotite. The depth of the 2390 nm feature decreases with increasing Fe content; therefore red, green, and yellow shifts indicate increasing chlorite content relative to biotite. White intervals represent the development of all three features indicative of Mg-bearing biotite. The ternary diagram also identifies kaolinite due to its strongly developed 2390 nm feature displayed as blue pixels.

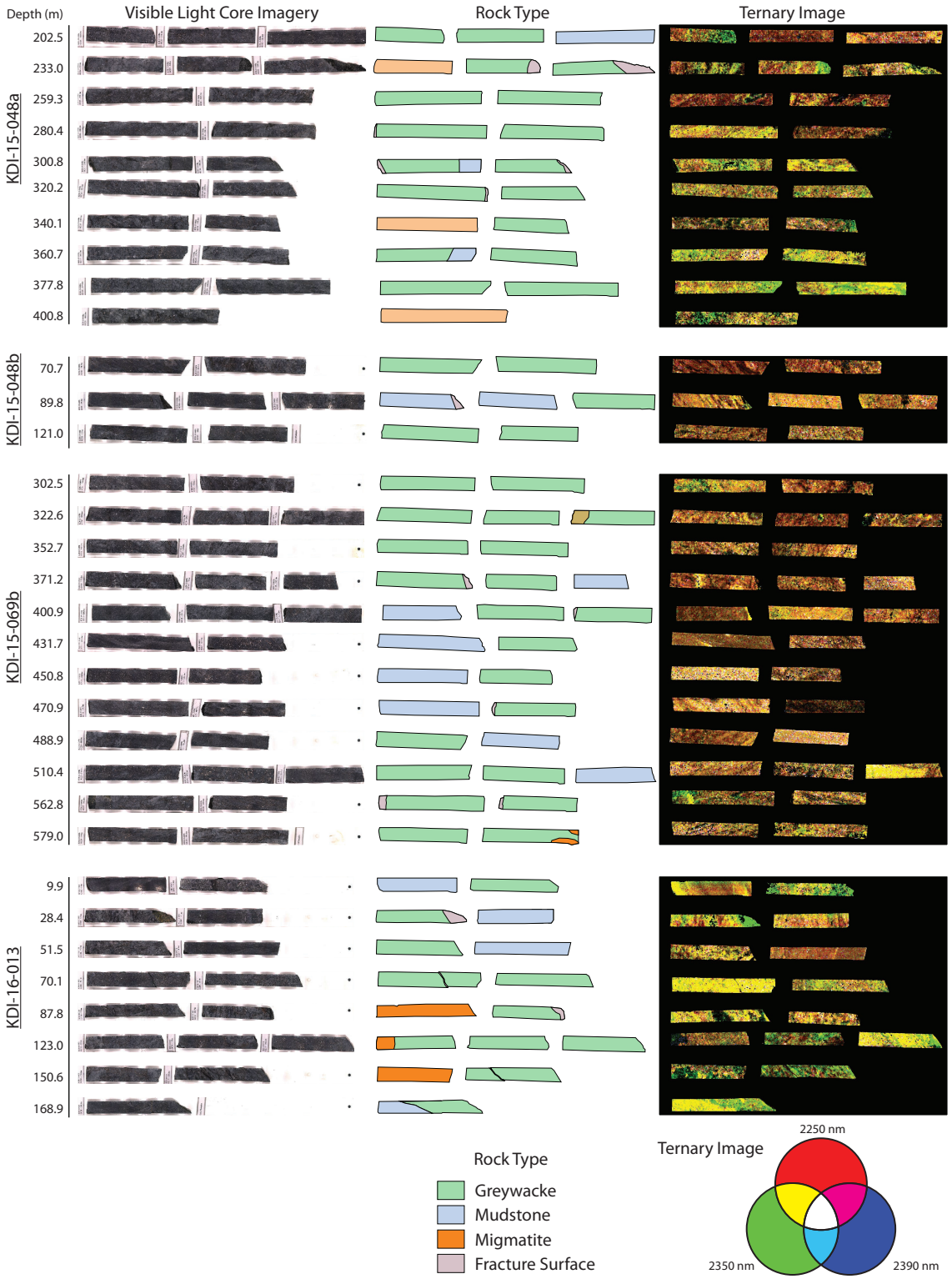

Figure 3.14: Profile through drill holes analyzed by hyperspectral imaging showing general patterns of dark mica/biotite - chlorite ternary image. Ternary images are produced based on the depth of the 2250 nm, 2350 nm, and 2390 nm features and colored red, green, and blue, respectively.

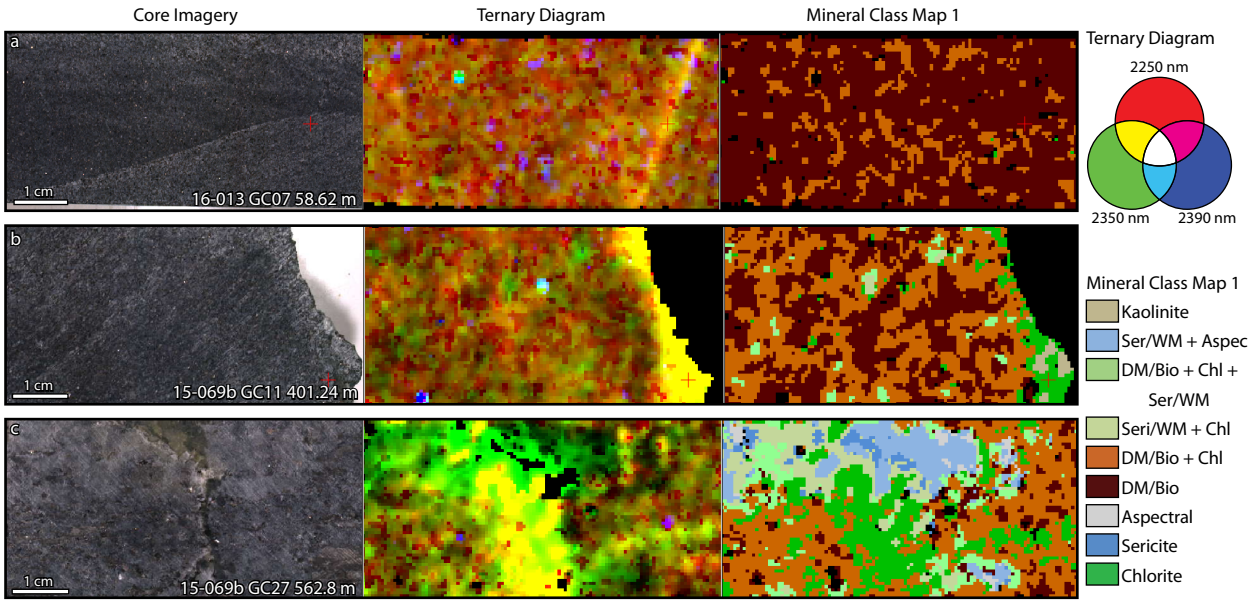

Figure 3.15: (a) Ternary images identifying <0.5 mm thick quartz and carbonate veins otherwise not identified in mineral maps and mineral class maps. **(b)** A quartz-pyrite vein coating a core fracture with a 2 mm diffuse quartz selvage. Ternary images clearly identify yellow shifts, from red-dominated pixels, within the selvage. **(c)** Ternary image identifying chlorite-biotite compositional shifts surrounding a quartz-pyrite vein in association with kaolinite and sericite.

Mudstones generally display more yellow, white, cyan, and magenta pixels evidencing better development of the 2390 nm feature characteristic of biotite. This supports mudstones' increased bioitite modal content and decreased chlorite modal content. In mudstones, compositional shifts in the ternary images also highlight bedding otherwise obscured by the dark color of the rock. Strongly banded gneisses display intimate mixing between strongly developed 2250 nm and 2350 nm features of the chlorite-biotite mixture. Although no carbonates are identified by hypersepctral imaging, the ternary map highlights biotite-chlorite compositional shifts in selvages surrounding several discrete <0.5 mm thick quartz-pyrite and carbonate veins. Ternary diagrams shift largely from green to yellow indicating deeper 2250 nm features which become more prominent with the (Fe,Mg)Al-OH bond (Figure 3.15). These subtle relationships between chlorite and biotite are often subtle or unrecognizable in mineral class maps (Figure 3.15a). These selvages are closely associated with sericite, and have an inverse relationship with the presence of kaolinite.

3.3.3.6 Discussion

Several hyperspectral parameters display significant background variation and do not vector towards the deposit. The aspectral slope log indicates the Fe content of unaltered anhydrous silicates does not vary with proximity to the deposit and is not an effective hyperspectral exploration vector for the kimberlite (Figure 3.16a). Aspectral pixel count, in accordance with visual core logging, also indicates there is no appreciable quartz leaching in any samples surrounding the deposit.

Increasing chloritization of biotite vaguely appears to produce more Mg-rich chlorite of clinochlore composition (Figure 3.9b). Distal samples from drill hole 15-048a display shorter 2250 nm wavelength

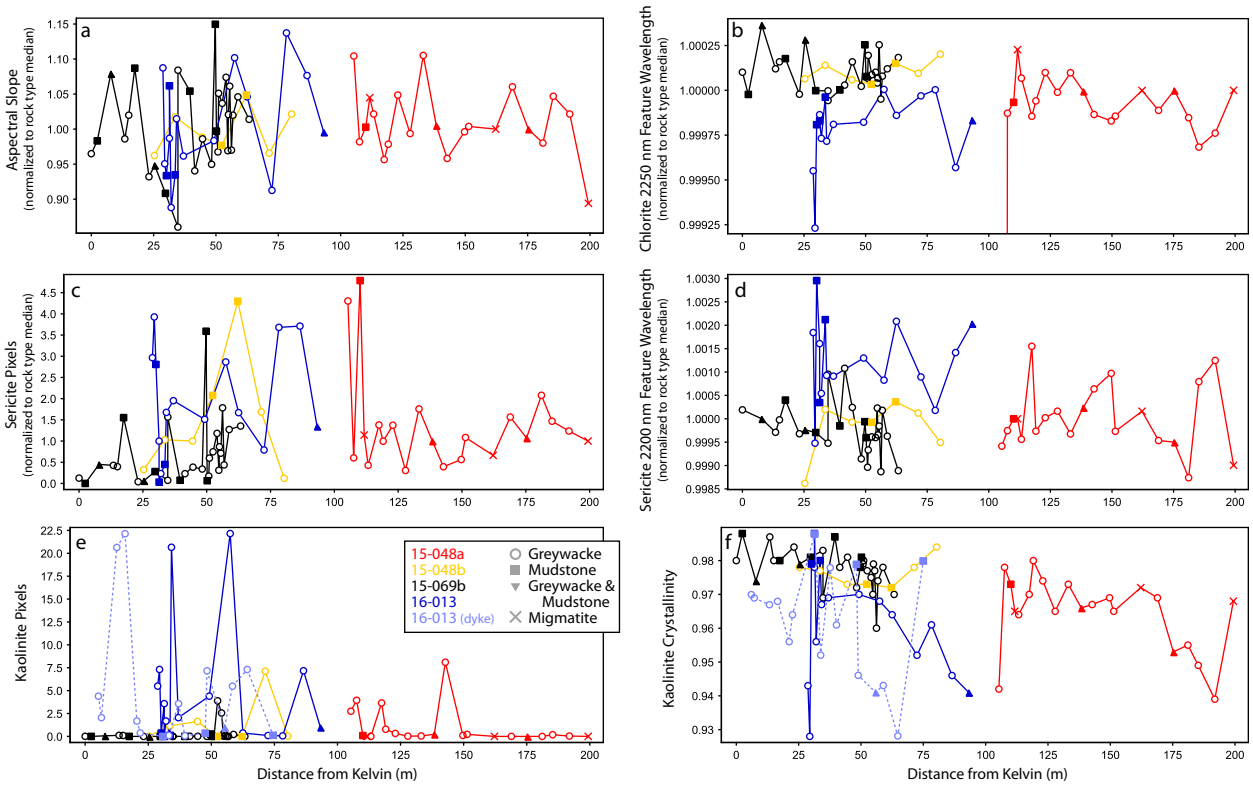

Figure 3.16: Various mineral logs plotted against sample distance from Kelvin plotted. Aspectral slope, chlorite 2250 nm feature, sericite pixels and 2200 nm feature are normalized to the rock type median. *16-013* series (dark blue) plots the sample distance to the Kelvin pipe, whereas *16-013 (dyke)* in dashed blue plots the sample distance from the dyke intersection at 96.9 - 103.7 m depth.

features defining background for these clinochlore composition values. Chlorite composition appears to shift towards more chamosite compositions as the 2250 nm feature wavelength shifts towards longer wavelengths with proximity to the kimberlite indicative of more Mg-Fe-Al substitution (Figure 3.16b). However, the generally shorter wavelength values of 16-013 suggests the broad shift towards longer wavelengths with proximity to the deposit is instead an artefact of background variation within the country-rocks.

In spite of the intimate relationship between biotite and chlorite in the rocks, distinguishing spatial and chemical relationships between the two was made easy by hyperspectral imaging and calculating the depth of certain absorption features. The ternary maps highlighting the development of the 2250 nm, 2350 nm, and 2390 nm features display significant background variation. However, they prove useful in highlighting potential areas of subtle changes in chlorite and biotite abundances in <2 mm thick vein selvages surrounding carbonate and quartz-pyrite veins (Figure 3.15). Core samples preferentially fractured along these veins, which posed a difficulty in distinguishing them in core sample or capturing them in a thin section. These areas readily identified by the ternary maps highlight areas for detailed hand specimen and petrographic follow-up. Care must be taken, however, because gneissose banding and relict bedding may produce similar ternary features.

Kaolinite is rare or absent in most core samples but the highest levels appear in sample 16-013 within 20

m of the dyke intersection. Despite significant background variation, kaolinite crystallinity increases with proximity to the deposit in several drill holes possibly recording a high temperature source overprinting less crystalline background values. However, kaolinite abundance does not correlate with higher crystallinity values. This suggests that kaolinite is not crystallized from kimberlite fluids, but may instead record evidence of distal thermal alteration.

In hydrothermal systems, infrared spectroscopy measurements of white mica composition and crystallinity have been shown to reflect pH and temperature conditions of formation, respectively (Agus, 2011; Fulignati, 2020; Guidotti, 1984). Sericite alteration is notably absent in mudstones because of their decreased feldspar content (aspectral class). Predictably, sericite alteration is more prevalent in felsic luecosome segregates. There is no apparent intensification of sericitization with proximity to the kimberlite pipe or dyke (Figure 3.16c). Sericite abundance instead suggests that kimberlite-related sericitization of country-rock feldspar is not uniformly distributed around the kimberlite pipe and dyke (Figure 3.11), and may instead be focused along pre-existing fractures and jointing. Additionally, the composition of sericite/white mica based on the 2200 nm feature does not shift with proximity to the deposit (Figure 3.16d).

Corescan produced sericite crystallinity logs from 1 cm intervals based on the depth of the 2200 nm Al-OH vibrational absorption feature (Figure 3.17). Values from drill hole 15-069b show evidence of a broad trend of decreasing crystallinity with depth approaching the kimberlite intersection at 523.6 m - 532.8 m (Figure 3.17b). A sharp increase in crystallinity appears up to 8 m (<35 m along hole) from the kimberlite intersection in drill hole 15-069b. Although white mica crystallinity values in this drill hole appear to show sericite crystallinity trends related to the location of the kimberlite, these patterns are not observed in other dill holes, nor do the trends in 15-069b exceed background variation to a point where this parameter can be considered as a definitive vector. Many of these samples lie within 10 m of the deepest modelled part of the North Limb. Below -100 m amsl the pipe is unmodelled and spatial relationships to these samples are unknown.

3.3.4 Lithogeochemistry

3.3.4.1 Lithium Borate Fusion ICP-MS

Elements for which >50% of measured values are at or below the practical detection limit (10 $\times$ the reported lower limit of detection) include Sn, Ta, Cr_2O_3, MnO, SrO, and BaO. These elements are discussed no further.

Results

Niobium and Ti are the most conserved elements in drill core samples. Niobium plotted versus TiO_2 lie along a strongly correlated trend line (R^2=0.841) passing through the origin confirming these elements are conserved. The various rock suites (greywacke, mudstone, and migmatite) lie along the same trend indicating they are cogenetic and elemental abundances can be compared using Pearce element ratio (PER) normalized to a conservative element without needing to level the data by rock type (Figure 3.18). Herein,

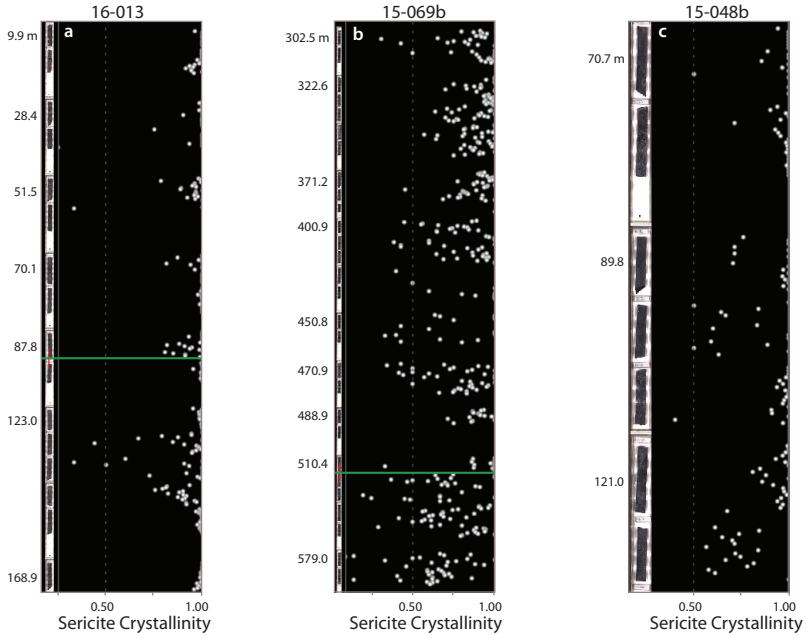

Figure 3.17: Down hole views of sericite crystallinity. Vertical axis (depth) is not to scale. Logs are produced from 1 cm intervals. Kimberlite intersections are shown in green.

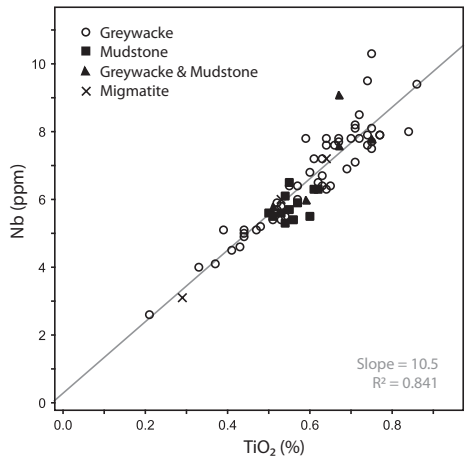

Figure 3.18: Conserved element biplot of TiO2 versus Nb for lithium borate fusion analysis.

TiO_2 is used as the conservative denominator in PERs due to it's lowest relative measurement error (Stanley, 2017).

Figure 3.19 and Figure 3.20 display downhole whole-rock PERs of elements expected to be mobilized in kimberlite - country-rock metasomatism. Iron and Mg are strongly positively correlated (r^2=0.73) and largely reflect changes in biotite and chlorite abundance. There are no apparent increases in MgO/TiO_2 and Fe_2O_3/TiO_2, disparate from background variation, with proximity to the kimberlite in downhole plots (Figure 3.19). Additionally, Al_2O_3/TiO_2 and SiO_2/TiO_2 values do not decrease near the kimberlite precluding evidence of Al or silica leaching in any country-rock samples (Figure 3.19 and Figure 3.20).

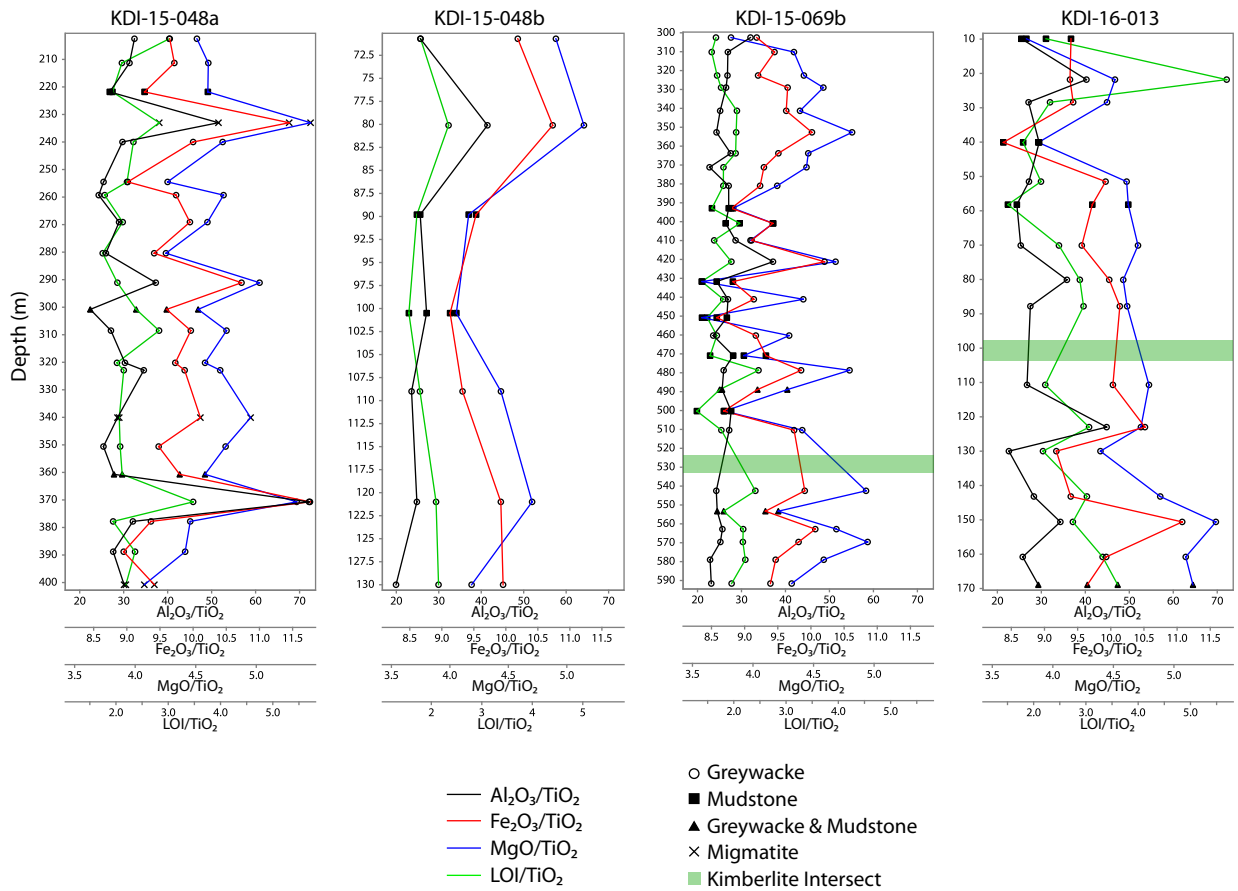

Figure 3.19: Downhole plots of total whole-rock Pearce Element Ratios Al_2O_3/TiO_2, Fe_2O_3/TiO_2, MgO/TiO_2, and LOI (%) by lithium borate fusion ICP-MS.

3.3.4.2 Weak Aqua Regia ICP-MS

Weak aqua regia digestion was employed on all core samples to detect secondary alteration mineralogy, specifically carbonates, oxides, and partial digestion of micas and clay minerals. Elements for which >50% of measured values are at or below the practical detection limit (10 × the reported lower limit of detection) include Au, B, Hg, In, Pd, Pt, Re, Sb, Se, Ta, and Te. These elements are not discussed further.

Results

Downhole plots of PERs from weak aqua regia ICP-MS are normalized to Zr because Ti is proven to be non-conserved in the aqua regia phases. Titanium, which can be hosted in biotite up to several percent compared to <<1% in chlorite, is conserved in whole rock concentrations during the chloritization of biotite. Chloritization presumably redistributes Ti from biotite into titanite as an alteration product (Eggleton and Banfield, 1985), thus causing decreased aqua regia soluble Ti concentrations with increasing chloritization (Figure 3.21).

Figure 3.22 displays downhole plots of elements from weak aqua regia ICP-MS analysis observed to be mobilized in kimberlite - country-rock alteration studies (Section 3.1.1). Overall, total carbon content

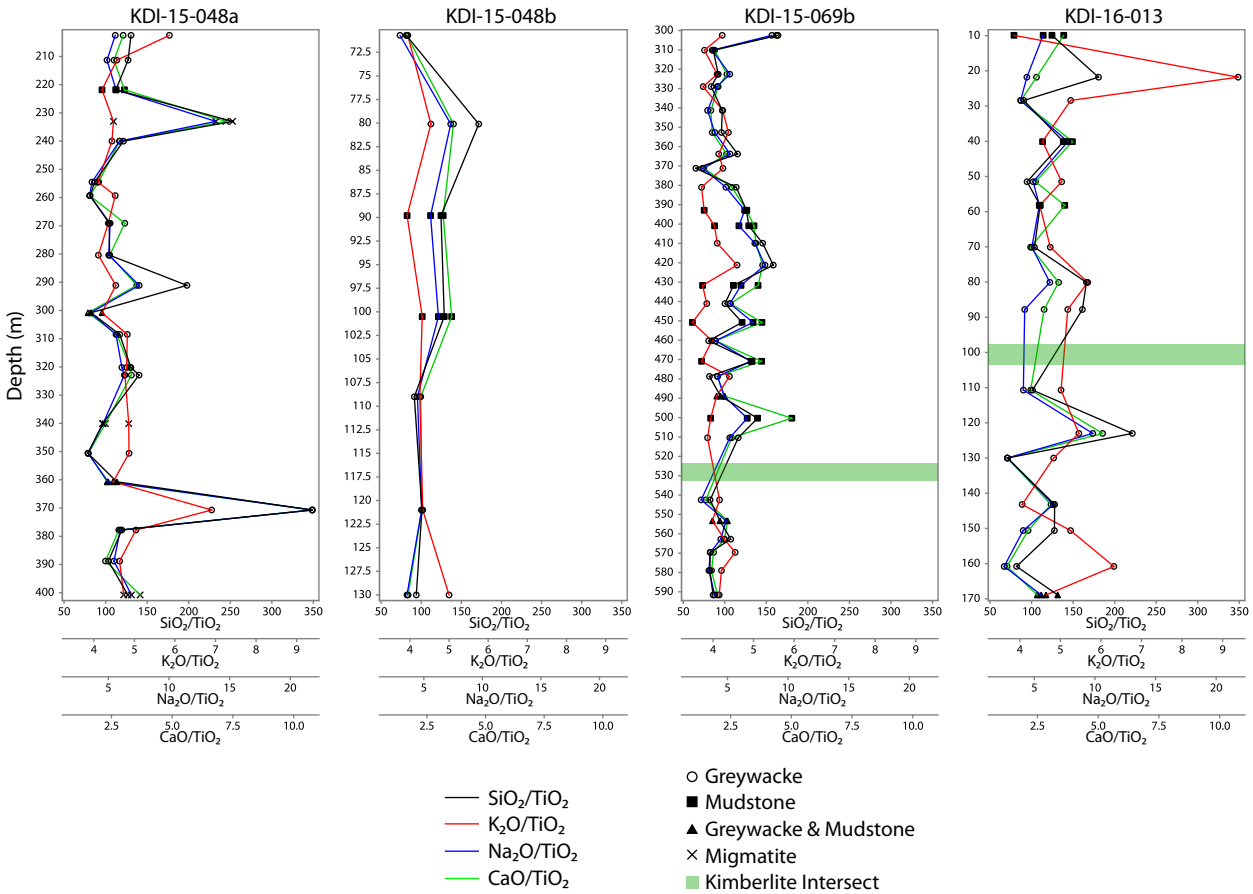

Figure 3.20: Downhole plots of whole-rock Pearce Element Ratios SiO_2/TiO_2, K_2O/TiO_2, Na_2O/TiO_2, and CaO/TiO_2 by lithium borate fusion ICP-MS.

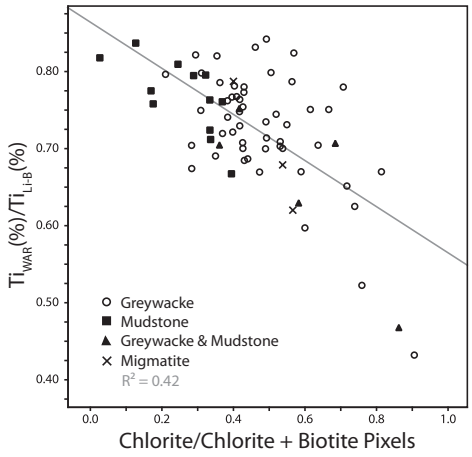

Figure 3.21: Chloritization intensity (calculated as chlorite pixels per total chlorite + biotite pixels) plotted against the recovery rate of Ti (calculated as the concentration of Ti_{WAR}/Ti_{Fusion}. Titanium recovery rate by weak aqua regia decreases as chloritization intensity increases supporting the process of Ti redistributed from biotite (partially recovered by weak aqua regia) to the insoluble alteration mineral titanite. This concept is operating on the assumption that phyllosilicates, particularly their cations, are partially digested by weak aqua regia.

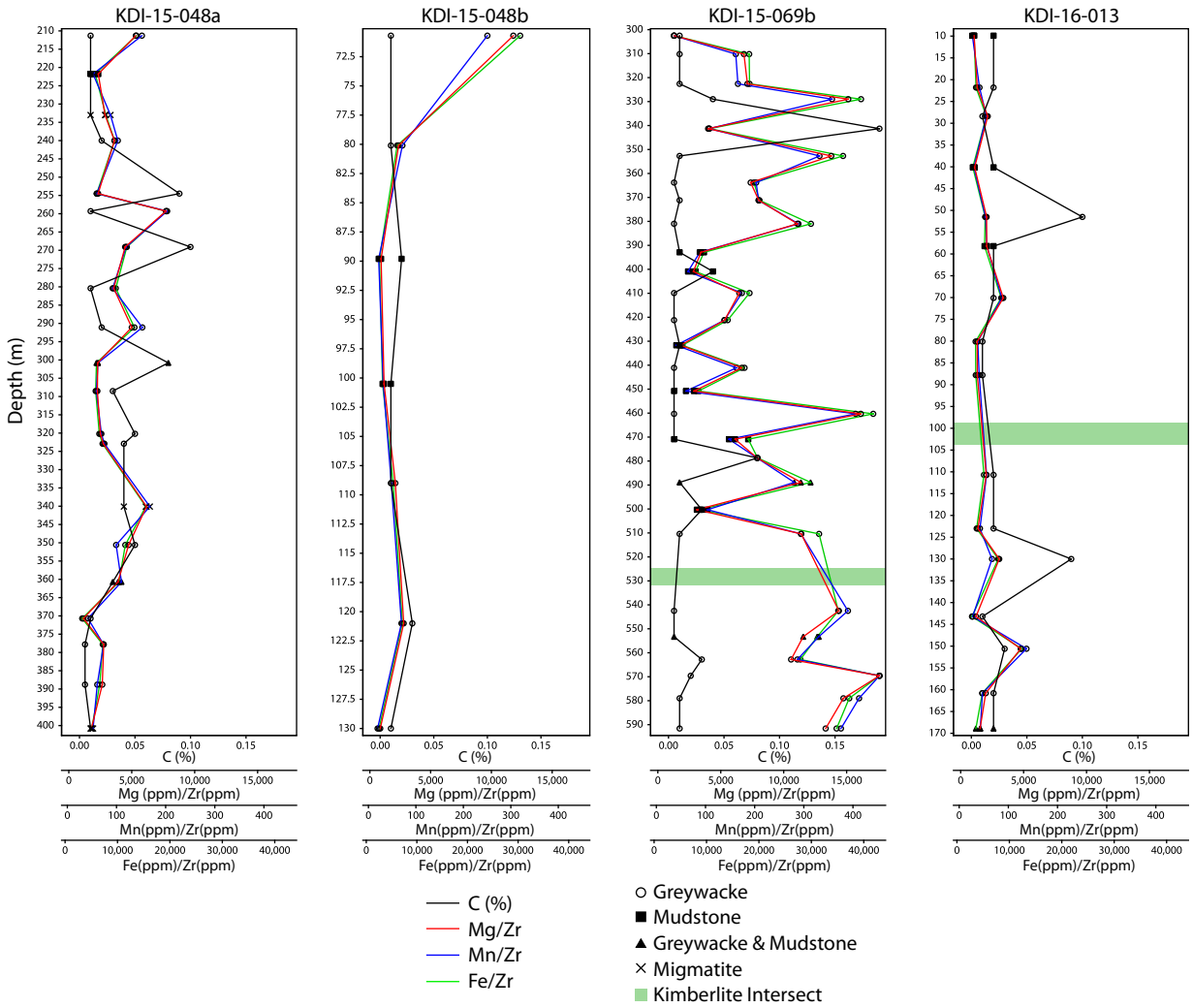

Figure 3.22: Downhole plots of total carbon (%) and Pearce Element Ratios Mg/Zr, Mn/Zr, and Fe/Zr by weak aqua regia ICP-MS.

is very low as carbonate was rarely observed in all rock types. Samples with carbonate veinlets observed in hand sample display elevated total carbon content, up to 0.19%. However, there is no evidence of carbonate content, or carbonate vein density, increasing with proximity to kimberlite intersections in any drill holes (Figure 3.22). In addition, weak aqua regia soluble Mg, Mn, and Fe show no discernible trends with proximity to the kimberlite. Volatile elements, Cs and Rb, have commonly been observed in elevated concentrations in country rock proximal to kimberlite contact (Fesq et al., 1975). However Cs_{WAR} and Rb_{WAR} do not show evidence of increasing concentrations with proximity to Kelvin (Figure 3.23).

3.3.4.3 Discussion

Spatial distribution and geochemical data fail to provide evidence that the carbonate veinlets observed in metaturbidite country-rock are associated with the kimberlite pipe or sheet dyke. Weak aqua regia soluble Mg and Sr do not correlate to carbonate abundance (Figure 3.24a, b). This lack of correlation between total

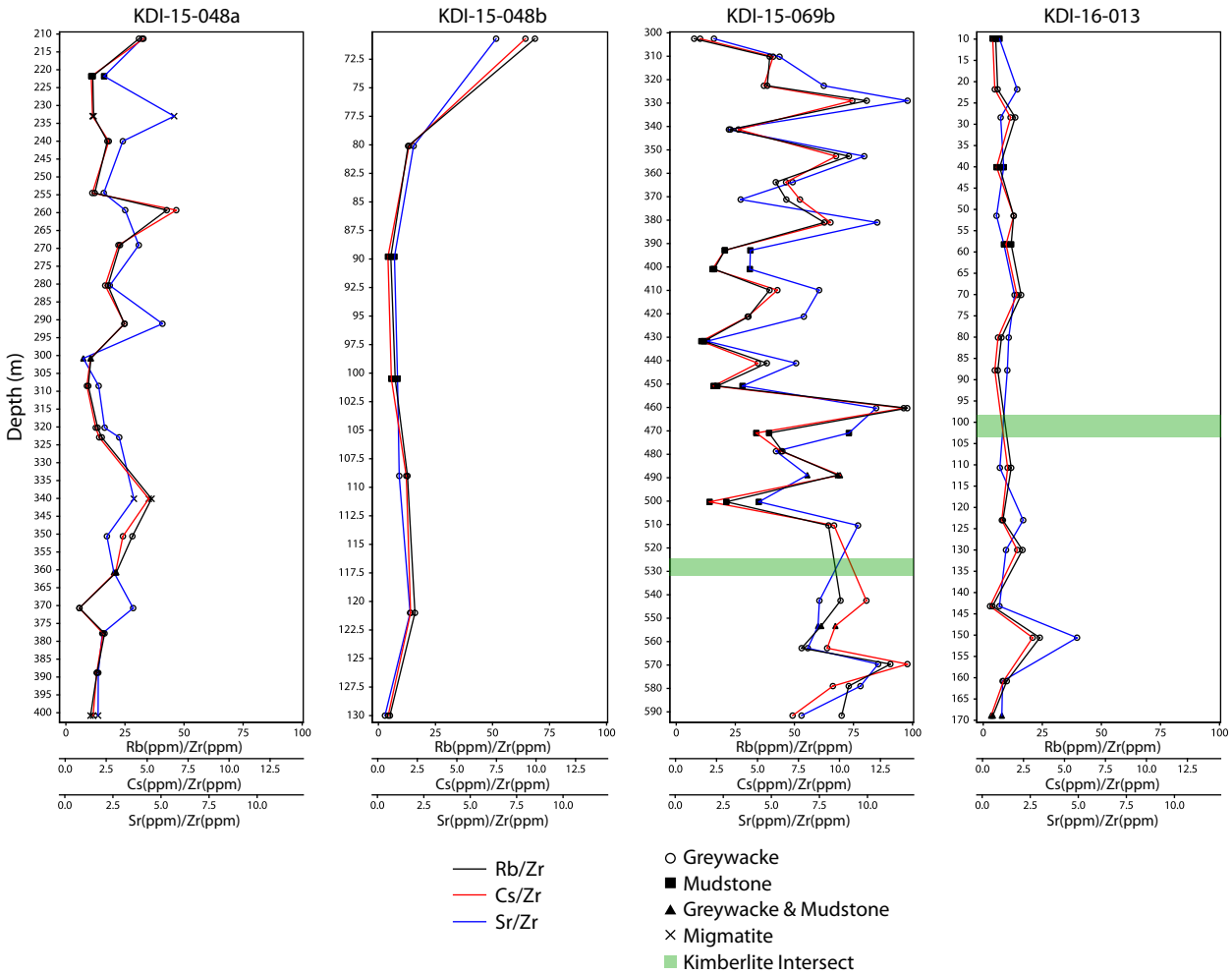

Figure 3.23: Downhole plots of Pearce Element Ratios Rb/Zr, Cs/Zr, and Sr/Zr by weak aqua regia ICP-MS.

carbon and Mg_{WAR} and Sr_{WAR} does not support evidence of Mg or Sr leaching from the kimberlite and concentrating in carbonate veinlets, and instead suggests the source of these carbonate veinlets hosted in metaturbidite country-rocks are not related to the Kelvin kimberlite.

Whole rock lithogeochemistry of distal core samples by lithium borate fusion and weak aqua regia digestion show no definitive evidence of metasomatism associated with distance to the kimberlite pipe or dyke (KDYKE-EXT). Few indicator elements ($Mg_{Li\text{-}B}$, $Fe_{Li\text{-}B}$, Rb_{WAR}, Cs_{WAR}) display elevated values proximal to known kimberlite intersections, however, these values are not readily distinguishable from background variation within, and between, drill holes. In a blind exploration exercise, these values would be insignificant and likely attributed to lithological variation in the metasedimentary country-rocks.

Several other trace elements have been observed to leach from the kimberlite near wall rock contacts during and post-emplacement. Fesq et al. (1975) documented large ion lithophile alkali elements Cs, Rb, and K behaving as mobile volatile elements within kimberlites near wallrock contacts suggesting these elements can be enriched in the surrounding country-rocks. Metaturbidite samples surrounding Kelvin do not display

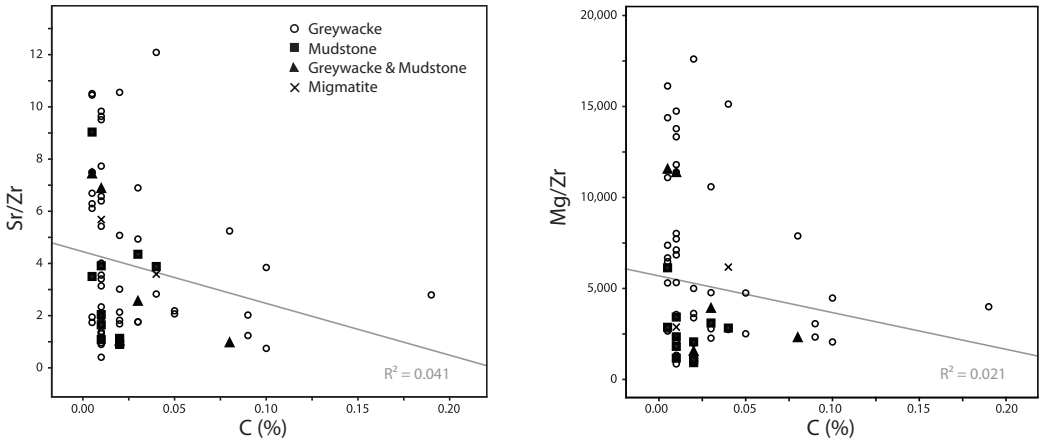

Figure 3.24: Biplots of total carbon (%) plotted against weak aqua regia ICP-MS **(a)** Sr(ppm)/Zr(ppm) and **(b)** Mg(ppm)/Zr(ppm).

increased Cs or Rb concentrations mobilized from the kimberlite, however samples within the kimberlite and across a contact may shed more light on the mobility of these volatile elements during emplacement of kimberlites (Figure 3.23).

3.4 Discussion and Conclusions

This research represents a compendious attempt to detect country-rock alteration surrounding a dominantly pyroclastic kimberlite body with cost-effective geochemical and mineralogical analyses. The absence of any definitive geochemical or mineralogical vectors in the country-rock proven in this research does not, however, indicate that the emplacement processes of the Kelvin kimberlite failed to produce metasomatic reactions with the metaturbidite country-rock. Detailed research on similar kimberlites hosted in silicic country-rocks have proven the potential to produce alteration, likely on a single-meter scale (Fulop et al., 2018; Harder et al., 2013; Hetman et al., 2004).

Many documented cases of kimberlite induced country-rock alteration rely on core logging, petrography, and whole rock lithogeochemistry - similar to the analyses and methods applied in this research (Section 3.1.1). However, these detailed publications had access to thousands of meters of continuous drill core, hundreds of thin sections, underground rock faces, and X-ray diffractometry among other methods (Fulop et al., 2018; Harder et al., 2013; Hetman et al., 2004; Muntener and Gaudet, 2018; Muntener and Scott Smith, 2013; Smith et al., 2004). It is important to note these documented examples are based on datasets at least an order of magnitude larger than that of this research. Additionally, most examples documented alteration within several meters of the kimberlite contact, with few examples documenting alteration up to 50 m or 100 m away (Hetman et al., 2004; Smith et al., 2004). Due to the spacing of the core samples in this research, identifying proximal alteration on a single-meter scale was expected to be a challenge.

Using similar whole-rock lithogeochemical analytical methods, examples from literature most commonly recorded Ca, Mg, and Fe concentrations elevated in country-rocks, and occasional silica leaching. These elements, among others, represent the most efficacious elements to use as lithogeochemical vectors

in drill core. Metasomatism across kimberlite - country-rock contacts have been best observed surrounding hypabyssal units at the Snap Lake kimberlite and Gahcho Kué cluster, however, only exist on a single-meter scale (Fulop et al., 2018; Hetman et al., 2004). Dyke contacts in core box photos appear very sharp (Figure 3.7d), whereas contacts between fresh country-rock and transitional-hypabyssal kimberlite (KIMB4/7) are gradational contacts over 1-2 meters (Figure 3.7b,d). At Kelvin, drill hole 16-013 provided a section through the hypabyssal dyke south of the South Limb with the closest sample within seven meters of the dyke contact. Four acid and weak aqua regia ICP-MS results failed to identify a larger cryptic alteration zone beyond the visually-obvious sharp contacts.

Several textures identified in the country-rock surrounding Kelvin are analogous to observations made in other publications. Country-rock breccias surrounding several dominantly-volcaniclastic pipes at the Renard kimberlite cluster (Muntener and Gaudet, 2018; Muntener and Scott Smith, 2013) draw comparison to discontinuous zones of clast-supported country-rock breccias found along the upper hangingwall contact of the Kelvin pipe documented in corebox photos and thin sections (Section 3.3.2). At Kelvin, evidence of distal country-rock alteration is limited to one occurrence of calcite veining, some hosting remnant olivine phenocrysts, penetrating up to five meters into metaturbidite country-rock (Figure 3.6g). These textures are analogous to country-rocks described at the Murowa and Sese pipes in Zimbabwe (Smith et al., 2004), and the Renard cluster (Muntener and Gaudet, 2018). Calcite veins (sometimes hosting remnant olivine phenocrysts at the Murowa and Sese pipes) form a halo up to 120 meters from kimberlite contacts and "likely facilitated the subsequent kimberlite magma emplacement and pipe formation by pre-conditioning the host rock" (Muntener and Gaudet, 2018). These kimberlite-derived <1 mm thick calcite veins in the fractured halo are observed on a meter-scale density and are only slightly more common than background country-rock fracturing, decreasing in density with distance from the kimberlite. However, these distal alteration halos likely represent rare occurrences surrounding kimberlites given their very limited acknowledgement in literature. Despite this research having access to core samples up to 200 m from the kimberlite and identifying few fractures containing carbonate in the matrix, the discontinuous nature of the core samples precluded the identification of a large continuous halo of dispersed fractures.

Although many of these documented cases of country-rock alteration observe evidence of mechanical and chemical processes, no conclusions have been made regarding the application of these parameters as exploration vectors for the discovery of kimberlites in near-miss drilling scenarios. The scope of many of these publications is instead to document the altered and brecciated country-rock units which "are important in understanding ultimate pipe shapes and emplacement" and ultimately contribute to resource classification and calculation (Muntener and Scott Smith, 2013).

Hyperspectral imaging of kimberlite drill core has been used to map and calculate hypabyssal kimberlite dilution by crustal rocks (Tappert et al., 2015), however, there is only one published application of hyperspectral scanning of country-rock drill core in an exploration setting (Tappert and Tappert, 2018). Several factors may contribute to this apparent lack in application of hyperspectral imaging in kimberlite exploration: (1) it has been proven that kimberlites do not produce large alteration footprints and do not

lend themselves to traditional alteration-based exploration methods; (2) geophysical methods are most commonly used to identify individual targets prior to drilling; (3) hyperspectral core scanning is an emerging technology; and (4) the few, if any, private applications will likely be held as an undisclosed proprietary technology for the immediate future.

Using a portable point spectrometer and proprietary SWIR spectra analysis, Tappert and Tappert (2018) detected subtle "hydration halos, which are most likely caused by kimberlite-derived hydrous fluids, [extending] more than 65 meters into the country-rocks, but their size strongly depends on the size of the kimberlite body." At several Canadian kimberlites, halos of measurable adsorbed water were observed independent of country-rock lithological variation. This provided the first example of reflectance spectroscopy successfully applied to kimberlite exploration in drill core. Detecting adsorbed water with hyperspectroscopy is proving to being more effective than measuring structurally bound water dependent instead on lithology, evidenced by loss on ignition (LOI) results (Figure 3.19).

Hyperspectral imaging computes several mineralogical and compositional parameters, some of which show potential as exploration vectors at Kelvin that warrant further investigation and application. Most notably, trends in sericite crystallinity from one drill hole (15-069b) spatially correlate with hydration halos observed by Tappert and Tappert (2018) where a proximal, <3 m thick, high temperature dehydration zone is surrounded by a <65 m hydration halo around several Slave kimberlites (Section 3.1.2). Apart from Tappert and Tappert (2018), there are no published applications of hyperspectral parameters (e.g. white mica crystallinity, chorite composition, biotite composition) recording evidence of kimberlite-induced country-rock alteration. Similar SWIR measurements of illite and chlorite maturity from point spectrometers have proven to be well correlated to more accurate X-ray diffraction crystallinity indices (Doublier et al., 2010). These SWIR spectral maturity values have been used to estimate temperature of formation of low-temperature metamorphic rocks and Carlin-type Au deposits (Barker, 2017; Doublier et al., 2010). Further investigation is suggested to examine the potential application of these clay mineral hyperspectral crystallinity measurements to estimate thermal alteration regimes and potentially record distal alteration.

This research concludes that the metaturbidite country-rocks showed no systematic changes in partial or whole-rock composition with respect to proximity to the kimberlite pipe or dyke. Mineral abundance, composition, and crystallinity measured by hyperspectral scanning also failed to identify trends in the data attributed to the proximity to the deposit. More detailed studies at the Kelvin and Faraday kimberlites suggest the presence of country-rock alteration, brecciation, and hydration on a single-meter scale along the margins of the kimberlite (Barnett et al., 2018; Tappert and Tappert, 2018). However, the hyperspectral and geochemical methods applied in this research failed to identify distal country-rock metasomatism at this scale and resolution. If drill core logging is used to vector towards kimberlites, it is recommended to focus attention on fault and joint sets that may facilitate the most distal evidence (tens of meters) of alteration.

Chapter 4

Conclusions

4.1 Conclusions and Exploration Implications

4.1.1 Surficial Geochemistry

Shallow till sampling at the Kelvin kimberlite detected geochemical signatures of proximal clastic glacial dispersion in two recent glacial directions. Geochemical interpretations, however, are qualified by the consistency of the surficial material and samples collected. In northern Canada, new surficial mapping programs are providing resources to aid surficial mapping and sampling planning prior to field investigations (Kerr et al., 2014; Knight, 2017). Developing a landscape evolution model since glaciation significantly aids in the spatial interpretation of the geochemical data. The primary mode of geochemical dispersion at Kelvin was westward glacial dispersion from the most recent glaciation, and unworked basal till provided the most ideal sample material with the simplest transport history.

Anomalous signatures were observed in both B-horizon soils and shallow frost boil samples in four acid and aqua regia ICP-MS datasets. Although the aqua regia dataset appeared to reduce background variation, four acid was preferred to ensure clastic kimberlite material is fully digested. Complete digestions also have the added benefit of comparison to regional till and bedrock geochemical datasets if available in the district. The pathfinder elements extracted by four acid digestion that effectively detect clastic signatures from the kimberlite included Cr, Mg, Mn, Nb, Ni, Ta, and Ti. These pathfinder elements were sufficiently enriched in the kimberlite to provide contrast against the metasediment and granitoid country rocks in the region. Additionally, these elements were shown to be largely unaffected by secondary soil formation processes because redistribution within the soil profile was minimal. Soils proved to be very immature allowing their direct comparison to cryoturbated fresh till samples, and may prove applicable in similar sub-actic environments in the northern Slave province. Additionally, size fraction results indicated the -180 µm fraction may be more suitable than the commonly used -63 µm fraction. However, an orientation survey (and possibly targeted sieving) may help identify the textural biases imposed by grain-size distributions and the strong control of

the fine fractions on bulk geochemistry.

In situ field physicochemical ORP and pH measurements did not detect the presence of a reduced column or effects of alkaline groundwater above and surrounding the Kelvin kimberlite. The formation of an electrochemical cell was likely disrupted by several factors including the continuous permafrost, inclined pipe morphology, thick bedrock cover over the North Limb, and small subcrop expression under the lake. However, pH and ORP conditions of the soils may provide important context for the mobility of trace metals.

4.1.2 Lithogeochemical Exploration

Hyperspectral and geochemical analyses in this research were applied to four drill holes surrounding the Kelvin kimberlite pipe and dyke system on a nearly 10-meter interval up to several hundred meters from the deposit contacts. Partial and whole-rock geochemistry results failed to detect evidence of metasomatism surrounding the kimberlite both proximal ad distal to kimberlite-country rock contacts. Instead, the small-scale lithologic changes within the metaturbidite country-rock produced significant geochemical background variation obscuring any subtle metasomatic signatures of enrichments or depletion. Short wave infrared hyperspectral scanning of the drill core by Corescan analyzed mineralogical abundance, composition, and crystallinity of hydrated minerals, as well. Results did not identify trends in the data that could be clearly attributed to proximity to the kimberlite, however, the results did highlight several possible cryptic alteration vectors including sericite crystallinity and subtle compositional shifts in chlorite and biotite.

4.2 Recommendations for Further Research

4.2.1 Surficial Geochemistry

The following research is recommended to expand on the till geochemistry results observed in this research:

1. The geochemical partitioning into the various size fractions of the till should be further evaluated by analyzing samples from additional kimberlites with known geochemical dispersion and KIM trains, such as Cayer (2017).

2. Additional work regarding hydrocarbon responses is also recommended to determine possible inorganic controls on the hydrocarbon responses observed at Kelvin in ActLabs's SGH report. This proposed research would require coordination between the research facility and the laboratories who perform the proprietary analyses and interpretations.

4.2.2 Lithogeochemical Exploration

The following research is recommended to test and challenge the results observed in this research, and to hopefully develop robust and novel mineralogical and lithogeochemical exploration vectors for kimberlites:

1. This research is recommended to be replicated at another known kimberlite at a higher-resolution

scale. Analyses should be performed on continuous intervals of core, ideally across a known kimberlite-country rock contact, to identify proximal alteration signatures and the processes by which they are created. In order to evaluate distal alteration and the possible presence of a halo of dispersed fractures, a comprehensive dataset of drill logging would be necessary. Several opportunities exist at active open pit mining operations and late-stage exploration projects in the Slave province to provide a robust dataset and ample access to core, drill logs, and background knowledge.

2. Hyperspectral results highlighted sericite crystallinity as having the potential to be applied as an alteration vector. However, trends did not correlate with sericite/white mica compositions suggesting metasomatism is limited and absent on a tens-of-meters scale. Further investigation is suggested to examine the potential for clay mineral crystallinity to record distal thermal alteration regimes and evaluate it's application as a cryptic alteration vector.

Bibliography

Agashev, A. M., Pokhilenko, N. P., Takazawa, E., McDonald, J. A., Vavilov, M. A., Watanabe, T., and Sobolev, N. V. (2008). Primary melting sequence of a deep (¿ 250 km) lithospheric mantle as recorded in the geochemistry of kimberlite-carbonatite assemblages, Snap Lake dyke system, Canada. *Chemical Geology*, 255(3-4):317–328.

Agus, A. J. L. (2011). *Mapping white mica in milled porphyry copper pebbles using hyperspectral imagery: An exploratory study*. PhD thesis, University of Twente.

ALS Geochemistry (2016). Geochemical Procedure: ME-MS61L: Lowest Detection Limit Super Trace Multi-Element Analysis by Four-Acid Digestion and ICP-MS/ICP-AES. Technical Report February.

Amplified Geochemical Imaging LLC (2015). A comparison of surface geochemical techniques.

Anand, R. R., Aspandiar, M. F., and Noble, R. R. P. (2016). A review of metal transfer mechanisms through transported cover with emphasis on the vadose zone within the Australian regolith. *Ore Geology Reviews*, 73(2007):394–416.

Ault, A. K., Flowers, R. M., and Bowring, S. A. (2013). Phanerozoic surface history of the Slave craton. *Tectonics*, 32(5):1066–1083.

Baragar, W. R. A. and McGlynn, J. C. (1976). Geological Survey of Canada Early Archean Basement in the Canadian Shield: A Review of the Evidence. *Geological Survey of Canada*.

Barker, R. (2017). *GEOCHEMICAL AND MINERALOGICAL INVESTIGATION OF BRECCIAS AT THE EL NIÑO AU-AG DEPOSIT ELKO COUNTY, NEVADA*. PhD thesis, Colorado State University.

Barnes, S. J., Cruden, A. R., Arndt, N., and Saumur, B. M. (2016). The mineral system approach applied to magmatic Ni – Cu – PGE sulphide deposits. *Ore Geology Reviews*, 76:296–316.

Barnett, W., Stubley, M., Hetman, C., Uken, R., Hrkac, C., and McCandless, T. (2018). Kelvin and Faraday kimberlite emplacement geometries and implications for subterranean magmatic processes. *Mineralogy and Petrology*, 112:447–462.

Barnett, W. P., Kurszlaukis, S., Tait, M., and Dirks, P. H. G. M. (2011). Kimberlite wall-rock fragmentation processes : Venetia K08 pipe development. *Bulletin of Volcanology*, 73(8):941–958.

Beard, A. D., Downes, H., Hegner, E., and Sablukov, S. (2000). Geochemistry and mineralogy of kimberlites from the Arkhangelsk Region , NW Russia : evidence for transitional kimberlite magma types. *Lithos*, 51:47–73.

Bell, K. and Franklin, J. M. (1993). Application of lead isotopes to mineral exploration in glaciated terrains. *Geology*, 21:1143–1146.

Benn, C., Sader, J. A., Zhivkov, N., Jeleva, T., and Anderson, R. (2016). Benefits of Soil Clay Fraction Geochemistry for Surficial Exploration: A Case Study from the Tethyan Belt. In *SEG-MJD 2016 Conference*, page 1. Society of Economic Geologists Inc.

Bezzola, M., Hetman, C., Garlick, G., Creaser, R., Hrkac, C., Vivian, G., Diering, M., and Nowicki, T. (2018). Geology and resource development of the Kelvin kimberlite pipe, Northwest Territories, Canada. *Mineralogy and Petrology*, 112(11):463–475.

Bleeker, W. (2001). The ca. 2680 Ma Raquette Lake Formation and correlative units across the Slave Province, Northwest Territories: evidence for a craton-scale overlap sequence. *Current Research, Geological Survey of Canada*.

Bleeker, W. (2002). Archaean tectonics: a review, with illustrations from the Slave craton. In Fowler, C. M. R., Ebinger, C. J., and Hawkesworth, C. J., editors, *The Early Earth: Physical, Chemical and Biological Development*, pages 151–181. The Geological Society London, geological edition.

Bleeker, W. (2003). The late Archean record: A puzzle in ca. 35 pieces. *Lithos*, 71(2-4):99–134.

Bleeker, W., Ketchum, J., Davis, B., and Sircombe, K. (2004). The Slave Craton From On Top: The Crustal View. (October 2015):1–5.

Bleeker, W., Ketchum, J. W. F., Jackson, V. A., and Villeneuve, M. E. (1999). The Central Slave Basement Complex, Part I: its structural topology and autochthonous cover. *Canadian Journal of Earth Sciences*, 36(7):1083–1109.

Bleeker, W., Stern, R., and Sircombe, K. (2000). Why the Slave Province, Northwest Territories, got a little bigger. *Geological Survey of Canada, Current Research*, 2000-C2:9.

Bockheim, J. G. (2015). *Cryopedology*. Springer International Publishing.

Bodnar, M. M. (2017). *Modelling geochemical dispersion above a buried polymetallic volcanogenic massive sulphide deposit in a recently glaciated terrain*. PhD thesis, University of British Columbia, Vancouver.

Bowring, S. A., Williams, I. S., and Compston, W. (1989). 3.96 Ga gneisses from the Slave province, Northwest Territories, Canada. *Geology*, 17:971–975.

Brown, R. J., Kavanagh, J., Sparks, R. S., Tait, M., and Field, M. (2007). Mechanically disrupted and chemically weakened zones in segmented dike systems cause vent localization: Evidence from kimberlite volcanic systems. *Geology*, 35(9):815–818.

Burt, A. K. and Hamilton, S. M. (2004). Comparison of Selective Leach Signatures over Kimberlites and Other Targets. Technical report.

Cairns, S. R. (2003). Bedrock mapping in the Walmsley Lake area, southeastern Slave Province , Northwest Territories. Technical report, Geological Survey of Canada.

Cairns, S. R., MacLachlan, K., Relf, C., Renaud, J., and Davis, W. J. (2003). Walmsley Lake Digital Atlas Extended Marginal Notes. Technical Report April.

Cameron, E. M., Hamilton, S. M., Leybourne, M. I., Hall, G. E. M., and McClenaghan, M. B. (2004). Finding deeply buried deposits using geochemistry. *Geochemistry: Exploration, Environment, Analysis*, 4(1):7–32.

Caro, G., Kopylova, M. G., and Creaser, R. A. (2004). The hypabyssal 5034 kimberlite of the Gahcho Kue cluster, southeastern Slave craton, northwest territories, Canada: A granite-contaminated group-I kimberlite. *Canadian Mineralogist*, 42(1):183–207.

Cayer, E. M. (2017). *The development of surface geochemical technologies for the detection of kimberlites concealed by glacial drift in the Northwest Territories, Canada*. PhD thesis, University of British Columbia, Vancouver.

Chouinard, R. L. M. (2018). *Surficial geochemical tools for Cu-Mo porphyry exploration in till-covered terrain*. PhD thesis, University of British Columbia, Vancouver.

Clement, C. R. (1982). *A comparative geological study of some major kimberlite pipes in the Northern Cape and Orange Free State*. PhD thesis, Univeristy of Cape Town.

Cummings, D. I., Kjarsgaard, B. A., Russell, H. A. J., and Sharpe, D. R. (2014). Comminution of indicator minerals in a tumbling mill: implications for mineral exploration. Technical report.

Davis, W. J. and Bleeker, W. (1999). Timing of plutonism, deformation, and metamorphism in the Yellowknife Domain, Slave Province, Canada. *Canadian Journal of Earth Sciences*, 36(7):1169–1187.

Davis, W. J., Gariepy, C., and Van Breemen, O. (1996). Pb isotopic composition of late Archaean granites and the extent of recycling early Archaean crust in the Slave Province, northwest Canada. *Chemical Geology*, 130(3-4):255–269.

Davis, W. J. and Hegner, E. (1992). Neodymium isotopic evidence for the tectonic assembly of Late Archean crust in the Slave Province, northwest Canada. *Contributions to Mineralogy and Petrology*, 111:493–504.

Davis, W. J., Jones, A. G., Bleeker, W., and Grütter, H. (2003). Lithosphere development in the Slave craton: a linked crustal and mantle perspective. *Lithos*, 71:575–589.

Dawson, J. B. (1967). Geochemistry and origin of kimberlite. In Wyllie, P. J., editor, *Ultramafic and Related Rocks*, pages 269–278. Wiley, New York.

De Beers Canada (2018). *Gahcho Kué Mine Environmental Screening Assessment*. Number March.

DiLabio, R. N. W. (1995). Residence sites of trace elements in oxidized till. Technical report, Ministry of Energy, Mines, and Petroleum Resources.

Doublier, M. P., Roache, A., and Potel, S. (2010). *Application of SWIR spectroscopy in very low-grade metamorphic environments: a comparison with XRD methods*, volume 2010.

Dredge, L. A., Ward, B. C., and Kerr, D. E. (1994). Glacial geology and implications for drift prospecting in the Lac de Gras, Winter Lake, and Aylmer Lake map areas, central Slave Province. Technical report.

Dreimanis, A. and Vagners, U. J. . (1971). Bimodal Distribution of Rock and Mineral Fragments in Basal Tills. *Till / a Symposium: edited by Goldthwait, R. P.*, pages 237–250.

Dyke, A. S. and Prest, V. K. (1987a). Late Wisconsinan and Holocene History of the Laurentide Ice Sheet. *Géographie physique et Quaternaire*, 41(2):237.

Dyke, A. S. and Prest, V. K. (1987b). Paleogeography of Northern North America, 18,000 - 5,000 years ago. *Geological Survey of Canada*, Map 1703A(Scale:1:12,500,000).

Dyke, A. S. and Zoltai, S. C. (1980). Radiocarbon-Dated Mudboils Central Canadian Arctic. *Current Research, Part B*, Paper 80-1:271–275.

Eggleton, R. A. and Banfield, J. F. (1985). The alteration of granitic biotite to chlorite. *American Mineralogist*, 70(9-10):902–910.

Fesq, H., Kable, E., and Gurney, J. (1975). Aspects of the geochemistry of kimberlites from the Premier Mine, and other selected South African occurences with particular reference to the rare earth elements. *Physics and Chemistry of the Earth*, 9:687–707.

Fulignati, P. (2020). Clay minerals in hydrothermal systems. *Minerals*, 10(10):1–17.

Fulop, A., Kopylova, M. G., Kurszlaukis, S., Hilchie, L., Ellemers, P., and Squibb, C. (2018). Petrography of snap lake kimberlite dyke (Northwest Territories, Canada) and its interaction with country rock granitoids. *Journal of Petrology*, 59(12):2493–2518.

Gaudet, M., Kopylova, M. G., Muntener, C., Zhuk, V., and Nathwani, C. (2018). Geology of the Renard 65 kimberlite pipe, Québec, Canada. *Mineralogy and Petrology*, 112:433–445.

Guidotti, C. V. (1984). Micas in metamorphic rocks. In S.W. Bailey, editor, *Micas*, pages 357–467. Mineralogical Society of America.

Gulson, B. (1986). *Lead Isotopes in Mineral Exploration*.

Gulson, B., Kamenov, G. D., Manton, W., and Rabinowitz, M. (2018). Concerns about quadrupole ICP-MS lead isotopic data and interpretations in the environment and health fields. *International Journal of Environmental Research and Public Health*, 15(4).

Hall, G. E. M. (1991). Analytical methods used in exploration geochemistry. Technical report.

Hall, G. E. M. (1998). Analytical perspective on trace element species of interest in exploration. *Journal of Geochemical Exploration*, 61:1–19.

Hall, G. E. M., Vaive, J. E., Beer, R., and Hoashi, M. (1996). Selective leaches revisited, with emphasis on the amorphous Fe oxyhydroxide phase extraction. *Journal of Geochemical Exploration*, 56(1):59–78.

Hamilton, S. M. (2007a). A Prospector's Guide to the Use of Selective Leach and Other Deep Penetrating Geochemical Techniques in Mineral Exploration. pages 1–58.

Hamilton, S. M. (2007b). Major Advances in Soil Geochemical Exploration Methods for Areas of Thick Glacial Drift Cover. *in Proceedings of Exploration 07: Fifth Decennial Internation Conference on Mineral Exploration*, (Advances in Prospect-Scale Geochemical Methods):263–280.

Harder, M., Nowicki, T. E., Hetman, C. M., Freeman, L., and Abedu, B. (2013). Geology and Evaluation of the K2 Kimberlite, Koidu Mine, Sierra Leone, West Africa. In Pearson, D. G., editor, *Proceedings of 10th International Kimberlite Conference*, volume 2.

Hardy, F., Eichenberg, D. J., and Poniatowski, B. T. (1997). Appendix 1: Quaternary Geology of the AK Property. Technical report, Mountain Province Mining Inc.

Hattori, K. H., Hamilton, S. M., Kong, J., and Gravel, J. (2009). Soil geochemical survey over concealed kimberlites in the Attawapiskat area in northern Canada. *Geochemistry: Exploration, Environment, Analysis*, 9(2):139–150.

Heaman, L. M., Kjarsgaard, B. A., and Creaser, R. A. (2004). The temporal evolution of North American kimberlites. *Lithos*, 76(1-4 SPEC. ISS.):377–397.

Heberlein, D. R. (2010). An Assessment of Soil Geochemical Methods for Detecting Copper-Gold Porphyry Mineralization through Quaternary Glaciofluvial Sediments at the WBX-MBX and 66 Zones, Mt. Milligan, North-Central British Columbia. *Geoscience BC Report*.

Helmstaedt, H. (2009). Crust-mantle coupling revisited: The Archean Slave craton, NWT, Canada. *Lithos*, 112(November 2009):1055–1068.

Henderson, J. B. (1970). STRATIGRAPHY OF THE ARCHEAN YELLOWKNIFE SUPERGROUP, YELLOWKNIFE BAY - PROSPEROUS LAKE AREA, DISTRICT OF MACKENZIE. Technical report.

Hetman, C., Smith, B. H. S., Paul, J. L., and Winter, F. (2004). Geology of the Gahcho Kue kimberlite pipes, NWT, Canada: root to diatreme magmatic transition zones. *Lithos*, 76:51–74.

Hetman, C. M. (2008). Tuffisitic Kimberlite (TK): A Canadian perspective on a distinctive textural variety of kimberlite. *Journal of Volcanology and Geothermal Research*, 174(1-3):57–67.

Hoffman, P. F. (1988). UNITED PLATES OF AMERICA , THE BIRTH OF A CRATON : and Growth of Laurentia. *Annual Review of Earth and Planetary Sciences*, 16:543–603.

Holk, G. J., Kyser, T. K., Chipley, D., Hiatt, E. E., and Marlatt, J. (2003). Mobile Pb-isotopes in Proterozoic sedimentary basins as guides for exploration of uranium deposits. *Journal of Geochemical Exploration*, 80(2-3):297–320.

Hunt, G. R. (1977). Spectral Signatures of Particulate Minerals in the Visible and Near Infrared. *Geophysics*, 42(3):501–513.

Hussein, A. A., Lochner, C., and Bell, K. (2003). Application of Pb Isotopes to Mineral Exploration in the Halfmile Lake Area, Bathurst, New Brunswick. *Economic Geology*, Monograph:679–688.

Isachsen, C. E., Bowring, S. A., and Padgham, W. A. (1991). U-Pb Zircon Geochronology of the Yellowknife Volcanic Belt, NWT, Canada: New Constraints on the Timing and Duration of Greenstone Belt Magmatism. *The Journal of Geology*, 99(1):55–67.

Johnson, D. D., Makarenko, M., Meikle, K., Prince-Wright, B., Jakubec, J., and Jones, K. (2010). Gahcho Kué Project Definitive Feasibility Study NI 43 - 101 Technical Report Northwest Territories, Canada. Technical report.

Kaiser, J. A. (2003). Express 2003-06: De Beers decides to pursue prefeasibility study for Gahcho Kue. (April).

Kelley, S. E., Ross, M., Elliott, B., and Normandeau, P. X. (2019). Effect of shifting ice flow and basal topography in shaping three-dimensional dispersal patterns, Lac de Gras region, Northwest Territories, Canada. *Journal of Geochemical Exploration*, 199(April 2018):105–127.

Kerr, D. E., Knight, R. D., Sharpe, D. R., and Cummings, D. I. (2014). Surficial geology, Walmsley Lake, Northwest Territories, NTS 75-N. Technical report.

Kerr, D. E., Knight, R. D., Sharpe, D. R., Cummings, D. I., Russell, H. A. J., and Kjarsgaard, B. A. (2013). Surficial Geology of the Proposed National Park Reserve on the East Arm of Great Slave Lake. Technical report, Geologicla Survey of Canada, Open File 7196.

Knight, J. (2017). NWT Open Report 2017-018 An interpretation of the deglaciation history of the southern Slave Province using 1 : 50 000 surficial geology maps.

Kramers, J. D. (1977). Lead and strontium isotopes in Cretaceous kimberlites and mantle-derived xenoliths from Southern Africa. *Earth and Planetary Science Letters*, 34(3):419–431.

Kusky, T. M. (1989). Accretion of Archean Slave province Geology. *Geology*, 17:63–67.

Kusky, T. M. (1993). Collapse of Archean orogens and the generation of late- to postkinematic granitoids. *Geology*, 21(10):925–928.

Langmuir, D. (1971). Eh-pH Determination. In *Procedures in Sedimentary Petrology*, chapter Eh-pH Dete, pages 597–636.

Laukamp, C. (2011). Short Wave Infrared Functional Groups of Rock- forming Minerals: Report Number EP115222. Technical Report August, CSIRO.

LeCheminant, A. N., Heaman, L. M., van Breemen, O., Ernst, R. E., Baragar, W. R. A., and Buchan, K. L. (1996). Mafic magmatism, mantle roots, and kimbelites in the Slave craton. *Searching for Diamonds in Canada: Open File Report 3228*, pages 161–169.

Maas, R., Sciences, E., Institut, M.-p., Sobolev, A. V., and Institut, M.-p. (2005). Sr, Nd, and Pb isotope evidence for a mantle origin of alkali chlorides and carbonates in the Udachnaya kimberlite, Siberia. *Geology*, 33(7):549–552.

Mackay, J. R. (1980). The origin of hummocks , western Arctic coast , Canada susceptible soils will always be such that water will Objections to the Cryostatic Theory Although cryostatic pressures are often pro- be attracted to the freezing zone , that is , the water. *Canadian Journal Earth Science*, 17(1978):996–1006.

Maclachlan, K., Relf, C., Cairns, S. R., Renaud, J., and Mills, A. (2002). Current Research 2002-C1 New bedrock mapping and preliminary U / Pb geochronology in the Walmsley Lake area , southeastern Slave Province , Northwest Territories. Technical report.

Mann, A. W., Birrell, R. D., Fedikow, M. A. F., and de Souza, H. A. F. (2005). Vertical ionic migration: mechanisms, soil anomalies, and sampling depth for mineral exploration. *Geochemistry: Exploration, Environment, Analysis*, 5(3):201–210.

Mann, A. W., Birrell, R. D., Mann, A. T., Humphreys, D. B., and Perdrix, J. L. (1998). Application of the mobile metal ion technique to routine geochemical exploration. *Journal of Geochemical Exploration*, 61(1-3):87–102.

McCandless, T. (1990). Kimberlite xenocryst wear in high-energy fluvial systems: experimental studies. *Journal of Geochemical Exploration*, 37(3):323–331.

McCandless, T. and Nash, W. P. (1996). Detrital mantle indicator minerals in Southwestern Wyoming, U.S.A.: Evaluation of mantle environment, igneous host, and diamond exploration significance. *Exploration and Mining Geology*, 5(1):33–44.

McClenaghan, M. B. (2005). Indicator mineral methods in mineral exploration. *Geochemistry: Exploration, Environment, Analysis*, 5(3):233–245.

McClenaghan, M. B., Hamilton, S. M., Hall, G. E. M., Burt, A. K., and Kjarsgaard, B. A. (2006). Selective Leach Geochemistry of Soils Overlying the 95-2, B30, and A4 Kimberlites, Northeastern Ontario. Technical report.

McClenaghan, M. B. and Kjarsgaard, B. A. (2001). Indicator mineral and geochemical methods for diamond exploration in glaciated terrain in Canada. *Geological Society, London, Special Publications*, 185(1):83–123.

McClenaghan, M. B. and Kjarsgaard, B. A. (2007). Indicator Mineral and Surficial Geochemical Exploration Methods for Kimberlite in Glaciated Terrain; Examples From Canada. (5):983–1006.

McClenaghan, M. B., Kjarsgaard, B. A., Kjarsgaard, I. M., Paulen, R. C., and Sterling, J. A. R. (1999a). GEOLOGICAL SURVEY OF CANADA OPEN FILE 3775 Mineralogy and geochemistry of the Peddie kimberlite and associated glacial sediments , Lake Timiskaming , Ontario. Technical report.

McClenaghan, M. B., Kjarsgaard, I. M., and Kjarsgaard, B. A. (2004). Geological Survey of Canada Open File 4822: Kimberlite indicator mineral chemistry and till geochemistry around the Seed and Triple B kimberlites, Lake Timiskaming, Ontario. Technical report, Geological Survey of Canada.

McClenaghan, M. B., Kjarsgaard, I. M., Kjarsgaard, B. A., Sterling, J. A. R., Pringle, G., and Berger, B. (1999b). GEOLOGICAL SURVEY OF CANADA OPEN FILE 3769 Mineralogy and geochemistry of the A4 kimberlite and associated glacial sediments, Kirkland Lake, Ontario. Technical report.

McClenaghan, M. B., Kjarsgaard, I. M., Sterling, J. A. R., Pringle, G., Kjarsgaard, B. A., and Berger, B. (1999c). GEOLOGICAL SURVEY OF CANADA OPEN FILE 3719 Mineralogy and geochemistry of the C14 kimberlite and associated glacial sediments, Kirkland Lake, Ontario. Technical report.

McClenaghan, M. B., Layton-Matthews, D., and Matile, G. (2011). Till geochemical signatures of magmatic Ni–Cu deposits, Thompson Nickel Belt, Manitoba, Canada. *Geochemistry: Exploration, Environment, Analysis*, 11(2):145–159.

McClenaghan, M. B. and Paulen, R. C. (2018). *Application of Till Mineralogy and Geochemistry to Mineral Exploration*.

McClenaghan, M. B., Paulen, R. C., and Oviatt, N. M. (2018). Geometry of indicator mineral and till geochemistry dispersal fans from the Pine Point Mississippi Valley-type Pb-Zn district , Northwest Territories , Canada. *Journal of Geochemical Exploration*, 190(June 2017):69–86.

McClenaghan, M. B., Plouffe, A., McMartin, I., Campbell, J. E., Spirito, W. A., Paulen, R. C., Garrett, R. G., and Hall, G. E. M. (2013). Till sampling and geochemical analytical protocols used by the Geological Survey of Canada. *Geochemistry: Exploration, Environment, Analysis*, 13(4):285–301.

McGlynn, J. C. and Henderson, J. B. (1970). Archean Volcanism and Sedimentation in the Slave Structural Province. (1):31–44.

McLean, J. E. and Bledsoe, B. E. (1992). Behavior of Metals in Soils. Technical report.

McMartin, I. and McClenaghan, M. B. (2001). Till geochemistry and sampling techniques in glaciated shield terrain: a review. *Geological Society, London, Special Publications*, 185(1):19–43.

Ming, D., Morris, R., and Clark, B. (2007). Chatper 23: Aqueous Alteration on Mars. In *The Martian Surface: Composition, Mineralogy, and Physical Properties*, page 636. J.f. bell edition.

Mitchell, R. H. (1986). *Kimberlites: Mineralogy, Geochmistry, and Petrology*. Plenum Publishing Corporation.

Mitchell, R. H. (1995). *Kimberlites, Orangeites, and Related Rocks*. Spring Science+Business Media New York.

Mitchell, R. H. and Scott Smith, B. H. (2017). Mineralogy of Kimberley-type Pyroclastic Kimberlite and the Transition to Hypabyssal Kimberlite. (11):2–4.

Muntener, C. and Gaudet, M. (2018). Geology of the Renard 2 pipe to 1000 m depth, Renard Mine, Québec, Canada: insights into Kimberley-type pyroclastic kimberlite emplacement. *Mineralogy and Petrology*, 112:421–432.

Muntener, C. and Scott Smith, B. H. (2013). Economic Geology of Renard 3, Quebec, Canada: A Diamondiferous, Multi-Phase Pipe Infilled with Hypabyssal and Tuffisitic Kimberlite. *Proceedings of 10th International Kimberlite Conference*, 2.

Nesbitt, H. W. and Young, G. M. (1984). Prediction of some weathering trends of plutonic and volcanic rocks based on thermodynamic and kinetic considerations. *Geochimica et Cosmochimica Acta*, 48(7):1523–1534.

Noble, R. R. P., Lintern, M. J., Townley, B., Anand, R. R., Gray, D. G., and Reid, N. (2013). Metal migration at the North Miitel Ni sulphide deposit in the southern Yilgarn Craton: Part 3, gas and overview. *Geochemistry: Exploration, Environment, Analysis*, 13(2):99–113.

Noble, R. R. P., Morris, P. A., Anand, R. R., Lau, I. C., and Pinchand, G. T. (2019). Application of ultrafine fraction soil extraction and analysis for mineral exploration. *Geochemistry: Exploration, Environment, Analysis*, (2015).

Noble, R. R. P., Seneshen, D. M., Lintern, M. J., Anand, R. R., Pages, A., and Pinchand, G. T. (2018). Soil-gas and weak partial soil extractions for nickel exploration through transported cover in Western Australia. *Geochemistry: Exploration, Environment, Analysis*, 18:31–45.

Padgham, W. A. and Fyson, W. K. (1991). The Slave Province: a distinct Archean craton. *Canadian Journal of Earth Sciences*, 29:2072–2086.

Palandri, J. L. and Reed, M. H. (2004). Geochemical models of metasomatism in ultramafic systems: Serpentinization, rodingitization, and sea floor carbonate chimney precipitation. *Geochimica et Cosmochimica Acta*, 68(5):1115–1133.

Parent, M., Paradis, S. J., and Doiron, A. (1996). Palimpsest glacial dispersal trains and their significance for drift prospecting. *Journal of Geochemical Exploration*, 56(2):123–140.

Paterson, S. R. and Fowler, T. K. (1993). Re-examining pluton explacement processes. *Journal of Structural Geology*, 15(2):191–206.

Paulen, R. C., McClenaghan, M. B., and Hicken, A. K. (2013). Regional and local ice-flow history in the vicinity of the Izok Lake Zn-Cu-Pb-Ag deposit, Nunavut. *Canadian Journal of Earth Sciences*, 50:1209–1222.

Pehrsson, S. J., van Breemen, O., and Hanmer, S. (1993). Ages of diabase dyke intrusions, Great Slave Lake shear zone, Northwest Territories. pages 23–28.

Pell, J. A. (1997). Kimberlites in the Slave Craton, Northwest Territories, Canada. *Geoscience Canada*, 24(2):77–90.

Peltier, L. C. (1950). The Geographic Cycle in Periglacial Regions as It is Related to Climatic Geomorphology. *Annals of the Association of American Geographers*, 40:214–236.

Percival, J. A. and Pysklywec, R. N. (2007). Are Archean lithospheric keels inverted? *Earth and Planetary Science Letters*, 254:393–403.

Power, M., Belcourt, G., and Rockel, E. (2004). Geophysical methods for kimberlite exploration in northern Canada. *The Leading Edge*, 23(11):1124–1129.

Power, M. and Hildes, D. (2007). Geophysical strategies for kimberlite exploration in northern Canada. *Procedings of Exploration 07: Fifth Decennial International Conference on Mineral Exploration*, pages 1025–1031.

Rate, A. W. (2010). Formation of soil geochemical anomalies by plant uptake of trace elements. *19th World Congress of Soil Science, Soil Solutions for a Changing World*, August:86–89.

Renaud, J., Maclachlan, K., and Cairns, S. R. (2002). Stratigraphy and structure of the Aylmer Lake volcanic belt and surrounding metasedimentary rocks , Northwest Territories. Technical report.

Rich, S. D. (2016). *Geochemical mapping of porphyry deposits and associated alteration through transported overburden*. PhD thesis.

Ridley, W. I. (2005). Plumbo-Isotopy : The Measurement of Lead Isotopes by Multi-Collector Inductively Coupled Mass Spectrometry. Technical report.

Rukhlov, A. S. and Ferbey, T. (2015). Application of lead isotopes in till for mineral exploration: a simplified method using ICP-MS. Technical report.

Sacco, D., McKillop, R., Ward, B. C., and Ellis, S. (2018). Surficial Geology and Till Sampling Suitability for NTS Map Sheets 075M09, parts of 075N05/06/11/12 , and parts of 075D05/06/10/11/12, Slave Geological Province, Northwest Territories. Technical report.

Sader, J. A., Hattori, K. H., Kong, J. M., Hamilton, S. M., and Brauneder, K. (2011). Geochemical responses in peat groundwater over Attawapiskat kimberlites, James Bay Lowlands, Canada and their application to diamond exploration. *Geochemistry: Exploration, Environment, Analysis*, 11(3):193–210.

Sader, J. A., Ii, H. S. A., Fenstermacher, R. F., and Hattori, K. (2009). Imaging a buried diamondiferous kimberlite using conventional geochemistry and Amplified Geochemical Imaging Technology [extended abstract]. *Proceedings of the 24th International Applied Geochemistry Symposium, Fredericton, Extended Abstracts*, 2:581–584.

Sader, J. A., Leybourne, M. I., and McClenaghan, M. B. (2007). Low-temperature serpentinization processes and kimberlite groundwater signatures in the Kirkland Lake and Lake Timiskiming kimberlite fields , Ontario , Low-temperature serpentinization processes and kimberlite groundwater signatures in the Kirkland Lake. *Geochemistry: Exploration, Environment, Analysis*, 7:3–21.

Schmidberger, S. S., Simonetti, A., and Francis, D. (2001). Sr-Nd-Pb isotope systematics of mantle xenoliths from Somerset Island kimberlites : Evidence for lithosphere stratification beneath Arctic Canada. *Geochimica et Cosmochimica Acta*, 65(22):4243–4255.

Schwedt, G. (2001). *The essential guide to environmental chemistry*.

Scott Smith, B. H., Nowicki, T., and Mitchell, R. H. (2013). Kimberlite Terminology and Classification. *Special Issue of the Journal of the Geological Society of India*, 2(January):17.

Seneshen, D. M., Grunsky, E. C., Rencz, A., Hall, G. E. M., and Dunn, C. E. (2001). Geochemical orientation surveys (fiscal year 2000-2001) for kimberlites in northern Alberta. Technical report.

Sharpe, D. R., Kjarsgaard, B. A., Knight, R. D., Russell, H. A. J., and Kerr, D. E. (2017). Glacial dispersal and flow history, East Arm area of Great Slave Lake, NWT, Canada. *Quaternary Science Reviews*, 165:49–72.

Sharpe, D. R., Russell, H. A. J., and Knight, R. D. (2013). Glaciofluvial features and their significance in the proposed national park reserve, East Arm of Great Slave Lake. Technical report, Geological Survey of Canada, Open File 7196.

Shilts, W. W. (1971). Till studies and their application to regional drift prospecting. *Canadian Mining Journal*, 92(4):45–50.

Shilts, W. W. (1993). Geological Survey of Canada's contributions to understanding the composition of glacial sediments. *Canadian Journal of Earth Sciences*, 30(2):333–353.

Shilts, W. W. (1995). Geochemical Partitioning in Till. *Drift Exploration in the Canadian Cordillera*, 2:149–163.

Simonetti, A., Bell, K., and Hall, G. E. M. (1996). Pb isotopic ratios and elemental abundances for selective leachates from near-surface till: implications for mineral exploration. *Applied Geochemistry*, 11:721–734.

Sircombe, K. N., Bleeker, W., and Stern, R. A. (2001). Detrital zircon geochronology and grain-size analysis of a ∼2800 Ma Mesoarchean proto-cratonic cover succession, Slave Province, Canada. *Earth and Planetary Science Letters*, 189:207–220.

Smee, B. W. (1999). Theory behind the use of soil pH measurements as an inexpensive guide to buried mineralization, with examples. (1):1–14.

Smee, B. W. (2009). Soil micro-layer, airborne particles, and pH: the Govett connection. *Proceedings of the 24th International Applied Geochemistry Symposium*, pages 91–95.

Smith, C. B. (1983). Pb, Sr, Nd isotopic evidence for sources of southern African Cretaceous kimberlites. *Nature*, 304(7):51–54.

Smith, C. B., Sims, K., Chimuka, L., Duffin, A., Beard, A. D., and Townend, R. (2004). Kimberlite metasomatism at Murowa and Sese pipes, Zimbabwe. *Lithos*, 76(1-4 SPEC. ISS.):219–232.

Soil Classification Working Group (1998). The Canadian System of Soil Classification. Technical report, National Research Council of Canada.

Sparks, R. S. J., Baker, L., Brown, R. J., Field, M., Schumacher, J., Stripp, G., and Walters, A. (2006). Dynamical constraints on kimberlite volcanism. *Journal of Volcanology and Geothermal Research*, 155:18–48.

Spirito, W. A., McClenaghan, M. B., Plouffe, A., Mcmartin, I., Campbell, J. E., Paulen, R. C., Garrett, R. G., and Hall, G. E. M. (2011). Till Sampling and Analytical Protocols for GEM Projects : from field to archive. *Geological Survey of Canada*, (Open File 6850):73.

Stanley, C. R. (2017). Molar Element Ratio Analysis of Lithogeochemical Data: A Toolbox for Use in Mineral Exploration and Mining. In Tschirhart, V. and Thomas, M., editors, *Proceedings of Exploration 17: Sixth Decennial International Conference on Mineral Exploration*, volume 33, pages 471–494.

Stubley, M. (2005). Slave Craton : Interpretive Bedrock Compilation; Digital files and 2 maps. Technical report.

Stubley, M. (2015). Bedrock Hosts to the Kelvin-Farada, MZ and Doyle Kimberlite Bodies, Southeastern Slave Craton. Accompanies three bedrock geological maps. Internal Report. Technical report.

Sutherland, D. (2018). A Spatiotemporal Geochemical Hydrocarbon Interpretation for NWT Geoscience Kimberlite SGH Project. Technical report.

Tan, K. H. (1998). *Principles of Soil Chemistry*. Marcel Dekker Inc, 3 edition.

Tappert, M. C., Rivard, B., Fulop, A., Rogge, D., Feng, J., Tappert, R., and Stalder, R. (2015). Characterizing kimberlite dilution by crustal rocks at the Snap Lake diamond mine (Northwest Territories, Canada) using SWIR (1.90-2.36 µm) and LWIR (8.1-11.1 µm) hyperspectral imagery collected from drill core. *Economic Geology*, 110(6):1375–1387.

Tappert, M. C. and Tappert, R. (2018). Novel exploration tools : Using reflectance spectroscopy to detect hydration halos around kimberlites. Technical Report September.

Thorpe, R. I., Cumming, G. L., and Mortensen, J. K. (1992). A Significant Pb Isotope Boundary in the Slave Province and its Probably Relation to Ancient Basement in the Western Slave Province. Technical report.

Tosdal, R. M., Wooden, J. L., and Bouse, R. M. (1999). Pb Isotopes, Ore Deposits, and Metallogenic Terranes. In *Application of Radiogenic Isotopes to Ore Deposit Research and Exploration*, volume 12.

Van Breemen, O., Davis, W. J., and King, J. E. (1992). Temporal distribution of granitoid plutonic rocks in the Archean Slave Province, northwest Canadian Shield. *Canadian Journal of Earth Sciences*, 29:2186–2199.

Vivian, G. and Nowicki, T. (2017). 2016 Technical Report; Project Exploration Update and Maiden Mineral Resources Estimate, Kennady North Project, Northwest Territories, Canada. Technical report.

Vivian, G., Revering, C., and Hetman, C. (2019). 2019 Technical Report, Project Exploration and Faraday Inferred Resource Estimate Update, Kennady North Project, Northwest Territories, Canada. Technical report, Mountain Province Diamonds.

Vivian, G. and Wyllie, R. (2012). TECHNICAL REPORT 2012 KENNADY LAKE NORTH - Northwest Territories , Canada Kennady Diamonds Inc . Technical report.

Walker, D. A., Epstein, H. E., Gould, W. A., Kelley, A. M., Kade, A. N., Knudson, J. A., Krantz, W. B., Michaelson, G., Peterson, R. A., Ping, C. L., Raynolds, M. K., Romanovsky, V. E., and Shur, Y. (2004). Frost-boil ecosystems: Complex interactions between landforms, soil, vegetation and climate. *Permafrost and Periglacial Processes*, 15(2):171–188.

Weis, D. and Demaiffe, D. (1985). A depleted mantle source for kimberlites from Zaire : Nd , Sr and Pb isotopic evidence. *Earth and Planetary Science Letters*, 73:269–277.

Wilkinson, L., Kjarsgaard, B. A., Lecheminant, A. N., and Harris, J. (2001). Diabase dyke swarms in the Lac de Gras area, Northwest Territories, and their significance to kimberlite exploration: initial results. *Current*.

Appendices

Appendix A

Methodologies

A.1 Soil Sampling

Equipment List:

- GPS
- Camera
- Steel mattock pick (paint removed)
- Spade shovel (paint removed)
- Plastic trowel
- ExTech Soil Moisture Meter MO750
- Soil horizon markers
- Measuring tape or sewing tape
- Stainless steel 6.3 mm ($^1/_4$ inch) sieve
- Plastic 5 x 8 inch 8 MIL poly sample bags
- Plastic 8 x 14 inch 6 MIL poly sample bags
- Numbered sample tags with barcodes
- Packaging tape
- Pens and black marker
- Plastic ”rice bags” and 5-gallon buckets for sample transport

- Hand lens
- Flagging tape

Procedure:

1. Select sample size based on predetermined coordinates. Relocate hole if needed accounting for infrastructure and bogs.
2. Describe vegetation, surface materials, and any notable features.
3. Photograph numbered sample tag and sample location with shovel or pick pointing north.
4. With mattock pick and shovel, dig 30 x 30 x 30 cm pit, preserving vegetation cap. Clear profile with plastic trowel to expose representative profile.
5. Identify, mark, and measure all soil horizons. Photograph representative profile with measuring tape. Record color, grain size, structures of B horizon.
6. Measure in situ moisture of B horizon by gently inserting *ExTech Soil Moisture Meter MO750* six centimeters below the contact with overlying A horizon, carefully avoiding creating voids around the probe.
7. Rinse the top, bottom, sides, and pan of the sieve with excavated soil to clean sieve from previous sample and 'pre-contaminate' the equipment.
8. Collect B horizon sample using plastic trowel. Target the upper 10 cm of the B horizon leaving a 1 cm buffer from overlying horizons to avoid contamination. Care must be taken for thin B horizons, high clast content, and mottled or broken horizons. Sieve 1 kg of sample and place in 8 x 14 inch plastic sample bag. Insert barcoded sample tag into bag and seal with packaging tape. Label outside of sample bag and store in "rice bag" or 5-gallon bucket for transportation.
9. Collect 0.25 kg of B horizon following Step 8 procedures. Place in 5 x 8 inch sample bag, label, and store for SGH analysis.
10. Record clast abundance, lithology, and rounding from +6.3 mm fraction.
11. Backfill hole and replace vegetation cap to minimize landscape disturbance.
12. Clean trowel, shovel, pick, and moisture meter between sites.
13. Field duplicates are taken nearly every 20 samples. Duplicate pit should be no more than three meters from original pit, and follow the same sampling procedure.
14. Certified Reference Materials (CRM) are inserted every 20 samples. Sample tags should be skipped and packaged with CRM at a later time.

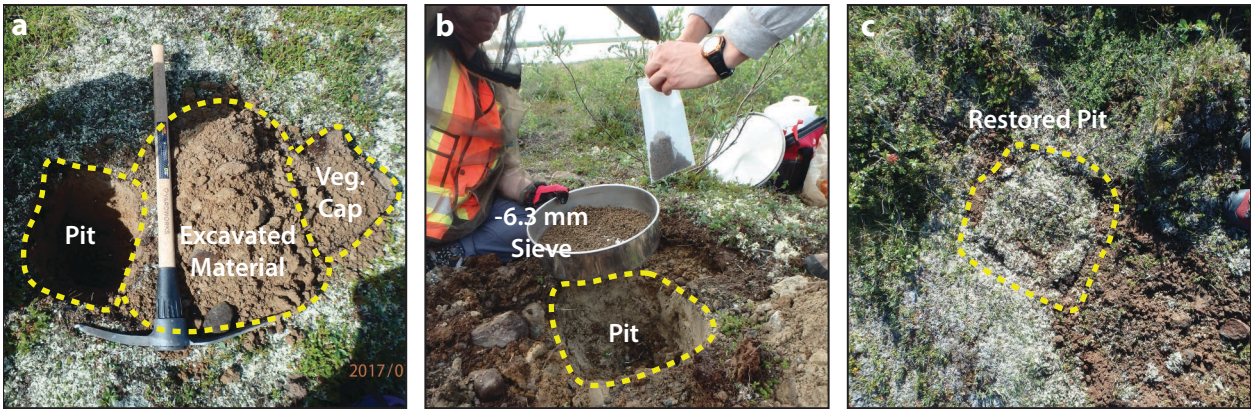

Figure A.1: **(a)** Excavated pit with preserved vegetation cap. **(b)** Packaging sieved material for SGH analysis. **(c)** Restored pit with replaced vegetation cap.

A.2 Physicochemical Measurements

Equipment List:

- Nitrile gloves
- Eutech Instruments Oakton Multi-Parameter PTTestr^{TM} 35 pH & TDS Meter
- Oakton pH 7.00 & 4.01 buffer - 20mL packets
- Oakton 1413 μS/cm Conductivity Standard - 20mL packets
- Oakton Waterproof ORP Test 10 Meter with Ag/AgCl electrode and 3M KCl electrolyte
- YSI 3682 Zobell ORP Calibration Solution
- 100 mL plastic cups
- Deionized water
- 15 mL measuring spoon
- Stir rod
- Dropper bottle 10% hydrochloric acid
- Kim wipes

Procedure:

1. The *Oakton Multi-Parameter PTTestr^{TM} 35 pH & TDS Meter* is calibrated twice a day using the *Oakton pH 4.01 and 7.00 buffer 20 mL packets* following instrument instructions. Conductivity is calibrated using *Oakton 1413 μS/cm Conductivity Standard 20mL packets*.

2. The Oakton ORP Test 10 Meter is calibrated twice a day following instrument instructions using YSI 3682 Zobell Calibration Solution.
3. Soil physicochemical property measurements were conducted at UBC after -180μm sieved and dried soil sample splits were returned from commercial analysis by ALS Minerals.
4. Wearing nitrile gloves, mix 30 mL of soil and 30 mL of deionized water in plastic cup and stir for 30 seconds.
5. Insert Oakton Multi-Parameter PTTestr^{TM} 35 pH & TDS Meter and record pH and TDS allowing 60 seconds to stabilize.
6. For select samples, insert Oakton ORP Test 10 Meter and record ORP value after 60 seconds of stabilization. Remove and rinse with tap water.
7. Add one drop of 10% hydrochloric acid from an acid dropper bottle and stir for 15 seconds.
8. Rinse Oakton Multi-Parameter PTTestr^{TM} 35 Meter with deionized water and reinsert into slurry. Record pH and TDS after 60 seconds.
9. Empty slurry into proper sediment disposal system and rinse meter, stir rod, plastic cup, measuring spoon with tap water followed by deionized water.
10. Perform a lab duplicate every 20 samples (5%) following the same procedure.

A.3 Sieving

Procedure:

1. Select soils were sieved conducted at UBC after -180μm sieved and dried soil sample splits were returned from commercial analysis by ALS Minerals.
2. Arrange desired sieves ($\leq$7 sieves) in the *Gilson GilSonic Ultrasiever GA-8*.
3. Measure approximately 80 g of sample into top sieve.
4. Run the Ultrasiever at 3600 pulses per minute at 50 / 60 Hz and at an amplitude of 33 (0 - 99 unitless scale) for 30 minutes.
5. Individually remove, weigh, label, and package sieved fractions for shipment for multi-element geochemical analyses at commercial laboratory.
6. Rinse sieves with water, and place in *Limplus Ultrasonic Cleaner LS-10D* for two minutes at 40,000 Hz and 25°C.
7. Completely air dry sieves, or gently use air hose.

A.4 Geochemical Analyses - ALS Minerals

Geochemical analyses on both soils and core were executed by ALS Minerals in North Vancouver. Detailed digestion and analytical procedures were provided by Katerina Paley, Client Services Manager, Geochemistry, Western Canada, ALS Minerals. All soils were prepared using PREP-41: drying at <60°C and sieved to -180 μm (80 mesh). The coarse +180 μ fraction was stored and returned the the author, the -180 μ fraction was analyzed and excess sample was returned to author for storage. Two-inch drill core was cut by the author at UBC. Half was returned to KDI, $^1/_4$ delivered to ALS Minerals for analysis, and $^1/_4$ delivered to Corescan in Denver, Colorado for hyperspectral analysis. Core analyzed by ALS Minerals was prepared according to PREP-31B: crush 70% <2 mm, rifle split,and pulverize 1000 g to 85% <75 μm.

A.4.1 ME-MS41L - Aqua Regia ICP-MS

A sample aliquot of 0.5 g is digested in a graphite heated block with a 3:1 ratio of HCl:HNO_3. The solution is analyzed by *Super Trace* inductively coupled plasma - mass spectrometry (ICP-MS) for ultra-low detection limits ideal in generative exploration using soils and sediment. Results are corrected for spectral inter-elemental interferences. Solutions can also be analyzed by inductively coupled plasma - atomic emission spectrometry (ICP-AES) to return major oxides.

A.4.2 ME-MS61L - Four Acid ICP-MS

A 0.25 g aliquot is first digested using 1.5 mL HNO_3 and $HClO_4$, followed by HF acid. The solution is dried at 185°C and leached with 50% HCl. Prior to analysis by ICP-MS and/or ICP-AES, the solution may be diluted with additional weak HCl. Final results are corrected for inter-element spectral interferences.

A.4.3 C-IR06a - Organic Carbon

A sample aliquot (0.10 - 0.20 g) is digested in boiling dilute HCl acid to remove carbonate-based carbon. Organic carbon is filtered from the solution with a Leco crucible. The crucible is washed with deionized water, dried, and analyzed by direct combustion and infrared absorption in an oxygen steam by high frequency Leco induction furnace. Results are processed and reported to a lower limit of detection of 0.01% organic carbon.

A.4.4 PbIS-RAT61 - Pb Isotope Ratios by Four Acid ICP-MS

Following the same four acid digestion procedure (ME-MS61L), a 0.5 g aliquot is digested by four acids: $HClO_4$ and HF, followed by HNO_3, and finally leached by HCl at 185°C. The solution is then diluted with 10% HCl to 25 mL. High precision isotope ICP-MS analyzes the solution and reports six Pb isotope ratios. Internal and certified Pb isotope standard materials are used to audit accuracy and precision. For a suitable analysis, total Pb concentration of the sample must exceed 2 ppm. The analytical method can be paired with various digestion methods for soils, sediment, and rock (e.g. Modified Weak Aqua Regia).

A.4.5 ME-MS41W - Modified Weak Aqua Regia ICP-MS

ME-MS41W is a weak digestion method modified from a traditional aqua regia digestion. A 0.5 g aliquot is digested in a graphite heat block by a HCl:HNO_3 1:1 ratio. The solution is analyzed by ICP-MS for ultra-low detection limits and results are corrected for spectral inter-elemental interferences.

A.4.6 ME-MS03-07 - Sequential Extraction

The following analyses are performed in sequential order on each sample. After each extraction, the final solution in separated from the solids by centrifuging and decanting. The supernatant solution is then analyzed by pH electrode and ICP-MS for ultra-low detection limits and results are corrected for spectral inter-elemental interferences.

1. ME-MS03 - Deionized Water Leach. A 1.0 g aliquot is leached with deionized water at 60°C for two hours.
2. ME-MS04 - Ammonium Acetate Leach. Sample is leached with a 1:40 ratio of ammonium acetate solution in acetic acid and shaken for two hours.
3. ME-MS05 - Cold Hydroxylamine Hydrochloride. At room temperature, sample is leached in a 1:25 ratio of hydroxylamine hydrochloride solution and rolled for two hours.
4. ME-MS06 - Hot Hydroxylamine Hydrochloride. Sample is leached in a 1:25 ratio of hydroxylamine hydrochloride solution. The sample is placed in a 60°C water bath for two hours before centrifuging.
5. ME-MS07 - Sodium Pyrophosphate. The sample is mixed with sodium pyrophosphate at 1:25 ratio and rolled for one hour at room temperature.

A.4.7 MS41W-PbIS - Pb Isotope by Modified Weak Aqua Regia ICP-MS

MS41W-PbIS is an supplemental analysis added to a digestion and ICP-MS analysis of soils, sediment or rock. Following traditional digestion protocols, concentrations of four Pb isotopes (204, 206, 207, 208) are analyzed by ICP-MS with a 0.005 ppm lower limit of detection. Results are corrected for mass bias, however ^{204}Pb and ^{204}Hg interference corrections are not accounted for. This package was paired with a modified weak aqua regia digestion of core samples.

A.4.8 ME-MS81d - Lithium Borate Fusion ICP

ME-MS81d consists lithium borate fusion followed by both trace element analysis by ICP-MS and major oxides by ICP-AES. Trace element analysis begins with mixing $LiBO_2$/LiB_4O_7 (lithium borate/lithium tetraborate flux) with 0.100 g of sample. The mixture is fused at 1025°C, cooled, and dissolved in a mixture of HNO_3, HCl, and HF. Anlysis of the solution is completed by ICP-MS. Lithium borate fusion is revered as a total digestion method, however some resistate minerals may not be fully digested including ziron, some metal oxides, some REE-phosphates, and some sulfides.

Lithium borate fusion ICP-AES analysis mixes lithium borate/lithium tetraborate flux with 0.100 g of sample and fused at 1000°C. After cooling, the material is dissolved in 100 mL of 4% HNO_3 and 2% HCl and analyzed by ICP-AES. Results are corrected for inter-element spectral interferences and reported as oxide concentration. LOI) is measured by heating a 1.0 g sample to 1000°C for one hour by furnace or thermogravimetric analysis (TGA). The final mass is measured to determine the difference in weight and mass loss.

A.4.9 C-IR07 - Total Carbon

A sample aliquot (0.10 g) is placed in a Leco crucible and washed with deionized water, dried, and analyzed by direct combustion and infrared absorption in an oxygen steam by high frequency Leco induction furnace. Results are processed and reported to a lower limit of detection of 0.01% total carbon.

A.5 Spatiotemporal Geochemical Hydrocarbons (SGH)

B horizon soil samples were analyzed by Activation Laboratories Ltd. (ActLabs) in Ancaster, Ontario. The samples are dried at <60°C and sieved to -250 μm (60 mesh). A very weak leach (nearly aqueous) extracts surface-bound and interstitial hydrocarbons compounds, which are separated into 162 hydrocarbon compounds by high resolution gas chromatography (HR-GC) and analyzed by mass spectrometry (MS) with a 1 ppt detection limit. Reported compounds range from the $C_(5)$ - C_{17} carbon series. Additional details can be found in the ActLabs Interpretation Report (Appendix C).

Appendix B

QA/QC

B.1 Slurry QAQC

The QA/QC protocol for the soil slurry measurements included calculating the MPD (%) for field duplicate pairs, and is included in this section.

Soil Slurry Duplicate MPD (%)

		Field Dup Pair 1				Field Dup Pair 2			
Analyte	**Units**	**Q515258L**	**Q515258U**	**Mean**	**MPD (%)**	**Q515276**	**Q515277**	**Mean**	**MPD (%)**
pH	s.u.	5.6	5.9	5.75	5.22	5.5	5.6	5.55	1.80
TDS	ppm	20	13	16.5	42.42	21	16	18.5	27.03
Temp	°C	23.3	23.5	23.4	0.85	23.3	23.5	23.4	0.85
Acidified pH	s.u.	4.2	4	4.1	4.88	4.3	3.8	4.05	12.35
Acidified TDS	ppm	99	111	105	11.43	126	150	138	17.39

		Field Dup Pair 3				Field Dup Pair 4			
Analyte	**Units**	**Q515308**	**Q515309**	**Mean**	**MPD (%)**	**Q515324**	**Q515325**	**Mean**	**MPD (%)**
pH	s.u.	5.1	5.3	5.2	3.85	4.9	5	4.95	2.02
TDS	ppm	8	8	8	0.00	15	13	14	14.29
Temp (°C)	°C	23.6	23.7	23.65	0.42	22.6	22.8	22.7	0.88
Acidified pH	s.u.	3.8	4.2	4	10.00	3.5	3.5	3.5	0.00
Acidified TDS	ppm	85	55	70	42.86	178	155	166.5	13.81

		Field Dup Pair 5				Field Dup Pair 6			
Analyte	**Units**	**Q515359**	**Q515360**	**Mean**	**MPD (%)**	**Q515381**	**Q515382**	**Mean**	**MPD (%)**
pH	s.u.	4.6	4.7	4.65	2.15	4.4	4.5	4.45	2.25
TDS	ppm	20	15	17.5	28.57	36	35	35.5	2.82
Temp (°C)	°C	22.8	22.9	22.85	0.44	22.8	22.9	22.85	0.44
Acidified pH	s.u.	3.6	3.4	3.5	5.71	3.3	3.5	3.4	5.88
Acidified TDS	ppm	142	123	132.5	14.34	186	151	168.5	20.77

		Field Dup Pair 7				Field Dup Pair 8			
Analyte	**Units**	**Q515421**	**Q515422**	**Mean**	**MPD (%)**	**Q515439**	**Q515440**	**Mean**	**MPD (%)**
pH	s.u.	5.2	5.1	5.15	1.94	5.5	5.6	5.55	1.80
TDS	ppm	11	12	11.5	8.70	6	8	7	28.57
Temp (°C)	°C	22.7	22.6	22.65	0.44	23	23	23	0.00
Acidified pH	s.u.	3.7	3.7	3.7	0.00	3.7	3.5	3.6	5.56
Acidified TDS	ppm	165	172	168.5	4.15	144	202	173	33.53

		Field Dup Pair 9					
Analyte	**Units**	**Q515451**	**Q515452**	**Mean**	**MPD (%)**	**Avg. Mean**	**Averag MPD (%)**
pH	s.u.	5.8	6.2	6	6.67	5.25	3.08
TDS	ppm	10	12	11	18.18	15.50	18.95
Temp (°C)	°C	22.9	23.3	23.1	1.73	23.07	0.67
Acidified pH	s.u.	3.7	4	3.85	7.79	3.74	5.80
Acidified TDS	ppm	130	138	134	5.97	139.56	18.25

B.2 Till Four Acid ICP-MS QAQC

The QA/QC protocol for the till four acid ICP-MS analyses included the analysis of OREAS-25a certified reference material, and the calculation of the MPD (%) for field duplicate pairs. The results of this QA/QC protocol are summarized in this section.

Analytical Results of OREAS-25a certified reference material - Four Acid ICP-MS

SAMPLE	Ag	Al	As	Ba	Be	Bi	Ca	Cd
	ppm	%	ppm	ppm	ppm	ppm	%	ppm
OREAS 25a Certified		8.87		147	1.02	0.35	0.309	
OREAS 25a Indicated	0.168		9.94					0.041
Q515259	0.043	9.51	10.9	166	0.85	0.362	0.31	0.047
Q515279	0.05	9.57	10.4	160	0.92	0.346	0.3	0.041
Q515310	0.045	9.3	11.1	158	0.97	0.349	0.3	0.04
Q515353	0.045	9.36	9.14	159	0.93	0.332	0.3	0.038
Q515361	0.042	9.33	10.05	160	0.95	0.346	0.31	0.049
Q515369	0.046	9.86	9.72	170	1	0.365	0.33	0.044
Q515383	0.047	8.66	10	155	0.89	0.347	0.28	0.041
Q515424	0.036	9.27	9.86	158	0.99	0.313	0.3	0.051
Q515453	0.045	9.19	9.54	163	1.02	0.335	0.31	0.038
Q515476	0.045	9.61	11.65	159	0.83	0.352	0.33	0.043

SAMPLE	Ce	Co	Cr	Cs	Cu	Fe	Ga	Ge
	ppm	ppm	ppm	ppm	ppm	%	ppm	ppm
OREAS 25a Certified	48.9	8.20	115	6.46	33.9	6.60	25.9	
OREAS 25a Indicated								0.22
Q515259	53.7	7.98	116.5	6.89	32	6.65	26.6	0.14
Q515279	51.6	7.8	112	6.79	32	6.62	26.1	0.17
Q515310	51.6	8.01	112	6.9	31.5	6.45	26.7	0.18
Q515353	50.1	7.56	112.5	6.67	29.6	6.57	27.3	0.13
Q515361	51	7.8	112.5	6.68	30.3	6.55	27.6	0.13
Q515369	53.3	8.15	117.5	7.16	32.8	6.92	29.3	0.17
Q515383	47.1	7.63	116.5	5.83	30.5	6.05	27	0.17
Q515424	53.8	7.85	113	6.71	32.6	6.54	26.3	0.16
Q515453	55	7.86	112.5	6.95	32.9	6.47	26.1	0.16
Q515476	50.6	8.29	124.5	7.06	33.7	6.69	29.2	0.05

SAMPLE	Hf	In	K	La	Li	Mg	Mn	Mo
	ppm	ppm	%	ppm	ppm	%	ppm	ppm
OREAS 25a Certified	4.53		0.482	21.8	36.7	0.327	474.433	2.55
OREAS 25a Indicated		0.091						
Q515259	4.77	0.1	0.49	22.7	38.3	0.32	487	2.6
Q515279	4.72	0.097	0.48	23.5	37.5	0.31	483	2.55
Q515310	4.62	0.092	0.47	23.5	39.2	0.31	472	2.58
Q515353	4.73	0.091	0.48	22.9	40.6	0.31	481	2.77
Q515361	4.79	0.087	0.48	23.1	40.8	0.31	474	2.82
Q515369	5.07	0.095	0.51	24.7	42.8	0.33	505	2.89
Q515383	4.45	0.077	0.45	20.7	32.5	0.3	470	2.52
Q515424	4.97	0.101	0.48	24	39.5	0.31	488	2.68
Q515453	5.18	0.104	0.48	24.5	40.3	0.31	486	2.68
Q515476	5	0.089	0.49	23.5	31.2	0.32	497	2.67

SAMPLE	Na	Nb	Ni	P	Pb	Rb	Re	S
	%	ppm	ppm	%	ppm	ppm	ppm	%
OREAS 25a Certified	0.134	22.4	45.8	0.048	25.2	61		0.051
OREAS 25a Indicated								
Q515259	0.135	23.8	45.5	0.0500	24.2	66.1	<0.002	0.06
Q515279	0.135	24.6	47	0.0530	23.8	62.2	<0.002	0.07
Q515310	0.132	24.4	47.1	0.0500	23.3	64	<0.002	0.07
Q515353	0.133	23.5	44.1	0.0500	22.9	62.8	<0.002	0.05
Q515361	0.134	23.6	45.5	0.0510	23	63.3	<0.002	0.05
Q515369	0.142	25	47.6	0.0530	24.4	68.7	<0.002	0.06
Q515383	0.122	23.6	41.7	0.0490	23.7	55.4	<0.002	0.05
Q515424	0.135	24.8	43.9	0.0500	23.5	65.2	<0.002	0.08
Q515453	0.135	25.1	45.1	0.0500	24	66.4	<0.002	0.06
Q515476	0.135	24.7	49.3	0.0540	24.3	66.9	<0.002	0.05

SAMPLE	Sb	Sc	Se	Sn	Sr	Ta	Te	Th
	ppm	ppm	ppm	ppm	ppm	ppm	ppm	ppm
OREAS 25a Certified	0.67	13.7		4.06	48.5	1.60		15.8
OREAS 25a Indicated			2.86				0.10	
Q515259	0.69	14.3	2.6	3.89	48.9	1.78	0.05	16.6
Q515279	0.74	15.2	2.5	4.16	47.4	1.72	0.04	16.95
Q515310	0.72	15.65	2.8	4	47.9	1.71	<0.04	16.8
Q515353	0.65	14.6	2.7	3.83	47.7	1.65	0.06	16.7
Q515361	0.72	14.55	2.3	4.03	48.7	1.66	0.06	16.85
Q515369	0.69	15.7	2.9	4.25	51.5	1.78	0.05	17.6
Q515383	0.64	13.85	2.8	3.67	44.3	1.64	0.05	14.5
Q515424	0.67	14.75	3	4.11	46.2	1.71	0.1	16.15
Q515453	0.68	14.9	2.9	4.11	47.7	1.72	0.07	16.6
Q515476	0.68	15.8	2.8	4.1	50	1.7	0.06	17.05

SAMPLE	Ti	Tl	U	V	W	Y	Zn	Zr	C(org)
	%	ppm	ppm	ppm	ppm	ppm	ppm	ppm	%
OREAS 25a Certified	0.977	0.35	2.94	157	2.10	12.3	44.4		1.561
OREAS 25a Indicated								159	
Q515259	1.04	0.351	2.98	158.5	2.42	13.25	47.5	172.5	0.75
Q515279	1.025	0.346	2.91	158.5	2.36	12.75	46.6	170.5	0.82
Q515310	0.999	0.327	2.85	159	2.24	13.25	46.2	169	0.74
Q515353	1.045	0.341	2.84	156.5	2.51	12.75	44.7	174.5	0.71
Q515361	1.03	0.357	2.87	157	2.51	12.9	45.3	174	0.74
Q515369	1.09	0.364	3.02	167.5	2.63	14.8	48.6	186	0.75
Q515383	0.956	0.33	2.55	152	2.36	11.7	46.7	157.5	0.75
Q515424	0.999	0.325	2.91	160	2.39	12.75	46.8	178.5	0.73
Q515453	0.999	0.366	3.02	160	2.45	13.45	47.9	185.5	0.75
Q515476	1.015	0.349	2.87	166.5	2.35	13.5	48.7	180	0.71

Four Acid - Certified CRM Values - OREAS 25a

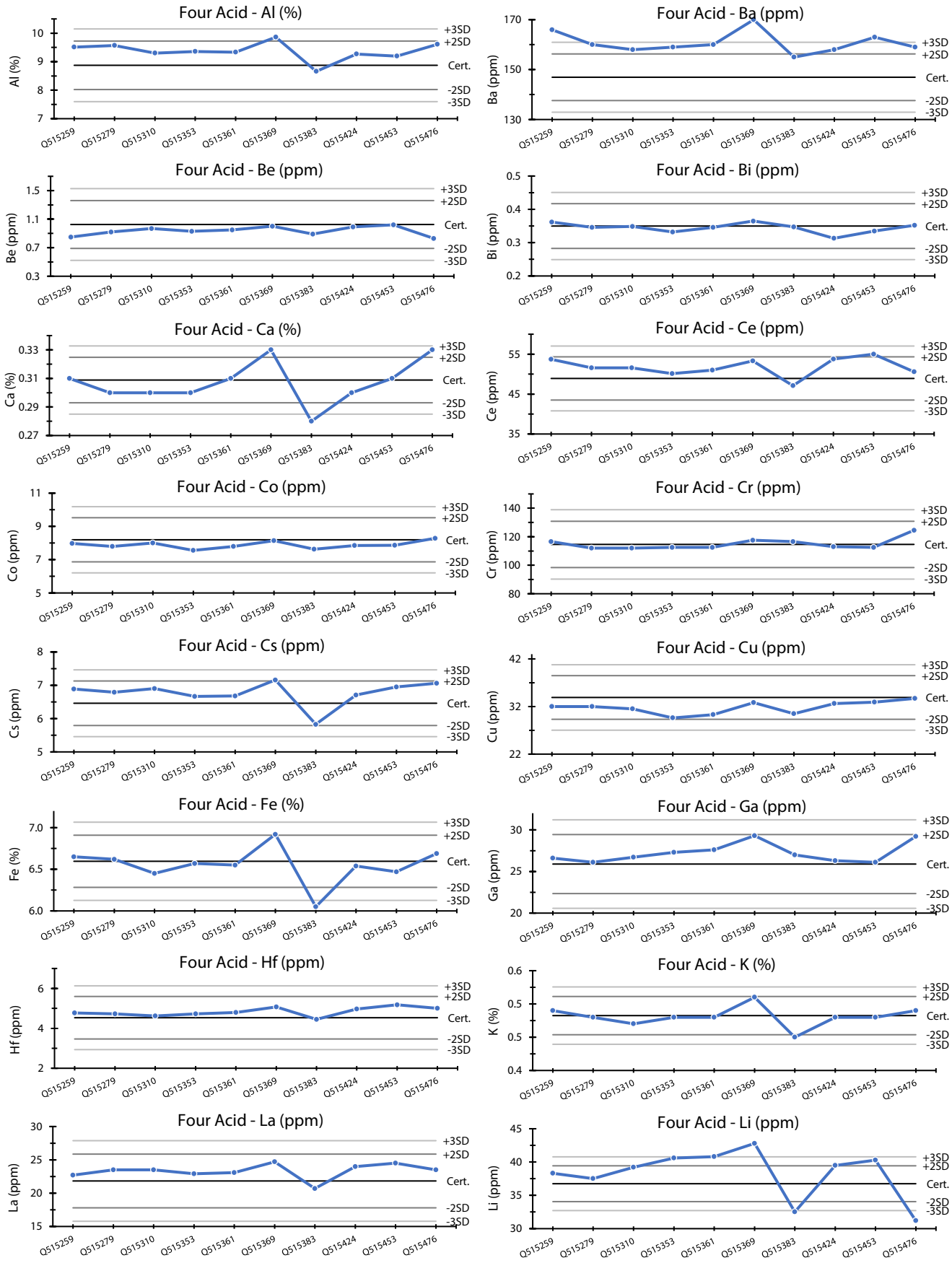

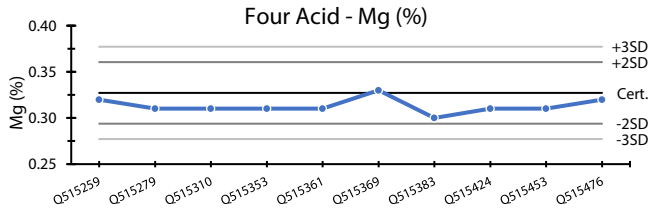
Four Acid - Mg (%)
Mg (%)
0.40
0.35
0.30
0.25
+3SD
+2SD
Cert.
-2SD
-3SD
Q515259
Q515279
Q515310
Q515353
Q515361
Q515369
Q515383
Q515424
Q515453
Q515476

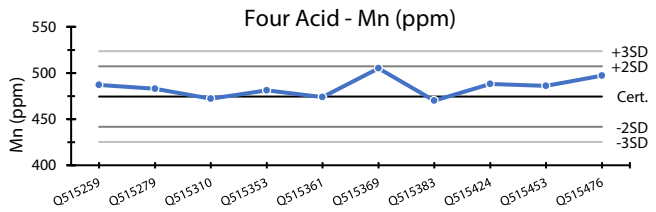
Four Acid - Mn (ppm)
Mn (ppm)
550
500
450
400
+3SD
+2SD
Cert.
-2SD
-3SD
Q515259
Q515279
Q515310
Q515353
Q515361
Q515369
Q515383
Q515424
Q515453
Q515476

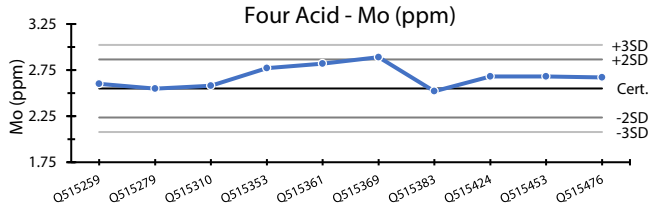
Four Acid - Mo (ppm)
Mo (ppm)
3.25
2.75
2.25
1.75
+3SD
+2SD
Cert.
-2SD
-3SD
Q515259
Q515279
Q515310
Q515353
Q515361
Q515369
Q515383
Q515424
Q515453
Q515476

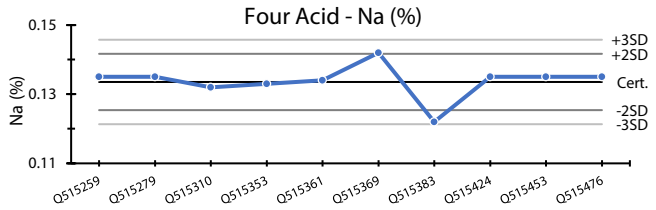
Four Acid - Na (%)
Na (%)
0.15
0.13
0.11
+3SD
+2SD
Cert.
-2SD
-3SD
Q515259
Q515279
Q515310
Q515353
Q515361
Q515369
Q515383
Q515424
Q515453
Q515476

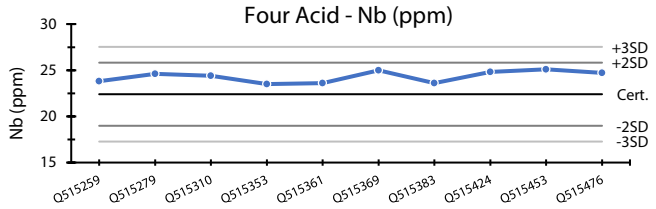
Four Acid - Nb (ppm)
Nb (ppm)
30
25
20
15
+3SD
+2SD
Cert.
-2SD
-3SD
Q515259
Q515279
Q515310
Q515353
Q515361
Q515369
Q515383
Q515424
Q515453
Q515476

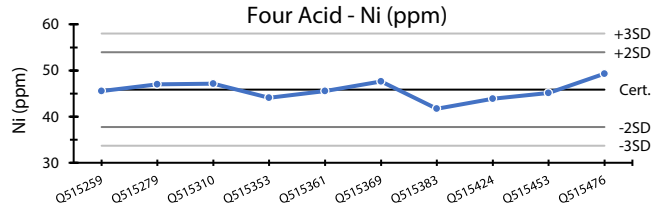
Four Acid - Ni (ppm)
Ni (ppm)
60
50
40
30
+3SD
+2SD
Cert.
-2SD
-3SD
Q515259
Q515279
Q515310
Q515353
Q515361
Q515369
Q515383
Q515424
Q515453
Q515476

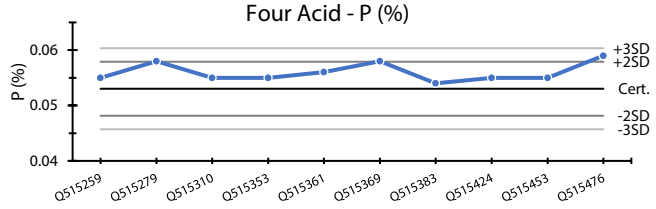
Four Acid - P (%)
P (%)
0.06
0.05
0.04
+3SD
+2SD
Cert.
-2SD
-3SD
Q515259
Q515279
Q515310
Q515353
Q515361
Q515369
Q515383
Q515424
Q515453
Q515476

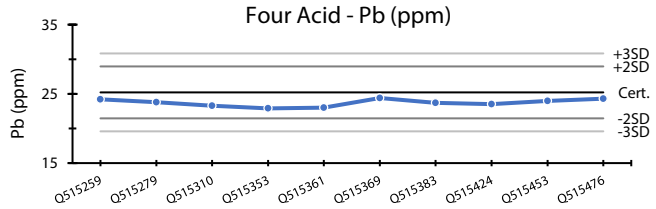
Four Acid - Pb (ppm)
Pb (ppm)
35
25
15
+3SD
+2SD
Cert.
-2SD
-3SD
Q515259
Q515279
Q515310
Q515353
Q515361
Q515369
Q515383
Q515424
Q515453
Q515476

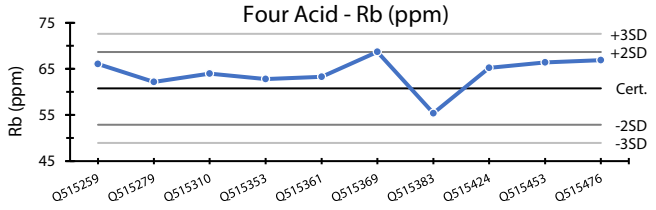
Four Acid - Rb (ppm)
Rb (ppm)
75
65
55
45
+3SD
+2SD
Cert.
-2SD
-3SD
Q515259
Q515279
Q515310
Q515353
Q515361
Q515369
Q515383
Q515424
Q515453
Q515476

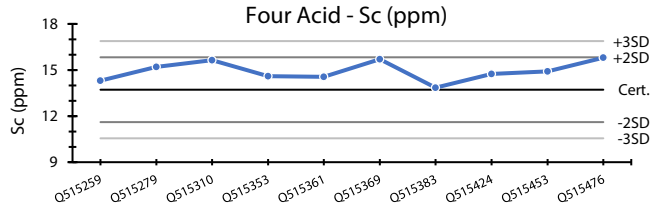
Four Acid - Sc (ppm)
Sc (ppm)
18
15
12
9
+3SD
+2SD
Cert.
-2SD
-3SD
Q515259
Q515279
Q515310
Q515353
Q515361
Q515369
Q515383
Q515424
Q515453
Q515476

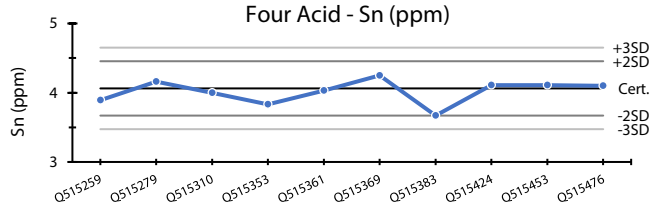
Four Acid - Sn (ppm)
Sn (ppm)
5
4
3
+3SD
+2SD
Cert.
-2SD
-3SD
Q515259
Q515279
Q515310
Q515353
Q515361
Q515369
Q515383
Q515424
Q515453
Q515476

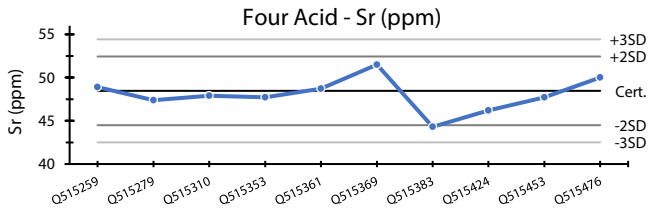
Four Acid - Sr (ppm)
Sr (ppm)
55
50
45
40
+3SD
+2SD
Cert.
-2SD
-3SD
Q515259
Q515279
Q515310
Q515353
Q515361
Q515369
Q515383
Q515424
Q515453
Q515476

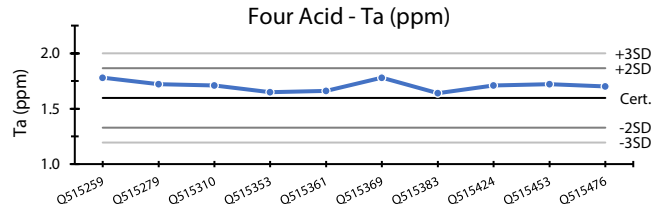
Four Acid - Ta (ppm)
Ta (ppm)
2.0
1.5
1.0
+3SD
+2SD
Cert.
-2SD
-3SD
Q515259
Q515279
Q515310
Q515353
Q515361
Q515369
Q515383
Q515424
Q515453
Q515476

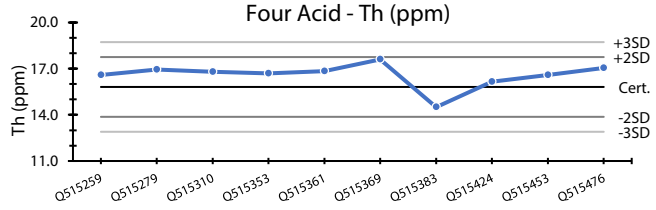
Four Acid - Th (ppm)
Th (ppm)
20.0
17.0
14.0
11.0
+3SD
+2SD
Cert.
-2SD
-3SD
Q515259
Q515279
Q515310
Q515353
Q515361
Q515369
Q515383
Q515424
Q515453
Q515476

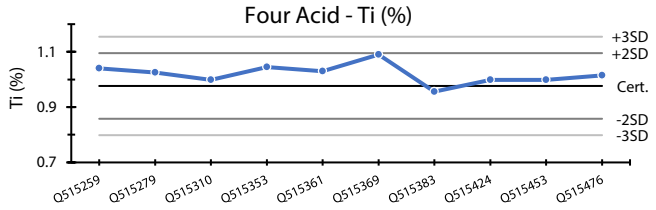
Four Acid - Ti (%)
Ti (%)
1.1
0.9
0.7
+3SD
+2SD
Cert.
-2SD
-3SD
Q515259
Q515279
Q515310
Q515353
Q515361
Q515369
Q515383
Q515424
Q515453
Q515476

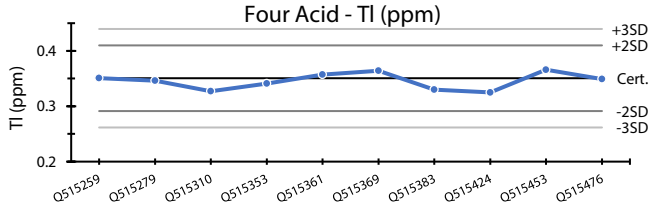
Four Acid - Tl (ppm)
Tl (ppm)
0.4
0.3
0.2
+3SD
+2SD
Cert.
-2SD
-3SD
Q515259
Q515279
Q515310
Q515353
Q515361
Q515369
Q515383
Q515424
Q515453
Q515476

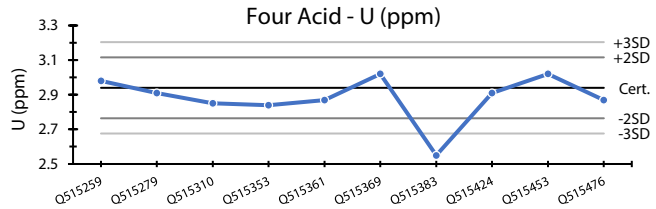

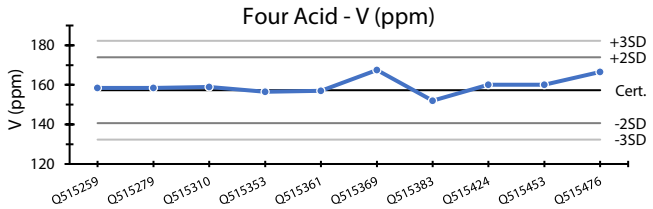

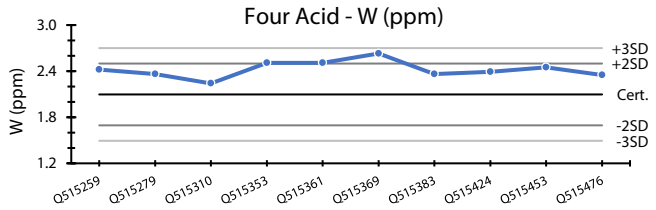

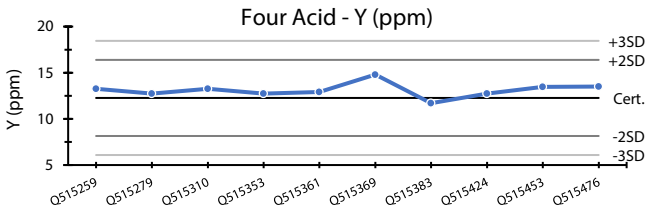

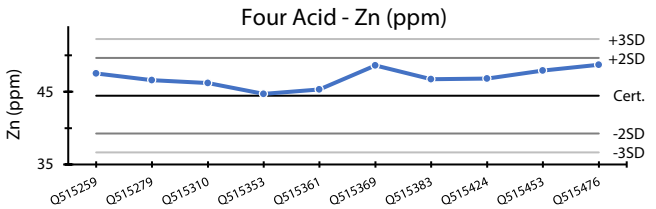

Four Acid - Indicated CRM Values - OREAS 25a

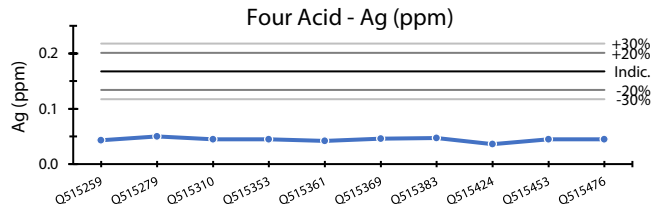

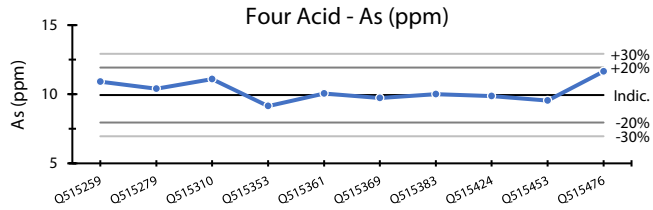

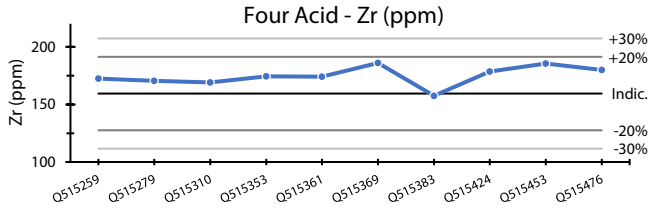

Cd, Ge, In, Re, S, Sb, Se, and Te are excluded as >50% of their values are under ten times the lower limit of detection.

Till Four Acid ICP-MS Field Duplicate MPD (%)

		Duplicate Pair 1				Duplicate Pair 2			
		Q515258L	Q515258U	Mean	MPD (%)	Q515276	Q515277	Mean	MPD (%)
Ag	ppm	0.042	0.04	0.041	4.88	0.042	0.041	0.0415	2.41
Al	%	5.42	5.01	5.215	7.86	5.24	5.16	5.2	1.54
As	ppm	1.77	0.58	1.175	101.28	1.39	1.16	1.275	18.04
Ba	ppm	630	610	620	3.23	600	590	595	1.68
Be	ppm	1.1	1.02	1.06	7.55	1.11	1.03	1.07	7.48
Bi	ppm	0.153	0.089	0.121	52.89	0.093	0.081	0.087	13.79
Ca	%	1.25	1.36	1.305	8.43	1.25	1.28	1.265	2.37
Cd	ppm	0.055	0.062	0.0585	11.97	0.047	0.053	0.05	12.00
Ce	ppm	60.9	53.9	57.4	12.20	55.9	55.9	55.9	0.00
Co	ppm	8.36	6.54	7.45	24.43	4.84	4.63	4.735	4.44
Cr	ppm	41	29.5	35.25	32.62	24.2	23	23.6	5.08
Cs	ppm	1.98	1.07	1.525	59.67	1.13	1.08	1.105	4.52
Cu	ppm	18.6	9.38	13.99	65.90	14.75	11.5	13.125	24.76
Fe	%	2.09	1.73	1.91	18.85	1.39	1.34	1.365	3.66
Ga	ppm	13.85	11.55	12.7	18.11	11.05	10.7	10.875	3.22
Ge	ppm	0.11	0.11	0.11	0.00	0.16	0.13	0.145	20.69
Hf	ppm	4.22	5.04	4.63	17.71	3.54	4	3.77	12.20
In	ppm	0.032	0.035	0.0335	8.96	0.018	0.012	0.015	40.00
K	%	1.8	1.68	1.74	6.90	1.69	1.67	1.68	1.19
La	ppm	27.2	23.9	25.55	12.92	27.8	26.5	27.15	4.79
Li	ppm	27.7	18	22.85	42.45	19.5	16.9	18.2	14.29
Mg	%	0.67	0.54	0.605	21.49	0.46	0.44	0.45	4.44
Mn	ppm	315	303	309	3.88	228	235	231.5	3.02
Mo	ppm	0.48	0.24	0.36	66.67	0.3	0.21	0.255	35.29
Na	%	1.54	1.53	1.535	0.65	1.67	1.68	1.675	0.60
Nb	ppm	5.9	6.04	5.97	2.35	4.69	4.83	4.76	2.94
Ni	ppm	20.1	13.85	16.975	36.82	14.3	12.75	13.525	11.46
P	%	0.061	0.071	0.066	15.15	0.063	0.062	0.0625	1.60
Pb	ppm	11.8	10.65	11.225	10.24	10.6	10.2	10.4	3.85
Rb	ppm	63.6	51.5	57.55	21.03	48.4	45.4	46.9	6.40
Re	ppm	0.001	0.001	0.001	0.00	0.001	0.001	0.001	0.00
S	%	0.005	0.005	0.005	0.00	0.005	0.005	0.005	0.00
Sb	ppm	0.07	0.07	0.07	0.00	0.06	0.06	0.06	0.00
Sc	ppm	7.44	6.83	7.135	8.55	5.82	5.84	5.83	0.34
Se	ppm	0.1	0.1	0.1	0.00	0.1	0.1	0.1	0.00
Sn	ppm	1.13	1.03	1.08	9.26	0.85	0.83	0.84	2.38
Sr	ppm	233	236	234.5	1.28	247	246	246.5	0.41
Ta	ppm	0.45	0.48	0.465	6.45	0.43	0.35	0.39	20.51
Te	ppm	0.02	0.02	0.02	0.00	0.02	0.02	0.02	0.00
Th	ppm	8.35	5.92	7.135	34.06	7.69	6.37	7.03	18.78
Ti	%	0.235	0.239	0.237	1.69	0.187	0.194	0.1905	3.67
Tl	ppm	0.342	0.257	0.2995	28.38	0.269	0.25	0.2595	7.32
U	ppm	1.64	1.33	1.485	20.88	1.51	1.63	1.57	7.64
V	ppm	51	43.4	47.2	16.10	33.4	31.8	32.6	4.91
W	ppm	0.44	0.329	0.3845	28.87	0.289	1.12	0.7045	117.96
Y	ppm	11.8	12.8	12.3	8.13	11.65	11.55	11.6	0.86
Zn	ppm	40.9	29	34.95	34.05	27.5	25.2	26.35	8.73
Zr	ppm	154	183.5	168.75	17.48	134.5	152.5	143.5	12.54

Underlined elements indicate elements with significant natural variability (MPD>20%)

		Duplicate Pair 3				Duplicate Pair 4			
		Q515308	Q515309	Mean	MPD (%)	Q515324	Q515325	Mean	MPD (%)
Ag	ppm	0.019	0.024	0.0215	23.26	0.035	0.044	0.0395	22.78
Al	%	4.32	5.06	4.69	15.78	5.19	5.23	5.21	0.77
As	ppm	1.67	2.34	2.005	33.42	1.86	1.13	1.495	48.83
Ba	ppm	530	560	545	5.50	460	447	453.5	2.87
Be	ppm	0.86	1.01	0.935	16.04	1.05	1.14	1.095	8.22
Bi	ppm	0.08	0.093	0.0865	15.03	0.145	0.149	0.147	2.72
Ca	%	1	1.11	1.055	10.43	1.11	1.13	1.12	1.79
Cd	ppm	0.042	0.051	0.0465	19.35	0.044	0.048	0.046	8.70
Ce	ppm	28.3	57.4	42.85	67.91	50.4	45.1	47.75	11.10
Co	ppm	3.64	4.73	4.185	26.05	2.7	2.47	2.585	8.90
Cr	ppm	22	29.6	25.8	29.46	17	15.8	16.4	7.32
Cs	ppm	0.86	0.99	0.925	14.05	0.91	0.8	0.855	12.87
Cu	ppm	1.94	3.33	2.635	52.75	5.52	4.77	5.145	14.58
Fe	%	1.54	1.96	1.75	24.00	0.91	0.76	0.835	17.96
Ga	ppm	11	11.4	11.2	3.57	11.05	11	11.025	0.45
Ge	ppm	0.11	0.14	0.125	24.00	0.12	0.13	0.125	8.00
Hf	ppm	3.5	4.1	3.8	15.79	3.83	3.14	3.485	19.80
In	ppm	0.018	0.033	0.0255	58.82	0.012	0.012	0.012	0.00
K	%	1.39	1.43	1.41	2.84	1.6	1.59	1.595	0.63
La	ppm	13.4	29	21.2	73.58	24.7	21.3	23	14.78
Li	ppm	12.2	16.5	14.35	29.97	15.8	15.5	15.65	1.92
Mg	%	0.36	0.43	0.395	17.72	0.27	0.26	0.265	3.77
Mn	ppm	223	256	239.5	13.78	149.5	156.5	153	4.58
Mo	ppm	0.28	0.32	0.3	13.33	0.39	0.24	0.315	47.62
Na	%	1.32	1.39	1.355	5.17	1.87	1.915	1.8925	2.38
Nb	ppm	4.34	5.55	4.945	24.47	2.83	2.61	2.72	8.09
Ni	ppm	7.53	10.35	8.94	31.54	7.52	7.36	7.44	2.15
P	%	0.021	0.034	0.0275	47.27	0.066	0.069	0.0675	4.44
Pb	ppm	9.09	11.55	10.32	23.84	10.65	10.3	10.475	3.34
Rb	ppm	40.7	44.6	42.65	9.14	37.3	36.2	36.75	2.99
Re	ppm	0.001	0.001	0.001	0.00	0.001	0.001	0.001	0.00
S	%	0.01	0.01	0.01	0.00	0.005	0.005	0.005	0.00
Sb	ppm	0.07	0.07	0.07	0.00	0.05	0.04	0.045	22.22
Sc	ppm	5.41	6.51	5.96	18.46	3.6	3.49	3.545	3.10
Se	ppm	0.1	0.1	0.1	0.00	0.1	0.2	0.15	66.67
Sn	ppm	0.84	0.82	0.83	2.41	0.56	0.49	0.525	13.33
Sr	ppm	205	224	214.5	8.86	242	246	244	1.64
Ta	ppm	0.27	0.36	0.315	28.57	0.21	0.18	0.195	15.38
Te	ppm	0.02	0.02	0.02	0.00	0.02	0.02	0.02	0.00
Th	ppm	3.2	11.8	7.5	114.67	5.87	4.78	5.325	20.47
Ti	%	0.184	0.225	0.2045	20.05	0.121	0.115	0.118	5.08
Tl	ppm	0.212	0.244	0.228	14.04	0.206	0.194	0.2	6.00
U	ppm	0.71	0.98	0.845	31.95	1.9	1.57	1.735	19.02
V	ppm	38.6	43.9	41.25	12.85	23.9	19.7	21.8	19.27
W	ppm	0.283	0.973	0.628	109.87	0.238	0.198	0.218	18.35
Y	ppm	7.52	9.66	8.59	24.91	9.02	9.01	9.015	0.11
Zn	ppm	17.6	22.4	20	24.00	15.5	13.8	14.65	11.60
Zr	ppm	133	153.5	143.25	14.31	150.5	124.5	137.5	18.91

Underlined elements indicate elements with significant natural variability (MPD>20%)

		Duplicate Pair 5				Duplicate Pair 6			
		Q515359	Q515360	Mean	MPD (%)	Q515381	Q515382	Mean	MPD (%)
Ag	ppm	0.036	0.035	0.0355	2.82	0.048	0.044	0.046	8.70
Al	%	5.41	5.41	5.41	0.00	5.29	5.27	5.28	0.38
As	ppm	1.53	0.71	1.12	73.21	1.29	1.13	1.21	13.22
Ba	ppm	490	510	500	4.00	460	447	453.5	2.87
Be	ppm	1.07	1.14	1.105	6.33	1.05	1.17	1.11	10.81
Bi	ppm	0.172	0.158	0.165	8.48	0.149	0.165	0.157	10.19
Ca	%	1.13	1.21	1.17	6.84	1.12	1.15	1.135	2.64
Cd	ppm	0.04	0.062	0.051	43.14	0.055	0.056	0.0555	1.80
Ce	ppm	44.5	55	49.75	21.11	48.7	46.7	47.7	4.19
Co	ppm	3.54	3.73	3.635	5.23	2.99	3.08	3.035	2.97
Cr	ppm	21.8	23.9	22.85	9.19	18.3	17.5	17.9	4.47
Cs	ppm	1.39	1.37	1.38	1.45	1.03	1	1.015	2.96
Cu	ppm	6.54	6.35	6.445	2.95	6.18	6.43	6.305	3.97
Fe	%	1.21	1.19	1.2	1.67	0.93	0.92	0.925	1.08
Ga	ppm	12.05	12.45	12.25	3.27	11.45	11.35	11.4	0.88
Ge	ppm	0.09	0.12	0.105	28.57	0.11	0.14	0.125	24.00
Hf	ppm	3.55	4.13	3.84	15.10	3.12	3.55	3.335	12.89
In	ppm	0.013	0.017	0.015	26.67	0.011	0.012	0.0115	8.70
K	%	1.66	1.68	1.67	1.20	1.66	1.62	1.64	2.44
La	ppm	21.9	26.7	24.3	19.75	23.3	22.3	22.8	4.39
Li	ppm	17.8	19.2	18.5	7.57	16.2	16.2	16.2	0.00
Mg	%	0.36	0.39	0.375	8.00	0.29	0.28	0.285	3.51
Mn	ppm	186.5	205	195.75	9.45	148.5	156.5	152.5	5.25
Mo	ppm	0.52	0.43	0.475	18.95	0.47	0.43	0.45	8.89
Na	%	1.9	1.89	1.895	0.53	1.95	1.97	1.96	1.02
Nb	ppm	3.59	4.22	3.905	16.13	2.53	2.39	2.46	5.69
Ni	ppm	8.89	9.35	9.12	5.04	8.74	9.09	8.915	3.93
P	%	0.044	0.064	0.054	37.04	0.066	0.067	0.0665	1.50
Pb	ppm	10.35	10.65	10.5	2.86	10.5	10.55	10.525	0.48
Rb	ppm	45.2	46.3	45.75	2.40	41.1	39.7	40.4	3.47
Re	ppm	0.001	0.001	0.001	0.00	0.001	0.001	0.001	0.00
S	%	0.005	0.005	0.005	0.00	0.01	0.005	0.0075	66.67
Sb	ppm	0.05	0.04	0.045	22.22	0.06	0.04	0.05	40.00
Sc	ppm	4.42	5.03	4.725	12.91	3.61	3.68	3.645	1.92
Se	ppm	0.1	0.1	0.1	0.00	0.1	0.1	0.1	0.00
Sn	ppm	0.71	0.86	0.785	19.11	0.51	0.53	0.52	3.85
Sr	ppm	246	248	247	0.81	246	248	247	0.81
Ta	ppm	0.27	0.3	0.285	10.53	0.18	0.18	0.18	0.00
Te	ppm	0.02	0.02	0.02	0.00	0.02	0.02	0.02	0.00
Th	ppm	5.72	7.1	6.41	21.53	5.85	5.81	5.83	0.69
Ti	%	0.155	0.181	0.168	15.48	0.118	0.116	0.117	1.71
Tl	ppm	0.231	0.245	0.238	5.88	0.197	0.205	0.201	3.98
U	ppm	1.46	1.77	1.615	19.20	1.87	1.71	1.79	8.94
V	ppm	28	30.9	29.45	9.85	24	23.5	23.75	2.11
W	ppm	0.307	0.316	0.3115	2.89	0.206	0.236	0.221	13.57
Y	ppm	7.97	10.7	9.335	29.24	9.28	9.65	9.465	3.91
Zn	ppm	19.3	22	20.65	13.08	15.4	15.5	15.45	0.65
Zr	ppm	127	149.5	138.25	16.27	119.5	136	127.75	12.92

Underlined elements indicate elements with significant natural variability (MPD>20%)

		Duplicate Pair 7				Duplicate Pair 8			
		Q515421	Q515422	Mean	MPD (%)	Q515439	Q515440	Mean	MPD (%)
Ag	ppm	0.025	0.035	0.03	33.33	0.041	0.054	0.0475	27.37
Al	%	4.71	4.41	4.56	6.58	5.18	5.19	5.185	0.19
As	ppm	0.97	1.3	1.135	29.07	2.52	1.54	2.03	48.28
Ba	ppm	550	510	530	7.55	440	430	435	2.30
Be	ppm	0.98	0.96	0.97	2.06	1.05	1.14	1.095	8.22
Bi	ppm	0.073	0.053	0.063	31.75	0.149	0.104	0.1265	35.57
Ca	%	1.1	0.99	1.045	10.53	1.09	1.14	1.115	4.48
Cd	ppm	0.044	0.039	0.0415	12.05	0.048	0.049	0.0485	2.06
Ce	ppm	55.3	36.4	45.85	41.22	46.1	56.7	51.4	20.62
Co	ppm	5.24	4	4.62	26.84	3.04	3.45	3.245	12.63
Cr	ppm	27.4	18.5	22.95	38.78	16.5	14.6	15.55	12.22
Cs	ppm	1.09	0.87	0.98	22.45	0.79	0.84	0.815	6.13
Cu	ppm	5.87	5.57	5.72	5.24	7.9	7.53	7.715	4.80
Fe	%	1.67	1.14	1.405	37.72	0.83	0.76	0.795	8.81
Ga	ppm	11.45	10.2	10.825	11.55	9.86	10.45	10.155	5.81
Ge	ppm	0.13	0.11	0.12	16.67	0.12	0.14	0.13	15.38
Hf	ppm	3.87	2.68	3.275	36.34	2.72	2.36	2.54	14.17
In	ppm	0.017	0.013	0.015	26.67	0.013	0.013	0.013	0.00
K	%	1.63	1.51	1.57	7.64	1.55	1.52	1.535	1.95
La	ppm	26	16.75	21.375	43.27	20.4	25.8	23.1	23.38
Li	ppm	18.7	17	17.85	9.52	14.8	14.3	14.55	3.44
Mg	%	0.5	0.37	0.435	29.89	0.25	0.23	0.24	8.33
Mn	ppm	276	198	237	32.91	148.5	140	144.25	5.89
Mo	ppm	0.19	0.2	0.195	5.13	0.38	0.26	0.32	37.50
Na	%	1.455	1.44	1.4475	1.04	1.875	1.95	1.9125	3.92
Nb	ppm	4.88	3.07	3.975	45.53	2.43	2.19	2.31	10.39
Ni	ppm	11.85	9.03	10.44	27.01	8.82	7.53	8.175	15.78
P	%	0.05	0.046	0.048	8.33	0.06	0.064	0.062	6.45
Pb	ppm	9.87	9.08	9.475	8.34	10.85	10.65	10.75	1.86
Rb	ppm	48.7	45.1	46.9	7.68	33.5	34.5	34	2.94
Re	ppm	0.001	0.001	0.001	0.00	0.001	0.001	0.001	0.00
S	%	0.01	0.03	0.02	100.00	0.005	0.005	0.005	0.00
Sb	ppm	0.08	0.07	0.075	13.33	0.04	0.04	0.04	0.00
Sc	ppm	6.1	4.39	5.245	32.60	3.1	3.07	3.085	0.97
Se	ppm	0.2	0.1	0.15	66.67	0.1	0.1	0.1	0.00
Sn	ppm	0.9	0.69	0.795	26.42	0.54	0.48	0.51	11.76
Sr	ppm	212	205	208.5	3.36	245	255	250	4.00
Ta	ppm	0.3	0.22	0.26	30.77	0.33	0.18	0.255	58.82
Te	ppm	0.02	0.02	0.02	0.00	0.02	0.02	0.02	0.00
Th	ppm	8.82	4.66	6.74	61.72	5.05	6.69	5.87	27.94
Ti	%	0.215	0.129	0.172	50.00	0.102	0.096	0.099	6.06
Tl	ppm	0.257	0.234	0.2455	9.37	0.184	0.191	0.1875	3.73
U	ppm	1.31	0.86	1.085	41.47	1.66	2.06	1.86	21.51
V	ppm	40.8	27	33.9	40.71	19.5	19.7	19.6	1.02
W	ppm	0.258	0.18	0.219	35.62	0.195	0.162	0.1785	18.49
Y	ppm	9.62	7.31	8.465	27.29	7.77	9.01	8.39	14.78
Zn	ppm	26.4	19.6	23	29.57	14	13.3	13.65	5.13
Zr	ppm	143.5	98.4	120.95	37.29	107	95.6	101.3	11.25

Underlined elements indicate elements with significant natural variability (MPD>20%)

		Duplicate Pair 9				Mean MPD
		Q515451	Q515452	Mean	MPD (%)	
Ag	ppm	0.039	0.044	0.0415	12.05	5.59
Al	%	5.79	5.45	5.62	6.05	5.46
As	ppm	0.82	1.17	0.995	35.18	6.12
Ba	ppm	490	460	475	6.32	392.92
Be	ppm	1.33	1.41	1.37	5.84	1.31
Bi	ppm	0.153	0.126	0.1395	19.35	5.39
Ca	%	1.3	1.26	1.28	3.13	2.72
Cd	ppm	0.062	0.052	0.057	17.54	2.05
Ce	ppm	60.1	54.8	57.45	9.23	48.78
Co	ppm	4.57	3.78	4.175	18.92	7.64
Cr	ppm	23.4	19.2	21.3	19.72	22.34
Cs	ppm	1.29	1.09	1.19	16.81	4.57
Cu	ppm	12.95	10.4	11.675	21.84	8.51
Fe	%	1.12	0.97	1.045	14.35	7.11
Ga	ppm	12.2	11.75	11.975	3.76	10.99
Ge	ppm	0.14	0.13	0.135	7.41	2.88
Hf	ppm	4.78	3.82	4.3	22.33	8.89
In	ppm	0.018	0.018	0.018	0.00	4.46
K	%	1.74	1.65	1.695	5.31	2.61
La	ppm	27.5	25.5	26.5	7.55	26.25
Li	ppm	18.5	16.8	17.65	9.63	15.34
Mg	%	0.35	0.3	0.325	15.38	5.24
Mn	ppm	193	176.5	184.75	8.93	150.24
Mo	ppm	0.42	0.39	0.405	7.41	1.14
Na	%	2.12	2.08	2.1	1.90	1.75
Nb	ppm	3.86	3.41	3.635	12.38	10.14
Ni	ppm	10.8	9.7	10.25	10.73	12.35
P	%	0.072	0.072	0.072	0.00	1.44
Pb	ppm	11.55	11.15	11.35	3.52	10.32
Rb	ppm	44.8	42.4	43.6	5.50	34.78
Re	ppm	0.001	0.001	0.001	0.00	0.00
S	%	0.01	0.005	0.0075	66.67	16.68
Sb	ppm	0.06	0.05	0.055	18.18	2.27
Sc	ppm	4.71	4.15	4.43	12.64	8.72
Se	ppm	0.3	0.1	0.2	100.00	11.24
Sn	ppm	0.86	0.68	0.77	23.38	4.96
Sr	ppm	266	258	262	3.05	205.23
Ta	ppm	0.3	0.24	0.27	22.22	5.36
Te	ppm	0.02	0.02	0.02	0.00	0.02
Th	ppm	6.66	6.28	6.47	5.87	15.07
Ti	%	0.164	0.145	0.1545	12.30	8.44
Tl	ppm	0.241	0.226	0.2335	6.42	1.74
U	ppm	2.08	1.91	1.995	8.52	8.32
V	ppm	29.5	26.4	27.95	11.09	27.38
W	ppm	0.373	0.255	0.314	37.58	6.14
Y	ppm	10.95	10.35	10.65	5.63	12.06
Zn	ppm	19.3	17.5	18.4	9.78	19.09
Zr	ppm	163	136.5	149.75	17.70	109.46

Underlined elements indicate elements with significant natural variability (MPD>20%)

B.3 Till Aqua Regia ICP-MS QAQC

The QA/QC protocol for the aqua regia ICP-MS analyses included the analysis of OREAS-25a certified reference material, and the calculation of the MPD (%) for field duplicate pairs. The results of this QA/QC protocol are summarized in this section.

Analytical Results of OREAS-25a certified reference material - Aqua Regia ICP-MS

SAMPLE	Au	Ag	Al	As	B	Ba	Be	Bi
	ppm	ppm	%	ppm	ppm	ppm	ppm	ppm
OREAS 25a Certified			5.85			56		0.3
OREAS 25a Indicated	0.94	0.035		2.84	5.92		0.65	
Q515259	0.0007	0.025	5.65	2.86	<10	52.9	0.52	0.252
Q515279	0.0008	0.03	5.88	2.63	<10	54.5	0.58	0.26
Q515310	0.001	0.051	5.73	2.58	<10	58.6	0.58	0.292
Q515353	0.0007	0.025	5.62	3.15	<10	55.1	0.63	0.262
Q515361	0.0007	0.03	5.87	2.84	<10	58	0.66	0.287
Q515369	0.0009	0.028	6.2	3	<10	60.7	0.68	0.288
Q515383	0.0011	0.031	6.28	2.92	<10	59.9	0.65	0.29
Q515424	0.0006	0.027	5.83	2.83	<10	53	0.61	0.259
Q515453	0.0004	0.029	5.67	2.69	<10	56.3	0.6	0.238
Q515476	0.0006	0.028	5.5	2.97	<10	54.5	0.58	0.252

SAMPLE	Ca	Cd	Ce	Co	Cr	Cs	Cu	Fe
	%	ppm	ppm	ppm	ppm	ppm	ppm	%
OREAS 25a Certified	0.15		33.1	5.72	73	4.45	24.9	5.99
OREAS 25a Indicated		0.041						
Q515259	0.14	0.035	30.5	5.16	70	3.71	22.2	5.87
Q515279	0.14	0.035	29.4	5.24	69.8	3.83	22	6.01
Q515310	0.16	0.049	32.1	5.65	71.4	3.69	23.1	5.93
Q515353	0.14	0.039	32.1	5.41	76	3.62	23.8	5.9
Q515361	0.13	0.024	32.5	5.48	72.4	3.93	23.8	5.86
Q515369	0.14	0.034	33.2	5.77	77.3	4.05	24.9	6.1
Q515383	0.14	0.029	33.5	5.65	75.2	4.24	24.9	6.07
Q515424	0.14	0.043	29.1	5.3	74.3	3.54	22.7	6.05
Q515453	0.13	0.04	30	5.35	72.6	3.58	22.1	6.01
Q515476	0.16	0.028	29.7	5.18	72.8	3.73	24.7	5.79

SAMPLE	Ga	Ge	Hf	Hg	In	K	La	Li
	ppm	ppm	ppm	ppm	ppm	%	ppm	ppm
OREAS 25a Certified	20.6					0.131		
OREAS 25a Indicated		0.13	0.47	0.053	0.081		13.0	23.7
Q515259	19.4	0.087	0.34	0.1	0.062	0.13	11.75	16.5
Q515279	19.55	0.086	0.321	0.088	0.069	0.13	12	19.2
Q515310	21.2	0.088	0.409	0.085	0.079	0.13	14	19.6
Q515353	20.3	0.06	0.33	0.061	0.07	0.12	11.8	19.6
Q515361	20.5	0.062	0.352	0.147	0.074	0.13	13.3	20.8
Q515369	20.9	0.096	0.407	0.065	0.067	0.14	13.55	22.3
Q515383	21.1	0.069	0.37	0.062	0.068	0.14	13.75	22.9
Q515424	19.4	0.083	0.353	0.078	0.069	0.13	12.5	20.3
Q515453	20.5	0.06	0.341	0.062	0.069	0.14	12.85	19.4
Q515476	19	0.078	0.356	0.12	0.069	0.12	12.35	20.6

SAMPLE	Mg	Mn	Mo	Na	Nb	Ni	P	Pb
	%	ppm	ppm	%	ppm	ppm	%	ppm
OREAS 25a Certified		424.739				26.9	0.037	21.0
OREAS 25a Indicated	0.193		1.36	0.040	0.52			
Q515259	0.18	409	1.39	0.032	0.571	26.6	0.037	19.15
Q515279	0.18	412	1.4	0.033	0.534	26.9	0.038	19.1
Q515310	0.18	411	1.38	0.034	0.723	27.9	0.038	20
Q515353	0.18	411	1.42	0.031	0.548	26.7	0.038	20.1
Q515361	0.19	413	1.51	0.034	0.632	27.2	0.038	20.7
Q515369	0.19	432	1.42	0.036	0.975	28.9	0.039	20.6
Q515383	0.19	427	1.43	0.036	0.627	29	0.039	20.4
Q515424	0.18	407	1.37	0.034	0.59	26.6	0.039	18.75
Q515453	0.18	415	1.43	0.033	0.602	25.8	0.039	18.45
Q515476	0.18	400	1.36	0.033	0.719	27.2	0.038	18.5

SAMPLE	Pd	Pt	Rb	Re	S	Sb	Sc	Se
	ppm	ppm	ppm	ppm	%	ppm	ppm	ppm
OREAS 25a Certified							8.64	
OREAS 25a Indicated	< 0.01	0.004	31.4	< 0.05	0.050	0.18		0.87
Q515259	<0.001	0.002	28	<0.001	0.04	0.185	8.71	0.6
Q515279	<0.001	<0.002	28.9	<0.001	0.04	0.166	8.88	0.7
Q515310	0.001	<0.002	30.9	<0.001	0.03	0.166	9.35	0.6
Q515353	<0.001	0.002	29.8	<0.001	0.03	0.199	9.5	0.7
Q515361	<0.001	<0.002	29.8	<0.001	0.03	0.643	8.95	0.7
Q515369	<0.001	<0.002	31.8	<0.001	0.03	0.215	9.74	0.9
Q515383	0.002	<0.002	32.5	<0.001	0.03	0.189	9.33	0.8
Q515424	0.001	<0.002	28.6	<0.001	0.04	0.163	9.2	0.6
Q515453	<0.001	0.002	28.3	<0.001	0.07	0.186	9.2	0.6
Q515476	<0.001	<0.002	29.9	<0.001	0.04	0.177	9.23	0.7

SAMPLE	Sn	Sr	Ta	Te	Th	Ti	Tl	U
	ppm	ppm	ppm	ppm	ppm	%	ppm	ppm
OREAS 25a Certified	2.70	17.3			10.7		0.20	1.49
OREAS 25a Indicated			0.099	< 0.02		0.036		
Q515259	2.5	16.65	<0.005	0.05	9.05	0.054	0.162	1.365
Q515279	2.53	17.45	<0.005	0.1	9.13	0.053	0.167	1.36
Q515310	2.71	17.95	<0.005	0.05	9.61	0.063	0.18	1.445
Q515353	2.52	17.2	<0.005	0.02	9.46	0.052	0.167	1.485
Q515361	5.86	17.3	<0.005	0.05	9.54	0.062	0.172	1.435
Q515369	2.8	18.4	0.015	0.02	9.72	0.074	0.18	1.5
Q515383	2.73	18.55	<0.005	<0.01	9.64	0.069	0.174	1.45
Q515424	2.55	16.85	<0.005	0.04	9.26	0.059	0.184	1.375
Q515453	2.53	16.9	<0.005	0.02	9.1	0.061	0.163	1.395
Q515476	2.47	17.35	<0.005	0.07	8.94	0.062	0.164	1.33

SAMPLE	V	W	Y	Zn	Zr	C (org)
	ppm	ppm	ppm	ppm	ppm	%
OREAS 25a Certified	117		4.56	30.1		1.561
OREAS 25a Indicated					19.0	
Q515259	127.5	0.028	4.27	29.5	14.45	0.75
Q515279	126	0.021	4.29	29.7	14.45	0.82
Q515310	123.5	0.026	4.45	31.1	16.55	0.74
Q515353	128	0.031	4.24	30.2	14.45	0.71
Q515361	123	0.032	4.27	32.1	15.8	0.74
Q515369	127.5	0.047	4.49	33.6	17.9	0.75
Q515383	126	0.026	4.5	33	16.2	0.75
Q515424	123.5	0.027	4.16	30	15.65	0.73
Q515453	122.5	0.026	4.13	28.9	15.8	0.75
Q515476	125	0.032	4.3	30.8	14.9	0.71

Aqua Regia - Certified CRM Values - OREAS 25a

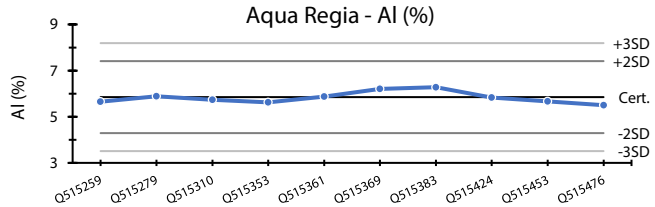

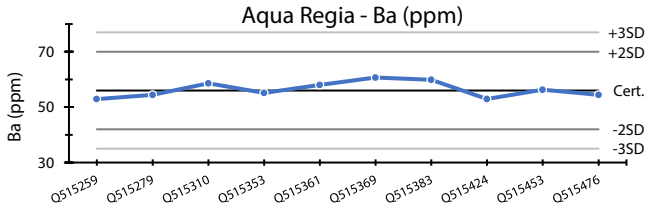

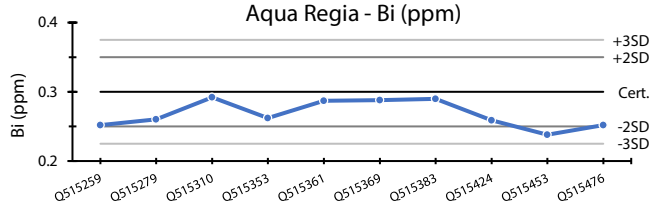

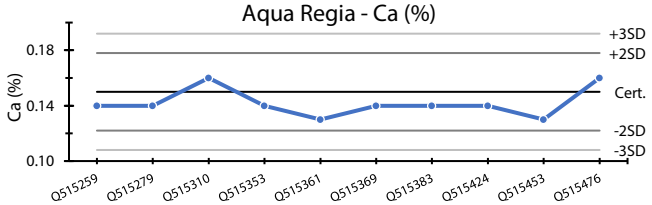

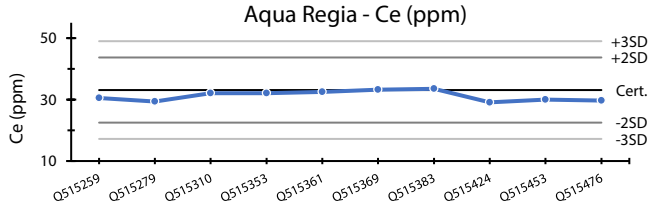

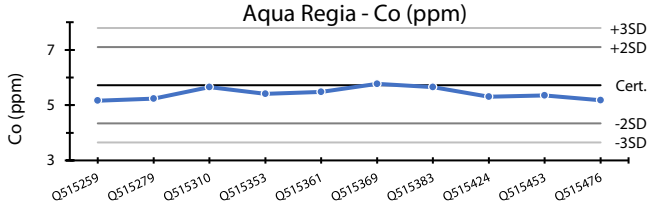

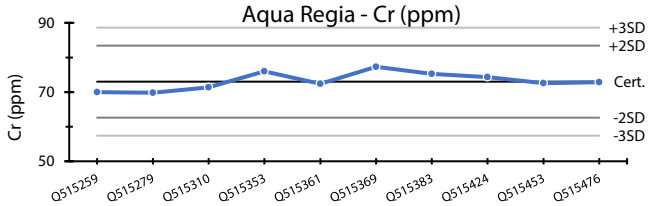

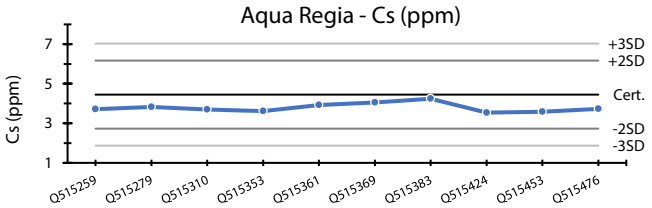

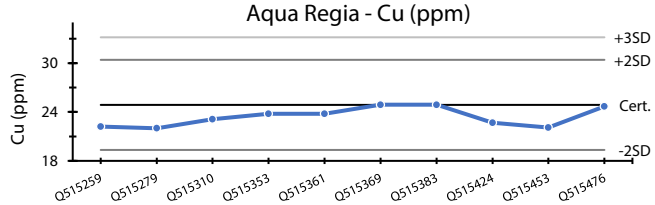

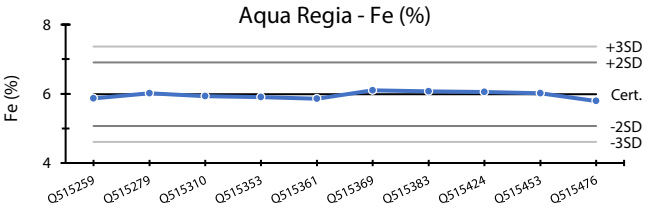

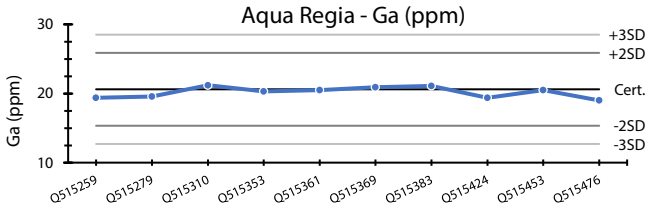

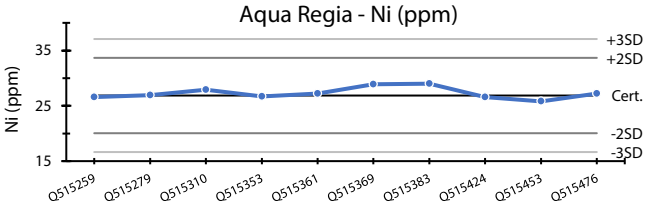

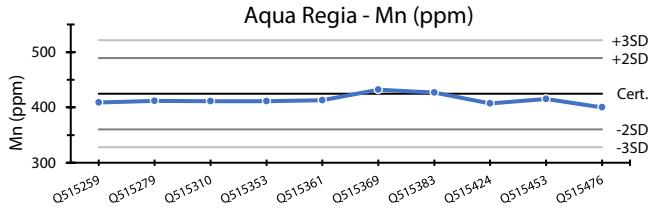

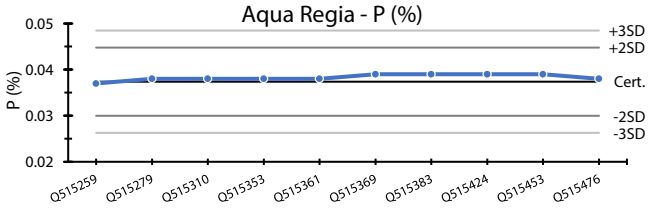

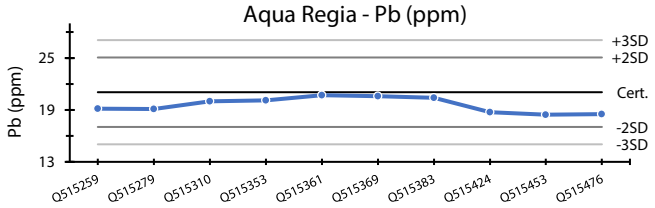

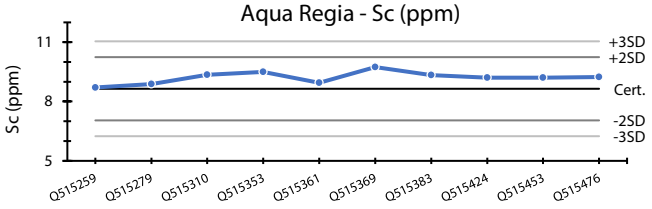

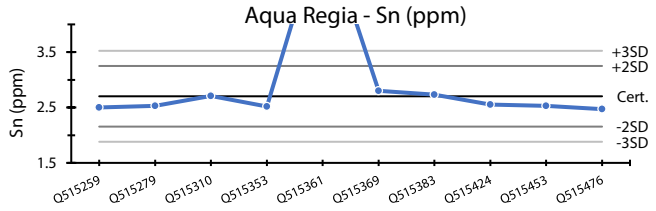

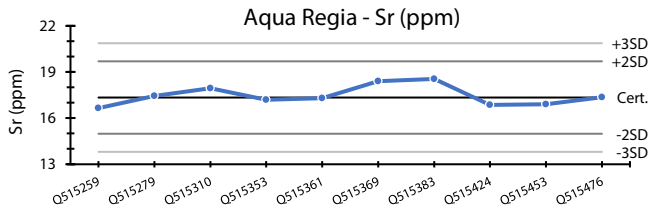

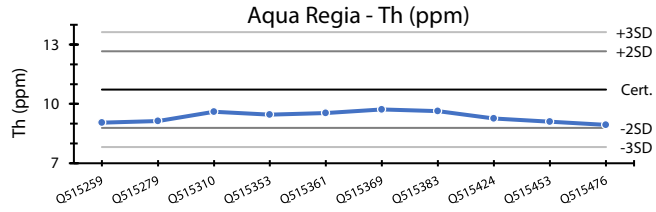

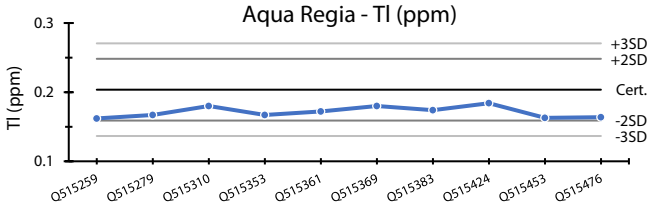

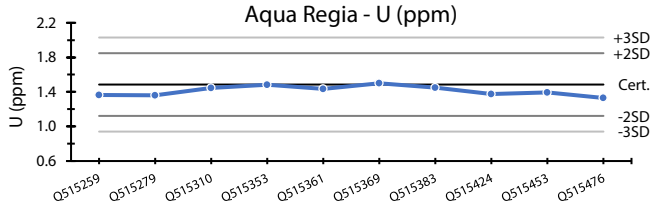

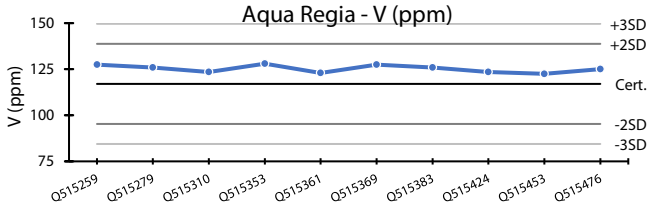

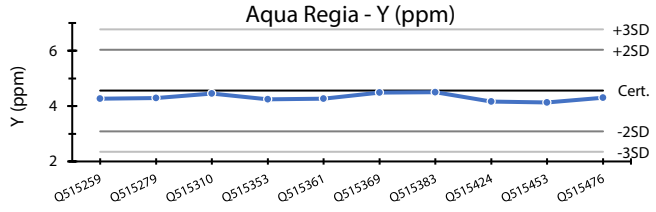

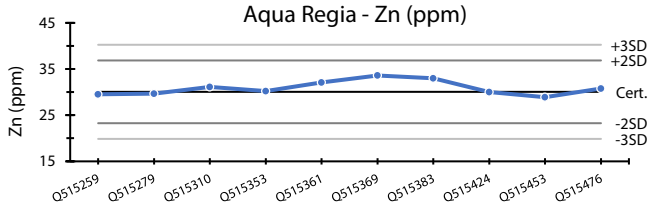

Aqua Regia - Indicated CRM Values - OREAS 25a

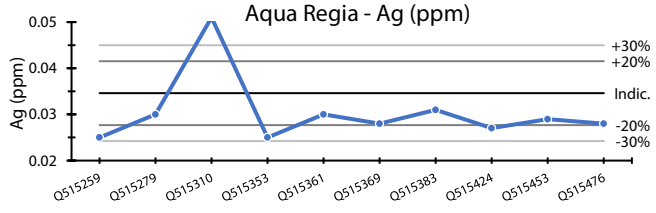

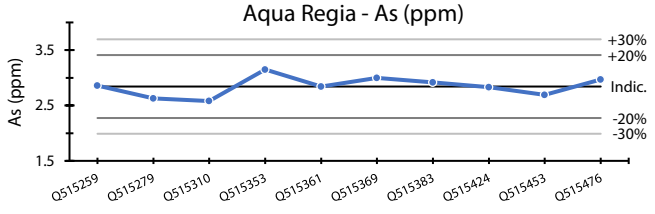

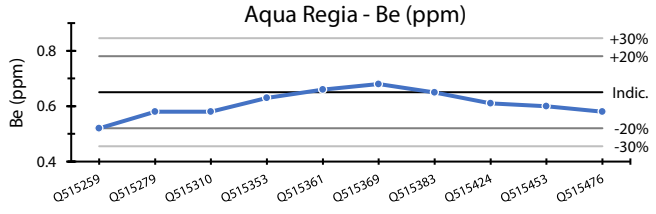

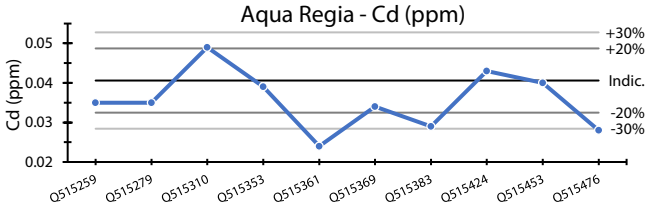

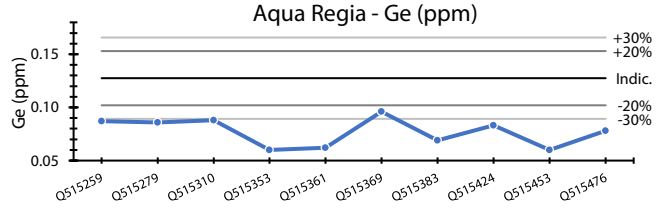

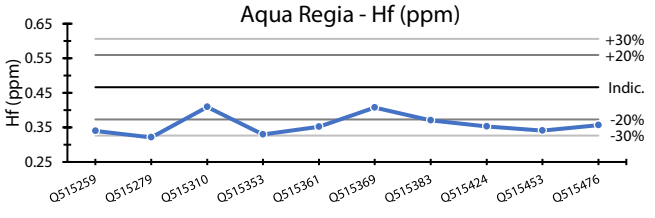

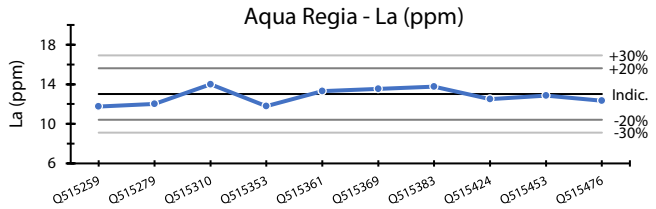

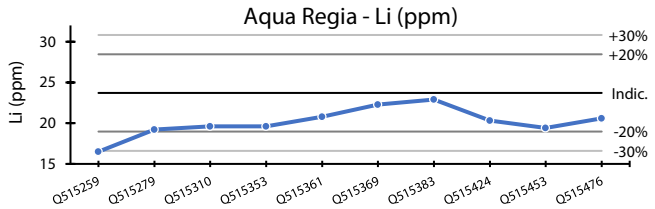

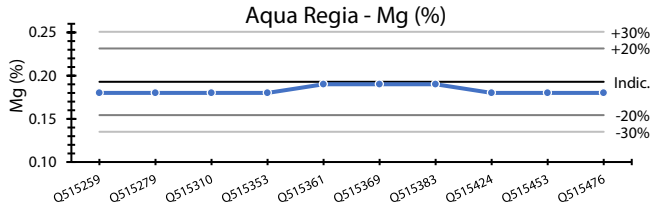

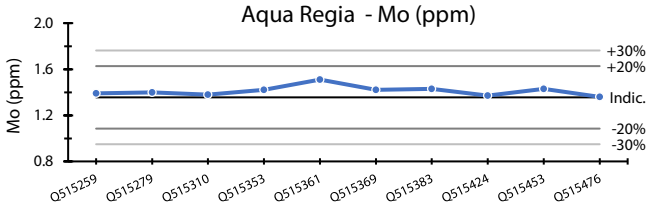

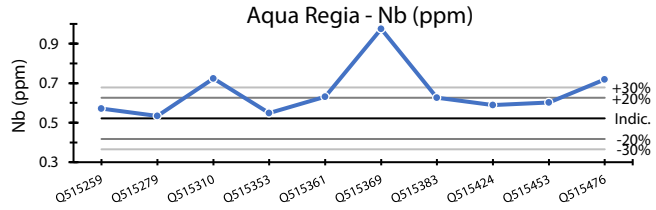

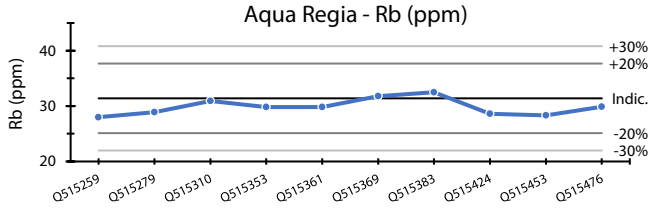

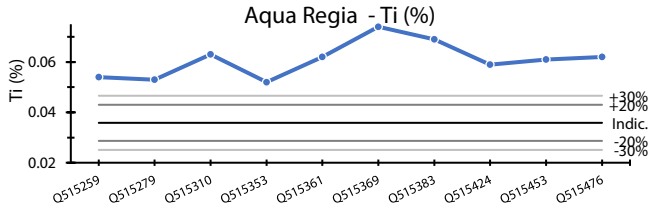

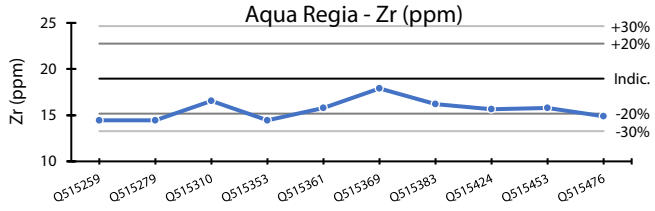

Au, B, Hg, In, K, Na, Pd, Pt, Re, S, Sb, Se, Ta, and Te are excluded as >50% of their values are under ten times the lower limit of detection.

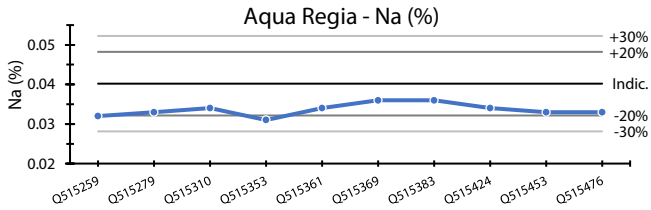

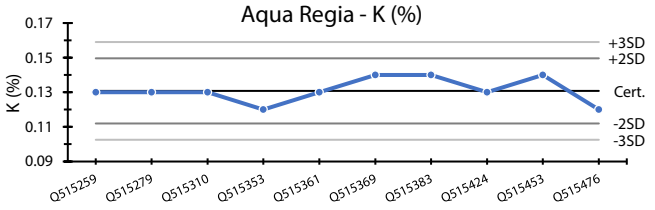

Till Aqua Regia ICP-MS Field Duplicate MPD (%)

		Duplicate Pair 1				Duplicate Pair 2			
		Q515258L	Q515258U	Mean	MPD (%)	Q515276	Q515277	Mean	MPD (%)
Au	ppm	0.0008	0.0008	0.0008	0.00	0.0003	0.0009	0.0006	100.00
Ag	ppm	0.011	0.007	0.009	44.44	0.012	0.011	0.0115	8.70
Al	%	0.84	0.49	0.665	52.63	0.51	0.43	0.47	17.02
As	ppm	2.15	1.04	1.595	69.59	1	0.9	0.95	10.53
B	ppm	5	5	5	0.00	5	5	5	0.00
Ba	ppm	38.4	24.4	31.4	44.59	23.1	21.6	22.35	6.71
Be	ppm	0.23	0.14	0.185	48.65	0.14	0.13	0.135	7.41
Bi	ppm	0.104	0.058	0.081	56.79	0.07	0.095	0.0825	30.30
Ca	%	0.16	0.18	0.17	11.76	0.14	0.16	0.15	13.33
Cd	ppm	0.026	0.028	0.027	7.41	0.022	0.024	0.023	8.70
Ce	ppm	33.2	36.9	35.05	10.56	33	36.7	34.85	10.62
Co	ppm	5.77	3.75	4.76	42.44	2.56	2.51	2.535	1.97
Cr	ppm	23.6	14.2	18.9	49.74	12.3	11.6	11.95	5.86
Cs	ppm	1.18	0.58	0.88	68.18	0.609	0.521	0.565	15.58
Cu	ppm	18.75	9.33	14.04	67.09	13.45	11.2	12.325	18.26
Fe	%	1.29	0.87	1.08	38.89	0.73	0.67	0.7	8.57
Ga	ppm	3.8	2.36	3.08	46.75	2.16	1.945	2.0525	10.48
Ge	ppm	0.067	0.069	0.068	2.94	0.056	0.06	0.058	6.90
Hf	ppm	0.041	0.086	0.0635	70.87	0.024	0.058	0.041	82.93
Hg	ppm	0.004	0.002	0.003	66.67	0.002	0.002	0.002	0.00
In	ppm	0.011	0.007	0.009	44.44	0.0025	0.007	0.00475	94.74
K	%	0.12	0.08	0.1	40.00	0.08	0.07	0.075	13.33
La	ppm	14.95	17	15.975	12.83	14.55	16.1	15.325	10.11
Li	ppm	17.3	10.4	13.85	49.82	11.5	10.3	10.9	11.01
Mg	%	0.36	0.23	0.295	44.07	0.21	0.19	0.2	10.00
Mn	ppm	129	90.7	109.85	34.87	60.6	62.4	61.5	2.93
Mo	ppm	0.44	0.18	0.31	83.87	0.2	0.17	0.185	16.22
Na	%	0.011	0.01	0.0105	9.52	0.008	0.007	0.0075	13.33
Nb	ppm	0.837	0.423	0.63	65.71	0.566	0.365	0.4655	43.18
Ni	ppm	15.55	9	12.275	53.36	9.26	8.56	8.91	7.86
P	%	0.047	0.06	0.0535	24.30	0.049	0.054	0.0515	9.71
Pb	ppm	2.93	2.17	2.55	29.80	2.16	2.04	2.1	5.71
Pd	ppm	0.0005	0.0005	0.0005	0.00	0.0005	0.0005	0.0005	0.00
Pt	ppm	0.001	0.001	0.001	0.00	0.001	0.001	0.001	0.00
Rb	ppm	12.3	7.15	9.725	52.96	6.79	6.42	6.605	5.60
Re	ppm	0.0005	0.0005	0.0005	0.00	0.0005	0.0005	0.0005	0.00
S	%	0.005	0.005	0.005	0.00	0.005	0.005	0.005	0.00
Sb	ppm	0.009	0.012	0.0105	28.57	0.007	0.008	0.0075	13.33
Sc	ppm	2.14	1.55	1.845	31.98	1.37	1.42	1.395	3.58
Se	ppm	0.1	0.1	0.1	0.00	0.1	0.1	0.1	0.00
Sn	ppm	0.38	0.25	0.315	41.27	0.24	0.24	0.24	0.00
Sr	ppm	8.23	7.49	7.86	9.41	6.22	6.78	6.5	8.62
Ta	ppm	0.0025	0.0025	0.0025	0.00	0.0025	0.0025	0.0025	0.00
Te	ppm	0.005	0.005	0.005	0.00	0.02	0.005	0.0125	120.00
Th	ppm	4.07	4.97	4.52	19.91	3.76	4.17	3.965	10.34
Ti	%	0.065	0.044	0.0545	38.53	0.037	0.037	0.037	0.00
Tl	ppm	0.084	0.051	0.0675	48.89	0.053	0.049	0.051	7.84
U	ppm	0.801	0.71	0.7555	12.05	0.992	1.04	1.016	4.72
V	ppm	30.6	20.7	25.65	38.60	15.4	15	15.2	2.63
W	ppm	0.097	0.067	0.082	36.59	0.077	0.11	0.0935	35.29
Y	ppm	4.66	5.16	4.91	10.18	4.84	5.79	5.315	17.87
Zn	ppm	28.8	16.8	22.8	52.63	17	15.9	16.45	6.69
Zr	ppm	2.03	3.95	2.99	64.21	1.27	2.87	2.07	77.29

Underlined elements indicate elements with significant natural variability (MPD>20%)

		Duplicate Pair 3				Duplicate Pair 4			
		Q515308	Q515309	Mean	MPD (%)	Q515324	Q515325	Mean	MPD (%)
Au	ppm	0.0003	0.0003	0.0003	0.00	0.0004	0.0009	0.00065	76.92
Ag	ppm	0.007	0.009	0.008	25.00	0.01	0.01	0.01	0.00
Al	%	0.4	0.91	0.655	77.86	0.29	0.26	0.275	10.91
As	ppm	1.15	1.76	1.455	41.92	1.33	0.95	1.14	33.33
B	ppm	5	5	5	0.00	5	5	5	0.00
Ba	ppm	13.7	15.6	14.65	12.97	20.1	16.4	18.25	20.27
Be	ppm	0.11	0.18	0.145	48.28	0.12	0.1	0.11	18.18
Bi	ppm	0.058	0.062	0.06	6.67	0.135	0.109	0.122	21.31
Ca	%	0.04	0.06	0.05	40.00	0.13	0.13	0.13	0.00
Cd	ppm	0.015	0.037	0.026	84.62	0.018	0.019	0.0185	5.41
Ce	ppm	15.75	19.1	17.425	19.23	37.2	37.2	37.2	0.00
Co	ppm	1.275	2.12	1.6975	49.78	1.52	1.33	1.425	13.33
Cr	ppm	8.55	12.7	10.625	39.06	9.75	8.92	9.335	8.89
Cs	ppm	0.394	0.435	0.4145	9.89	0.443	0.368	0.4055	18.50
Cu	ppm	1.39	2.67	2.03	63.05	5.05	4.29	4.67	16.27
Fe	%	0.84	1.1	0.97	26.80	0.54	0.37	0.455	37.36
Ga	ppm	3.58	3.24	3.41	9.97	1.72	1.52	1.62	12.35
Ge	ppm	0.041	0.048	0.0445	15.73	0.047	0.058	0.0525	20.95
Hf	ppm	0.023	0.033	0.028	35.71	0.013	0.011	0.012	16.67
Hg	ppm	0.002	0.014	0.008	150.00	0.002	0.002	0.002	0.00
In	ppm	0.0025	0.008	0.00525	104.76	0.0025	0.0025	0.0025	0.00
K	%	0.02	0.03	0.025	40.00	0.07	0.06	0.065	15.38
La	ppm	7.8	9.35	8.575	18.08	17.85	15.1	16.475	16.69
Li	ppm	4.9	8.5	6.7	53.73	7	6.7	6.85	4.38
Mg	%	0.1	0.15	0.125	40.00	0.14	0.12	0.13	15.38
Mn	ppm	31.3	42.3	36.8	29.89	40.2	35.3	37.75	12.98
Mo	ppm	0.21	0.21	0.21	0.00	0.32	0.17	0.245	61.22
Na	%	0.004	0.004	0.004	0.00	0.008	0.006	0.007	28.57
Nb	ppm	0.868	1.08	0.974	21.77	0.516	0.326	0.421	45.13
Ni	ppm	3.22	5.08	4.15	44.82	5.38	5.13	5.255	4.76
P	%	0.016	0.025	0.0205	43.90	0.053	0.057	0.055	7.27
Pb	ppm	1.735	2.52	2.1275	36.90	2.25	2.05	2.15	9.30
Pd	ppm	0.002	0.002	0.002	0.00	0.0005	0.0005	0.0005	0.00
Pt	ppm	0.001	0.001	0.001	0.00	0.001	0.001	0.001	0.00
Rb	ppm	2.4	3.57	2.985	39.20	4.33	3.68	4.005	16.23
Re	ppm	0.0005	0.0005	0.0005	0.00	0.0005	0.0005	0.0005	0.00
S	%	0.005	0.005	0.005	0.00	0.005	0.005	0.005	0.00
Sb	ppm	0.01	0.011	0.0105	9.52	0.007	0.009	0.008	25.00
Sc	ppm	0.801	1.46	1.1305	58.29	0.946	0.82	0.883	14.27
Se	ppm	0.1	0.2	0.15	66.67	0.05	0.1	0.075	66.67
Sn	ppm	0.24	0.24	0.24	0.00	0.18	0.15	0.165	18.18
Sr	ppm	3.33	4.21	3.77	23.34	4.12	3.49	3.805	16.56
Ta	ppm	0.0025	0.013	0.00775	135.48	0.0025	0.0025	0.0025	0.00
Te	ppm	0.03	0.005	0.0175	142.86	0.005	0.02	0.0125	120.00
Th	ppm	2.41	2.81	2.61	15.33	3.84	3.57	3.705	7.29
Ti	%	0.037	0.038	0.0375	2.67	0.025	0.02	0.0225	22.22
Tl	ppm	0.025	0.034	0.0295	30.51	0.025	0.023	0.024	8.33
U	ppm	0.255	0.295	0.275	14.55	1.205	1.21	1.2075	0.41
V	ppm	20.2	21.9	21.05	8.08	12.6	9.2	10.9	31.19
W	ppm	0.108	0.175	0.1415	47.35	0.083	0.094	0.0885	12.43
Y	ppm	1.425	1.93	1.6775	30.10	4.96	4.9	4.93	1.22
Zn	ppm	6.7	9.5	8.1	34.57	8	7.1	7.55	11.92
Zr	ppm	1.11	1.53	1.32	31.82	0.7	0.63	0.665	10.53

Underlined elements indicate elements with significant natural variability (MPD>20%)

		Duplicate Pair 5				Duplicate Pair 6			
		Q515359	Q515360	Mean	MPD (%)	Q515381	Q515382	Mean	MPD (%)
Au	ppm	0.0009	0.0016	0.00125	56.00	0.0016	0.0013	0.00145	20.69
Ag	ppm	0.01	0.012	0.011	18.18	0.014	0.013	0.0135	7.41
Al	%	0.45	0.47	0.46	4.35	0.34	0.35	0.345	2.90
As	ppm	1.06	1.3	1.18	20.34	1.37	1.6	1.485	15.49
B	ppm	5	5	5	0.00	5	5	5	0.00
Ba	ppm	24.8	26.3	25.55	5.87	22	22.5	22.25	2.25
Be	ppm	0.13	0.15	0.14	14.29	0.12	0.13	0.125	8.00
Bi	ppm	0.123	0.123	0.123	0.00	0.142	0.127	0.1345	11.15
Ca	%	0.09	0.13	0.11	36.36	0.11	0.12	0.115	8.70
Cd	ppm	0.013	0.02	0.0165	42.42	0.02	0.015	0.0175	28.57
Ce	ppm	33	43	38	26.32	36.5	35.6	36.05	2.50
Co	ppm	2.29	2.36	2.325	3.01	1.87	1.99	1.93	6.22
Cr	ppm	14.4	14.25	14.325	1.05	11	11.05	11.025	0.45
Cs	ppm	0.83	0.784	0.807	5.70	0.525	0.522	0.5235	0.57
Cu	ppm	7.05	6.59	6.82	6.74	6.03	6.51	6.27	7.66
Fe	%	0.75	0.69	0.72	8.33	0.58	0.58	0.58	0.00
Ga	ppm	2.68	2.69	2.685	0.37	1.86	1.73	1.795	7.24
Ge	ppm	0.054	0.073	0.0635	29.92	0.056	0.061	0.0585	8.55
Hf	ppm	0.009	0.017	0.013	61.54	0.024	0.027	0.0255	11.76
Hg	ppm	0.002	0.002	0.002	0.00	0.005	0.002	0.0035	85.71
In	ppm	0.0025	0.007	0.00475	94.74	0.0025	0.0025	0.0025	0.00
K	%	0.08	0.09	0.085	11.76	0.08	0.08	0.08	0.00
La	ppm	13.6	18.5	16.05	30.53	17.15	16.35	16.75	4.78
Li	ppm	11.7	12.2	11.95	4.18	9	9.1	9.05	1.10
Mg	%	0.19	0.21	0.2	10.00	0.15	0.15	0.15	0.00
Mn	ppm	60.9	59.4	60.15	2.49	44.3	44.6	44.45	0.67
Mo	ppm	0.4	0.33	0.365	19.18	0.38	0.43	0.405	12.35
Na	%	0.006	0.01	0.008	50.00	0.009	0.008	0.0085	11.76
Nb	ppm	0.699	0.699	0.699	0.00	0.492	0.501	0.4965	1.81
Ni	ppm	6.52	6.86	6.69	5.08	6.48	6.84	6.66	5.41
P	%	0.03	0.052	0.041	53.66	0.052	0.05	0.051	3.92
Pb	ppm	2.35	2.54	2.445	7.77	2.26	2.37	2.315	4.75
Pd	ppm	0.0005	0.0005	0.0005	0.00	0.0005	0.0005	0.0005	0.00
Pt	ppm	0.001	0.001	0.001	0.00	0.001	0.001	0.001	0.00
Rb	ppm	6.73	7.03	6.88	4.36	5.06	4.76	4.91	6.11
Re	ppm	0.0005	0.0005	0.0005	0.00	0.0005	0.0005	0.0005	0.00
S	%	0.005	0.005	0.005	0.00	0.005	0.005	0.005	0.00
Sb	ppm	0.0025	0.006	0.00425	82.35	0.009	0.007	0.008	25.00
Sc	ppm	1.25	1.425	1.3375	13.08	0.985	0.968	0.9765	1.74
Se	ppm	0.1	0.1	0.1	0.00	0.05	0.1	0.075	66.67
Sn	ppm	0.25	0.21	0.23	17.39	0.17	0.18	0.175	5.71
Sr	ppm	4.16	4.56	4.36	9.17	3.71	3.95	3.83	6.27
Ta	ppm	0.0025	0.0025	0.0025	0.00	0.0025	0.0025	0.0025	0.00
Te	ppm	0.01	0.01	0.01	0.00	0.01	0.005	0.0075	66.67
Th	ppm	2.55	4.41	3.48	53.45	4.01	3.8	3.905	5.38
Ti	%	0.038	0.039	0.0385	2.60	0.027	0.027	0.027	0.00
Tl	ppm	0.051	0.052	0.0515	1.94	0.028	0.027	0.0275	3.64
U	ppm	1.115	1.185	1.15	6.09	1.16	1.19	1.175	2.55
V	ppm	16.4	16.8	16.6	2.41	12.6	12.4	12.5	1.60
W	ppm	0.07	0.076	0.073	8.22	0.066	0.062	0.064	6.25
Y	ppm	3.55	4.77	4.16	29.33	4.92	5.06	4.99	2.81
Zn	ppm	13.5	13.9	13.7	2.92	9.8	9.8	9.8	0.00
Zr	ppm	0.44	0.9	0.67	68.66	0.91	1.25	1.08	31.48

Underlined elements indicate elements with significant natural variability (MPD>20%)

		Duplicate Pair 7				Duplicate Pair 8			
		Q515421	Q515422	Mean	MPD (%)	Q515439	Q515440	Mean	MPD (%)
Au	ppm	0.0001	0.0002	0.00015	66.67	0.001	0.0004	0.0007	85.71
Ag	ppm	0.01	0.013	0.0115	26.09	0.012	0.008	0.01	40.00
Al	%	0.5	0.39	0.445	24.72	0.35	0.23	0.29	41.38
As	ppm	1.24	1.23	1.235	0.81	1.94	0.77	1.355	86.35
B	ppm	5	5	5	0.00	5	5	5	0.00
Ba	ppm	24	20.8	22.4	14.29	16	14.2	15.1	11.92
Be	ppm	0.13	0.14	0.135	7.41	0.12	0.08	0.1	40.00
Bi	ppm	0.056	0.052	0.054	7.41	0.104	0.076	0.09	31.11
Ca	%	0.13	0.1	0.115	26.09	0.09	0.1	0.095	10.53
Cd	ppm	0.014	0.016	0.015	13.33	0.019	0.013	0.016	37.50
Ce	ppm	26.1	21.3	23.7	20.25	27.8	24.1	25.95	14.26
Co	ppm	3.24	2.59	2.915	22.30	1.795	2.3	2.0475	24.66
Cr	ppm	15.4	11.5	13.45	29.00	8.51	7.19	7.85	16.82
Cs	ppm	0.619	0.493	0.556	22.66	0.329	0.307	0.318	6.92
Cu	ppm	5.43	5.2	5.315	4.33	6.32	6.17	6.245	2.40
Fe	%	0.92	0.65	0.785	34.39	0.49	0.43	0.46	13.04
Ga	ppm	2.85	1.98	2.415	36.02	1.32	1.135	1.2275	15.07
Ge	ppm	0.055	0.038	0.0465	36.56	0.043	0.038	0.0405	12.35
Hf	ppm	0.022	0.014	0.018	44.44	0.03	0.03	0.03	0.00
Hg	ppm	0.002	0.006	0.004	100.00	0.005	0.002	0.0035	85.71
In	ppm	0.005	0.0025	0.00375	66.67	0.0025	0.0025	0.0025	0.00
K	%	0.09	0.07	0.08	25.00	0.06	0.06	0.06	0.00
La	ppm	12.25	10.05	11.15	19.73	12.8	11.4	12.1	11.57
Li	ppm	12.6	10.2	11.4	21.05	7.4	6.7	7.05	9.93
Mg	%	0.23	0.17	0.2	30.00	0.12	0.11	0.115	8.70
Mn	ppm	82.2	59.6	70.9	31.88	34.8	38	36.4	8.79
Mo	ppm	0.16	0.17	0.165	6.06	0.29	0.2	0.245	36.73
Na	%	0.007	0.005	0.006	33.33	0.006	0.005	0.0055	18.18
Nb	ppm	0.694	0.491	0.5925	34.26	0.356	0.213	0.2845	50.26
Ni	ppm	7.98	6.69	7.335	17.59	5.59	4.74	5.165	16.46
P	%	0.049	0.04	0.0445	20.22	0.049	0.049	0.049	0.00
Pb	ppm	1.87	1.665	1.7675	11.60	2.23	1.595	1.9125	33.20
Pd	ppm	0.001	0.0005	0.00075	66.67	0.0005	0.001	0.00075	66.67
Pt	ppm	0.001	0.001	0.001	0.00	0.001	0.001	0.001	0.00
Rb	ppm	7.63	5.7	6.665	28.96	3.19	3.44	3.315	7.54
Re	ppm	0.0005	0.0005	0.0005	0.00	0.0005	0.0005	0.0005	0.00
S	%	0.005	0.005	0.005	0.00	0.02	0.02	0.02	0.00
Sb	ppm	0.0025	0.0025	0.0025	0.00	0.005	0.005	0.005	0.00
Sc	ppm	1.415	0.987	1.201	35.64	0.769	0.655	0.712	16.01
Se	ppm	0.05	0.05	0.05	0.00	0.05	0.05	0.05	0.00
Sn	ppm	0.3	0.21	0.255	35.29	0.14	0.12	0.13	15.38
Sr	ppm	5.57	4.71	5.14	16.73	3.02	3.14	3.08	3.90
Ta	ppm	0.0025	0.0025	0.0025	0.00	0.0025	0.0025	0.0025	0.00
Te	ppm	0.005	0.01	0.0075	66.67	0.01	0.02	0.015	66.67
Th	ppm	3.2	2.55	2.875	22.61	3.56	3.37	3.465	5.48
Ti	%	0.039	0.026	0.0325	40.00	0.02	0.019	0.0195	5.13
Tl	ppm	0.062	0.046	0.054	29.63	0.024	0.025	0.0245	4.08
U	ppm	0.453	0.423	0.438	6.85	0.821	0.812	0.8165	1.10
V	ppm	21.2	14.6	17.9	36.87	9.4	9	9.2	4.35
W	ppm	0.073	0.062	0.0675	16.30	0.077	0.066	0.0715	15.38
Y	ppm	3.71	3	3.355	21.16	3.76	3.79	3.775	0.79
Zn	ppm	16.1	12.3	14.2	26.76	6.5	6	6.25	8.00
Zr	ppm	1.21	0.51	0.86	81.40	1.25	1.43	1.34	13.43

Underlined elements indicate elements with significant natural variability (MPD>20%)

		Duplicate Pair 9				Mean MPD
		Q515451	Q515452	Mean	MPD (%)	
Au	ppm	0.138	0.0003	0.06915	199.13	47.47
Ag	ppm	0.023	0.008	0.0155	96.77	22.80
Al	%	0.44	0.33	0.385	28.57	11.91
As	ppm	1.38	0.95	1.165	36.91	21.24
B	ppm	5	5	5	0.00	3.33
Ba	ppm	27.6	20.9	24.25	27.63	20.17
Be	ppm	0.18	0.11	0.145	48.28	14.79
Bi	ppm	0.131	0.099	0.115	27.83	9.87
Ca	%	0.14	0.12	0.13	15.38	4.40
Cd	ppm	0.019	0.02	0.0195	5.13	7.12
Ce	ppm	40.9	34.6	37.75	16.69	23.24
Co	ppm	3.11	2.25	2.68	32.09	11.24
Cr	ppm	13.2	10.05	11.625	27.10	15.00
Cs	ppm	0.687	0.451	0.569	41.48	8.39
Cu	ppm	12.15	8.69	10.42	33.21	10.20
Fe	%	0.68	0.56	0.62	19.35	5.85
Ga	ppm	2.09	1.65	1.87	23.53	7.78
Ge	ppm	0.073	0.061	0.067	17.91	5.08
Hf	ppm	0.05	0.064	0.057	24.56	4.12
Hg	ppm	0.004	0.002	0.003	66.67	25.40
In	ppm	0.0025	0.0025	0.0025	0.00	0.00
K	%	0.11	0.08	0.095	31.58	5.31
La	ppm	19.85	16.65	18.25	17.53	13.43
Li	ppm	10	7.7	8.85	25.99	12.39
Mg	%	0.18	0.14	0.16	25.00	5.73
Mn	ppm	64.8	50.3	57.55	25.20	45.90
Mo	ppm	0.37	0.31	0.34	17.65	9.20
Na	%	0.009	0.008	0.0085	11.76	5.00
Nb	ppm	0.539	0.316	0.4275	52.16	17.37
Ni	ppm	7.9	6.19	7.045	24.27	11.16
P	%	0.06	0.056	0.058	6.90	1.18
Pb	ppm	2.47	2.07	2.27	17.62	9.69
Pd	ppm	0.0005	0.0005	0.0005	0.00	11.11
Pt	ppm	0.001	0.002	0.0015	66.67	11.11
Rb	ppm	6.37	4.7	5.535	30.17	10.02
Re	ppm	0.0005	0.0005	0.0005	0.00	0.00
S	%	0.03	0.03	0.03	0.00	0.01
Sb	ppm	0.0025	0.006	0.00425	82.35	13.73
Sc	ppm	1.38	1.02	1.2	30.00	8.38
Se	ppm	0.05	0.1	0.075	66.67	11.15
Sn	ppm	0.21	0.17	0.19	21.05	6.21
Sr	ppm	4.69	4.17	4.43	11.74	5.61
Ta	ppm	0.0025	0.0025	0.0025	0.00	0.00
Te	ppm	0.01	0.01	0.01	0.00	11.12
Th	ppm	4.6	4.2	4.4	9.09	4.70
Ti	%	0.038	0.029	0.0335	26.87	5.35
Tl	ppm	0.045	0.035	0.04	25.00	4.88
U	ppm	1.315	1.215	1.265	7.91	1.99
V	ppm	14.8	11.7	13.25	23.40	14.59
W	ppm	0.162	0.064	0.113	86.73	17.06
Y	ppm	5.73	5.04	5.385	12.81	4.92
Zn	ppm	11.4	8.6	10	28.00	13.48
Zr	ppm	2.55	2.55	2.55	0.00	3.25

Underlined elements indicate elements with significant natural variability (MPD>20%)

B.4 Till Pb Isotope Q-ICP-MS QAQC

The QA/QC protocol for the Pb isotope analysis of till samples included the calculation of the MPD (%) for labortory duplicate pairs, and is summarized in this section.

Till Pb Isotope Q-ICP-MS Duplicate MPD (%)

Pb Isotope Ratio	Lab Duplicate Pair 1				Lab Duplicate Pair 2				Avg. MPD (%)
	Q515300	Q515300d	Mean	MPD (%)	Q515449	Q515449d	Mean	MPD (%)	
206/204	18.11	18.15	18.13	0.22	18.45	18.77	18.61	1.72	0.97
207/204	15.57	15.68	15.63	0.70	15.61	15.58	15.60	0.19	0.45
208/204	39.16	38.39	38.78	1.99	37.24	37.41	37.33	0.46	1.22
208/206	2.162	2.115	2.14	2.20	2.019	1.993	2.01	1.30	1.75
208/207	2.516	2.448	2.48	2.74	2.385	2.401	2.39	0.67	1.70
206/207	1.163	1.162	1.16	0.09	1.181	1.204	1.19	1.93	1.01

B.5 Till Size Fraction Four Acid ICP-MS QAQC

The QA/QC protocol for the four acid ICP-MS analyses of the various size fractions of till samples included the calculation of the MPD (%) for laboratory duplicate pairs. Additionally, the reconstituted trace element geochemistry was calculated as the weighted sum of all size fractions, and was compared to the -180 micron results. The results of this QA/QC protocol are summarized in this section.

Till Size Fraction Four Acid ICP-MS Duplicate MPD (%)

		Duplicate Pair 1				Duplicate Pair 2			
		125-106 µm				25-5 µm			
		515300-3	515300-9	Mean	MPD (%)	515300-7	515300-8	Mean	MPD (%)
Ag	ppm	0.033	0.032	0.0325	3.1	0.045	0.045	0.045	0.0
Al	%	4.7	4.46	4.58	5.2	6.08	6.46	6.27	6.1
As	ppm	1.53	1.18	1.355	25.8	3.05	3.57	3.31	15.7
Ba	ppm	520	510	515	1.9	730	780	755	6.6
Be	ppm	0.94	1.03	0.985	9.1	1.27	1.43	1.35	11.9
Bi	ppm	0.078	0.057	0.0675	31.1	0.16	0.176	0.168	9.5
Ca	%	1.06	1.05	1.055	0.9	1.22	1.3	1.26	6.3
Cd	ppm	0.045	0.034	0.0395	27.8	0.05	0.061	0.0555	19.8
Ce	ppm	30.7	22.1	26.4	32.6	58.5	63.9	61.2	8.8
Co	ppm	4.98	4.03	4.505	21.1	8.2	8.91	8.555	8.3
Cr	ppm	26.4	22.6	24.5	15.5	52	54.9	53.45	5.4
Cs	ppm	1.33	0.99	1.16	29.3	2.42	2.6	2.51	7.2
Cu	ppm	9.64	7.38	8.51	26.6	19.2	20.6	19.9	7.0
Fe	%	1.57	1.34	1.455	15.8	2.58	2.76	2.67	6.7
Ga	ppm	10.85	9.77	10.31	10.5	15.9	17.5	16.7	9.6
Ge	ppm	0.06	0.05	0.055	18.2	0.08	0.1	0.09	22.2
Hf	ppm	1.75	2.07	1.91	16.8	5.15	5.52	5.335	6.9
In	ppm	0.017	0.016	0.0165	6.1	0.037	0.036	0.0365	2.7
K	%	1.42	1.36	1.39	4.3	2.05	2.18	2.115	6.1
La	ppm	14	10.6	12.3	27.6	29	31.5	30.25	8.3
Li	ppm	18.4	15.5	16.95	17.1	30.8	33.2	32	7.5
Mg	%	0.49	0.42	0.455	15.4	0.76	0.81	0.785	6.4
Mn	ppm	240	212	226	12.4	306	326	316	6.3
Mo	ppm	0.25	0.22	0.235	12.8	0.6	0.61	0.605	1.7
Na	%	1.44	1.445	1.4425	0.3	1.52	1.61	1.565	5.8
Nb	ppm	3.87	3.33	3.6	15.0	8.47	9.22	8.845	8.5
Ni	ppm	13.3	10.45	11.875	24.0	25.2	26.4	25.8	4.7
P	%	0.026	0.024	0.025	8.0	0.041	0.043	0.042	4.8
Pb	ppm	8.69	8.15	8.42	6.4	12.1	13.15	12.625	8.3
Rb	ppm	42.3	37.8	40.05	11.2	68.1	72.2	70.15	5.8
Re	ppm	<0.002	<0.002	-	-	<0.002	<0.002	-	-
S	%	0.01	0.01	0.01	0.0	0.01	0.01	0.01	0.0
Sb	ppm	0.04	0.04	0.04	0.0	0.06	0.07	0.065	15.4
Sc	ppm	5.36	4.67	5.015	13.8	9.49	10.4	9.945	9.2
Se	ppm	0.2	0.4	0.3	66.7	0.3	0.5	0.4	50.0
Sn	ppm	0.79	0.66	0.725	17.9	1.51	1.63	1.57	7.6
Sr	ppm	215	216	215.5	0.5	237	251	244	5.7
Ta	ppm	0.27	0.23	0.25	16.0	0.62	0.67	0.645	7.8
Te	ppm	<0.04	<0.04	-	-	<0.04	<0.04	-	-
Th	ppm	3.17	2.03	2.6	43.8	7.14	7.64	7.39	6.8
Ti	%	0.168	0.153	0.1605	9.3	0.328	0.352	0.34	7.1
Tl	ppm	0.224	0.205	0.2145	8.9	0.375	0.405	0.39	7.7
U	ppm	0.72	0.56	0.64	25.0	1.72	1.82	1.77	5.6
V	ppm	38	32.9	35.45	14.4	67.1	71	69.05	5.6
W	ppm	0.304	0.244	0.274	21.9	0.667	0.718	0.6925	7.4
Y	ppm	7.1	6.03	6.565	16.3	11.7	12.3	12	5.0
Zn	ppm	25.7	20.9	23.3	20.6	43.5	45.9	44.7	5.4
Zr	ppm	62.4	78.8	70.6	23.2	197	211	204	6.9

underlined values exhibit significant natural variability (MPD > 20%)

		Duplicate Pair 3				Duplicate Pair 4			
		150-125 µm				106-75 µm			
		515396-2	515396-8	Mean	MPD (%)	515396-4	515396-9	Mean	MPD (%)
Ag	ppm	0.033	0.035	0.034	5.9	0.033	0.04	0.0365	19.2
Al	%	4.33	4.35	4.34	0.5	4.18	4.35	4.265	4.0
As	ppm	1.09	1.48	1.285	30.4	1.13	1.02	1.075	10.2
Ba	ppm	530	540	535	1.9	530	560	545	5.5
Be	ppm	0.87	0.79	0.83	9.6	0.78	0.85	0.815	8.6
Bi	ppm	0.054	0.067	0.0605	21.5	0.042	0.069	0.0555	48.6
Ca	%	0.95	0.89	0.92	6.5	1.03	1.02	1.025	1.0
Cd	ppm	0.027	0.024	0.0255	11.8	0.032	0.029	0.0305	9.8
Ce	ppm	33.5	28.5	31	16.1	41.8	30	35.9	32.9
Co	ppm	4.43	5.03	4.73	12.7	4.1	4.41	4.255	7.3
Cr	ppm	17.7	19.5	18.6	9.7	17	18	17.5	5.7
Cs	ppm	0.82	1.01	0.915	20.8	0.72	0.82	0.77	13.0
Cu	ppm	6.45	7.44	6.945	14.3	5.13	5.85	5.49	13.1
Fe	%	1.08	1.12	1.1	3.6	1.14	1.11	1.125	2.7
Ga	ppm	8.92	8.95	8.935	0.3	8.81	9.25	9.03	4.9
Ge	ppm	0.05	0.05	0.05	0.0	0.07	0.05	0.06	33.3
Hf	ppm	1.225	1.945	1.585	45.4	1.975	1.98	1.9775	0.3
In	ppm	0.011	0.012	0.0115	8.7	0.012	0.008	0.01	40.0
K	%	1.48	1.55	1.515	4.6	1.43	1.54	1.485	7.4
La	ppm	15.8	13.25	14.525	17.6	19.2	13.95	16.575	31.7
Li	ppm	15.7	17.7	16.7	12.0	14.2	15.9	15.05	11.3
Mg	%	0.35	0.38	0.365	8.2	0.36	0.36	0.36	0.0
Mn	ppm	224	199	211.5	11.8	231	211	221	9.0
Mo	ppm	0.18	0.24	0.21	28.6	0.17	0.17	0.17	0.0
Na	%	1.4	1.38	1.39	1.4	1.385	1.425	1.405	2.8
Nb	ppm	2.71	3.11	2.91	13.7	2.65	2.63	2.64	0.8
Ni	ppm	8.9	10.25	9.575	14.1	8.14	8.67	8.405	6.3
P	%	0.031	0.029	0.03	6.7	0.044	0.04	0.042	9.5
Pb	ppm	7.97	7.88	7.925	1.1	8.08	8.36	8.22	3.4
Rb	ppm	41.5	44.6	43.05	7.2	39.1	43.2	41.15	10.0
Re	ppm	<0.002	<0.002	-	-	<0.002	<0.002	-	-
S	%	<0.01	<0.01	-	-	<0.01	<0.01	-	-
Sb	ppm	0.05	0.04	0.045	22.2	0.04	0.05	0.045	22.2
Sc	ppm	3.79	3.65	3.72	3.8	4.21	4.06	4.135	3.6
Se	ppm	0.3	0.3	0.3	0.0	0.4	0.2	0.3	66.7
Sn	ppm	0.5	0.67	0.585	29.1	0.54	0.56	0.55	3.6
Sr	ppm	204	199	201.5	2.5	209	215	212	2.8
Ta	ppm	0.19	0.23	0.21	19.0	0.17	0.17	0.17	0.0
Te	ppm	<0.04	<0.04	-	-	<0.04	0.05	0.05	-
Th	ppm	3.79	2.87	3.33	27.6	4.78	3.08	3.93	43.3
Ti	%	0.118	0.126	0.122	6.6	0.127	0.116	0.1215	9.1
Tl	ppm	0.2	0.227	0.2135	12.6	0.214	0.221	0.2175	3.2
U	ppm	0.63	0.63	0.63	0.0	0.68	0.59	0.635	14.2
V	ppm	25.5	25	25.25	2.0	26.4	25.6	26	3.1
W	ppm	0.183	0.214	0.1985	15.6	0.16	0.163	0.1615	1.9
Y	ppm	5.96	5.29	5.625	11.9	7.22	6.35	6.785	12.8
Zn	ppm	17.5	20	18.75	13.3	17.1	17.7	17.4	3.4
Zr	ppm	41.3	70.5	55.9	52.2	76.7	75.3	76	1.8

underlined values exhibit significant natural variability (MPD > 20%)

		Duplicate Pair 5				Duplicate Pair 6				Average MPD (%)
		25-5 µm				53-25 µm				
		515414-7	515414-8	Mean	MPD (%)	515469-6	515469-8	Mean	MPD (%)	
Ag	ppm	0.06	0.053	0.0565	12.4	0.035	0.033	0.034	5.9	7.7
Al	%	5.27	5.53	5.4	4.8	4.37	4.46	4.415	2.0	3.8
As	ppm	2.68	2.65	2.665	1.1	0.99	1.21	1.1	20.0	17.2
Ba	ppm	490	510	500	4.0	560	570	565	1.8	3.6
Be	ppm	1.24	1.28	1.26	3.2	0.84	1.15	0.995	31.2	12.3
Bi	ppm	0.162	0.175	0.1685	7.7	0.053	0.059	0.056	10.7	21.5
Ca	%	1.35	1.41	1.38	4.3	1.28	1.31	1.295	2.3	3.6
Cd	ppm	0.053	0.06	0.0565	12.4	0.042	0.037	0.0395	12.7	15.7
Ce	ppm	71.8	75.7	73.75	5.3	42.7	40.9	41.8	4.3	16.7
Co	ppm	3.8	4.03	3.915	5.9	4.74	4.89	4.815	3.1	9.7
Cr	ppm	24.2	26.7	25.45	9.8	24.6	24.2	24.4	1.6	8.0
Cs	ppm	1.02	1.09	1.055	6.6	0.76	0.77	0.765	1.3	13.0
Cu	ppm	9.77	10.4	10.085	6.2	6.01	5.99	6	0.3	11.3
Fe	%	1.17	1.24	1.205	5.8	1.55	1.56	1.555	0.6	5.9
Ga	ppm	9.66	10.85	10.255	11.6	8.86	9.2	9.03	3.8	6.8
Ge	ppm	0.1	0.1	0.1	0.0	0.08	0.09	0.085	11.8	14.3
Hf	ppm	5.24	5.91	5.575	12.0	3.98	4.46	4.22	11.4	15.5
In	ppm	0.017	0.013	0.015	26.7	0.014	0.017	0.0155	19.4	17.3
K	%	1.67	1.76	1.715	5.2	1.51	1.54	1.525	2.0	5.0
La	ppm	34.4	37.3	35.85	8.1	20.4	18.8	19.6	8.2	16.9
Li	ppm	14	15.7	14.85	11.4	14.1	14	14.05	0.7	10.0
Mg	%	0.33	0.34	0.335	3.0	0.46	0.46	0.46	0.0	5.5
Mn	ppm	184	194	189	5.3	283	287	285	1.4	7.7
Mo	ppm	0.4	0.47	0.435	16.1	0.2	0.18	0.19	10.5	11.6
Na	%	1.955	2.06	2.0075	5.2	1.345	1.38	1.3625	2.6	3.0
Nb	ppm	3.51	3.95	3.73	11.8	3.8	3.72	3.76	2.1	8.7
Ni	ppm	11.05	12.4	11.725	11.5	9.9	10.15	10.025	2.5	10.5
P	%	0.083	0.089	0.086	7.0	0.059	0.061	0.06	3.3	6.5
Pb	ppm	11.25	12.1	11.675	7.3	8.57	8.64	8.605	0.8	4.6
Rb	ppm	40.8	44.1	42.45	7.8	42.8	43.6	43.2	1.9	7.3
Re	ppm	<0.002	<0.002	-	-	<0.002	<0.002	-	-	-
S	%	<0.01	<0.01	-	-	<0.01	<0.01	-	-	0.0
Sb	ppm	0.05	0.05	0.05	0.0	0.05	0.06	0.055	18.2	13.0
Sc	ppm	4.4	4.91	4.655	11.0	5.84	5.99	5.915	2.5	7.3
Se	ppm	0.2	0.2	0.2	0.0	0.3	0.3	0.3	0.0	30.6
Sn	ppm	0.65	0.8	0.725	20.7	0.69	0.69	0.69	0.0	13.2
Sr	ppm	256	270	263	5.3	219	222	220.5	1.4	3.0
Ta	ppm	0.27	0.39	0.33	36.4	0.26	0.25	0.255	3.9	13.8
Te	ppm	<0.04	<0.04	-	-	<0.04	<0.04	-	-	-
Th	ppm	8.74	9.48	9.11	8.1	5.44	5.69	5.565	4.5	22.4
Ti	%	0.167	0.176	0.1715	5.2	0.18	0.18	0.18	0.0	6.2
Tl	ppm	0.196	0.213	0.2045	8.3	0.208	0.221	0.2145	6.1	7.8
U	ppm	2.58	2.73	2.655	5.6	0.96	0.94	0.95	2.1	8.8
V	ppm	30.1	32.3	31.2	7.1	34.3	35	34.65	2.0	5.7
W	ppm	0.292	0.31	0.301	6.0	0.192	0.2	0.196	4.1	9.5
Y	ppm	12.6	13.4	13	6.2	10	9.93	9.965	0.7	8.8
Zn	ppm	17.3	18.4	17.85	6.2	21.1	21.5	21.3	1.9	8.5
Zr	ppm	195.5	217	206.25	10.4	158	179	168.5	12.5	17.8

underlined values exhibit significant natural variability (MPD > 20%)

Till Size Fraction Four Acid ICP-MS QA/QC Reconstituted Sums

Sample		Ba	Cr	Fe (%)	Mg (%)	Mn	Nb	Ni	Ta	Ti (%)
	Reconstituted	634	37.3	1.99	0.61	272	5.92	17.66	0.42	0.244
515300	Bulk (-180 µm Four Acid)	650	38.2	2.08	0.63	274	6.62	19.15	0.46	0.256
	% Error	*-2.5*	*-2.4*	*-4.5*	*-3.5*	*-0.8*	*-10.6*	*-7.8*	*-9.8*	*-4.8*
	Reconstituted	637	32.6	1.77	0.57	310	5.10	15.35	0.36	0.209
515396	Bulk (-180 µm Four Acid)	630	35.4	1.82	0.60	321	5.85	15.35	0.42	0.210
	% Error	*1.1*	*-7.9*	*-2.8*	*-5.0*	*-3.4*	*-12.8*	*0.0*	*-14.7*	*-0.3*
	Reconstituted	403	13.2	0.72	0.22	128	1.93	6.54	0.15	0.092
515414	Bulk (-180 µm Four Acid)	421	15.9	0.80	0.24	146	2.57	6.73	0.20	0.101
	% Error	*-4.3*	*-16.8*	*-10.1*	*-8.3*	*-12.6*	*-24.9*	*-2.8*	*-22.6*	*-8.5*
	Reconstituted	556	22.4	1.36	0.41	247	3.45	10.07	0.25	0.156
515469	Bulk (-180 µm Four Acid)	580	25.2	1.47	0.43	271	4.16	10.95	0.27	0.183
	% Error	*-4.2*	*-11.1*	*-7.8*	*-3.5*	*-8.9*	*-17.0*	*-8.0*	*-8.7*	*-14.6*

*ppm unless otherlise noted. % error calculated as the difference between reconstituted and bulk values, divided by bulk value. Negative error values indicate reconstituted sums fall below bulk values.

Size Fraction Bulk -180 µm vs Reconstituted -180 µm Sum Plots

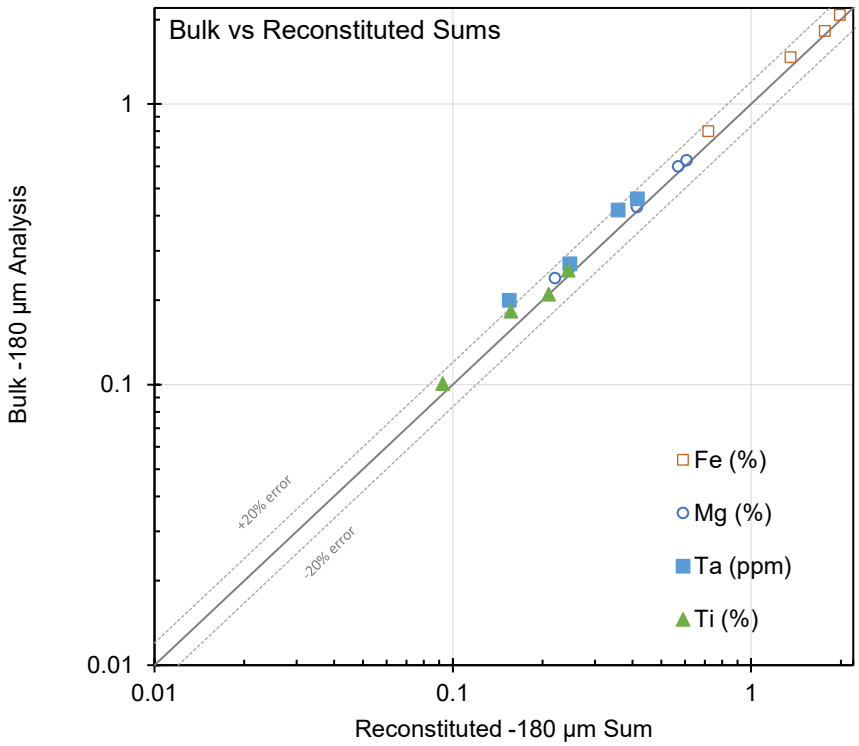

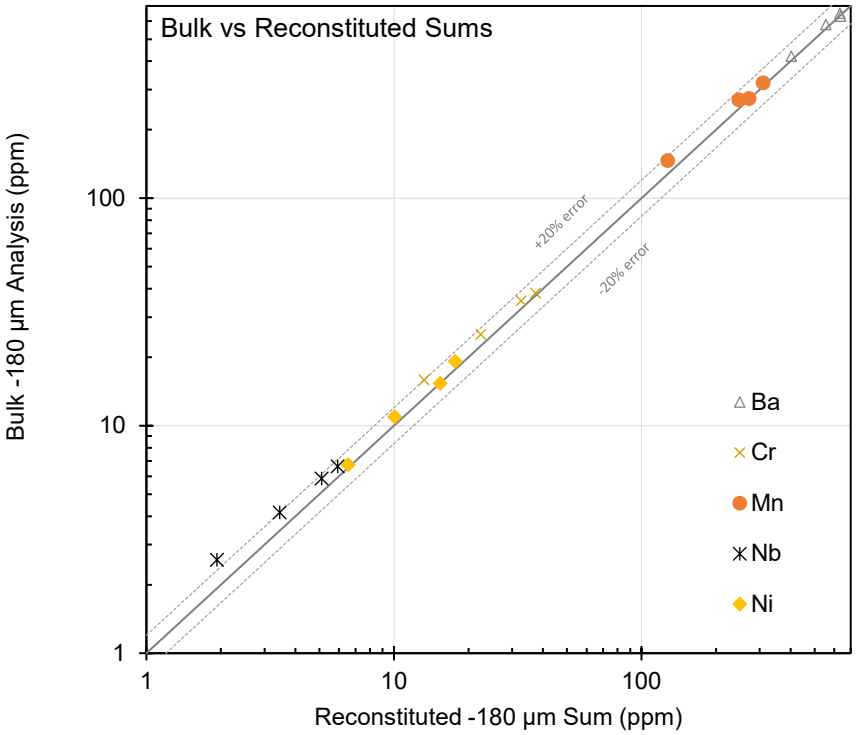

Appendix C

ActLabs SGH Interpretation Report

The complete Interpretation Report on the data and results of SGH analyses by ActLabs is included.

3D - SGH

"A SPATIOTEMPORAL GEOCHEMICAL HYDROCARBON INTERPRETATION"

for NWT Geoscience

"Kimberlite SGH PROJECT"

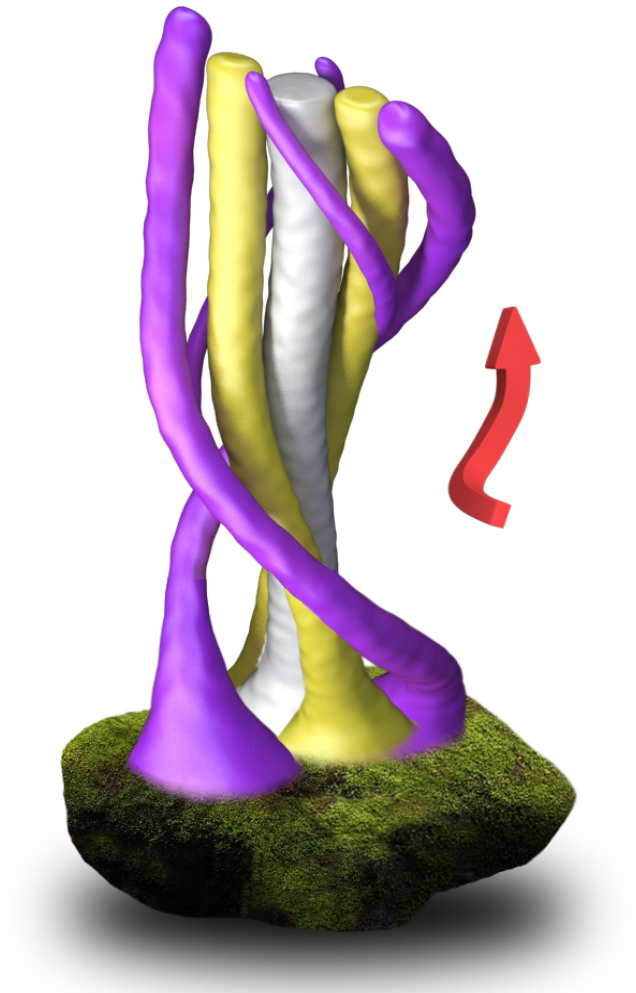

41 Bittern St. • Ancaster, ON • L9G 4V5 • CANADA • Tel: (905) 648-9611 • Fax: (905) 648-9613 • Toll Free: 1-888-ACTLABS

E-mail: dalesutherland@actlabs.com • Web Site: www.actlabs.com

(this page purposely left blank)

41 Bittern St. ● Ancaster, ON ● L9G 4V5 ● CANADA ● Tel: (905) 648-9611 ● Fax: (905) 648-9613 ● Toll Free: 1-888-ACTLABS

E-mail: dalesutherland@actlabs.com ● Web Site: www.actlabs.com

3D - SGH

"A SPATIOTEMPORAL GEOCHEMICAL HYDROCARBON INTERPRETATION"

for NWT Geoscience

"Kimberlite SGH PROJECT"

February 13, 2018

**** Dale Sutherland,***

Activation Laboratories Ltd

(* - author, originator)

EVALUATION OF SURFICIAL SOIL SAMPLES

EXPLORATION FOR: "Kimberlite "TARGETS

SGH KIMBERLITE TEMPLATE IS USED FOR THIS REPORT

Workorder: A18-00040

41 Bittern St. ● Ancaster, ON ● L9G 4V5 ● CANADA ● Tel: (905) 648-9611 ● Fax: (905) 648-9613 ● Toll Free: 1-888-ACTLABS

E-mail: dalesutherland@actlabs.com ● Web Site: www.actlabs.com

PREFACE

THIS SGH INTERPRETATION REPORT:

The purpose of this Spatio-temporal Geochemical Hydrocarbon (SGH, previously called Soil Gas Hydrocarbons) interpretation report is to provide more insight and knowledge that clients and other potential reviewers of the results have with regard to SGH, an organic, deep penetrating geochemistry. As SGH provides such a large data set and is not interpreted in the same way as inorganic geochemical methods, this interpretation and report enables the user to realize the results in a timely fashion and capitalizes on years of research and development since the inception of SGH in 1976 and includes the knowledge obtained by Activation Laboratories through the interpretation of SGH data from over hundreds of surveys for a wide variety of target types in various lithologies and from many geographical locations. Although referenced today as a "nano-technology", the analysis of SGH has not changed since inception. This interpretation and report is mandatory as it is the only known organic geochemistry that, in spite of the name, uses non-gaseous semi-volatile organic compounds interpreted using a forensic signature approach. The interpretation is based solely on SGH data (unless otherwise mentioned) and does not include the consideration or interpretation from any other geochemistry (inorganic), geology, or geophysics that may exist related to this survey area. This report can also provide evidence of project maintenance to government assessors. To keep the price to a minimum and to provide as short a turnaround time as practically possible, usually only one SGH Pathfinder Class map is illustrated in a typical report with an applied interpretation although several other SGH Pathfinder Class maps are used and referenced.

The interpretation in this report has used the results from some of the research with SGH in recent years which has focused on the fact that the SGH data is sometimes able to further dissect the relationships between the chemical Redox conditions in the overburden, the development of an electrochemical cell, and its affect in shaping geochemical anomalies. This research has resulted in the development by Activation Laboratories of a new enhanced model of the Electrochemical/ Redox Cell theory originated by Govett (1976) that was further developed to the model by Hamilton (2004, 2009). The new enhanced model developed by Sutherland (2011) takes the general anomalies expected by the Hamilton model to a higher level of detail and specificity. This has resulted in a more confident level of interpretation which has been referenced as 3D-SGH or **3D-Spatiotemporal Geochemical Hydrocarbons**. This model was first formally introduced at the International Applied Geochemistry Symposium (IAGS) organized by The Association of Applied Geochemists that took place in Rovaniemi, Finland, in August 2011. This new level of understanding of the expected anomaly types that can be observed with SGH provides a new level of quality control in the interpretation process as the symmetry of SGH anomalies can assure the interpreter which anomalies are truly as a result of a buried target. With the enhanced 3D-SGH interpretation that was introduced in 2012, we also mark the beginning of the ability to make some statements regarding the possible depth to mineralization for some projects as we dissect the Redox cell relative to the new Electrochemical Cell theory. The cover of this report is an artist's rendering of the pathways of different chemical classes of Spatiotemporal Geochemical Hydrocarbons which migrate through the overburden. This model is used as the new 3D-SGH interpretation approach.

41 Bittern St. ● Ancaster, ON ● L9G 4V5 ● CANADA ● Tel: (905) 648-9611 ● Fax: (905) 648-9613 ● Toll Free: 1-888-ACTLABS

E-mail: dalesutherland@actlabs.com ● Web Site: www.actlabs.com

DISCLAIMER

This "SGH Interpretation Report" has been prepared to assist the user in understanding the development and capabilities of this Organic based Geochemistry. The interpretation of the Soil Gas Hydrocarbon (SGH) data is in reference to a template or group of SGH classes of compounds specific to a type of mineralization or target that is chosen by the client (i.e. the template for gold, copper, VMS, uranium, etc.). The various templates of SGH Pathfinder Classes that together define the forensic identification signature for a wide range of commodity target types; Gold, Nickel, VMS, SEDEX, Uranium, Cu-Ni-PGE, IOCG, Base Metal, Tungsten, Lithium, Polymetallic, and Copper, as well as for Kimberlites, Coal Seam, Wet Gas and Oil Play, have been developed through years of research and have been further refined from review of case studies and orientation studies has proven to be able to also address a wide range of lithologies. Even with 20+ years of development and experience with SGH, Activation Laboratories Ltd. cannot guarantee that the templates used are applicable to every type of target in every type of environment. The interpretation in this report attempts to identify an anomaly that has the best SGH signature in the survey for the type of mineralization or target chosen by the client. However, this interpretation is not exhaustive and there may be additional SGH anomalies that may warrant interest. It should not be viewed due to the generation of this SGH report, that Activation Laboratories Ltd. has the expertise or is in the business of interpreting any type of geochemical data as a general service. As the author is the originator of the SGH geochemistry, has researched and developed this exploration tool since 1996, and has produced similar interpretations using SGH data for 1,100+ surveys, he is perhaps the best qualified to prepare this interpretation as assistance to clients wishing to use this SGH geochemistry. Activation Laboratories Ltd. can offer assistance in general suggestions for sampling protocols and in sample grid design; however we accept no responsibility to the appropriateness of the samples taken. Activation Laboratories Ltd. has made every attempt to ensure the accuracy and reliability of the information provided in this report. Activation Laboratories Ltd. or its employees do not accept any responsibility or liability for the accuracy, content, completeness, legality, or reliability of the information or description of processes contained in this report. The information is provided "as is" without a guarantee of any kind in the interpretation or use of the results of the SGH geochemistry. The client or user accepts all risks and responsibility for losses, damages, costs and other consequences resulting directly or indirectly from using any information or material contained in this report or using data from the associated spreadsheet of results.

41 Bittern St. ● Ancaster, ON ● L9G 4V5 ● CANADA ● Tel: (905) 648-9611 ● Fax: (905) 648-9613 ● Toll Free: 1-888-ACTLABS

E-mail: dalesutherland@actlabs.com ● Web Site: www.actlabs.com

Cautionary Note Regarding Assumptions and Forward Looking Statements

The statements and target rating made in the Soil Gas Hydrocarbon (SGH) interpretive report or in other communications may contain or imply certain forward-looking information related to the quality of a target or SGH anomaly.

Statements related to the rating of a target are based on comparison of the SGH signatures derived by Activation Laboratories Ltd. through previous research on known case studies. The rating is not derived from any statistics or other formula. The rating is a subjective value on a scale of 0 to 6 relative to the similarity of the SGH signature reviewed compared to the results of previous scientific research and case studies based on the analysis of surficial samples over known ore bodies. No information on the results from other geochemical methods, geophysics, or geology is usually available as additional information for the interpretation and assignment of a rating value unless otherwise stated. The rating does not imply ore grade and is not to be used in mineral resource estimate calculations. References to the rating should be viewed as forward-looking statements to the extent that it involves a subjective comparison to known SGH case studies. As with other geochemical methods, an implied rating and associated anticipated target characteristics may be different than that actually encountered if the target is drilled tested or the property developed.

Activation Laboratories Ltd. may also make a scientifically based reference in this interpretive report to an area that might be used as a drill target. Usually the nearest sample is identified as an approximation to a "possible drill target" location. This is based only on SGH results and is to be regarded as a guide based on the current state of this science. Unless otherwise stated, Activation Laboratories Ltd. has not physically observed the exploration site and has no prior knowledge of any site description or details or previous test results. Actlabs makes general recommendations for sampling and shipping of samples. Unless stated, the laboratory does not witness sampling, does not take into consideration the specific sampling procedures used, or factors such as the season of sampling, samples handling, packaging, or shipping methods. The majority of the time, Activation Laboratories Ltd. has had no input into sampling survey design. Where specified Activation Laboratories Ltd. may not have conducted sample preparation procedures as it may have been conducted at the client's assigned laboratory external to Actlabs. Although Actlabs has attempted to identify important factors that could cause actual actions, events or results to differ scientifically which may impact the associated interpretation and target rating from those described in forward-looking statements, there may be other factors that cause actions, events or results that are not anticipated, estimated or intended.

In general, any statements that express or involve discussions with respect to predictions, expectations, beliefs, plans, projections, objectives, assumptions, future events or performance are not statements of historical fact. These "scientifically based educated theories" should be viewed as "forward-looking statements". Readers of this interpretive report are cautioned not to place undue reliance on forward-looking information. Forward looking statements are made based on scientific beliefs, estimates and opinions on the date the statements are made and the interpretive report issued. The Company undertakes no obligation to update forward-looking statements or otherwise revise previous reports if these beliefs, estimates and opinions, future scientific developments, other new information, or other circumstances should change that may affect the analytical results, rating, or interpretation. Actlabs nor its employees shall be liable for any claims or damages as a result of this report, any interpretation, omissions in preparation, or in the test conducted. This report is to be reproduced in full, unless approved in writing.

41 Bittern St. ● Ancaster, ON ● L9G 4V5 ● CANADA ● Tel: (905) 648-9611 ● Fax: (905) 648-9613 ● Toll Free: 1-888-ACTLABS

E-mail: dalesutherland@actlabs.com ● Web Site: www.actlabs.com

SPATIOTEMPORAL GEOCHEMICAL HYDROCARBONS (SGH) GEOCHEMISTRY OVERVIEW

In the search for minerals and elements, geology requires tools to assess the location and potential quantity of minerals and ores. In the past people looked at the landscape to find the deposit. Similar landscapes indicate similar mineral and metal deposits. This is searching on a macro level, while geochemistry is searching on a micro level. Organic material requires many minerals and elements, so organic materials can be biomarkers of the presence of minerals and elements.

SGH is a deep penetrating geochemistry that involves the analysis of surficial samples from over potential mineral or petroleum targets. The analysis involves the testing for 162 hydrocarbon compounds in the C5-C17 carbon series range applicable to a wide variety of sample types. The hydrocarbons are residues from the decomposition of bacteria and microbe that feed on the target commodity as they require inorganic metallic's to catalyze the reactions necessary to develop hydrocarbons and grow in their life cycle. Specific classes of hydrocarbons (SGH) have been successful for delineating targets found at over 900 metres in depth. Samples of various media have been successfully analyzed such as soil (any horizon), sand, till, drill core, rock, peat, humus, lake-bottom sediments and even snow. After preparation in the laboratory, the SGH analysis incorporates a very weak leach, essentially aqueous, that only extracts the surficial bound hydrocarbon compounds and those compounds in interstitial spaces around the sample particles. These are the hydrocarbons that have been mobilized from the target depth. SGH is unique and should not be confused with other hydrocarbon tests or traditional analyses that measure C1 (Methane) to C5 (Pentane) or other gases. Thus, in spite of the name, SGH does not analyze for any hydrocarbons that are actually gaseous at room temperature and can be used to analyze for hydrocarbons in sample types other than soil. SGH is also different from soil hydrocarbon tests that thermally extracts or desorbs all of the hydrocarbons from the whole soil sample. This test is less specific as it does not separate the hydrocarbons and thus does not identify or measure the responses as precisely. These tests also do not use a forensic approach to identification. The hydrocarbons in the SGH extract are separated by high resolution capillary column gas chromatography and then detected by mass spectrometry to isolate, confirm, and measure the presence of only the individual hydrocarbons that have been found to be of interest from initial research and development and from performance testing especially from the two Canadian Mining Industry Research Organization (CAMIRO) projects (97E04 and 01E02).

Over the past 20+ years of research, Activation Laboratories Ltd. has developed an in-depth understanding of the unique SGH signatures associated with different commodity targets. Using a forensic approach we have developed target signatures or templates for identification, and the understanding of the expected geochromatography that is exhibited by each class of SGH compounds. In 2004 we began to include an SGH interpretation report delivered with the data to enable our clients to realize the complete value and understanding of the SGH results in the shortest time frame and provide the benefit from past research sponsored by Actlabs, CAMIRO, OMET and other industrial sponsors. In 2011, a new model of Electrochemical/Redox Cell theory was proposed and the new 3D-SGH interpretation approach based on this theory was incorporated in 2012 on a routine basis for SGH interpretation reports.

SGH has attracted the attention of a large number of Exploration companies. In the above mentioned research surveys, the sponsors have included (in no order): Western Mining Corporation, BHP-Billiton, Inco, Noranda, Outokumpu, Xstrata, Cameco, Cominco, Rio Algom, Alberta Geological Survey, Ontario Geological Survey, Manitoba Geological Survey and OMET. Further, beyond this research, Activation Laboratories Ltd. has interpreted the SGH data for over 700 targets from clients since January of 2004. In both CAMIRO projects, research surveys over known mineralization and in

41 Bittern St. ● Ancaster, ON ● L9G 4V5 ● CANADA ● Tel: (905) 648-9611 ● Fax: (905) 648-9613 ● Toll Free: 1-888-ACTLABS

E-mail: dalesutherland@actlabs.com ● Web Site: www.actlabs.com

exploration projects over unknown targets, SGH has performed exceptionally well. As an example, in the first CAMIRO research project that commenced in 1997 (Project 97E04), there were 10 study areas that were submitted blindly to Actlabs. These study sites were selected since other inorganic geochemical methods were unsuccessful at illustrating anomalies related to the target.

Although Actlabs was only provided with the samples and their coordinates, SGH was able to locate the blind mineralization with exceptional accuracy in 9 of the 10 surveys. SGH has consistently demonstrated this rate of success. SGH has been very successful in exploration and discovery of unknown targets e.g. as just one example Golden Band Resources drilled an SGH anomaly and discovered a significant vein containing "visible" gold. (www.goldenbandresources.com)

41 Bittern St. ● Ancaster, ON ● L9G 4V5 ● CANADA ● Tel: (905) 648-9611 ● Fax: (905) 648-9613 ● Toll Free: 1-888-ACTLABS

E-mail: dalesutherland@actlabs.com ● Web Site: www.actlabs.com

INTERPRETATION OF SGH RESULTS - A18-00040
NWT Geoscience – Kimberlite SGH PROJECT

SGH INTERPRETATION RATING AND CLARIFICATION

Often a geochemistry such as SGH is used as an economical exploration investigation tool to provide more information on an exploration target as some geological body or geophysical target. Field sampling is hoped to pick up changes in the chemistry of the immediate overburden which in turn is expected to result in a chemical anomaly. The author believes that it is important to convey to the client of an anomaly even if it is only a part of the mineral signature or template requested. The anomaly illustrated in the report may not be representative of the mineralization sought as only a part of the SGH signature is present and thus will have a low rating, but the anomaly may confirm the presence of the geological or geophysical target which may be valuable to the client. In addition it would confirm the ability and sensitivity of SGH to show geological or geophysical occurrences. Example: A well defined rabbit-ear anomaly on the SGH Pathfinder Class map in a report, even though it may have a lower rating of 2.0 or 3.0, may illustrate to the exploration geologist that SGH does agree that there is some geological body at depth that is changing the chemistry and forming a Redox cell in the overburden. However the SGH forensic signature Rating indicates that there is a lower confidence that the "identification" of that body is likely to be say Gold (if the SGH Gold template is requested). This information would provide a confirmation that a target does exist, however if the SGH Rating indicates that the target has a lower level of confidence then the target does not have the forensic signature of the mineralization sought. SGH would thus provide a savings to the exploration program and divert focus to potentially other targets having a higher confidence in the identification Rating.

Thus, the SGH rating must always be considered in conjunction with the SGH Pathfinder Class map(s) shown in the report. It is this rating that provides an insight into the authors' complete interpretation and is a measure of the confidence and to what degree the complete SGH signature compares with the SGH results from over case studies of similar known deposits. Unfortunately, the interpretation of a visual, as the SGH map provided, is so ingrained in humans that the reader may erroneously disregard the author's subjective rating to a large degree. As of November 25, 2011, the author now highlights the rating directly on the page having the plan view of the SGH Pathfinder Class map chosen to be illustrated. Thus to the reader of the report, the authors Rating is actually **MORE IMPORTANT** than the readers instinctive interpretation of the one map provided. Again, SGH should not be used in isolation from other site information, and that a Rating of 4.0 is when, in the authors' estimation, a signature only starts to have a good identification relative to that type of mineralization, and that the survey may warrant further study although it is not a specific recommendation to drill test the anomaly. As the SGH interpretation is represented by a signature, the SGH Pathfinder Class map(s) illustrated in reports is always only "PART" of the specific SGH signature or template that the client requests. No one SGH map can represent the complete signature due to the different amounts of spatial dispersion expected for the variety of SGH chemical classes within each signature. Thus the author selects the one SGH Class Map relative to the mineralization requested that best represents an anomaly that estimates the overall signature found in the survey.

41 Bittern St. ● Ancaster, ON ● L9G 4V5 ● CANADA ● Tel: (905) 648-9611 ● Fax: (905) 648-9613 ● Toll Free: 1-888-ACTLABS

E-mail: dalesutherland@actlabs.com ● Web Site: www.actlabs.com

INTERPRETATION OF SGH RESULTS - A18-00040
NWT Geoscience – Kimberlite SGH PROJECT

This report is based on the SGH results from the analysis of a total of 215 soil samples to determine the presence of Kimberlite SGH Project. The project area was covered by a condensed grouping of sample with 7 transect of wider spaced samples taken at increasing distances away from the grouped area. This is shown on the map below.

The high bias in this survey necessitated that it be interpreted twice, once as the whot survey and once with just the densely sampled portion,ac of 127 samples, which had samples taken at roughly 25 metres that appears on the next page. The SGH data is only reviewed for the specific target type requested, in this case for the presence of Kimberlite type deposits.

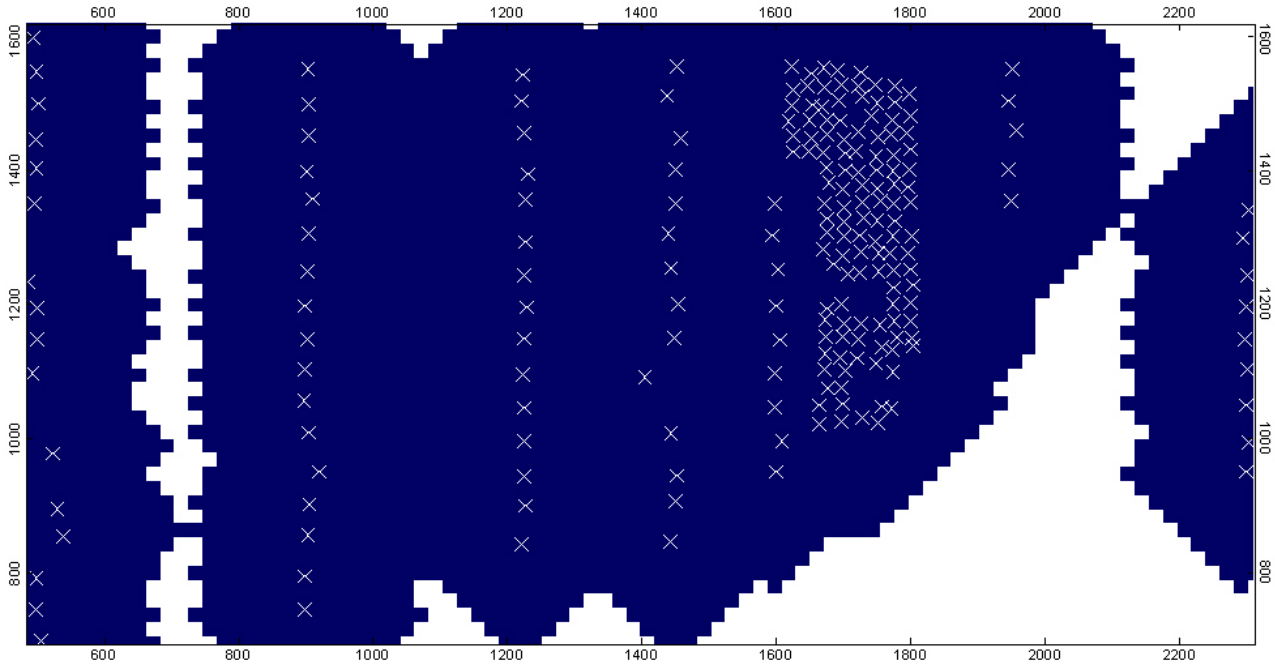

41 Bittern St. ● Ancaster, ON ● L9G 4V5 ● CANADA ● Tel: (905) 648-9611 ● Fax: (905) 648-9613 ● Toll Free: 1-888-ACTLABS

E-mail: dalesutherland@actlabs.com ● Web Site: www.actlabs.com

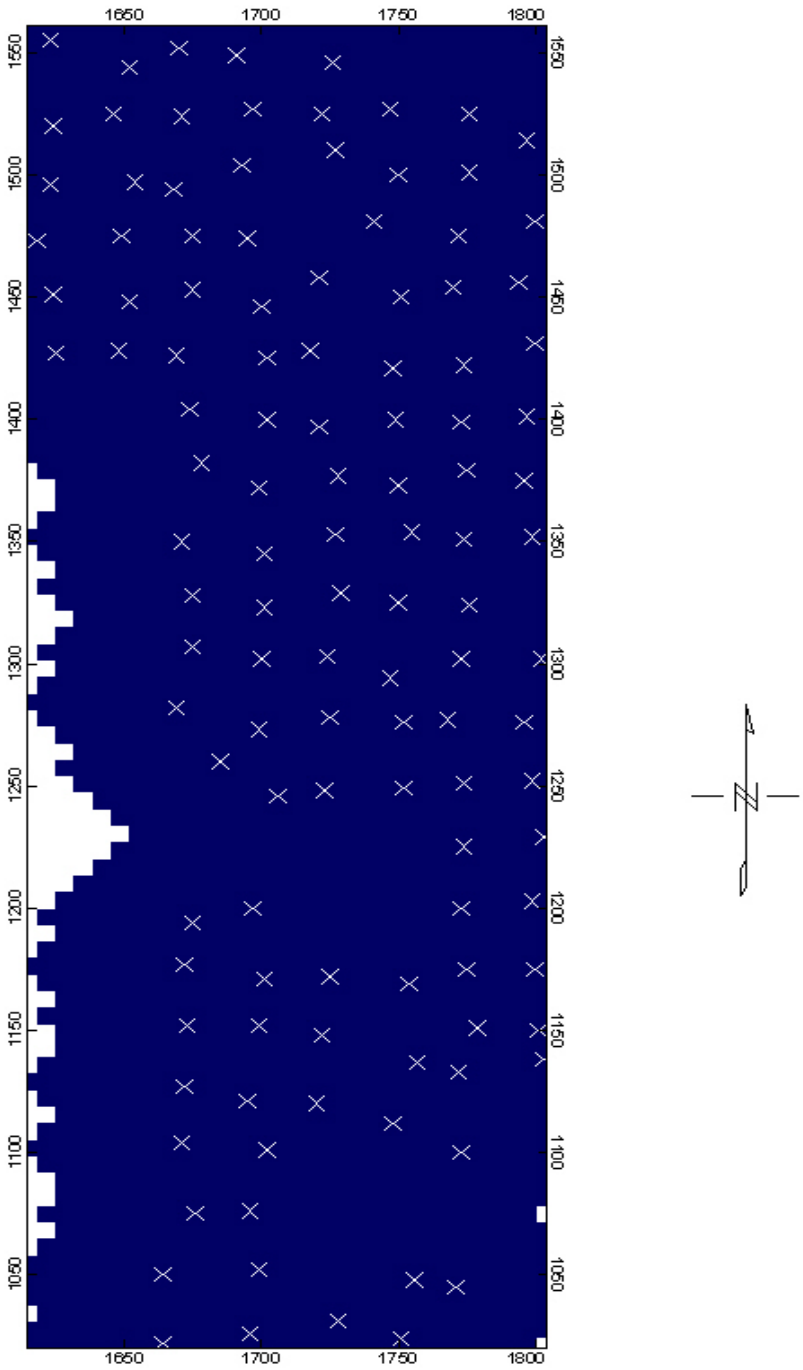

Condensed grouping portion of the survey with samples taken at about 25 metres.

41 Bittern St. ● Ancaster, ON ● L9G 4V5 ● CANADA ● Tel: (905) 648-9611 ● Fax: (905) 648-9613 ● Toll Free: 1-888-ACTLABS

E-mail: dalesutherland@actlabs.com ● Web Site: www.actlabs.com

INTERPRETATION OF SGH RESULTS - A18-00040
NWT Geoscience – Kimberlite SGH PROJECT

Note that the associated SGH results used for the maps shown in this report are presented in a separate Excel spreadsheet. This data must accompany this report. This data is semi-quantitative and is presented in units of pg/g or *parts-per-trillion* (ppt) as the concentration of specific hydrocarbons in the sample. The number of samples submitted for this survey is adequate to use SGH as an exploration tool. The recommended "minimum" number of samples is 50. As SGH is an organic geochemistry it is essentially "blind" to the elemental presence of any inorganic species as actual metallic gold, nickel, silver, uranium, etc. content in each sample analyzed. SGH only detects the hydrocarbon decomposition products of the bacteria that have used the mineralized target as a food source. Note that this geochemistry does not detect all organic hydrocarbons in the samples but only targets relatively rare hydrocarbons that have been proven to be associated with microbial degradation products and mineralization.

The overall precision of the SGH analysis for these soil samples at the Kimberlite SGH Project was very good as demonstrated by 15 different samples taken from this SGH survey which were used for laboratory replicate analysis. The average Coefficient of Variation (%CV) of the replicate results for the survey samples in this submission was 11.4% which represents a very good level of analytical performance especially at the low level parts-per-trillion (ppt) concentrations measured. The 7 field duplicates submitted was also quite good at 19.5%. It is typically observed that the variability of field duplicates is 5% to 8% CV higher than for laboratory duplicates of random samples taken from the survey.

The method of determination of the estimate of error expressed as a coefficient of variation that is used in SGH reports. With even a small survey of 50 samples, the analysis of 162 compounds in each sample in the SGH geochemistry represents a possible total of 8,100 measurements. Thus a method for the estimate of error had to be applicable to large data sets. Even the use of 3 pairs of different samples from a survey represents 972 measurements. A method of reporting the performance of sample replicates also has to recognize that values are at ultra-trace concentrations of low parts-per-trillion (ppt) values. Thus the method used is by Stanley and Lawie (Geochemistry: Exploration, Environment, Analysis, Vol. 8 2007, pp. 173-182) which was entitled: "Thompson-Howarth error analysis: unbiased alternative to the large sample method for assessing non-normally distributed measurement error in geochemical samples". No other statistics were used on the data for this report for mapping or interpretation purposes aside from the use of a Kriging trending algorithm in the GeoSoft Oasis Montaj mapping software. Note the blanking distance for this Kimberlite survey was not optimized as the distances between samples and for transects varied so much. This is best left to professional GIS personnel. **This interpretation is conducted blindly and is based only on the SGH results from this submission. No other geographical, geochemical or geophysical data was reviewed.** A template or group of SGH Pathfinder Classes that have been found to be associated with Kimberlite targets has been used as the basis for the interpretation of the Kimberlite SGH Project. The final interpretation is customized and conducted by the author. Although the term "template" or "signature" often appears in an SGH Interpretation Report, a computerized interpretation is not used.

41 Bittern St. ● Ancaster, ON ● L9G 4V5 ● CANADA ● Tel: (905) 648-9611 ● Fax: (905) 648-9613 ● Toll Free: 1-888-ACTLABS

E-mail: dalesutherland@actlabs.com ● Web Site: www.actlabs.com

A18-00040 – NWT Geoscience – Kimberlite SGH PROJECT
SGH INTERPRETATION – KIMBERLITE PATHFINDER CLASS MAPS

The KIMBERLITE template of SGH Pathfinder Classes uses medium and high molecular weight classes of hydrocarbon compounds. At least three Pathfinder Class maps, associated with the SGH signature developed for Kimberlite must be present to begin to be considered for assignment of a good rating relative to the SGH performance in case studies over known Kimberlite types of mineralization. These SGH classes must also concur and support a consistent interpretation in relation to the expected geochromatographic characteristics of the Pathfinder Class. The *overall* SGH interpretation Rating has even a higher level of confidence as it further implies the consensus between at least two additional pathfinder classes. A combination of these SGH Pathfinder Classes potentially defines the signature of a target at depth if present. Each of the SGH Pathfinder Class maps shown in this report is a specific *portion* of the SGH signature considered in the interpretation relative to the presence of Kimberlite occurances. Each pathfinder class map shown is still just one of the Pathfinder Class maps used in each of the interpretation templates (other SGH Pathfinder Class maps are usually not shown at this price point and report turnaround time except at the discretion of the Author).

SGH has been described by the Ontario Geological Survey of Canada (OGS) as a "Redox cell locator". Many SGH surveys for Gold and other mineral targets can result in multiple types of anomalies, depending on the class of SGH compounds, even over the same target and in the same set of samples. Thus "Apical", "Segmented-Nested-Halo", and "Rabbit-Ear" or "Segmented Halo" type anomalies are all typically observed within the SGH data set from the effect of Redox cells that have developed over mineralization or specific target types. Redox cells are also related to the presence of bacteriological activity and the presence of geological bodies such as Granite Gneiss, Dunite, etc. Recently SGH has been shown to be far more sensitive to depicting Redox conditions than any measurements using pH or ORP tests. Thus it is important to understand that; not only is SGH a Redox cell locator, due to the forensic signature of mineralization used in the interpretation process, SGH can discriminate mineral targets and other target types from geological bodies and other magnetically detected targets, mineralized versus non-mineralized conductors, cultural effects, etc. even in surveys over highly difficult or exotic terrain that results in the unavoidable collection of multiple sample types. SGH has been proven to discriminate between false or mobilized soil anomalies and is able to actually locate the source target deposition. SGH is a deep-penetrating geochemistry and has been proven to locate Gold and other types of mineralization at several hundred metres below the surface irrespective of the type of overburden.

41 Bittern St. ● Ancaster, ON ● L9G 4V5 ● CANADA ● Tel: (905) 648-9611 ● Fax: (905) 648-9613 ● Toll Free: 1-888-ACTLABS

E-mail: dalesutherland@actlabs.com ● Web Site: www.actlabs.com

A18-00040 – NWT Geoscience – Kimberlite SGH PROJECT
SGH KIMBERLITE INTERPRETATION

As a general comment in regard to the data from the Kimberlite SGH Project, the interpretation is quite fairly complex in the SGH interpretation of results for Kimberlite Pipes.

The maps from the SGH anomalies detected were of a good response, however the objective of the SGH geochemistry is not necessarily to obtain values/anomalies with the highest contrast based on a signal:noise interpretation of any one sample, SGH is a more powerful exploration tool by maximizing the overall spatial contrast of the survey to observe specific hydrocarbon signatures that can vector to and identify buried mineralization. This survey has enough samples for interpretation. A survey design of one or two transects is often used with SGH, especially in research or orientation surveys, however it does not allow for the full capabilities of 3D-SGH and the symmetry it seeks to provide the optimum confidence in predicting the presence of Gold or other mineralization and the pathfinders that describe the SGH signature for "buried or blind" Gold targets.

The 3D-SGH approach successfully observed some good symmetry of the primarily anomaly at the Kimberlite SGH Project which in this case illustrated the existence of one particular Redox zone in the central portion of this survey. The symmetry of this Redox cell, as seen with the 3D-SGH interpretation approach, is important at improving the confidence of the predicted location and identification of mineralization that may be present in the northern portion of the survey. SGH has proven to have a significantly higher level of confidence than other geochemical methods.

The KIMBERLITE Pathfinder Classes shown and other SGH Pathfinder Classes for this occurence are able to illustrate the presence of an SGH hydrocarbon signature that has usually been associated with Kimberlite type targets as the detection of those hydrocarbon residues produced by the decomposition of bacteria in the death phase that have been feeding on material containing Kimberlite that have subsequently migrated to the surface as a flux of different classes of hydrocarbons. The SGH predicted KIMBERLITE trends at the Kimberlite SGH Project is expected to be a direct vertical projection of the location of KIMBERLITE Mineral Indicators or Kimberlite Pipes unless a situation is encountered such as that of a major fault or shear zone that may result is a "slight" deflection of the path of migration to surface of these specific hydrocarbons.

41 Bittern St. ● Ancaster, ON ● L9G 4V5 ● CANADA ● Tel: (905) 648-9611 ● Fax: (905) 648-9613 ● Toll Free: 1-888-ACTLABS

E-mail: dalesutherland@actlabs.com ● Web Site: www.actlabs.com

A18-00040 – NWT Geoscience - Kimberlite SGH PROJECT
SGH REDOX INTERPRETATION

The mapped results shown on the next page of this report, and in 3D-view on the page thereafter, shows the SGH results from one of the most reliable SGH Pathfinder Classes in predicting the presence of Kimberlite for the complete survey. Note that the Kriging trending algorithm applied emphasizes the response obtained in the discreet transects away from the main grouping of samples. It is hypothesized that these increasingly distant transects were collected in this research study to determine the present of glacial mobilized Kimberlite indicator minerals. The map on the next page may indicate that enough Kimberlite related minerals were scrapped away by glacial events that are able to support microbial colonies. SGH appears to detect these mineral indicator trails that vector to the Kimberlite pipes in the cluster of 25m spacing, Again the magnitude of the anomalies on the transects are artificially enhanced.

The three dashed yellow lines are a representation of the Kimberlite indicator trails. This is the first time SGH has been used to view these pathways. Many other SGH Pathfinder Classes support this interpretation.

41 Bittern St. ● Ancaster, ON ● L9G 4V5 ● CANADA ● Tel: (905) 648-9611 ● Fax: (905) 648-9613 ● Toll Free: 1-888-ACTLABS

E-mail: dalesutherland@actlabs.com ● Web Site: www.actlabs.com

A16-10292 – NWT Geoscience – Kimberlite SGH PROJECT
SGH KIMBERLITE PATHFINDER CLASS MAP

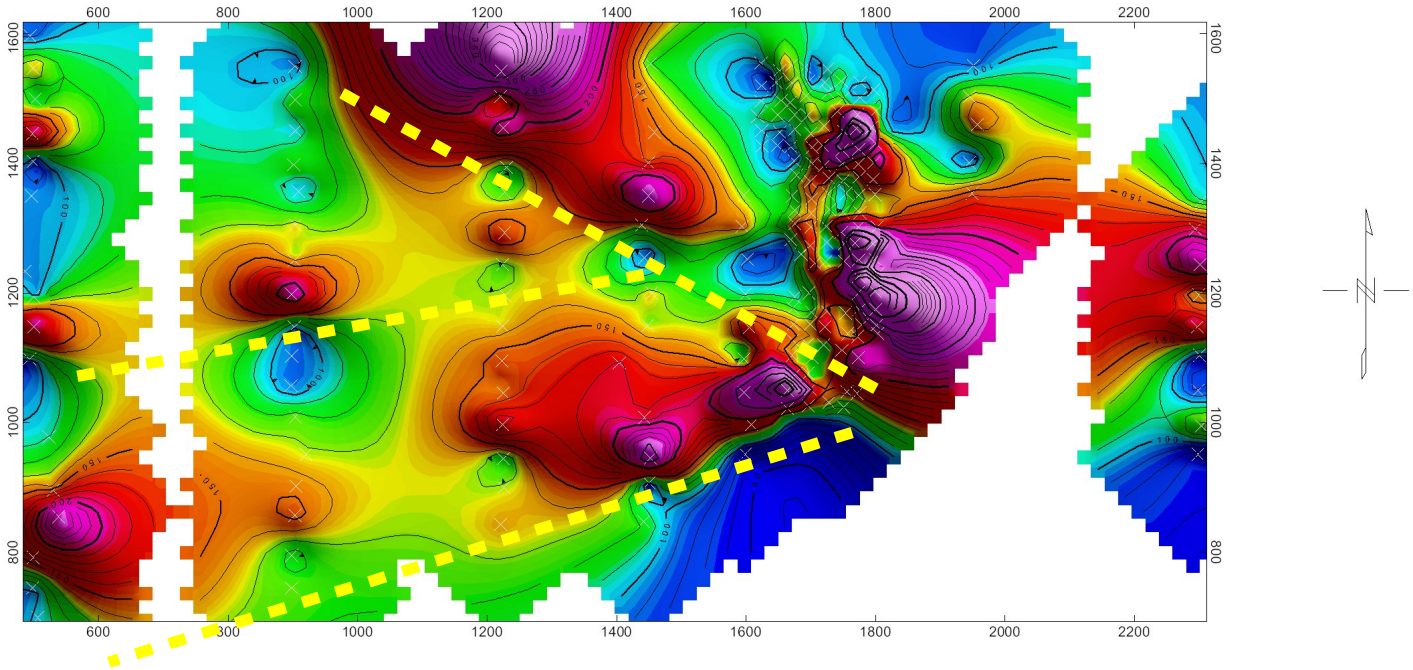

THREE PROPOSED KIMBERLITE MINERAL PATHWAYS REPRESENTED BY DASHED YELLOW LINES THAT VECTOR TO THE SOURCE KIMBERLITE PIPES - **SGH CONFIDENCE RATING 4.5 OUT OF 6.0**

Results represent only the material tested. Actlabs is not liable for any claim/damage from the use of this report in excess of the test cost. Samples are discarded in 90 days unless requested otherwise. This report is only to be reproduced in full.

41 Bittern St. ● Ancaster, ON ● L9G 4V5 ● CANADA ● Tel: (905) 648-9611 ● Fax: (905) 648-9613 ● Toll Free: 1-888-ACTLABS

E-mail: dalesutherland@actlabs.com ● Web Site: www.actlabs.com

A16-10292 – NWT Geoscience – Kimberlite SGH PROJECT
SGH KIMBERLITE PATHFINDER CLASS MAP

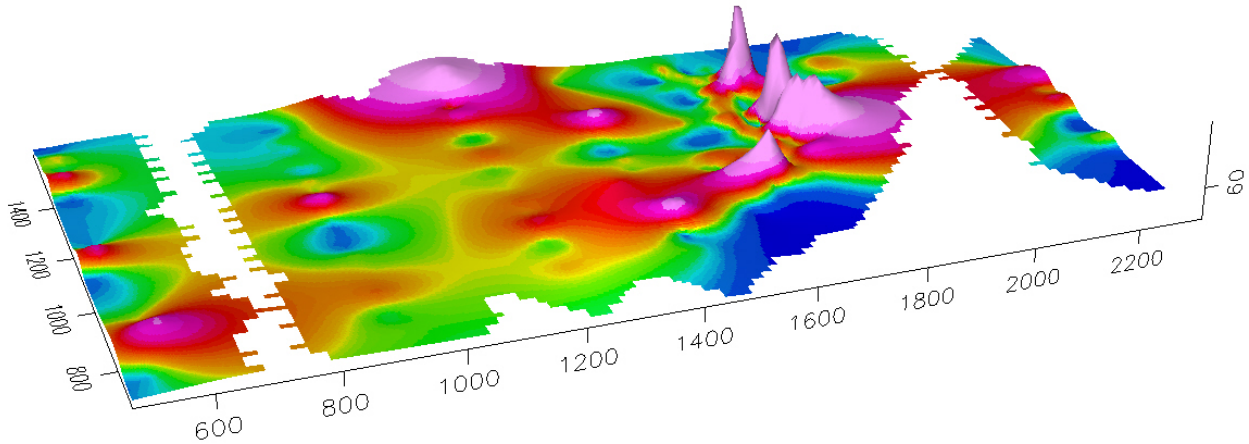

Results represent only the material tested. Actlabs is not liable for any claim/damage from the use of this report in excess of the test cost. Samples are discarded in 90 days unless requested otherwise. This report is only to be reproduced in full.

41 Bittern St. ● Ancaster, ON ● L9G 4V5 ● CANADA ● Tel: (905) 648-9611 ● Fax: (905) 648-9613 ● Toll Free: 1-888-ACTLABS

E-mail: dalesutherland@actlabs.com ● Web Site: www.actlabs.com

A16-10292 – NWT Geoscience - Kimberlite SGH PROJECT
SGH KIMBERLITE INTERPRETATION

The next page of this report, and in 3D-view on the following page is an SGH interpretation of the 25m gridded area in the eastern part of this survey. These maps are of the same SGH pathfinder class as was shownfor the complete survey. Due to the significantly lower sample spacing it was interpreted separately. Again the maps show the SGH anomalies from the most reliable SGH Pathfinder Classes in predicting the presence of Kimberlite occurrences.

This map shows quite complex anomalies in this area of the survey. Other Kimberlite class maps also support this interpretation. We believe that there are two Kimberlites present, as represented by the dashed yellow circles, however there is not sufficient with to this area to confidently states their location. Thus the SGH Confidence Rating has been reduced. Several other SGH Pathfinder Class Maps support this interpretation at the Kimberlite SGH Project.

Again, the prediction of these anomalies as outlining Kimberlite Pipes is based only on SGH. The SGH Confidence Rating in determining the location of the Kimberlite pipes is 4.5 out of a possible 6.0.

41 Bittern St. ● Ancaster, ON ● L9G 4V5 ● CANADA ● Tel: (905) 648-9611 ● Fax: (905) 648-9613 ● Toll Free: 1-888-ACTLABS

E-mail: dalesutherland@actlabs.com ● Web Site: www.actlabs.com

A16-10292 – NWT Geoscience - Kimberlite SGH PROJECT SGH "KIMBERLITE" PATHFINDER CLASS MAP

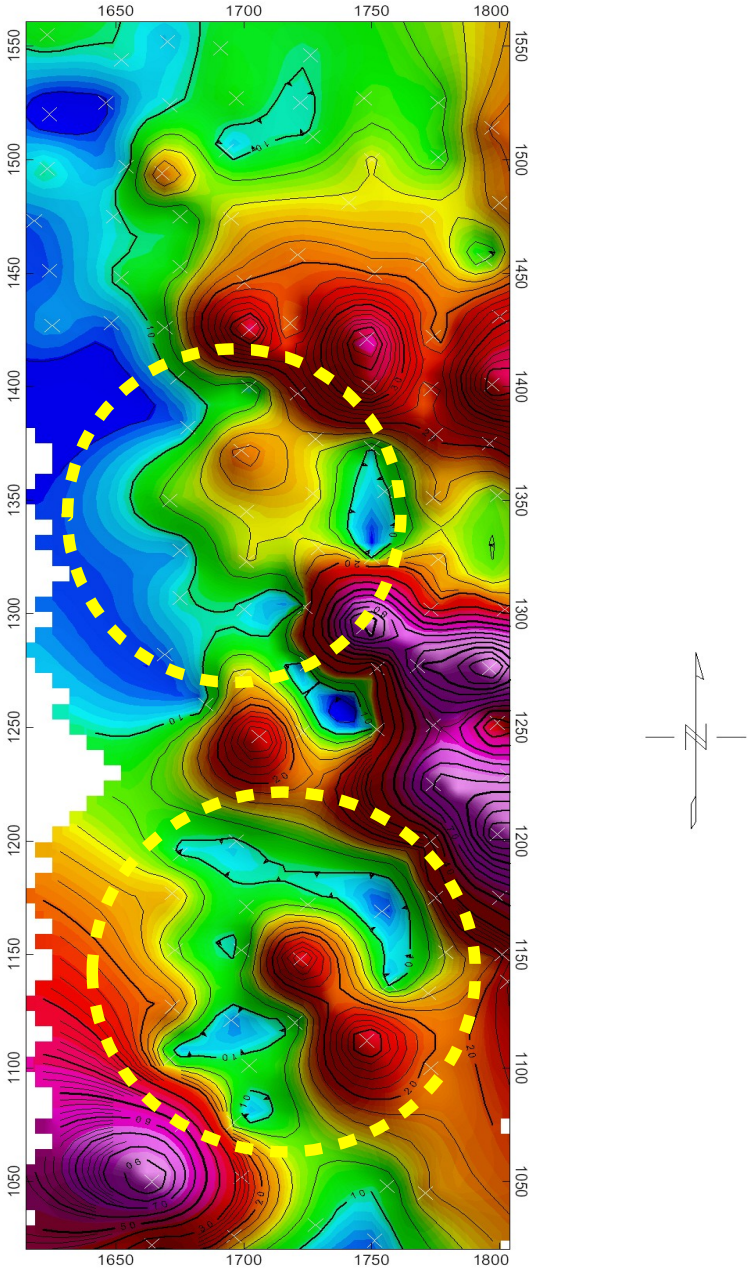

PREDICTED KIMBERLITE PIPE LOCATION REPRESENTED BY DASHED YELLOW CIRCLES

SGH CONFIDENCE RATING 5.0 OUT OF 6.0

Results represent only the material tested. Actlabs is not liable for any claim/damage from the use of this report in excess of the test cost. Samples are discarded in 90 days unless requested otherwise. This report is only to be reproduced in full.

41 Bittern St. ● Ancaster, ON ● L9G 4V5 ● CANADA ● Tel: (905) 648-9611 ● Fax: (905) 648-9613 ● Toll Free: 1-888-ACTLABS

E-mail: dalesutherland@actlabs.com ● Web Site: www.actlabs.com

A16-10292 – NWT Geoscience – Kimberlite SGH PROJECT
SGH "KIMBERLITE" PATHFINDER CLASS MAP

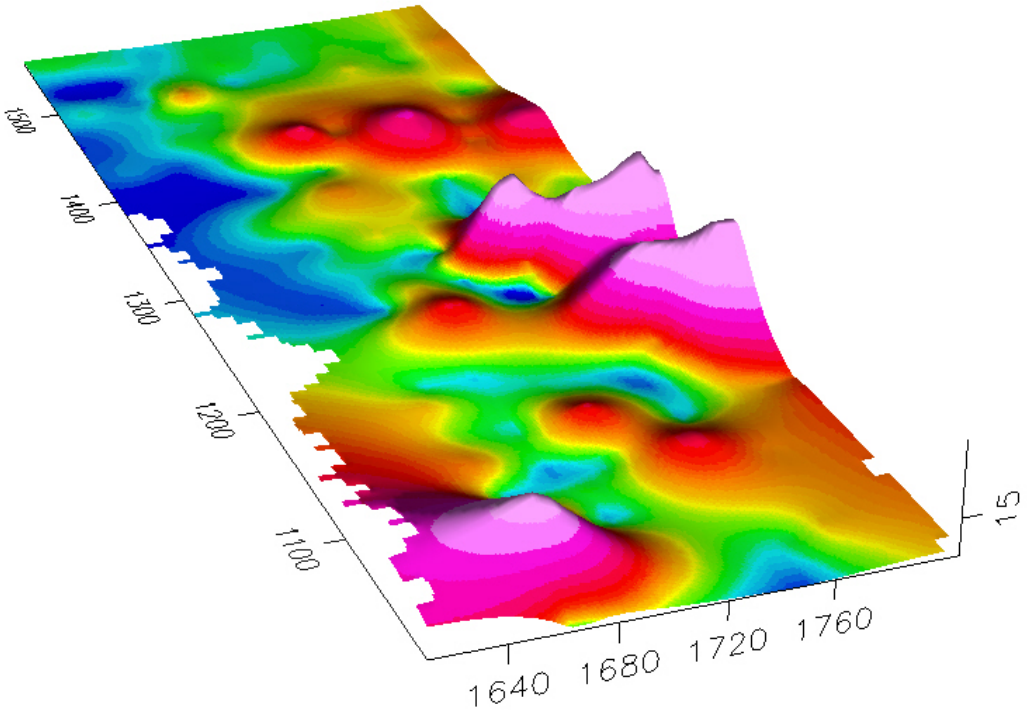

Results represent only the material tested. Actlabs is not liable for any claim/damage from the use of this report in excess of the test cost. Samples are discarded in 90 days unless requested otherwise. This report is only to be reproduced in full.

41 Bittern St. ● Ancaster, ON ● L9G 4V5 ● CANADA ● Tel: (905) 648-9611 ● Fax: (905) 648-9613 ● Toll Free: 1-888-ACTLABS

E-mail: dalesutherland@actlabs.com ● Web Site: www.actlabs.com

A18-00040 – NWT Geoscience
Kimberlite SGH PROJECT

IMPORTANT NOTE:

The intensity of the anomalies, i.e. red and purple colours, do not say anything about the grade or how much mineralization is present. SGH is a locator of mineralization under cover. It does not reveal the depth at the A2 Project either. Higher resolution sampling at say 50 metre may have to be employed to obtain more precise locations of mineralizations and possibly some statement regarding depth to mineralization.

The interpretation of SGH data by the author, the originator of this geochemistry, is not exhaustive. All anomalies are not necessarily interpreted and discussed, especially if they occur near the edges of the survey area. The primary purpose of this interpretation is to show the client the clearest, the most significant, and the most confident anomalies for the target type that the client has requested. This is based on the interpretation of SGH data for over 1,100 surveys conducted in the last 20 years. Thus, other anomalies may be valid targets but to consider each and interpret them all would result in a significantly longer turnaround time for results.

This interpretation is complex, based on our commitment to continued support, the client is invited to call or meet with the author directly to discuss the SGH results shown and other anomalies that may be coincident with other geochemical or geophysical methods.

41 Bittern St. ● Ancaster, ON ● L9G 4V5 ● CANADA ● Tel: (905) 648-9611 ● Fax: (905) 648-9613 ● Toll Free: 1-888-ACTLABS

E-mail: dalesutherland@actlabs.com ● Web Site: www.actlabs.com

In general, the number of samples was adequate to show what the author believes to be valuable information at the Kimberlite SGH Project. The use of a regularly spaced survey design contributes greatly to the results achieved by SGH. The grided area of about 170 should have been wider to more confidently describe the location of the Kimberlite Pipes. The other transects, if they were taken to track Kimberlite Indicator Minerals may be of value as they appeared to vector to the Kimberlite targets. In this survey, it appears that SGH was successful in indicating these pathways and indicating that a sizable amount of the mineral indicators were mobilized by Glacial transport that were able to support bacteriological biofilms. SGH responds to the bacteriological degradation components from these biofilms. The biofilms do not have to be from sulphate-reducing bacteria.

SGH indicates the presence of sulphides associated with the Kimberlite Pipes presumably as Nickel Sulphides.

With the advent of the development of 3D-SGH in 2012, that also interprets the spatial symmetry of anomalous areas, the ultimate rating of confidence as 6.0 on a scale of 6.0 is more difficult to obtain. To observe this symmetry a larger, and more unbiased, survey is often needed.

41 Bittern St. ● Ancaster, ON ● L9G 4V5 ● CANADA ● Tel: (905) 648-9611 ● Fax: (905) 648-9613 ● Toll Free: 1-888-ACTLABS

E-mail: dalesutherland@actlabs.com ● Web Site: www.actlabs.com

A18-00040 – NWT Geoscience Kimberlite SGH PROJECT
SGH SURVEY RECOMMENDATIONS

The SGH signature or template has been proven effective from the interpretation over many other surveys in many different geographical regions and for different types of KIMBERLITE targets as well as for other mineralization. Again, the degree of confidence in the rating only starts to be "good" at a level of 4.0. A Rating of 4.0 is an indication that the SGH geochemistry predicts that the zones described may warrant more work or more consideration. It must be remembered that there are still many other SGH Class maps used in the interpretation process that are not shown in this report due to turnaround time considerations.

From client feedback in recent years, a few true exploration surveys that have been interpreted with an SGH Confidence Rating of 4.0 (±0.5) have been drill tested with successful target intersections. However the frequency of success is much more prevalent for those targets that have had an SGH Rating Scores of ≥5.0.

With 3D-SGH, this geochemistry is capable of recommending drill locations with the highest associated confidence if symmetrical anomalies are found, and is the only geochemistry known to be able to estimate the depth to mineralization for some projects that achieve a high confidence rating. When a drill target is implied it is to ensure that the reader is aware of the location having the highest confidence of being the location of the vertical projection of the target, based only on SGH data. This would not necessarily be a recommendation for vertical drilling. Vertical drilling may or may not be the best approach to test the SGH anomaly in a project area. Activation Laboratories Ltd. has no experience in actual exploration drilling techniques. Other geological, geochemical and/or geophysical information should also be considered.

It must be remembered that many other SGH Class maps not shown in this report have been reviewed to support the interpretation shown. The client should use a combination of the SGH results shown in this report with additional geochemical, geophysical, and geological information to possibly obtain a more confident and precise target location. This is not a statement to convey some lower level of confidence in SGH results as blind independent research studies have consistently indicated that SGH is by far the most reliable geochemistry regardless of geographical location, sampling terrain, environmental conditions or lithology. The statement to not rely solely on SGH is made to recognize the proper use and interpretation of any scientific data. Whenever possible, multiple methods should always be employed so that any decisions do not rely on any one technique.

41 Bittern St. ● Ancaster, ON ● L9G 4V5 ● CANADA ● Tel: (905) 648-9611 ● Fax: (905) 648-9613 ● Toll Free: 1-888-ACTLABS

E-mail: dalesutherland@actlabs.com ● Web Site: www.actlabs.com

Contract Approval: January 2, 2018

Date Preparation Completed: January 5, 2018

Date Analysis Completed: February 1, 2018

SGH Interpretation Report: February 13, 2018

NWT Geoscience

Department of the NWT Industry, Tourism & Investment

Northwest Territories Geological Survey

4601B 52 Avenue, PO Box 1320

Yellowknife, NT, X1A 2LS, Canada

Attention: Barrett Elliott

RE: Your Reference: Kimberlite SGH Project

Activation Laboratories Workorder: A18-00040

CERTIFICATE OF ANALYSIS

This Certificate applies to the associated Excel Spreadsheet of Hydrocarbon results combined with the discussion and SGH Pathfinder Class maps of the data shown as the SGH Geochemical Method.

215 Soil Samples were analyzed for this submission

Sample preparation –Actlabs Ancaster - S4: Drying at 60°C and Sieving with -60 mesh collected

Interpretation relative to KIMBERLITE based targets was conducted.

The following analytical package was requested and analyzed at Actlabs Ancaster Canada:

Analysis Code SGH – Soil Gas Hydrocarbon Geochemistry using High Resolution Gas Chromatography/Mass Spectrometry (HRGC/MS)

41 Bittern St. ● Ancaster, ON ● L9G 4V5 ● CANADA ● Tel: (905) 648-9611 ● Fax: (905) 648-9613 ● Toll Free: 1-888-ACTLABS

E-mail: dalesutherland@actlabs.com ● Web Site: www.actlabs.com

Notes: The SGH – Spatio-temporal Geochemical Hydrocarbon Geochemistry is a semi-quantitative analytical procedure to detect and measure 162 hydrocarbon compounds as the organic signature in the sample material collected from a survey area. It is not an assay of mineralization but is a predictive geochemical tool used for exploration. This certificate pertains only to the SGH data presented in the associated Microsoft Excel spreadsheet of results.

The author of this SGH Interpretation Report, Mr. Dale Sutherland, is the creator of the SGH and OSG organic geochemical methods. He is a Chartered Chemist (C.Chem.) and Forensic Scientist specializing in organic chemistry. As an Organic Geochemist he is a member of the Association of the Chemical Profession of Ontario, the Association of Applied Geochemists, the International Association of Geochemistry, the Ontario Prospectors Association, the Association for Mineral Exploration of British Columbia, the British Organic Geochemical Society, the Ontario Petroleum institute, the Chemical Institute of Canada, and the Canadian Society for Chemistry, as well as having memberships in several national and international Forensic associations. He is not a professional geologist. Based on the interpretation of over 1,100+ SGH surveys in the last 20 years, he is a geochemist with respect to SGH only.

CERTIFIED BY:

Dale Sutherland, B.Sc.,B.Sc.,B.Ed.,C.Chem.,MCIC
Forensic Scientist, Organics Manager,
Director of Research
Activation Laboratories Ltd.

41 Bittern St. ● Ancaster, ON ● L9G 4V5 ● CANADA ● Tel: (905) 648-9611 ● Fax: (905) 648-9613 ● Toll Free: 1-888-ACTLABS

E-mail: dalesutherland@actlabs.com ● Web Site: www.actlabs.com

APPENDIX

NOTE: THERE IS NEW REQUIREMENTS FOR THE SGH GEOCHEMISTRY AS OF NOVEMBER 2017.

SURVEYS OF LESS THAN 50 SAMPLES PER SURVEY WILL NOT BE ACCEPTED.

Recently there has been several submissions of less than 50 samples that have limited findings which produced more questions, have required the same amount of work, and yet have provided less confident results. To ensure that SGH continues to provide top quality and highly confident information, a survey of at least a "minimum" of 50 samples will only be accepted.

SGH DATA and GIS PACKAGE: (included in the SGH analysis)

The SGH data used to create the SGH maps shown in this report is included as a separate Excel file and is included in the price of the SGH analysis. In addition a Georeferenced map file (tif and tfw files) is included for each map of the report and is provided for ease of import into the clients GIS software.

41 Bittern St. ● Ancaster, ON ● L9G 4V5 ● CANADA ● Tel: (905) 648-9611 ● Fax: (905) 648-9613 ● Toll Free: 1-888-ACTLABS

E-mail: dalesutherland@actlabs.com ● Web Site: www.actlabs.com

Appendix D

Raw Data

D.1 Soil Sample Locations and Sample ID Numbers

This section includes the location of till samples on a map of the study area and in the included inset. All sample IDs are prefixed with 'Q515'.

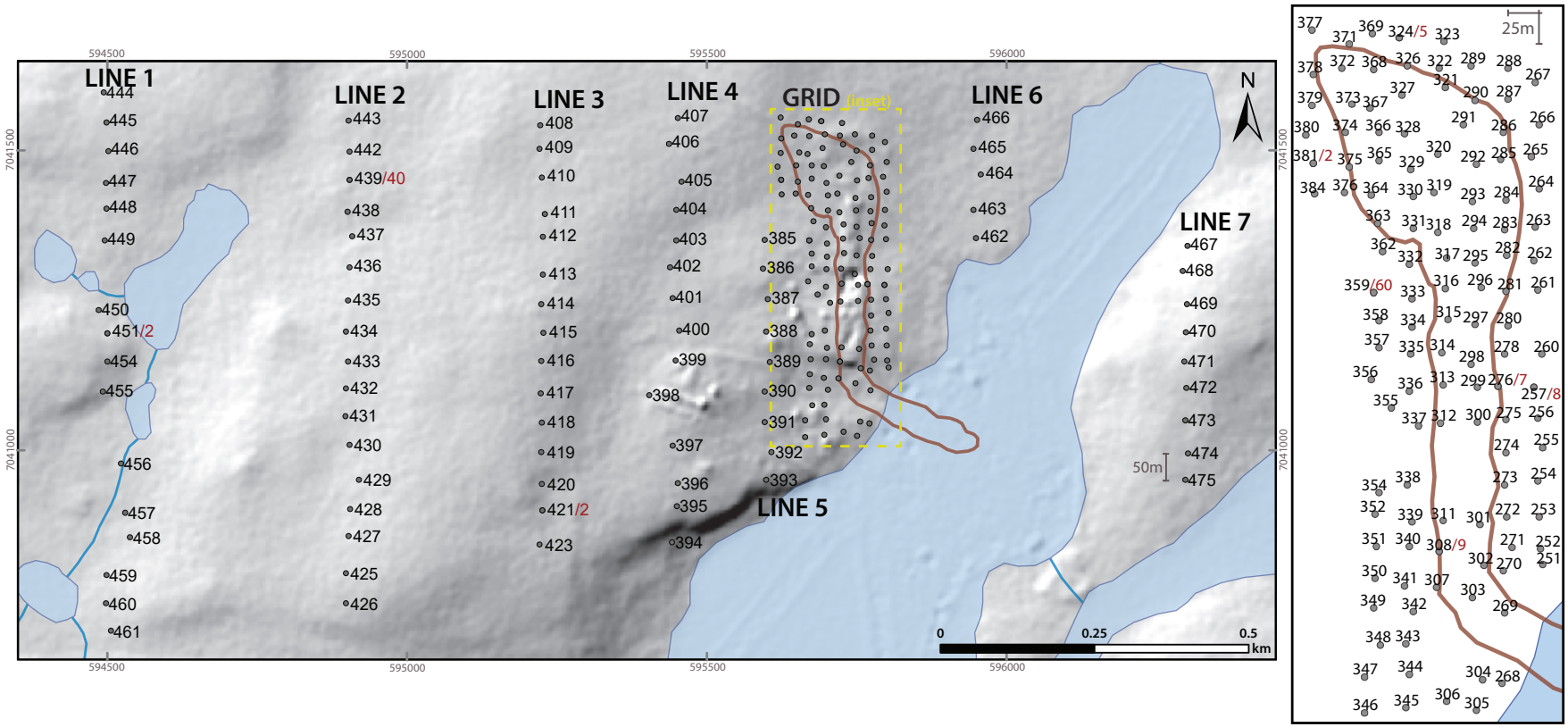

Figure D.1: B horizon soil sample locations and ID number. All samples are prefixed with 'Q515' - excluded in figure for simplicity. Field duplicates labelled in red. Samples spacing in transects is 50 m, and 25×25 m spacing in the grid.

D.2 Soil Profile Field Measurements

Measurements were recorded in the field at each sample location, and included UTM coordinates, depth to the various soil horizons, and the moisture content, soil texture, and clast content of the B-horizon.

Kelvin Soil Sample Field Measurements

Sample ID	Traverse ID	UTM Easting	UTM Northing	Elevation (m amsl)	Frost Boil	Depth to Base of O Horizon (cm)	Depth to Base of Ah Horizon (cm)	Depth to Base of Ae Horizon (cm)	Depth to Base of B Upper Horizon (cm)	Depth to Base of B Horizon (cm)	Hole Depth (cm)
Q515251	Grid	595803	7041138	409	Y	2.5	-	-	-	6.0	6.0
Q515252	Grid	595801	7041150	412	-	6.5	-	8.5	-	23	23
Q515253	Grid	595800	7041175	416	-	4.0	-	7	-	27	27
Q515254	Grid	595799	7041203	417	-	5.0	-	10	-	25	25
Q515255	Grid	595803	7041229	414	-	9.0	12	20	-	35	35
Q515256	Grid	595799	7041252	419	-	5	17	-	-	24.0	30
Q515257	Grid	595796	7041276	419	-	5	8	-	-	25	25
Q515258	Grid	595796	7041276	419	-	6	-	-	16	33	33
Q515260	Grid	595802	7041302	418	Y	9	-	-	12	28	28
Q515261	Grid	595799	7041352	415	-	7	10.5	-	22	33	41
Q515262	Grid	595796	7041375	417	-	3	10	-	-	32	32
Q515263	Grid	595797	7041401	414	-	3	8.0	-	-	35	35
Q515264	Grid	595800	7041431	415	-	2	5.5	-	-	27	27
Q515265	Grid	595794	7041456	415	-	2.5	5.5	-	-	30	30
Q515266	Grid	595800	7041481	415	-	3	6	-	-	34	34
Q515267	Grid	595797	7041514	414	-	2	4.5	-	-	34	34
Q515268	Grid	595771	7041045	425	-	6	14	-	-	32	32
Q515269	Grid	595773	7041100	410	-	3.0	7	-	-	25.0	25.0
Q515270	Grid	595772	7041133	408	-	3	6	12	-	30	30
Q515271	Grid	595779	7041151	409	-	4	8	-	18.0	34	34
Q515272	Grid	595775	7041175	412	-	8	10	15	25	36	36
Q515273	Grid	595773	7041200	411	-	2	5	8	17	30	30
Q515274	Grid	595774	7041225	414	-	5	8	12	-	30	30
Q515275	Grid	595774	7041251	416	-	3.5	5.5	6	-	25	25
Q515276	Grid	595768	7041277	418	-	3.5	5	-	-	35	35

Kelvin Soil Sample Field Measurements

Sample ID	Traverse ID	UTM Easting	UTM Northing	Elevation (m amsl)	Frost Boil	Depth to Base of O Horizon (cm)	Depth to Base of Ah Horizon (cm)	Depth to Base of Ae Horizon (cm)	Depth to Base of B Upper Horizon (cm)	Depth to Base of B Horizon (cm)	Hole Depth (cm)
Q515277	Grid	595768	7041277	418	-	-	2	-	-	30	30
Q515278	Grid	595773	7041302	416	-	5	9	-	-	35	35
Q515280	Grid	595776	7041324	417	-	6.5	10	12	-	30	30
Q515281	Grid	595774	7041351	418	-	6	13	-	-	25	25
Q515282	Grid	595775	7041379	416	-	6	8	12	-	30	30
Q515283	Grid	595773	7041399	415	-	3	9	12	-	32	32
Q515284	Grid	595774	7041422	415	Y	2	7	10	-	30	30
Q515285	Grid	595770	7041454	412	Y	3	-	-	-	23	23
Q515286	Grid	595772	7041475	411	-	4	6	-	-	20	20
Q515287	Grid	595776	7041501	412	-	2.5	4.5	7	-	25	25
Q515288	Grid	595776	7041525	413	-	2.5	4	5	-	30	30
Q515289	Grid	595747	7041527	414	-	3.5	7	8	-	32	32
Q515290	Grid	595750	7041500	414	-	2.5	5	6.5	-	30	30
Q515291	Grid	595741	7041481	415	-	2.5	5	-	-	35	35
Q515292	Grid	595751	7041450	420	-	3.5	5	7	-	31	31
Q515293	Grid	595748	7041421	419	Y	3	-	-	-	20	20
Q515294	Grid	595749	7041400	419	-	3	-	-	-	24	24
Q515295	Grid	595750	7041373	419	-	2	4	7.5	-	30	30
Q515296	Grid	595755	7041354	415	Y	1.5	3	-	17	20	20
Q515297	Grid	595750	7041325	416	-	2	6	9	17	25	25
Q515298	Grid	595747	7041294	415	-	2.5	5	-	11	25	25
Q515299	Grid	595752	7041276	417	-	2	5	-	-	25	25
Q515300	Grid	595752	7041249	419	-	3	9	-	-	30	30
Q515301	Grid	595754	7041169	416	-	-	3	-	11	27	27
Q515302	Grid	595757	7041137	413	-	-	5	-	-	30	30

Kelvin Soil Sample Field Measurements

Sample ID	Traverse ID	UTM Easting	UTM Northing	Elevation (m amsl)	Frost Boil	Depth to Base of O Horizon (cm)	Depth to Base of Ah Horizon (cm)	Depth to Base of Ae Horizon (cm)	Depth to Base of B Upper Horizon (cm)	Depth to Base of B Horizon (cm)	Hole Depth (cm)
Q515303	Grid	595748	7041112	411	-	2.5	6	-	-	27	27
Q515304	Grid	595756	7041048	415	-	3	-	7	14	35	35
Q515305	Grid	595751	7041024	415	Y	-	3	-	-	27	27
Q515306	Grid	595728	7041031	414	-	3	5	-	-	30	30
Q515307	Grid	595720	7041120	414	-	2	5	-	-	30	30
Q515308	Grid	595722	7041148	416	-	2	4	-	-	32	32
Q515309	Grid	595722	7041148	416	-	2	5	-	-	30	30
Q515311	Grid	595725	7041172	412	-	1	6	9	-	30	30
Q515312	Grid	595723	7041248	413	-	2	6	-	-	30	30
Q515313	Grid	595725	7041278	413	-	4	6	-	-	30	30
Q515314	Grid	595724	7041303	413	-	3.5	6.5	8	-	34	34
Q515315	Grid	595729	7041329	415	-	9	14.5	17	-	44	44
Q515316	Grid	595727	7041353	416	-	7.5	10	12.5	-	32	32
Q515317	Grid	595728	7041377	417	-	3	6	-	-	30	30
Q515318	Grid	595721	7041397	423	-	3	5	5.5	-	32	32
Q515319	Grid	595718	7041428	424	-	2	5	-	-	33	33
Q515320	Grid	595721	7041458	425	-	2	6	-	-	28	28
Q515321	Grid	595727	7041510	424	-	4	6.5	-	-	30	30
Q515322	Grid	595722	7041525	422	-	2	5	6	-	25	25
Q515323	Grid	595726	7041546	419	-	2	5	7	-	28	28
Q515324	Grid	595691	7041549	422	-	3	5	6	-	31	31
Q515325	Grid	595691	7041549	422	-	3	5	6.5	-	23	23
Q515326	Grid	595697	7041527	421	-	3	5	7	-	30	30
Q515327	Grid	595693	7041504	420	-	2.5	4	5	-	27	27
Q515328	Grid	595695	7041474	421	-	2	4	5	-	25	25

Kelvin Soil Sample Field Measurements

Sample ID	Traverse ID	UTM Easting	UTM Northing	Elevation (m amsl)	Frost Boil	Depth to Base of O Horizon (cm)	Depth to Base of Ah Horizon (cm)	Depth to Base of Ae Horizon (cm)	Depth to Base of B Upper Horizon (cm)	Depth to Base of B Horizon (cm)	Hole Depth (cm)
Q515329	Grid	595700	7041446	421	-	8	12	-	-	26	26
Q515330	Grid	595702	7041425	420	-	3	5	-	-	25	25
Q515331	Grid	595702	7041400	421	-	3	5.5	-	-	26	26
Q515332	Grid	595699	7041372	421	-	3.5	6	-	-	27	27
Q515333	Grid	595701	7041345	419	-	3.5	6	-	-	24	24
Q515334	Grid	595701	7041323	419	-	7	9	11	-	30	30
Q515335	Grid	595700	7041302	418	-	2.5	4	7.5	-	30	30
Q515336	Grid	595699	7041273	421	-	3	5	12	-	30	30
Q515337	Grid	595706	7041246	421	-	4.5	8	9	-	30	30
Q515338	Grid	595697	7041200	421	-	2	4	6.5	-	30	30
Q515339	Grid	595701	7041171	419	-	3.5	8	-	-	25	25
Q515340	Grid	595699	7041152	418	-	-	5	11	-	30	30
Q515341	Grid	595695	7041121	415	-	3	6	-	-	30	30
Q515342	Grid	595702	7041101	412	-	7	10	12	-	30	30
Q515343	Grid	595696	7041076	411	-	2.5	3.5	-	-	30	30
Q515344	Grid	595699	7041052	410	-	2.5	-	-	-	26	26
Q515345	Grid	595696	7041026	411	-	2.5	6	8	-	30	30
Q515346	Grid	595664	7041022	413	-	1.5	4	6	-	30	30
Q515347	Grid	595664	7041050	413	Y	2	-	-	-	32	32
Q515348	Grid	595676	7041075	414	-	3	7	-	-	28	28
Q515349	Grid	595671	7041104	414	Y	2.5	-	-	-	29	29
Q515350	Grid	595672	7041127	416	-	5	8	-	-	33	33
Q515351	Grid	595673	7041152	418	-	2.5	4.5	-	-	32	32
Q515352	Grid	595672	7041177	421	-	4.5	8	-	-	30	30
Q515354	Grid	595675	7041194	418	-	2	6	-	-	30	30

Kelvin Soil Sample Field Measurements

Sample ID	Traverse ID	UTM Easting	UTM Northing	Elevation (m amsl)	Frost Boil	Depth to Base of O Horizon (cm)	Depth to Base of Ah Horizon (cm)	Depth to Base of Ae Horizon (cm)	Depth to Base of B Upper Horizon (cm)	Depth to Base of B Horizon (cm)	Hole Depth (cm)
Q515355	Grid	595685	7041260	418	-	2	4	5	-	29	29
Q515356	Grid	595669	7041282	420	-	2	4	5	-	32	32
Q515357	Grid	595675	7041307	418	Y	2	-	-	-	28	28
Q515358	Grid	595675	7041328	416	Y	5	8.5	13	-	32	32
Q515359	Grid	595671	7041350	416	Y	2	-	-	-	29	29
Q515360	Grid	595671	7041350	416	Y	2	-	-	-	37	37
Q515362	Grid	595678	7041382	422	-	3	6	8	-	34	34
Q515363	Grid	595674	7041404	421	Y	3	5	-	-	31	31
Q515364	Grid	595669	7041426	421	Y		3	-	-	29	29
Q515365	Grid	595675	7041453	415	-	3.5	7	8.5	-	27	27
Q515366	Grid	595675	7041475	416	-	2.5	4	6	-	29	29
Q515367	Grid	595668	7041494	-	-	4	7	10.5	-	30	30
Q515368	Grid	595671	7041524	424	-	2	3.5	5	-	25	25
Q515370	Grid	595670	7041552	425	-	3	7	8.5	-	27	27
Q515371	Grid	595652	7041544	-	-	2	5	-	-	25	25
Q515372	Grid	595646	7041525	420	-	5	10	-	-	28	28
Q515373	Grid	595654	7041497	417	-	2.5	5	5.5	-	29	29
Q515374	Grid	595649	7041475	420	Y	3	6	8.5	-	29	29
Q515375	Grid	595652	7041448	414	-	5	6	9	-	29	29
Q515376	Grid	595648	7041428	414	-	3	5	-	-	27	27
Q515377	Grid	595623	7041555	423	-	4	9.5	11	-	31	31
Q515378	Grid	595624	7041520	422	-	2	6.5	7.5	-	27	27
Q515379	Grid	595623	7041496	420	-	2.5	5	6	-	27	27
Q515380	Grid	595618	7041473	417	-	3	5	6	-	29	29
Q515381	Grid	595624	7041451	414	-	4	6	8	-	27	27

Kelvin Soil Sample Field Measurements

Sample ID	Traverse ID	UTM Easting	UTM Northing	Elevation (m amsl)	Frost Boil	Depth to Base of O Horizon (cm)	Depth to Base of Ah Horizon (cm)	Depth to Base of Ae Horizon (cm)	Depth to Base of B Upper Horizon (cm)	Depth to Base of B Horizon (cm)	Hole Depth (cm)
Q515382	Grid	595624	7041451	414	-	2.5	5	7.5	-	27	27
Q515384	Grid	595625	7041427	418	Y	3	-	-	-	32	32
Q515385	T5	595597	7041351	418	-	3.5	5.5	7.5	-	27	27
Q515386	T5	595594	7041303	421	-	3	-	-	13	27	27
Q515387	T5	595602	7041252	419	-	3	-	-	13	32	32
Q515388	T5	595599	7041198	422	-	3	6	-	-	28	28
Q515389	T5	595605	7041147	418	-	8	11	-	-	34	34
Q515390	T5	595597	7041098	420	-	3	-	-	-	20	20
Q515391	T5	595597	7041047	414	-	3	-	-	-	22	22
Q515392	T5	595608	7040997	421	-	9	-	-	-	30	30
Q515393	T5	595599	7040951	420	-	7.5	-	-	-	32	32
Q515394	T4	595442	7040847	418	Y	2	-	-	-	25	25
Q515395	T4	595450	7040907	424	Y	4	-	-	-	28	28
Q515396	T4	595452	7040945	421	Y	0.5	-	-	-	32	32
Q515397	T4	595443	7041008	426	Y	1.5	3.5	-	-	32	32
Q515398	T4	595404	7041092	423	Y	2	-	-	-	30	30
Q515399	T4	595448	7041150	420	-	4.5	6	8	-	32	32
Q515400	T4	595454	7041200	418	-	6	8	11	-	29	29
Q515401	T4	595443	7041254	416	-	2.5	5	-	-	25	25
Q515402	T4	595439	7041305	415	Y	3	5	-	-	25	25
Q515403	T4	595449	7041350	417	-	3.5	6	8.5	-	24	24
Q515404	T4	595449	7041401	420	-	4	8	-	-	28	28
Q515405	T4	595458	7041448	423	Y	4	8.5	-	-	35	35
Q515406	T4	595437	7041511	425	-	4	8	-	-	29	29
Q515407	T4	595452	7041554	426	-	5	7	10.5	-	33	33

Kelvin Soil Sample Field Measurements

Sample ID	Traverse ID	UTM Easting	UTM Northing	Elevation (m amsl)	Frost Boil	Depth to Base of O Horizon (cm)	Depth to Base of Ah Horizon (cm)	Depth to Base of Ae Horizon (cm)	Depth to Base of B Upper Horizon (cm)	Depth to Base of B Horizon (cm)	Hole Depth (cm)
Q515408	T3	595222	7041542	429	Y	3	-	-	-	22	22
Q515409	T3	595221	7041503	430	Y	2.5	-	-	-	25	25
Q515410	T3	595225	7041455	429	Y	3	-	-	-	27	27
Q515411	T3	595230	7041394	430	-	6	-	-	-	25	25
Q515412	T3	595227	7041356	434	-	2.5	5.5	-	-	27	27
Q515413	T3	595227	7041293	437	-	3	5.5	-	-	34	34
Q515414	T3	595224	7041244	440	Y	2.5	-	-	-	28	28
Q515415	T3	595228	7041196	439	Y	3	6	-	-	24	24
Q515416	T3	595224	7041149	437	Y	4	-	-	-	26	26
Q515417	T3	595223	7041095	437	-	6	9	-	-	28	28
Q515418	T3	595225	7041046	436	Y	4	6	-	-	31	31
Q515419	T3	595224	7040997	432	Y	3	-	-	-	31	31
Q515420	T3	595225	7040944	431	-	7	12	13	-	30	30
Q515421	T3	595226	7040900	431	-	2	3.5	5	-	33	33
Q515422	T3	595226	7040900	431	-	3	6	7	-	28	28
Q515423	T3	595221	7040843	430	Y	3	-	-	-	24	24
Q515425	T2	594898	7040795	432	-	5	7	-	-	30	30
Q515426	T2	594898	7040745	430	-	2	4	6	-	28	28
Q515427	T2	594903	7040857	430	Y	4	-	-	-	26	26
Q515428	T2	594905	7040902	431	-	4	7	-	-	24	24
Q515429	T2	594920	7040951	435	-	8	-	-	-	26	26
Q515430	T2	594904	7041009	436	-	4	-	-	-	30	30
Q515431	T2	594897	7041057	436	Y	4	-	-	-	24	24
Q515432	T2	594898	7041103	432	-	7	11.5	12.5	-	34	34
Q515433	T2	594902	7041148	432	-	4	7.5	-	-	0.3	0.3

Kelvin Soil Sample Field Measurements

Sample ID	Traverse ID	UTM Easting	UTM Northing	Elevation (m amsl)	Frost Boil	Depth to Base of O Horizon (cm)	Depth to Base of Ah Horizon (cm)	Depth to Base of Ae Horizon (cm)	Depth to Base of B Upper Horizon (cm)	Depth to Base of B Horizon (cm)	Hole Depth (cm)
Q515434	T2	594898	7041198	428	Y	2.5	-	-	-	24	24
Q515435	T2	594902	7041250	425	-	3	5	-	-	22	22
Q515436	T2	594904	7041305	423	-	4	5.5	-	-	28	28
Q515437	T2	594909	7041357	423	-	6	8	-	-	29	29
Q515438	T2	594901	7041398	423	-	3	6	-	14	28	28
Q515439	T2	594904	7041451	429	-	5	8	-	-	30	30
Q515440	T2	594904	7041451	429	-	4	7	-	-	24	24
Q515442	T2	594904	7041498	427	-	3	6	-	-	30	30
Q515443	T2	594903	7041550	426	-	2.5	4	6	-	32	32
Q515444	T1	594494	7041597	431	Y	4	-	-	-	24	24
Q515445	T1	594499	7041547	431	Y	4	-	-	-	28	28
Q515446	T1	594502	7041499	429	-	5	7	8	-	23	23
Q515447	T1	594498	7041446	428	Y	4.5	-	-	-	23	23
Q515448	T1	594499	7041403	429	Y	5	-	-	-	21	21
Q515449	T1	594496	7041350	428	-	2	4	5	-	24	24
Q515450	T1	594486	7041234	431	Y	3	-	-	-	24	24
Q515451	T1	594500	7041195	432	Y	4	-	-	-	29	29
Q515452	T1	594500	7041195	432	Y	3.5	-	-	-	28	28
Q515454	T1	594500	7041148	432	Y	4.5	-	-	-	25	25
Q515455	T1	594493	7041098	428	Y	3	6	-	-	28	28
Q515456	T1	594523	7040978	427	Y	3	-	-	7	29	29
Q515457	T1	594530	7040896	425	Y	3	-	-	-	22	22
Q515458	T1	594538	7040855	425	Y	3.5	-	-	-	28	28
Q515459	T1	594499	7040792	422	Y	3	-	-	-	24	24
Q515460	T1	594498	7040745	423	-	4	7	-	-	26	26

Kelvin Soil Sample Field Measurements

Sample ID	Traverse ID	UTM Easting	UTM Northing	Elevation (m amsl)	Frost Boil	Depth to Base of O Horizon (cm)	Depth to Base of Ah Horizon (cm)	Depth to Base of Ae Horizon (cm)	Depth to Base of B Upper Horizon (cm)	Depth to Base of B Horizon (cm)	Hole Depth (cm)
Q515461	T1	594506	7040699	422	-	3	6	-	-	31	31
Q515462	T6	595949	7041354	418	-	5	7	-	-	25	25
Q515463	T6	595945	7041401	415	-	4	-	-	-	30	30
Q515464	T6	595957	7041460	412	-	5	-	-	-	23	23
Q515465	T6	595945	7041503	412	Y	3	-	-	-	27	27
Q515466	T6	595951	7041551	414	-	5	-	7	-	31	31
Q515467	T7	596302	7041341	416	-	4	-	-	-	30	30
Q515468	T7	596294	7041299	416	Y	3	-	-	-	20	20
Q515469	T7	596301	7041244	418	-	3	-	-	-	29	29
Q515470	T7	596299	7041197	419	Y	2	-	-	-	25	25
Q515471	T7	596297	7041148	419	-	11	-	-	-	30	30
Q515472	T7	596300	7041104	418	-	5	7	-	-	27	27
Q515473	T7	596298	7041050	417	-	3	5	6.5	-	32	32
Q515474	T7	596303	7040995	415	Y	2	-	-	-	25	25
Q515475	T7	596298	7040951	417	-	2.5	7	-	-	25	25

Kelvin Soil Sample Field Measurements

Sample ID	B Horizon Color	B Horizon Moisture (%)	B Horizon Texture	B Horizon % Clasts	B Horizon Clast Composition
Q515251	Light Brown	0	Silt with clay	30	granite
Q515252	Light Brown	0	Silt with clay	2	granite
Q515253	Light Grey	0	Med sand with silt	5	granite
Q515254	Light Brown	0	Med sand with pebbles	25	-
Q515255	Light Brown	0	Poor sort sand w/ silt & pebbles	30	-
Q515256	Light Brown	0	-	15	gniess
Q515257	Light Brown	0	Fine sand with silt and clay	15	granite
Q515258	Light Grey	0	Fine sand with silt and clay	15	granite
Q515260	Light Brown	0	Mod well sort sand w/ silt	10	granite, gneiss
Q515261	Light Grey	1.8	Mod well sort sand w/ silt	15	gniess
Q515262	Light Brown	7.9	Mod well sort sand w/ silt	5	-
Q515263	Light Brown	7.3	Mod well sort fine sand	5	granite
Q515264	Light Brown	0	Mod well sort med-fine sand	5	-
Q515265	Light Brown	1.8	Poor sort sand	-	-
Q515266	Light Brown	0	Poor sort sand	-	-
Q515267	Light Brown	0	Mod well sort sand w/ silt	10	-
Q515268	Grey	0	-	7	-
Q515269	Light Brown	0	Sand w/ silt and pebbles	15	granite, gneiss
Q515270	Light Brown	0	Fine sand w/ silt	-	-
Q515271	Light Brown	0	Silt with clay	5	granite, gneiss
Q515272	Light Brown	0	Med-fine sand w/ silt	5	schist
Q515273	Light Brown	0	Fine sand, silt w/ minor clay	8	granite
Q515274	Light Brown	0	Poor sort med-coarse sand	20	granite
Q515275	Light Brown	0	Poor sort sand w/ silt & pebbles	15	granite, gneiss
Q515276	Light Grey	0	Well sort silt w/ clay	3	-

Kelvin Soil Sample Field Measurements

Sample ID	B Horizon Color	B Horizon Moisture (%)	B Horizon Texture	B Horizon % Clasts	B Horizon Clast Composition
Q515277	Light Grey	0	Well sort silt w/ clay	3	-
Q515278	Light Brown	0	Well sort med sand w/ silt	5	granite
Q515280	Light Grey	0.7	Well sort sand	10	-
Q515281	Light Brown	2.3	Well sort fine sand w/ silt	15	-
Q515282	Light Brown	1.6	Well sort fine sand w/ silt	15	-
Q515283	Light Brown	7.9	Mod Well sort med sand w/ granules	15	-
Q515284	Light Grey	7.6	Mostly silt w minor clays	7	-
Q515285	Light Grey	5.5	Fine sand w/ silt & minor clay	10	-
Q515286	Light Brown	7.5	Mod well sort med-fine sand	2	-
Q515287	Light Brown	4.3	Mod poor sort sand and silt	5	-
Q515288	Light Brown	0	Mod well sort fine sand w/ silt	10	-
Q515289	Light Brown	0	Poor sort sand w/ silt	15	gniess
Q515290	Light Brown	0	Poor sort sand w/ silt & pebbles	15	gneiss
Q515291	Light Brown	11.1	Poor sort sand w/ silt & pebbles	15	gneiss
Q515292	Light Brown	0	mod sort sand w/ granules	5	gneiss
Q515293	Light Brown	16.2	Well sort fine sand w/ minor clay	5	-
Q515294	Light Brown	0	Mod well sort med-fine sand w/ minor clay	-	-
Q515295	Light Brown	5.5	Mod well sort sand	-	-
Q515296	Light Brown	8.5	fine sand / silt & minor clay	15	gniess
Q515297	Light Grey	0	well sorted fine sand w/ silt	2	-
Q515298	Light Brown	2	Mod well sort med-fine sand	5	-
Q515299	Light Brown	0	Mod well sort med-fine sand w/ silt	10	-
Q515300	Light Brown	0	Mod well sort med sand	15	gniess
Q515301	Light Brown	0	Mod poor sort med sand	-	granite
Q515302	Light Brown	0	Mod well wort med-fine sand w/ silt	15	gniess

Kelvin Soil Sample Field Measurements

Sample ID	B Horizon Color	B Horizon Moisture (%)	B Horizon Texture	B Horizon % Clasts	B Horizon Clast Composition
Q515303	Light Brown	0	Mod well wort med-fine sand w/ silt	15	gniess
Q515304	Light Brown	0	Very fine sand, silt, w/ clay	5	-
Q515305	Light Grey	0	Well sorted silt w/ clay	15	-
Q515306	Light Grey	0	Fine sand, silt w/ minor clay	20	-
Q515307	Light Brown	0	Well sorted fine sand	15	gniess
Q515308	Light Brown	0	Very well sort fine sand and silt	2	-
Q515309	Light Brown	0	Very well sort fine sand and silt	2	-
Q515311	Light Brown	0	Mod well sort sand and silt	20	granite
Q515312	Light Brown	0	Did not screen	-	-
Q515313	Light Brown	0	-	15	-
Q515314	Light Brown	2.2	Well sort fine sand and silt	15	-
Q515315	Light Brown	0	Fine sand, silt w/ minor clay	2	-
Q515316	Light Brown	0	Fine sand, silt w/ minor clay	3	granite
Q515317	Light Brown	10.7	Mod well sort med sand	3	-
Q515318	Light Brown	0	Mod well sort med-fine sand	3	gniess
Q515319	Light Brown	0	Mod poor sort med sand w/ silt	10	-
Q515320	Light Brown	0	Mod poor sort med sand w/ silt & pebbles	10	-
Q515321	Light Brown	0	Mod poor sort med sand w/ silt & pebbles	10	-
Q515322	Light Brown	0	Mod poor sort coarse-fine sand	10	granite
Q515323	Light Brown	0	Poorly sort coarse-fine sand w/ silt	15	-
Q515324	Light Brown	0	Mod well wsort med sand and silt	15	-
Q515325	Light Brown	0	Mod well wsort med sand and silt	15	gneiss
Q515326	Light Brown	0	Mod well sort Med-fine sand	10	-
Q515327	Light Brown	0	Mod well sort med sand and silt	10	-
Q515328	Light Brown	0	Mod poorly sort coase-med sand	10	-

Kelvin Soil Sample Field Measurements

Sample ID	B Horizon Color	B Horizon Moisture (%)	B Horizon Texture	B Horizon % Clasts	B Horizon Clast Composition
Q515329	Light Brown	0	Mod poorly sort coase-med sand	15	-
Q515330	Light Brown	0	Mod well sort fine sand, silt, minor clay	3	-
Q515331	Light Brown	7.8	Mod well sort fine sand, silt, minor clay	20	gneiss
Q515332	Light Brown	0	well sort fine sand w/ silt	5	-
Q515333	Light Brown	0	Poorly sort med-fine sand w/ silt, minor clay, pebbles	10	-
Q515334	Light Brown	0	Mod well sort med-fine sand w/ silt	15	-
Q515335	Light Brown	0.3	Poor sort Med-fine sand w/ silt and pebbles	-	-
Q515336	Light Brown	0	Well sort fine sand w/ silt	5	-
Q515337	Light Brown	0	Well sort fine sand w/ silt	3	-
Q515338	Light Brown	0	Mod poor wort med sand w/ silt and pebbles	-	-
Q515339	Light Brown	0	Mod poor sort fine sand, silt, w/ clay and pebbles	25	-
Q515340	Light Brown	0	Mod poor sort fine sand, silt, w/ clay and pebbles	20	-
Q515341	Light Brown	0	Mod poor sort fine sand, silt, w/ clay and pebbles	20	-
Q515342	Light Brown	0	Mod poor sort med-fine sand w/ silt	15	gneiss
Q515343	Light Brown	0	Very fine sand w/ silt and clay	Did not seive	-
Q515344	Light Grey	0	Fine sand, silt w/ minor clay and pebbles	7	granite
Q515345	Light Brown	0	Med-fine sand w/ silt	10	gneiss
Q515346	Light Brown	0	Med-fine sand w/ granules/pebbles	35	-
Q515347	Light Grey	0	Fine sand w/ silt & minor clay	7	-
Q515348	Light Brown	0	Fine sand w/ granules	7	granite
Q515349	Light Brown	0	Fine sand w/ granules	7	-
Q515350	Light Brown	0	mod poor sort med sand	25	granite, gneiss
Q515351	Light Brown	0	Fine sand w/ silt	15	-
Q515352	Light Brown	0	med-fine sand w/ silt and granule	15	gneiss
Q515354	Light Brown	0	Mod well sort fine sand	5	-

Kelvin Soil Sample Field Measurements

Sample ID	B Horizon Color	B Horizon Moisture (%)	B Horizon Texture	B Horizon % Clasts	B Horizon Clast Composition
Q515355	Light Brown	0	Mod well sort fine sand	5	-
Q515356	Light Brown	0	Mod well sort med-fine sand	3	-
Q515357	Light Grey	5.3	Fine sand w/ silt	10	-
Q515358	Light Brown	0	Mod poor sort fine sand, silt, w/ clay	20	-
Q515359	Light Brown	0	Mod poor sort med-fine sand	-	-
Q515360	Light Brown	0.7	Mod poor sort med-fine sand	-	-
Q515362	Light Brown	0	Mod poor sort med-fine sand	-	-
Q515363	Light Brown	9	Mod poor sort med-fine sand	Did not seive	-
Q515364	Light Brown	8.4	Mod poor sort med-fine sand w/ silt	10	-
Q515365	Light Brown	0	Mod poor sort med sand	-	-
Q515366	Light Brown	0	Mod poor sort med-coarse sand	15	-
Q515367	Light Brown	0	Mod poor sort med-coarse sand	15	-
Q515368	Light Brown	0	Mod poor sort med-coarse sand	10	-
Q515370	Light Brown	0	Mod poor sort med-coarse sand	25	-
Q515371	Light Brown	0	Mod poor sort med sand w/ silt	20	-
Q515372	Light Brown	0	Mod poor sort coarse sand	20	-
Q515373	Light Brown	0	Mod Well sort med sand w/ granules	10	-
Q515374	Light Brown	0	Fine sand w/ silt and granules	7	-
Q515375	Light Brown	8.1	Poor sort coarse sand	20	-
Q515376	Light Brown	10.1	Poor sort med sand w/ granules	15	-
Q515377	Light Brown	0	Mod poor sort med-fine sand	20	-
Q515378	Light Brown	0	Mod poor sort med-fine sand	25	-
Q515379	Light Brown	8.7	Mod poor sort med sand	20	-
Q515380	Light Brown	8.9	Mod well sort med-fine sand	15	granite
Q515381	Light Brown	0	Mod well sort med sand	15	-

Kelvin Soil Sample Field Measurements

Sample ID	B Horizon Color	B Horizon Moisture (%)	B Horizon Texture	B Horizon % Clasts	B Horizon Clast Composition
Q515382	Light Brown	0.9	Mod well sort med sand	15	-
Q515384	Light Brown	10.1	Didn't seive	-	-
Q515385	Light Brown	0	Mod well sort med-fine sand	15	ganite, gneiss
Q515386	Light Brown	0	Mod well sort fine sand w/ silt and minor clay	20	-
Q515387	Light Brown	0	Well sort fine sand	10	gneiss
Q515388	Light Brown	0	Mod well sort med-fine sand w/ granules	10	granite
Q515389	Light Grey	0	Mod well sort med sand	30	granite
Q515390	Light Brown	0	Mod well sort fine sand w/ silt and granules	20	-
Q515391	Light Grey	0	Mod well sort fine sand w/ silt, minor clay, granules	15	-
Q515392	Light Brown	0	Poor sort med sand w/ granules	30	granite
Q515393	Light Brown	0	Mod well sort fine sand and silt	15	-
Q515394	Light Brown	0	Poor sort fine sand	30	granite, gneiss
Q515395	Light Brown	0	Mod poor sort med-fine sand w/ granules	20	-
Q515396	Light Brown	0	-	20	-
Q515397	Light Brown	0	Didn't seive	-	-
Q515398	Light Grey	0	Didn't seive	-	-
Q515399	Light Brown	0	Mod poor sort coarse-med sand	10	granite
Q515400	Light Brown	0	Mod poor sort med sand and silt	7	-
Q515401	Light Brown	0	Mod poor sort med sand w/ granules	15	granite
Q515402	Light Brown	0	Mod poor sort coarse-med sand	20	-
Q515403	Light Brown	0	Mod well sort coarse-med sand	5	-
Q515404	Light Brown	0	Mod poor sort med sand w/ granules	15	-
Q515405	Light Brown	0	Mod well sort med sand w/ silt	-	-
Q515406	Light Brown	0	Mod well wort fine sand and silt	15	-
Q515407	Light Brown	1.2	Mod poor sort coarse-med sand	10	-

Kelvin Soil Sample Field Measurements

Sample ID	B Horizon Color	B Horizon Moisture (%)	B Horizon Texture	B Horizon % Clasts	B Horizon Clast Composition
Q515408	Light Grey	0	Mod well sort med-fine sand	10	-
Q515409	Light Brown	0	Mod well sort coarse-med sand	20	-
Q515410	Light Grey	0	Mod poor sort med sand w/ silt	20	-
Q515411	Light Brown	0	Mod poor sort coarse-med sand	25	granite
Q515412	Light Brown	0	Mod poor sort coarse-med sand w/ pebbles	25	granite, gneiss
Q515413	Light Brown	0	Poor sort coarse-med sand w/ silt and pebbles	25	-
Q515414	Light Grey	0	Poor sort coarse-med sand w/ silt and pebbles	10	-
Q515415	Light Grey	0	Mod well sort med sand w/ silt and granules	20	-
Q515416	Light Brown	0	Mod poor sort med-fine sand w/ silt and granules	20	-
Q515417	Light Brown	0	Mod poor sort coarse-med sand w/ granules	30	granite
Q515418	Light Brown	0	Mod poor sort coarse-med sand w/ granules	15	granite
Q515419	Light Grey	0	Mod wel wort fine sand w/ silt, clay, granules	15	-
Q515420	Light Brown	0	Mod poor sort fine sand and silt	25	granite
Q515421	Light Brown	0	Well sort med sand w/ granules	15	-
Q515422	Light Brown	0	Well sort med sand w/ granules	5	-
Q515423	Light Grey	0	Well sort sand w/ silt and minor clay	10	-
Q515425	Light Brown	0	Mod well sort fine sand, silt, w/ granules	7	-
Q515426	Light Brown	0	Mod well sort fine sand, silt, w/ granules	25	-
Q515427	Light Brown	0	-	15	-
Q515428	Light Brown	0	Mod poor sort med-coarse sand	15	-
Q515429	Light Brown	0	Mod well sort fine-med sand w/ silt and ganules	15	-
Q515430	Light Brown	0	Mod poor sort coarse-med sand w/ silt and granules	10	-
Q515431	Light Grey	0	Mod well sort fine sand w/ silt and minor clay	10	-
Q515432	Light Brown	0	Mod well sort fine sand w/ silt	10	-
Q515433	Light Brown	0	Mod well sort med sand w/ silt and pebbles	20	granite

Kelvin Soil Sample Field Measurements

Sample ID	B Horizon Color	B Horizon Moisture (%)	B Horizon Texture	B Horizon % Clasts	B Horizon Clast Composition
Q515434	Light Grey	0	Mod well word fine sand, silt, and minor clay	10	-
Q515435	Light Brown	0	Mod well word fine sand, silt, and minor clay	-	-
Q515436	Light Brown	0	Mod poor sort coarse-med sand	10	-
Q515437	Light Brown	0	Mod poor sort coarse-med sand w/ silt	7	-
Q515438	Light Brown	0	Poor sort coarse-med sand w/ silt	5	-
Q515439	Light Brown	0	Mod poor sort coarse-med sand	7	-
Q515440	Light Grey	0	Mod poor sort coarse-med sand	7	-
Q515442	Light Brown	0	Mod poor sort coarse-med sand w/ silt	20	granite, schist
Q515443	Light Brown	0	Mod poor sort med-fine sand w/ silt	25	schist
Q515444	Light Grey	0	Mod poor sort fine sand w/ silt	3	-
Q515445	Light Grey	0	mod well sort fine sand w/ silt	3	-
Q515446	Light Brown	0	Mod poor sort med-fine sand w/ silt	7	granite, schist
Q515447	Light Grey	0	Mod poor sort med-fine sand w/ silt and granules	12	granite, schist
Q515448	Light Brown	0	Mod well sort fine sand and silt	7	granite
Q515449	Light Brown	0	Mod well sort coarse-med sand w/ granules	10	granite
Q515450	Light Grey	0	Mod well sort med-fine sand w/ silt	7	-
Q515451	Light Grey	0	Mod poor sort med sand w/ silt and granules	10	-
Q515452	Light Grey	0	Mod poor sort med sand w/ silt and granules	5	-
Q515454	Light Brown	0		-	-
Q515455	Light Brown	0	Mod well sort med-fine sand w/ silt and granules	5	granite
Q515456	Light Grey	0	Mod well sort fine sand and silt w/ minor clay	-	-
Q515457	Light Grey	0	Mod well sort fine sand and silt w/ minor clay	-	-
Q515458	Light Grey	0	Poor sort coarse-fine sand and silt w/ minor clay	15	-
Q515459	Light Grey	0	Mod well sort med-fine sand w/ silt and minor clay	15	-
Q515460	Light Brown	0	Mod poor sort coarse-med sand w/ silt	15	-

Kelvin Soil Sample Field Measurements

Sample ID	B Horizon Color	B Horizon Moisture (%)	B Horizon Texture	B Horizon % Clasts	B Horizon Clast Composition
Q515461	Light Brown	0	-	-	-
Q515462	Light Brown	3.6	Mod poor sort coarse-med sand	25	-
Q515463	Light Brown	5.7	Mod poor sort med-fine sand w/ silt	15	-
Q515464	Light Brown	0	Mod poor sort med-fine sand w/ silt	10	-
Q515465	Light Grey	0	Mod well sort fine sand w/ silt	10	-
Q515466	Light Brown	0	Mod well sort coarse-med sand w/ silt	10	-
Q515467	Light Brown	0	Mod well sort fine sand	15	-
Q515468	Light Grey	0	Mod well sort fine sand w/ silt	7	-
Q515469	Light Brown	0	Mod poor sort med sand	5	-
Q515470	Light Grey	0	Mod well sort fine sand w/ silt	5	-
Q515471	Light Brown	0	Mod poor sort med-fine sand	20	granite
Q515472	Light Brown	0	Mod poor sort med-fine sand w/ silt and granules	30	granite, schist
Q515473	Light Brown	0	Mod poor sort sand w/ silt and granules	20	-
Q515474	Light Grey	0	Mod well sort fine sand, silt, minor clay	15	-
Q515475	Light Brown	0	Mod well sort med-fine sand	-	-

D.3 Soil Slurry Physicochemical Results

Physicochemical measurements of soil slurries included the 1:1 mixture of soil and deionized water (by volume) and the measurement of pH, TDS, temperature, acidified pH, acidified TDS, and the Eh for select samples.

Soil Slurry Physicochemical Results

Sample	pH	TDS	Temperature	Acidified pH	Acidified TDS	Eh
	s.u.	ppm	°C	s.u.	ppm	Volts
Q515251	5.2	22	24.1	4.4	108	-
Q515252	4.9	16	24.1	4.1	85	-
Q515253	6.1	12	24.4	3.5	146	-
Q515254	5	30	24.5	4.2	118	-
Q515255	4.6	23	23.8	3.9	109	-
Q515256	4.7	21	23.5	3.9	108	-
Q515257	6	16	23.2	4.7	79	-
Q515258L	5.6	20	23.3	4.2	99	-
Q515258U	5.9	13	23.5	4	111	-
Q515260	5	21	23.5	3.6	120	-
Q515261	4.6	22	23.5	3.7	133	-
Q515262	4.4	40	23.8	3.8	109	-
Q515263	4.5	79	23.7	3.6	205	-
Q515264	4.7	25	23.7	3.8	109	-
Q515265	4.4	49	23.5	3.6	133	-
Q515266	4.9	18	23.8	4	98	-
Q515267	5.2	9	23.6	3.8	107	-
Q515268	5.8	13	23.5	4.2	99	-
Q515269	5.9	8	23.6	4.2	81	-
Q515270	5	20	23.4	4.1	95	-
Q515271	5.3	9	23.2	3.8	117	-
Q515272	5	10	23.5	3.8	99	-
Q515273	4.9	13	23.4	3.8	94	-
Q515274	4.7	22	23.5	4	96	-
Q515275	4.5	25	23.3	3.7	109	-
Q515276	5.5	21	23.3	4.3	126	-
Q515277	5.6	16	23.5	3.8	150	-
Q515278	4.8	30	23.5	4.1	105	-
Q515280	4.3	39	22.8	3.7	113	-
Q515281	4.5	68	23.3	4	139	-
Q515282	4.6	23	23.1	3.8	94	-
Q515283	4.4	69	23.1	3.9	129	-
Q515284	4.7	68	23.1	3.7	186	-
Q515285	4.5	38	23.1	3.5	150	-
Q515286	4.4	94	23.3	3.5	212	-
Q515287	4.6	30	23.4	3.7	134	-
Q515288	5.1	14	23.4	3.6	114	-
Q515289	4.6	34	23.5	3.5	160	0.460
Q515290	4.7	20	23.1	3.7	107	0.477
Q515291	4.2	99	23.4	3.5	196	0.511
Q515292	4.7	21	23.4	3.7	114	0.497
Q515293	4.3	386	23.2	3.9	462	0.509
Q515294	4.8	31	23.2	3.8	114	0.494
Q515295	4.4	35	23.4	3.7	114	0.498
Q515296	4.3	46	23.2	3.5	172	0.517
Q515297	4.6	26	23.5	3.8	108	0.492

Soil Slurry Physicochemical Results

Sample	pH	TDS	Temperature	Acidified pH	Acidified TDS	Eh
	s.u.	ppm	°C	s.u.	ppm	Volts
Q515298	5.1	30	23.5	4.1	111	0.504
Q515299	5.1	18	23.3	4.1	101	0.490
Q515300	4.9	29	23.6	4.1	95	-
Q515301	5.1	13	23.6	3.9	85	0.491
Q515302	5	16	23.5	4	98	0.475
Q515303	5.2	16	23.3	4.3	94	0.479
Q515304	5	25	23.5	4.1	129	0.484
Q515305	6.4	17	23.5	4.6	117	0.448
Q515306	6	16	23.6	4	140	-
Q515307	5	12	23.5	4	87	-
Q515308	5.1	8	23.6	3.8	85	-
Q515309	5.3	8	23.7	4.2	55	-
Q515311	5.3	7	23.7	4	69	-
Q515312	5.2	17	23.6	4.1	98	-
Q515313	5.5	20	23.6	4.3	114	-
Q515314	4.5	25	23.1	3.6	113	-
Q515315	4.6	26	23.2	3.7	130	-
Q515316	4.8	29	23.3	3.7	143	-
Q515317	4.3	66	23.2	3.6	178	-
Q515318	4.8	21	23.2	3.6	157	-
Q515319	5.4	10	23.2	3.7	107	-
Q515320	4.7	21	22.7	3.5	106	-
Q515321	4.8	13	22.9	3.4	141	-
Q515322	5	13	22.9	3.6	150	-
Q515323	5.1	13	22.7	3.2	166	-
Q515324	4.9	15	22.6	3.5	178	0.496
Q515325	5	13	22.8	3.5	155	0.492
Q515326	4.9	16	22.7	3.3	144	0.496
Q515327	4.9	13	22.5	3.2	177	0.489
Q515328	4.9	14	22.4	3.6	161	0.491
Q515329	4.5	27	23	3.6	125	0.503
Q515330	4.9	19	23.1	3.4	175	0.488
Q515331	4.4	40	23.1	3.3	196	0.512
Q515332	4.6	19	23	3.4	179	0.508
Q515333	5.2	20	23	4.1	102	0.476
Q515334	4.9	16	23.1	3.9	88	0.502
Q515335	4.4	27	23	3.4	158	0.534
Q515336	5.1	19	23.1	3.9	95	0.506
Q515337	4.9	14	23.2	3.6	116	0.503
Q515338	5.3	10	23.2	3.8	115	0.495
Q515339	4.9	13	23.4	4	92	0.524
Q515340	5.3	9	22.8	3.7	104	0.525
Q515341	5.3	10	22.7	3.4	167	0.513
Q515342	5.2	14	22.8	3.6	131	0.493
Q515343	5.1	18	23	4	104	0.501
Q515344	5.8	14	23	4.4	102	0.489

Soil Slurry Physicochemical Results

Sample	pH	TDS	Temperature	Acidified pH	Acidified TDS	Eh
	s.u.	ppm	°C	s.u.	ppm	Volts
Q515345	4.9	16	23.1	3.8	110	0.507
Q515346	5	14	23.1	3.8	119	-
Q515347	6	16	23.1	4.6	113	-
Q515348	5.1	18	23.1	3.9	133	-
Q515349	5.8	19	23.3	4.2	132	-
Q515350	4.8	19	23.6	3.7	132	-
Q515351	5	12	23.5	3.8	111	-
Q515352	4.8	16	23.6	3.8	112	-
Q515354	4.9	14	23.5	3.9	118	-
Q515355	4.9	9	22.9	3.6	117	-
Q515356	4.8	17	22.9	3.7	110	-
Q515357	4.6	52	22.9	3.6	162	-
Q515358	4.7	13	22.8	3.3	142	-
Q515359	4.6	20	22.8	3.6	142	-
Q515360	4.7	15	22.9	3.4	123	-
Q515362	4.9	23	23.2	3.7	138	-
Q515363	4.4	63	23	3.5	167	-
Q515364	4.5	54	23.1	3.7	137	-
Q515365	4.8	19	23.1	3.6	159	-
Q515366	5	12	23	3.2	132	-
Q515367	5.4	14	23	3.3	186	-
Q515368	5.4	12	22.5	3.4	150	-
Q515370	5.3	8	22.5	3.4	147	-
Q515371	5.6	9	22.6	3.6	115	-
Q515372	5.3	10	22.6	3.7	100	-
Q515373	5	17	22.6	3.5	129	-
Q515374	4.4	34	22.6	3.3	192	-
Q515375	4.3	84	23.1	3.8	193	-
Q515376	4.4	71	23	3.8	186	-
Q515377	4.9	14	22.6	3.5	150	-
Q515378	4.8	18	22.8	3.3	159	-
Q515379	3.7	114	22.7	3.1	275	-
Q515380	3.9	78	22.7	3.3	232	-
Q515381	4.4	36	22.8	3.3	186	-
Q515382	4.5	35	22.9	3.5	151	-
Q515384	3.8	79	22.8	3.3	92	-
Q515385	5.1	12	22.9	3.5	147	-
Q515386	5.3	9	22.9	3.6	117	-
Q515387	5.1	9	22.5	3.5	117	-
Q515388	5	9	22.5	3.6	110	-
Q515389	4.6	28	22.5	3.4	166	-
Q515390	4.9	11	22.5	3.7	86	-
Q515391	5.9	11	22.5	3.9	125	-
Q515392	5.3	19	22.6	4	143	-
Q515393	4.9	13	22.8	3.3	139	-
Q515394	5.4	14	22.7	4.1	104	-

Soil Slurry Physicochemical Results

Sample	pH	TDS	Temperature	Acidified pH	Acidified TDS	Eh
	s.u.	ppm	°C	s.u.	ppm	Volts
Q515395	5.1	26	22.8	4.2	148	-
Q515396	5.4	13	22.9	3.6	114	-
Q515397	5.5	14	22.9	4.4	72	-
Q515398	5.6	13	23.2	4.1	128	-
Q515399	4.9	14	23.1	3.5	139	-
Q515400	4.6	19	23.2	3.6	115	-
Q515401	4.8	12	23.3	3.6	124	-
Q515402	5.1	15	23.3	3.8	132	-
Q515403	5.1	12	23.3	3.7	112	-
Q515404	4.9	15	22.6	3.6	131	-
Q515405	5.3	10	22.6	3.7	124	-
Q515406	5.9	31	22.7	4.8	142	-
Q515407	4.9	22	22.6	3.7	135	-
Q515408	6.4	15	22.7	4.3	141	-
Q515409	6.3	13	22.6	4.6	116	-
Q515410	6	18	22.8	4.3	142	-
Q515411	5.3	14	22.7	3.7	123	-
Q515412	5.8	13	22.7	4.1	130	-
Q515413	5	13	23	3.5	138	-
Q515414	5.5	6	22.9	3	228	-
Q515415	5.5	9	22.9	3.4	145	-
Q515416	5.2	8	22.5	3.6	144	-
Q515417	4.9	18	22.6	3.7	147	-
Q515418	5.5	12	22.4	3.6	165	-
Q515419	5.9	14	22.5	4	155	-
Q515420	4.8	20	22.7	3.6	170	-
Q515421	5.2	11	22.7	3.7	165	-
Q515422	5.1	12	22.6	3.7	172	-
Q515423	5.6	9	22.8	3.6	144	-
Q515425	4.9	11	23	3.7	127	-
Q515426	5.1	13	23	4.1	110	-
Q515427	5.7	16	22.9	4.3	126	-
Q515428	5.2	15	23	3.7	157	-
Q515429	5.1	9	23	3.7	143	-
Q515430	5.4	17	23	4.2	116	-
Q515431	6.3	13	22.7	4.1	145	-
Q515432	5.6	11	22.7	3.8	154	-
Q515433	5.2	14	22.8	4	108	-
Q515434	6.1	10	22.7	4	118	-
Q515435	5.9	9	22.8	3.7	122	-
Q515436	5	21	22.8	3.7	164	-
Q515437	5.2	15	23	3.9	138	-
Q515438	6.1	10	22.9	3.9	151	-
Q515439	5.5	6	23	3.7	144	-
Q515440	5.6	8	23	3.5	202	-
Q515442	4.9	17	23	3.7	156	-

Soil Slurry Physicochemical Results

Sample	pH	TDS	Temperature	Acidified pH	Acidified TDS	Eh
	s.u.	ppm	°C	s.u.	ppm	Volts
Q515443	5.5	10	23.1	3.9	129	-
Q515444	5.7	13	23.2	4.1	112	-
Q515445	6.5	11	23.2	4.7	107	-
Q515446	4.9	14	23.4	3.7	142	-
Q515447	5.6	16	23.2	4.2	101	-
Q515448	5.6	20	23.3	4.4	124	-
Q515449	5.3	9	22.7	3.7	120	-
Q515450	5.9	12	22.9	4	114	-
Q515451	5.8	10	22.9	3.7	130	-
Q515452	6.2	12	23.3	4	138	-
Q515454	6.2	11	23.4	4.4	108	-
Q515455	5.4	10	23.2	4.1	89	-
Q515456	5.8	14	23.1	4	111	-
Q515457	6.4	24	23.3	5.1	122	-
Q515458	6.4	14	23.1	4.4	136	-
Q515459	6.8	23	23.2	4.9	140	-
Q515460	5.8	11	23.1	3.9	130	-
Q515461	5.7	10	23.3	3.8	134	-
Q515462	4.5	50	23.2	3.7	176	-
Q515463	4.7	49	23.1	4.1	146	-
Q515464	5.4	38	23.3	4.3	152	-
Q515465	5.3	15	23.3	3.8	142	-
Q515466	5.9	20	23.3	4.6	137	-
Q515467	5.6	8	22.4	3.6	130	-
Q515468	5.7	21	22.5	4.1	147	-
Q515469	5.4	15	22.4	4	115	-
Q515470	6.1	23	22.5	4.3	148	-
Q515471	5.2	12	22.6	3.7	154	-
Q515472	5	14	22.7	3.9	116	-
Q515473	5.4	11	22.6	3.8	129	-
Q515474	6	17	22.5	4.3	131	-
Q515475	5.5	9	22.7	3.7	129	-

- not measured

D.4 Till Four Acid ICP-MS Results

Multi-element results are presented for the four acid digestion and ICP-MS analysis of the -180 micron fraction of till samples.

Till Four Acid ICP-MS Results

Sample	Ag	Al	As	Ba	Be	Bi	Ca	Cd	Ce	Co
	ppm	%	ppm	ppm	ppm	ppm	%	ppm	ppm	ppm
Q515251	0.042	5.05	1.14	530	1.48	0.107	1.12	0.055	41.5	4.97
Q515252	0.027	4.83	0.75	570	0.9	0.09	0.97	0.05	43.2	3.35
Q515253	0.041	5.3	0.91	540	1.01	0.097	1.29	0.068	52.8	4.5
Q515254	0.038	4.97	2.78	580	0.92	0.128	1.13	0.073	40.1	5.83
Q515255	0.027	5.4	3.09	580	1.06	0.156	1.25	0.093	53.2	9.1
Q515256	0.04	5.04	1.8	520	0.99	0.124	1.22	0.06	32.5	5.96
Q515257	0.044	4.97	0.16	620	0.85	0.093	1.31	0.046	60.8	6.17
Q515258L	0.042	5.42	1.77	630	1.1	0.153	1.25	0.055	60.9	8.36
Q515258U	0.04	5.01	0.58	610	1.02	0.089	1.36	0.062	53.9	6.54
Q515260	0.045	5.13	1.32	490	0.96	0.114	1.19	0.045	42.2	3.68
Q515261	0.028	4.93	0.59	500	0.88	0.183	1.13	0.038	29.2	2.97
Q515262	0.04	4.97	0.89	460	0.85	0.127	1.15	0.042	38.7	2.94
Q515263	0.037	4.92	1.23	480	0.88	0.11	1.08	0.037	29.3	3.28
Q515264	0.035	4.67	0.79	510	0.87	0.091	1.1	0.032	36.5	3.77
Q515265	0.049	5.06	1.08	429	1.02	0.135	1.13	0.046	39.4	2.61
Q515266	0.03	4.67	1.25	560	0.88	0.11	1.14	0.041	39.9	4.1
Q515267	0.042	4.85	1.46	490	0.99	0.144	1.09	0.047	43.6	4.52
Q515268	0.043	4.7	1.24	550	1.01	0.085	1.15	0.062	58.5	6.05
Q515269	0.031	4.66	1.02	510	1.24	0.103	1.1	0.043	40.5	4.95
Q515270	0.036	4.29	1.37	520	0.82	0.067	1.01	0.04	31	4.09
Q515271	0.038	4.89	0.97	550	0.91	0.101	1.15	0.053	46.4	5.69
Q515272	0.021	4.57	1.43	540	0.81	0.087	1.02	0.039	29.8	4.2
Q515273	0.039	4.73	0.76	560	0.86	0.059	1.11	0.045	31.1	4.15
Q515274	0.025	4.95	7.2	520	0.9	0.17	1.22	0.057	43.3	7.18
Q515275	0.022	4.5	1.5	560	0.94	0.079	0.96	0.037	23.5	4.05
Q515276	0.042	5.24	1.39	600	1.11	0.093	1.25	0.047	55.9	4.84
Q515277	0.041	5.16	1.16	590	1.03	0.081	1.28	0.053	55.9	4.63
Q515278	0.041	5.29	2.61	500	1.09	0.156	1.16	0.032	51.1	4.29
Q515280	0.028	5.19	1.24	520	1.09	0.1	1.09	0.034	36.1	3.34
Q515281	0.04	5.27	1.61	540	1.03	0.139	1.18	0.045	44.1	4.27
Q515282	0.028	5.02	1.83	530	0.99	0.148	1.13	0.044	42	3.77
Q515283	0.033	5.05	1.96	530	0.96	0.131	1.09	0.048	30	3.85
Q515284	0.044	5.39	1.75	480	1.14	0.133	1.22	0.047	59.1	4.28
Q515285	0.046	5.5	1.99	480	1.18	0.154	1.22	0.049	57.9	3.98
Q515286	0.04	5.53	1.53	480	1.08	0.155	1.24	0.042	57.2	3.37
Q515287	0.045	5.15	2.47	490	1.03	0.17	1.12	0.043	44.6	3.59
Q515288	0.048	5.2	1.49	480	1.06	0.174	1.16	0.039	41.6	2.93
Q515289	0.049	5.34	2.09	470	1.1	0.149	1.15	0.045	58.3	3.22
Q515290	0.03	5.23	2.52	520	1.06	0.168	1.15	0.052	53.1	3.99
Q515291	0.041	5.29	1.96	460	1.1	0.175	1.16	0.043	52.5	2.93
Q515292	0.039	5.51	2.4	490	1.1	0.204	1.17	0.048	58.9	3.68

Till Four Acid ICP-MS Results

Sample	Ag	Al	As	Ba	Be	Bi	Ca	Cd	Ce	Co
	ppm	%	ppm	ppm	ppm	ppm	%	ppm	ppm	ppm
Q515293	0.044	5.51	2.09	520	1.1	0.156	1.27	0.051	60	4.91
Q515294	0.035	5.06	1.79	421	1.06	0.13	1.05	0.049	46.5	2.71
Q515295	0.026	5.19	1.19	470	1.03	0.207	1.05	0.039	34.3	2.79
Q515296	0.049	5.59	1.82	490	1.22	0.149	1.21	0.04	51.2	3.61
Q515297	0.024	4.25	0.98	590	0.8	0.068	1.05	0.028	38.7	3.15
Q515298	0.054	5.75	2.33	670	1.24	0.149	1.23	0.067	58.3	8.09
Q515299	0.045	5.15	2.49	600	1.18	0.111	1.19	0.05	63.3	5.83
Q515300	0.043	5.67	2.06	650	1.2	0.116	1.22	0.051	47	6.98
Q515301	0.037	5.03	1.54	540	1.01	0.069	1.18	0.042	37.1	4.13
Q515302	0.03	4.92	1.37	580	0.97	0.074	1.19	0.05	50.8	4.29
Q515303	0.031	4.74	1.7	570	0.92	0.087	1.13	0.042	38.6	5.97
Q515304	0.039	4.9	1.89	570	1.04	0.091	1.15	0.063	60.1	6.52
Q515305	0.044	4.91	1.2	610	1.07	0.073	1.28	0.05	47.6	6.39
Q515306	0.048	5.14	1.79	570	1.1	0.09	1.24	0.049	67.2	6.32
Q515307	0.041	4.61	1.56	560	0.97	0.068	1.15	0.044	39.9	5.17
Q515308	0.019	4.32	1.67	530	0.86	0.08	1	0.042	28.3	3.64
Q515309	0.024	5.06	2.34	560	1.01	0.093	1.11	0.051	57.4	4.73
Q515311	0.024	5.01	1.95	550	0.95	0.085	1.15	0.059	43.8	5.55
Q515312	0.026	5.08	1.15	630	1.03	0.086	1.19	0.029	40.7	5.34
Q515313	0.042	5.06	1.47	600	1.02	0.088	1.19	0.046	57	5.18
Q515314	0.031	4.62	1.79	530	0.96	0.104	1.13	0.042	46.3	3.51
Q515315	0.026	4.86	0.64	570	0.89	0.095	1.13	0.028	45.7	3.19
Q515316	0.041	5.47	0.89	490	1.04	0.137	1.22	0.048	50.2	3.23
Q515317	0.033	4.76	1.56	510	0.9	0.117	1.11	0.041	42.9	3.53
Q515318	0.032	5.16	1.41	480	0.99	0.115	1.14	0.054	39.4	2.9
Q515319	0.034	5.1	1.48	490	0.97	0.127	1.13	0.041	42.4	3.17
Q515320	0.035	5.12	1.62	440	0.97	0.143	1.06	0.044	42	2.66
Q515321	0.04	5.05	1.27	440	1.05	0.131	1.08	0.042	60.2	2.4
Q515322	0.048	5.06	1.79	440	1.01	0.163	1.11	0.041	45.8	2.54
Q515323	0.052	5.34	1.78	447	1.05	0.138	1.18	0.055	49.9	3.18
Q515324	0.035	5.19	1.86	460	1.05	0.145	1.11	0.044	50.4	2.7
Q515325	0.044	5.23	1.13	447	1.14	0.149	1.13	0.048	45.1	2.47
Q515326	0.04	5.27	1.71	439	1.12	0.134	1.14	0.043	47	2.58
Q515327	0.043	5.3	2.36	448	1.19	0.121	1.16	0.046	43.8	2.66
Q515328	0.04	5.28	1.38	460	1.09	0.138	1.16	0.047	69.7	2.81
Q515329	0.034	5.3	1.35	449	1.11	0.135	1.08	0.041	31.4	3.05
Q515330	0.043	5.07	1.37	480	0.98	0.113	1.15	0.046	41.5	3.07
Q515331	0.047	5.28	1.64	470	1.19	0.184	1.15	0.041	51.3	3.05
Q515332	0.027	5.12	0.26	430	1.13	0.114	1.06	0.036	41.1	2.16
Q515333	0.036	5.57	1.5	500	1.23	0.163	1.22	0.05	52.8	4.69
Q515334	0.04	5.38	1.96	448	1.13	0.135	1.18	0.048	45.5	2.92

Till Four Acid ICP-MS Results

Sample	Ag	Al	As	Ba	Be	Bi	Ca	Cd	Ce	Co
	ppm	%	ppm	ppm	ppm	ppm	%	ppm	ppm	ppm
Q515335	0.044	5.38	2.14	444	1.2	0.163	1.18	0.045	51.8	3.17
Q515336	0.036	4.87	1.76	510	1.12	0.101	1.16	0.048	37	3.83
Q515337	0.03	4.41	1.38	570	0.91	0.059	1.11	0.034	44.3	3.82
Q515338	0.038	4.91	1.57	560	0.98	0.084	1.14	0.055	50	4.49
Q515339	0.022	4.84	1.76	570	0.98	0.089	0.96	0.045	31.6	4.2
Q515340	0.031	4.63	1.79	540	0.93	0.075	1.08	0.039	37.1	4.54
Q515341	0.044	4.32	1.1	530	0.87	0.054	1.09	0.035	36.4	5.17
Q515342	0.042	4.65	1.29	550	0.91	0.061	1.12	0.034	50.9	4.25
Q515343	0.047	5.31	2.42	610	1.1	0.12	1.2	0.063	49	6.87
Q515344	0.044	5.07	1.53	590	1.24	0.104	1.23	0.045	52.1	6.1
Q515345	0.025	4.49	2.03	530	0.89	0.086	1.07	0.049	35.3	4.66
Q515346	0.028	4.43	2.12	520	0.85	0.079	1.04	0.047	38.1	4.71
Q515347	0.041	5.11	1.61	620	1.01	0.087	1.24	0.044	45.2	6.26
Q515348	0.04	4.58	0.94	560	0.94	0.062	1.14	0.04	45.1	4.37
Q515349	0.04	4.75	0.82	590	0.92	0.076	1.2	0.058	44.8	5.59
Q515350	0.036	4.69	1.05	580	0.95	0.084	1.15	0.045	36.3	4.95
Q515351	0.04	4.55	0.92	540	0.94	0.067	1.09	0.049	29.7	4.61
Q515352	0.024	4.77	1.14	570	0.96	0.075	1.07	0.043	29.6	4.17
Q515354	0.018	4.78	0.63	510	0.87	0.082	1.08	0.054	55	3.81
Q515355	0.044	4.95	0.94	500	0.96	0.097	1.14	0.049	38.2	3.22
Q515356	0.029	4.62	0.89	510	0.95	0.088	1.08	0.043	32.6	3.44
Q515357	0.043	5.26	0.85	520	1.16	0.147	1.25	0.06	56.1	4.4
Q515358	0.037	5.01	1.94	439	1.06	0.154	1.12	0.041	42.1	2.67
Q515359	0.036	5.41	1.53	490	1.07	0.172	1.13	0.04	44.5	3.54
Q515360	0.035	5.41	0.71	510	1.14	0.158	1.21	0.062	55	3.73
Q515362	0.026	5.06	0.8	530	1.34	0.106	1.2	0.033	39.3	3.44
Q515363	0.032	5.23	0.38	500	1.12	0.156	1.22	0.043	48.6	3.4
Q515364	0.037	5.4	0.78	500	1.12	0.16	1.23	0.041	59.9	3.74
Q515365	0.04	4.96	1.08	520	0.98	0.155	1.09	0.041	36.1	3.89
Q515366	0.041	5.11	0.93	449	1.05	0.145	1.14	0.043	59.9	2.8
Q515367	0.044	5.12	1.71	480	1.03	0.162	1.16	0.054	49.3	3.22
Q515368	0.043	5.13	1.23	447	1.1	0.123	1.13	0.052	48.4	3.02
Q515370	0.046	5.23	1.56	460	0.96	0.158	1.15	0.048	49.6	2.82
Q515371	0.041	5.03	2.34	480	1.04	0.178	1.09	0.053	53	3.41
Q515372	0.034	5.2	0.88	447	1.04	0.183	1.06	0.042	50.9	2.76
Q515373	0.043	5.31	1.57	470	1.78	0.163	1.11	0.052	51.4	3
Q515374	0.035	5.12	1.17	500	1.04	0.116	1.15	0.043	57.4	3.77
Q515375	0.056	4.95	1.56	500	0.94	0.168	1.03	0.044	36.3	4.01
Q515376	0.036	4.98	0.63	480	0.98	0.127	1.11	0.044	48.7	3.1
Q515377	0.025	4.95	4.42	500	1.02	0.19	0.94	0.053	41.5	3.5
Q515378	0.042	5.11	2.42	510	1.02	0.173	1.09	0.045	55.8	3.75

Till Four Acid ICP-MS Results

Sample	Ag	Al	As	Ba	Be	Bi	Ca	Cd	Ce	Co
	ppm	%	ppm	ppm	ppm	ppm	%	ppm	ppm	ppm
Q515379	0.043	5.05	1.04	439	0.97	0.132	1.11	0.041	46.6	2.61
Q515380	0.039	4.82	2.53	460	0.94	0.197	1.09	0.048	57.9	3.24
Q515381	0.048	5.29	1.29	460	1.05	0.149	1.12	0.055	48.7	2.99
Q515382	0.044	5.27	1.13	447	1.17	0.165	1.15	0.056	46.7	3.08
Q515384	0.029	4.96	1.24	480	0.97	0.135	1.16	0.045	40.4	4.01
Q515385	0.03	4.94	1.81	430	1.05	0.13	1.16	0.054	37.7	2.52
Q515386	0.028	5.15	1.18	480	1.21	0.131	1.19	0.038	37.4	3.43
Q515387	0.022	4.79	1.33	490	1.12	0.148	1.12	0.051	36.6	3.51
Q515388	0.037	4.89	1.95	470	1.01	0.11	1.15	0.05	37.2	3.95
Q515389	0.018	4.11	0.75	540	0.74	0.093	1.08	0.028	40.2	3.96
Q515390	0.023	4.55	1.53	500	0.9	0.109	1.1	0.044	39.8	3.55
Q515391	0.046	5.26	2.16	480	1.18	0.136	1.22	0.06	54.6	4.32
Q515392	0.037	4.5	1.57	550	0.93	0.085	1.08	0.04	44.5	6.13
Q515393	0.034	4.5	2.29	560	0.95	0.071	1.11	0.052	34.3	5.34
Q515394	0.041	4.91	3.08	580	1.17	0.136	1.12	0.049	38	7.25
Q515395	0.022	4.66	2.14	570	1.01	0.129	1.1	0.045	35.9	4.9
Q515396	0.033	5.07	1.97	630	1.08	0.104	1.21	0.049	42.3	8.25
Q515397	0.03	4.81	1.6	600	1.01	0.096	1.28	0.042	48.5	6.34
Q515398	0.048	5.34	2.78	620	1.15	0.146	1.21	0.06	49.8	8.13
Q515399	0.024	4.64	2.82	580	0.85	0.133	1.1	0.054	35.9	4.68
Q515400	0.02	4.22	0.47	560	0.91	0.046	1.06	0.026	27.3	3.41
Q515401	0.035	4.62	1	520	0.92	0.067	1.05	0.037	38.8	4.04
Q515402	0.04	5.1	1.93	470	1.19	0.137	1.17	0.044	42.8	4.06
Q515403	0.034	5.04	1.59	443	1.13	0.146	1.14	0.048	31.8	3.2
Q515404	0.038	4.83	2.01	446	1.1	0.137	1.07	0.049	36.4	3.03
Q515405	0.044	4.91	1.87	430	1.16	0.152	1.1	0.041	47.3	2.65
Q515406	0.027	5.04	3.5	600	1.09	0.11	1.14	0.041	49.3	6.15
Q515407	0.036	4.67	1.76	530	1.02	0.126	0.99	0.022	37.7	4.72
Q515408	0.038	5.07	2.16	550	1.11	0.101	1.22	0.043	56.4	5.51
Q515409	0.036	4.99	1.64	540	0.98	0.098	1.13	0.038	45.3	5.7
Q515410	0.048	5	1.62	590	1.04	0.106	1.21	0.04	53.3	6.04
Q515411	0.034	4.68	1.43	550	0.98	0.061	1.11	0.047	53.4	5.22
Q515412	0.036	4.67	1.27	510	0.98	0.084	1.07	0.046	36.8	4.56
Q515413	0.036	4.93	2.02	470	1.13	0.135	1.07	0.047	49.4	3.68
Q515414	0.041	4.95	1.19	421	1.12	0.103	1.15	0.047	43.2	2.71
Q515415	0.042	4.75	2.17	480	0.95	0.123	1.08	0.045	44.7	4.66
Q515416	0.03	4.53	1.12	510	0.96	0.053	1	0.038	30.7	4.26
Q515417	0.028	4.58	1.39	510	0.95	0.083	1.02	0.053	41.8	4.19
Q515418	0.036	4.36	1.06	550	0.98	0.048	1.07	0.042	35.5	4.43
Q515419	0.031	4.93	0.93	580	1.09	0.063	1.2	0.044	45.8	5.52
Q515420	0.027	4.85	1.58	560	0.87	0.089	1.03	0.045	42.8	4.82

Till Four Acid ICP-MS Results

Sample	Ag	Al	As	Ba	Be	Bi	Ca	Cd	Ce	Co
	ppm	%	ppm	ppm	ppm	ppm	%	ppm	ppm	ppm
Q515421	0.025	4.71	0.97	550	0.98	0.073	1.1	0.044	55.3	5.24
Q515422	0.035	4.41	1.3	510	0.96	0.053	0.99	0.039	36.4	4
Q515423	0.041	5.05	2.69	530	1.03	0.149	1.11	0.054	67.4	6.37
Q515425	0.029	4.63	1.32	520	0.93	0.077	0.96	0.046	38.6	4.06
Q515426	0.03	5.06	2.35	490	1.04	0.096	1.01	0.058	44.2	4.61
Q515427	0.042	5.25	1.32	610	1.24	0.086	1.19	0.052	58.7	6.36
Q515428	0.038	4.54	0.84	500	0.86	0.064	0.99	0.041	46.8	4.38
Q515429	0.037	4.67	0.76	510	1.01	0.059	0.93	0.041	53.8	5.01
Q515430	0.025	4.76	0.92	540	1.04	0.075	1.04	0.051	39.8	5.77
Q515431	0.045	5.05	0.4	560	1.16	0.083	1.25	0.056	64.5	5.3
Q515432	0.036	4.31	0.69	520	0.9	0.061	1.05	0.04	36.9	3.96
Q515433	0.025	4.65	1.09	540	0.96	0.072	1.11	0.057	39.3	4.45
Q515434	0.034	5.58	1.11	510	1.23	0.132	1.25	0.06	51.2	4.94
Q515435	0.048	5.45	1.25	460	1.32	0.146	1.21	0.058	55.8	4.01
Q515436	0.031	4.74	1.6	510	0.93	0.12	1.05	0.041	47.7	3.74
Q515437	0.035	5.13	0.83	530	1.09	0.11	1.09	0.042	39.5	3.49
Q515438	0.034	4.95	1.74	490	1.05	0.082	1.07	0.036	47.1	4.13
Q515439	0.041	5.18	2.52	440	1.05	0.149	1.09	0.048	46.1	3.04
Q515440	0.054	5.19	1.54	430	1.14	0.104	1.14	0.049	56.7	3.45
Q515442	0.037	5.01	1.39	430	1.11	0.17	1.05	0.032	45.7	2.3
Q515443	0.038	5.32	1.24	520	1.08	0.124	1.19	0.056	64.4	3.77
Q515444	0.036	5.6	2.06	540	1.2	0.148	1.25	0.046	55.5	5.57
Q515445	0.044	5.69	0.66	500	1.3	0.14	1.36	0.056	67.5	3.99
Q515446	0.028	4.76	1.33	480	0.96	0.079	1.07	0.043	35.3	3.39
Q515447	0.046	5.62	2.51	530	1.13	0.157	1.17	0.04	49.9	5.91
Q515448	0.045	5.49	1.11	540	1.11	0.148	1.21	0.051	65.4	5.66
Q515449	0.039	5.27	1.17	430	1.26	0.093	1.16	0.046	36.4	2.51
Q515450	0.045	5.68	0.11	500	1.22	0.15	1.33	0.068	62	3.63
Q515451	0.039	5.79	0.82	490	1.33	0.153	1.3	0.062	60.1	4.57
Q515452	0.044	5.45	1.17	460	1.41	0.126	1.26	0.052	54.8	3.78
Q515454	0.036	5.71	1.06	500	1.21	0.147	1.27	0.064	63.5	4.45
Q515455	0.027	5.41	1.97	450	0.91	0.164	1.08	0.048	43.2	3.23
Q515456	0.04	5.29	1.03	560	0.97	0.1	1.28	0.049	55.5	4.25
Q515457	0.045	5.26	2.55	640	0.91	0.123	1.22	0.055	50.8	7.58
Q515458	0.039	4.94	1.51	570	0.88	0.083	1.22	0.047	54.5	5.35
Q515459	0.036	4.82	1.58	600	0.88	0.063	1.25	0.041	49.6	5.6
Q515460	0.04	5.31	1.52	540	0.98	0.098	1.21	0.045	42.9	4.2
Q515461	0.033	4.36	1.19	550	0.7	0.049	1.05	0.029	33.1	4.96
Q515462	0.027	4.2	1.47	530	0.69	0.06	1.05	0.038	32.6	3.87
Q515463	0.031	4.45	1.49	570	0.84	0.122	1.06	0.029	44.1	4.51
Q515464	0.034	5.18	1.88	590	0.89	0.104	1.26	0.062	50.2	5.78

Till Four Acid ICP-MS Results

Sample	Ag	Al	As	Ba	Be	Bi	Ca	Cd	Ce	Co
	ppm	%	ppm	ppm	ppm	ppm	%	ppm	ppm	ppm
Q515465	0.025	4.92	2.1	600	0.89	0.098	1.16	0.041	35.4	4.42
Q515466	0.037	5.23	1.57	630	0.95	0.09	1.31	0.048	48.3	6.01
Q515467	0.031	4.49	1.65	570	0.78	0.059	1.12	0.033	41	5.55
Q515468	0.031	4.69	1.54	590	0.81	0.065	1.21	0.039	48.1	5.4
Q515469	0.033	4.58	1.46	580	0.77	0.078	1.16	0.039	35.5	5.37
Q515470	0.037	4.97	1.69	630	0.93	0.078	1.26	0.049	49.4	5.99
Q515471	0.029	4.67	2.08	590	0.81	0.076	1.14	0.063	37.5	5.1
Q515472	0.038	4.72	2.02	560	0.82	0.083	1.1	0.045	36.8	5.35
Q515473	0.031	4.81	0.93	590	0.82	0.076	1.16	0.04	34.7	4.45
Q515474	0.039	5.11	1.25	630	0.86	0.073	1.27	0.038	56.6	6.81
Q515475	0.029	4.68	1.82	580	0.83	0.069	1.16	0.042	36.5	4.54

Till Four Acid

Sample	Cr	Cs	Cu	Fe	Ga	Ge	Hf	In	K	La
	ppm	ppm	ppm	%	ppm	ppm	ppm	ppm	%	ppm
Q515251	24.8	1.02	19.55	1.47	10.7	0.07	3.22	0.022	1.56	18
Q515252	27.1	0.92	2.17	1.75	12.95	0.09	4.49	0.023	1.53	19.3
Q515253	25.2	0.97	6.62	1.32	11.4	0.09	4.33	0.016	1.67	23.3
Q515254	35.6	1.21	8.13	2.31	13.35	0.08	3.92	0.023	1.54	17.75
Q515255	47.3	1.92	12.75	3.05	16.5	0.1	4.95	0.035	1.6	23.9
Q515256	30.1	1.29	9.55	1.88	12.25	0.09	3.15	0.014	1.51	14.6
Q515257	30.6	1.11	10.5	1.67	11.9	0.11	5.07	0.031	1.69	26.9
Q515258L	41	1.98	18.6	2.09	13.85	0.11	4.22	0.032	1.8	27.2
Q515258U	29.5	1.07	9.38	1.73	11.55	0.11	5.04	0.035	1.68	23.9
Q515260	18.8	0.93	12.8	1.22	10.15	0.1	2.6	0.015	1.57	18.7
Q515261	19	0.93	3.37	1.02	10.15	0.06	2.62	0.019	1.54	13.55
Q515262	17.3	0.87	5.66	0.99	10.25	0.08	3.09	0.014	1.53	17.1
Q515263	17.3	0.91	6.14	0.98	10.15	0.06	2.36	0.011	1.52	13.35
Q515264	20.1	0.84	5.26	1.16	9.97	0.08	2.55	0.019	1.51	16.05
Q515265	15.2	0.91	5	0.8	10.35	0.08	2.81	0.01	1.54	17.5
Q515266	24.6	0.92	10.65	1.29	10.55	0.07	4.61	0.016	1.55	17.85
Q515267	20.4	1.02	6.85	1.1	10.85	0.08	3.11	0.016	1.57	19.25
Q515268	28.6	1.13	7.83	1.5	11.4	0.11	3.8	0.022	1.55	25.7
Q515269	24	0.98	12.5	1.29	10.85	0.09	3.13	0.017	1.47	18.4
Q515270	24	0.92	9.73	1.34	10.2	0.1	2.43	0.018	1.37	14.4
Q515271	26.3	1.02	13.65	1.46	11.35	0.09	3.82	0.025	1.56	21.1
Q515272	26.5	0.92	4.39	1.63	11.15	0.08	3.75	0.023	1.41	13.45
Q515273	24.2	0.8	4.64	1.41	10.1	0.07	2.82	0.015	1.5	13.6
Q515274	42.1	1.3	7.75	2.73	13.85	0.1	4.26	0.034	1.38	18.55
Q515275	23.1	1.02	4.99	1.5	10.75	0.08	2.07	0.016	1.5	11.2
Q515276	24.2	1.13	14.75	1.39	11.05	0.16	3.54	0.018	1.69	27.8
Q515277	23	1.08	11.5	1.34	10.7	0.13	4	0.012	1.67	26.5
Q515278	22	1.48	17.85	1.41	10.15	0.13	2.76	0.018	1.56	24.3
Q515280	22.7	1.14	3.99	1.19	10.5	0.09	2.92	0.015	1.59	16.3
Q515281	23	1.24	7.61	1.39	10.55	0.12	4.03	0.017	1.61	20.2
Q515282	21.8	1.12	4.66	1.27	10.25	0.1	2.88	0.013	1.56	19.25
Q515283	21.8	1.22	7.63	1.33	10.4	0.1	2.65	0.018	1.56	14.5
Q515284	17.8	1.01	8.52	1.07	10.3	0.13	4.09	0.012	1.65	28
Q515285	18.1	1.04	8.68	1.05	10.7	0.13	3.43	0.015	1.66	27.6
Q515286	19	1.06	6	1	10.7	0.13	4.18	0.013	1.67	27.4
Q515287	19.5	1.1	7.45	1.18	10.15	0.12	2.87	0.012	1.6	20.9
Q515288	16	0.92	5.74	0.97	9.74	0.12	2.57	0.011	1.61	18.75
Q515289	17.3	1	8.46	0.98	10.55	0.12	3.22	0.012	1.64	27.4
Q515290	22.6	1.2	7.34	1.25	10.65	0.13	4.1	0.019	1.65	26.2
Q515291	16.2	0.94	7.6	0.94	10.2	0.13	3.18	0.014	1.58	24.9
Q515292	19.9	1.18	6.98	1.1	10.85	0.13	3.72	0.016	1.67	28.2

Till Four Acid

Sample	Cr	Cs	Cu	Fe	Ga	Ge	Hf	In	K	La
	ppm	ppm	ppm	%	ppm	ppm	ppm	ppm	%	ppm
Q515293	21.9	1.13	10.9	1.19	10.85	0.13	4.13	0.02	1.69	28.9
Q515294	15.4	1.13	6.45	0.86	9.84	0.11	2.2	0.009	1.48	22
Q515295	16.7	1.13	3.37	0.94	10.6	0.1	2.52	0.014	1.58	16.35
Q515296	20.2	1.21	8.47	1.15	10.9	0.13	3.43	0.017	1.65	24.6
Q515297	20	0.72	2.56	1.08	9.11	0.1	3.18	0.017	1.46	18
Q515298	40.1	1.99	22.6	1.91	13.45	0.14	3.84	0.025	1.89	28.1
Q515299	32.9	1.41	24.8	1.76	11.55	0.16	4.05	0.028	1.66	31.1
Q515300	38.2	1.81	13.1	2.08	13.1	0.14	4.22	0.032	1.77	23.5
Q515301	21.3	0.78	5.36	1.34	9.88	0.13	3.47	0.016	1.51	17.3
Q515302	25.8	0.96	6.21	1.56	10.9	0.13	3.58	0.021	1.54	24.6
Q515303	24.5	1.05	13.7	1.59	9.87	0.12	3.23	0.026	1.49	18.5
Q515304	28.7	1.21	7.28	1.8	11.4	0.16	4.34	0.022	1.59	28.7
Q515305	28.7	1.06	6.76	1.63	10.95	0.14	4.52	0.025	1.67	23
Q515306	27.1	1.31	8.06	1.51	11.6	0.15	4.58	0.021	1.71	31.7
Q515307	23.9	0.87	7.16	1.41	10.2	0.12	4.24	0.015	1.49	18.35
Q515308	22	0.86	1.94	1.54	11	0.11	3.5	0.018	1.39	13.4
Q515309	29.6	0.99	3.33	1.96	11.4	0.14	4.1	0.033	1.43	29
Q515311	26.5	0.85	5.37	1.86	9.76	0.12	4.32	0.026	1.4	20.1
Q515312	27.1	1.16	9.62	1.4	11.8	0.11	3.73	0.022	1.68	19.15
Q515313	27.2	1.18	20.1	1.44	12.25	0.15	4.24	0.019	1.64	28.1
Q515314	19.8	0.78	10.1	1.25	10.6	0.16	3.47	0.02	1.45	22.5
Q515315	21.9	0.96	2.23	0.98	11.3	0.13	4.47	0.017	1.63	23
Q515316	19.7	1.08	5.36	1	11.75	0.14	3.72	0.015	1.63	24.8
Q515317	21.6	0.99	4.91	1.12	10.45	0.13	3.18	0.013	1.52	19.45
Q515318	17.3	0.89	4.79	1.02	10.5	0.12	3.53	0.012	1.56	18.55
Q515319	17.3	0.94	6.49	0.98	10.8	0.13	2.83	0.013	1.58	20
Q515320	15.4	0.96	5.14	0.89	10.45	0.1	2.68	0.01	1.55	19.7
Q515321	14.6	0.79	4.73	0.82	10.25	0.13	3.18	0.01	1.52	29.3
Q515322	15.7	0.83	5.39	0.86	10.5	0.11	3.19	0.013	1.54	21.6
Q515323	21.4	0.87	7.23	0.91	10.95	0.11	3.14	0.013	1.58	24.1
Q515324	17	0.91	5.52	0.91	11.05	0.12	3.83	0.012	1.6	24.7
Q515325	15.8	0.8	4.77	0.76	11	0.13	3.14	0.012	1.59	21.3
Q515326	15.1	0.86	5.83	0.85	10.85	0.12	3.31	0.011	1.58	21.8
Q515327	15.1	0.81	6.82	0.83	10.7	0.12	3.14	0.009	1.58	21.1
Q515328	16.7	0.9	5.69	0.91	11	0.14	3.51	0.011	1.61	33.1
Q515329	17.7	1.21	7.76	0.93	11.2	0.1	2.6	0.009	1.58	14.8
Q515330	17.1	0.9	5.44	0.96	10.35	0.12	3.29	0.011	1.57	20.1
Q515331	17.7	0.96	6.84	0.99	11.55	0.15	3.22	0.016	1.55	24.7
Q515332	14.2	1.02	1.94	0.62	11.2	0.12	3.54	0.009	1.52	19.05
Q515333	26.2	1.43	7.34	1.26	12.75	0.14	4.07	0.018	1.62	25.4
Q515334	18.1	0.98	5.66	0.97	11.5	0.13	3.63	0.011	1.56	21.7

Till Four Acid

Sample	Cr	Cs	Cu	Fe	Ga	Ge	Hf	In	K	La
	ppm	ppm	ppm	%	ppm	ppm	ppm	ppm	%	ppm
Q515335	19.3	1.04	7.54	1.01	11.6	0.14	3.42	0.013	1.55	25.1
Q515336	21.3	0.92	9.8	1.24	10.8	0.12	3.4	0.018	1.49	17.55
Q515337	21.8	0.72	4.58	1.29	10.3	0.13	3.6	0.021	1.46	20.9
Q515338	23.9	0.88	6.82	1.34	11.2	0.15	3.01	0.017	1.54	23.7
Q515339	27	1	4.52	1.67	12.9	0.13	4.5	0.025	1.43	14.95
Q515340	24.1	0.79	4.7	1.56	10.75	0.13	3.65	0.018	1.4	17.4
Q515341	20.9	0.7	6.84	1.31	10.05	0.14	3.32	0.014	1.42	16.85
Q515342	23.1	0.94	5.57	1.35	10.6	0.13	3.37	0.02	1.54	25
Q515343	38.8	1.68	13.9	1.97	13.6	0.15	4.97	0.023	1.71	23.9
Q515344	28.9	1.14	8.14	1.55	12.2	0.15	3.94	0.025	1.67	25.4
Q515345	26.8	1.07	3.97	1.64	11.55	0.13	4.29	0.021	1.38	16.65
Q515346	24.9	0.89	6.07	1.56	10.4	0.13	3.93	0.023	1.36	18.1
Q515347	29	1.19	8.26	1.65	12.35	0.14	3.96	0.023	1.71	21.4
Q515348	23.2	0.95	6.63	1.51	11.3	0.08	3.07	0.018	1.52	21.3
Q515349	26.4	1.15	9.21	1.62	11.8	0.1	3.88	0.021	1.63	21.9
Q515350	26.1	1.03	8.46	1.54	11.3	0.09	3.57	0.023	1.57	17.45
Q515351	22.6	0.83	9.31	1.43	10.5	0.08	3.27	0.019	1.45	14.55
Q515352	23.7	1.02	4.85	1.49	11.6	0.08	3.13	0.023	1.55	14.5
Q515354	27.6	0.89	2.97	1.9	12.35	0.1	5.23	0.025	1.36	26.1
Q515355	16.6	0.94	5.68	1.06	10.85	0.08	3.35	0.02	1.51	18.3
Q515356	20.3	0.89	5.75	1.16	10.95	0.07	3.05	0.019	1.46	15.55
Q515357	20.6	1.06	10.55	1.13	12.25	0.11	4.44	0.015	1.66	26.9
Q515358	17	0.93	5.69	1.05	11	0.09	3.52	0.007	1.51	19.9
Q515359	21.8	1.39	6.54	1.21	12.05	0.09	3.55	0.013	1.66	21.9
Q515360	23.9	1.37	6.35	1.19	12.45	0.12	4.13	0.017	1.68	26.7
Q515362	20.2	0.99	4.74	1.3	10.7	0.09	3.38	0.016	1.63	18.65
Q515363	20.3	1.06	7.49	1.08	11.3	0.11	3.89	0.022	1.64	22.7
Q515364	21.8	1.15	10.3	1.21	11.8	0.12	4.29	0.014	1.69	29
Q515365	22.3	1.28	7.83	1.21	11.5	0.09	3.2	0.023	1.62	17.6
Q515366	14.9	0.85	6.7	0.88	10.7	0.13	2.99	0.01	1.58	28.4
Q515367	18.4	0.9	6.53	1.04	11.25	0.1	3.98	0.009	1.63	23.3
Q515368	17.4	0.97	7.13	0.92	10.95	0.11	3.38	0.016	1.62	23.1
Q515370	16.7	0.89	7.56	0.92	10.6	0.11	3.91	0.01	1.66	23.3
Q515371	20.7	0.94	8.96	1.1	10.9	0.14	3.96	0.017	1.61	25.4
Q515372	17.2	0.96	6.41	0.84	11	0.13	2.98	0.017	1.6	24.3
Q515373	18	1.03	6.94	1	11.25	0.11	3.45	0.018	1.64	24.7
Q515374	18.5	0.84	7.97	1.1	11.2	0.13	3.32	0.015	1.63	27.3
Q515375	28.4	1.44	7.09	1.25	11.45	0.09	2.81	0.016	1.64	17.75
Q515376	19.9	1.14	5.11	1.04	11.15	0.12	2.64	0.013	1.6	23.1
Q515377	24.5	1.38	5.56	1.4	11.75	0.1	2.85	0.015	1.64	20.2
Q515378	24.2	1.19	9.32	1.26	11.35	0.12	3.7	0.013	1.74	27.4

Till Four Acid

Sample	Cr	Cs	Cu	Fe	Ga	Ge	Hf	In	K	La
	ppm	ppm	ppm	%	ppm	ppm	ppm	ppm	%	ppm
Q515379	16.6	0.79	5.31	0.88	10.65	0.12	3.16	0.013	1.59	22.1
Q515380	20.3	0.98	5.71	1.19	11.05	0.13	4.32	0.014	1.55	27.5
Q515381	18.3	1.03	6.18	0.93	11.45	0.11	3.12	0.011	1.66	23.3
Q515382	17.5	1	6.43	0.92	11.35	0.14	3.55	0.012	1.62	22.3
Q515384	21.9	1.05	15.3	1.12	11.05	0.1	3.34	0.012	1.57	17.9
Q515385	16.7	0.85	4.06	0.86	10.75	0.1	3.17	0.007	1.45	17.4
Q515386	20.4	0.93	4.78	1.04	11.6	0.12	3.41	0.011	1.54	17.55
Q515387	21.2	0.81	5.66	1.11	10.85	0.11	3.63	0.015	1.46	16
Q515388	20.4	0.8	6.35	1.08	10.85	0.1	3.49	0.011	1.43	16.75
Q515389	27	1.12	1.92	1.55	12.05	0.11	5.18	0.013	1.37	19.15
Q515390	22.2	0.79	3.64	1.35	11.1	0.12	4.07	0.015	1.41	18.7
Q515391	24.1	1.15	9.29	1.16	12.8	0.15	3.91	0.015	1.63	25.9
Q515392	28.7	1.15	7.9	1.42	11.45	0.13	3.37	0.019	1.53	21.4
Q515393	27.1	0.93	5.41	1.47	11.25	0.13	3.34	0.014	1.52	16.1
Q515394	32.3	1.48	9.81	1.7	13.15	0.12	4.21	0.014	1.74	17.35
Q515395	33.1	1.69	6.09	1.49	13.2	0.13	4.05	0.025	1.57	16.95
Q515396	35.4	1.43	10.75	1.82	13.1	0.13	3.53	0.017	1.79	19.4
Q515397	32.7	1.14	9.57	1.72	12.7	0.13	4.54	0.021	1.62	22.1
Q515398	38.1	1.72	11.95	1.94	13.85	0.13	4.28	0.026	1.89	22.9
Q515399	27.9	1.03	5.45	1.52	11.6	0.12	3.92	0.012	1.6	16.6
Q515400	20.9	0.79	1.76	1	10.9	0.08	3.07	0.015	1.49	13.2
Q515401	23	1.18	3.4	1.3	12.25	0.13	3.23	0.018	1.62	17.55
Q515402	22.8	1.11	7.31	1.1	12	0.14	3.33	0.013	1.6	20
Q515403	20.3	0.99	6.19	0.96	11.6	0.1	3.04	0.009	1.53	15.15
Q515404	18.2	0.91	7.33	0.9	11.3	0.1	3.43	0.011	1.53	17.45
Q515405	16.4	0.88	7.28	0.64	11.05	0.12	2.84	0.01	1.51	23.5
Q515406	33.7	1.41	19.9	1.64	13.7	0.13	4.2	0.018	1.78	22.3
Q515407	31.6	1.4	6.48	1.34	11.95	0.12	4.11	0.015	1.68	17.3
Q515408	28.2	1.05	7.91	1.37	12.65	0.15	4.56	0.014	1.75	26.5
Q515409	27.1	1.11	6.84	1.38	11.5	0.13	3.61	0.015	1.74	20.5
Q515410	31.6	1.26	9.69	1.56	12.95	0.15	4.49	0.018	1.78	24.1
Q515411	25.1	0.89	5.78	1.45	12.35	0.14	4.36	0.02	1.66	23.9
Q515412	23.2	0.99	5.99	1.23	11.45	0.1	3.36	0.017	1.59	17.15
Q515413	23.4	1.13	6.14	1.16	12.15	0.14	3.38	0.012	1.55	23.8
Q515414	15.9	0.78	6.17	0.8	11.2	0.12	3.56	0.009	1.44	19.15
Q515415	22.5	0.9	8.21	1.09	10.45	0.12	3.48	0.019	1.59	20.3
Q515416	21.9	0.82	4.9	1.26	11.3	0.12	3.1	0.014	1.59	13.85
Q515417	22	1.08	5.26	1.21	11.75	0.13	2.51	0.013	1.55	19.75
Q515418	23.3	0.85	4.06	1.33	11.4	0.12	3.71	0.016	1.55	16.2
Q515419	25.9	1.06	7.7	1.54	11.85	0.13	3.97	0.013	1.75	21
Q515420	27.2	1.22	4.31	1.75	12.25	0.1	3.82	0.012	1.66	20.3

Till Four Acid

Sample	Cr	Cs	Cu	Fe	Ga	Ge	Hf	In	K	La
	ppm	ppm	ppm	%	ppm	ppm	ppm	ppm	%	ppm
Q515421	27.4	1.09	5.87	1.67	11.45	0.13	3.87	0.017	1.63	26
Q515422	18.5	0.87	5.57	1.14	10.2	0.11	2.68	0.013	1.51	16.75
Q515423	28.7	1.33	9.84	1.41	11.6	0.14	4.41	0.016	1.76	31.2
Q515425	22.8	0.98	3.99	1.46	10.95	0.11	2.92	0.014	1.52	18.65
Q515426	26.4	1.23	5.71	1.74	11.4	0.1	3.35	0.017	1.45	20.8
Q515427	32.4	1.5	10.15	1.78	12.85	0.14	4.44	0.023	1.85	27.2
Q515428	20.7	1.08	4.65	1.2	10.5	0.11	2.9	0.012	1.63	21.4
Q515429	20.2	1.19	5.26	1.25	11.1	0.13	2.62	0.013	1.68	24.2
Q515430	22.6	1.31	7.21	1.52	11.6	0.11	3.49	0.016	1.7	17.95
Q515431	27.2	1.22	7.96	1.45	12.05	0.15	5.06	0.01	1.71	30.3
Q515432	20.4	0.92	4.99	1.25	10.15	0.12	3.12	0.015	1.51	17.1
Q515433	24.2	0.96	5.16	1.43	10.8	0.1	3.76	0.014	1.56	18.35
Q515434	25.1	1.35	9.77	1.25	12.55	0.12	4.31	0.016	1.74	23.7
Q515435	21.6	1.31	8.11	1.11	11.95	0.14	4	0.013	1.64	25.7
Q515436	22.8	0.92	4.5	1.25	10.8	0.11	3.56	0.016	1.57	21.7
Q515437	22.9	1.17	3.08	1.07	11.4	0.11	3.85	0.019	1.72	16.55
Q515438	20	0.98	7.43	1.16	10.6	0.12	2.88	0.019	1.6	20.8
Q515439	16.5	0.79	7.9	0.83	9.86	0.12	2.72	0.013	1.55	20.4
Q515440	14.6	0.84	7.53	0.76	10.45	0.14	2.36	0.013	1.52	25.8
Q515442	13.9	0.91	5.25	0.77	10.4	0.12	3.16	0.008	1.55	21
Q515443	21.9	1.1	6.48	1.25	11.15	0.13	4.01	0.012	1.75	29.4
Q515444	27.2	1.45	13.5	1.43	12.1	0.14	4.29	0.018	1.8	25.7
Q515445	20.7	1.12	11	1.12	11.8	0.17	4.96	0.014	1.72	31.7
Q515446	18.5	0.86	8.15	1.11	9.59	0.1	2.57	0.008	1.49	16.45
Q515447	29	1.67	12.6	1.49	12.2	0.13	3.86	0.016	1.8	23.4
Q515448	27.9	1.6	13.9	1.32	12.05	0.14	4.01	0.014	1.78	30.7
Q515449	14.4	0.94	5.54	0.78	10.4	0.1	2.99	0.005	1.55	16.6
Q515450	21.5	1.16	9.72	1.04	11.85	0.13	4.53	0.02	1.73	29.1
Q515451	23.4	1.29	12.95	1.12	12.2	0.14	4.78	0.018	1.74	27.5
Q515452	19.2	1.09	10.4	0.97	11.75	0.13	3.82	0.018	1.65	25.5
Q515454	23.7	1.28	11.3	1.24	12.4	0.16	4.41	0.017	1.69	29.4
Q515455	19.7	1.07	7.24	1.13	11.7	<0.05	3.57	0.017	1.51	20.1
Q515456	24.7	1.05	7.86	1.16	12.05	<0.05	4.54	0.016	1.7	27.5
Q515457	37.4	1.81	14.15	1.93	13.95	<0.05	4.65	0.017	1.84	24.3
Q515458	27.8	1.17	7.72	1.47	11.9	<0.05	4.31	0.025	1.66	27.6
Q515459	28.9	1.08	6.26	1.56	11.75	<0.05	4.6	0.023	1.67	23.6
Q515460	22.4	1	5.03	1.16	12.05	<0.05	3.96	0.016	1.69	19.85
Q515461	22.5	0.8	4.56	1.18	10.2	<0.05	2.78	0.014	1.49	15.35
Q515462	23.3	0.76	3.48	1.28	9.95	<0.05	3.33	0.017	1.39	15.55
Q515463	25.9	0.94	6.83	1.3	10.5	<0.05	3.43	0.014	1.5	21.2
Q515464	30.6	1.32	10.3	1.5	12.45	<0.05	4.2	0.017	1.7	24.6

Till Four Acid

Sample	Cr	Cs	Cu	Fe	Ga	Ge	Hf	In	K	La
	ppm	ppm	ppm	%	ppm	ppm	ppm	ppm	%	ppm
Q515465	26.9	1	6.48	1.36	11.9	<0.05	3.92	0.016	1.64	16.45
Q515466	36.1	1.35	10.45	1.63	12.75	<0.05	4.4	0.022	1.76	23.2
Q515467	26	0.82	4.69	1.42	10.5	<0.05	3.92	0.02	1.5	18.6
Q515468	29.4	0.96	6.97	1.52	11.8	<0.05	5.37	0.024	1.61	22.8
Q515469	25.2	0.9	6.58	1.47	11	<0.05	3.69	0.017	1.53	16.55
Q515470	32.2	1.19	9.23	1.68	12.75	<0.05	5.26	0.017	1.71	24.9
Q515471	27.1	0.98	5.09	1.61	11.8	<0.05	4.15	0.018	1.54	17.45
Q515472	28.7	0.97	6.23	1.59	11.65	<0.05	4.53	0.024	1.49	17.3
Q515473	26.5	0.98	3.83	1.28	11.5	<0.05	4.1	0.02	1.59	16.3
Q515474	30.6	1.27	7.08	1.69	13.4	<0.05	4.93	0.022	1.82	28
Q515475	26.4	0.83	5.32	1.48	11	<0.05	3.43	0.023	1.54	17.2

Till Four Acid

Sample	Li	Mg	Mn	Mo	Na	Nb	Ni	P	Pb	Rb
	ppm	%	ppm	ppm	%	ppm	ppm	%	ppm	ppm
Q515251	17.8	0.44	220	0.32	1.61	3.79	15.05	0.045	9.51	41.8
Q515252	14.5	0.34	197.5	0.54	1.33	5.53	7.37	0.025	11.3	45.1
Q515253	16	0.4	235	0.2	1.87	4.29	10.6	0.067	10.85	43.6
Q515254	21	0.54	260	0.61	1.43	5.8	14.1	0.038	11.05	48.8
Q515255	26.1	0.75	379	0.97	1.395	8.04	17.95	0.057	12.2	54.3
Q515256	18.4	0.54	266	0.62	1.585	4.35	13	0.041	10.3	47.7
Q515257	18.8	0.54	292	0.29	1.54	6.27	13.95	0.063	11	53.9
Q515258L	27.7	0.67	315	0.48	1.54	5.9	20.1	0.061	11.8	63.6
Q515258U	18	0.54	303	0.24	1.53	6.04	13.85	0.071	10.65	51.5
Q515260	15.2	0.34	192.5	0.41	1.84	2.95	9.84	0.058	9.99	38.7
Q515261	12.7	0.34	183	0.32	1.755	2.99	7.71	0.044	9.29	40
Q515262	13.8	0.29	159.5	0.39	1.815	2.7	7.75	0.058	9.97	38.4
Q515263	15.4	0.3	156	0.32	1.72	2.37	8.73	0.055	9.36	41.2
Q515264	14.8	0.36	190.5	0.51	1.57	3.16	8.84	0.051	9.45	43.4
Q515265	14	0.25	139.5	0.48	1.93	2.22	6.78	0.067	10.35	38.9
Q515266	16.5	0.39	211	0.46	1.49	3.82	11.55	0.048	10.4	47.3
Q515267	16	0.33	187.5	0.85	1.705	3.01	9.71	0.058	10.55	44.2
Q515268	18.6	0.46	247	0.2	1.47	4.66	14.4	0.057	10.8	49.4
Q515269	18.3	0.4	213	0.32	1.52	3.98	12.6	0.045	9.79	46
Q515270	14.2	0.38	206	0.48	1.34	3.32	9.66	0.038	9.49	42.5
Q515271	17.9	0.44	248	0.45	1.55	4.28	12.9	0.044	10.35	47.9
Q515272	16.9	0.42	231	0.28	1.36	3.98	9.47	0.023	9.35	41.8
Q515273	15.1	0.39	214	0.2	1.505	3.61	9.14	0.038	9.39	43.3
Q515274	18.9	0.64	296	0.79	1.385	5.92	14.8	0.07	11.5	44.9
Q515275	16.1	0.38	183	0.33	1.385	3.43	9.23	0.022	9.33	46
Q515276	19.5	0.46	228	0.3	1.67	4.69	14.3	0.063	10.6	48.4
Q515277	16.9	0.44	235	0.21	1.68	4.83	12.75	0.062	10.2	45.4
Q515278	19.2	0.41	202	0.76	1.73	3.09	13.6	0.062	10.6	43.8
Q515280	12.6	0.39	181.5	0.45	1.76	3.3	8.85	0.018	9.06	39
Q515281	17.6	0.43	203	0.64	1.735	3.82	11.15	0.055	10.15	43.5
Q515282	14.7	0.38	204	0.6	1.69	3.61	9.7	0.049	10.15	42.2
Q515283	16.6	0.39	179	0.66	1.635	3.26	9.48	0.041	9.56	42.7
Q515284	14.8	0.32	187.5	0.37	1.945	3.19	9.28	0.077	10.65	39
Q515285	16.5	0.3	177.5	0.69	1.995	3.13	10.05	0.074	11.05	40.1
Q515286	16.1	0.32	179.5	0.45	1.995	3.27	9.69	0.076	11.05	40.9
Q515287	16	0.34	189	0.81	1.76	3.08	9.7	0.061	10.25	42
Q515288	14.9	0.3	158.5	0.46	1.865	2.69	8.51	0.063	9.96	38.5
Q515289	15.6	0.29	155.5	0.53	1.915	2.71	9.43	0.067	11	40.3
Q515290	17.2	0.38	207	0.85	1.76	3.73	10.9	0.057	11.1	45.5
Q515291	15.3	0.28	154.5	0.77	1.925	2.55	9.18	0.067	10.9	38.6
Q515292	17.2	0.32	178.5	0.91	1.935	3	10	0.066	11.6	42.8

Till Four Acid

Sample	Li	Mg	Mn	Mo	Na	Nb	Ni	P	Pb	Rb
	ppm	%	ppm	ppm	%	ppm	ppm	%	ppm	ppm
Q515293	16.7	0.37	202	0.49	1.93	4.05	11.55	0.077	11.6	44.9
Q515294	14.8	0.26	132	0.52	1.83	2.2	8.23	0.059	9.94	37.3
Q515295	12.7	0.29	156	0.6	1.88	2.91	7.06	0.023	9.48	40.1
Q515296	17.3	0.33	169.5	0.51	2.01	3.35	10.2	0.07	10.75	42.7
Q515297	10.5	0.36	209	0.31	1.355	3.79	7.35	0.028	9.98	40.2
Q515298	26.6	0.63	258	0.36	1.6	6.23	21.9	0.061	11.65	65.4
Q515299	22.3	0.51	255	0.47	1.5	6.91	17.35	0.056	11.5	53.9
Q515300	24.3	0.63	274	0.42	1.565	6.62	19.15	0.039	11.1	57.7
Q515301	15.1	0.38	229	0.18	1.65	3.53	9.79	0.053	9.87	39.9
Q515302	14.9	0.43	231	0.31	1.565	4.62	10.7	0.033	10	43.5
Q515303	19.1	0.46	279	0.42	1.44	3.98	14.9	0.045	9.52	45.1
Q515304	20	0.51	297	0.29	1.44	5.25	14.25	0.054	10.1	49.5
Q515305	17.5	0.5	292	0.19	1.535	5.69	13.15	0.061	9.95	50.6
Q515306	19.5	0.47	257	0.2	1.645	5.4	14.1	0.07	10.55	52.3
Q515307	15.1	0.41	250	0.19	1.47	3.94	11.4	0.051	9.79	45.2
Q515308	12.2	0.36	223	0.28	1.32	4.34	7.53	0.021	9.09	40.7
Q515309	16.5	0.43	256	0.32	1.39	5.55	10.35	0.034	11.55	44.6
Q515311	16.8	0.47	291	0.27	1.44	4.36	12.3	0.034	10.2	38
Q515312	19.5	0.5	234	0.2	1.505	5.28	13.85	0.045	10.1	47.3
Q515313	20.9	0.49	230	0.25	1.505	5.88	15.5	0.052	10.5	48.2
Q515314	16.6	0.36	200	0.63	1.515	3.48	9.54	0.049	9.9	37.6
Q515315	12.1	0.38	209	0.16	1.6	4.04	7.62	0.032	10.05	40.2
Q515316	17.1	0.34	179	0.27	1.96	3.23	9.34	0.067	10.25	37.9
Q515317	15.6	0.36	183	0.36	1.59	3.66	8.95	0.05	9.47	39.4
Q515318	14.5	0.31	166.5	0.57	1.835	2.95	7.63	0.058	9.65	36.9
Q515319	16.8	0.32	167.5	0.71	1.775	2.9	8.7	0.056	9.95	38.3
Q515320	15.9	0.27	147	0.8	1.845	2.58	7.83	0.054	9.79	35.4
Q515321	14.1	0.24	140.5	0.51	1.875	2.26	6.74	0.063	10.3	33.3
Q515322	14.5	0.25	139.5	0.41	1.875	2.43	7.27	0.07	9.92	34.3
Q515323	16	0.27	163	0.55	1.975	2.59	8.14	0.067	10.4	36.1
Q515324	15.8	0.27	149.5	0.39	1.87	2.83	7.52	0.066	10.65	37.3
Q515325	15.5	0.26	156.5	0.24	1.915	2.61	7.36	0.069	10.3	36.2
Q515326	14.8	0.25	138	0.44	1.975	2.24	7.25	0.07	10.5	35.7
Q515327	15.3	0.25	147.5	0.31	1.975	2.25	7.76	0.066	10.4	35.4
Q515328	15.7	0.28	151	0.51	1.925	2.8	7.87	0.069	10.7	37
Q515329	18.3	0.32	159	0.57	1.855	2.43	9.64	0.055	9.25	38.7
Q515330	15.3	0.3	162.5	0.58	1.83	2.88	8.56	0.064	10.1	38.7
Q515331	17.8	0.3	161	0.54	1.89	2.88	8.47	0.064	10.2	37.9
Q515332	13.9	0.24	139	0.14	1.92	2.44	6.07	0.041	9.82	36.2
Q515333	22.6	0.4	192	0.41	1.88	4.1	11.3	0.062	10.9	43.5
Q515334	17	0.29	154.5	0.37	1.99	2.87	8.27	0.067	10.25	37.1

Till Four Acid

Sample	Li	Mg	Mn	Mo	Na	Nb	Ni	P	Pb	Rb
	ppm	%	ppm	ppm	%	ppm	ppm	%	ppm	ppm
Q515335	18	0.29	165.5	0.37	1.96	3.25	8.73	0.064	10.75	39
Q515336	17.5	0.36	198.5	0.36	1.64	3.78	9.99	0.057	10.1	41
Q515337	15.5	0.39	209	0.19	1.38	3.83	9.19	0.047	9.94	41.6
Q515338	18.4	0.4	209	0.24	1.545	3.95	10.3	0.047	10.25	43.1
Q515339	17.1	0.36	207	0.38	1.32	5.68	9.3	0.017	10.65	44
Q515340	16.8	0.4	232	0.26	1.39	4.33	9.98	0.031	9.15	39.9
Q515341	15.7	0.38	243	0.21	1.415	3.73	10.65	0.046	9.19	41.3
Q515342	18.2	0.42	223	0.23	1.48	4.17	10.5	0.052	9.57	44.9
Q515343	26.1	0.62	297	0.43	1.455	6.19	16.95	0.057	10.45	55.7
Q515344	20	0.48	268	0.2	1.565	5.16	13.15	0.063	10.25	49.1
Q515345	18.2	0.45	249	0.32	1.34	4.19	10.2	0.035	9.43	40.1
Q515346	18	0.42	244	0.28	1.325	3.94	10.6	0.038	9.28	40.5
Q515347	20.7	0.52	276	0.23	1.545	5.47	13.4	0.055	10.15	53.2
Q515348	16.9	0.44	251	0.27	1.44	3.68	10.3	0.054	9.44	44.9
Q515349	19.7	0.51	285	0.32	1.485	4.86	12.95	0.053	9.76	50.2
Q515350	18.9	0.48	250	0.41	1.435	4.87	12.5	0.047	9.31	47.5
Q515351	17.7	0.4	234	0.29	1.39	3.38	11.1	0.045	9.15	41.8
Q515352	18.6	0.42	214	0.36	1.475	4.19	9.62	0.03	9.68	44.5
Q515354	14	0.36	280	0.25	1.45	5.28	7.82	0.029	10.05	38.8
Q515355	15.2	0.31	183.5	0.39	1.765	2.9	8.82	0.051	9.66	40.8
Q515356	14.6	0.37	192	0.39	1.525	3.22	8.42	0.043	9.08	42.2
Q515357	17	0.36	192	0.4	1.95	4.07	10.1	0.07	10.7	44.5
Q515358	14.5	0.27	140	0.73	1.885	2.68	7.1	0.073	10.35	37.8
Q515359	17.8	0.36	186.5	0.52	1.9	3.59	8.89	0.044	10.35	45.2
Q515360	19.2	0.39	205	0.43	1.89	4.22	9.35	0.064	10.65	46.3
Q515362	15.8	0.38	193.5	0.36	1.735	3.22	8.81	0.061	9.88	42.1
Q515363	16.6	0.35	184.5	0.41	1.85	3.71	9.16	0.072	10.3	41.8
Q515364	18	0.37	195.5	0.55	1.91	3.74	10.35	0.07	10.85	43.3
Q515365	17.7	0.37	184.5	0.69	1.67	3.18	10.05	0.053	10.1	46.1
Q515366	14.3	0.25	143.5	0.58	1.935	2.42	7.45	0.071	11.15	37.2
Q515367	15.2	0.3	167.5	0.46	1.865	3.01	8.71	0.075	10.75	40.4
Q515368	15.2	0.28	153	0.41	1.915	2.63	8.15	0.065	10.35	38.7
Q515370	14.7	0.27	148.5	0.49	1.96	2.43	8.55	0.07	10.75	38.9
Q515371	16.4	0.31	168.5	0.53	1.77	3.11	10	0.064	11.15	41.3
Q515372	16.1	0.27	131.5	0.43	1.88	2.24	8.37	0.055	10.55	38.9
Q515373	16.2	0.29	151.5	0.73	1.95	2.59	8.45	0.067	10.8	39.5
Q515374	16.3	0.33	178	0.52	1.81	2.82	9.33	0.062	11.05	41.3
Q515375	17.6	0.42	184.5	0.95	1.635	3.41	15.3	0.039	9.12	45.5
Q515376	15.9	0.33	173.5	0.48	1.75	3.02	8.87	0.058	9.99	43
Q515377	19.5	0.38	180	0.45	1.57	3.17	9.57	0.043	9.73	41.8
Q515378	18.7	0.36	180.5	0.8	1.735	3.36	10.95	0.072	10.8	45.1

Till Four Acid

Sample	Li	Mg	Mn	Mo	Na	Nb	Ni	P	Pb	Rb
	ppm	%	ppm	ppm	%	ppm	ppm	%	ppm	ppm
Q515379	14.3	0.25	143	0.34	1.905	2.45	7.71	0.065	10.2	37.3
Q515380	15.2	0.32	195	0.58	1.69	3.24	8.22	0.068	10.75	40
Q515381	16.2	0.29	148.5	0.47	1.95	2.53	8.74	0.066	10.5	41.1
Q515382	16.2	0.28	156.5	0.43	1.97	2.39	9.09	0.067	10.55	39.7
Q515384	13.3	0.36	177	0.48	1.72	3.45	9.1	0.064	10.65	37.9
Q515385	12.7	0.26	148.5	0.4	1.875	2.57	6.92	0.065	10.55	31.8
Q515386	14.2	0.31	166	0.28	1.85	3.47	8.11	0.054	11.1	36.4
Q515387	14.4	0.31	171.5	0.34	1.65	3.49	8.49	0.049	10.75	36.3
Q515388	11.8	0.32	185	0.32	1.73	3.19	8.75	0.053	10.3	34.8
Q515389	8.6	0.4	292	1.12	1.305	5.44	7.4	0.01	9.93	39.4
Q515390	12.9	0.35	210	0.25	1.56	3.71	7.72	0.038	10.35	35.6
Q515391	17.7	0.36	193.5	0.34	1.885	4.14	11.75	0.074	11.5	41
Q515392	18.4	0.46	245	0.29	1.4	4.41	12.85	0.051	10.1	45.7
Q515393	17.7	0.45	252	0.21	1.385	4.34	11.4	0.04	9.87	41.2
Q515394	23.8	0.55	270	0.38	1.45	5.19	15.1	0.06	11	53.4
Q515395	20.3	0.5	249	0.5	1.335	5.81	12.9	0.044	11.55	50.9
Q515396	23	0.6	321	0.31	1.485	5.85	15.35	0.058	10.95	53.8
Q515397	20.8	0.56	282	0.32	1.45	5.6	13.6	0.066	11.05	48.1
Q515398	27	0.64	315	0.37	1.545	6.31	16.95	0.072	11.3	57.7
Q515399	15.4	0.45	226	0.69	1.435	4.27	11.05	0.051	10.45	44.2
Q515400	12.5	0.38	199.5	0.15	1.365	3.55	7.83	0.044	9.35	40.4
Q515401	18	0.44	211	0.67	1.475	4.18	9.18	0.049	10	46.4
Q515402	17.4	0.35	182	0.54	1.825	3.42	10.5	0.068	11	41.2
Q515403	15.7	0.29	160.5	0.66	1.855	2.96	9.27	0.055	10.7	37.7
Q515404	13.9	0.26	153.5	0.41	1.78	3.11	8	0.054	10.9	36.8
Q515405	14.1	0.25	132	0.12	1.825	2.56	7.85	0.064	11.2	34
Q515406	22.2	0.56	243	0.41	1.495	5.83	16.05	0.052	11.55	57.4
Q515407	20.4	0.46	205	0.35	1.425	3.92	13.15	0.057	9.82	46.3
Q515408	17.8	0.44	232	0.27	1.68	5.32	12.05	0.068	11.25	47.5
Q515409	17.4	0.45	226	0.25	1.63	4.5	12	0.065	10.85	48.9
Q515410	19.8	0.52	252	0.25	1.54	5.75	13.85	0.069	11.1	51.9
Q515411	17.6	0.45	247	0.26	1.465	4.64	11.55	0.058	10.75	48.4
Q515412	16.4	0.39	206	0.29	1.545	3.91	10.9	0.06	10.05	43
Q515413	16	0.35	168	0.45	1.705	3.46	9.91	0.062	11.15	39.1
Q515414	12.7	0.24	146	0.23	1.945	2.57	6.73	0.066	10.4	32.5
Q515415	14.9	0.34	186.5	0.25	1.645	3.43	10.05	0.063	10.5	39.5
Q515416	17.6	0.4	207	0.15	1.45	3.59	9.41	0.046	9.03	44.4
Q515417	17.2	0.4	199.5	0.21	1.495	3.54	9.73	0.044	9.96	44.1
Q515418	15.8	0.4	232	0.23	1.4	4.11	8.78	0.057	9.9	44.7
Q515419	17.6	0.5	270	0.19	1.565	5.1	11.8	0.062	9.61	50.1
Q515420	18.5	0.5	235	0.31	1.455	4.5	11.35	0.037	9.55	48.3

Till Four Acid

Sample	Li	Mg	Mn	Mo	Na	Nb	Ni	P	Pb	Rb
	ppm	%	ppm	ppm	%	ppm	ppm	%	ppm	ppm
Q515421	18.7	0.5	276	0.19	1.455	4.88	11.85	0.05	9.87	48.7
Q515422	17	0.37	198	0.2	1.44	3.07	9.03	0.046	9.08	45.1
Q515423	22.1	0.47	231	0.47	1.62	4.42	13.7	0.075	10.7	49.7
Q515425	20.4	0.41	206	0.23	1.375	3.8	9.49	0.031	9.38	44.2
Q515426	22	0.46	211	0.35	1.445	3.95	10.9	0.051	9.86	42.6
Q515427	25.2	0.59	288	0.3	1.55	5.99	15.1	0.061	10.9	60.6
Q515428	18.2	0.41	211	0.2	1.475	3.37	9.85	0.06	9.3	49
Q515429	23.7	0.44	215	0.22	1.44	3.6	10.1	0.053	9.43	55.2
Q515430	24.4	0.49	237	0.32	1.455	4.43	11.2	0.065	10.05	59
Q515431	20.3	0.47	252	0.2	1.655	5.55	12	0.064	11	52.7
Q515432	17.8	0.41	218	0.27	1.37	3.45	9.64	0.048	8.93	47.2
Q515433	17.3	0.44	242	0.24	1.44	4.28	10.6	0.048	9.77	47.6
Q515434	19.6	0.4	210	0.45	1.965	4.16	11.15	0.067	11.35	49.6
Q515435	19.1	0.34	183	0.48	2	3.44	10	0.071	11.25	44.9
Q515436	15.2	0.37	204	0.31	1.55	3.65	9.38	0.05	9.95	41
Q515437	17.9	0.39	191.5	0.14	1.675	3.73	9.65	0.064	10	44.4
Q515438	17	0.35	199	0.19	1.62	3.18	9.42	0.059	10	42.4
Q515439	14.8	0.25	148.5	0.38	1.875	2.43	8.82	0.06	10.85	33.5
Q515440	14.3	0.23	140	0.26	1.95	2.19	7.53	0.064	10.65	34.5
Q515442	15.3	0.24	135	0.34	1.87	2.15	6.33	0.056	10.6	38
Q515443	18.4	0.38	195	0.32	1.815	3.5	9.7	0.073	11.25	45.2
Q515444	22.2	0.45	226	0.58	1.87	4.51	13.75	0.072	11.7	49.4
Q515445	16.8	0.34	204	0.35	2.15	4.16	9.82	0.08	11.7	43
Q515446	16	0.32	181.5	0.44	1.63	2.83	8.42	0.047	9.41	40.3
Q515447	24.7	0.48	226	0.47	1.83	4.27	14.2	0.063	11	51.6
Q515448	22.7	0.45	214	0.34	1.82	4.6	13.9	0.064	11.95	53.4
Q515449	14.7	0.24	133	0.42	2.04	2.38	7.06	0.06	10	38.5
Q515450	17.5	0.35	193.5	0.24	2.08	4.18	10.1	0.079	11.65	44.3
Q515451	18.5	0.35	193	0.42	2.12	3.86	10.8	0.072	11.55	44.8
Q515452	16.8	0.3	176.5	0.39	2.08	3.41	9.7	0.072	11.15	42.4
Q515454	18.9	0.37	195.5	0.51	2.02	4.27	11.55	0.066	11.7	45.2
Q515455	12.3	0.27	157	0.45	1.925	2.92	8.77	0.042	10.6	36.1
Q515456	13.2	0.42	228	0.17	1.81	4.99	11.3	0.067	10.85	47.4
Q515457	21.1	0.61	320	0.37	1.52	5.84	19.7	0.064	11	61.9
Q515458	14.6	0.47	264	0.23	1.59	4.97	12.6	0.064	10.1	48.8
Q515459	14.7	0.49	282	0.29	1.51	5.68	13.1	0.059	10.1	51.1
Q515460	13.2	0.35	210	0.26	1.895	3.92	10.2	0.065	10.55	45.1
Q515461	11.6	0.37	228	0.19	1.43	3.08	9.98	0.044	8.95	44.6
Q515462	10.5	0.38	230	0.23	1.37	3.52	9.37	0.044	8.97	40
Q515463	13.9	0.39	218	0.31	1.395	3.97	11.75	0.046	9.84	46.7
Q515464	16.3	0.49	251	0.28	1.655	5.03	14.4	0.067	10.95	51.7

Till Four Acid

Sample	Li	Mg	Mn	Mo	Na	Nb	Ni	P	Pb	Rb
	ppm	%	ppm	ppm	%	ppm	ppm	%	ppm	ppm
Q515465	15.6	0.42	231	0.52	1.595	3.82	12.65	0.052	10.3	48.8
Q515466	18.3	0.54	286	0.37	1.62	5.91	17.25	0.063	10.95	55.1
Q515467	12.8	0.42	266	0.23	1.405	3.94	11.8	0.053	9.41	45.5
Q515468	13.9	0.47	270	0.24	1.48	5.46	12.85	0.061	9.98	50
Q515469	12.6	0.43	271	0.23	1.455	4.16	10.95	0.055	9.42	46.7
Q515470	15.7	0.51	296	0.26	1.54	5.88	13.6	0.066	10.5	55.6
Q515471	13.4	0.42	267	0.26	1.42	4.61	11.25	0.048	10.2	46.4
Q515472	13.4	0.43	249	0.35	1.415	4.43	11.8	0.046	10.55	46.8
Q515473	14.1	0.45	242	0.21	1.485	4.49	10.8	0.065	10.2	48.8
Q515474	16.5	0.54	303	0.24	1.575	6.04	13.6	0.072	10.5	59.6
Q515475	13.6	0.43	247	0.26	1.45	3.94	11.05	0.052	9.84	46

Till Four Acid

Sample	Re	S	Sb	Sc	Se	Sn	Sr	Ta	Te	Th
	ppm	%	ppm	ppm	ppm	ppm	ppm	ppm	ppm	ppm
Q515251	<0.002	0.01	0.05	4.98	<0.2	0.71	227	0.28	<0.04	4.68
Q515252	<0.002	0.01	0.09	5.38	<0.2	0.86	207	0.39	<0.04	5.98
Q515253	<0.002	<0.01	0.06	5.03	<0.2	0.73	255	0.33	<0.04	6.31
Q515254	<0.002	<0.01	0.08	6.05	<0.2	0.96	220	0.41	<0.04	4.87
Q515255	<0.002	0.01	0.06	8.08	<0.2	1.42	220	0.56	<0.04	7.19
Q515256	<0.002	<0.01	0.07	5.63	<0.2	0.85	231	0.3	<0.04	3.65
Q515257	<0.002	<0.01	0.07	6.84	<0.2	1.04	238	0.48	<0.04	6.85
Q515258L	<0.002	<0.01	0.07	7.44	<0.2	1.13	233	0.45	<0.04	8.35
Q515258U	<0.002	<0.01	0.07	6.83	<0.2	1.03	236	0.48	<0.04	5.92
Q515260	<0.002	0.02	0.06	3.78	<0.2	0.59	245	0.21	<0.04	5.11
Q515261	<0.002	0.01	0.06	3.84	<0.2	0.62	239	0.2	<0.04	3.17
Q515262	<0.002	<0.01	0.07	3.59	<0.2	0.51	240	0.25	<0.04	4.53
Q515263	<0.002	<0.01	0.06	3.44	<0.2	0.55	229	0.18	<0.04	3.02
Q515264	<0.002	<0.01	0.05	4.3	<0.2	0.66	221	0.22	<0.04	4.58
Q515265	<0.002	<0.01	0.04	3	<0.2	0.46	243	0.17	<0.04	4.45
Q515266	<0.002	<0.01	0.06	5.41	<0.2	0.57	224	0.28	<0.04	5.08
Q515267	<0.002	<0.01	0.05	4.19	<0.2	0.62	229	0.21	<0.04	5.44
Q515268	<0.002	<0.01	0.07	5.87	<0.2	0.89	217	0.35	<0.04	9.03
Q515269	<0.002	<0.01	0.06	5.02	<0.2	0.61	218	0.41	<0.04	5.29
Q515270	<0.002	<0.01	0.07	4.81	<0.2	0.65	202	0.23	<0.04	5.53
Q515271	<0.002	<0.01	0.07	5.61	<0.2	0.79	226	0.35	<0.04	6.44
Q515272	<0.002	<0.01	0.06	5.46	<0.2	0.75	208	0.28	<0.04	3.85
Q515273	<0.002	<0.01	0.06	4.81	<0.2	0.67	225	0.29	<0.04	3.39
Q515274	<0.002	<0.01	0.08	6.72	0.2	1.02	218	0.38	<0.04	4.85
Q515275	<0.002	<0.01	0.07	4.38	<0.2	0.65	209	0.26	<0.04	2.5
Q515276	<0.002	<0.01	0.06	5.82	<0.2	0.85	247	0.43	<0.04	7.69
Q515277	<0.002	<0.01	0.06	5.84	<0.2	0.83	246	0.35	<0.04	6.37
Q515278	<0.002	<0.01	0.05	4.42	<0.2	0.63	239	0.22	<0.04	5.81
Q515280	<0.002	0.02	0.06	4.34	<0.2	0.65	247	0.26	<0.04	4.59
Q515281	<0.002	0.02	0.06	4.99	<0.2	0.71	243	0.27	<0.04	4.9
Q515282	<0.002	0.01	0.06	4.55	<0.2	0.66	240	0.25	<0.04	5.57
Q515283	<0.002	0.01	0.06	4.47	<0.2	0.67	233	0.23	<0.04	3.3
Q515284	<0.002	0.01	0.06	4.03	<0.2	0.64	251	0.24	<0.04	7.52
Q515285	<0.002	0.02	0.06	4.08	<0.2	0.62	255	0.24	<0.04	7.29
Q515286	<0.002	0.01	0.05	4.17	<0.2	0.62	259	0.24	<0.04	7.1
Q515287	<0.002	<0.01	0.05	4.22	<0.2	0.57	238	0.22	<0.04	5.17
Q515288	<0.002	<0.01	0.06	3.65	<0.2	0.55	245	0.19	<0.04	4.82
Q515289	<0.002	<0.01	0.04	3.73	<0.2	0.52	249	0.24	<0.04	7.16
Q515290	<0.002	0.01	0.06	4.8	<0.2	0.72	244	0.26	<0.04	5.94
Q515291	<0.002	<0.01	0.06	3.58	<0.2	0.56	251	0.18	<0.04	6.56
Q515292	<0.002	0.01	0.07	4.13	<0.2	0.59	254	0.23	<0.04	8

Till Four Acid

Sample	Re	S	Sb	Sc	Se	Sn	Sr	Ta	Te	Th
	ppm	%	ppm	ppm	ppm	ppm	ppm	ppm	ppm	ppm
Q515293	<0.002	<0.01	0.05	4.71	<0.2	0.75	257	0.31	<0.04	8.12
Q515294	<0.002	<0.01	0.04	3.19	<0.2	0.49	232	0.16	<0.04	6.05
Q515295	<0.002	<0.01	0.05	3.58	<0.2	0.57	247	0.21	<0.04	3.78
Q515296	<0.002	<0.01	0.04	4.26	<0.2	0.62	258	0.24	<0.04	5.87
Q515297	<0.002	0.01	0.06	4.77	<0.2	0.61	220	0.25	<0.04	5.41
Q515298	<0.002	0.01	0.08	7.88	<0.2	1.25	241	0.45	<0.04	6.9
Q515299	<0.002	0.01	0.12	7.06	0.2	1	228	0.48	<0.04	8.12
Q515300	<0.002	0.01	0.08	7.7	<0.2	1.19	239	0.46	<0.04	5.5
Q515301	<0.002	<0.01	0.05	4.93	0.2	0.61	237	0.24	<0.04	4.26
Q515302	<0.002	<0.01	0.07	5.62	<0.2	0.81	238	0.32	<0.04	6.54
Q515303	<0.002	<0.01	0.08	5.53	<0.2	0.77	223	0.26	<0.04	6.04
Q515304	<0.002	0.01	0.06	6.71	<0.2	0.97	219	0.37	<0.04	7.51
Q515305	<0.002	<0.01	0.05	6.75	<0.2	0.94	236	0.39	<0.04	4.93
Q515306	<0.002	<0.01	0.06	6.35	<0.2	0.89	238	0.39	<0.04	8.84
Q515307	<0.002	<0.01	0.08	5.61	<0.2	0.72	226	0.26	<0.04	5.73
Q515308	<0.002	0.01	0.07	5.41	<0.2	0.84	205	0.27	<0.04	3.2
Q515309	<0.002	0.01	0.07	6.51	<0.2	0.82	224	0.36	<0.04	11.8
Q515311	<0.002	0.02	0.07	6.1	<0.2	0.77	222	0.28	<0.04	10.25
Q515312	<0.002	<0.01	0.06	6.03	<0.2	0.89	233	0.39	<0.04	4.47
Q515313	<0.002	0.01	0.08	6.63	<0.2	0.98	230	0.41	<0.04	7.11
Q515314	<0.002	0.01	0.06	4.63	<0.2	0.61	225	0.25	<0.04	6.82
Q515315	<0.002	0.01	0.06	4.99	<0.2	0.81	237	0.28	<0.04	6.62
Q515316	<0.002	<0.01	0.05	4.17	<0.2	0.62	257	0.25	<0.04	5.72
Q515317	<0.002	0.01	0.06	4.43	<0.2	0.65	226	0.26	<0.04	5.86
Q515318	<0.002	<0.01	0.05	3.71	<0.2	0.52	242	0.25	<0.04	4.44
Q515319	<0.002	0.01	0.05	3.91	<0.2	0.64	240	0.21	<0.04	4.97
Q515320	<0.002	0.01	0.03	3.26	<0.2	0.51	238	0.19	<0.04	4.84
Q515321	<0.002	0.01	0.04	3.07	<0.2	0.47	241	0.18	<0.04	8.06
Q515322	<0.002	<0.01	0.05	3.21	<0.2	0.49	239	0.19	<0.04	4.84
Q515323	<0.002	<0.01	0.05	3.47	<0.2	0.53	253	0.19	<0.04	5.69
Q515324	<0.002	<0.01	0.05	3.6	<0.2	0.56	242	0.21	<0.04	5.87
Q515325	<0.002	<0.01	0.04	3.49	0.2	0.49	246	0.18	<0.04	4.78
Q515326	<0.002	<0.01	0.04	3.05	<0.2	0.5	252	0.22	<0.04	5.21
Q515327	<0.002	<0.01	0.04	3.17	<0.2	0.5	251	0.17	<0.04	4.52
Q515328	<0.002	<0.01	0.04	3.44	<0.2	0.56	246	0.21	<0.04	7.18
Q515329	<0.002	0.01	0.05	3.54	0.2	0.58	241	0.19	<0.04	3.72
Q515330	<0.002	<0.01	0.05	3.65	<0.2	0.61	243	0.21	<0.04	4.51
Q515331	<0.002	<0.01	0.05	3.96	0.2	0.56	245	0.22	<0.04	6.06
Q515332	<0.002	<0.01	0.05	3.26	<0.2	0.57	242	0.2	<0.04	4.84
Q515333	<0.002	0.01	0.07	5.21	<0.2	0.84	249	0.36	<0.04	6.3
Q515334	<0.002	<0.01	0.04	3.89	0.2	0.63	251	0.22	<0.04	4.92

Till Four Acid

Sample	Re	S	Sb	Sc	Se	Sn	Sr	Ta	Te	Th
	ppm	%	ppm	ppm	ppm	ppm	ppm	ppm	ppm	ppm
Q515335	<0.002	<0.01	0.04	3.9	<0.2	0.62	251	0.27	<0.04	5.75
Q515336	<0.002	<0.01	0.06	4.73	0.2	0.73	231	0.27	<0.04	3.81
Q515337	<0.002	0.01	0.05	5.08	<0.2	0.71	219	0.27	<0.04	8.87
Q515338	<0.002	0.01	0.06	5.12	0.2	0.71	228	0.28	<0.04	5.81
Q515339	<0.002	0.01	0.08	5.74	0.3	1	210	0.4	<0.04	4.24
Q515340	<0.002	0.01	0.08	5.45	<0.2	0.73	215	0.29	<0.04	4.48
Q515341	<0.002	<0.01	0.07	4.95	<0.2	0.74	212	0.26	<0.04	4.34
Q515342	<0.002	<0.01	0.06	5	0.2	0.78	220	0.29	<0.04	7.52
Q515343	<0.002	0.01	0.07	7.76	<0.2	1.11	224	0.45	<0.04	5.96
Q515344	<0.002	0.01	0.06	6.16	<0.2	0.95	236	0.36	<0.04	7.57
Q515345	<0.002	0.01	0.08	5.78	0.2	0.78	207	0.29	<0.04	4.93
Q515346	<0.002	0.01	0.08	5.27	0.2	0.74	204	0.26	<0.04	5.45
Q515347	<0.002	<0.01	0.07	6.5	<0.2	1	235	0.38	<0.04	5.07
Q515348	<0.002	<0.01	0.07	5.37	<0.2	0.7	217	0.27	<0.04	6.85
Q515349	<0.002	<0.01	0.07	6.17	<0.2	0.85	225	0.33	<0.04	5.93
Q515350	<0.002	<0.01	0.06	5.74	<0.2	0.8	218	0.33	<0.04	4.51
Q515351	<0.002	<0.01	0.06	5.3	<0.2	0.65	211	0.23	<0.04	4.15
Q515352	<0.002	<0.01	0.06	5.34	<0.2	0.81	220	0.3	<0.04	3.84
Q515354	<0.002	<0.01	0.09	6.02	<0.2	0.88	214	0.41	<0.04	8.58
Q515355	<0.002	<0.01	0.05	3.92	<0.2	0.57	238	0.21	<0.04	4.74
Q515356	<0.002	<0.01	0.07	4.56	<0.2	0.6	219	0.22	<0.04	3.99
Q515357	<0.002	<0.01	0.07	4.78	<0.2	0.73	256	0.32	<0.04	6.71
Q515358	<0.002	<0.01	0.04	3.48	0.3	0.48	240	0.35	0.04	5.37
Q515359	<0.002	<0.01	0.05	4.42	<0.2	0.71	246	0.27	<0.04	5.72
Q515360	<0.002	<0.01	0.04	5.03	<0.2	0.86	248	0.3	<0.04	7.1
Q515362	<0.002	0.01	0.06	4.61	<0.2	0.63	239	0.22	<0.04	6.69
Q515363	<0.002	0.01	0.05	4.51	0.2	0.65	245	0.31	<0.04	6.16
Q515364	<0.002	<0.01	0.05	4.86	<0.2	0.66	252	0.28	<0.04	7.44
Q515365	<0.002	<0.01	0.05	4.61	<0.2	0.65	230	0.24	<0.04	4.75
Q515366	<0.002	<0.01	0.05	3.24	<0.2	0.49	246	0.18	<0.04	8.41
Q515367	<0.002	<0.01	0.05	3.98	<0.2	0.58	242	0.22	<0.04	6.59
Q515368	<0.002	<0.01	0.04	3.61	<0.2	0.52	241	0.21	<0.04	5.72
Q515370	<0.002	<0.01	0.05	3.44	<0.2	0.44	250	0.18	<0.04	6.3
Q515371	<0.002	<0.01	0.04	4.16	<0.2	0.58	234	0.23	0.04	6.75
Q515372	<0.002	<0.01	0.06	3.33	<0.2	0.52	241	0.16	0.04	6.33
Q515373	<0.002	0.02	0.05	3.69	<0.2	0.5	245	0.19	<0.04	6.67
Q515374	<0.002	<0.01	0.05	4.16	<0.2	0.58	241	0.21	<0.04	10.85
Q515375	<0.002	0.02	0.04	4.53	<0.2	0.77	222	0.25	<0.04	4.69
Q515376	<0.002	0.01	0.05	4.02	<0.2	0.65	234	0.21	<0.04	7.18
Q515377	<0.002	0.01	0.05	4.58	<0.2	0.66	212	0.25	<0.04	5.55
Q515378	<0.002	0.01	0.06	4.56	<0.2	0.68	231	0.25	<0.04	9.13

Till Four Acid

Sample	Re	S	Sb	Sc	Se	Sn	Sr	Ta	Te	Th
	ppm	%	ppm	ppm	ppm	ppm	ppm	ppm	ppm	ppm
Q515379	<0.002	0.01	0.05	3.43	<0.2	0.45	240	0.19	<0.04	5.51
Q515380	<0.002	0.01	0.06	4.43	<0.2	0.6	226	0.23	<0.04	7.62
Q515381	<0.002	0.01	0.06	3.61	<0.2	0.51	246	0.18	<0.04	5.85
Q515382	<0.002	<0.01	0.04	3.68	<0.2	0.53	248	0.18	<0.04	5.81
Q515384	<0.002	<0.01	0.05	4.16	<0.2	0.61	235	0.26	<0.04	4.59
Q515385	<0.002	<0.01	0.05	3.25	<0.2	0.47	242	0.19	<0.04	4.56
Q515386	<0.002	<0.01	0.04	3.98	0.3	0.56	246	0.25	<0.04	4.49
Q515387	<0.002	<0.01	0.06	4.08	<0.2	0.56	232	0.23	<0.04	4.19
Q515388	<0.002	<0.01	0.06	3.94	0.3	0.54	235	0.25	<0.04	4.74
Q515389	<0.002	<0.01	0.09	6.18	<0.2	0.96	207	0.34	<0.04	5.8
Q515390	<0.002	<0.01	0.06	4.5	<0.2	0.62	223	0.24	<0.04	5.03
Q515391	<0.002	<0.01	0.06	4.87	<0.2	0.71	247	0.33	<0.04	7.2
Q515392	<0.002	<0.01	0.08	5.49	<0.2	0.86	211	0.32	<0.04	4.82
Q515393	<0.002	<0.01	0.06	5.65	<0.2	0.77	212	0.32	<0.04	4.24
Q515394	<0.002	<0.01	0.08	6.37	<0.2	0.92	216	0.39	<0.04	5.45
Q515395	<0.002	<0.01	0.08	6.51	<0.2	0.93	212	1.2	<0.04	4.8
Q515396	<0.002	<0.01	0.09	6.88	<0.2	1.05	228	0.42	<0.04	4.79
Q515397	<0.002	<0.01	0.08	7.06	<0.2	0.94	226	0.39	<0.04	7.17
Q515398	<0.002	<0.01	0.08	7.28	<0.2	1.12	231	0.5	<0.04	5.82
Q515399	<0.002	<0.01	0.06	5.47	<0.2	0.7	222	0.29	<0.04	5.2
Q515400	<0.002	<0.01	0.07	4.78	<0.2	0.66	213	0.25	<0.04	3.19
Q515401	<0.002	<0.01	0.06	5.18	<0.2	0.84	212	0.29	<0.04	5.28
Q515402	<0.002	<0.01	0.07	4.37	<0.2	0.63	238	0.31	<0.04	4.44
Q515403	<0.002	<0.01	0.06	3.65	<0.2	0.58	243	0.22	<0.04	3.99
Q515404	<0.002	<0.01	0.06	3.72	<0.2	0.56	234	0.22	<0.04	4.49
Q515405	<0.002	<0.01	0.06	3.3	<0.2	0.47	240	0.2	<0.04	5.75
Q515406	<0.002	<0.01	0.08	7.06	0.3	1.18	223	0.41	<0.04	6.25
Q515407	<0.002	<0.01	0.06	5.41	0.2	0.78	206	0.3	<0.04	5.07
Q515408	<0.002	<0.01	0.08	5.73	<0.2	0.97	239	0.39	<0.04	6.81
Q515409	<0.002	<0.01	0.05	4.83	<0.2	0.97	226	0.46	<0.04	5.93
Q515410	<0.002	<0.01	0.05	6.65	0.3	1	229	0.42	<0.04	6.22
Q515411	<0.002	<0.01	0.08	5.7	0.2	0.9	214	0.3	<0.04	8.03
Q515412	<0.002	<0.01	0.07	4.77	<0.2	0.77	218	0.29	<0.04	4.6
Q515413	<0.002	<0.01	0.06	4.39	<0.2	0.67	227	0.25	<0.04	6.56
Q515414	<0.002	<0.01	0.07	3.31	<0.2	0.46	245	0.2	<0.04	4.11
Q515415	<0.002	<0.01	0.06	4.04	<0.2	0.62	225	0.25	<0.04	5.37
Q515416	<0.002	<0.01	0.06	4.8	<0.2	0.71	206	0.25	<0.04	3.47
Q515417	<0.002	<0.01	0.07	4.74	<0.2	0.77	214	0.24	<0.04	8.36
Q515418	<0.002	<0.01	0.08	5.1	<0.2	0.77	210	0.31	<0.04	4.56
Q515419	<0.002	0.02	0.06	6.27	0.3	0.88	226	0.34	<0.04	6.72
Q515420	<0.002	0.02	0.08	5.53	<0.2	0.97	210	0.32	<0.04	6.21

Till Four Acid

Sample	Re	S	Sb	Sc	Se	Sn	Sr	Ta	Te	Th
	ppm	%	ppm	ppm	ppm	ppm	ppm	ppm	ppm	ppm
Q515421	<0.002	0.01	0.08	6.1	0.2	0.9	212	0.3	<0.04	8.82
Q515422	<0.002	0.03	0.07	4.39	<0.2	0.69	205	0.22	<0.04	4.66
Q515423	<0.002	0.01	0.05	5.66	0.3	0.95	224	0.31	<0.04	7.31
Q515425	<0.002	0.01	0.05	4.96	0.2	0.74	201	0.26	<0.04	5.42
Q515426	<0.002	0.01	0.07	5.3	<0.2	0.83	206	0.26	<0.04	18.2
Q515427	<0.002	0.01	0.08	7.13	<0.2	1.13	229	0.43	<0.04	6.5
Q515428	<0.002	0.01	0.06	4.53	0.2	0.8	203	0.23	<0.04	6.76
Q515429	<0.002	0.01	0.04	4.7	<0.2	0.94	199.5	0.33	<0.04	8.09
Q515430	<0.002	0.01	0.06	5.49	<0.2	1.13	205	0.29	<0.04	5.71
Q515431	<0.002	<0.01	0.07	6.27	0.2	0.98	236	0.37	<0.04	7.87
Q515432	<0.002	0.01	0.07	5	<0.2	0.73	201	0.22	<0.04	4.24
Q515433	<0.002	0.01	0.06	5.54	0.2	0.83	215	0.27	0.04	5.7
Q515434	<0.002	<0.01	0.06	5.25	0.2	0.82	254	0.31	<0.04	5.9
Q515435	<0.002	0.01	0.06	4.51	<0.2	0.74	250	0.26	<0.04	6.5
Q515436	<0.002	<0.01	0.07	4.75	<0.2	0.8	224	0.23	<0.04	6.35
Q515437	<0.002	<0.01	0.06	4.82	<0.2	0.87	234	0.26	<0.04	4.45
Q515438	<0.002	<0.01	0.04	4.28	<0.2	0.74	224	0.22	<0.04	6.4
Q515439	<0.002	<0.01	0.04	3.1	<0.2	0.54	245	0.33	<0.04	5.05
Q515440	<0.002	<0.01	0.04	3.07	<0.2	0.48	255	0.18	<0.04	6.69
Q515442	<0.002	0.01	0.05	3.13	0.4	0.51	234	0.15	<0.04	5.14
Q515443	<0.002	0.01	0.05	4.64	0.3	0.74	242	0.25	<0.04	7.99
Q515444	<0.002	0.01	0.05	5.53	0.2	0.89	248	0.33	<0.04	6.13
Q515445	<0.002	<0.01	0.04	4.69	<0.2	0.76	273	0.31	<0.04	7.64
Q515446	<0.002	0.01	0.05	3.89	<0.2	0.6	224	0.19	<0.04	4.73
Q515447	<0.002	0.01	0.07	5.59	<0.2	0.86	244	0.3	<0.04	5.7
Q515448	<0.002	0.01	0.06	5.58	0.2	0.92	245	0.3	<0.04	8.21
Q515449	<0.002	0.01	0.04	3.1	0.3	0.55	251	0.2	<0.04	3.85
Q515450	<0.002	0.01	0.06	4.82	<0.2	0.75	268	0.36	<0.04	7.06
Q515451	<0.002	0.01	0.06	4.71	0.3	0.86	266	0.3	<0.04	6.66
Q515452	<0.002	<0.01	0.05	4.15	<0.2	0.68	258	0.24	<0.04	6.28
Q515454	<0.002	0.01	0.07	4.98	<0.2	0.78	259	0.31	<0.04	7.33
Q515455	<0.002	0.01	0.03	3.66	<0.2	0.53	245	0.2	<0.04	5.57
Q515456	<0.002	<0.01	0.05	5.61	<0.2	0.87	249	0.34	<0.04	6.62
Q515457	<0.002	<0.01	0.07	7.51	<0.2	1.2	231	0.44	<0.04	6.72
Q515458	<0.002	<0.01	0.06	5.93	<0.2	0.9	231	0.35	<0.04	7.66
Q515459	<0.002	<0.01	0.09	6.36	<0.2	1.03	229	0.42	0.04	6.2
Q515460	<0.002	<0.01	0.06	4.69	<0.2	0.75	251	0.29	<0.04	4.8
Q515461	<0.002	<0.01	0.06	4.56	<0.2	0.62	209	0.22	<0.04	3.91
Q515462	<0.002	<0.01	0.04	4.92	<0.2	0.62	205	0.23	<0.04	5.91
Q515463	<0.002	<0.01	0.06	5.05	<0.2	0.71	214	0.26	<0.04	11.15
Q515464	<0.002	0.01	0.04	6.15	<0.2	0.9	242	0.35	<0.04	6.97

Till Four Acid

Sample	Re	S	Sb	Sc	Se	Sn	Sr	Ta	Te	Th
	ppm	%	ppm	ppm	ppm	ppm	ppm	ppm	ppm	ppm
Q515465	<0.002	<0.01	0.06	5.46	0.2	0.74	236	0.26	<0.04	5.68
Q515466	<0.002	<0.01	0.05	6.93	<0.2	1.34	243	0.41	<0.04	5.59
Q515467	<0.002	<0.01	0.05	5.35	0.2	0.74	215	0.27	<0.04	4.85
Q515468	<0.002	<0.01	0.06	6.32	<0.2	0.93	223	0.44	<0.04	6.31
Q515469	<0.002	<0.01	0.05	5.4	<0.2	0.74	220	0.27	<0.04	3.9
Q515470	<0.002	<0.01	0.07	6.86	<0.2	1.01	233	0.41	<0.04	6.31
Q515471	<0.002	<0.01	0.07	5.87	<0.2	0.85	218	0.32	<0.04	4.9
Q515472	<0.002	0.01	0.06	5.74	<0.2	0.87	213	0.29	<0.04	4.89
Q515473	<0.002	<0.01	0.05	5.77	<0.2	0.83	223	0.29	0.04	4.62
Q515474	<0.002	<0.01	0.06	6.85	<0.2	1.06	235	0.41	<0.04	7.86
Q515475	<0.002	<0.01	0.06	5.55	<0.2	0.72	220	0.26	<0.04	5.45

Till Four Acid

Sample	Ti	Tl	U	V	W	Y	Zn	Zr
	%	ppm	ppm	ppm	ppm	ppm	ppm	ppm
Q515251	0.16	0.229	1.31	31.7	0.284	8.89	25.1	121.5
Q515252	0.207	0.251	1.36	38.7	0.343	8.08	16.9	171
Q515253	0.175	0.218	1.74	32.9	0.257	11.2	21.5	157.5
Q515254	0.225	0.254	0.96	49.5	0.405	8.43	31.2	140
Q515255	0.345	0.312	1.42	72.6	0.492	12	44.2	180
Q515256	0.194	0.24	1.04	43.8	0.262	8.09	30.4	121.5
Q515257	0.238	0.283	1.68	41.5	0.357	13.45	30.1	185.5
Q515258L	0.235	0.342	1.64	51	0.44	11.8	40.9	154
Q515258U	0.239	0.257	1.33	43.4	0.329	12.8	29	183.5
Q515260	0.127	0.194	1.49	25	0.195	8.54	19.3	93.9
Q515261	0.125	0.205	0.84	23.7	0.205	7.4	16	93.3
Q515262	0.119	0.199	1.26	23.4	0.261	8.13	15.6	110
Q515263	0.101	0.212	0.85	23.9	0.229	7.45	16.4	83.6
Q515264	0.132	0.217	0.96	27.2	0.175	8.34	19.1	91.8
Q515265	0.098	0.187	1.3	20.4	0.221	8.26	12.9	101.5
Q515266	0.153	0.254	1.23	30.2	0.249	9.42	23.5	172
Q515267	0.126	0.214	1.35	27.8	0.19	9.14	20.1	113.5
Q515268	0.189	0.254	1.45	38	0.296	11.05	25	142
Q515269	0.147	0.23	1.01	30.3	0.208	9.16	24.7	117
Q515270	0.14	0.229	0.7	31.2	0.199	7.79	20.3	87.3
Q515271	0.174	0.254	1.21	35.1	0.278	9.59	23.3	142
Q515272	0.172	0.211	0.8	36.7	0.253	7.43	21.6	135.5
Q515273	0.152	0.21	0.75	32.4	0.225	7.77	19.2	106
Q515274	0.261	0.235	1.01	63	0.424	10.4	37.6	159.5
Q515275	0.132	0.226	0.57	30.4	0.276	5.61	20.2	75.4
Q515276	0.187	0.269	1.51	33.4	0.289	11.65	27.5	134.5
Q515277	0.194	0.25	1.63	31.8	1.12	11.55	25.2	152.5
Q515278	0.139	0.231	1.45	30.6	0.236	10	27.1	108
Q515280	0.144	0.215	1.07	27	0.197	6.11	18.5	110.5
Q515281	0.16	0.232	1.44	31.5	2.49	9.84	23.4	152.5
Q515282	0.151	0.225	1.28	30.8	0.435	8.53	19.5	111
Q515283	0.141	0.237	0.88	31.1	0.243	6.86	20.4	99.4
Q515284	0.137	0.205	2.01	25.5	0.218	11	16.9	156
Q515285	0.141	0.218	2.05	26.2	0.567	10.7	17.5	132
Q515286	0.147	0.205	1.95	26.2	0.248	11.25	17.3	150.5
Q515287	0.139	0.216	1.36	27.1	0.465	8.61	19.1	112
Q515288	0.119	0.21	1.25	22.9	0.186	8.36	16.2	96.2
Q515289	0.122	0.202	1.75	24.2	0.307	9.55	16.5	120.5
Q515290	0.159	0.244	1.77	30.5	0.227	10.4	21.5	146.5
Q515291	0.118	0.214	1.74	23.1	0.167	9.42	16.4	119.5
Q515292	0.134	0.223	2.16	28.1	0.228	10.25	18.4	141.5

Till Four Acid

Sample	Ti	Tl	U	V	W	Y	Zn	Zr
	%	ppm	ppm	ppm	ppm	ppm	ppm	ppm
Q515293	0.173	0.235	1.99	31.4	0.286	11.7	21.2	152.5
Q515294	0.107	0.189	1.83	21	0.183	8.5	15.6	81.5
Q515295	0.132	0.21	1.06	25.1	0.247	5.91	15	93.8
Q515296	0.142	0.227	1.9	27.2	0.216	10.25	19.5	125.5
Q515297	0.162	0.211	1.24	26.9	0.187	7.86	16.5	123
Q515298	0.24	0.37	1.8	48.1	0.47	11.85	42.1	145.5
Q515299	0.247	0.308	1.85	44.6	0.45	12.9	33.8	158
Q515300	0.256	0.322	1.3	49.5	0.456	10.5	34.3	158
Q515301	0.154	0.217	1.01	28.6	0.203	8.59	20.1	131
Q515302	0.205	0.237	1	39.2	0.239	9.51	21.5	138.5
Q515303	0.182	0.235	0.91	34.4	0.397	9.24	29.2	128
Q515304	0.213	0.256	1.2	41.4	0.332	11.35	29	161.5
Q515305	0.23	0.27	1.23	41.5	0.316	11.85	26.2	170
Q515306	0.22	0.276	1.66	40.6	0.286	12.75	26.6	172.5
Q515307	0.164	0.246	0.93	33.9	0.222	9.53	22.1	146
Q515308	0.184	0.212	0.71	38.6	0.283	7.52	17.6	133
Q515309	0.225	0.244	0.98	43.9	0.973	9.66	22.4	153.5
Q515311	0.197	0.215	1.06	38.8	0.792	9.07	22.7	157.5
Q515312	0.197	0.283	1.02	36	0.34	9.38	26.4	144.5
Q515313	0.21	0.283	1.64	37	0.442	11.05	33.4	168.5
Q515314	0.14	0.208	1.02	28.5	0.21	8.38	20.7	138
Q515315	0.161	0.231	1.44	23.8	0.28	8.59	18	173.5
Q515316	0.138	0.216	1.64	24.9	0.243	9.48	19.4	147.5
Q515317	0.142	0.219	1.06	27	1.41	7.9	20.1	130
Q515318	0.122	0.197	1.37	24.8	0.183	7.88	16.4	140
Q515319	0.124	0.207	1.52	23.9	0.208	8.51	17.2	110.5
Q515320	0.108	0.186	1.35	22.3	0.166	7.15	15.1	105.5
Q515321	0.101	0.185	1.56	20.4	0.185	8.62	12.8	128
Q515322	0.105	0.188	1.46	21.4	0.196	8.7	13.5	122.5
Q515323	0.112	0.197	1.53	23.8	0.229	9.47	16	124.5
Q515324	0.121	0.206	1.9	23.9	0.238	9.02	15.5	150.5
Q515325	0.115	0.194	1.57	19.7	0.198	9.01	13.8	124.5
Q515326	0.101	0.192	1.58	21.3	0.252	8.63	13.6	129
Q515327	0.1	0.185	1.72	21.4	0.164	8.58	13.8	124
Q515328	0.119	0.205	1.68	23.5	0.201	9.73	15.6	138.5
Q515329	0.108	0.211	0.9	22.9	0.186	6.39	17.7	103.5
Q515330	0.125	0.206	1.46	25.5	0.192	8.7	17.2	129.5
Q515331	0.122	0.202	1.44	24.5	0.195	8.94	17.3	124.5
Q515332	0.115	0.193	1.43	16.8	0.151	7.51	12.9	135.5
Q515333	0.165	0.249	1.7	31.1	0.36	10.65	25.8	156.5
Q515334	0.122	0.2	1.58	25	0.292	9.08	15.8	140

Till Four Acid

Sample	Ti	Tl	U	V	W	Y	Zn	Zr
	%	ppm	ppm	ppm	ppm	ppm	ppm	ppm
Q515335	0.134	0.217	1.89	26.1	0.225	9.93	17.8	133.5
Q515336	0.15	0.232	1.01	30.2	0.236	9.14	21.8	129.5
Q515337	0.152	0.226	0.88	31.4	0.203	9.11	21.1	137
Q515338	0.152	0.237	1.06	32.5	0.299	9.55	23.3	117.5
Q515339	0.218	0.257	0.94	43.1	0.367	7.77	20	173.5
Q515340	0.177	0.216	0.79	36	0.294	8.48	20.2	142.5
Q515341	0.154	0.214	0.74	32.6	0.193	9.02	21.4	132
Q515342	0.165	0.24	1.07	33	0.221	9.28	23.7	133.5
Q515343	0.229	0.315	1.49	47.1	0.698	11	36.6	192
Q515344	0.2	0.294	1.34	40.3	0.299	11.15	27.1	159.5
Q515345	0.179	0.227	0.92	38.3	0.294	8.22	24.8	170.5
Q515346	0.163	0.227	0.9	35.1	0.244	8.34	24.3	157
Q515347	0.209	0.303	1.2	41.8	0.299	10.75	28.8	158
Q515348	0.165	0.237	1.01	34.3	0.244	9.52	24.5	115.5
Q515349	0.206	0.276	1.26	38.2	0.328	10.7	29.4	146
Q515350	0.193	0.254	0.83	37.3	0.273	9.04	25.9	133
Q515351	0.145	0.222	0.72	30	0.232	8.38	21.9	123.5
Q515352	0.173	0.222	0.75	34.4	0.304	7.49	21	114.5
Q515354	0.239	0.204	1.35	44.5	0.383	10.2	17.9	195
Q515355	0.133	0.205	1.2	24.9	0.24	8.39	17	122
Q515356	0.132	0.233	0.92	27.3	0.211	7.88	18.6	97.5
Q515357	0.169	0.232	1.83	29.7	0.386	11.45	20.5	158
Q515358	0.111	0.208	1.62	26.6	0.199	8.77	13.5	116
Q515359	0.155	0.231	1.46	28	0.307	7.97	19.3	127
Q515360	0.181	0.245	1.77	30.9	0.316	10.7	22	149.5
Q515362	0.146	0.231	1.02	28.7	0.242	8.62	19.4	125
Q515363	0.152	0.229	1.65	26.3	0.31	10.35	19.4	146
Q515364	0.162	0.231	2.06	28.5	0.304	11.25	19.4	159.5
Q515365	0.14	0.249	1.14	29.3	0.262	7.96	21.2	117.5
Q515366	0.113	0.183	2.55	20.9	0.18	10.15	12.8	108
Q515367	0.133	0.199	1.84	25.9	0.245	10.35	15.4	145
Q515368	0.116	0.191	1.85	24.3	0.227	9.31	14.4	127
Q515370	0.115	0.196	1.85	22.5	0.389	9.77	14.1	148
Q515371	0.135	0.207	2.13	26.1	0.295	10.2	17	145
Q515372	0.108	0.207	1.71	21.4	0.227	8.62	14.1	110.5
Q515373	0.123	0.222	1.92	24.4	0.245	9.67	15.9	127
Q515374	0.126	0.212	2	26.2	0.266	9.81	17.4	125.5
Q515375	0.149	0.24	1.13	31.2	0.851	7.13	21.7	101.5
Q515376	0.132	0.217	1.35	24.6	0.24	8.82	17.5	96.4
Q515377	0.149	0.212	1.2	36.4	0.265	7.66	18.2	112.5
Q515378	0.145	0.231	1.75	30.6	0.282	10.2	19.8	135

Till Four Acid

Sample	Ti	Tl	U	V	W	Y	Zn	Zr
	%	ppm	ppm	ppm	ppm	ppm	ppm	ppm
Q515379	0.111	0.181	1.75	22.2	0.186	9.25	12.6	116.5
Q515380	0.155	0.196	2.08	30.4	0.248	11.5	17	157.5
Q515381	0.118	0.197	1.87	24	0.206	9.28	15.4	119.5
Q515382	0.116	0.205	1.71	23.5	0.236	9.65	15.5	136
Q515384	0.133	0.233	1.38	25	0.258	8.23	20.5	117
Q515385	0.105	0.19	1.28	21.9	0.189	8.06	13.8	115
Q515386	0.129	0.219	1.23	25.3	0.275	8.21	16.3	121
Q515387	0.124	0.214	1.12	26.2	0.22	8.22	16.4	127
Q515388	0.126	0.216	1.09	25.6	0.238	7.94	17.5	124
Q515389	0.238	0.23	0.92	45.3	0.37	8.38	19.6	185
Q515390	0.146	0.225	0.89	33	0.272	7.68	18	145
Q515391	0.157	0.257	1.95	31.2	0.287	10.85	21.6	142
Q515392	0.163	0.272	0.94	35.4	0.294	8.59	26.7	121
Q515393	0.165	0.258	0.72	35.8	0.278	8.22	26.6	119.5
Q515394	0.194	0.31	1.14	42.6	0.345	9.97	35.6	146.5
Q515395	0.198	0.295	0.93	36.3	0.499	9.17	29.6	146
Q515396	0.21	0.341	0.99	44	0.357	9.44	33.4	125.5
Q515397	0.215	0.288	1.18	39.7	0.318	11.2	33.5	162.5
Q515398	0.227	0.366	1.29	47.6	0.577	10.9	39.7	149
Q515399	0.156	0.272	0.88	36.8	0.388	8.57	25.4	141
Q515400	0.14	0.228	0.67	23.3	0.24	7.58	19.7	109.5
Q515401	0.162	0.275	0.94	31.8	0.269	8.4	24.3	117.5
Q515402	0.137	0.23	1.38	28.3	0.258	9.4	22.6	119.5
Q515403	0.121	0.206	1.03	24.5	0.189	7.6	18.5	105
Q515404	0.122	0.22	1.24	24.1	0.217	8.12	14.2	122.5
Q515405	0.105	0.209	1.72	16.8	0.155	8.62	14.4	105
Q515406	0.213	0.344	2	43	0.327	11.5	35.2	150.5
Q515407	0.153	0.277	1.12	33.6	0.29	8.41	25	146
Q515408	0.197	0.28	1.74	36.9	0.335	11.4	26.1	165.5
Q515409	0.165	0.295	1.3	34.4	0.269	9.96	27.3	130
Q515410	0.215	0.296	1.54	40.4	0.366	11.3	30.4	162
Q515411	0.177	0.296	1.26	33.5	0.23	10.9	27.8	152
Q515412	0.146	0.25	1.06	31.8	0.244	9.19	24.3	121
Q515413	0.132	0.225	1.61	29.3	0.413	8.82	20	120
Q515414	0.101	0.196	1.38	20.8	0.309	8.7	13.4	129
Q515415	0.135	0.243	1.27	28	0.233	8.8	19.4	123.5
Q515416	0.141	0.283	0.76	29.1	0.197	7.62	22.3	109
Q515417	0.139	0.258	0.76	30	0.237	7.24	23.1	85.6
Q515418	0.157	0.273	0.82	32.9	0.231	8.98	22.6	133.5
Q515419	0.208	0.276	1.66	38.7	0.304	10.3	25.8	152
Q515420	0.192	0.253	0.89	41.8	0.299	7.33	27.5	141.5

Till Four Acid

Sample	Ti	Tl	U	V	W	Y	Zn	Zr
	%	ppm	ppm	ppm	ppm	ppm	ppm	ppm
Q515421	0.215	0.257	1.31	40.8	0.258	9.62	26.4	143.5
Q515422	0.129	0.234	0.86	27	0.18	7.31	19.6	98.4
Q515423	0.186	0.264	1.76	37.2	0.351	10.95	26.3	165
Q515425	0.152	0.233	0.82	31.8	0.261	6.82	22.9	112.5
Q515426	0.173	0.245	1.03	37.9	0.293	8.03	26.8	122
Q515427	0.23	0.323	1.57	44.3	0.395	11.3	32.6	165.5
Q515428	0.14	0.262	1.04	29.5	0.189	8.91	22.2	106
Q515429	0.14	0.28	1.1	29.8	0.199	8.63	25.6	92.9
Q515430	0.174	0.322	1.15	35.4	0.247	9.69	34.2	127
Q515431	0.223	0.281	1.99	38.8	0.344	12.45	27.1	180.5
Q515432	0.147	0.257	0.92	29.9	0.229	8.14	23.7	116.5
Q515433	0.18	0.265	0.91	35.3	0.211	9.49	23.8	143
Q515434	0.175	0.254	1.75	32.7	0.306	10.1	23.2	156
Q515435	0.148	0.228	2.04	30.2	0.325	10.7	20.8	144
Q515436	0.153	0.231	0.96	30.8	0.201	8.61	21.6	140
Q515437	0.153	0.253	1.24	24.1	0.24	8.29	23.2	148.5
Q515438	0.131	0.251	1.17	26.5	0.931	8.35	21.4	113
Q515439	0.102	0.184	1.66	19.5	0.195	7.77	14	107
Q515440	0.096	0.191	2.06	19.7	0.162	9.01	13.3	95.6
Q515442	0.101	0.186	1.51	19.4	0.166	7.76	12.7	114
Q515443	0.154	0.225	2.4	30.9	0.243	11	21.1	147
Q515444	0.186	0.264	1.76	35.3	0.354	10.9	25.7	159
Q515445	0.182	0.235	2.48	29.9	0.353	12.1	18.6	176
Q515446	0.127	0.208	0.9	24.8	0.176	7.15	17	94.3
Q515447	0.181	0.269	1.43	37.3	0.354	9.37	27.4	137.5
Q515448	0.189	0.289	2.27	34.3	0.332	11.1	27.2	147
Q515449	0.106	0.193	1.13	21.4	0.168	7.6	14	110
Q515450	0.174	0.231	2.12	27.7	1.415	11.65	20.3	164.5
Q515451	0.164	0.241	2.08	29.5	0.373	10.95	19.3	163
Q515452	0.145	0.226	1.91	26.4	0.255	10.35	17.5	136.5
Q515454	0.177	0.242	2.08	32.4	0.302	11.25	20.4	161
Q515455	0.137	0.203	1.48	27.8	0.234	7.71	15.5	131
Q515456	0.21	0.255	1.67	33.4	0.389	11.65	24.3	169.5
Q515457	0.23	0.361	1.9	49.3	0.426	11.65	38.5	168
Q515458	0.206	0.267	1.44	38.7	0.319	11.15	25.6	160
Q515459	0.229	0.285	1.24	40.7	0.312	11.3	26	171
Q515460	0.173	0.246	1.33	31	0.249	9.86	19.7	143
Q515461	0.139	0.254	0.74	30.1	0.162	7.82	19.2	105.5
Q515462	0.162	0.223	0.74	32.4	0.321	8.26	19.2	124.5
Q515463	0.162	0.241	0.95	30	0.238	9.01	23.4	128
Q515464	0.209	0.284	1.6	38	0.811	11.4	28.9	154.5

Till Four Acid

Sample	Ti	Tl	U	V	W	Y	Zn	Zr
	%	ppm	ppm	ppm	ppm	ppm	ppm	ppm
Q515465	0.165	0.259	1	34.1	0.203	9.1	23.4	140.5
Q515466	0.245	0.295	1.32	44.1	0.468	11.9	31.5	162.5
Q515467	0.171	0.247	0.8	35	0.227	9.33	22.7	142.5
Q515468	0.22	0.262	1.28	41.3	0.311	11.4	26.7	198.5
Q515469	0.183	0.255	0.84	36.5	0.284	9.24	23.7	142
Q515470	0.242	0.31	1.48	44.7	0.321	12.4	28.7	189.5
Q515471	0.203	0.254	0.96	40.8	0.278	9.8	27.9	156
Q515472	0.187	0.251	1.1	38	0.264	9.85	24.5	157
Q515473	0.191	0.252	0.95	31.9	0.269	10.05	29	139
Q515474	0.241	0.316	1.47	45.2	0.312	12.4	30.5	180
Q515475	0.17	0.256	0.87	34.1	0.26	9.26	24.5	127

D.5 Till Aqua Regia ICP-MS Results

Multi-element results are presented for the aqua regia digestion and ICP-MS analysis of the -180 micron fraction of till samples.

Till Aqua Regia ICP-MS Results

	Au	Ag	Al	As	B	Ba	Be	Bi	Ca	Cd	Ce
	ppm	ppm	%	ppm	ppm	ppm	ppm	ppm	%	ppm	ppm
Q515251	0.0004	0.018	0.61	1.58	<10	20.6	0.2	0.092	0.1	0.033	32.9
Q515252	<0.0002	0.014	0.91	1.19	<10	12.4	0.14	0.063	0.04	0.02	24
Q515253	<0.0002	0.011	0.4	1.29	<10	21.6	0.13	0.071	0.15	0.026	33.8
Q515254	0.0002	0.021	0.74	2.81	<10	23.6	0.18	0.104	0.07	0.034	22.2
Q515255	0.0006	0.021	1.14	3.32	<10	35.4	0.34	0.131	0.09	0.054	28.6
Q515256	0.0003	0.018	0.69	2.05	<10	28.7	0.19	0.096	0.1	0.028	22.4
Q515257	0.0004	0.01	0.51	1.12	<10	26.1	0.15	0.065	0.18	0.026	38.7
Q515258L	0.0008	0.011	0.84	2.15	<10	38.4	0.23	0.104	0.16	0.026	33.2
Q515258U	0.0008	0.007	0.49	1.04	<10	24.4	0.14	0.058	0.18	0.028	36.9
Q515260	0.0006	0.014	0.35	1.61	<10	19.3	0.13	0.089	0.12	0.021	24.9
Q515261	0.0004	0.01	0.31	0.65	<10	16.1	0.07	0.089	0.08	0.01	21
Q515262	0.0009	0.011	0.29	1.16	<10	16.6	0.09	0.081	0.1	0.011	24.6
Q515263	0.0008	0.009	0.3	1.12	<10	19.3	0.09	0.074	0.09	0.011	20
Q515264	0.0003	0.008	0.33	1.16	<10	18.2	0.1	0.069	0.11	0.017	26.9
Q515265	0.0012	0.013	0.25	1.1	<10	14.7	0.08	0.093	0.11	0.014	32
Q515266	0.0006	0.012	0.4	1.41	<10	19.7	0.11	0.085	0.11	0.016	22.1
Q515267	0.0006	0.012	0.35	1.69	<10	21	0.1	0.118	0.12	0.015	27.2
Q515268	0.0004	0.013	0.52	1.51	<10	26.7	0.15	0.061	0.15	0.025	30.1
Q515269	0.0003	0.009	0.47	1.23	<10	22.5	0.15	0.077	0.12	0.021	24.9
Q515270	0.0003	0.011	0.45	1.48	<10	17.2	0.12	0.057	0.09	0.019	19.15
Q515271	0.0004	0.008	0.55	1.43	<10	23.3	0.17	0.07	0.1	0.022	29.5
Q515272	<0.0002	0.004	0.57	1.54	<10	14	0.14	0.06	0.05	0.014	22.1
Q515273	<0.0002	0.01	0.47	0.82	<10	12.9	0.11	0.039	0.08	0.016	18.55
Q515274	0.0011	0.018	0.95	6.68	<10	33	0.24	0.141	0.09	0.029	23.5
Q515275	0.0003	0.009	0.47	1.21	<10	14.7	0.12	0.061	0.05	0.017	12
Q515276	0.0003	0.012	0.51	1	<10	23.1	0.14	0.07	0.14	0.022	33
Q515277	0.0009	0.011	0.43	0.9	<10	21.6	0.13	0.095	0.16	0.024	36.7
Q515278	0.0005	0.014	0.51	2.47	<10	27.2	0.2	0.125	0.09	0.016	25.5
Q515280	0.001	0.012	0.36	0.72	<10	23.6	0.07	0.071	0.04	0.006	26.4
Q515281	0.0076	0.015	0.44	1.39	<10	25	0.12	0.107	0.11	0.019	27.3
Q515282	0.0045	0.008	0.36	1.4	<10	19	0.09	0.104	0.1	0.017	23.9
Q515283	0.0003	0.009	0.47	1.6	<10	19.4	0.12	0.103	0.08	0.017	18.8
Q515284	0.0011	0.01	0.36	1.28	<10	20.3	0.11	0.118	0.14	0.019	41
Q515285	0.0003	0.01	0.35	1.48	<10	20.8	0.12	0.125	0.13	0.019	37.5
Q515286	0.0019	0.01	0.34	1.54	<10	21.3	0.1	0.12	0.14	0.017	42.5
Q515287	0.0004	0.014	0.37	1.8	<10	22.2	0.1	0.137	0.1	0.015	26.1
Q515288	0.0007	0.011	0.3	1.08	<10	19.4	0.09	0.146	0.11	0.012	33
Q515289	0.0008	0.017	0.31	1.41	<10	20.6	0.08	0.139	0.13	0.022	34.8
Q515290	0.0008	0.009	0.38	2.19	<10	21.8	0.1	0.145	0.11	0.031	31.6
Q515291	0.0005	0.006	0.28	1.5	<10	17.7	0.11	0.115	0.12	0.025	26.6
Q515292	0.0015	0.012	0.35	1.81	<10	25.4	0.1	0.12	0.12	0.02	32.5

Till Aqua Regia ICP-MS Results

	Au	Ag	Al	As	B	Ba	Be	Bi	Ca	Cd	Ce
	ppm	ppm	%	ppm	ppm	ppm	ppm	ppm	%	ppm	ppm
Q515293	0.0006	0.009	0.38	1.77	<10	23.9	0.13	0.124	0.18	0.023	45.1
Q515294	0.0007	0.013	0.34	1.29	<10	22.9	0.09	0.114	0.11	0.018	23.4
Q515295	0.0004	0.008	0.26	0.88	<10	18.3	0.08	0.102	0.04	0.012	32
Q515296	0.0009	0.01	0.38	1.49	<10	27.4	0.12	0.127	0.14	0.021	38.4
Q515297	0.0003	0.008	0.23	0.54	<10	12.7	0.07	0.044	0.05	0.012	15.8
Q515298	0.0004	0.022	0.79	1.55	<10	42.2	0.2	0.132	0.16	0.037	39.1
Q515299	0.0005	0.017	0.56	1.67	<10	27.8	0.2	0.094	0.14	0.035	35.8
Q515300	0.0007	0.017	0.85	1.76	<10	34.5	0.26	0.099	0.12	0.03	36.6
Q515301	0.0003	0.012	0.41	1.01	<10	14.2	0.1	0.056	0.12	0.017	29.4
Q515302	0.0005	0.01	0.38	0.94	<10	15.8	0.1	0.055	0.09	0.018	20.7
Q515303	0.0008	0.011	0.49	1.44	<10	24.6	0.18	0.078	0.11	0.023	19.55
Q515304	0.0003	0.014	0.54	1.77	<10	26.6	0.14	0.074	0.14	0.04	30.8
Q515305	0.0008	0.015	0.4	1.05	<10	26.3	0.11	0.051	0.19	0.02	35.6
Q515306	0.0043	0.015	0.43	1.49	<10	30.4	0.12	0.069	0.18	0.023	42.6
Q515307	0.0002	0.013	0.37	0.95	<10	20.7	0.09	0.051	0.12	0.021	24.6
Q515308	0.0003	0.007	0.4	1.15	<10	13.7	0.11	0.058	0.04	0.015	15.75
Q515309	0.0003	0.009	0.91	1.76	<10	15.6	0.18	0.062	0.06	0.037	19.1
Q515311	0.0005	0.007	0.72	1.85	<10	19.1	0.17	0.072	0.07	0.036	23.6
Q515312	0.0003	0.006	0.58	0.72	<10	26.5	0.15	0.063	0.13	0.019	29.7
Q515313	0.0014	0.022	0.56	0.76	<10	28.3	0.21	0.076	0.16	0.025	40
Q515314	0.0002	0.007	0.33	1.5	<10	16.6	0.1	0.075	0.11	0.013	23.2
Q515315	0.0003	0.007	0.3	0.17	<10	17	0.05	0.077	0.08	0.009	30.1
Q515316	0.0002	0.013	0.35	0.6	<10	27.4	0.1	0.119	0.15	0.018	44.2
Q515317	0.0054	0.011	0.34	1.61	<10	22.9	0.08	0.105	0.12	0.017	26
Q515318	0.0005	0.011	0.29	0.88	<10	21.6	0.1	0.121	0.11	0.011	28.9
Q515319	0.0003	0.009	0.33	1.21	<10	21.1	0.11	0.098	0.12	0.017	31.1
Q515320	0.0005	0.007	0.3	1.21	<10	18.6	0.09	0.111	0.09	0.016	29
Q515321	0.0019	0.015	0.24	0.96	<10	16.7	0.08	0.135	0.13	0.024	34.5
Q515322	0.0003	0.016	0.26	1.41	<10	17.2	0.09	0.147	0.13	0.018	37.1
Q515323	0.0011	0.02	0.29	1.57	<10	20.5	0.12	0.117	0.14	0.023	34.2
Q515324	0.0004	0.01	0.29	1.33	<10	20.1	0.12	0.135	0.13	0.018	37.2
Q515325	0.0009	0.01	0.26	0.95	<10	16.4	0.1	0.109	0.13	0.019	37.2
Q515326	0.0005	0.008	0.25	1.55	<10	16.5	0.09	0.112	0.11	0.015	33.6
Q515327	0.0002	0.009	0.27	1.03	<10	18.3	0.09	0.098	0.11	0.014	34.3
Q515328	0.0002	0.009	0.28	1.13	<10	18.7	0.09	0.147	0.12	0.016	33
Q515329	0.0004	0.011	0.39	1.15	<10	25.4	0.11	0.118	0.09	0.014	27
Q515330	0.0007	0.009	0.28	1.17	<10	19.4	0.07	0.085	0.13	0.018	29.1
Q515331	0.0003	0.01	0.34	1.57	<10	21.9	0.12	0.098	0.13	0.018	38.3
Q515332	0.0004	0.005	0.22	0.28	<10	14.5	0.06	0.082	0.07	0.008	31.4
Q515333	0.0002	0.011	0.51	1.33	<10	28	0.18	0.109	0.15	0.019	39.4
Q515334	0.0004	0.008	0.31	1.73	<10	21.4	0.1	0.106	0.13	0.015	40.5

Till Aqua Regia ICP-MS Results

	Au	Ag	Al	As	B	Ba	Be	Bi	Ca	Cd	Ce
	ppm	ppm	%	ppm	ppm	ppm	ppm	ppm	%	ppm	ppm
Q515335	0.0007	0.009	0.37	2.12	<10	21.6	0.1	0.112	0.13	0.018	41.5
Q515336	0.0006	0.012	0.36	1.4	<10	19.2	0.14	0.074	0.12	0.019	27.5
Q515337	0.0003	0.014	0.38	1.08	<10	14.8	0.12	0.052	0.11	0.016	20.5
Q515338	<0.0002	0.009	0.49	1.18	<10	18.2	0.12	0.051	0.11	0.023	23
Q515339	<0.0002	0.005	0.83	1.27	<10	14.8	0.21	0.067	0.03	0.039	21.1
Q515340	<0.0002	0.011	0.58	1.43	<10	14.3	0.2	0.063	0.07	0.026	21.4
Q515341	0.0002	0.014	0.3	0.78	<10	16.2	0.11	0.036	0.12	0.014	23.2
Q515342	0.0006	0.012	0.37	1.25	<10	20.4	0.11	0.043	0.13	0.018	24.6
Q515343	0.0005	0.018	0.79	2.07	<10	39.7	0.23	0.092	0.15	0.035	37.4
Q515344	0.0015	0.011	0.5	1.34	<10	25.4	0.16	0.063	0.15	0.024	34.7
Q515345	<0.0002	0.009	0.54	1.68	<10	21.3	0.12	0.063	0.08	0.027	23.2
Q515346	<0.0002	0.012	0.56	1.91	<10	22.2	0.15	0.059	0.11	0.021	23
Q515347	<0.0002	0.011	0.51	1.13	<10	26.4	0.16	0.054	0.15	0.018	32.5
Q515348	<0.0002	0.017	0.42	1.43	<10	22.2	0.14	0.054	0.12	0.019	23.5
Q515349	<0.0002	0.01	0.49	1.44	<10	26.8	0.14	0.062	0.16	0.036	32.2
Q515350	0.0005	0.011	0.48	1.56	<10	23.3	0.15	0.057	0.13	0.015	25.1
Q515351	<0.0002	0.015	0.55	1.25	<10	17.7	0.18	0.049	0.1	0.02	23.9
Q515352	0.0009	0.008	0.56	1.3	<10	15.9	0.18	0.074	0.07	0.017	23.1
Q515354	0.0004	0.004	0.62	1.06	<10	14.1	0.16	0.055	0.03	0.028	25.8
Q515355	0.0008	0.017	0.37	1.38	<10	16.2	0.13	0.08	0.1	0.019	27.6
Q515356	0.0002	0.009	0.41	1.27	<10	18.1	0.12	0.072	0.09	0.015	20.1
Q515357	0.0015	0.014	0.37	1.24	<10	21.2	0.14	0.088	0.16	0.027	43.5
Q515358	0.0006	0.009	0.32	3.01	<10	18.8	0.13	0.136	0.13	0.012	34.6
Q515359	0.0009	0.01	0.45	1.06	<10	24.8	0.13	0.123	0.09	0.013	33
Q515360	0.0016	0.012	0.47	1.3	<10	26.3	0.15	0.123	0.13	0.02	43
Q515362	0.0002	0.01	0.39	1.34	<10	23.5	0.11	0.091	0.13	0.014	25.3
Q515363	0.001	0.011	0.43	1.12	<10	27.4	0.14	0.148	0.14	0.018	41.2
Q515364	0.0009	0.013	0.45	1.42	<10	25	0.15	0.148	0.15	0.021	47.1
Q515365	0.0004	0.014	0.43	1.56	<10	27.1	0.11	0.125	0.1	0.019	26.8
Q515366	0.0008	0.012	0.29	1.46	<10	18.3	0.13	0.126	0.1	0.018	33
Q515367	0.0006	0.013	0.37	2.32	<10	21.8	0.12	0.141	0.13	0.024	37.7
Q515368	0.001	0.013	0.34	1.54	<10	21.8	0.11	0.122	0.12	0.022	42.7
Q515370	0.0009	0.017	0.31	1.82	<10	19.9	0.13	0.319	0.13	0.017	36.7
Q515371	0.0006	0.015	0.44	2.71	<10	22.9	0.14	0.157	0.12	0.023	36.7
Q515372	0.0014	0.011	0.39	1.53	<10	19	0.14	0.161	0.09	0.017	29.9
Q515373	0.0008	0.012	0.41	2.1	<10	24.9	0.15	0.148	0.12	0.016	39.3
Q515374	0.0007	0.014	0.39	1.47	<10	20.1	0.14	0.115	0.12	0.016	35.5
Q515375	0.0007	0.034	0.49	1.97	<10	32.5	0.14	0.154	0.09	0.017	25
Q515376	0.0011	0.016	0.38	1.02	<10	24.6	0.11	0.141	0.11	0.019	29.6
Q515377	0.0014	0.01	0.57	5.18	<10	24.1	0.15	0.174	0.07	0.014	36.7
Q515378	0.0009	0.01	0.47	3.15	<10	32.2	0.15	0.163	0.13	0.021	46.5

Till Aqua Regia ICP-MS Results

	Au	Ag	Al	As	B	Ba	Be	Bi	Ca	Cd	Ce
	ppm	ppm	%	ppm	ppm	ppm	ppm	ppm	%	ppm	ppm
Q515379	0.0011	0.012	0.28	1.69	<10	18.8	0.1	0.128	0.12	0.018	39
Q515380	0.0004	0.01	0.35	2.9	<10	18.2	0.13	0.188	0.12	0.017	45
Q515381	0.0016	0.014	0.34	1.37	<10	22	0.12	0.142	0.11	0.02	36.5
Q515382	0.0013	0.013	0.35	1.6	<10	22.5	0.13	0.127	0.12	0.015	35.6
Q515384	0.0006	0.016	0.45	1.15	<10	25.5	0.15	0.133	0.13	0.026	35.1
Q515385	0.0011	0.013	0.32	1.83	<10	19.3	0.1	0.124	0.12	0.011	37
Q515386	0.0005	0.012	0.45	1.09	<10	20.5	0.12	0.099	0.1	0.019	36.2
Q515387	0.0007	0.01	0.47	1.39	<10	17.3	0.13	0.134	0.09	0.018	26.1
Q515388	0.0005	0.012	0.5	1.61	<10	20.3	0.15	0.1	0.1	0.027	35.7
Q515389	0.0008	0.007	0.24	0.62	<10	14.9	0.04	0.066	0.04	0.006	26.8
Q515390	0.0003	0.007	0.39	1.15	<10	12.3	0.12	0.079	0.07	0.02	22.2
Q515391	0.0042	0.013	0.45	1.61	<10	32.5	0.15	0.111	0.16	0.022	44.3
Q515392	0.0007	0.014	0.53	1.14	<10	32.6	0.18	0.068	0.14	0.019	30.9
Q515393	0.0003	0.012	0.54	1.98	<10	22.2	0.17	0.061	0.12	0.025	28.3
Q515394	0.0007	0.013	0.71	2.41	<10	41	0.22	0.111	0.17	0.023	38
Q515395	0.0006	0.012	0.68	1.81	<10	34.4	0.16	0.105	0.11	0.01	24.5
Q515396	0.0014	0.011	0.74	1.43	<10	35.9	0.26	0.082	0.18	0.026	35.5
Q515397	0.0004	0.014	0.55	1.28	<10	28.7	0.16	0.076	0.18	0.025	33.9
Q515398	<0.0002	0.017	0.74	2.2	<10	49.5	0.22	0.116	0.19	0.028	36
Q515399	<0.0002	0.007	0.46	2.22	<10	23.5	0.12	0.114	0.1	0.014	23.1
Q515400	<0.0002	0.006	0.28	0.08	<10	15.5	0.07	0.021	0.08	0.005	17.65
Q515401	<0.0002	0.01	0.44	0.6	<10	20.8	0.12	0.055	0.1	0.013	25.6
Q515402	0.0008	0.014	0.37	1.26	<10	22.5	0.13	0.115	0.13	0.019	34.2
Q515403	0.0002	0.012	0.32	0.99	<10	20	0.1	0.103	0.1	0.018	21.4
Q515404	<0.0002	0.008	0.28	1.31	<10	16	0.1	0.116	0.1	0.014	36.2
Q515405	0.0003	0.015	0.3	0.11	<10	16.1	0.11	0.157	0.11	0.015	32
Q515406	0.0007	0.013	0.64	2.74	<10	30.1	0.19	0.114	0.15	0.022	41.3
Q515407	<0.0002	0.014	0.56	1.54	<10	40.2	0.14	0.093	0.12	0.018	27.2
Q515408	<0.0002	0.01	0.41	0.92	<10	21.7	0.14	0.062	0.16	0.021	40.6
Q515409	<0.0002	0.011	0.46	0.77	<10	25.1	0.13	0.061	0.14	0.018	41.6
Q515410	0.0014	0.01	0.52	1.06	<10	31.5	0.16	0.082	0.18	0.026	37.7
Q515411	0.0002	0.01	0.46	0.78	<10	20.7	0.12	0.047	0.12	0.021	29.3
Q515412	<0.0002	0.014	0.43	0.92	<10	25.4	0.09	0.072	0.13	0.019	26.4
Q515413	0.0025	0.012	0.47	1.75	<10	25.5	0.14	0.119	0.13	0.022	35.1
Q515414	0.0005	0.011	0.22	0.75	<10	13.9	0.1	0.071	0.11	0.017	27
Q515415	<0.0002	0.01	0.37	1.63	<10	20.9	0.14	0.081	0.13	0.019	30.8
Q515416	<0.0002	0.009	0.43	0.62	<10	15.5	0.12	0.033	0.1	0.016	27.2
Q515417	<0.0002	0.008	0.44	0.76	<10	22	0.14	0.051	0.09	0.018	17.65
Q515418	<0.0002	0.016	0.36	0.43	<10	17.4	0.1	0.034	0.12	0.02	26.2
Q515419	<0.0002	0.01	0.46	0.98	<10	25.4	0.13	0.061	0.17	0.016	34.5
Q515420	<0.0002	0.012	0.56	1.86	<10	22.8	0.18	0.08	0.08	0.022	26.2

Till Aqua Regia ICP-MS Results

	Au	Ag	Al	As	B	Ba	Be	Bi	Ca	Cd	Ce
	ppm	ppm	%	ppm	ppm	ppm	ppm	ppm	%	ppm	ppm
Q515421	<0.0002	0.01	0.5	1.24	<10	24	0.13	0.056	0.13	0.014	26.1
Q515422	0.0002	0.013	0.39	1.23	<10	20.8	0.14	0.052	0.1	0.016	21.3
Q515423	0.0006	0.012	0.58	2.72	<10	39.5	0.17	0.139	0.16	0.022	39.6
Q515425	0.0005	0.01	0.62	1.37	<10	14.5	0.18	0.06	0.05	0.016	18.15
Q515426	<0.0002	0.011	0.93	2.28	<10	23	0.25	0.093	0.08	0.03	28.5
Q515427	<0.0002	0.01	0.63	1.32	<10	32.3	0.18	0.077	0.15	0.011	35.5
Q515428	<0.0002	0.008	0.4	0.84	<10	23.5	0.11	0.064	0.11	0.014	23.8
Q515429	<0.0002	0.012	0.55	0.73	<10	27.3	0.14	0.087	0.1	0.017	24.5
Q515430	<0.0002	0.009	0.58	1.12	<10	26.8	0.17	0.063	0.13	0.021	24
Q515431	0.0003	0.012	0.44	0.45	<10	24.4	0.13	0.068	0.17	0.02	36.4
Q515432	<0.0002	0.012	0.4	0.77	<10	21.6	0.11	0.057	0.11	0.014	21.4
Q515433	<0.0002	0.008	0.5	1.01	<10	16.8	0.16	0.04	0.11	0.019	28.5
Q515434	<0.0002	0.01	0.43	0.85	<10	27.1	0.12	0.096	0.13	0.018	37.1
Q515435	0.0007	0.012	0.42	1.37	<10	28	0.12	0.144	0.13	0.015	35.6
Q515436	<0.0002	0.009	0.34	0.89	<10	17.1	0.09	0.077	0.09	0.016	23.4
Q515437	0.0002	0.012	0.45	0.21	<10	24.7	0.09	0.088	0.1	0.013	30.5
Q515438	0.0002	0.01	0.45	1.16	<10	19.8	0.14	0.052	0.11	0.017	27.3
Q515439	0.001	0.012	0.35	1.94	<10	16	0.12	0.104	0.09	0.019	27.8
Q515440	0.0004	0.008	0.23	0.77	<10	14.2	0.08	0.076	0.1	0.013	24.1
Q515442	0.0009	0.011	0.26	1.56	<10	14.3	0.07	0.11	0.08	0.012	26.9
Q515443	0.0004	0.009	0.41	1.52	<10	21.4	0.13	0.1	0.12	0.016	36.6
Q515444	0.0006	0.008	0.55	1.91	<10	31.6	0.14	0.135	0.13	0.021	34.5
Q515445	0.0026	0.011	0.34	0.62	<10	23.3	0.12	0.11	0.16	0.021	46.2
Q515446	0.0005	0.009	0.42	1.31	<10	21.3	0.14	0.083	0.1	0.016	29.4
Q515447	0.0007	0.01	0.62	2.27	<10	38	0.19	0.127	0.13	0.018	30.7
Q515448	0.031	0.018	0.55	1.48	<10	33.7	0.18	0.111	0.12	0.025	33.5
Q515449	<0.0002	0.011	0.28	1.14	<10	17.3	0.08	0.076	0.1	0.011	25.5
Q515450	0.0157	0.014	0.38	0.32	<10	23	0.12	0.129	0.13	0.023	46.5
Q515451	0.138	0.023	0.44	1.38	<10	27.6	0.18	0.131	0.14	0.019	40.9
Q515452	0.0003	0.008	0.33	0.95	<10	20.9	0.11	0.099	0.12	0.02	34.6
Q515454	0.0005	0.009	0.51	1.07	<10	26.8	0.17	0.127	0.12	0.019	38.8
Q515455	0.0002	0.009	0.5	1.22	<10	16	0.15	0.13	0.06	0.018	30
Q515456	0.0005	0.01	0.39	0.15	<10	20.7	0.12	0.058	0.15	0.022	42.1
Q515457	0.001	0.014	0.73	1.71	<10	41.5	0.2	0.09	0.18	0.022	34.8
Q515458	0.0015	0.012	0.46	0.7	<10	26.5	0.14	0.063	0.17	0.022	36.8
Q515459	0.0007	0.011	0.42	0.64	<10	24.9	0.12	0.044	0.16	0.018	38.1
Q515460	0.0005	0.012	0.35	0.79	<10	21.6	0.1	0.065	0.14	0.016	34.4
Q515461	<0.0002	0.011	0.33	0.56	<10	17	0.1	0.026	0.08	0.011	17.85
Q515462	<0.0002	0.007	0.29	1.05	<10	15.1	0.08	0.039	0.09	0.016	23.3
Q515463	<0.0002	0.011	0.45	0.9	<10	22.5	0.15	0.05	0.1	0.013	21.9
Q515464	0.0004	0.011	0.48	0.99	<10	25.5	0.13	0.073	0.15	0.026	35.4

Till Aqua Regia ICP-MS Results

	Au	Ag	Al	As	B	Ba	Be	Bi	Ca	Cd	Ce
	ppm	ppm	%	ppm	ppm	ppm	ppm	ppm	%	ppm	ppm
Q515465	0.0003	0.007	0.39	1.56	<10	26.2	0.11	0.064	0.1	0.012	18.5
Q515466	0.0006	0.011	0.51	0.68	<10	27.9	0.15	0.061	0.16	0.021	34
Q515467	0.0002	0.01	0.44	1.24	<10	20.1	0.12	0.04	0.12	0.02	30.5
Q515468	0.0014	0.009	0.43	0.7	<10	22.6	0.14	0.057	0.15	0.018	32.4
Q515469	0.0004	0.009	0.38	1.11	<10	22.7	0.11	0.048	0.16	0.016	26.3
Q515470	0.0005	0.011	0.47	1.18	<10	26.6	0.15	0.052	0.21	0.02	34.8
Q515471	0.0002	0.01	0.48	1.41	<10	19.4	0.16	0.058	0.12	0.036	22
Q515472	0.0004	0.017	0.58	1.52	<10	17.7	0.16	0.054	0.11	0.026	23.7
Q515473	0.0003	0.008	0.49	0.75	<10	19.1	0.12	0.048	0.14	0.019	20.9
Q515474	0.0005	0.011	0.46	0.98	<10	26.4	0.14	0.048	0.21	0.021	37
Q515475	0.0004	0.01	0.47	1.29	<10	18.6	0.16	0.047	0.14	0.021	27

Till Aqua Regia

	Co	Cr	Cs	Cu	Fe	Ga	Ge	Hf	Hg	In	K
	ppm	ppm	ppm	ppm	%	ppm	ppm	ppm	ppm	ppm	%
Q515251	3.28	14.15	0.612	20.6	0.86	2.5	0.05	0.013	0.006	<0.005	0.06
Q515252	1.45	12.15	0.455	1.75	1.05	4.04	0.04	0.02	0.011	<0.005	0.02
Q515253	2.39	10.9	0.441	5.76	0.7	1.685	0.051	0.085	<0.004	<0.005	0.07
Q515254	3.69	18.3	0.71	7.63	1.49	4.35	0.052	0.025	0.016	0.01	0.06
Q515255	5.99	25.8	1.21	12.6	2.06	7.28	0.064	0.024	0.015	0.011	0.1
Q515256	4.02	15.2	0.879	9.37	1.24	3.55	0.05	0.014	0.01	0.005	0.11
Q515257	3.67	15	0.644	10.35	0.87	2.43	0.064	0.084	<0.004	0.006	0.08
Q515258L	5.77	23.6	1.18	18.75	1.29	3.8	0.067	0.041	0.004	0.011	0.12
Q515258U	3.75	14.2	0.58	9.33	0.87	2.36	0.069	0.086	<0.004	0.007	0.08
Q515260	2.3	10.9	0.526	13.9	0.7	1.58	0.043	0.029	<0.004	<0.005	0.07
Q515261	1.495	9.32	0.496	3.1	0.49	1.765	0.041	0.01	<0.004	<0.005	0.05
Q515262	1.5	8.41	0.43	5.15	0.51	1.505	0.044	0.016	0.004	<0.005	0.06
Q515263	1.82	8.07	0.428	5.29	0.51	1.43	0.038	0.022	<0.004	<0.005	0.06
Q515264	1.995	9.5	0.427	5.08	0.6	1.7	0.047	0.018	<0.004	<0.005	0.06
Q515265	1.275	7.41	0.355	4.24	0.45	1.255	0.051	0.014	<0.004	<0.005	0.06
Q515266	1.875	10.05	0.477	10	0.62	1.73	0.042	0.015	0.006	<0.005	0.07
Q515267	2.78	10.7	0.526	6.32	0.63	1.815	0.052	0.016	<0.004	0.005	0.08
Q515268	3.69	14.1	0.659	7.14	0.84	2.2	0.054	0.032	<0.004	0.006	0.09
Q515269	3	11.65	0.522	12.75	0.73	2.01	0.042	0.019	0.004	<0.005	0.06
Q515270	2.16	10.8	0.526	9.45	0.79	2.28	0.041	0.015	0.006	0.005	0.04
Q515271	3.43	12.75	0.585	13.05	0.77	2.07	0.048	0.068	0.004	0.007	0.06
Q515272	1.99	11.9	0.518	3.98	0.91	2.83	0.035	0.043	0.006	<0.005	0.03
Q515273	1.985	9.84	0.385	3.95	0.72	1.97	0.039	0.029	0.005	<0.005	0.04
Q515274	4.33	22.9	0.862	6.86	1.89	6.03	0.057	0.021	0.015	0.006	0.1
Q515275	2.16	11.35	0.564	4.6	0.97	2.47	0.032	0.019	0.004	<0.005	0.05
Q515276	2.56	12.3	0.609	13.45	0.73	2.16	0.056	0.024	<0.004	<0.005	0.08
Q515277	2.51	11.6	0.521	11.2	0.67	1.945	0.06	0.058	<0.004	0.007	0.07
Q515278	2.45	12.35	0.839	16	0.83	2.33	0.046	0.019	<0.004	0.006	0.08
Q515280	1.72	12.65	0.719	3.36	0.63	2.5	0.041	0.007	0.004	<0.005	0.09
Q515281	2.39	12.65	0.686	6.71	0.78	2.14	0.051	0.014	<0.004	0.006	0.08
Q515282	1.89	10.65	0.575	4.1	0.67	2.01	0.044	0.011	<0.004	0.008	0.07
Q515283	2.01	11.55	0.666	6.73	0.77	2.46	0.041	0.018	0.005	0.005	0.07
Q515284	2.73	10.4	0.524	8	0.63	1.68	0.062	0.036	<0.004	<0.005	0.09
Q515285	2.26	9.94	0.494	7.48	0.59	1.57	0.058	0.051	<0.004	0.005	0.09
Q515286	1.805	10.15	0.55	5.27	0.56	1.62	0.062	0.028	<0.004	0.005	0.09
Q515287	1.91	10.85	0.618	6.84	0.65	1.845	0.04	0.008	<0.004	0.007	0.08
Q515288	1.49	8.92	0.443	5.16	0.51	1.45	0.048	0.012	<0.004	<0.005	0.07
Q515289	1.85	10.05	0.474	8.05	0.57	1.705	0.07	0.021	<0.004	<0.005	0.07
Q515290	2.18	11.75	0.556	6.41	0.69	2.27	0.053	0.009	<0.004	<0.005	0.08
Q515291	1.585	8.62	0.43	6.4	0.49	1.625	0.057	0.016	<0.004	<0.005	0.06
Q515292	2.24	11.1	0.523	5.97	0.66	2	0.056	0.013	<0.004	<0.005	0.08

Till Aqua Regia

	Co	Cr	Cs	Cu	Fe	Ga	Ge	Hf	Hg	In	K
	ppm	ppm	ppm	ppm	%	ppm	ppm	ppm	ppm	ppm	%
Q515293	3.2	11.75	0.54	10.05	0.69	1.915	0.072	0.079	<0.004	<0.005	0.09
Q515294	1.77	9.91	0.488	6.02	0.57	1.87	0.04	0.014	0.005	0.006	0.08
Q515295	1.49	9.39	0.519	2.99	0.53	1.97	0.035	0.006	<0.004	<0.005	0.06
Q515296	2.19	11.7	0.59	7.88	0.73	1.915	0.074	0.034	<0.004	<0.005	0.09
Q515297	1.085	6.76	0.311	2.06	0.4	2.11	0.033	0.002	<0.004	<0.005	0.03
Q515298	5.33	21.4	1.105	19.9	1.16	3.74	0.071	0.034	0.006	0.008	0.12
Q515299	3.21	13.9	0.572	21.8	1	2.57	0.067	0.029	<0.004	<0.005	0.07
Q515300	4.59	20.2	0.962	12.45	1.28	4.23	0.058	0.028	<0.004	<0.005	0.08
Q515301	2.17	9.87	0.328	4.85	0.69	1.725	0.059	0.038	0.005	<0.005	0.04
Q515302	1.85	11.25	0.445	5.21	0.79	2.75	0.044	0.018	<0.004	<0.005	0.03
Q515303	3.62	11.8	0.62	12.65	0.83	2.5	0.047	0.012	<0.004	<0.005	0.07
Q515304	4.13	14.75	0.686	6.73	1	3.07	0.058	0.043	0.007	<0.005	0.09
Q515305	3.47	13.4	0.541	5.8	0.86	2.2	0.068	0.132	<0.004	0.005	0.08
Q515306	3.86	14.15	0.683	6.92	0.85	2.5	0.07	0.112	<0.004	<0.005	0.11
Q515307	2.89	10.55	0.403	6.3	0.71	1.945	0.048	0.025	<0.004	<0.005	0.05
Q515308	1.275	8.55	0.394	1.39	0.84	3.58	0.041	0.023	<0.004	<0.005	0.02
Q515309	2.12	12.7	0.435	2.67	1.1	3.24	0.048	0.033	0.014	0.008	0.03
Q515311	3.16	12.9	0.414	4.98	0.95	2.38	0.067	0.034	0.007	<0.005	0.03
Q515312	3.27	13.9	0.694	8.82	0.74	2.95	0.069	0.03	<0.004	0.007	0.06
Q515313	3.29	13.85	0.571	19.3	0.8	2.61	0.065	0.034	<0.004	<0.005	0.06
Q515314	1.755	8.85	0.36	8.97	0.65	1.94	0.053	0.028	<0.004	<0.005	0.04
Q515315	1.275	9.38	0.601	1.77	0.38	2.66	0.058	0.002	<0.004	<0.005	0.06
Q515316	1.995	11.3	0.656	4.77	0.56	1.99	0.063	0.031	<0.004	<0.005	0.08
Q515317	2.11	11.3	0.589	4.62	0.64	1.95	0.049	0.021	<0.004	<0.005	0.07
Q515318	1.545	9.32	0.465	4.2	0.54	1.88	0.053	0.01	<0.004	<0.005	0.06
Q515319	1.84	9.35	0.483	5.91	0.55	1.82	0.05	0.01	<0.004	<0.005	0.07
Q515320	1.515	8.91	0.422	4.62	0.51	1.8	0.052	0.012	<0.004	<0.005	0.06
Q515321	1.42	8.45	0.361	4.33	0.47	1.43	0.039	0.014	<0.004	<0.005	0.06
Q515322	1.55	8.64	0.397	4.87	0.52	1.535	0.061	0.017	<0.004	<0.005	0.06
Q515323	1.835	8.97	0.391	6.21	0.54	1.52	0.055	0.042	<0.004	<0.005	0.07
Q515324	1.52	9.75	0.443	5.05	0.54	1.72	0.047	0.013	<0.004	<0.005	0.07
Q515325	1.33	8.92	0.368	4.29	0.37	1.52	0.058	0.011	<0.004	<0.005	0.06
Q515326	1.435	8.58	0.353	5.35	0.47	1.45	0.052	0.011	<0.004	<0.005	0.06
Q515327	1.49	8.7	0.356	6.11	0.46	1.34	0.047	0.06	<0.004	<0.005	0.06
Q515328	1.555	9.65	0.439	5.26	0.5	1.615	0.051	0.026	<0.004	<0.005	0.07
Q515329	1.97	12.4	0.719	7.61	0.57	2.13	0.043	0.018	<0.004	0.007	0.09
Q515330	1.605	9.31	0.417	5.16	0.5	1.545	0.041	0.016	<0.004	<0.005	0.07
Q515331	1.765	11.05	0.454	6.68	0.56	1.775	0.059	0.029	<0.004	0.005	0.07
Q515332	0.985	7.97	0.486	1.54	0.26	1.69	0.043	0.004	<0.004	<0.005	0.05
Q515333	3.03	15.6	0.798	6.97	0.77	2.49	0.06	0.016	0.004	0.008	0.09
Q515334	1.65	11	0.476	5.2	0.57	1.8	0.058	0.041	<0.004	0.005	0.07

Till Aqua Regia

	Co	Cr	Cs	Cu	Fe	Ga	Ge	Hf	Hg	In	K
	ppm	ppm	ppm	ppm	%	ppm	ppm	ppm	ppm	ppm	%
Q515335	1.83	11.45	0.506	7.05	0.6	1.785	0.062	0.051	<0.004	0.006	0.08
Q515336	2.06	10.8	0.445	9.42	0.66	1.88	0.045	0.029	0.005	0.006	0.06
Q515337	1.845	10.1	0.364	4.33	0.66	2.02	0.036	0.028	<0.004	0.006	0.04
Q515338	2.52	12.05	0.379	6.22	0.71	1.92	0.039	0.019	0.008	0.006	0.05
Q515339	2.13	12.95	0.446	3.89	0.99	4.58	0.026	0.037	0.006	<0.005	0.03
Q515340	2.41	11.55	0.43	4.37	0.85	2.48	0.041	0.047	0.006	0.005	0.03
Q515341	2.99	9.73	0.301	6.41	0.62	1.58	0.042	0.04	<0.004	0.005	0.05
Q515342	2.41	12.25	0.472	5.24	0.7	1.94	0.044	0.054	<0.004	0.006	0.07
Q515343	4.43	21.4	1.065	13.4	1.15	3.73	0.056	0.028	<0.004	0.009	0.11
Q515344	3.79	15.1	0.656	7.33	0.84	2.45	0.059	0.05	<0.004	<0.005	0.08
Q515345	2.55	14.35	0.66	3.78	0.92	3.24	0.039	0.024	0.006	0.007	0.05
Q515346	2.79	13.7	0.561	6.11	0.86	2.47	0.039	0.042	0.005	0.006	0.06
Q515347	3.84	14.7	0.661	7.29	0.87	2.49	0.05	0.092	0.004	0.008	0.09
Q515348	2.38	12.45	0.544	6.71	0.76	2.2	0.038	0.027	<0.004	0.008	0.07
Q515349	3.89	15	0.641	10.05	0.89	2.5	0.054	0.078	<0.004	0.007	0.09
Q515350	2.93	13.9	0.612	8.81	0.79	2.51	0.047	0.036	<0.004	0.005	0.06
Q515351	2.69	12.25	0.476	9.94	0.75	1.975	0.038	0.03	<0.004	0.005	0.05
Q515352	2.33	12.45	0.575	4.9	0.83	2.85	0.037	0.033	<0.004	0.006	0.04
Q515354	1.6	12.55	0.449	2.58	0.98	3.51	0.038	0.016	0.014	<0.005	0.02
Q515355	1.93	9.61	0.441	5.98	0.55	1.805	0.047	0.031	0.004	0.005	0.05
Q515356	1.895	10.85	0.464	5.79	0.61	1.955	0.038	0.045	0.004	0.005	0.06
Q515357	2.69	11.95	0.502	11.1	0.62	1.95	0.065	0.058	<0.004	<0.005	0.07
Q515358	1.595	11	0.474	6.4	0.68	1.96	0.055	0.019	<0.004	0.006	0.06
Q515359	2.29	14.4	0.83	7.05	0.75	2.68	0.054	0.009	<0.004	<0.005	0.08
Q515360	2.36	14.25	0.784	6.59	0.69	2.69	0.073	0.017	<0.004	0.007	0.09
Q515362	1.93	10.75	0.528	4.75	0.7	1.955	0.05	0.026	0.006	<0.005	0.07
Q515363	2.18	11.8	0.643	8.1	0.62	2.1	0.073	0.038	<0.004	0.005	0.09
Q515364	2.34	12.55	0.629	11	0.72	2.15	0.074	0.015	0.005	<0.005	0.1
Q515365	2.43	12.75	0.707	7.82	0.69	2.37	0.049	0.009	<0.004	<0.005	0.09
Q515366	1.66	8.18	0.365	6.87	0.47	1.385	0.048	0.018	<0.004	<0.005	0.06
Q515367	1.865	10.65	0.437	6.66	0.61	1.835	0.062	0.031	0.006	<0.005	0.07
Q515368	1.755	10.05	0.463	7.04	0.56	1.695	0.068	0.024	0.006	<0.005	0.07
Q515370	1.65	9.66	0.393	7.41	0.52	1.51	0.051	0.034	0.004	<0.005	0.07
Q515371	2.21	12.5	0.491	9.08	0.67	1.85	0.063	0.029	0.004	<0.005	0.08
Q515372	1.545	10.3	0.467	6.06	0.45	1.65	0.049	0.013	0.004	<0.005	0.06
Q515373	2.01	11.9	0.553	7.47	0.61	1.935	0.066	0.032	0.005	<0.005	0.08
Q515374	2.57	10.7	0.443	8.39	0.63	1.76	0.056	0.033	0.004	<0.005	0.07
Q515375	2.79	17.7	0.907	7.55	0.79	2.72	0.046	0.017	0.004	0.006	0.12
Q515376	1.86	12.05	0.576	5.26	0.58	2.18	0.05	0.016	<0.004	<0.005	0.08
Q515377	2.25	16.1	0.879	5.83	0.91	3.25	0.053	0.009	0.007	<0.005	0.08
Q515378	2.45	15.05	0.72	9.85	0.81	2.21	0.075	0.052	0.005	0.006	0.12

Till Aqua Regia

	Co	Cr	Cs	Cu	Fe	Ga	Ge	Hf	Hg	In	K
	ppm	ppm	ppm	ppm	%	ppm	ppm	ppm	ppm	ppm	%
Q515379	1.55	9.59	0.374	5.6	0.51	1.45	0.056	0.023	<0.004	<0.005	0.06
Q515380	1.76	10.95	0.499	5.61	0.64	2.14	0.066	0.014	0.004	<0.005	0.06
Q515381	1.87	11	0.525	6.03	0.58	1.86	0.056	0.024	0.005	<0.005	0.08
Q515382	1.99	11.05	0.522	6.51	0.58	1.73	0.061	0.027	<0.004	<0.005	0.08
Q515384	2.73	12.75	0.669	16.05	0.7	2.13	0.062	0.019	0.005	0.007	0.1
Q515385	1.495	9.71	0.446	4.02	0.52	1.675	0.057	0.022	<0.004	<0.005	0.06
Q515386	2.01	10.5	0.484	4.54	0.62	1.92	0.055	0.02	0.004	<0.005	0.06
Q515387	1.9	9.87	0.397	5.38	0.63	1.845	0.04	0.018	0.005	<0.005	0.05
Q515388	2.37	10.35	0.445	6.27	0.66	1.76	0.054	0.039	0.006	<0.005	0.06
Q515389	1.4	10.45	0.696	1.36	0.72	3.13	0.046	0.021	0.004	<0.005	0.04
Q515390	1.59	10	0.462	3.35	0.75	2.22	0.037	0.022	0.004	0.005	0.03
Q515391	2.9	14.55	0.735	9.33	0.76	2.2	0.074	0.115	0.004	0.006	0.12
Q515392	4.22	17.45	0.783	7.71	0.9	2.57	0.056	0.048	<0.004	0.005	0.1
Q515393	3.38	14.25	0.598	5.52	0.88	2.49	0.047	0.061	0.005	<0.005	0.06
Q515394	5.19	19.2	1.065	9.9	1.13	3.38	0.06	0.065	<0.004	0.008	0.16
Q515395	2.7	16.5	1.145	5.93	0.82	3.75	0.04	0.011	0.004	0.007	0.1
Q515396	6.07	19.4	0.962	10.75	1.14	3.26	0.056	0.105	0.005	0.005	0.13
Q515397	4.19	17.75	0.682	10.1	0.93	2.98	0.073	0.072	0.004	0.009	0.1
Q515398	5.86	25.7	1.155	11.9	1.25	3.97	0.08	0.114	0.008	0.01	0.21
Q515399	2.5	15.45	0.583	4.93	0.81	2.49	0.056	0.022	0.007	0.005	0.08
Q515400	1.28	8.77	0.387	1.27	0.39	2.04	0.041	0.006	0.009	<0.005	0.05
Q515401	2.28	12.35	0.652	3.16	0.73	2.88	0.059	0.013	0.006	0.006	0.09
Q515402	2.4	13.05	0.538	6.79	0.67	2.08	0.065	0.018	0.004	<0.005	0.09
Q515403	1.64	10.5	0.454	5.29	0.54	1.685	0.046	0.015	0.004	<0.005	0.07
Q515404	1.595	9.71	0.381	6.76	0.51	1.85	0.068	0.016	0.006	<0.005	0.05
Q515405	1.435	8.62	0.387	6.55	0.32	1.62	0.051	0.013	0.006	<0.005	0.06
Q515406	4.21	21.5	0.911	20.9	1.03	3.82	0.08	0.073	0.007	0.01	0.13
Q515407	3.36	22.8	1.04	6.65	0.9	3.16	0.065	0.023	0.004	<0.005	0.16
Q515408	3.2	14.1	0.546	6.91	0.77	2.43	0.082	0.09	0.004	0.006	0.1
Q515409	3.44	16.15	0.592	6.16	0.81	2.69	0.072	0.043	0.004	<0.005	0.12
Q515410	3.85	18.1	0.787	9.2	0.92	2.82	0.077	0.072	0.004	0.007	0.14
Q515411	2.87	12.5	0.421	5.31	0.75	2.33	0.063	0.025	0.007	<0.005	0.07
Q515412	2.72	13.9	0.532	5.61	0.73	2.25	0.06	0.037	0.006	<0.005	0.09
Q515413	2.39	15.25	0.662	6.21	0.78	2.78	0.072	0.027	0.007	0.007	0.1
Q515414	1.5	8.35	0.33	5.66	0.43	1.175	0.052	0.058	0.007	<0.005	0.06
Q515415	2.99	13.1	0.463	7.79	0.64	2.02	0.057	0.049	0.005	0.006	0.08
Q515416	2.59	12.25	0.43	4.72	0.71	2.41	0.06	0.029	0.008	0.005	0.07
Q515417	2.39	12.45	0.574	4.9	0.71	2.53	0.04	0.021	0.006	0.005	0.07
Q515418	2.41	11.05	0.442	3.54	0.73	2.17	0.055	0.017	<0.004	<0.005	0.07
Q515419	3.69	15.65	0.643	7.29	0.88	2.59	0.07	0.102	0.005	0.007	0.11
Q515420	3.13	17.85	0.77	4.02	1.13	3.89	0.049	0.017	0.006	0.005	0.08

Till Aqua Regia

	Co	Cr	Cs	Cu	Fe	Ga	Ge	Hf	Hg	In	K
	ppm	ppm	ppm	ppm	%	ppm	ppm	ppm	ppm	ppm	%
Q515421	3.24	15.4	0.619	5.43	0.92	2.85	0.055	0.022	<0.004	0.005	0.09
Q515422	2.59	11.5	0.493	5.2	0.65	1.98	0.038	0.014	0.006	<0.005	0.07
Q515423	4.84	19.5	0.873	9.44	0.97	2.91	0.078	0.098	0.006	0.005	0.16
Q515425	2.2	11.9	0.495	3.42	0.86	2.64	0.051	0.034	0.009	0.006	0.05
Q515426	3.07	18.6	0.764	5.28	1.14	3.44	0.054	0.038	0.015	0.01	0.06
Q515427	3.96	18.5	0.821	8.7	1.04	3.12	0.066	0.058	0.006	0.009	0.13
Q515428	2.91	12.9	0.595	4.25	0.73	2.43	0.061	0.02	<0.004	0.006	0.11
Q515429	3.33	13.05	0.714	4.76	0.78	2.61	0.059	0.03	0.005	0.005	0.14
Q515430	4.01	12.9	0.719	6.69	0.96	3.03	0.063	0.028	0.013	0.006	0.13
Q515431	3.32	14	0.603	6.95	0.79	2.44	0.067	0.102	0.005	0.005	0.1
Q515432	2.2	12.4	0.503	4.67	0.68	2.1	0.043	0.035	0.007	<0.005	0.07
Q515433	2.27	11.05	0.454	4.42	0.72	2.22	0.054	0.029	0.007	<0.005	0.06
Q515434	2.97	13.55	0.661	8.15	0.75	2.14	0.06	0.047	<0.004	0.006	0.11
Q515435	2.35	12.55	0.633	6.97	0.72	1.975	0.066	0.074	<0.004	<0.005	0.12
Q515436	1.985	10.65	0.456	3.67	0.71	2.2	0.041	0.009	0.004	<0.005	0.07
Q515437	1.95	11.9	0.657	2.35	0.59	2.6	0.058	0.012	0.005	<0.005	0.1
Q515438	2.5	9.2	0.453	6.09	0.67	2.01	0.048	0.021	<0.004	<0.005	0.08
Q515439	1.795	8.51	0.329	6.32	0.49	1.32	0.043	0.03	0.005	<0.005	0.06
Q515440	2.3	7.19	0.307	6.17	0.43	1.135	0.038	0.03	<0.004	<0.005	0.06
Q515442	1.115	7.48	0.369	4.13	0.43	1.425	0.045	0.009	0.004	<0.005	0.05
Q515443	2.06	11.35	0.484	5.32	0.72	2.08	0.066	0.007	0.006	<0.005	0.09
Q515444	3.51	15.7	0.802	11.5	0.87	2.46	0.064	0.037	0.005	<0.005	0.14
Q515445	2.62	11.7	0.627	10.7	0.62	1.96	0.081	0.074	0.004	<0.005	0.09
Q515446	2.01	10.85	0.46	8.27	0.67	1.85	0.046	0.029	0.006	<0.005	0.07
Q515447	3.87	18.1	0.948	10.9	0.97	2.89	0.059	0.025	0.007	0.008	0.16
Q515448	3.58	16.25	0.85	11.85	0.83	2.61	0.066	0.01	0.006	0.005	0.15
Q515449	1.475	8.35	0.381	4.65	0.43	1.36	0.043	0.009	<0.004	<0.005	0.06
Q515450	1.89	11.35	0.528	8.33	0.55	1.875	0.07	0.031	<0.004	<0.005	0.1
Q515451	3.11	13.2	0.687	12.15	0.68	2.09	0.073	0.05	0.004	<0.005	0.11
Q515452	2.25	10.05	0.451	8.69	0.56	1.65	0.061	0.064	<0.004	<0.005	0.08
Q515454	2.7	13.1	0.627	9.97	0.75	2.36	0.064	0.023	<0.004	0.006	0.09
Q515455	1.78	11.15	0.513	6.04	0.75	2.31	0.059	0.019	0.005	<0.005	0.04
Q515456	2.07	11.8	0.516	6.81	0.56	2.05	0.078	0.111	<0.004	<0.005	0.09
Q515457	4.67	21	1.03	12.4	1.28	3.58	0.069	0.216	<0.004	0.008	0.18
Q515458	3.23	15	0.648	7.28	0.87	2.51	0.073	0.128	<0.004	0.005	0.1
Q515459	3.05	14.85	0.575	5.6	0.83	2.49	0.063	0.11	<0.004	0.006	0.09
Q515460	2.5	12.25	0.468	4.47	0.62	1.965	0.059	0.048	0.004	0.009	0.07
Q515461	2.91	9.38	0.412	3.88	0.55	1.585	0.036	0.04	<0.004	<0.005	0.05
Q515462	1.76	11	0.354	2.91	0.62	2.08	0.045	0.008	0.009	0.005	0.05
Q515463	2.27	10.95	0.45	5.86	0.72	2.05	0.048	0.024	0.006	<0.005	0.07
Q515464	3.1	14.5	0.628	8.57	0.84	2.36	0.071	0.021	0.008	0.008	0.1

Till Aqua Regia

	Co	Cr	Cs	Cu	Fe	Ga	Ge	Hf	Hg	In	K
	ppm	ppm	ppm	ppm	%	ppm	ppm	ppm	ppm	ppm	%
Q515465	2.1	12	0.517	5.08	0.7	1.955	0.041	0.02	<0.004	<0.005	0.09
Q515466	2.94	15.4	0.641	8.3	0.85	2.58	0.064	0.038	0.005	<0.005	0.1
Q515467	3.05	12.1	0.408	4.01	0.76	2.01	0.052	0.04	<0.004	0.005	0.06
Q515468	2.88	13	0.506	6.07	0.83	2.27	0.056	0.081	0.004	<0.005	0.08
Q515469	2.99	12.25	0.469	6.55	0.73	1.9	0.049	0.048	<0.004	0.005	0.06
Q515470	3.45	15.4	0.665	8.93	0.9	2.47	0.067	0.081	<0.004	0.006	0.09
Q515471	2.72	12.25	0.455	4.76	0.8	2.66	0.047	0.023	<0.004	<0.005	0.05
Q515472	2.73	12.95	0.474	5.45	0.85	2.51	0.044	0.035	0.012	0.006	0.05
Q515473	2.02	11.7	0.513	3.52	0.57	2.13	0.042	0.012	<0.004	<0.005	0.06
Q515474	4.01	14.55	0.66	6.65	0.89	2.53	0.067	0.127	<0.004	0.006	0.1
Q515475	2.19	11.8	0.401	4.88	0.74	1.855	0.05	0.032	<0.004	<0.005	0.05

Till Aqua Regia

	La	Li	Mg	Mn	Mo	Na	Nb	Ni	P	Pb	Pd
	ppm	ppm	%	ppm	ppm	%	ppm	ppm	%	ppm	ppm
Q515251	14.45	13.3	0.22	59.9	0.27	0.009	0.685	11.95	0.035	2.67	<0.001
Q515252	10.6	8.3	0.11	31.9	0.48	0.007	1.2	3.54	0.019	3.1	<0.001
Q515253	14.9	9.7	0.18	59.5	0.16	0.009	0.364	6.36	0.057	2.14	<0.001
Q515254	9.54	11.6	0.26	80.8	0.56	0.007	1.23	9.6	0.029	2.72	0.001
Q515255	12.85	16.7	0.42	147.5	0.97	0.009	1.625	13.1	0.042	4.06	<0.001
Q515256	10.15	11.1	0.31	87.7	0.59	<0.001	0.805	9.98	0.038	2.58	<0.001
Q515257	18.5	10.1	0.25	92.1	0.21	0.01	0.375	9.35	0.054	2.2	<0.001
Q515258L	14.95	17.3	0.36	129	0.44	0.011	0.837	15.55	0.047	2.93	<0.001
Q515258U	17	10.4	0.23	90.7	0.18	0.01	0.423	9	0.06	2.17	<0.001
Q515260	10.8	8.6	0.16	55.5	0.37	0.006	0.43	8.02	0.047	1.945	<0.001
Q515261	9.41	6.1	0.14	36.8	0.28	0.003	0.438	4.86	0.031	1.52	<0.001
Q515262	10.9	6.9	0.12	35.9	0.31	0.005	0.368	5.24	0.043	1.71	0.001
Q515263	8.96	7.6	0.13	38.7	0.28	0.004	0.303	5.59	0.038	1.555	<0.001
Q515264	12	8.2	0.15	47.4	0.49	0.006	0.414	5.67	0.043	1.885	<0.001
Q515265	13.95	6.6	0.12	34.2	0.39	0.004	0.29	4.74	0.052	1.86	<0.001
Q515266	9.73	9	0.14	40.4	0.41	0.008	0.47	7.13	0.041	1.955	<0.001
Q515267	12.15	8.8	0.16	60.3	0.78	0.006	0.456	6.5	0.05	2.04	<0.001
Q515268	13.45	11.2	0.23	80.8	0.17	0.009	0.578	9.93	0.053	2.28	<0.001
Q515269	11.05	12	0.19	63.3	0.31	0.006	0.509	9.45	0.041	1.995	<0.001
Q515270	8.77	7.9	0.16	46.3	0.37	0.006	0.567	6.52	0.035	2.02	<0.001
Q515271	13.65	10.7	0.2	74.4	0.34	0.005	0.523	8.55	0.034	2.41	<0.001
Q515272	10.55	9.9	0.17	45.1	0.24	0.005	0.747	5.55	0.018	2.11	<0.001
Q515273	8.4	8.6	0.14	43.3	0.15	0.006	0.513	5.09	0.032	1.465	<0.001
Q515274	9.98	13.1	0.34	85.9	0.72	0.008	1.42	9.82	0.06	4.01	<0.001
Q515275	5.89	9.3	0.18	51.7	0.28	0.007	0.662	6.04	0.018	1.755	<0.001
Q515276	14.55	11.5	0.21	60.6	0.2	0.008	0.566	9.26	0.049	2.16	<0.001
Q515277	16.1	10.3	0.19	62.4	0.17	0.007	0.365	8.56	0.054	2.04	<0.001
Q515278	11.3	12.5	0.2	48.2	0.64	0.006	0.554	9.32	0.039	2.55	<0.001
Q515280	12.4	6	0.18	38.4	0.43	0.007	0.618	5.34	0.009	1.615	<0.001
Q515281	11.9	10	0.2	55.9	0.57	0.007	0.619	7.11	0.043	2.06	<0.001
Q515282	10.9	7.7	0.17	48	0.53	0.005	0.515	5.49	0.039	1.97	0.001
Q515283	8.53	9.3	0.18	43.5	0.58	0.008	0.589	5.88	0.028	1.93	<0.001
Q515284	19.55	8.9	0.16	60.5	0.35	0.007	0.358	6.46	0.06	2.45	<0.001
Q515285	16.6	9	0.15	54.4	0.55	0.008	0.378	6.76	0.056	2.41	<0.001
Q515286	19.2	8.7	0.16	47.1	0.35	0.008	0.437	6.43	0.06	2.57	<0.001
Q515287	11.55	8.9	0.16	46.3	0.73	0.007	0.445	6.45	0.046	2.32	<0.001
Q515288	15.2	7.7	0.13	38.4	0.43	0.005	0.387	5.72	0.049	2.12	<0.001
Q515289	16.55	7.5	0.14	43.2	0.49	0.005	0.468	6.72	0.05	2.31	0.001
Q515290	15	9	0.17	48	0.78	0.006	0.616	6.79	0.042	2.36	<0.001
Q515291	12.65	7.5	0.12	36.1	0.61	0.005	0.399	5.92	0.051	1.955	0.003
Q515292	15.5	8.7	0.16	49.2	0.82	0.005	0.596	6.86	0.051	2.36	<0.001

Till Aqua Regia

	La	Li	Mg	Mn	Mo	Na	Nb	Ni	P	Pb	Pd
	ppm	ppm	%	ppm	ppm	%	ppm	ppm	%	ppm	ppm
Q515293	20.6	8.8	0.18	65.1	0.43	0.009	0.452	8.1	0.061	2.58	0.001
Q515294	11.4	8.5	0.15	39.7	0.56	0.006	0.45	6.37	0.045	2.02	<0.001
Q515295	16.15	5.3	0.14	33.1	0.6	0.004	0.488	4.3	0.012	1.75	0.001
Q515296	17.65	9.3	0.18	53.1	0.5	0.008	0.646	7.27	0.052	2.45	0.001
Q515297	8.13	4.3	0.1	24.8	0.24	0.004	0.411	3.07	0.018	1.65	<0.001
Q515298	18.15	15.3	0.34	91.5	0.26	0.011	1.055	15.2	0.049	3.01	0.002
Q515299	17.45	12.3	0.23	69.1	0.39	0.007	0.848	11.15	0.044	2.94	<0.001
Q515300	18.4	14.8	0.33	89.8	0.36	0.01	1.28	13.65	0.03	3.07	0.003
Q515301	14.15	7.2	0.14	48.8	0.15	0.006	0.548	5.89	0.041	2.41	<0.001
Q515302	10.05	7.7	0.16	43.6	0.27	0.007	0.746	5.74	0.025	1.855	<0.001
Q515303	9.49	12.4	0.2	72.7	0.35	0.007	0.659	10.1	0.038	2.11	0.001
Q515304	14.95	11.6	0.23	96.2	0.26	0.008	0.958	9.15	0.044	2.3	<0.001
Q515305	17.2	8.9	0.22	97.6	0.13	0.01	0.266	7.38	0.055	1.95	0.001
Q515306	19.65	11.2	0.23	86.9	0.15	0.009	0.336	8.99	0.058	2.07	0.002
Q515307	11.6	7.8	0.16	68.4	0.15	0.007	0.526	6.7	0.041	1.84	0.001
Q515308	7.8	4.9	0.1	31.3	0.21	0.004	0.868	3.22	0.016	1.735	0.002
Q515309	9.35	8.5	0.15	42.3	0.21	0.004	1.08	5.08	0.025	2.52	0.002
Q515311	10.6	10.5	0.16	50.9	0.22	0.005	0.839	8.17	0.026	2.62	<0.001
Q515312	14.4	11.4	0.24	64.5	0.17	0.009	0.823	9.82	0.036	2.26	0.003
Q515313	19.25	11.6	0.24	62.8	0.19	0.01	0.713	11.4	0.045	2.77	<0.001
Q515314	11.2	8	0.13	37.1	0.53	0.006	0.746	6.27	0.04	2.11	<0.001
Q515315	14.75	5	0.14	35	0.11	0.006	0.538	4.18	0.021	1.87	<0.001
Q515316	20.7	8.9	0.17	49.5	0.19	0.007	0.606	6.72	0.055	2.24	0.001
Q515317	12.5	7.7	0.17	49	0.36	0.006	0.669	6.26	0.043	2.02	<0.001
Q515318	14	7.1	0.14	37.9	0.51	0.006	0.508	5.04	0.046	1.84	0.001
Q515319	15.1	8.2	0.15	41.4	0.63	0.006	0.558	6.09	0.043	2.03	<0.001
Q515320	13.95	7.3	0.13	35.4	0.72	0.005	0.455	5.75	0.041	1.97	0.001
Q515321	16.5	6.3	0.12	35	0.47	0.006	0.412	4.73	0.051	2.15	<0.001
Q515322	17.5	6.6	0.12	37.7	0.43	0.006	0.408	5.18	0.052	2.17	0.001
Q515323	16.15	7.3	0.13	41.5	0.57	0.008	0.492	5.76	0.054	2.24	<0.001
Q515324	17.85	7	0.14	40.2	0.32	0.008	0.516	5.38	0.053	2.25	<0.001
Q515325	15.1	6.7	0.12	35.3	0.17	0.006	0.326	5.13	0.057	2.05	<0.001
Q515326	13.85	6.5	0.11	35	0.34	0.005	0.293	5.12	0.053	2.14	<0.001
Q515327	14	6.6	0.12	35.4	0.24	0.005	0.306	5.56	0.05	2.11	<0.001
Q515328	13.3	7.3	0.13	39.2	0.4	0.007	0.38	5.74	0.054	1.945	0.001
Q515329	10.5	9	0.18	40.3	0.54	0.006	0.425	7.41	0.04	1.76	<0.001
Q515330	11.8	7.7	0.13	41.4	0.47	0.007	0.333	5.46	0.054	1.82	<0.001
Q515331	15.7	8.7	0.15	44.6	0.52	0.007	0.457	6.22	0.057	2.26	<0.001
Q515332	13	5.7	0.1	27.2	0.08	0.005	0.31	3.73	0.028	1.575	<0.001
Q515333	16.15	12.5	0.22	60.8	0.35	0.007	0.663	8.07	0.055	2.54	<0.001
Q515334	16.75	8.7	0.14	44.1	0.29	0.006	0.486	5.66	0.055	2.26	<0.001

Till Aqua Regia

	La	Li	Mg	Mn	Mo	Na	Nb	Ni	P	Pb	Pd
	ppm	ppm	%	ppm	ppm	%	ppm	ppm	%	ppm	ppm
Q515335	18.5	9.1	0.15	47.8	0.31	0.007	0.483	6.07	0.054	2.49	<0.001
Q515336	11.3	9.2	0.15	46.7	0.29	0.007	0.483	6.72	0.049	2.16	<0.001
Q515337	8.29	8	0.15	45.4	0.15	0.007	0.579	5.36	0.042	1.62	<0.001
Q515338	9.2	9.2	0.16	50.5	0.15	0.007	0.545	6.37	0.042	1.78	0.001
Q515339	8.7	8.6	0.12	34	0.29	0.006	0.944	4.97	0.012	2.63	<0.001
Q515340	9.06	9.3	0.15	44.1	0.19	0.007	0.655	5.61	0.026	1.755	<0.001
Q515341	9.42	7.8	0.14	63.5	0.13	0.008	0.337	6.64	0.043	1.54	<0.001
Q515342	10.15	10.3	0.18	61.3	0.2	0.008	0.53	6.96	0.046	1.64	<0.001
Q515343	15.4	16.7	0.32	94.5	0.31	0.01	0.923	11.7	0.049	2.98	<0.001
Q515344	14.35	12.1	0.23	92.3	0.16	0.008	0.455	8.69	0.048	2.18	<0.001
Q515345	9.59	10.8	0.19	56.5	0.3	0.006	0.75	6.64	0.03	2.46	0.002
Q515346	9.23	11.6	0.18	60.8	0.26	0.006	0.679	7.37	0.036	2.35	<0.001
Q515347	13.25	11.7	0.25	96.2	0.17	0.011	0.333	7.99	0.044	1.845	0.001
Q515348	9.7	10.4	0.18	55.6	0.2	0.006	0.5	6.81	0.042	1.875	<0.001
Q515349	13.3	13.1	0.25	109	0.24	0.01	0.367	9.45	0.049	2.18	0.001
Q515350	10.45	11.9	0.22	69.6	0.31	0.009	0.639	9.01	0.041	2	<0.001
Q515351	9.69	10.6	0.16	54.9	0.22	0.007	0.522	7.9	0.038	2.49	<0.001
Q515352	9.51	11.5	0.18	48.9	0.28	0.007	0.739	6.24	0.023	2.26	<0.001
Q515354	10.7	7.1	0.09	28.8	0.16	0.006	0.689	3.87	0.021	2.44	<0.001
Q515355	11.3	9	0.13	39.8	0.27	0.007	0.468	6.59	0.039	2.07	<0.001
Q515356	8.29	9.1	0.16	44.8	0.28	0.008	0.549	5.33	0.032	1.75	<0.001
Q515357	17.9	9.8	0.17	61.2	0.29	0.008	0.341	7.48	0.058	2.43	<0.001
Q515358	14.1	8.2	0.13	40.9	0.66	0.006	0.5	5.63	0.061	2.82	<0.001
Q515359	13.6	11.7	0.19	60.9	0.4	0.006	0.699	6.52	0.03	2.35	<0.001
Q515360	18.5	12.2	0.21	59.4	0.33	0.01	0.699	6.86	0.052	2.54	<0.001
Q515362	11.35	9	0.17	46.8	0.34	0.008	0.604	5.92	0.051	2.07	0.002
Q515363	18.55	10.2	0.18	52.7	0.33	0.011	0.659	6.76	0.058	2.65	<0.001
Q515364	23	10.9	0.19	56.4	0.45	0.011	0.637	7.36	0.06	2.72	0.001
Q515365	12.2	10	0.18	50.7	0.6	0.01	0.624	6.97	0.044	2.26	<0.001
Q515366	14.9	7.5	0.11	34	0.43	0.009	0.375	5.52	0.049	2.27	<0.001
Q515367	17.05	8.4	0.14	44.2	0.39	0.01	0.548	6.02	0.059	2.57	<0.001
Q515368	21.1	8.3	0.14	42.9	0.35	0.008	0.488	6	0.057	2.64	<0.001
Q515370	16.75	7.8	0.12	38.4	0.4	0.008	0.435	6.52	0.058	2.53	0.001
Q515371	16.65	9.7	0.16	48.2	0.46	0.009	0.56	7.53	0.054	2.93	<0.001
Q515372	13.45	8.8	0.13	34.6	0.35	0.007	0.487	6.24	0.044	2.27	<0.001
Q515373	17.55	9.2	0.16	46.9	0.59	0.011	0.559	6.94	0.054	2.63	0.001
Q515374	16	9.4	0.15	48.9	0.46	0.009	0.53	6.74	0.051	2.48	<0.001
Q515375	11.15	11.1	0.25	59.6	0.81	0.011	0.699	10.5	0.033	1.87	0.001
Q515376	13.3	9.6	0.17	43.9	0.38	0.01	0.598	6.7	0.047	2.02	<0.001
Q515377	16.65	12.2	0.22	50.1	0.41	0.007	0.838	7.22	0.036	2.87	<0.001
Q515378	22.6	12.2	0.2	58.5	0.76	0.01	0.631	8.46	0.06	2.87	<0.001

Till Aqua Regia

	La	Li	Mg	Mn	Mo	Na	Nb	Ni	P	Pb	Pd
	ppm	ppm	%	ppm	ppm	%	ppm	ppm	%	ppm	ppm
Q515379	17.7	7.6	0.12	37.6	0.29	0.008	0.44	5.53	0.053	2.43	<0.001
Q515380	22	8.1	0.15	42.4	0.5	0.007	0.535	5.6	0.054	3.04	<0.001
Q515381	17.15	9	0.15	44.3	0.38	0.009	0.492	6.48	0.052	2.26	<0.001
Q515382	16.35	9.1	0.15	44.6	0.43	0.008	0.501	6.84	0.05	2.37	<0.001
Q515384	16.9	11	0.19	59	0.47	0.01	0.628	7.09	0.054	2.44	<0.001
Q515385	16.6	8.3	0.13	36.2	0.41	0.008	0.503	5.51	0.055	2.45	<0.001
Q515386	16.7	8.6	0.14	45.3	0.2	0.008	0.602	5.78	0.044	2.37	0.001
Q515387	11.3	8.5	0.13	38.7	0.25	0.008	0.616	5.7	0.037	2.2	<0.001
Q515388	16.05	9.6	0.15	47.8	0.26	0.008	0.556	6.22	0.046	2.27	<0.001
Q515389	12.35	3.2	0.11	36.1	1.04	0.007	0.981	3.28	0.005	1.985	<0.001
Q515390	9.98	8	0.13	40	0.19	0.007	0.637	4.34	0.028	1.75	<0.001
Q515391	22.1	11.8	0.22	74.5	0.28	0.011	0.349	8.92	0.066	2.43	<0.001
Q515392	14.1	13.1	0.26	100.5	0.25	0.012	0.643	10.3	0.047	2.04	0.001
Q515393	12.7	13.4	0.22	71.9	0.17	0.01	0.759	8.24	0.036	1.985	0.001
Q515394	16.95	18.2	0.33	120	0.31	0.013	0.916	11.85	0.054	2.84	0.001
Q515395	11.3	13.8	0.24	59.5	0.36	0.01	0.9	8.57	0.036	3.1	<0.001
Q515396	16.15	17.6	0.33	158.5	0.27	0.016	0.903	11.8	0.051	2.62	<0.001
Q515397	16.4	12.9	0.25	89.7	0.28	0.008	0.793	9.86	0.056	2.55	<0.001
Q515398	17.6	18	0.37	136.5	0.32	0.011	0.783	13.8	0.06	2.66	<0.001
Q515399	11.2	9.8	0.19	60.2	0.58	0.005	0.706	7.34	0.039	1.99	<0.001
Q515400	8.46	5.9	0.14	35	0.1	0.006	0.402	4.42	0.035	1.125	<0.001
Q515401	11.9	11.9	0.22	62.9	0.64	0.006	0.717	6.26	0.04	1.735	<0.001
Q515402	15.9	10.1	0.18	60.8	0.46	0.006	0.525	7.79	0.052	2.39	<0.001
Q515403	10.1	8.4	0.14	40.5	0.53	0.005	0.399	6.14	0.047	1.705	<0.001
Q515404	17.6	7.2	0.11	37	0.37	0.003	0.416	5.76	0.046	2.35	<0.001
Q515405	15.35	7.4	0.12	36.1	0.06	0.004	0.337	5.71	0.049	2.01	<0.001
Q515406	19.95	16.5	0.31	92.9	0.38	0.008	0.88	12.65	0.044	2.96	<0.001
Q515407	12.75	15	0.28	80.9	0.28	0.007	0.803	10.75	0.048	1.78	<0.001
Q515408	19.5	11.5	0.22	81.4	0.21	0.009	0.299	7.46	0.057	2.07	<0.001
Q515409	19.95	13.2	0.23	85.9	0.21	0.008	0.517	8.89	0.054	2.19	<0.001
Q515410	18.05	13.2	0.28	93.7	0.2	0.008	0.484	9.8	0.058	2.25	<0.001
Q515411	13.8	11.3	0.2	73.6	0.2	0.007	0.541	7.71	0.044	1.965	<0.001
Q515412	12.8	10.7	0.2	66.7	0.22	0.006	0.463	7.87	0.05	1.795	<0.001
Q515413	16.95	10.7	0.19	62.6	0.45	0.008	0.7	7.9	0.052	2.7	<0.001
Q515414	12.9	6.2	0.1	37.2	0.15	0.004	0.22	4.76	0.052	1.665	<0.001
Q515415	14.5	10.5	0.17	62.9	0.2	0.005	0.399	7.34	0.053	1.86	<0.001
Q515416	12.25	11.4	0.2	65.4	0.13	0.006	0.589	6.49	0.04	1.405	<0.001
Q515417	8.18	11.5	0.21	62.8	0.21	0.007	0.603	6.55	0.035	1.385	<0.001
Q515418	12.35	9.1	0.18	69.2	0.17	0.007	0.513	5.6	0.048	1.595	<0.001
Q515419	16.6	12.2	0.25	99.6	0.16	0.009	0.352	8.32	0.055	1.885	<0.001
Q515420	12.55	12.7	0.25	75.2	0.26	0.008	1.03	8.07	0.028	2.1	<0.001

Till Aqua Regia

	La	Li	Mg	Mn	Mo	Na	Nb	Ni	P	Pb	Pd
	ppm	ppm	%	ppm	ppm	%	ppm	ppm	%	ppm	ppm
Q515421	12.25	12.6	0.23	82.2	0.16	0.007	0.694	7.98	0.049	1.87	0.001
Q515422	10.05	10.2	0.17	59.6	0.17	0.005	0.491	6.69	0.04	1.665	<0.001
Q515423	18.95	15	0.28	102	0.41	0.008	0.58	10.65	0.067	2.68	<0.001
Q515425	8.91	12.7	0.18	52.2	0.17	0.004	0.795	5.85	0.022	1.79	<0.001
Q515426	13.55	14.3	0.23	66.2	0.33	0.006	1.005	8.15	0.041	2.85	<0.001
Q515427	17.15	14.2	0.3	103.5	0.21	0.01	0.524	9.8	0.051	2.27	<0.001
Q515428	11.35	12.4	0.22	79.8	0.17	0.006	0.508	6.59	0.048	1.635	<0.001
Q515429	11.55	15.9	0.26	87.4	0.16	0.006	0.711	7.37	0.043	1.61	<0.001
Q515430	11.15	16.8	0.28	98.1	0.26	0.007	0.746	7.7	0.053	2.09	<0.001
Q515431	17.8	11.5	0.23	83.4	0.15	0.01	0.299	7.5	0.057	2.04	<0.001
Q515432	10.1	10.9	0.18	57.1	0.27	0.007	0.519	6.61	0.041	1.46	<0.001
Q515433	13.45	10.6	0.17	55.6	0.17	0.007	0.641	5.81	0.042	1.92	<0.001
Q515434	17.4	10.8	0.21	71.9	0.36	0.01	0.536	7	0.056	2.15	0.002
Q515435	17	10.5	0.19	61.9	0.36	0.008	0.585	6.84	0.062	2.43	<0.001
Q515436	10.95	9	0.17	52.9	0.26	0.007	0.483	5.16	0.042	1.64	<0.001
Q515437	14.5	11.3	0.21	54.6	0.11	0.007	0.698	5.88	0.05	1.97	0.001
Q515438	12.55	11.1	0.18	63.3	0.16	0.007	0.583	5.67	0.05	1.77	<0.001
Q515439	12.8	7.4	0.12	34.8	0.29	0.006	0.356	5.59	0.049	2.23	<0.001
Q515440	11.4	6.7	0.11	38	0.2	0.005	0.213	4.74	0.049	1.595	0.001
Q515442	12.6	6.8	0.11	30.4	0.25	0.004	0.333	3.76	0.046	1.865	0.001
Q515443	17.65	10	0.18	55.3	0.26	0.006	0.518	6.26	0.057	2.3	<0.001
Q515444	16.25	13	0.23	76.9	0.51	0.01	0.644	9.53	0.058	2.98	<0.001
Q515445	22.5	9.3	0.16	62	0.31	0.01	0.32	6.84	0.066	2.57	<0.001
Q515446	14.05	9.6	0.14	45.3	0.4	0.006	0.596	6.16	0.043	1.91	<0.001
Q515447	14.2	16	0.28	85.2	0.39	0.011	0.73	10.4	0.055	2.36	<0.001
Q515448	15.9	14.8	0.26	71.7	0.27	0.009	0.749	9.56	0.052	2.51	<0.001
Q515449	11.9	7	0.11	34.3	0.26	0.008	0.387	4.89	0.047	1.62	<0.001
Q515450	21.9	8.6	0.17	50.2	0.15	0.009	0.477	6.35	0.065	2.51	<0.001
Q515451	19.85	10	0.18	64.8	0.37	0.009	0.539	7.9	0.06	2.47	<0.001
Q515452	16.65	7.7	0.14	50.3	0.31	0.008	0.316	6.19	0.056	2.07	<0.001
Q515454	18.55	10.4	0.19	59.7	0.41	0.01	0.617	7.84	0.052	2.6	<0.001
Q515455	14.4	10.3	0.13	35	0.39	0.007	0.637	5.25	0.03	2.28	<0.001
Q515456	20.1	9.9	0.2	59.7	0.11	0.011	0.312	6.44	0.058	2.1	<0.001
Q515457	16.9	16.7	0.35	144	0.29	0.016	0.278	13	0.053	2.59	0.001
Q515458	17.85	11.1	0.24	93.2	0.2	0.012	0.353	7.86	0.057	2.11	<0.001
Q515459	18.1	11.6	0.22	86	0.22	0.011	0.364	7.58	0.05	1.985	0.001
Q515460	16.4	9.1	0.16	63.6	0.21	0.009	0.488	6.45	0.053	1.975	0.001
Q515461	7.89	7.9	0.14	62.9	0.14	0.005	0.371	5.34	0.032	1.14	<0.001
Q515462	11.25	6.5	0.14	44.9	0.21	0.007	0.52	5.3	0.036	1.545	0.001
Q515463	10.55	10.1	0.17	55.8	0.25	0.008	0.584	6.55	0.039	1.685	<0.001
Q515464	17	11.9	0.24	74	0.23	0.013	0.705	8.52	0.053	2.15	<0.001

Till Aqua Regia

	La	Li	Mg	Mn	Mo	Na	Nb	Ni	P	Pb	Pd
	ppm	ppm	%	ppm	ppm	%	ppm	ppm	%	ppm	ppm
Q515465	8.74	10.9	0.18	50.3	0.41	0.008	0.493	6.82	0.04	1.65	<0.001
Q515466	16.3	14.3	0.26	78.4	0.28	0.011	0.549	9.36	0.054	2.07	0.003
Q515467	14.75	9.4	0.17	77.2	0.2	0.008	0.564	6.75	0.049	1.905	<0.001
Q515468	15.5	10.6	0.21	85.2	0.17	0.01	0.311	6.85	0.053	1.805	<0.001
Q515469	11.85	8.6	0.17	74.1	0.17	0.007	0.481	6.83	0.048	1.82	<0.001
Q515470	17.6	11.8	0.24	102	0.18	0.01	0.403	8.32	0.056	1.995	0.001
Q515471	9.72	11.2	0.16	68	0.2	0.008	0.752	6.73	0.039	2.09	<0.001
Q515472	10.65	10.3	0.16	58.4	0.28	0.008	0.898	6.88	0.036	2.57	<0.001
Q515473	9.5	10.1	0.19	51.1	0.11	0.009	0.728	6.26	0.052	1.785	<0.001
Q515474	18	12.6	0.25	114.5	0.15	0.01	0.344	8.38	0.061	1.935	<0.001
Q515475	12.4	10.1	0.16	52.7	0.19	0.007	0.642	6.55	0.046	1.81	<0.001

Till Aqua Regia

	Pt	Rb	Re	S	Sb	Sc	Se	Sn	Sr	Ta	Te
	ppm	ppm	ppm	%	ppm	ppm	ppm	ppm	ppm	ppm	ppm
Q515251	<0.002	5.54	<0.001	<0.01	0.015	1.36	0.2	0.27	5.89	<0.005	0.02
Q515252	<0.002	3.22	<0.001	0.01	0.021	1.18	0.2	0.4	4.49	0.014	0.01
Q515253	<0.002	4.68	<0.001	<0.01	0.007	1.155	<0.1	0.23	5.92	<0.005	0.01
Q515254	<0.002	6.14	<0.001	<0.01	0.019	1.355	0.1	0.38	5.27	<0.005	0.01
Q515255	<0.002	10.2	<0.001	<0.01	0.023	2.07	0.3	0.61	6.97	<0.005	0.01
Q515256	<0.002	8.66	<0.001	<0.01	0.01	1.265	0.1	0.3	5.49	<0.005	<0.01
Q515257	<0.002	7.84	<0.001	<0.01	0.014	1.7	0.1	0.27	8.25	<0.005	<0.01
Q515258L	<0.002	12.3	<0.001	<0.01	0.009	2.14	0.1	0.38	8.23	<0.005	<0.01
Q515258U	<0.002	7.15	<0.001	<0.01	0.012	1.55	0.1	0.25	7.49	<0.005	<0.01
Q515260	<0.002	5.24	<0.001	<0.01	0.008	0.957	0.1	0.16	4.36	<0.005	0.01
Q515261	<0.002	4.22	<0.001	<0.01	0.007	0.849	0.1	0.18	3.83	<0.005	<0.01
Q515262	<0.002	3.85	<0.001	<0.01	0.005	0.81	0.1	0.14	3.84	<0.005	<0.01
Q515263	<0.002	4.49	<0.001	<0.01	0.005	0.788	0.1	0.14	3.52	<0.005	<0.01
Q515264	<0.002	4.94	<0.001	<0.01	0.006	0.915	0.1	0.18	4.62	<0.005	<0.01
Q515265	<0.002	3.65	<0.001	<0.01	<0.005	0.722	0.1	0.13	3.51	<0.005	<0.01
Q515266	<0.002	5.65	<0.001	<0.01	0.007	0.972	0.2	0.18	5.95	<0.005	<0.01
Q515267	<0.002	5.54	<0.001	<0.01	<0.005	0.983	0.1	0.18	4.54	<0.005	0.01
Q515268	<0.002	7.46	<0.001	<0.01	0.007	1.365	<0.1	0.22	6.48	<0.005	<0.01
Q515269	<0.002	5.6	<0.001	<0.01	0.005	1.11	0.1	0.21	5.6	<0.005	0.01
Q515270	<0.002	4.28	<0.001	<0.01	0.012	0.925	0.1	0.22	5.05	<0.005	<0.01
Q515271	<0.002	6.19	<0.001	<0.01	0.006	1.225	<0.1	0.23	4.83	<0.005	<0.01
Q515272	<0.002	4.01	<0.001	<0.01	0.01	1.025	0.1	0.29	3.74	<0.005	0.01
Q515273	<0.002	3.43	<0.001	<0.01	0.006	0.914	0.1	0.18	3.76	<0.005	<0.01
Q515274	<0.002	7.59	<0.001	<0.01	0.107	1.59	0.2	0.44	5.23	0.006	0.02
Q515275	<0.002	4.45	<0.001	<0.01	0.013	0.946	0.1	0.21	3.83	<0.005	0.01
Q515276	<0.002	6.79	<0.001	<0.01	0.007	1.37	0.1	0.24	6.22	<0.005	0.02
Q515277	<0.002	6.42	<0.001	<0.01	0.008	1.42	0.1	0.24	6.78	<0.005	<0.01
Q515278	<0.002	7.15	<0.001	<0.01	0.007	1.16	0.1	0.23	4.89	<0.005	<0.01
Q515280	<0.002	5.71	<0.001	<0.01	0.006	1.025	0.1	0.26	3.56	<0.005	<0.01
Q515281	<0.002	6.25	<0.001	<0.01	0.01	1.15	0.1	0.23	5.46	<0.005	0.01
Q515282	<0.002	5.22	<0.001	<0.01	0.005	0.97	0.1	0.2	4.65	<0.005	<0.01
Q515283	<0.002	5.59	<0.001	<0.01	0.005	1.045	0.1	0.22	4.33	<0.005	<0.01
Q515284	<0.002	5.58	<0.001	<0.01	0.005	1.11	0.1	0.17	4.5	<0.005	<0.01
Q515285	<0.002	5.29	<0.001	<0.01	0.007	1.08	0.1	0.16	4.21	<0.005	<0.01
Q515286	<0.002	5.32	<0.001	<0.01	0.007	1.07	0.1	0.16	4.59	<0.005	<0.01
Q515287	<0.002	5.52	<0.001	<0.01	0.007	0.944	0.1	0.19	4.28	<0.005	0.01
Q515288	<0.002	4.43	<0.001	<0.01	0.006	0.816	<0.1	0.15	4.04	<0.005	<0.01
Q515289	0.002	4.7	<0.001	<0.01	0.006	0.977	<0.1	0.18	4.18	<0.005	<0.01
Q515290	<0.002	5.68	<0.001	<0.01	0.006	1.115	<0.1	0.19	4.24	<0.005	<0.01
Q515291	0.002	4.27	<0.001	<0.01	0.009	0.895	<0.1	0.12	4.26	<0.005	0.01
Q515292	<0.002	5.97	<0.001	<0.01	0.006	1.06	0.1	0.19	4.19	<0.005	<0.01

Till Aqua Regia

	Pt	Rb	Re	S	Sb	Sc	Se	Sn	Sr	Ta	Te
	ppm	ppm	ppm	%	ppm	ppm	ppm	ppm	ppm	ppm	ppm
Q515293	0.002	5.87	<0.001	<0.01	0.008	1.25	<0.1	0.2	6.94	<0.005	0.01
Q515294	<0.002	5.32	<0.001	<0.01	0.008	0.968	0.1	0.15	3.6	<0.005	0.01
Q515295	<0.002	3.97	<0.001	<0.01	<0.005	0.788	<0.1	0.19	3.37	<0.005	<0.01
Q515296	<0.002	6.4	<0.001	<0.01	0.007	1.24	0.1	0.22	4.48	<0.005	0.01
Q515297	0.002	2.95	<0.001	<0.01	0.011	0.473	0.1	0.2	3.81	<0.005	0.01
Q515298	<0.002	13.45	<0.001	<0.01	0.013	2.3	0.1	0.37	8.29	<0.005	<0.01
Q515299	<0.002	7.27	<0.001	<0.01	0.031	1.525	0.1	0.32	7.26	<0.005	0.01
Q515300	<0.002	8.86	<0.001	<0.01	0.027	1.995	0.2	0.41	7.02	<0.005	0.02
Q515301	<0.002	3.5	<0.001	<0.01	0.007	0.894	<0.1	0.19	4.27	<0.005	<0.01
Q515302	<0.002	3.56	<0.001	<0.01	0.009	1.035	0.1	0.2	5.54	<0.005	<0.01
Q515303	<0.002	7.13	<0.001	<0.01	0.009	1.18	<0.1	0.26	5.66	<0.005	<0.01
Q515304	0.002	7.94	<0.001	<0.01	0.012	1.455	<0.1	0.35	6.57	<0.005	0.04
Q515305	0.002	7.69	<0.001	<0.01	<0.005	1.525	<0.1	0.27	8.07	<0.005	0.01
Q515306	<0.002	8.82	<0.001	<0.01	0.011	1.725	<0.1	0.27	6.99	<0.005	<0.01
Q515307	<0.002	5.04	<0.001	<0.01	0.016	0.986	<0.1	0.16	5.45	<0.005	<0.01
Q515308	<0.002	2.4	<0.001	<0.01	0.01	0.801	0.1	0.24	3.33	<0.005	0.03
Q515309	<0.002	3.57	<0.001	<0.01	0.011	1.46	0.2	0.24	4.21	0.013	<0.01
Q515311	<0.002	3.61	<0.001	<0.01	0.02	1.275	<0.1	0.27	4.3	0.008	0.03
Q515312	0.003	7.07	<0.001	<0.01	0.007	1.645	<0.1	0.35	6.89	<0.005	<0.01
Q515313	<0.002	7.27	<0.001	<0.01	0.015	1.725	<0.1	0.3	8.51	<0.005	0.01
Q515314	<0.002	3.82	<0.001	<0.01	0.015	0.899	<0.1	0.17	4.96	<0.005	0.01
Q515315	<0.002	4	<0.001	<0.01	0.006	0.834	<0.1	0.23	4.3	<0.005	0.01
Q515316	<0.002	5.33	<0.001	<0.01	0.006	1.175	0.1	0.25	4.51	<0.005	<0.01
Q515317	<0.002	5.88	<0.001	<0.01	0.009	1.07	<0.1	0.2	5.41	<0.005	<0.01
Q515318	<0.002	4.57	<0.001	<0.01	0.005	0.898	<0.1	0.23	4.01	<0.005	0.01
Q515319	<0.002	4.84	<0.001	<0.01	0.005	0.974	<0.1	0.21	4.5	<0.005	<0.01
Q515320	<0.002	4.41	<0.001	<0.01	<0.005	0.904	<0.1	0.17	3.23	<0.005	0.01
Q515321	<0.002	3.49	<0.001	<0.01	0.005	0.821	<0.1	0.18	3.93	<0.005	0.01
Q515322	<0.002	4.05	<0.001	<0.01	0.008	0.828	<0.1	0.16	3.81	<0.005	<0.01
Q515323	<0.002	4.21	<0.001	<0.01	<0.005	0.944	<0.1	0.13	3.99	<0.005	0.02
Q515324	<0.002	4.33	<0.001	<0.01	0.007	0.946	<0.1	0.18	4.12	<0.005	<0.01
Q515325	<0.002	3.68	<0.001	<0.01	0.009	0.82	0.1	0.15	3.49	<0.005	0.02
Q515326	<0.002	3.85	<0.001	<0.01	0.005	0.721	0.2	0.12	3.11	<0.005	0.02
Q515327	<0.002	3.85	<0.001	<0.01	0.011	0.754	0.1	0.13	3.05	<0.005	0.01
Q515328	<0.002	4.33	<0.001	<0.01	0.012	0.849	0.1	0.15	3.65	<0.005	0.02
Q515329	<0.002	5.82	<0.001	<0.01	0.009	1.06	0.1	0.2	3.46	<0.005	0.01
Q515330	<0.002	4.56	<0.001	<0.01	0.007	0.868	0.1	0.16	3.93	<0.005	0.01
Q515331	<0.002	5.17	<0.001	<0.01	0.009	1.015	0.1	0.17	3.98	<0.005	0.01
Q515332	<0.002	3.45	<0.001	<0.01	<0.005	0.702	<0.1	0.13	2.59	<0.005	0.02
Q515333	<0.002	7.01	<0.001	<0.01	0.014	1.4	0.1	0.29	5.32	<0.005	0.01
Q515334	<0.002	4.52	<0.001	<0.01	0.008	1.015	<0.1	0.18	3.88	<0.005	<0.01

Till Aqua Regia

	Pt	Rb	Re	S	Sb	Sc	Se	Sn	Sr	Ta	Te
	ppm	ppm	ppm	%	ppm	ppm	ppm	ppm	ppm	ppm	ppm
Q515335	<0.002	5.08	<0.001	<0.01	0.006	1.045	<0.1	0.15	3.8	<0.005	0.02
Q515336	<0.002	4.86	<0.001	<0.01	0.011	0.925	0.1	0.17	4.49	<0.005	0.02
Q515337	<0.002	4.16	<0.001	<0.01	0.009	0.895	0.1	0.22	4.58	<0.005	0.01
Q515338	<0.002	4.56	<0.001	<0.01	0.012	0.99	0.1	0.19	4.36	<0.005	<0.01
Q515339	<0.002	3.3	<0.001	<0.01	0.018	1.24	0.1	0.33	3.52	0.013	0.01
Q515340	<0.002	3.57	<0.001	<0.01	0.013	1.05	0.1	0.22	3.81	0.006	0.02
Q515341	<0.002	4.2	<0.001	<0.01	0.007	0.778	0.1	0.14	4.67	<0.005	0.02
Q515342	<0.002	6.67	<0.001	<0.01	0.009	1.1	0.1	0.21	5.16	<0.005	0.01
Q515343	<0.002	12.4	<0.001	<0.01	0.02	1.955	0.2	0.35	7.36	<0.005	0.02
Q515344	<0.002	8.27	<0.001	<0.01	0.007	1.455	0.1	0.98	6.29	<0.005	0.02
Q515345	<0.002	5.8	<0.001	<0.01	0.005	1.055	0.1	0.26	4.4	<0.005	0.01
Q515346	<0.002	6.32	<0.001	<0.01	0.015	1.115	0.1	0.22	4.72	<0.005	0.02
Q515347	<0.002	9.63	<0.001	<0.01	0.01	1.485	0.1	0.26	7.39	<0.005	0.02
Q515348	<0.002	6.69	<0.001	<0.01	0.01	0.994	0.1	0.22	5.13	<0.005	0.01
Q515349	<0.002	8.64	<0.001	<0.01	0.011	1.66	0.1	0.25	7.92	<0.005	0.01
Q515350	<0.002	6.62	<0.001	<0.01	0.013	1.25	<0.1	0.25	5.9	<0.005	0.02
Q515351	<0.002	4.93	<0.001	<0.01	<0.005	1.035	0.1	0.17	4.67	<0.005	0.02
Q515352	<0.002	4.17	<0.001	<0.01	0.012	1.155	0.1	0.26	4.23	<0.005	0.01
Q515354	<0.002	3.47	<0.001	<0.01	0.006	0.803	0.1	0.28	3.39	0.011	0.02
Q515355	<0.002	4.06	<0.001	<0.01	0.009	0.844	<0.1	0.16	4.08	<0.005	0.01
Q515356	<0.002	5.09	<0.001	<0.01	0.018	0.931	0.2	0.19	4.24	<0.005	0.02
Q515357	<0.002	5.43	<0.001	<0.01	0.006	1.285	0.1	0.19	5.63	<0.005	0.01
Q515358	<0.002	4.14	<0.001	<0.01	0.006	0.915	0.2	0.15	3.67	<0.005	0.01
Q515359	<0.002	6.73	<0.001	<0.01	<0.005	1.25	0.1	0.25	4.16	<0.005	0.01
Q515360	<0.002	7.03	<0.001	<0.01	0.006	1.425	0.1	0.21	4.56	<0.005	0.01
Q515362	<0.002	5.58	<0.001	<0.01	0.012	1	0.1	0.22	6.04	<0.005	<0.01
Q515363	<0.002	6.5	<0.001	<0.01	0.012	1.245	0.1	0.24	5.51	<0.005	<0.01
Q515364	<0.002	6.18	<0.001	<0.01	0.009	1.275	0.1	0.22	5.4	<0.005	0.01
Q515365	<0.002	6.37	<0.001	<0.01	0.005	1.085	<0.1	0.25	4.99	<0.005	0.01
Q515366	<0.002	3.54	<0.001	<0.01	0.007	0.742	0.2	0.12	3.84	<0.005	0.01
Q515367	<0.002	4.5	<0.001	<0.01	<0.005	0.962	0.1	0.18	4.5	<0.005	<0.01
Q515368	<0.002	4.38	<0.001	<0.01	0.008	0.944	0.1	0.16	4.15	<0.005	<0.01
Q515370	<0.002	4.06	<0.001	<0.01	<0.005	0.834	<0.1	0.14	3.86	<0.005	0.01
Q515371	<0.002	5.02	<0.001	<0.01	<0.005	1.075	0.1	0.18	4.28	<0.005	0.01
Q515372	<0.002	4.01	<0.001	<0.01	0.006	0.854	0.1	0.15	3.63	<0.005	<0.01
Q515373	<0.002	5.08	<0.001	<0.01	0.009	1.09	<0.1	0.18	4.39	<0.005	0.02
Q515374	<0.002	4.61	<0.001	<0.01	0.007	0.965	<0.1	0.17	4.73	<0.005	0.01
Q515375	<0.002	8.22	<0.001	<0.01	0.011	1.295	0.1	0.28	5.04	<0.005	0.01
Q515376	<0.002	6.22	<0.001	<0.01	0.011	1.055	0.1	0.21	4.9	<0.005	0.01
Q515377	<0.002	5.16	<0.001	<0.01	0.011	1.47	0.1	0.27	3.78	<0.005	0.02
Q515378	<0.002	7.11	<0.001	<0.01	0.009	1.415	0.1	0.23	4.64	<0.005	<0.01

Till Aqua Regia

	Pt	Rb	Re	S	Sb	Sc	Se	Sn	Sr	Ta	Te
	ppm	ppm	ppm	%	ppm	ppm	ppm	ppm	ppm	ppm	ppm
Q515379	<0.002	3.7	<0.001	<0.01	<0.005	0.808	<0.1	0.14	4.22	<0.005	0.01
Q515380	<0.002	4.3	<0.001	<0.01	0.01	0.904	0.1	0.19	4.51	<0.005	<0.01
Q515381	<0.002	5.06	<0.001	<0.01	0.009	0.985	<0.1	0.17	3.71	<0.005	0.01
Q515382	<0.002	4.76	<0.001	<0.01	0.007	0.968	0.1	0.18	3.95	<0.005	<0.01
Q515384	<0.002	7.22	<0.001	<0.01	0.006	1.34	0.1	0.23	5.37	<0.005	<0.01
Q515385	<0.002	3.8	<0.001	<0.01	0.007	0.854	0.1	0.17	4.41	<0.005	0.01
Q515386	<0.002	4.26	<0.001	<0.01	0.007	0.953	0.1	0.2	4.55	<0.005	0.01
Q515387	<0.002	3.67	<0.001	<0.01	0.007	0.879	0.1	0.2	4.43	<0.005	<0.01
Q515388	<0.002	4.44	<0.001	<0.01	0.01	0.983	<0.1	0.17	4.28	<0.005	<0.01
Q515389	<0.002	5.61	<0.001	<0.01	0.009	0.756	<0.1	0.43	3.96	<0.005	<0.01
Q515390	<0.002	3.01	<0.001	<0.01	0.009	0.813	<0.1	0.2	3.99	<0.005	<0.01
Q515391	<0.002	7.49	<0.001	<0.01	0.008	1.47	0.1	0.25	5.91	<0.005	<0.01
Q515392	<0.002	9.4	<0.001	<0.01	0.009	1.475	0.2	0.28	7.04	<0.005	<0.01
Q515393	<0.002	5.76	<0.001	<0.01	0.009	1.345	<0.1	0.27	6.22	<0.005	<0.01
Q515394	<0.002	13.15	<0.001	<0.01	0.007	1.85	0.1	0.43	7.86	<0.005	<0.01
Q515395	<0.002	10.85	<0.001	<0.01	0.012	1.33	0.1	0.41	7.87	<0.005	<0.01
Q515396	<0.002	12.15	<0.001	<0.01	0.018	1.96	0.1	0.36	9.42	<0.005	0.01
Q515397	<0.002	10	<0.001	<0.01	0.014	1.75	0.1	0.31	7.8	<0.005	<0.01
Q515398	<0.002	15.4	<0.001	<0.01	0.014	2.61	0.1	0.39	7.74	<0.005	0.01
Q515399	<0.002	6.6	<0.001	<0.01	0.007	1.21	<0.1	0.23	4.88	<0.005	<0.01
Q515400	<0.002	4.27	<0.001	<0.01	<0.005	0.758	0.1	0.19	4.21	<0.005	0.01
Q515401	<0.002	8.12	<0.001	<0.01	0.007	1.17	<0.1	0.31	4.64	<0.005	0.01
Q515402	<0.002	6.3	<0.001	<0.01	0.006	1.135	0.1	0.19	4.33	<0.005	<0.01
Q515403	<0.002	4.71	<0.001	<0.01	0.005	0.884	<0.1	0.17	3.58	<0.005	<0.01
Q515404	<0.002	3.58	<0.001	<0.01	<0.005	0.837	<0.1	0.17	3.89	<0.005	0.01
Q515405	<0.002	4.08	<0.001	<0.01	<0.005	0.881	<0.1	0.14	3.43	<0.005	<0.01
Q515406	<0.002	13.35	<0.001	<0.01	0.019	2.47	0.2	0.45	8.23	<0.005	0.01
Q515407	<0.002	11.1	<0.001	<0.01	0.01	1.94	0.2	0.31	5.15	<0.005	<0.01
Q515408	<0.002	7.65	<0.001	<0.01	0.006	1.53	<0.1	0.27	7.02	<0.005	<0.01
Q515409	<0.002	8.99	<0.001	<0.01	<0.005	1.4	<0.1	0.3	5.59	<0.005	0.01
Q515410	<0.002	10.3	<0.001	<0.01	0.012	1.825	<0.1	0.34	8.22	<0.005	0.01
Q515411	<0.002	6.74	<0.001	<0.01	0.009	1.05	0.1	0.25	5	<0.005	<0.01
Q515412	<0.002	6.83	<0.001	<0.01	0.006	1.19	<0.1	0.43	5.36	<0.005	<0.01
Q515413	<0.002	7.21	<0.001	<0.01	<0.005	1.385	0.1	0.26	4.66	<0.005	<0.01
Q515414	<0.002	3.53	<0.001	<0.01	0.005	0.699	<0.1	0.12	3.15	<0.005	<0.01
Q515415	<0.002	5.69	<0.001	<0.01	0.006	1.215	0.1	0.2	4.26	<0.005	0.01
Q515416	<0.002	6.97	<0.001	<0.01	0.006	1.095	0.1	0.22	4.32	<0.005	<0.01
Q515417	<0.002	7.15	<0.001	<0.01	0.007	1.175	<0.1	0.26	4.51	<0.005	0.01
Q515418	<0.002	6.22	<0.001	<0.01	0.008	0.962	0.1	0.24	5.14	<0.005	0.01
Q515419	<0.002	9.25	<0.001	<0.01	0.008	1.67	<0.1	0.33	8.34	<0.005	0.01
Q515420	<0.002	7	<0.001	<0.01	0.008	1.425	0.1	0.36	5.18	<0.005	0.01

Till Aqua Regia

	Pt	Rb	Re	S	Sb	Sc	Se	Sn	Sr	Ta	Te
	ppm	ppm	ppm	%	ppm	ppm	ppm	ppm	ppm	ppm	ppm
Q515421	<0.002	7.63	<0.001	<0.01	<0.005	1.415	<0.1	0.3	5.57	<0.005	<0.01
Q515422	<0.002	5.7	<0.001	<0.01	<0.005	0.987	<0.1	0.21	4.71	<0.005	0.01
Q515423	<0.002	10.25	<0.001	<0.01	<0.005	2	<0.1	0.32	5.92	<0.005	0.01
Q515425	<0.002	4.77	<0.001	<0.01	0.01	1.1	0.1	0.22	3.78	<0.005	0.01
Q515426	<0.002	5.95	<0.001	<0.01	0.014	1.59	0.2	0.29	4.33	0.008	0.01
Q515427	<0.002	11.3	<0.001	0.01	0.01	1.885	0.1	0.33	7.64	<0.005	0.01
Q515428	<0.002	8.21	<0.001	<0.01	0.005	1.24	<0.1	0.29	4.42	<0.005	<0.01
Q515429	<0.002	10.75	<0.001	<0.01	<0.005	1.335	0.1	0.36	4.13	<0.005	<0.01
Q515430	<0.002	12.1	<0.001	<0.01	0.005	1.415	<0.1	0.38	5.78	<0.005	0.04
Q515431	<0.002	8.18	<0.001	<0.01	<0.005	1.585	0.1	0.26	7.53	<0.005	0.01
Q515432	<0.002	6.94	<0.001	<0.01	0.008	1.015	0.1	0.23	5.04	<0.005	0.01
Q515433	<0.002	5.1	<0.001	0.01	0.012	1.045	<0.1	0.24	4.88	<0.005	<0.01
Q515434	<0.002	7.21	<0.001	0.02	<0.005	1.385	<0.1	0.24	4.8	<0.005	0.01
Q515435	<0.002	6.63	<0.001	0.02	0.005	1.275	<0.1	0.21	4.21	<0.005	0.01
Q515436	<0.002	5.35	<0.001	0.02	0.006	0.894	<0.1	0.23	4.23	<0.005	0.11
Q515437	<0.002	7.03	<0.001	0.02	0.006	1.21	<0.1	0.27	4.53	<0.005	0.01
Q515438	<0.002	6.3	<0.001	0.02	0.009	1	0.1	0.27	4.26	<0.005	<0.01
Q515439	<0.002	3.19	<0.001	0.02	0.005	0.769	<0.1	0.14	3.02	<0.005	0.01
Q515440	<0.002	3.44	<0.001	0.02	0.005	0.655	<0.1	0.12	3.14	<0.005	0.02
Q515442	<0.002	2.92	<0.001	0.02	0.005	0.685	<0.1	0.12	2.62	<0.005	0.01
Q515443	<0.002	5.49	<0.001	0.02	0.014	1.01	<0.1	0.23	4.24	<0.005	<0.01
Q515444	<0.002	8.48	<0.001	0.02	0.006	1.54	<0.1	0.27	5.18	<0.005	0.01
Q515445	<0.002	5.87	<0.001	0.01	0.006	1.31	<0.1	0.23	5.6	<0.005	0.01
Q515446	<0.002	5.26	<0.001	0.01	0.006	0.988	<0.1	0.19	4.34	<0.005	0.01
Q515447	<0.002	9.66	<0.001	0.02	0.008	1.84	0.1	0.32	5.23	<0.005	0.02
Q515448	<0.002	9.03	<0.001	0.02	0.011	1.665	0.1	0.31	5.72	<0.005	0.01
Q515449	<0.002	3.67	<0.001	0.03	<0.005	0.739	0.1	0.15	3.28	<0.005	0.01
Q515450	<0.002	5.58	<0.001	0.03	0.005	1.22	0.1	0.2	4.75	<0.005	0.01
Q515451	<0.002	6.37	<0.001	0.03	<0.005	1.38	<0.1	0.21	4.69	<0.005	0.01
Q515452	0.002	4.7	<0.001	0.03	0.006	1.02	0.1	0.17	4.17	<0.005	0.01
Q515454	<0.002	5.81	<0.001	0.02	0.009	1.405	<0.1	0.24	5.34	<0.005	0.02
Q515455	<0.002	2.97	<0.001	0.02	0.009	1.08	0.1	0.19	2.86	<0.005	0.04
Q515456	<0.002	6.5	<0.001	0.02	0.006	1.41	0.1	0.25	6.4	<0.005	0.01
Q515457	0.002	13.5	<0.001	0.02	0.01	2.35	<0.1	0.44	9.74	<0.005	<0.01
Q515458	<0.002	8.79	<0.001	0.02	0.009	1.625	0.1	0.33	8.19	<0.005	0.02
Q515459	<0.002	7.91	<0.001	0.01	0.013	1.555	<0.1	0.46	8.42	<0.005	<0.01
Q515460	<0.002	5.75	<0.001	0.01	0.007	1.09	<0.1	0.26	5.34	<0.005	0.01
Q515461	<0.002	5.47	<0.001	<0.01	0.007	0.782	<0.1	0.19	4.36	<0.005	<0.01
Q515462	<0.002	3.76	<0.001	0.01	0.006	0.747	<0.1	0.22	4.77	<0.005	<0.01
Q515463	<0.002	6.14	<0.001	0.02	0.006	1.015	0.1	0.22	5.46	<0.005	<0.01
Q515464	<0.002	8.01	<0.001	0.02	0.007	1.48	0.1	0.3	7.46	<0.005	<0.01

Till Aqua Regia

	Pt	Rb	Re	S	Sb	Sc	Se	Sn	Sr	Ta	Te
	ppm	ppm	ppm	%	ppm	ppm	ppm	ppm	ppm	ppm	ppm
Q515465	<0.002	6	<0.001	0.02	0.006	1.065	<0.1	0.23	4.64	<0.005	0.01
Q515466	<0.002	7.81	<0.001	0.02	0.009	1.63	0.1	0.3	7.89	<0.005	<0.01
Q515467	<0.002	5.38	<0.001	0.02	0.006	1.01	<0.1	0.23	5.48	<0.005	0.01
Q515468	<0.002	6.87	<0.001	0.02	0.008	1.425	<0.1	0.27	7.05	<0.005	0.01
Q515469	<0.002	6.87	<0.001	<0.01	0.009	1.02	0.1	0.21	5.63	<0.005	<0.01
Q515470	<0.002	9.94	<0.001	<0.01	0.01	1.695	0.1	0.29	8.6	<0.005	0.01
Q515471	<0.002	5.26	<0.001	<0.01	0.012	1.19	0.1	0.25	5.03	<0.005	0.01
Q515472	<0.002	5.01	<0.001	0.01	0.012	1.205	0.1	0.24	5.01	<0.005	0.01
Q515473	<0.002	5.87	<0.001	<0.01	0.005	1.08	0.1	0.22	5.23	<0.005	0.01
Q515474	<0.002	11.15	<0.001	<0.01	0.007	1.67	0.1	0.29	8.47	<0.005	0.01
Q515475	<0.002	5.47	<0.001	<0.01	0.007	1.015	0.1	0.19	5.08	<0.005	0.01

Till Aqua Regia

	Th	Ti	Tl	U	V	W	Y	Zn	Zr
	ppm	%	ppm	ppm	ppm	ppm	ppm	ppm	ppm
Q515251	2.44	0.038	0.05	1.18	18.2	0.254	4.66	17.7	0.4
Q515252	2.87	0.048	0.034	0.541	23.5	0.12	2.29	7.3	0.82
Q515253	3.66	0.033	0.033	0.887	14.9	0.073	5.29	10.6	3.13
Q515254	2.52	0.069	0.049	0.364	32.2	0.159	2.13	19.9	0.93
Q515255	2.46	0.112	0.071	0.63	50.9	0.159	3.25	30.8	0.93
Q515256	2.13	0.063	0.061	0.572	30.4	0.111	3.07	20.8	0.54
Q515257	5.06	0.047	0.06	0.846	20.3	0.09	5.28	18.3	4.12
Q515258L	4.07	0.065	0.084	0.801	30.6	0.097	4.66	28.8	2.03
Q515258U	4.97	0.044	0.051	0.71	20.7	0.067	5.16	16.8	3.95
Q515260	2.63	0.027	0.038	0.653	15.7	0.15	4.07	12.6	1.28
Q515261	2.23	0.028	0.033	0.498	12.1	0.05	2.81	9	0.45
Q515262	2.7	0.022	0.032	0.798	12.3	0.066	3.77	8.4	0.69
Q515263	2.22	0.021	0.028	0.663	11.4	0.045	3.36	9.3	1.01
Q515264	3.99	0.026	0.03	0.604	14.1	0.046	3.74	10.7	0.95
Q515265	3.9	0.019	0.024	1.025	10.6	1.56	4.75	7	0.79
Q515266	2.35	0.026	0.046	0.509	13.4	0.103	3.15	12.6	0.66
Q515267	2.85	0.028	0.04	0.848	15.1	0.06	4.29	12.3	0.87
Q515268	3.67	0.038	0.053	0.602	18.9	0.071	4.25	14.8	1.7
Q515269	2.87	0.033	0.042	0.559	16.6	0.151	3.73	16	1.14
Q515270	1.785	0.031	0.04	0.328	19.4	0.071	2.53	11.2	0.53
Q515271	4.2	0.034	0.054	0.677	17.1	0.07	3.51	13.3	3.09
Q515272	3.21	0.041	0.035	0.32	21.3	0.085	1.825	12.2	1.65
Q515273	2.45	0.027	0.027	0.344	16.1	0.06	2.55	8.9	1.17
Q515274	2.46	0.09	0.055	0.426	43.9	0.164	2.64	24.6	0.72
Q515275	1.45	0.035	0.032	0.235	17.5	0.068	1.475	11.7	0.7
Q515276	3.76	0.037	0.053	0.992	15.4	0.077	4.84	17	1.27
Q515277	4.17	0.037	0.049	1.04	15	0.11	5.79	15.9	2.87
Q515278	2.64	0.031	0.05	0.79	18.4	0.071	3.49	18.1	0.83
Q515280	2.89	0.037	0.038	0.679	16.1	0.06	1.82	11	0.29
Q515281	2.56	0.035	0.044	0.738	17.7	0.066	3.81	14.7	0.65
Q515282	2.31	0.033	0.038	0.554	16.7	0.092	3.26	10.7	0.49
Q515283	1.895	0.034	0.04	0.502	18	0.079	2.42	11.9	0.62
Q515284	4.95	0.028	0.038	1.315	13.7	0.09	5.59	10	1.73
Q515285	4.39	0.026	0.036	1.205	13	0.193	5.37	9.6	2.06
Q515286	4.81	0.028	0.036	1.45	13.1	0.983	5.95	10.3	1.37
Q515287	2.27	0.028	0.035	0.798	15.3	0.295	3.99	11.6	0.39
Q515288	3.41	0.024	0.029	1.045	12.3	0.429	4.57	9.4	0.56
Q515289	3.84	0.026	0.035	1.125	13	0.075	4.93	9.8	0.97
Q515290	3.29	0.032	0.037	0.922	15.5	0.122	3.82	12.5	0.58
Q515291	2.72	0.022	0.028	0.91	11.2	0.058	4.41	8.5	0.91
Q515292	3.3	0.028	0.041	1.16	15.4	0.059	4.68	11	0.88

Till Aqua Regia

	Th	Ti	Tl	U	V	W	Y	Zn	Zr
	ppm	%	ppm	ppm	ppm	ppm	ppm	ppm	ppm
Q515293	5.16	0.034	0.044	1.255	15.1	0.075	5.9	12.7	3.29
Q515294	2.54	0.025	0.04	0.76	12.4	0.059	3.73	10.1	0.58
Q515295	4.08	0.029	0.025	0.67	13.6	0.057	2.16	8.5	0.23
Q515296	4.33	0.032	0.04	1.25	15	0.07	5.25	12	2.09
Q515297	0.27	0.024	0.022	0.283	11	0.051	1.41	6.6	0.07
Q515298	3.9	0.06	0.086	1.125	25.5	0.1	5.47	28	1.61
Q515299	4.12	0.041	0.059	0.92	20	0.104	4.58	21.1	1.81
Q515300	4.29	0.067	0.069	0.72	27.8	0.124	4.01	22.3	1.42
Q515301	3.8	0.025	0.026	0.908	14.9	0.073	3.87	10.6	1.4
Q515302	2.14	0.038	0.035	0.408	19.4	0.136	2.47	10.3	0.53
Q515303	2.48	0.033	0.048	0.378	17.4	0.084	2.82	18.9	0.87
Q515304	3.83	0.045	0.053	0.486	23.4	0.106	4.09	18.1	1.81
Q515305	5.07	0.042	0.059	0.659	19	0.098	4.86	13.8	4.59
Q515306	5.39	0.042	0.062	0.962	18.5	0.078	5.5	16	4.2
Q515307	2.74	0.028	0.037	0.432	15.5	0.054	3.25	10.8	1.11
Q515308	2.41	0.037	0.025	0.255	20.2	0.108	1.425	6.7	1.11
Q515309	2.81	0.038	0.034	0.295	21.9	0.175	1.93	9.5	1.53
Q515311	3.34	0.035	0.032	0.506	19.9	0.118	2.32	11.4	1.36
Q515312	3.71	0.045	0.048	0.585	17.6	0.081	3.81	16.1	1.21
Q515313	4.63	0.047	0.057	1.035	16.8	0.168	5.22	22.6	2.13
Q515314	2.83	0.028	0.026	0.636	14.7	0.07	3.2	10.8	1.08
Q515315	0.947	0.031	0.034	0.688	8.2	0.052	2.68	8.1	0.1
Q515316	4.63	0.033	0.036	1.315	12.7	0.082	5.46	11.7	1.51
Q515317	2.65	0.032	0.041	0.691	15	0.057	3.63	12	1.03
Q515318	3.13	0.026	0.033	0.819	12.6	0.061	4.46	9.3	0.45
Q515319	3.43	0.028	0.042	0.785	12.7	0.065	4.11	9.6	0.59
Q515320	2.9	0.025	0.03	1.045	11.8	0.061	4.09	8.5	0.5
Q515321	3.76	0.022	0.027	1.12	10.9	0.061	4.82	7.1	0.86
Q515322	4.12	0.022	0.026	1.195	11.6	0.14	5.25	7.4	0.71
Q515323	4.19	0.023	0.025	1.13	11.7	0.103	5.24	8.4	1.86
Q515324	3.84	0.025	0.025	1.205	12.6	0.083	4.96	8	0.7
Q515325	3.57	0.02	0.023	1.21	9.2	0.094	4.9	7.1	0.63
Q515326	3.36	0.019	0.023	1.14	11.8	0.061	4.62	7.2	0.54
Q515327	4.03	0.019	0.026	1.25	10.9	0.076	4.7	7.2	1.67
Q515328	3.37	0.023	0.029	0.996	12.6	0.305	4.39	8.1	1.07
Q515329	2.93	0.029	0.043	0.793	14.4	0.084	3.36	10.8	0.48
Q515330	3.28	0.023	0.033	0.841	12.7	0.056	4.31	9.7	1.05
Q515331	4.14	0.025	0.038	1.1	14	0.06	4.82	9.8	1.08
Q515332	2.57	0.021	0.023	0.943	6.4	0.043	3.25	6.1	0.22
Q515333	3.63	0.037	0.051	1.29	17.5	0.085	5.09	16.5	0.75
Q515334	4.78	0.026	0.03	1.155	14.3	0.077	5.16	9	1.48

Till Aqua Regia

	Th	Ti	Tl	U	V	W	Y	Zn	Zr
	ppm	%	ppm	ppm	ppm	ppm	ppm	ppm	ppm
Q515335	5	0.027	0.035	1.585	14.2	0.073	5.36	10.2	1.95
Q515336	2.94	0.027	0.034	0.635	16.5	0.082	3.86	12.1	1.05
Q515337	2.24	0.028	0.033	0.326	16.5	0.068	2.73	10.4	1.09
Q515338	2.22	0.028	0.031	0.476	17.6	0.071	3.04	12.1	0.72
Q515339	3.03	0.048	0.037	0.385	27.3	0.129	1.625	8.5	1.48
Q515340	2.6	0.034	0.035	0.342	20.9	0.155	2.22	9.5	1.72
Q515341	2.85	0.022	0.03	0.334	16.1	0.219	2.99	10.3	1.96
Q515342	3.15	0.031	0.05	0.449	17.4	0.052	3.4	13.5	2.27
Q515343	3.67	0.054	0.086	0.919	26.6	0.131	4.29	24.1	1.07
Q515344	4.03	0.041	0.063	0.714	21.1	0.078	4.37	15	2.52
Q515345	2.61	0.042	0.043	0.417	24.7	0.093	2.38	15.2	0.82
Q515346	2.95	0.034	0.044	0.406	21.7	0.079	2.71	14.6	1.61
Q515347	3.49	0.041	0.067	0.641	20.2	0.078	3.96	16	3.84
Q515348	2.79	0.03	0.045	0.418	18.6	0.096	2.91	14.2	1.17
Q515349	3.6	0.043	0.057	0.812	20.3	0.084	4.35	19.7	3.94
Q515350	3.05	0.038	0.054	0.409	20.2	0.642	3.15	16.3	1.81
Q515351	3.53	0.028	0.042	0.4	17.1	0.086	2.85	14	1.45
Q515352	3.16	0.039	0.04	0.395	20	0.088	2.2	12.5	1.54
Q515354	3.32	0.038	0.029	0.515	27.3	0.107	1.715	6.7	0.55
Q515355	3.32	0.025	0.031	0.783	13.8	0.102	3.45	9.7	1.33
Q515356	2.45	0.031	0.042	0.461	15.6	0.184	2.49	11.2	1.47
Q515357	5	0.033	0.039	1.375	15.4	0.078	5.76	13	2.73
Q515358	3.48	0.026	0.035	1.03	18.8	0.081	4.83	8.8	0.79
Q515359	2.55	0.038	0.051	1.115	16.4	0.07	3.55	13.5	0.44
Q515360	4.41	0.039	0.052	1.185	16.8	0.076	4.77	13.9	0.9
Q515362	2.58	0.029	0.048	0.619	14.2	0.375	3.94	12.1	1.08
Q515363	4.56	0.036	0.049	1.285	13.9	0.183	5.53	13.7	1.83
Q515364	4.65	0.034	0.045	1.545	14.2	0.096	6.11	13	1.16
Q515365	2.33	0.034	0.046	0.775	15.4	0.102	3.58	13.3	0.36
Q515366	3.73	0.019	0.024	1.17	10.1	0.85	4.59	7.8	1.01
Q515367	4.31	0.027	0.031	1.155	13.8	0.075	5.2	9.5	1.52
Q515368	5.14	0.025	0.031	1.47	12.5	0.066	5.68	9.1	1.2
Q515370	3.99	0.023	0.028	1.31	11.4	0.137	5.4	8.6	1.73
Q515371	4.01	0.028	0.033	1.18	13.5	0.102	4.98	11	1.47
Q515372	3.13	0.024	0.027	1.04	10.1	0.132	4.38	8.9	0.69
Q515373	4.2	0.03	0.033	1.205	13.6	0.141	5.29	10.4	1.51
Q515374	4.18	0.028	0.032	1.23	13.6	0.065	4.86	11.4	1.51
Q515375	2.14	0.041	0.045	0.62	18.5	0.183	2.9	16	0.68
Q515376	2.78	0.031	0.043	0.76	13.2	0.101	3.91	11.6	0.62
Q515377	4.13	0.043	0.039	0.959	23	0.611	3.52	12.5	0.57
Q515378	5.85	0.035	0.051	1.51	17.4	0.215	5.88	13	2.22

Till Aqua Regia

	Th	Ti	Tl	U	V	W	Y	Zn	Zr
	ppm	%	ppm	ppm	ppm	ppm	ppm	ppm	ppm
Q515379	4.58	0.022	0.024	1.375	11.3	0.055	5.42	7.7	1.33
Q515380	4.96	0.03	0.025	1.44	15	0.091	5.46	9.2	0.63
Q515381	4.01	0.027	0.028	1.16	12.6	0.066	4.92	9.8	0.91
Q515382	3.8	0.027	0.027	1.19	12.4	0.062	5.06	9.8	1.25
Q515384	3.58	0.035	0.057	1.23	13.7	0.077	4.97	14.4	1.06
Q515385	4.25	0.024	0.027	1.13	12.4	0.064	4.9	8.3	0.83
Q515386	4.2	0.032	0.029	1.025	13.8	0.095	4.46	9.3	1.1
Q515387	2.91	0.027	0.028	0.74	13.2	0.085	3.39	8.6	1.06
Q515388	4.18	0.027	0.031	1.17	13.6	0.102	4.54	10.1	1.69
Q515389	4	0.058	0.027	0.467	26.8	0.108	1.595	7.9	0.88
Q515390	2.89	0.032	0.023	0.492	17.5	0.084	2.66	8.9	1.27
Q515391	5.07	0.039	0.05	1.475	16.7	0.107	6.43	14.3	4.18
Q515392	3.89	0.044	0.063	0.593	19.8	0.111	4.08	19	2.41
Q515393	3.85	0.041	0.045	0.452	19.2	0.08	3.5	16.8	2.75
Q515394	4.82	0.058	0.077	0.642	24.6	1.365	4.63	26.5	3.35
Q515395	2.07	0.051	0.074	0.452	17.5	0.11	2.9	18.5	0.58
Q515396	4.26	0.059	0.082	0.631	23.7	0.096	4.56	23.1	4.8
Q515397	5.41	0.048	0.076	0.668	22	0.171	4.65	22.6	3.51
Q515398	4.99	0.066	0.108	0.849	29	0.124	5.12	28.7	4.81
Q515399	3.33	0.037	0.056	0.4	20.9	0.097	2.97	14.8	1.08
Q515400	1.225	0.024	0.037	0.231	7.5	0.042	2.19	9	0.16
Q515401	2.65	0.041	0.05	0.476	17.1	0.075	3.44	16.1	0.68
Q515402	3.81	0.03	0.048	1.195	15.4	0.155	4.79	13.7	0.95
Q515403	2.29	0.023	0.035	0.705	12	0.059	3.65	9.6	0.59
Q515404	4.19	0.023	0.028	1.18	12.5	0.107	4.63	7.6	0.71
Q515405	3.44	0.021	0.029	1.14	7.1	0.121	4.53	7.9	0.48
Q515406	5.74	0.058	0.098	1.55	26.3	0.083	6.13	25.8	4.1
Q515407	2.81	0.048	0.079	0.65	22.9	0.16	3.79	18.8	0.94
Q515408	5.23	0.036	0.06	1.19	16.8	0.103	5.47	14.1	3.75
Q515409	6.55	0.036	0.066	0.853	18.1	0.062	4.85	16.3	2.3
Q515410	6.28	0.048	0.072	1.005	20.7	0.107	5.4	19.2	3.69
Q515411	3.73	0.032	0.054	0.544	17	0.095	3.98	16.4	0.98
Q515412	3.35	0.032	0.055	0.623	16.5	0.099	4.06	14.8	1.74
Q515413	4.36	0.037	0.056	1.415	19.5	0.127	5.08	13.8	1.28
Q515414	3.28	0.019	0.026	0.92	10	0.05	4.41	6.8	2.04
Q515415	3.68	0.028	0.042	0.872	14.8	0.078	4.43	12	2.19
Q515416	3.24	0.03	0.056	0.435	16	0.055	3.4	14	1.33
Q515417	2.24	0.034	0.052	0.337	16.6	0.088	2.61	14.3	0.99
Q515418	3.43	0.03	0.047	0.382	16.5	0.057	3.49	12.9	0.99
Q515419	4.91	0.043	0.068	0.897	20.5	0.071	4.9	16.6	4.1
Q515420	5.27	0.053	0.057	0.377	27.3	0.099	2.35	19.9	0.76

Till Aqua Regia

	Th	Ti	Tl	U	V	W	Y	Zn	Zr
	ppm	%	ppm	ppm	ppm	ppm	ppm	ppm	ppm
Q515421	3.2	0.039	0.062	0.453	21.2	0.073	3.71	16.1	1.21
Q515422	2.55	0.026	0.046	0.423	14.6	0.062	3	12.3	0.51
Q515423	4.98	0.048	0.076	1.01	21.3	0.103	5.55	17.1	3.76
Q515425	2.6	0.032	0.043	0.329	16.7	0.097	1.86	13.7	1.46
Q515426	4.09	0.047	0.052	0.531	25.6	0.142	3.01	18.7	1.14
Q515427	4.68	0.05	0.083	0.817	21.8	0.09	4.53	19.4	3.13
Q515428	3.11	0.032	0.059	0.491	15.8	0.06	3.61	15.1	0.98
Q515429	3.92	0.037	0.076	0.459	15.9	0.055	3.29	17	1.6
Q515430	3.35	0.044	0.083	0.512	19.8	0.061	3.95	24.4	1.52
Q515431	4.57	0.04	0.058	0.883	17.6	0.084	5.05	14.8	4.16
Q515432	2.75	0.028	0.056	0.422	14.8	0.055	3.07	14.7	1.58
Q515433	3.99	0.033	0.043	0.492	16.4	0.055	3.51	12.2	1.23
Q515434	4.06	0.039	0.047	1.155	15	0.32	5.05	13.3	2.16
Q515435	4.55	0.036	0.045	1.23	14.8	0.1	5.27	11.7	2.79
Q515436	2.38	0.032	0.033	0.476	15.4	0.171	3.01	11.8	0.34
Q515437	3.03	0.039	0.053	0.914	11	0.074	4.25	12.8	0.64
Q515438	3.11	0.03	0.041	0.719	12.8	0.061	3.72	12.2	0.86
Q515439	3.56	0.02	0.024	0.821	9.4	0.077	3.76	6.5	1.25
Q515440	3.37	0.019	0.025	0.812	9	0.066	3.79	6	1.43
Q515442	2.4	0.02	0.02	1	9.2	0.065	3.78	6	0.36
Q515443	2.67	0.03	0.039	1.11	14.8	0.068	4.8	11.4	0.28
Q515444	3.96	0.044	0.056	1.04	17.4	0.321	4.8	14.8	1.66
Q515445	5.41	0.036	0.042	1.78	14	0.096	6.92	10.1	3.57
Q515446	3.13	0.029	0.035	0.615	14	0.071	3.6	10.5	1.13
Q515447	3.37	0.05	0.062	0.917	19.8	0.105	4.39	17.8	1.36
Q515448	3.26	0.044	0.059	1.035	16	0.109	4.36	17	0.63
Q515449	2.13	0.022	0.027	0.804	9.8	0.064	3.85	7.3	0.34
Q515450	5.1	0.034	0.037	1.56	11.7	0.113	6.17	10.5	1.48
Q515451	4.6	0.038	0.045	1.315	14.8	0.162	5.73	11.4	2.55
Q515452	4.2	0.029	0.035	1.215	11.7	0.064	5.04	8.6	2.55
Q515454	4.15	0.04	0.047	1.31	15.5	0.091	5.35	11.1	1.32
Q515455	3.43	0.032	0.028	1.025	14.8	0.114	3.4	8.3	0.79
Q515456	5.27	0.039	0.046	1.045	12.1	0.063	5.34	12.9	3.86
Q515457	5.1	0.062	0.098	1.155	24.5	0.109	4.99	24.9	8.47
Q515458	4.65	0.049	0.066	0.882	18.7	0.082	4.97	16.2	5.03
Q515459	4.85	0.048	0.057	0.737	18.4	0.083	4.47	14.7	4.37
Q515460	3.81	0.035	0.042	0.924	14.7	0.069	4.84	11	2.43
Q515461	2.79	0.026	0.044	0.258	12.1	0.05	2.28	8.9	1.81
Q515462	2.47	0.031	0.026	0.312	16.5	0.051	2.37	9.5	0.4
Q515463	2.83	0.03	0.051	0.463	13.1	0.082	2.89	12.6	1.08
Q515464	3.81	0.042	0.062	0.997	16.5	0.088	4.67	15.5	1.41

Till Aqua Regia

	Th	Ti	Tl	U	V	W	Y	Zn	Zr
	ppm	%	ppm	ppm	ppm	ppm	ppm	ppm	ppm
Q515465	2.24	0.032	0.04	0.436	14.2	0.089	2.73	11.8	0.97
Q515466	3.8	0.047	0.056	0.799	16.7	0.074	4.6	16.8	2
Q515467	4.87	0.031	0.043	0.45	16	0.066	3.48	11.9	1.8
Q515468	4.25	0.041	0.05	0.638	16.8	0.067	4.22	13.5	3.56
Q515469	3.54	0.03	0.047	0.424	18.6	0.098	3.7	13.7	2.09
Q515470	4.32	0.048	0.066	0.812	21.5	0.076	5.28	17.6	3.73
Q515471	2.38	0.037	0.034	0.383	20.6	0.082	3.01	16	1.01
Q515472	3.33	0.037	0.039	0.523	19.1	0.149	3.07	13.2	1.47
Q515473	1.885	0.034	0.042	0.371	13.2	0.057	3.2	17.3	0.55
Q515474	4.97	0.048	0.071	0.732	20.8	0.066	5.26	18	4.87
Q515475	3.79	0.029	0.039	0.417	16	0.053	3.35	13.1	1.27

D.6 Till Pb Isotope Ratios Q-ICP-MS Results

Lead isotope ratio results are presented for the Q-ICP-MS analysis of the -180 micron fraction of till samples.

Till Pb Isotopes Ratios Q-ICP-MS Results

Sample	Pb^{206}/Pb^{204}	Pb^{207}/Pb^{204}	Pb^{208}/Pb^{204}	Pb^{208}/Pb^{206}	Pb^{208}/Pb^{207}	Pb^{206}/Pb^{207}
Q515282	17.97	15.48	37.77	2.102	2.439	1.16
Q515300	18.11	15.57	39.16	2.162	2.516	1.163
Q515300d	18.15	15.68	38.39	2.115	2.448	1.162
Q515344	18.09	15.58	39.46	2.181	2.532	1.161
Q515367	19.88	15.89	39.09	1.966	2.46	1.251
Q515396	18.26	15.58	38.8	2.125	2.49	1.171
Q515404	18.25	15.53	37.69	2.065	2.428	1.174
Q515414	18.89	15.67	37.66	1.994	2.404	1.204
Q515419	17.77	15.47	37.18	2.093	2.403	1.144
Q515425	17.85	15.47	37.46	2.099	2.421	1.15
Q515431	18.47	15.54	38.6	2.09	2.483	1.187
Q515438	18.16	15.49	37.3	2.054	2.409	1.17
Q515449	18.45	15.61	37.24	2.019	2.385	1.181
Q515449d	18.77	15.58	37.41	1.993	2.401	1.204
Q515458	18.27	15.5	38.15	2.089	2.461	1.176
Q515463	17.42	15.4	37.57	2.157	2.439	1.129
Q515470	17.89	15.44	38.32	2.142	2.482	1.156

D.7 Till Sequential Extraction Results

Multi-element results are presented for the sequential extraction digestions and ICP-MS analysis of the -180 micron fraction of till samples.

Till Sequential Extraction Results

Deionized Water Extraction

Sample	Ag ppm	Al ppm	Al %	As ppm	Au ppm	B ppm	Ba ppm	Be ppm	Bi ppm	Br ppm	Ca ppm	Cd ppm	Ce ppm	Co ppm	Cr ppm
Q515255	<0.002	27	0.0027	0.01	<0.001	0.2	0.32	<0.005	<0.003	1	10	0.002	0.0446	0.068	<0.05
Q515396	<0.002	8	0.0008	0.02	0.001	0.2	0.14	<0.005	<0.003	<1	10	<0.001	0.049	0.015	<0.05
Q515469	<0.002	7	0.0007	<0.01	<0.001	<0.2	0.22	<0.005	<0.003	1	<10	0.001	0.0183	0.014	<0.05
Q515414	<0.002	2	0.0002	0.04	<0.001	<0.2	0.06	<0.005	<0.003	<1	<10	<0.001	0.0055	0.004	<0.05

Ammonium Acetate pH 5 Extraction

Sample	Ag ppm	Al ppm	Al %	As ppm	Au ppm	B ppm	Ba ppm	Be ppm	Bi ppm	Br ppm	Ca ppm	Cd ppm	Ce ppm	Co ppm	Cr ppm
Q515255	<0.002	410	0.041	0.06	0.001	<0.2	3.9	0.029	<0.003	1	40	0.006	1.52	0.175	0.14
Q515396	<0.002	128	0.0128	<0.01	<0.001	<0.2	3.25	0.01	<0.003	<1	30	<0.001	1.16	0.053	0.09
Q515469	<0.002	96	0.0096	<0.01	0.001	<0.2	6.5	<0.005	0.003	<1	30	0.001	0.564	0.069	0.07
Q515414	<0.002	52	0.0052	0.02	<0.001	<0.2	2.1	<0.005	0.004	<1	20	0.002	0.124	0.013	<0.05

Cold HA-HC 0.14M @ 25°C Extraction

Sample	Ag ppm	Al ppm	Al %	As ppm	Au ppm	B ppm	Ba ppm	Be ppm	Bi ppm	Br ppm	Ca ppm	Cd ppm	Ce ppm	Co ppm	Cr ppm
Q515255	0.004	435	0.0435	<0.01	<0.001	<0.2	0.83	0.024	<0.003	<1	150	0.004	0.826	0.052	0.1
Q515396	<0.002	272	0.0272	0.1	<0.001	<0.2	0.57	0.01	<0.003	<1	590	0.001	1.715	0.2	0.17
Q515469	0.002	151	0.0151	0.05	<0.001	<0.2	0.73	<0.005	<0.003	<1	610	<0.001	1.135	0.162	0.05
Q515414	0.002	71	0.0071	0.08	<0.001	<0.2	0.51	<0.005	<0.003	<1	690	0.005	0.888	0.053	<0.05

Hot HA-HC 0.25M @ 60°C Extraction

Sample	Ag ppm	Al ppm	Al %	As ppm	Au ppm	B ppm	Ba ppm	Be ppm	Bi ppm	Br ppm	Ca ppm	Cd ppm	Ce ppm	Co ppm	Cr ppm
Q515255	0.014	3480	0.348	0.18	<0.001	<0.2	7.28	0.12	0.054	2	110	0.024	4.86	1.89	5.51
Q515396	0.004	865	0.0865	0.47	<0.001	<0.2	4.42	0.032	0.035	<1	200	0.012	4.51	1.455	1.63
Q515469	0.002	693	0.0693	0.34	<0.001	<0.2	4.12	0.024	0.03	<1	180	0.012	4.78	1.01	1.49
Q515414	0.002	313	0.0313	0.65	<0.001	<0.2	2.68	0.014	0.052	<1	250	0.009	2.4	0.405	0.81

Na pyro-phosphate (0.1M) Extraction

Sample	Ag ppm	Al ppm	Al %	As ppm	Au ppm	B ppm	Ba ppm	Be ppm	Bi ppm	Br ppm	Ca ppm	Cd ppm	Ce ppm	Co ppm	Cr ppm
Q515255	<0.002	182	0.0182	0.45	<0.001	<0.2	0.72	0.007	0.005	2	10	0.001	0.231	0.107	0.99
Q515396	<0.002	140	0.014	0.14	<0.001	<0.2	1.12	0.005	<0.003	<1	10	0.001	0.181	0.06	0.36
Q515469	<0.002	244	0.0244	0.08	<0.001	0.2	1.23	0.006	<0.003	<1	10	0.002	0.182	0.078	0.46
Q515414	<0.002	18	0.0018	<0.01	<0.001	<0.2	0.39	<0.005	<0.003	<1	<10	0.002	0.0746	0.01	0.09

Till Sequential Extraction Results

Deionized Water Extraction

Sample	Cu ppm	Dy ppm	Er ppm	Eu ppm	Fe ppm	Fe %	Ga ppm	Gd ppm	Ge ppm	Hf ppm	Hg ppm	Ho ppm	I ppm	In ppm	K ppm
Q515255	0.1	0.0044	0.0008	0.001	17	0.0017	<0.05	0.0029	<0.005	0.0008	<0.01	0.0001	0.06	<0.001	11
Q515396	0.05	0.0012	<0.0005	0.0007	4	0.0004	<0.05	0.0026	<0.005	<0.0005	<0.01	0.0001	<0.05	<0.001	5
Q515469	<0.05	0.0006	<0.0005	<0.0005	4	0.0004	<0.05	0.0014	<0.005	<0.0005	<0.01	0.0002	0.05	<0.001	6
Q515414	<0.05	0.0006	<0.0005	<0.0005	1	0.0001	<0.05	<0.0005	<0.005	<0.0005	<0.01	<0.0001	<0.05	<0.001	<5

Ammonium Acetate pH 5 Extraction

Sample	Cu ppm	Dy ppm	Er ppm	Eu ppm	Fe ppm	Fe %	Ga ppm	Gd ppm	Ge ppm	Hf ppm	Hg ppm	Ho ppm	I ppm	In ppm	K ppm
Q515255	0.5	0.057	0.028	0.0258	46	0.0046	<0.05	0.103	<0.005	0.0023	<0.01	0.0106	0.23	<0.001	8
Q515396	0.33	0.0212	0.007	0.011	31	0.0031	<0.05	0.0455	<0.005	0.0029	<0.01	0.0012	0.17	<0.001	<5
Q515469	0.1	0.0109	0.0051	0.0057	20	0.002	<0.05	0.0234	<0.005	0.0006	<0.01	0.002	0.16	<0.001	<5
Q515414	0.08	0.0028	0.0018	0.0023	12	0.0012	<0.05	0.0095	<0.005	0.0007	<0.01	0.0009	0.11	<0.001	<5

Cold HA-HC 0.14M @ 25°C Extraction

Sample	Cu ppm	Dy ppm	Er ppm	Eu ppm	Fe ppm	Fe %	Ga ppm	Gd ppm	Ge ppm	Hf ppm	Hg ppm	Ho ppm	I ppm	In ppm	K ppm
Q515255	0.22	0.0412	0.0236	0.0107	116	0.0116	<0.05	0.0492	<0.005	0.0014	<0.01	0.0082	0.12	<0.001	5
Q515396	0.28	0.207	0.0946	0.0364	88	0.0088	<0.05	0.245	<0.005	0.0048	<0.01	0.0338	0.1	<0.001	<5
Q515469	0.1	0.201	0.097	0.0353	42	0.0042	<0.05	0.236	<0.005	0.002	<0.01	0.0345	0.05	0.001	<5
Q515414	0.08	0.301	0.156	0.0416	22	0.0022	<0.05	0.336	<0.005	<0.0005	<0.01	0.0544	<0.05	<0.001	<5

Hot HA-HC 0.25M @ 60°C Extraction

Sample	Cu ppm	Dy ppm	Er ppm	Eu ppm	Fe ppm	Fe %	Ga ppm	Gd ppm	Ge ppm	Hf ppm	Hg ppm	Ho ppm	I ppm	In ppm	K ppm
Q515255	4.64	0.238	0.108	0.0798	4990	0.499	1.57	0.333	0.012	0.0053	<0.01	0.0343	0.71	0.003	44
Q515396	2.8	0.17	0.0766	0.0509	1420	0.142	0.32	0.277	0.01	0.0078	<0.01	0.029	0.09	0.001	89
Q515469	2.46	0.201	0.0699	0.0568	1130	0.113	0.35	0.294	0.008	0.0026	<0.01	0.0304	0.07	0.001	87
Q515414	2.55	0.2	0.0894	0.0469	602	0.0602	0.13	0.258	0.005	0.0015	<0.01	0.0348	<0.05	0.001	43

Na pyro-phosphate (0.1M) Extraction

Sample	Cu ppm	Dy ppm	Er ppm	Eu ppm	Fe ppm	Fe %	Ga ppm	Gd ppm	Ge ppm	Hf ppm	Hg ppm	Ho ppm	I ppm	In ppm	K ppm
Q515255	0.77	0.0117	0.0047	0.0055	961	0.0961	0.29	0.017	0.005	0.032	<0.01	0.0016	0.56	<0.001	24
Q515396	0.27	0.0089	0.0041	0.0019	150	0.015	<0.05	0.0089	<0.005	0.0302	<0.01	0.0017	<0.05	0.001	63
Q515469	0.36	0.0089	0.0047	0.0023	185	0.0185	0.07	0.0092	<0.005	0.0336	<0.01	0.0017	0.05	0.001	71
Q515414	0.11	<0.0005	0.0011	0.0009	22	0.0022	<0.05	0.0032	<0.005	0.0073	<0.01	0.0002	<0.05	<0.001	20

Till Sequential Extraction Results

Deionized Water Extraction

Sample	La ppm	Li ppm	Lu ppm	Mg ppm	Mg %	Mn ppm	Mo ppm	Na ppm	Nb ppm	Nd ppm	Ni ppm	P ppm	Pb ppm	Pr ppm	Rb ppm
Q515255	0.0226	0.06	0.0001	4.7	0.0005	0.76	<0.001	5	0.0013	0.023	0.11	1	0.005	0.0062	0.061
Q515396	0.022	0.02	<0.0001	2.7	0.0003	0.48	0.001	<5	0.0011	0.0079	<0.05	<1	<0.005	0.0115	0.05
Q515469	0.0049	0.03	<0.0001	2.8	0.0003	0.37	<0.001	<5	0.0012	0.0091	<0.05	<1	0.005	0.0015	0.053
Q515414	0.0009	0.03	<0.0001	0.5	5E-05	0.08	<0.001	<5	<0.0005	0.0026	<0.05	<1	<0.005	<0.0001	0.037

Ammonium Acetate pH 5 Extraction

Sample	La ppm	Li ppm	Lu ppm	Mg ppm	Mg %	Mn ppm	Mo ppm	Na ppm	Nb ppm	Nd ppm	Ni ppm	P ppm	Pb ppm	Pr ppm	Rb ppm
Q515255	0.707	0.03	0.0012	3.1	0.0003	1.17	0.001	<5	0.0015	0.681	0.35	2	0.166	0.19	0.194
Q515396	0.676	0.01	0.0009	2	0.0002	1	0.003	<5	0.0009	0.352	0.06	1	0.07	0.1	0.18
Q515469	0.215	0.01	0.0005	5.3	0.0005	1.3	<0.001	<5	0.0009	0.16	<0.05	2	0.126	0.0551	0.208
Q515414	0.048	<0.01	0.0002	0.8	8E-05	0.17	0.001	<5	<0.0005	0.0351	<0.05	1	0.063	0.0104	0.108

Cold HA-HC 0.14M @ 25°C Extraction

Sample	La ppm	Li ppm	Lu ppm	Mg ppm	Mg %	Mn ppm	Mo ppm	Na ppm	Nb ppm	Nd ppm	Ni ppm	P ppm	Pb ppm	Pr ppm	Rb ppm
Q515255	0.486	0.01	0.0016	1.6	0.0002	0.74	<0.001	<5	0.0022	0.292	0.14	23	0.09	0.0787	0.072
Q515396	0.783	0.01	0.009	0.7	7E-05	5.25	<0.001	<5	0.0019	0.923	0.05	245	0.117	0.195	0.039
Q515469	0.351	0.02	0.0082	1.6	0.0002	4.02	<0.001	<5	0.0018	0.797	<0.05	269	0.124	0.15	0.076
Q515414	0.257	0.02	0.0137	0.7	7E-05	3.29	<0.001	<5	0.0014	0.775	<0.05	308	0.095	0.136	0.027

Hot HA-HC 0.25M @ 60°C Extraction

Sample	La ppm	Li ppm	Lu ppm	Mg ppm	Mg %	Mn ppm	Mo ppm	Na ppm	Nb ppm	Nd ppm	Ni ppm	P ppm	Pb ppm	Pr ppm	Rb ppm
Q515255	2.12	3.9	0.011	1120	0.112	32.8	0.02	15	0.127	2.31	3.19	68	1.44	0.545	1.09
Q515396	1.795	1.54	0.007	287	0.0287	30.1	0.033	18	0.0406	1.935	1.59	96	0.565	0.437	1.145
Q515469	2.1	1.15	0.007	270	0.027	18.85	0.021	12	0.0366	2.05	1.41	90	0.707	0.508	1.1
Q515414	1.115	0.57	0.0084	112.5	0.0113	4.62	0.043	15	0.0219	1.335	0.96	112	0.387	0.3	0.347

Na pyro-phosphate (0.1M) Extraction

									ME-MS07	ME-MS07	ME-MS07		ME-MS07	ME-MS07	ME-MS07
Sample	La ppm	Li ppm	Lu ppm	Mg ppm	Mg %	Mn ppm	Mo ppm	Na ppm	Nb ppm	Nd ppm	Ni ppm	P ppm	Pb ppm	Pr ppm	Rb ppm
Q515255	0.0957	0.17	0.0005	38.6	0.0039	4.11	0.214	-	0.527	0.115	0.21	-	0.059	0.0288	0.165
Q515396	0.0934	0.15	0.0005	22.8	0.0023	0.63	0.048	-	0.0864	0.0614	0.33	-	0.015	0.0186	0.285
Q515469	0.0878	0.24	0.0005	40.5	0.0041	0.91	0.047	-	0.105	0.0684	0.31	-	0.019	0.0181	0.399
Q515414	0.036	0.03	0.0009	3.8	0.0004	0.14	0.028	-	0.0233	0.0295	0.1	-	<0.005	0.0116	0.055

- not measured

Till Sequential Extraction Results

Deionized Water Extraction

Sample	Re	Sb	Se	Sm	Sn	Sr	Ta	Tb	Te	Th	Ti	Tl	Tm	U	V
	ppm	ppm	ppm	ppm	ppm	ppm	ppm	ppm	ppm	ppm	ppm	ppm	ppm	ppm	ppm
Q515255	<0.0002	0.0005	<0.02	0.0032	<0.005	0.185	<0.001	0.0007	<0.005	0.006	0.71	<0.001	0.0004	0.0037	<0.05
Q515396	<0.0002	0.0016	<0.02	0.0273	<0.005	0.068	<0.001	0.0001	<0.005	0.0057	0.09	<0.001	<0.0001	0.0036	<0.05
Q515469	<0.0002	<0.0005	<0.02	0.0025	<0.005	0.055	<0.001	0.0006	<0.005	0.0046	0.38	0.001	0.0001	0.003	<0.05
Q515414	<0.0002	0.0005	<0.02	0.0013	<0.005	0.02	<0.001	0.0001	<0.005	0.001	<0.05	<0.001	<0.0001	0.0012	<0.05

Ammonium Acetate pH 5 Extraction

Sample	Re	Sb	Se	Sm	Sn	Sr	Ta	Tb	Te	Th	Ti	Tl	Tm	U	V
	ppm	ppm	ppm	ppm	ppm	ppm	ppm	ppm	ppm	ppm	ppm	ppm	ppm	ppm	ppm
Q515255	0.0002	<0.0005	<0.02	0.119	<0.005	0.428	<0.001	0.0096	<0.005	0.0775	0.61	0.002	0.0019	0.0752	0.07
Q515396	<0.0002	0.0011	<0.02	0.033	<0.005	0.238	<0.001	0.0037	0.009	0.101	<0.05	0.002	0.0008	0.0456	<0.05
Q515469	<0.0002	<0.0005	0.05	0.026	<0.005	0.228	<0.001	0.0029	<0.005	0.0701	0.33	0.001	0.0005	0.028	<0.05
Q515414	<0.0002	<0.0005	<0.02	0.0088	<0.005	0.062	<0.001	0.0008	0.012	0.0126	0.07	<0.001	0.0005	0.0101	<0.05

Cold HA-HC 0.14M @ 25°C Extraction

Sample	Re	Sb	Se	Sm	Sn	Sr	Ta	Tb	Te	Th	Ti	Tl	Tm	U	V
	ppm	ppm	ppm	ppm	ppm	ppm	ppm	ppm	ppm	ppm	ppm	ppm	ppm	ppm	ppm
Q515255	<0.0002	0.001	<0.02	0.0602	<0.005	0.222	<0.001	0.0061	0.006	0.0171	0.53	0.001	0.0036	0.0094	0.22
Q515396	<0.0002	<0.0005	<0.02	0.226	<0.005	0.921	<0.001	0.0342	<0.005	0.0493	0.2	<0.001	0.0138	0.0292	0.09
Q515469	<0.0002	0.001	<0.02	0.228	<0.005	0.898	<0.001	0.0331	0.007	0.0089	0.48	<0.001	0.0131	0.0164	0.1
Q515414	<0.0002	<0.0005	<0.02	0.289	<0.005	0.721	<0.001	0.0511	0.005	0.0042	0.22	<0.001	0.0226	0.049	<0.05

Hot HA-HC 0.25M @ 60°C Extraction

Sample	Re	Sb	Se	Sm	Sn	Sr	Ta	Tb	Te	Th	Ti	Tl	Tm	U	V
	ppm	ppm	ppm	ppm	ppm	ppm	ppm	ppm	ppm	ppm	ppm	ppm	ppm	ppm	ppm
Q515255	<0.0002	<0.0005	0.04	0.434	0.021	0.787	0.007	0.0399	<0.005	0.0153	113	0.009	0.0116	0.15	12.2
Q515396	<0.0002	0.0022	<0.02	0.361	0.011	0.649	0.001	0.029	<0.005	0.0297	31.6	0.008	0.0079	0.0997	2.63
Q515469	0.0002	<0.0005	0.07	0.389	0.013	0.586	0.001	0.0343	<0.005	0.0198	30.6	0.008	0.0116	0.0931	2.12
Q515414	<0.0002	0.0017	<0.02	0.293	0.008	0.561	0.001	0.0311	<0.005	0.0412	14.35	0.004	0.0101	0.108	1.07

Na pyro-phosp	ME-MS07	ME-MS07	ME-MS07	ME-MS07	ME-MS07	ME-MS07	ME-MS07	ME-MS07	ME-MS07	ME-MS07	ME-MS07	ME-MS07	ME-MS07	ME-MS07	ME-MS07
Sample	Re	Sb	Se	Sm	Sn	Sr	Ta	Tb	Te	Th	Ti	Tl	Tm	U	V
	ppm	ppm	ppm	ppm	ppm	ppm	ppm	ppm	ppm	ppm	ppm	ppm	ppm	ppm	ppm
Q515255	<0.0002	0.0067	<0.02	0.0262	0.051	0.122	0.016	0.0028	0.011	0.692	137.5	0.003	0.0007	0.0434	1.71
Q515396	0.0002	<0.0005	0.09	0.0149	0.009	0.093	0.006	0.0012	0.006	0.642	15.9	0.003	0.0006	0.0152	0.3
Q515469	<0.0002	0.0031	<0.02	0.0166	0.028	0.147	0.007	0.0008	0.012	0.642	20.6	0.002	0.0004	0.0165	0.4
Q515414	<0.0002	<0.0005	0.03	0.0076	<0.005	0.032	0.002	0.0005	0.006	0.247	2.98	0.001	0.0003	0.0034	<0.05

Till Sequential Extraction Results

Deionized Water Extraction

Sample	W ppm	Y ppm	Yb ppm	Zn ppm	Zr ppm	Final pH Unity
Q515255	0.001	0.0082	0.0013	0.09	0.009	5.2
Q515396	<0.001	0.0051	<0.0005	<0.05	0.011	5.3
Q515469	<0.001	0.0046	<0.0005	<0.05	0.017	5.1
Q515414	<0.001	<0.0005	<0.0005	<0.05	0.001	5.3

Ammonium Acetate pH 5 Extraction

Sample	W ppm	Y ppm	Yb ppm	Zn ppm	Zr ppm	Final pH Unity
Q515255	0.001	0.243	0.0116	0.33	0.041	4.9
Q515396	<0.001	0.0829	0.0041	0.08	0.056	4.9
Q515469	0.001	0.0649	0.0026	0.25	0.076	4.9
Q515414	<0.001	0.0169	0.0023	0.06	0.007	4.9

Cold HA-HC 0.14M @ 25°C Extraction

Sample	W ppm	Y ppm	Yb ppm	Zn ppm	Zr ppm	Final pH Unity
Q515255	<0.001	0.291	0.0176	0.23	0.03	2.3
Q515396	0.001	0.99	0.0655	0.07	0.103	2.3
Q515469	<0.001	1.03	0.0717	0.11	0.039	2.2
Q515414	0.002	1.55	0.127	0.26	0.02	2.2

Hot HA-HC 0.25M @ 60°C Extraction

Sample	W ppm	Y ppm	Yb ppm	Zn ppm	Zr ppm	Final pH Unity
Q515255	0.001	0.863	0.0731	9.27	0.103	1.1
Q515396	0.003	0.659	0.0551	2.97	0.236	1.1
Q515469	0.003	0.727	0.068	3.07	0.097	1.1
Q515414	0.009	0.785	0.0706	1.41	0.03	1.1

Na pyro-phos ME-MS07 ME-MS07 ME-MS07 ME-MS07 ME-MS07 pH-MS07

Sample	W ppm	Y ppm	Yb ppm	Zn ppm	Zr ppm	Final pH Unity
Q515255	0.045	0.0444	0.0064	0.36	0.853	9.6
Q515396	0.023	0.0377	0.0042	0.16	1.3	10.1
Q515469	0.03	0.0398	0.0041	0.34	1.52	10.2
Q515414	0.011	0.0121	<0.0005	<0.05	0.328	10.2

D.8 Till Size Fraction Four Acid ICP-MS Results

Multi-element results are presented for the four acid digestion and ICP-MS analysis of the various size fractions of till samples.

Till Size Fraction Four Acid ICP-MS Results

Sample ID	Lab ID	Size Fraction µm	Ag ppm	Al %	As ppm	Ba ppm	Be ppm	Bi ppm	Ca %	Cd ppm
515300	515300-1	180-150	0.027	4.23	1.04	470	0.83	0.041	0.99	0.03
515300	515300-2	150-125	0.031	4.52	1.19	490	0.93	0.062	1.07	0.036
515300	515300-3	125-106	0.033	4.7	1.53	520	0.94	0.078	1.06	0.045
515300	515300-4	106-75	0.031	4.55	1.12	510	0.89	0.06	1.12	0.035
515300	515300-5	75-53	0.037	4.96	1.42	580	0.9	0.072	1.24	0.043
515300	515300-6	25-53	0.032	5.23	1.66	630	0.95	0.084	1.31	0.041
515300	515300-7	5-25	0.045	6.08	3.05	730	1.27	0.16	1.22	0.05
515300	515300-8	5-25	0.045	6.46	3.57	780	1.43	0.176	1.3	0.061
515300	515300-9	125-106	0.032	4.46	1.18	510	1.03	0.057	1.05	0.034
515396	515396-1	180-150	0.043	3.88	0.9	480	0.79	0.045	0.82	0.021
515396	515396-2	150-125	0.033	4.33	1.09	530	0.87	0.054	0.95	0.027
515396	515396-3	125-106	0.036	4.61	1.5	560	0.97	0.07	1.02	0.04
515396	515396-4	106-75	0.033	4.18	1.13	530	0.78	0.042	1.03	0.032
515396	515396-5	75-53	0.039	4.63	1.28	600	0.93	0.058	1.18	0.032
515396	515396-6	25-53	0.039	5.08	1.43	660	1.05	0.068	1.36	0.046
515396	515396-7	5-25	0.041	6.3	3.18	750	1.45	0.146	1.45	0.061
515396	515396-8	150-125	0.035	4.35	1.48	540	0.79	0.067	0.89	0.024
515396	515396-9	106-75	0.04	4.35	1.02	560	0.85	0.069	1.02	0.029
515414	515414-1	180-150	0.034	4.17	0.63	296	0.88	0.048	0.91	0.036
515414	515414-2	150-125	0.034	4.51	0.45	336	0.87	0.109	0.92	0.036
515414	515414-3	125-106	0.036	4.6	1.64	338	0.88	0.096	0.99	0.03
515414	515414-4	106-75	0.033	4.37	0.55	327	0.94	0.057	0.97	0.033
515414	515414-5	75-53	0.039	5.11	0.72	407	1.19	0.067	1.21	0.05
515414	515414-6	25-53	0.055	5.11	1.05	448	1.01	0.075	1.3	0.047
515414	515414-7	5-25	0.06	5.27	2.68	490	1.24	0.162	1.35	0.053
515414	515414-8	5-25	0.053	5.53	2.65	510	1.28	0.175	1.41	0.06
515469	515469-1	180-150	0.037	3.97	0.76	490	0.74	0.035	0.83	0.017
515469	515469-2	150-125	0.033	4.02	0.74	490	0.86	0.04	0.93	0.029
515469	515469-3	125-106	0.039	4.08	0.91	510	0.85	0.037	0.92	0.023
515469	515469-4	106-75	0.043	4.17	0.92	530	0.94	0.044	1	0.028
515469	515469-5	75-53	0.043	4.25	1	550	0.95	0.051	1.13	0.034
515469	515469-6	25-53	0.035	4.37	0.99	560	0.84	0.053	1.28	0.042
515469	515469-7	5-25	0.034	5.39	2.64	660	1.19	0.118	1.58	0.064
515469	515469-8	25-53	0.033	4.46	1.21	570	1.15	0.059	1.31	0.037

Till Size Fraction Four Acid ICP-MS Results

Sample ID	Lab ID	Size Fraction µm	Ce ppm	Co ppm	Cr ppm	Cs ppm	Cu ppm	Fe %	Ga ppm	Ge ppm
515300	515300-1	180-150	16.35	3.23	14.9	0.84	5.53	1.02	9.22	0.05
515300	515300-2	150-125	39.2	4.26	22	0.98	6.66	1.35	10.45	0.06
515300	515300-3	125-106	30.7	4.98	26.4	1.33	9.64	1.57	10.85	0.06
515300	515300-4	106-75	23.5	4.75	24.4	1.05	7.78	1.48	9.98	0.05
515300	515300-5	75-53	41.3	5.02	27.1	1.08	8.36	1.59	11.1	0.07
515300	515300-6	25-53	48.2	5.66	33.4	1.29	10.05	1.78	11.3	0.07
515300	515300-7	5-25	58.5	8.2	52	2.42	19.2	2.58	15.9	0.08
515300	515300-8	5-25	63.9	8.91	54.9	2.6	20.6	2.76	17.5	0.1
515300	515300-9	125-106	22.1	4.03	22.6	0.99	7.38	1.34	9.77	0.05
515396	515396-1	180-150	17.75	3.09	10.8	0.58	4.1	0.75	8.31	<0.05
515396	515396-2	150-125	33.5	4.43	17.7	0.82	6.45	1.08	8.92	0.05
515396	515396-3	125-106	44.5	5.82	25.3	1.16	8.79	1.41	10.6	0.06
515396	515396-4	106-75	41.8	4.1	17	0.72	5.13	1.14	8.81	0.07
515396	515396-5	75-53	40	5.21	22	0.9	6.45	1.42	10.1	0.07
515396	515396-6	25-53	44.2	6.3	30.1	1.14	8.09	1.73	11.95	0.07
515396	515396-7	5-25	62.1	11.95	54.7	2.4	18.85	2.66	16.3	0.1
515396	515396-8	150-125	28.5	5.03	19.5	1.01	7.44	1.12	8.95	0.05
515396	515396-9	106-75	30	4.41	18	0.82	5.85	1.11	9.25	0.05
515414	515414-1	180-150	11.35	1.545	6.1	0.49	4.88	0.43	7.25	<0.05
515414	515414-2	150-125	19	1.385	6.7	0.55	5.13	0.42	7.84	0.05
515414	515414-3	125-106	20.6	1.595	7.5	0.54	4.99	0.49	7.91	0.05
515414	515414-4	106-75	18.4	1.62	7.8	0.59	5.04	0.43	7.53	0.05
515414	515414-5	75-53	36.3	2.15	11.3	0.7	5.69	0.67	9.18	0.07
515414	515414-6	25-53	54.1	2.45	14	0.7	5.6	0.81	8.83	0.07
515414	515414-7	5-25	71.8	3.8	24.2	1.02	9.77	1.17	9.66	0.1
515414	515414-8	5-25	75.7	4.03	26.7	1.09	10.4	1.24	10.85	0.1
515469	515469-1	180-150	18.25	3.02	9.8	0.57	4.28	0.67	7.42	0.05
515469	515469-2	150-125	24.3	3.09	11.7	0.57	4.57	0.8	7.98	0.06
515469	515469-3	125-106	22.4	3.35	12.9	0.65	4.74	0.8	7.85	0.06
515469	515469-4	106-75	29.1	3.75	16.1	0.67	5.06	1.03	8.5	0.06
515469	515469-5	75-53	31	4.13	20.1	0.73	5.43	1.21	8.45	0.06
515469	515469-6	25-53	42.7	4.74	24.6	0.76	6.01	1.55	8.86	0.08
515469	515469-7	5-25	64.8	8.44	43.6	1.36	12.65	2.42	12.2	0.11
515469	515469-8	25-53	40.9	4.89	24.2	0.77	5.99	1.56	9.2	0.09

Till Size Fraction Four Acid ICP-MS Results

Sample ID	Lab ID	Size Fraction µm	Hf ppm	In ppm	K %	La ppm	Li ppm	Mg %	Mn ppm	Mo ppm
515300	515300-1	180-150	2.02	0.009	1.25	8.15	12.5	0.33	178.5	0.16
515300	515300-2	150-125	2.24	0.014	1.33	19.9	15.5	0.44	218	0.24
515300	515300-3	125-106	1.75	0.017	1.42	14	18.4	0.49	240	0.25
515300	515300-4	106-75	2.3	0.013	1.37	11.1	15.8	0.47	242	0.22
515300	515300-5	75-53	3.73	0.018	1.55	19.55	17	0.51	252	0.22
515300	515300-6	25-53	4.39	0.023	1.68	22.3	18	0.57	271	0.26
515300	515300-7	5-25	5.15	0.037	2.05	29	30.8	0.76	306	0.6
515300	515300-8	5-25	5.52	0.036	2.18	31.5	33.2	0.81	326	0.61
515300	515300-9	125-106	2.07	0.016	1.36	10.6	15.5	0.42	212	0.22
515396	515396-1	180-150	0.853	0.011	1.29	8.54	12.7	0.24	149.5	0.18
515396	515396-2	150-125	1.225	0.011	1.48	15.8	15.7	0.35	224	0.18
515396	515396-3	125-106	2.22	0.016	1.6	20.8	20.1	0.45	255	0.23
515396	515396-4	106-75	1.975	0.012	1.43	19.2	14.2	0.36	231	0.17
515396	515396-5	75-53	3.39	0.019	1.62	18	16.8	0.44	269	0.19
515396	515396-6	25-53	4.5	0.023	1.8	20.3	20.4	0.55	311	0.24
515396	515396-7	5-25	5.42	0.032	2.23	30.9	37.3	0.87	432	0.44
515396	515396-8	150-125	1.945	0.012	1.55	13.25	17.7	0.38	199	0.24
515396	515396-9	106-75	1.98	0.008	1.54	13.95	15.9	0.36	211	0.17
515414	515414-1	180-150	0.792	0.005	1.1	5.8	8.1	0.13	90.5	0.07
515414	515414-2	150-125	0.681	<0.005	1.29	9.68	9.4	0.15	63.7	0.08
515414	515414-3	125-106	1.21	0.006	1.28	10.25	10.3	0.16	93.5	0.07
515414	515414-4	106-75	0.604	0.007	1.24	9.2	11	0.16	92.4	0.08
515414	515414-5	75-53	1.865	0.009	1.47	17.6	11.9	0.21	129.5	0.11
515414	515414-6	25-53	3.27	0.014	1.55	24.9	11.3	0.24	148	0.14
515414	515414-7	5-25	5.24	0.017	1.67	34.4	14	0.33	184	0.4
515414	515414-8	5-25	5.91	0.013	1.76	37.3	15.7	0.34	194	0.47
515469	515469-1	180-150	0.865	0.009	1.4	9.27	12	0.23	147	0.13
515469	515469-2	150-125	2.11	0.011	1.36	12.05	12.8	0.28	175.5	0.13
515469	515469-3	125-106	1.735	0.009	1.4	11.25	13.3	0.29	153.5	0.14
515469	515469-4	106-75	1.53	0.011	1.45	14	14.3	0.33	195.5	0.15
515469	515469-5	75-53	2.92	0.013	1.47	15.65	13.5	0.37	225	0.16
515469	515469-6	25-53	3.98	0.014	1.51	20.4	14.1	0.46	283	0.2
515469	515469-7	5-25	6.45	0.027	1.83	30.2	22.4	0.69	398	0.46
515469	515469-8	25-53	4.46	0.017	1.54	18.8	14	0.46	287	0.18

Till Size Fraction Four Acid ICP-MS Results

Sample ID	Lab ID	Size Fraction µm	Na %	Nb ppm	Ni ppm	P %	Pb ppm	Rb ppm	Re ppm	S %
515300	515300-1	180-150	1.46	2.28	7.77	0.015	7.43	34.4	<0.002	<0.01
515300	515300-2	150-125	1.495	3.15	10.6	0.02	8.74	38.4	<0.002	0.01
515300	515300-3	125-106	1.44	3.87	13.3	0.026	8.69	42.3	<0.002	0.01
515300	515300-4	106-75	1.45	3.86	11.65	0.033	8.44	38.8	<0.002	0.01
515300	515300-5	75-53	1.575	4.03	12.6	0.038	9.82	43	<0.002	0.01
515300	515300-6	25-53	1.585	4.97	14.5	0.041	10.7	47.5	<0.002	0.01
515300	515300-7	5-25	1.52	8.47	25.2	0.041	12.1	68.1	<0.002	0.01
515300	515300-8	5-25	1.61	9.22	26.4	0.043	13.15	72.2	<0.002	0.01
515300	515300-9	125-106	1.445	3.33	10.45	0.024	8.15	37.8	<0.002	0.01
515396	515396-1	180-150	1.325	1.745	5.59	0.026	7.07	35.2	<0.002	0.01
515396	515396-2	150-125	1.4	2.71	8.9	0.031	7.97	41.5	<0.002	<0.01
515396	515396-3	125-106	1.42	3.63	12	0.043	8.9	47.5	<0.002	<0.01
515396	515396-4	106-75	1.385	2.65	8.14	0.044	8.08	39.1	<0.002	<0.01
515396	515396-5	75-53	1.47	3.5	10.4	0.055	8.94	44.3	<0.002	<0.01
515396	515396-6	25-53	1.58	4.69	13.4	0.064	10.05	50.9	<0.002	<0.01
515396	515396-7	5-25	1.655	8.69	25.9	0.074	12.1	74.7	<0.002	0.01
515396	515396-8	150-125	1.38	3.11	10.25	0.029	7.88	44.6	<0.002	<0.01
515396	515396-9	106-75	1.425	2.63	8.67	0.04	8.36	43.2	<0.002	<0.01
515414	515414-1	180-150	1.645	1.095	3.84	0.032	6.46	27	<0.002	<0.01
515414	515414-2	150-125	1.745	0.808	3.9	0.029	7.25	29.7	<0.002	0.01
515414	515414-3	125-106	1.785	1.08	4.4	0.034	7.11	29.3	<0.002	<0.01
515414	515414-4	106-75	1.7	1.1	4.44	0.037	7.56	29.9	<0.002	<0.01
515414	515414-5	75-53	1.985	1.565	5.72	0.059	9.35	34.2	<0.002	0.01
515414	515414-6	25-53	1.985	2.17	6.45	0.074	9.85	35.3	<0.002	0.01
515414	515414-7	5-25	1.955	3.51	11.05	0.083	11.25	40.8	<0.002	<0.01
515414	515414-8	5-25	2.06	3.95	12.4	0.089	12.1	44.1	<0.002	<0.01
515469	515469-1	180-150	1.35	1.41	5.21	0.021	7.64	40	<0.002	<0.01
515469	515469-2	150-125	1.35	1.755	5.86	0.027	7.52	41.2	<0.002	<0.01
515469	515469-3	125-106	1.355	1.85	6.55	0.028	7.7	42.4	<0.002	<0.01
515469	515469-4	106-75	1.35	2.29	7.59	0.037	8.04	43.9	<0.002	<0.01
515469	515469-5	75-53	1.355	2.92	8.45	0.048	8.7	44.4	<0.002	<0.01
515469	515469-6	25-53	1.345	3.8	9.9	0.059	8.57	42.8	<0.002	<0.01
515469	515469-7	5-25	1.515	7.19	19.85	0.083	11.25	59.1	<0.002	0.01
515469	515469-8	25-53	1.38	3.72	10.15	0.061	8.64	43.6	<0.002	<0.01

Till Size Fraction Four Acid ICP-MS Results

Sample ID	Lab ID	Size Fraction µm	Sb ppm	Sc ppm	Se ppm	Sn ppm	Sr ppm	Ta ppm	Te ppm	Th ppm
515300	515300-1	180-150	0.03	3.71	0.4	0.49	209	0.15	<0.04	1.485
515300	515300-2	150-125	0.04	4.98	0.2	0.61	218	0.21	<0.04	4.91
515300	515300-3	125-106	0.04	5.36	0.2	0.79	215	0.27	<0.04	3.17
515300	515300-4	106-75	0.04	5.15	0.3	0.74	218	0.24	<0.04	1.955
515300	515300-5	75-53	0.04	5.89	0.2	0.78	239	0.27	<0.04	4.91
515300	515300-6	25-53	0.05	6.43	0.2	0.93	245	0.33	<0.04	5.76
515300	515300-7	5-25	0.06	9.49	0.3	1.51	237	0.62	<0.04	7.14
515300	515300-8	5-25	0.07	10.4	0.5	1.63	251	0.67	<0.04	7.64
515300	515300-9	125-106	0.04	4.67	0.4	0.66	216	0.23	<0.04	2.03
515396	515396-1	180-150	0.05	2.69	0.2	0.37	194	0.12	<0.04	1.765
515396	515396-2	150-125	0.05	3.79	0.3	0.5	204	0.19	<0.04	3.79
515396	515396-3	125-106	0.04	5.17	0.3	0.78	212	0.26	<0.04	5.5
515396	515396-4	106-75	0.04	4.21	0.4	0.54	209	0.17	<0.04	4.78
515396	515396-5	75-53	0.06	5.3	0.4	0.66	227	0.24	<0.04	4.75
515396	515396-6	25-53	0.05	6.83	0.3	0.87	246	0.31	<0.04	4.98
515396	515396-7	5-25	0.07	10.25	0.3	1.57	254	0.63	<0.04	7.45
515396	515396-8	150-125	0.04	3.65	0.3	0.67	199	0.23	<0.04	2.87
515396	515396-9	106-75	0.05	4.06	0.2	0.56	215	0.17	0.05	3.08
515414	515414-1	180-150	0.04	1.43	0.2	0.31	208	0.08	<0.04	0.948
515414	515414-2	150-125	0.03	1.39	0.2	0.27	215	0.06	<0.04	2.49
515414	515414-3	125-106	0.04	1.81	0.4	0.29	224	0.08	<0.04	2.45
515414	515414-4	106-75	0.04	1.72	0.2	0.27	213	0.08	<0.04	2.29
515414	515414-5	75-53	0.04	2.64	0.2	0.37	255	0.12	<0.04	5.1
515414	515414-6	25-53	0.04	3.09	0.3	0.44	261	0.16	<0.04	7.01
515414	515414-7	5-25	0.05	4.4	0.2	0.65	256	0.27	<0.04	8.74
515414	515414-8	5-25	0.05	4.91	0.2	0.8	270	0.39	<0.04	9.48
515469	515469-1	180-150	0.07	2.36	0.2	0.36	196	0.11	<0.04	1.5
515469	515469-2	150-125	0.06	3.24	0.2	0.47	199.5	0.13	<0.04	2.83
515469	515469-3	125-106	0.07	2.95	0.2	0.46	201	0.14	<0.04	2.81
515469	515469-4	106-75	0.08	3.91	0.2	0.49	206	0.16	<0.04	3.35
515469	515469-5	75-53	0.07	4.7	0.4	0.59	215	0.2	<0.04	5.24
515469	515469-6	25-53	0.05	5.84	0.3	0.69	219	0.26	<0.04	5.44
515469	515469-7	5-25	0.07	9.09	0.3	1.2	246	0.53	<0.04	8.89
515469	515469-8	25-53	0.06	5.99	0.3	0.69	222	0.25	<0.04	5.69

Till Size Fraction Four Acid ICP-MS Results

Sample ID	Lab ID	Size Fraction µm	Ti %	Tl ppm	U ppm	V ppm	W ppm	Y ppm	Zn ppm	Zr ppm
515300	515300-1	180-150	0.107	0.175	0.51	25.1	0.162	4.55	15.9	75.7
515300	515300-2	150-125	0.145	0.202	1.19	32	0.21	6.63	21.1	83.8
515300	515300-3	125-106	0.168	0.224	0.72	38	0.304	7.1	25.7	62.4
515300	515300-4	106-75	0.175	0.207	0.66	36.7	0.227	7.24	22.9	89.5
515300	515300-5	75-53	0.186	0.223	1.05	40.2	0.259	9.07	24.1	143
515300	515300-6	25-53	0.221	0.256	1.31	45.4	0.31	10.7	28.9	170.5
515300	515300-7	5-25	0.328	0.375	1.72	67.1	0.667	11.7	43.5	197
515300	515300-8	5-25	0.352	0.405	1.82	71	0.718	12.3	45.9	211
515300	515300-9	125-106	0.153	0.205	0.56	32.9	0.244	6.03	20.9	78.8
515396	515396-1	180-150	0.074	0.176	0.42	16.9	0.111	4.37	11.8	29.8
515396	515396-2	150-125	0.118	0.2	0.63	25.5	0.183	5.96	17.5	41.3
515396	515396-3	125-106	0.15	0.246	0.94	32.2	0.253	7.32	23.4	85.8
515396	515396-4	106-75	0.127	0.214	0.68	26.4	0.16	7.22	17.1	76.7
515396	515396-5	75-53	0.158	0.233	0.86	33.5	0.196	8.97	21.1	134.5
515396	515396-6	25-53	0.204	0.267	1.07	43.2	0.258	10.7	27.4	176.5
515396	515396-7	5-25	0.335	0.402	1.63	68.4	0.593	13.05	50.3	203
515396	515396-8	150-125	0.126	0.227	0.63	25	0.214	5.29	20	70.5
515396	515396-9	106-75	0.116	0.221	0.59	25.6	0.163	6.35	17.7	75.3
515414	515414-1	180-150	0.054	0.106	0.39	9.9	0.068	3.88	7.3	28
515414	515414-2	150-125	0.037	0.134	0.74	8.5	0.073	4.14	7.3	24.9
515414	515414-3	125-106	0.051	0.122	0.6	10.2	0.075	4.4	7.2	48
515414	515414-4	106-75	0.052	0.132	0.5	9.6	0.079	4.63	7.7	22.2
515414	515414-5	75-53	0.081	0.162	1.29	15.6	0.096	7.26	10.4	67.4
515414	515414-6	25-53	0.108	0.156	1.92	19.5	0.377	9.86	11.8	125
515414	515414-7	5-25	0.167	0.196	2.58	30.1	0.292	12.6	17.3	195.5
515414	515414-8	5-25	0.176	0.213	2.73	32.3	0.31	13.4	18.4	217
515469	515469-1	180-150	0.058	0.185	0.35	13.8	0.1	3.83	12.1	29.6
515469	515469-2	150-125	0.08	0.182	0.59	16.1	0.105	5.67	13.2	79.4
515469	515469-3	125-106	0.079	0.19	0.55	16.8	0.125	5.2	14.4	67.9
515469	515469-4	106-75	0.106	0.202	0.6	21.6	0.128	6.25	17.1	53.1
515469	515469-5	75-53	0.136	0.21	0.65	27.3	0.156	7.84	18.6	112
515469	515469-6	25-53	0.18	0.208	0.96	34.3	0.192	10	21.1	158
515469	515469-7	5-25	0.314	0.299	1.61	57.7	0.427	14.25	37	255
515469	515469-8	25-53	0.18	0.221	0.94	35	0.2	9.93	21.5	179

D.9 Till Size Fraction Sieving Mass Measurements

Mass measurements are presented for the dry ultra-sonic sieving process undetaken for the till samples selected for size fraction analysis. Sieving and mass measurements were conducted by the author at the MDRU EGI laboratory.

Size Fraction Sieving Mass Measurements

Sample	Size Fraction	Empty Sieve Mass	Final Sieve Mass	Sample Mass	*% of Total Mass*
515300	180-150	321.33	325.22	3.89	*4.40*
	150-125	324.39	331.28	6.89	*7.80*
	125-106	317.66	324.65	6.99	*7.91*
	106-75	311.35	320.88	9.53	*10.79*
	75-53	314.26	323.97	9.71	*10.99*
	53-25	309.08	325.11	16.03	*18.15*
	25-5	364.28	399.26	34.98	*39.60*
	<5	100.56	100.87	0.31	*0.35*
	Total Mass (Pre-Sieve)			**89.96**	
	Reconstituted Total Mass (Sum)			**88.33**	

Sample	Size Fraction	Empty Sieve Mass	Final Sieve Mass	Sample Mass	*% of Total Mass*
515396	180-150	321.27	324.35	3.08	*3.45*
	150-125	323.83	331.47	7.64	*8.57*
	125-106	316.83	325.56	8.73	*9.79*
	106-75	310.75	322.2	11.45	*12.84*
	75-53	313.1	325.75	12.65	*14.19*
	53-25	308.24	326.9	18.66	*20.93*
	25-5	363.22	389.98	26.76	*30.01*
	<5	100.59	100.78	0.19	*0.21*
	Total Mass (Pre-Sieve)			**89.88**	
	Reconstituted Total Mass (Sum)			**89.16**	

Sample	Size Fraction	Empty Sieve Mass	Final Sieve Mass	Sample Mass	*% of Total Mass*
515414	180-150	320.97	324.63	3.66	*4.07*
	150-125	323.78	333.5	9.72	*10.81*
	125-106	316.58	325.36	8.78	*9.76*
	106-75	310.42	325.54	15.12	*16.81*
	75-53	313.24	327.41	14.17	*15.76*
	53-25	308.08	326.95	18.87	*20.98*
	25-5	363.26	382.49	19.23	*21.38*
	<5	100.48	100.86	0.38	*0.42*
	Total Mass (Pre-Sieve)			**90.00**	
	Reconstituted Total Mass (Sum)			**89.93**	

Sample	Size Fraction	Empty Sieve Mass	Final Sieve Mass	Sample Mass	*% of Total Mass*
515469	180-150	321.23	326.55	5.32	*5.92*
	150-125	323.59	333.2	9.61	*10.68*
	125-106	316.66	326.13	9.47	*10.53*
	106-75	310.82	326.07	15.25	*16.96*
	75-53	313.09	327.86	14.77	*16.42*
	53-25	308.41	326.91	18.5	*20.57*
	25-5	363.43	380.06	16.63	*18.49*
	<5	100.56	100.95	0.39	*0.43*
	Total Mass (Pre-Sieve)			**89.99**	
	Reconstituted Total Mass (Sum)			**89.94**	

All values in grams
Gilsonic Sonic Sieve operated at manual settings: 45 minutes at 33 amplitude

D.10 Drill Core Fusion ICP-MS and Whole Rock ICP-AES Results

Major and trace element results are presented for the lithium borate fusion and ICP-MS and ICP-AES analysis of the drill core samples.

Drill Core Fusion ICP-MS and Whole Rock ICP-AES Results

Sample ID	Depth m	Length cm	Total C %	Ba ppm	Ce ppm	Cr ppm	Cs ppm	Dy ppm	Er ppm	Eu ppm	Ga ppm	Gd ppm	Hf ppm	Ho ppm
KDI-16-013 GC 02	9.9	17.5	0.02	404	63.6	170	6.81	2.16	1.25	1.08	16.3	3.19	4.4	0.44
KDI-16-013 GC 03	21.8	19	0.02	2840	35.3	90	6.82	2.28	1.37	1.17	17.8	2.73	2.3	0.47
KDI-16-013 GC 04	28.4	20	0.01	580	65.5	180	14.3	2.82	1.39	1.05	24.4	3.54	4	0.53
KDI-16-013 GC 05	40.1	17	0.02	460	44.6	120	8.28	2.43	1.45	1.39	16.9	2.84	3	0.5
KDI-16-013 GC 06	51.5	19	0.1	597	63.7	180	15.5	2.52	1.29	1.2	22.8	3.62	3.5	0.49
KDI-16-013 GC 07	58.2	21	0.02	381	78.2	210	11.2	2.82	1.56	1.22	18.9	3.96	5.7	0.56
KDI-16-013 GC 08	70.1	22	0.02	533	59.1	160	10.95	2.63	1.6	1.19	20.5	3.44	3.4	0.55
KDI-16-013 GC 09	80.1	21	0.01	796	43.4	100	7.89	2.83	1.67	1.17	16.5	3.02	2.8	0.57
KDI-16-013 GC 10	87.8	22	0.01	540	122.5	130	7.55	5.46	2.7	1.77	16.7	7.36	3	1.03
KDI-16-013 GC 12	110.7	16	0.02	475	52.6	150	12.4	2.29	1.14	0.89	20.2	2.96	2.9	0.45
KDI-16-013 GC 13	123.0	17	0.02	434	36	80	7.49	2.36	1.47	1.22	16	2.67	2.2	0.47
KDI-16-013 GC 14	130.0	17	0.09	816	87.7	240	14.55	3.68	2	1.28	25.4	5.25	4.7	0.67
KDI-16-013 GC 15	143.2	18	0.01	426	54.8	150	5.37	2.29	1.22	1.29	17.4	3.05	3.2	0.47
KDI-16-013 GC 16	150.6	16	0.03	588	42.3	140	9.22	1.95	1.01	1.05	21.9	2.84	2.7	0.39
KDI-16-013 GC 17	160.8	21	0.02	851	74.3	190	13.1	3.24	1.69	1.18	24.1	4.34	3.8	0.58
KDI-16-013 GC 18	168.9	23	0.02	450	53.2	140	5.49	2.3	1.1	1.28	17.5	3.09	4	0.44
KDI-15-048a GC 01	202.5	14.5	0.01	1245	50.7	140	10.25	3.09	1.75	1.32	19	3.44	3.8	0.65
KDI-15-048a GC 02	211.3	18	0.01	473	52.3	150	11.65	3.24	1.96	1.08	20.5	3.51	3.6	0.74
KDI-15-048a GC 03	221.8	21	0.01	399	56.3	170	9.06	2.56	1.35	1.13	17.6	3.26	3.4	0.52
KDI-15-048a GC 04	233.0	17	0.01	301	36.3	100	4.99	1.54	0.91	1.53	15.2	2	2.5	0.32
KDI-15-048a GC 05	240.0	16	0.02	538	53.8	150	10.3	2.47	1.41	1.26	18.3	3.36	3.4	0.54
KDI-15-048a GC 06	254.5	21.5	0.09	526	74.8	190	11.25	2.89	1.43	1.23	23	4.14	4.2	0.52
KDI-15-048a GC 07	259.3	22	0.01	753	72	200	16.35	2.94	1.59	1.17	23.5	3.88	4	0.56
KDI-15-048a GC 08	269.1	22	0.1	560	54.4	170	11	3.53	1.91	1.42	21.3	4.3	3	0.67
KDI-15-048a GC 09	280.4	23	0.01	531	69.7	180	10.1	3.01	1.45	1.27	20.4	3.7	4.2	0.57
KDI-15-048a GC 10	291.1	21	0.02	339	35.9	100	6.78	1.75	1.03	1.02	15.6	2.02	2.2	0.36
KDI-15-048a GC 11	300.8	22	0.08	798	70.4	200	12.3	2.9	1.49	1.17	21.8	3.96	4.2	0.57
KDI-15-048a GC 12	308.5	16	0.03	590	61.2	160	8.81	2.74	1.48	1.41	19	3.52	3.6	0.57
KDI-15-048a GC 13	320.2	23	0.05	480	52.3	140	9.72	3.35	1.91	1.35	19.4	3.59	3.4	0.71
KDI-15-048a GC 14	322.9	17.5	0.04	536	50	130	8.75	2.49	1.41	1.24	18.1	3.19	2.8	0.53

Drill Core Fusion ICP-MS and Whole Rock ICP-AES Results

Sample ID	Depth m	Length cm	Total C %	Ba ppm	Ce ppm	Cr ppm	Cs ppm	Dy ppm	Er ppm	Eu ppm	Ga ppm	Gd ppm	Hf ppm	Ho ppm
KDI-15-048a GC 15	340.1	21	0.04	633	60.8	170	13.05	2.83	1.55	1.21	21.8	3.36	3.1	0.57
KDI-15-048a GC 16	350.6	16	0.05	625	70.4	200	12.95	3.49	1.95	1.24	24.2	4.18	3.8	0.64
KDI-15-048a GC 17	360.7	21	0.03	588	64.3	180	10.6	2.32	1.25	1.28	20	3.39	4.4	0.48
KDI-15-048a GC 18	370.7	18	0.01	412	26.5	70	4.34	1.87	1.13	1.58	13.8	1.97	1.7	0.43
KDI-15-048a GC 19	377.8	23	0.005	470	53.3	160	11.35	2.69	1.54	1.31	22.1	3.25	3.2	0.54
KDI-15-048a GC 20	388.8	24	0.005	510	57.8	180	11.15	2.39	1.42	1.45	22	3.05	3.8	0.48
KDI-15-048a GC 21	400.8	26	0.01	460	54.6	160	10.95	3.48	1.82	1.46	18.8	3.9	3.9	0.69
KDI-15-048b GC 01	70.7	21	0.01	758	70.6	200	14	3.65	1.97	1.29	26.1	4.67	3.9	0.72
KDI-15-048b GC 02	80.1	21	0.01	502	46.3	120	9.25	1.85	0.89	1.1	19.6	2.59	2.8	0.32
KDI-15-048b GC 03	89.8	18	0.02	416	64.5	180	8.02	2.74	1.66	1.09	15.5	3.34	5	0.62
KDI-15-048b GC 04	100.5	16.5	0.01	508	56.2	150	8.29	2.23	1.22	1.12	16.3	3.12	3.5	0.44
KDI-15-048b GC 05	109.0	17	0.01	596	70.1	200	14.25	2.55	1.2	1.32	22	3.56	4.5	0.46
KDI-15-048b GC 06	121.0	20	0.03	708	70.1	180	11.55	2.45	1.47	1.2	19.8	3.59	3.6	0.52
KDI-15-048b GC 07	130.0	16	0.01	572	103.5	260	12.1	3.33	1.76	1.24	19.8	4.57	8.4	0.67
KDI-15-0069b GC 01	302.5	20	0.01	439	51.5	130	10.2	2.34	1.14	1.24	16.4	2.97	3.6	0.44
KDI-15-0069b GC 02	310.2	20	0.01	795	81.7	220	14.35	3.7	2.62	1.53	27.3	4.68	4.8	0.78
KDI-15-0069b GC 03	322.6	20	0.01	556	64	190	11.75	2.51	1.11	1.44	22.5	3.63	3.7	0.48
KDI-15-0069b GC 04	329.0	16	0.04	809	69.5	210	12.6	3.06	1.65	1.48	26.4	4.44	3.9	0.63
KDI-15-0069b GC 05	341.3	18	0.19	812	52.5	190	15.2	2.96	1.64	0.97	22.9	3.72	3.7	0.61
KDI-15-0069b GC 06	352.7	19	0.01	675	50.8	180	12.2	2.2	1.42	1.02	22.7	2.97	3.1	0.48
KDI-15-0069b GC 07	363.8	18.5	0.005	607	56	160	12.7	2.24	1.18	1.19	20.4	3.09	3.6	0.45
KDI-15-0069b GC 08	371.2	20.5	0.01	906	85.9	250	19.55	3.38	1.85	1.31	28.1	4.6	4.5	0.72
KDI-15-0069b GC 09	381.0	15	0.005	712	61.3	180	12	3.43	2.02	1.35	20.5	4	4.2	0.73
KDI-15-0069b GC 10	392.9	11.5	0.01	471	67.2	170	10.1	2.41	1.17	1.34	18.6	3.57	3.9	0.45
KDI-15-0069b GC 11	400.9	17	0.04	430	68.1	170	9.69	2.41	1.37	1.17	17.7	3.45	4.3	0.51
KDI-15-0069b GC 12	409.9	18.5	0.005	463	55.4	140	9.98	2.1	1.17	1.21	16.9	2.68	3.5	0.43
KDI-15-0069b GC 13	421.2	17	0.005	564	48.8	130	8.7	2.01	1.05	1.3	17.9	2.52	3.2	0.41
KDI-15-0069b GC 14	431.7	23	0.01	461	73.3	200	9.95	2.41	1.3	1.23	17.4	3.31	5.4	0.48
KDI-15-0069b GC 15	441.1	17	0.005	501	53.2	170	10.95	2.64	1.59	1.22	20.9	3.33	3.3	0.56

Drill Core Fusion ICP-MS and Whole Rock ICP-AES Results

Sample ID	Depth m	Length cm	Total C %	Ba ppm	Ce ppm	Cr ppm	Cs ppm	Dy ppm	Er ppm	Eu ppm	Ga ppm	Gd ppm	Hf ppm	Ho ppm
KDI-15-0069b GC 16	450.8	19	0.005	417	61.9	170	9.07	2.47	1.24	1.45	17.7	3.13	3.9	0.5
KDI-15-0069b GC 17	460.3	15	0.005	513	65.8	210	15.45	2.92	1.6	1.18	23.9	3.74	4.1	0.62
KDI-15-0069b GC 18	470.9	21.5	0.005	405	58.4	150	8.56	2.35	1.25	1.34	17.6	2.97	3.9	0.5
KDI-15-0069b GC 19	478.7	18	0.08	626	63.1	200	15.35	3.29	1.86	1.39	25	3.96	3.2	0.68
KDI-15-0069b GC 20	488.9	19	0.01	568	66.6	180	13.8	3.04	1.72	1.39	23	3.48	4.3	0.57
KDI-15-0069b GC 21	500.3	16	0.03	437	57.2	210	6.88	2.24	1.26	1.12	16.4	2.94	3.9	0.45
KDI-15-0069b GC 22	510.4	20	0.01	574	66.4	170	11.75	2.6	1.42	1.38	20.6	3.5	4	0.56
KDI-15-0069b GC 25	542.5	17.5	0.005	676	61.8	210	17.7	2.5	1.46	0.95	26	3.56	4	0.57
KDI-15-0069b GC 26	553.3	16.5	0.005	550	67	200	13.2	2.46	1.33	1.31	21.5	3.66	4.7	0.52
KDI-15-0069b GC 27	562.8	22.5	0.03	652	65	180	13.7	2.6	1.25	1.19	20.5	3.61	4	0.52
KDI-15-0069b GC 28	569.6	17	0.02	620	73.8	210	16.6	2.92	1.57	1.18	25.4	4.19	3.9	0.59
KDI-15-0069b GC 29	579.0	19	0.01	681	68.1	210	13.05	2.6	1.49	1.12	23.6	3.68	4	0.61
KDI-15-0069b GC 30	591.6	20	0.01	663	77.4	210	9.6	2.97	1.67	1.3	22.7	3.76	5	0.63

Drill Core Fusion ICP-MS and Whole Rock ICP-AES Results

Sample ID	Depth m	La ppm	Lu ppm	Nb ppm	Nd ppm	Pr ppm	Rb ppm	Sm ppm	Sn ppm	Sr ppm	Ta ppm	Tb ppm	Th ppm	Tm ppm	U ppm
KDI-16-013 GC 02	9.9	34.4	0.18	5.7	26.2	7.11	59.9	4.72	2	264	0.4	0.44	7.32	0.18	2.18
KDI-16-013 GC 03	21.8	17.7	0.21	5.1	16.7	4.23	77.9	3.21	3	211	0.7	0.4	3.56	0.22	2.02
KDI-16-013 GC 04	28.4	33.3	0.24	7.8	29.9	7.69	115.5	5.16	2	224	0.9	0.47	6.62	0.21	2.63
KDI-16-013 GC 05	40.1	22.4	0.2	5.6	20.1	5.27	66.2	4	2	341	0.6	0.43	4.43	0.21	1.9
KDI-16-013 GC 06	51.5	33	0.2	7.8	29.4	7.58	105.5	5.23	3	287	0.8	0.47	6.93	0.18	2.49
KDI-16-013 GC 07	58.2	39.1	0.26	6.3	32.3	8.79	90.1	5.58	1	353	0.5	0.53	9.73	0.22	2.74
KDI-16-013 GC 08	70.1	28.2	0.2	6.3	25.6	6.75	92.2	4.62	2	269	0.4	0.45	6.41	0.22	1.76
KDI-16-013 GC 09	80.1	21.1	0.23	4.6	19	5.11	66.2	3.61	1	271	0.5	0.46	4.46	0.24	1.84
KDI-16-013 GC 10	87.8	55.7	0.33	5.1	56.9	15.2	65.8	10.3	2	202	0.6	1	13.7	0.4	3.57
KDI-16-013 GC 12	110.7	24.9	0.16	6.4	22.9	6.07	95.4	4.2	2	221	0.8	0.4	5.53	0.17	2.1
KDI-16-013 GC 13	123.0	17.4	0.23	4	16	4.27	55.2	3.18	2	314	0.6	0.39	3.72	0.23	2.02
KDI-16-013 GC 14	130.0	42.7	0.26	8	39	10.25	127.5	6.92	3	200	0.6	0.67	9.28	0.26	2.78
KDI-16-013 GC 15	143.2	27	0.14	5.4	23.1	6.2	61.2	4.26	2	300	0.4	0.45	5.72	0.16	1.82
KDI-16-013 GC 16	150.6	19.8	0.13	5.9	20	5.22	90.1	3.56	1	195	0.7	0.42	5.13	0.15	1.71
KDI-16-013 GC 17	160.8	36.4	0.22	7.8	32.3	8.69	134.5	5.89	2	174.5	0.7	0.61	8.1	0.23	3.09
KDI-16-013 GC 18	168.9	26	0.15	5.8	22.8	6.3	60.5	3.96	2	258	0.6	0.42	6.14	0.14	2.2
KDI-15-048a GC 01	202.5	24.9	0.24	5.4	22.2	6.13	81.9	4.51	4	287	0.8	0.52	5.29	0.26	2.77
KDI-15-048a GC 02	211.3	25.5	0.29	5.8	23.8	6.28	81.1	4.07	2	231	0.8	0.52	5.59	0.3	2.54
KDI-15-048a GC 03	221.8	28.4	0.21	5.5	24.4	6.59	73	4.49	2	280	0.4	0.44	5.68	0.21	1.83
KDI-15-048a GC 04	233.0	18.1	0.11	3.1	15.7	4.37	40	2.82	1	386	0.4	0.29	3.58	0.13	1.44
KDI-15-048a GC 05	240.0	26.8	0.21	5.5	23.7	6.39	78.1	4.02	2	291	0.7	0.43	5.82	0.21	2.23
KDI-15-048a GC 06	254.5	36.9	0.19	7.1	32.8	8.81	93.5	5.86	2	245	0.8	0.51	7.01	0.19	2.65
KDI-15-048a GC 07	259.3	35.7	0.23	7.6	31.2	8.42	114	5.71	3	239	0.9	0.5	7.62	0.22	2.59
KDI-15-048a GC 08	269.1	26.2	0.26	6.5	25.6	6.61	87.1	5.27	2	298	0.9	0.63	5.39	0.27	2.45
KDI-15-048a GC 09	280.4	34.8	0.22	6.7	29.8	8.12	88	5.1	2	284	0.8	0.53	7.42	0.23	2.78
KDI-15-048a GC 10	291.1	17.7	0.15	4.1	16	4.31	53.3	2.7	1	239	0.5	0.3	3.78	0.15	1.49
KDI-15-048a GC 11	300.8	34.7	0.21	7.8	31.2	8.49	99.8	5.05	3	233	0.9	0.49	7.58	0.23	2.82
KDI-15-048a GC 12	308.5	30.2	0.22	6	26.6	7.06	80.3	4.94	2	285	0.6	0.49	6.33	0.23	2.34
KDI-15-048a GC 13	320.2	25.6	0.29	5.7	24.2	6.21	84.9	4.73	2	282	0.7	0.59	5.18	0.28	2.3
KDI-15-048a GC 14	322.9	24.5	0.21	5.1	22	5.96	72.9	4.18	2	267	0.6	0.44	4.92	0.2	2.08

Drill Core Fusion ICP-MS and Whole Rock ICP-AES Results

Sample ID	Depth m	La ppm	Lu ppm	Nb ppm	Nd ppm	Pr ppm	Rb ppm	Sm ppm	Sn ppm	Sr ppm	Ta ppm	Tb ppm	Th ppm	Tm ppm	U ppm
KDI-15-048a GC 15	340.1	29.7	0.23	7.2	26.3	7.13	110	4.8	3	263	0.8	0.49	6.13	0.25	2.34
KDI-15-048a GC 16	350.6	34.1	0.25	7.5	31.7	8.37	122	5.7	2	208	0.7	0.57	7.02	0.26	2.49
KDI-15-048a GC 17	360.7	32	0.2	6	28.3	7.46	86.3	5.07	2	257	0.6	0.43	6.99	0.18	2.56
KDI-15-048a GC 18	370.7	13.3	0.18	2.6	12.1	3.02	37.2	2.27	2	418	0.4	0.32	2.5	0.17	1.51
KDI-15-048a GC 19	377.8	26.1	0.26	6.4	23.3	6.24	94.9	4.2	2	290	0.7	0.48	5.59	0.22	2.46
KDI-15-048a GC 20	388.8	29.1	0.22	7.2	25.2	6.83	98.3	4.34	3	285	0.8	0.44	6.27	0.2	2.62
KDI-15-048a GC 21	400.8	26.1	0.27	6	24.9	6.48	79.2	4.76	3	334	0.6	0.58	5.8	0.26	2.88
KDI-15-048b GC 01	70.7	34.1	0.27	7.7	31.6	8.39	108	5.95	2	225	0.5	0.65	7.83	0.29	2.08
KDI-15-048b GC 02	80.1	22.8	0.14	4.5	19.7	5.39	65.7	3.5	2	280	0.9	0.35	4.85	0.13	2.31
KDI-15-048b GC 03	89.8	33.2	0.26	5.4	26.6	7.43	74.7	4.43	1	281	0.4	0.49	7.83	0.27	2.38
KDI-15-048b GC 04	100.5	28.4	0.15	5.3	23.6	6.48	78.2	3.93	1	308	0.4	0.4	5.6	0.17	1.63
KDI-15-048b GC 05	109.0	34.6	0.18	8.1	30.4	8.33	111	5.38	2	306	1.2	0.47	7.31	0.19	2.45
KDI-15-048b GC 06	121.0	35.2	0.21	7.6	30.4	8.35	96.2	5.17	1	293	1.2	0.51	7.16	0.2	2.8
KDI-15-048b GC 07	130.0	53.4	0.25	7.8	41.7	11.6	103.5	7.1	2	234	1.1	0.61	13.45	0.26	4.42
KDI-15-0069b GC 01	302.5	25.3	0.17	4.9	22.2	5.89	59.3	4.06	2	361	0.8	0.41	5.12	0.17	2.15
KDI-15-0069b GC 02	310.2	41	0.32	8.2	36.2	9.44	103.5	6.57	2	300	1.3	0.66	7.38	0.29	3.09
KDI-15-0069b GC 03	322.6	30.9	0.18	6.9	28.5	7.66	93.3	5.16	2	337	1	0.5	6.61	0.18	2.33
KDI-15-0069b GC 04	329.0	33.8	0.24	7.9	30.9	8.42	101.5	5.71	1	326	1.2	0.61	6.98	0.26	2.49
KDI-15-0069b GC 05	341.3	24.7	0.24	7.7	24.6	6.29	99.6	4.76	2	226	1.3	0.54	5.95	0.24	2.5
KDI-15-0069b GC 06	352.7	23.8	0.24	7.6	22.1	6.06	106.5	3.99	1	268	1.1	0.4	5.94	0.21	2.05
KDI-15-0069b GC 07	363.8	27.4	0.2	6.4	24.3	6.63	84.9	4.16	1	294	1.1	0.41	5.88	0.18	2.41
KDI-15-0069b GC 08	371.2	41.7	0.29	9.4	37.4	10.05	129	6.95	2	261	1.5	0.62	8.65	0.24	3.32
KDI-15-0069b GC 09	381.0	29.9	0.32	6.8	27	7.32	82.5	5.02	1	316	1.1	0.59	6.31	0.28	2.55
KDI-15-0069b GC 10	392.9	33.6	0.18	6.5	28.9	7.79	74.7	5.12	1	330	0.4	0.44	6.82	0.17	1.88
KDI-15-0069b GC 11	400.9	34.5	0.2	6.1	27.9	7.72	74.8	4.63	1	358	0.5	0.45	7.33	0.19	2.11
KDI-15-0069b GC 12	409.9	27.9	0.2	5.2	23.2	6.3	68.7	3.96	1	355	0.9	0.37	5.89	0.2	2.25
KDI-15-0069b GC 13	421.2	24.5	0.18	5	20.8	5.62	66.9	3.75	1	350	0.9	0.36	5.09	0.18	2.21
KDI-15-0069b GC 14	431.7	37.9	0.22	6.3	30.2	8.17	78.7	4.89	1	327	0.4	0.44	8.4	0.19	2.52
KDI-15-0069b GC 15	441.1	25.6	0.24	6.4	24	6.31	91.2	4.32	1	328	1.2	0.46	5.23	0.23	1.86

Drill Core Fusion ICP-MS and Whole Rock ICP-AES Results

Sample ID	Depth m	La ppm	Lu ppm	Nb ppm	Nd ppm	Pr ppm	Rb ppm	Sm ppm	Sn ppm	Sr ppm	Ta ppm	Tb ppm	Th ppm	Tm ppm	U ppm
KDI-15-0069b GC 16	450.8	31.5	0.21	5.9	25.8	7.17	70.6	4.34	1	386	0.4	0.46	6.38	0.22	2.02
KDI-15-0069b GC 17	460.3	31.7	0.26	7.9	29.3	7.81	116	5.28	1	285	0.8	0.55	7	0.23	2.18
KDI-15-0069b GC 18	470.9	29	0.19	5.6	24.3	6.72	73.7	4.25	1	376	0.7	0.4	5.98	0.17	1.76
KDI-15-0069b GC 19	478.7	29.5	0.3	9.5	28.9	7.49	117	5.34	1	285	1.3	0.55	6.99	0.3	2.68
KDI-15-0069b GC 20	488.9	32.3	0.27	9.1	28.9	7.69	101.5	5	1	310	1.5	0.48	6.89	0.25	2.66
KDI-15-0069b GC 21	500.3	28.9	0.18	5.5	24.4	6.63	73.2	4.37	1	317	0.4	0.39	5.85	0.17	1.9
KDI-15-0069b GC 22	510.4	33.3	0.23	7.8	28.1	7.79	83	4.92	1	331	1.5	0.47	6.52	0.19	2.16
KDI-15-0069b GC 25	542.5	29.7	0.23	10.3	27	7.23	119	5.01	2	219	1.4	0.47	6.96	0.22	2.92
KDI-15-0069b GC 26	553.3	33.3	0.2	7.6	29.5	7.96	93	4.9	1	319	0.9	0.45	7.26	0.2	2.52
KDI-15-0069b GC 27	562.8	31.8	0.21	7.2	28.6	7.67	90.9	5.02	2	277	0.8	0.47	6.79	0.19	2.94
KDI-15-0069b GC 28	569.6	35.3	0.24	8.1	32.4	8.56	123	5.53	2	258	0.9	0.53	7.97	0.2	2.53
KDI-15-0069b GC 29	579.0	32.7	0.26	7.9	30	7.94	113	5.38	2	263	0.9	0.53	7.62	0.24	2.74
KDI-15-0069b GC 30	591.6	38.1	0.29	8.5	33.2	8.88	108.5	5.85	2	296	0.9	0.54	8.24	0.24	3.34

Drill Core Fusion ICP-MS and Whole Rock ICP-AES Results

Sample ID	Depth m	V ppm	W ppm	Y ppm	Yb ppm	Zr ppm	SiO2 %	Al2O3 %	Fe2O3 %	CaO %	MgO %	Na2O %	K2O %	Cr2O3 %	TiO2 %
KDI-16-013 GC 02	9.9	91	1	12.6	1.15	190	68.5	14	5.17	1.97	2.08	3.15	2.12	0.02	0.55
KDI-16-013 GC 03	21.8	69	4	13	1.36	87	70.4	15.7	3.66	0.96	1.76	1.71	3.66	0.01	0.39
KDI-16-013 GC 04	28.4	133	3	14.7	1.51	159	60.7	18.15	6.32	1.22	2.98	2.59	3.52	0.03	0.67
KDI-16-013 GC 05	40.1	85	1	13.7	1.38	119	69.1	14.75	4.19	1.97	1.94	3.88	2.28	0.02	0.5
KDI-16-013 GC 06	51.5	125	2	13.2	1.23	139	60.5	17.4	6.35	1.55	2.95	3.14	3.22	0.02	0.64
KDI-16-013 GC 07	58.2	109	1	15.3	1.62	235	67.3	14.9	5.93	2.21	2.82	3.3	2.74	0.03	0.61
KDI-16-013 GC 08	70.1	122	1	14.7	1.46	135	66.2	16.2	6.12	1.42	3.01	3.07	3.04	0.02	0.64
KDI-16-013 GC 09	80.1	73	1	15.2	1.62	106	71.4	15.4	4.29	1.45	1.97	2.7	2.44	0.01	0.43
KDI-16-013 GC 10	87.8	94	3	27	2.46	115	70.9	12.1	4.46	1.22	2.03	1.85	2.28	0.02	0.44
KDI-16-013 GC 12	110.7	110	2	11.3	1.25	117	63.7	16.85	6.32	1.4	3.02	2.58	3.16	0.02	0.63
KDI-16-013 GC 13	123.0	63	1	13.6	1.59	81	73	14.8	3.47	1.71	1.56	3.24	1.8	0.01	0.33
KDI-16-013 GC 14	130.0	166	4	18.8	1.96	187	59.6	19	7.71	1.06	3.69	2.33	4.06	0.03	0.84
KDI-16-013 GC 15	143.2	100	2	11.9	1.15	132	67.7	15	4.98	1.62	2.59	3.48	2.15	0.02	0.53
KDI-16-013 GC 16	150.6	125	2	10.4	1.03	100	66.3	17.85	5.76	1.1	2.78	2.12	2.73	0.02	0.52
KDI-16-013 GC 17	160.8	159	3	16.8	1.52	152	59	18.55	7.15	0.9	3.67	1.81	4.55	0.03	0.72
KDI-16-013 GC 18	168.9	102	2	11.4	0.98	159	67	14.95	4.92	1.27	2.63	2.84	2.37	0.02	0.51
KDI-15-048a GC 01	202.5	106	4	16.5	1.64	150	66.6	16.55	4.92	1.52	2.3	2.84	2.99	0.02	0.51
KDI-15-048a GC 02	211.3	114	2	18.8	2.13	137	67.3	16.6	5.15	1.38	2.44	2.59	2.42	0.02	0.53
KDI-15-048a GC 03	221.8	108	14	14.2	1.53	141	67.4	16.1	5.56	1.82	2.76	3.38	2.52	0.03	0.6
KDI-15-048a GC 04	233.0	58	1	7.8	0.81	84	73.3	14.95	3.32	2.09	1.58	4.02	1.3	0.01	0.29
KDI-15-048a GC 05	240.0	112	2	14.2	1.44	125	65.6	16.05	5.4	1.53	2.55	3.2	2.4	0.02	0.54
KDI-15-048a GC 06	254.5	151	2	14.1	1.14	177	61.6	18.05	6.4	1.4	3.03	2.59	2.91	0.03	0.71
KDI-15-048a GC 07	259.3	155	4	15.4	1.47	157	60.2	18	7.21	1.19	3.5	2.56	3.35	0.03	0.74
KDI-15-048a GC 08	269.1	131	2	18.4	1.68	118	64.7	17.95	6.17	1.89	2.85	3.19	2.7	0.02	0.62
KDI-15-048a GC 09	280.4	123	2	15.2	1.54	167	66	16.35	5.93	1.53	2.68	3.17	2.59	0.02	0.63
KDI-15-048a GC 10	291.1	77	2	9.8	0.99	83	73.2	13.8	3.97	1.31	1.86	2.79	1.68	0.01	0.37
KDI-15-048a GC 11	300.8	146	3	15.6	1.6	172	61.9	16.8	7.2	1.15	3.39	2.64	3.15	0.03	0.75
KDI-15-048a GC 12	308.5	115	3	15.4	1.37	144	66.7	15.45	5.68	1.55	2.71	3.21	2.75	0.02	0.57
KDI-15-048a GC 13	320.2	103	1	18.5	1.76	135	67.8	15.75	5.06	1.7	2.38	3.18	2.5	0.02	0.52
KDI-15-048a GC 14	322.9	95	2	14.3	1.4	114	65.9	16.25	4.64	1.56	2.21	2.97	2.24	0.02	0.47

Drill Core Fusion ICP-MS and Whole Rock ICP-AES Results

Sample ID	Depth m	V ppm	W ppm	Y ppm	Yb ppm	Zr ppm	SiO2 %	Al2O3 %	Fe2O3 %	CaO %	MgO %	Na2O %	K2O %	Cr2O3 %	TiO2 %
KDI-15-048a GC 15	340.1	141	2	15	1.51	126	61.7	18.3	6.47	1.44	3.17	2.92	3.11	0.02	0.64
KDI-15-048a GC 16	350.6	162	6	17.7	1.68	138	59.1	19.05	7.11	1.16	3.56	2.49	3.65	0.03	0.75
KDI-15-048a GC 17	360.7	118	3	12	1.21	178	66.9	16.4	5.78	1.37	2.7	2.94	2.64	0.02	0.59
KDI-15-048a GC 18	370.7	37	6	10.8	1.13	75	73.2	15.15	2.47	2.26	1.12	4.58	1.45	0.01	0.21
KDI-15-048a GC 19	377.8	121	3	14.8	1.51	129	65.7	17.65	5.15	1.54	2.45	3.29	2.77	0.02	0.55
KDI-15-048a GC 20	388.8	127	2	13.9	1.36	157	65.1	17.4	5.64	1.42	2.78	3.44	2.92	0.02	0.63
KDI-15-048a GC 21	400.8	107	3	17.7	1.68	160	67.2	15.95	4.99	1.95	2.16	3.66	2.51	0.02	0.53
KDI-15-048b GC 01	70.7	167	2	18.2	1.61	147	61.1	19.25	7.64	1.23	3.68	2.22	2.96	0.03	0.75
KDI-15-048b GC 02	80.1	88	1	8.9	0.82	104	70.4	17	4.4	1.49	2.11	2.99	1.86	0.02	0.41
KDI-15-048b GC 03	89.8	95	1	16.2	1.51	210	69.8	14.35	5.34	1.79	2.33	3.12	2.2	0.03	0.56
KDI-15-048b GC 04	100.5	93	1	11.9	1.11	142	69.5	14.65	4.93	1.92	2.19	3.37	2.33	0.02	0.54
KDI-15-048b GC 05	109.0	144	4	12.4	1.13	177	64.9	16.75	6.62	1.59	3.15	3.16	3.02	0.03	0.71
KDI-15-048b GC 06	121.0	129	1	14.1	1.4	143	64.6	15.9	6.35	1.46	3.01	3.08	2.77	0.02	0.64
KDI-15-048b GC 07	130.0	122	2	17	1.61	341	65.7	13.95	6.97	1.19	2.93	2.49	3.5	0.03	0.7
KDI-15-0069b GC 01	302.5	80	3	11.5	1.09	140	72.2	14.1	4.04	1.93	1.68	3.81	1.86	0.02	0.44
KDI-15-0069b GC 02	310.2	166	2	20.5	1.92	194	61.2	19.1	6.71	1.31	3.08	2.65	2.69	0.03	0.71
KDI-15-0069b GC 03	322.6	137	1	12.6	1.55	145	63.6	18.5	6.35	1.62	3.05	3.58	2.83	0.03	0.69
KDI-15-0069b GC 04	329.0	169	2	17.3	1.7	155	61.9	19.6	7.14	1.47	3.39	3.07	2.78	0.03	0.74
KDI-15-0069b GC 05	341.3	144	2	16.2	1.66	135	65	16.85	6.45	1.13	2.94	2.25	2.84	0.03	0.67
KDI-15-0069b GC 06	352.7	140	2	13.9	1.48	123	63.4	16.05	6.61	1.15	3.18	2.61	2.89	0.03	0.66
KDI-15-0069b GC 07	363.8	119	2	12.2	1.25	137	65.8	15.7	5.42	1.33	2.54	2.97	2.36	0.02	0.57
KDI-15-0069b GC 08	371.2	190	4	18.6	1.7	175	56.1	19.55	7.99	1.2	3.82	2.55	3.65	0.03	0.86
KDI-15-0069b GC 09	381.0	126	2	20.1	1.99	164	68.3	16.25	5.54	1.53	2.52	2.92	2.23	0.02	0.6
KDI-15-0069b GC 10	392.9	102	3	12.4	1.11	165	69.4	14.9	4.84	1.74	2.11	3.53	2.08	0.02	0.55
KDI-15-0069b GC 11	400.9	99	1	13.1	1.33	176	69.6	14.25	5.09	1.87	2.25	3.21	2.18	0.02	0.54
KDI-15-0069b GC 12	409.9	87	2	11.9	1.21	147	69.9	13.75	4.37	1.7	1.91	3.48	1.97	0.02	0.48
KDI-15-0069b GC 13	421.2	79	2	10.7	1	127	69.7	16.35	4.49	1.68	2.06	3.56	2.02	0.02	0.44
KDI-15-0069b GC 14	431.7	102	1	13.3	1.23	229	68.5	15.1	5.47	2.25	2.22	3.79	2.32	0.03	0.62
KDI-15-0069b GC 15	441.1	125	3	15.1	1.46	134	65.2	17.5	5.94	1.62	2.87	3.38	2.5	0.02	0.65

Drill Core Fusion ICP-MS and Whole Rock ICP-AES Results

Sample ID	Depth m	V ppm	W ppm	Y ppm	Yb ppm	Zr ppm	SiO2 %	Al2O3 %	Fe2O3 %	CaO %	MgO %	Na2O %	K2O %	Cr2O3 %	TiO2 %
KDI-15-0069b GC 16	450.8	102	6	13.6	1.32	161	68.9	15.2	4.89	2.16	2.04	4.05	1.99	0.02	0.57
KDI-15-0069b GC 17	460.3	159	1	16.6	1.7	160	62.1	18.15	7.06	1.45	3.31	3.09	3.06	0.03	0.77
KDI-15-0069b GC 18	470.9	95	3	12.2	1.16	156	70.4	14.9	4.94	2	2.08	3.68	1.97	0.02	0.53
KDI-15-0069b GC 19	478.7	164	2	18.7	1.82	130	60.4	19.2	7.29	1.45	3.55	3.09	3.26	0.03	0.74
KDI-15-0069b GC 20	488.9	130	3	16.9	1.67	167	63.6	17.15	6.16	1.51	2.87	3.16	2.74	0.02	0.67
KDI-15-0069b GC 21	500.3	91	2	12	1.14	164	71.1	14.1	4.43	2.56	1.92	3.38	2.01	0.02	0.51
KDI-15-0069b GC 22	510.4	117	2	14.5	1.41	168	68.6	16.05	5.75	1.5	2.6	3.06	2.28	0.02	0.59
KDI-15-0069b GC 25	542.5	168	2	14.9	1.39	153	61.8	18.2	7.43	1.11	3.7	2.12	3.12	0.03	0.75
KDI-15-0069b GC 26	553.3	139	1	13.7	1.21	190	63.1	16.4	6.24	1.59	2.82	3.27	2.67	0.03	0.67
KDI-15-0069b GC 27	562.8	129	3	13.9	1.35	160	65.4	15.65	6.14	1.37	2.86	2.71	2.61	0.03	0.61
KDI-15-0069b GC 28	569.6	163	2	16.4	1.58	168	61.8	18.9	7.36	1.35	3.71	2.69	3.41	0.03	0.75
KDI-15-0069b GC 29	579.0	162	3	16	1.58	158	63.2	17.6	7.29	1.32	3.53	2.67	3.24	0.03	0.77
KDI-15-0069b GC 30	591.6	161	2	16.6	1.68	200	61.9	16.65	6.76	1.41	3.11	2.84	2.99	0.03	0.72

Drill Core Fusion ICP-MS and Whole Rock ICP-AES Results

Sample ID	Depth m	MnO %	P2O5 %	SrO %	BaO %	LOI %	Total %
KDI-16-013 GC 02	9.9	0.04	0.12	0.03	0.05	1.23	99.03
KDI-16-013 GC 03	21.8	0.04	0.31	0.02	0.31	2.22	101.15
KDI-16-013 GC 04	28.4	0.06	0.13	0.02	0.07	1.55	98.01
KDI-16-013 GC 05	40.1	0.04	0.24	0.04	0.05	0.9	99.9
KDI-16-013 GC 06	51.5	0.06	0.15	0.03	0.07	1.37	97.45
KDI-16-013 GC 07	58.2	0.06	0.13	0.04	0.04	0.92	101.03
KDI-16-013 GC 08	70.1	0.06	0.09	0.03	0.06	1.59	101.55
KDI-16-013 GC 09	80.1	0.04	0.23	0.03	0.09	1.24	101.72
KDI-16-013 GC 10	87.8	0.05	0.33	0.02	0.06	1.3	97.06
KDI-16-013 GC 12	110.7	0.06	0.16	0.03	0.06	1.4	99.39
KDI-16-013 GC 13	123.0	0.04	0.23	0.04	0.05	1.01	101.29
KDI-16-013 GC 14	130.0	0.06	0.13	0.02	0.09	1.83	100.45
KDI-16-013 GC 15	143.2	0.04	0.14	0.04	0.05	1.6	99.94
KDI-16-013 GC 16	150.6	0.06	0.14	0.02	0.07	1.43	100.9
KDI-16-013 GC 17	160.8	0.07	0.13	0.02	0.1	2.39	99.09
KDI-16-013 GC 18	168.9	0.05	0.16	0.02	0.05	1.84	98.63
KDI-15-048a GC 01	202.5	0.05	0.3	0.03	0.14	1.54	100.31
KDI-15-048a GC 02	211.3	0.05	0.25	0.02	0.05	1.12	99.92
KDI-15-048a GC 03	221.8	0.05	0.14	0.03	0.05	1.16	101.6
KDI-15-048a GC 04	233.0	0.04	0.16	0.04	0.03	0.82	101.95
KDI-15-048a GC 05	240.0	0.06	0.14	0.03	0.06	1.26	98.84
KDI-15-048a GC 06	254.5	0.06	0.12	0.03	0.06	1.57	98.56
KDI-15-048a GC 07	259.3	0.07	0.11	0.02	0.08	1.32	98.38
KDI-15-048a GC 08	269.1	0.06	0.34	0.03	0.06	1.32	101.9
KDI-15-048a GC 09	280.4	0.05	0.15	0.03	0.06	1.1	100.29
KDI-15-048a GC 10	291.1	0.04	0.09	0.03	0.04	0.75	99.94
KDI-15-048a GC 11	300.8	0.07	0.07	0.02	0.09	1.79	99.05
KDI-15-048a GC 12	308.5	0.05	0.14	0.03	0.06	1.61	100.53
KDI-15-048a GC 13	320.2	0.05	0.31	0.03	0.05	1.05	100.4
KDI-15-048a GC 14	322.9	0.05	0.23	0.03	0.06	1.01	97.64

Drill Core Fusion ICP-MS and Whole Rock ICP-AES Results

Sample ID	Depth m	MnO %	P2O5 %	SrO %	BaO %	LOI %	Total %
KDI-15-048a GC 15	340.1	0.07	0.14	0.03	0.07	1.32	99.4
KDI-15-048a GC 16	350.6	0.06	0.16	0.02	0.07	1.56	98.77
KDI-15-048a GC 17	360.7	0.06	0.13	0.03	0.07	1.25	100.88
KDI-15-048a GC 18	370.7	0.03	0.27	0.05	0.05	0.73	101.58
KDI-15-048a GC 19	377.8	0.05	0.17	0.03	0.05	1.07	100.49
KDI-15-048a GC 20	388.8	0.05	0.14	0.03	0.06	1.49	101.12
KDI-15-048a GC 21	400.8	0.05	0.37	0.04	0.05	1.16	100.64
KDI-15-048b GC 01	70.7	0.07	0.16	0.03	0.09	1.34	100.55
KDI-15-048b GC 02	80.1	0.05	0.12	0.03	0.06	0.96	101.9
KDI-15-048b GC 03	89.8	0.04	0.13	0.03	0.05	0.96	100.73
KDI-15-048b GC 04	100.5	0.04	0.12	0.03	0.06	0.84	100.54
KDI-15-048b GC 05	109.0	0.06	0.09	0.03	0.07	1.26	101.44
KDI-15-048b GC 06	121.0	0.06	0.09	0.03	0.08	1.34	99.43
KDI-15-048b GC 07	130.0	0.05	0.09	0.03	0.06	1.5	99.19
KDI-15-0069b GC 01	302.5	0.04	0.19	0.04	0.05	0.73	101.13
KDI-15-0069b GC 02	310.2	0.06	0.17	0.02	0.09	1.12	98.94
KDI-15-0069b GC 03	322.6	0.06	0.1	0.04	0.07	1.16	101.68
KDI-15-0069b GC 04	329.0	0.07	0.16	0.04	0.09	1.3	101.78
KDI-15-0069b GC 05	341.3	0.06	0.21	0.03	0.09	1.38	99.93
KDI-15-0069b GC 06	352.7	0.07	0.07	0.03	0.07	1.35	98.17
KDI-15-0069b GC 07	363.8	0.06	0.09	0.03	0.07	1.16	98.12
KDI-15-0069b GC 08	371.2	0.08	0.1	0.02	0.1	1.55	97.6
KDI-15-0069b GC 09	381.0	0.05	0.23	0.03	0.08	1.08	101.38
KDI-15-0069b GC 10	392.9	0.05	0.11	0.04	0.05	0.87	100.29
KDI-15-0069b GC 11	400.9	0.04	0.11	0.04	0.05	1.14	100.39
KDI-15-0069b GC 12	409.9	0.04	0.07	0.04	0.05	0.78	98.56
KDI-15-0069b GC 13	421.2	0.04	0.11	0.04	0.06	0.86	101.43
KDI-15-0069b GC 14	431.7	0.04	0.14	0.04	0.05	0.86	101.43
KDI-15-0069b GC 15	441.1	0.06	0.16	0.04	0.06	1.17	101.17

Drill Core Fusion ICP-MS and Whole Rock ICP-AES Results

Sample ID	Depth m	MnO %	P2O5 %	SrO %	BaO %	LOI %	Total %
KDI-15-0069b GC 16	450.8	0.03	0.13	0.04	0.05	0.85	100.92
KDI-15-0069b GC 17	460.3	0.07	0.11	0.03	0.06	1.29	100.58
KDI-15-0069b GC 18	470.9	0.04	0.14	0.04	0.05	0.82	101.61
KDI-15-0069b GC 19	478.7	0.08	0.09	0.04	0.07	1.83	101.12
KDI-15-0069b GC 20	488.9	0.06	0.07	0.03	0.06	1.16	99.26
KDI-15-0069b GC 21	500.3	0.05	0.1	0.03	0.05	0.66	100.92
KDI-15-0069b GC 22	510.4	0.05	0.09	0.03	0.06	1.04	101.72
KDI-15-0069b GC 25	542.5	0.08	0.13	0.02	0.07	1.81	100.37
KDI-15-0069b GC 26	553.3	0.06	0.12	0.04	0.06	1.21	98.28
KDI-15-0069b GC 27	562.8	0.06	0.14	0.03	0.07	1.33	99.01
KDI-15-0069b GC 28	569.6	0.08	0.13	0.03	0.07	1.63	101.94
KDI-15-0069b GC 29	579.0	0.08	0.1	0.03	0.08	1.71	101.65
KDI-15-0069b GC 30	591.6	0.07	0.09	0.03	0.07	1.41	98.08

D.11 Drill Core Aqua Regia ICP-MS Results

Major and trace element results are presented for the aqua regia digestion and ICP-MS analysis of the drill core samples.

Drill Core Aqua Regia ICP-MS Results

Sample ID	Depth m	Length cm	Total C %	Au ppm	Ag ppm	Al %	As ppm	B ppm	Ba ppm	Be ppm	Bi ppm	Ca %	Cd ppm
KDI-16-013 GC 02	9.9	17.5	0.02	0.0012	0.204	2.16	1.56	10	261	0.18	0.421	0.13	0.122
KDI-16-013 GC 03	21.8	19	0.02	0.0012	0.052	1.84	3.24	10	335	0.2	0.65	0.26	0.105
KDI-16-013 GC 04	28.4	20	0.01	0.0014	0.081	3.38	2.64	10	401	0.44	0.621	0.09	0.039
KDI-16-013 GC 05	40.1	17	0.02	0.001	0.117	2.12	1	<10	274	0.17	0.576	0.19	0.069
KDI-16-013 GC 06	51.5	19	0.1	0.0013	0.138	3.31	1.03	10	406	0.6	0.888	0.1	0.055
KDI-16-013 GC 07	58.2	21	0.02	0.0013	0.172	2.8	0.99	<10	286	0.44	0.313	0.12	0.067
KDI-16-013 GC 08	70.1	22	0.02	0.0005	0.125	3.09	3.08	10	338	0.67	0.289	0.07	0.083
KDI-16-013 GC 09	80.1	21	0.01	0.0032	0.092	2.25	1.35	20	489	0.33	0.393	0.19	0.113
KDI-16-013 GC 10	87.8	22	0.01	0.0018	0.12	2.32	0.82	20	347	0.49	0.898	0.3	0.143
KDI-16-013 GC 12	110.7	16	0.02	0.0015	0.099	3.42	0.51	10	371	0.69	0.581	0.13	0.044
KDI-16-013 GC 13	123.0	17	0.02	0.0015	0.077	1.92	0.39	10	272	0.24	0.472	0.19	0.042
KDI-16-013 GC 14	130.0	17	0.09	0.0009	0.12	3.79	3.19	10	585	0.7	0.488	0.11	0.054
KDI-16-013 GC 15	143.2	18	0.01	0.0012	0.116	2.34	0.83	<10	211	0.7	0.344	0.13	0.081
KDI-16-013 GC 16	150.6	16	0.03	0.0022	0.068	2.88	0.9	10	393	0.98	0.603	0.14	0.049
KDI-16-013 GC 17	160.8	21	0.02	0.0021	0.164	3.88	1.78	20	585	0.83	0.712	0.13	0.02
KDI-16-013 GC 18	168.9	23	0.02	0.0009	0.033	2.49	4.11	10	224	0.76	0.422	0.15	0.018
KDI-15-048a GC 01	202.5	14.5	0.01	0.0009	0.089	2.67	1.16	10	459	0.28	0.491	0.26	0.065
KDI-15-048a GC 02	211.3	18	0.01	0.001	0.087	2.82	0.6	<10	352	0.55	0.328	0.2	0.057
KDI-15-048a GC 03	221.8	21	0.01	0.0012	0.104	2.78	1.95	<10	267	0.76	0.251	0.12	0.032
KDI-15-048a GC 04	233.0	17	0.01	0.0007	0.1	1.71	1.22	<10	154.5	0.42	0.149	0.15	0.04
KDI-15-048a GC 05	240.0	16	0.02	0.0007	0.11	2.87	1.11	<10	371	0.61	0.319	0.12	0.045
KDI-15-048a GC 06	254.5	21.5	0.09	0.0007	0.092	3.45	2.55	10	440	0.7	0.352	0.13	0.14
KDI-15-048a GC 07	259.3	22	0.01	0.0006	0.104	3.77	0.42	<10	580	0.75	0.338	0.07	0.048
KDI-15-048a GC 08	269.1	22	0.1	0.0011	0.11	2.97	0.77	10	398	0.49	0.678	0.3	0.075
KDI-15-048a GC 09	280.4	23	0.01	0.0006	0.115	2.71	0.56	<10	331	0.47	0.37	0.1	0.047
KDI-15-048a GC 10	291.1	21	0.02	0.0009	0.069	1.98	0.58	<10	233	0.43	0.374	0.09	0.031
KDI-15-048a GC 11	300.8	22	0.08	0.0008	0.197	3.37	2.1	<10	506	0.68	0.588	0.05	0.063
KDI-15-048a GC 12	308.5	16	0.03	0.0005	0.119	2.72	1.47	10	327	0.55	0.263	0.15	0.028
KDI-15-048a GC 13	320.2	23	0.05	0.0006	0.097	2.44	1.7	<10	302	0.52	0.376	0.25	0.084

Drill Core Aqua Regia ICP-MS Results

Sample ID	Depth m	Length cm	Total C %	Au ppm	Ag ppm	Al %	As ppm	B ppm	Ba ppm	Be ppm	Bi ppm	Ca %	Cd ppm
KDI-15-048a GC 14	322.9	17.5	0.04	0.0004	0.083	2.45	0.28	<10	371	0.57	0.326	0.18	0.048
KDI-15-048a GC 15	340.1	21	0.04	0.0007	0.107	3.42	1.42	<10	449	1.11	0.381	0.1	0.049
KDI-15-048a GC 16	350.6	16	0.05	0.0009	0.095	3.75	1.34	<10	483	0.91	0.444	0.11	0.024
KDI-15-048a GC 17	360.7	21	0.03	0.0008	0.127	2.82	0.99	<10	386	0.88	0.625	0.1	0.049
KDI-15-048a GC 18	370.7	18	0.01	0.0006	0.102	1.28	3.03	<10	138.5	0.96	0.23	0.23	0.063
KDI-15-048a GC 19	377.8	23	0.005	0.0006	0.078	2.61	1.45	<10	297	0.76	0.531	0.13	0.038
KDI-15-048a GC 20	388.8	24	0.005	0.0006	0.069	2.92	3.15	<10	294	0.68	0.643	0.11	0.035
KDI-15-048a GC 21	400.8	26	0.01	0.0015	0.132	2.23	4.59	<10	222	0.36	1.11	0.29	0.102
KDI-15-048b GC 01	70.7	21	0.01	0.0014	0.086	4.02	0.37	10	687	1.56	0.291	0.14	0.042
KDI-15-048b GC 02	80.1	21	0.01	0.0011	0.066	2.29	0.38	10	346	0.8	0.25	0.09	0.035
KDI-15-048b GC 03	89.8	18	0.02	0.0039	0.135	2.57	0.94	<10	327	0.71	0.315	0.14	0.057
KDI-15-048b GC 04	100.5	16.5	0.01	0.0018	0.118	2.45	0.56	<10	376	0.51	0.182	0.11	0.046
KDI-15-048b GC 05	109.0	17	0.01	0.0021	0.119	3.42	4.51	10	451	0.63	0.367	0.08	0.054
KDI-15-048b GC 06	121.0	20	0.03	0.0039	0.113	3.23	0.75	10	525	0.57	0.394	0.09	0.036
KDI-15-048b GC 07	130.0	16	0.01	0.0048	0.329	3.18	0.98	10	391	0.5	0.59	0.07	0.024
KDI-15-0069b GC 01	302.5	20	0.01	0.0002	0.126	1.88	0.43	<10	260	0.29	0.178	0.15	0.056
KDI-15-0069b GC 02	310.2	20	0.01	0.0007	0.09	3.35	1.03	<10	611	0.59	0.338	0.13	0.044
KDI-15-0069b GC 03	322.6	20	0.01	0.0008	0.083	3.2	1.58	<10	396	0.93	0.296	0.09	0.03
KDI-15-0069b GC 04	329.0	16	0.04	0.0005	0.082	3.49	4.04	<10	616	0.72	0.261	0.12	0.037
KDI-15-0069b GC 05	341.3	18	0.19	0.0009	0.08	3.15	3.16	<10	588	0.86	0.521	0.16	0.053
KDI-15-0069b GC 06	352.7	19	0.01	0.0009	0.083	3.22	3.62	<10	406	0.93	0.632	0.05	0.03
KDI-15-0069b GC 07	363.8	18.5	0.005	0.0004	0.086	2.87	0.53	<10	456	0.74	0.459	0.07	0.03
KDI-15-0069b GC 08	371.2	20.5	0.01	0.0022	0.088	4.21	4.59	10	738	1	0.593	0.07	0.035
KDI-15-0069b GC 09	381.0	15	0.005	0.0005	0.101	2.8	0.25	<10	545	0.57	0.407	0.18	0.045
KDI-15-0069b GC 10	392.9	11.5	0.01	0.0005	0.111	2.47	0.52	<10	363	0.69	0.204	0.08	0.028
KDI-15-0069b GC 11	400.9	17	0.04	0.0007	0.143	2.45	0.56	10	293	0.8	0.325	0.21	0.045
KDI-15-0069b GC 12	409.9	18.5	0.005	0.0002	0.124	2.2	0.33	<10	311	0.63	0.289	0.06	0.041
KDI-15-0069b GC 13	421.2	17	0.005	0.001	0.096	2.25	0.36	<10	385	0.7	0.335	0.07	0.037
KDI-15-0069b GC 14	431.7	23	0.01	0.0015	0.201	2.38	0.86	<10	354	0.31	0.367	0.13	0.077

Drill Core Aqua Regia ICP-MS Results

Sample ID	Depth m	Length cm	Total C %	Au ppm	Ag ppm	Al %	As ppm	B ppm	Ba ppm	Be ppm	Bi ppm	Ca %	Cd ppm
KDI-15-0069b GC 15	441.1	17	0.005	0.0005	0.082	3.06	0.83	<10	390	0.51	0.25	0.12	0.034
KDI-15-0069b GC 16	450.8	19	0.005	0.0019	0.154	2.19	0.56	<10	291	0.24	0.419	0.13	0.046
KDI-15-0069b GC 17	460.3	15	0.005	0.0009	0.105	3.44	0.39	<10	397	0.87	0.355	0.08	0.035
KDI-15-0069b GC 18	470.9	21.5	0.005	0.0005	0.131	2.2	0.36	<10	269	0.65	0.181	0.12	0.037
KDI-15-0069b GC 19	478.7	18	0.08	0.001	0.091	3.71	0.68	10	471	1.45	0.369	0.06	0.036
KDI-15-0069b GC 20	488.9	19	0.01	0.0008	0.107	3.05	0.26	<10	412	1.19	0.282	0.05	0.026
KDI-15-0069b GC 21	500.3	16	0.03	0.0006	0.124	2.06	0.78	<10	325	0.12	0.259	0.15	0.059
KDI-15-0069b GC 22	510.4	20	0.01	0.0002	0.111	2.77	0.34	<10	418	0.91	0.213	0.05	0.035
KDI-15-0069b GC 25	542.5	17.5	0.005	0.0007	0.105	3.86	0.26	<10	487	2.19	0.347	0.11	0.049
KDI-15-0069b GC 26	553.3	16.5	0.005	0.0008	0.123	3.13	0.36	<10	397	1.29	0.352	0.08	0.043
KDI-15-0069b GC 27	562.8	22.5	0.03	0.0009	0.107	3	0.47	<10	450	1.16	0.516	0.12	0.047
KDI-15-0069b GC 28	569.6	17	0.02	0.0002	0.082	3.85	2.72	<10	446	0.88	0.286	0.1	0.053
KDI-15-0069b GC 29	579.0	19	0.01	0.0009	0.105	3.79	0.87	<10	514	0.88	0.72	0.08	0.047
KDI-15-0069b GC 30	591.6	20	0.01	0.0019	0.105	3.36	1.14	<10	455	0.78	0.662	0.05	0.035

Drill Core Aqua Regia ICP-MS Results

Sample ID	Depth m	Ce ppm	Co ppm	Cr ppm	Cs ppm	Cu ppm	Fe %	Ga ppm	Ge ppm	Hf ppm	Hg ppm	In ppm	K %
KDI-16-013 GC 02	9.9	31.7	25.2	160	6.89	112.5	3.61	10.85	0.118	0.267	<0.004	0.038	1.16
KDI-16-013 GC 03	21.8	20.5	12.75	56.2	4.79	23.4	2.33	6.64	0.047	0.166	<0.004	0.016	0.89
KDI-16-013 GC 04	28.4	28.5	25.4	142.5	13.2	43.6	4.34	14.3	0.115	0.244	<0.004	0.044	2.14
KDI-16-013 GC 05	40.1	25.4	16.8	107.5	8.15	30.8	2.87	9.34	0.108	0.243	<0.004	0.031	1.32
KDI-16-013 GC 06	51.5	20.8	27.7	147.5	15.9	62.4	4.5	14.2	0.146	0.242	<0.004	0.046	2.11
KDI-16-013 GC 07	58.2	28.4	25.8	194	11.05	85.6	4.06	11.95	0.175	0.186	<0.004	0.043	1.87
KDI-16-013 GC 08	70.1	26.4	24.4	138.5	10.4	35.4	4.19	12.75	0.098	0.153	<0.004	0.039	1.71
KDI-16-013 GC 09	80.1	20.6	15.8	77	7.5	32.5	2.82	8.14	0.078	0.227	<0.004	0.024	1.33
KDI-16-013 GC 10	87.8	53.5	17.95	99.9	6.69	42.7	3.21	9.5	0.124	0.246	<0.004	0.027	1.22
KDI-16-013 GC 12	110.7	20.4	25.4	141	13.35	46	4.49	14.15	0.133	0.257	<0.004	0.048	2.13
KDI-16-013 GC 13	123.0	19	12.6	60.4	7.23	28.3	2.31	6.94	0.082	0.167	<0.004	0.023	1.09
KDI-16-013 GC 14	130.0	27.7	31.3	182.5	13.85	67.7	5.15	15.2	0.114	0.18	<0.004	0.051	2.33
KDI-16-013 GC 15	143.2	26.7	20.6	119.5	5.37	61.1	3.35	9.54	0.078	0.29	<0.004	0.032	1.01
KDI-16-013 GC 16	150.6	20.7	19.85	91.8	9.3	43.6	3.75	10.35	0.095	0.081	<0.004	0.03	1.57
KDI-16-013 GC 17	160.8	32	28.1	141	12.7	45.1	4.81	14.7	0.097	0.305	<0.004	0.051	2.24
KDI-16-013 GC 18	168.9	36.2	18.95	114.5	5.19	61.1	3.59	9.98	0.083	0.281	<0.004	0.021	0.92
KDI-15-048a GC 01	202.5	28.5	18.7	93.4	10.3	38.8	3.32	9.19	0.074	0.176	<0.004	0.023	1.5
KDI-15-048a GC 02	211.3	26.3	20.4	103.5	12.55	40.5	3.58	10.65	0.124	0.077	<0.004	0.04	1.69
KDI-15-048a GC 03	221.8	24.3	21.5	150.5	10.05	39.6	3.64	10.65	0.106	0.176	<0.004	0.034	1.58
KDI-15-048a GC 04	233.0	18.35	11.55	75	4.64	27.8	2.16	5.92	0.072	0.076	<0.004	0.017	0.74
KDI-15-048a GC 05	240.0	29.7	21.1	116	10.85	45.6	3.85	10.55	0.101	0.108	<0.004	0.035	1.6
KDI-15-048a GC 06	254.5	38.1	23.9	150	12.15	37.9	4.43	13.65	0.141	0.187	<0.004	0.045	1.91
KDI-15-048a GC 07	259.3	27.7	27.4	157	17.55	54	5	14.1	0.147	0.068	<0.004	0.057	2.38
KDI-15-048a GC 08	269.1	24.3	22.9	122.5	11.1	55	4.03	11.15	0.121	0.094	<0.004	0.036	1.7
KDI-15-048a GC 09	280.4	28.9	22.5	126.5	9.71	53.8	3.85	10.55	0.099	0.107	<0.004	0.035	1.59
KDI-15-048a GC 10	291.1	20.3	13	72.1	7.18	23.4	2.62	7.31	0.081	0.063	<0.004	0.024	1.09
KDI-15-048a GC 11	300.8	28.7	30.8	155	12.55	85.5	4.88	13.1	0.113	0.221	<0.004	0.045	1.88
KDI-15-048a GC 12	308.5	30.5	21.8	123	8.57	44.8	3.78	10.9	0.09	0.199	<0.004	0.03	1.36
KDI-15-048a GC 13	320.2	21.1	18.15	104	9.5	41.3	3.33	9.24	0.101	0.147	<0.004	0.032	1.48

Drill Core Aqua Regia ICP-MS Results

Sample ID	Depth m	Ce ppm	Co ppm	Cr ppm	Cs ppm	Cu ppm	Fe %	Ga ppm	Ge ppm	Hf ppm	Hg ppm	In ppm	K %
KDI-15-048a GC 14	322.9	24.5	18.6	108	9.46	37.8	3.26	9.39	0.1	0.134	<0.004	0.033	1.47
KDI-15-048a GC 15	340.1	25.9	26.1	145.5	15.2	51.8	4.59	13.6	0.124	0.089	<0.004	0.049	2.11
KDI-15-048a GC 16	350.6	29.1	27.8	165.5	14.9	35	4.86	15.15	0.116	0.12	<0.004	0.054	2.38
KDI-15-048a GC 17	360.7	29.4	24.4	143.5	11.8	58.5	3.95	11.15	0.112	0.109	<0.004	0.043	1.64
KDI-15-048a GC 18	370.7	17.85	9.08	55.2	4.41	27.4	1.66	4.58	0.055	0.132	<0.004	0.012	0.63
KDI-15-048a GC 19	377.8	21.3	19.35	116	11.25	36.1	3.5	10.25	0.1	0.14	<0.004	0.041	1.61
KDI-15-048a GC 20	388.8	28.1	22.7	133.5	11.5	45.3	3.95	11.75	0.09	0.165	<0.004	0.037	1.57
KDI-15-048a GC 21	400.8	26.8	21.5	117.5	11.2	59.1	3.34	8.64	0.109	0.189	<0.004	0.026	1.29
KDI-15-048b GC 01	70.7	24.1	29.5	157	16.05	43.9	5.23	15.5	0.167	0.048	<0.004	0.051	2.3
KDI-15-048b GC 02	80.1	21	14.25	79.2	9.45	23.3	2.92	8.08	0.106	0.149	<0.004	0.023	1.24
KDI-15-048b GC 03	89.8	28.4	22.8	162.5	9.22	69.1	3.73	9.92	0.128	0.375	<0.004	0.036	1.51
KDI-15-048b GC 04	100.5	26.6	20.4	134	9.21	45.6	3.45	9.79	0.108	0.269	<0.004	0.035	1.54
KDI-15-048b GC 05	109.0	29	25.5	162	15.5	43.8	4.57	13.55	0.147	0.237	<0.004	0.047	2.11
KDI-15-048b GC 06	121.0	30.2	24.3	150	12.6	45.1	4.33	12.75	0.135	0.165	<0.004	0.044	1.87
KDI-15-048b GC 07	130.0	38.7	37.7	225	12.9	167.5	4.92	13.4	0.15	0.525	<0.004	0.048	1.98
KDI-15-0069b GC 01	302.5	26.2	17	103.5	10.7	52	2.72	7.76	0.106	0.213	<0.004	0.026	1.13
KDI-15-0069b GC 02	310.2	30.5	26.3	154.5	14.7	42.5	4.48	12.9	0.172	0.076	<0.004	0.049	1.97
KDI-15-0069b GC 03	322.6	27.4	22.4	152	12.35	24.4	4.17	12.6	0.129	0.068	<0.004	0.043	1.83
KDI-15-0069b GC 04	329.0	25	25.2	159	12.4	31.5	4.54	13.65	0.159	0.034	<0.004	0.049	1.94
KDI-15-0069b GC 05	341.3	22.2	23.4	146	15.65	43.3	4.31	11.95	0.144	0.123	<0.004	0.035	1.92
KDI-15-0069b GC 06	352.7	20.1	24	152	11.65	43.7	4.29	12.65	0.108	0.037	<0.004	0.039	1.76
KDI-15-0069b GC 07	363.8	23.8	20.6	131.5	13.35	35.5	3.77	10.8	0.121	0.061	<0.004	0.04	1.68
KDI-15-0069b GC 08	371.2	30.1	30.8	193	21.1	38.6	5.59	16.9	0.187	0.097	<0.004	0.052	2.6
KDI-15-0069b GC 09	381.0	24.9	22.4	135.5	12.1	45.4	3.83	10.6	0.136	0.035	<0.004	0.039	1.66
KDI-15-0069b GC 10	392.9	25.3	21.3	137	10.6	40.2	3.36	9.9	0.108	0.109	<0.004	0.034	1.47
KDI-15-0069b GC 11	400.9	23.4	21.8	145	9.9	60.2	3.47	9.72	0.107	0.125	<0.004	0.034	1.38
KDI-15-0069b GC 12	409.9	26.8	20	121	10.75	50.9	3.15	8.96	0.123	0.05	<0.004	0.031	1.35
KDI-15-0069b GC 13	421.2	23.2	17.1	104	9.37	40	2.99	8.26	0.107	0.067	<0.004	0.029	1.26
KDI-15-0069b GC 14	431.7	31.3	26.5	188	11.1	108	3.8	10.2	0.151	0.206	<0.004	0.045	1.56

Drill Core Aqua Regia ICP-MS Results

Sample ID	Depth m	Ce ppm	Co ppm	Cr ppm	Cs ppm	Cu ppm	Fe %	Ga ppm	Ge ppm	Hf ppm	Hg ppm	In ppm	K %
KDI-15-0069b GC 15	441.1	22.9	22.1	145.5	11.5	26.3	3.95	11.85	0.12	0.066	<0.004	0.041	1.67
KDI-15-0069b GC 16	450.8	24.8	20.6	146.5	9	71.9	3.26	9.47	0.128	0.116	<0.004	0.037	1.3
KDI-15-0069b GC 17	460.3	24.1	26.6	165	15.45	44.5	4.64	13.7	0.147	0.032	<0.004	0.049	2.08
KDI-15-0069b GC 18	470.9	22.4	19.2	125	8.67	57.4	3.16	9.02	0.117	0.049	<0.004	0.034	1.24
KDI-15-0069b GC 19	478.7	22.5	26.7	163.5	15.85	49.5	4.86	15	0.131	0.076	<0.004	0.049	2.05
KDI-15-0069b GC 20	488.9	23.8	23.3	145	13.95	41.6	4.15	12.35	0.139	0.042	<0.004	0.049	1.84
KDI-15-0069b GC 21	500.3	26	17.8	127	6.9	54.3	2.92	8.56	0.147	0.098	<0.004	0.032	1.32
KDI-15-0069b GC 22	510.4	20.5	22.3	139	11.8	53.2	3.84	10.7	0.123	0.035	<0.004	0.041	1.57
KDI-15-0069b GC 25	542.5	25.5	26.6	155.5	17	40.3	5.13	15.05	0.112	0.042	<0.004	0.049	2.06
KDI-15-0069b GC 26	553.3	27.4	25.2	164.5	13.85	53.7	4.42	12.8	0.12	0.036	<0.004	0.038	1.87
KDI-15-0069b GC 27	562.8	30.9	24.2	153	14.15	49.8	4.27	12.05	0.115	0.046	<0.004	0.04	1.7
KDI-15-0069b GC 28	569.6	29.9	27.3	168.5	16.55	30.1	5.03	14.9	0.112	0.034	<0.004	0.05	2.21
KDI-15-0069b GC 29	579.0	28.1	28.8	171.5	13.15	42.7	5.1	15.15	0.122	0.039	<0.004	0.045	2.11
KDI-15-0069b GC 30	591.6	32.3	25.9	172.5	9.64	41.8	4.7	13.85	0.126	0.04	<0.004	0.047	1.98

Drill Core Aqua Regia ICP-MS Results

Sample ID	Depth m	La ppm	Li ppm	Mg %	Mn ppm	Mo ppm	Na %	Nb ppm	Ni ppm	SiO2 %	Pb ppm	Pd ppm	Pt ppm
KDI-16-013 GC 02	9.9	15.95	39.7	1.18	296	1.55	0.077	0.111	71.4	0.039	8.44	<0.001	0.002
KDI-16-013 GC 03	21.8	9.3	47	0.84	264	0.93	0.042	0.077	41.3	0.115	3.18	<0.001	<0.002
KDI-16-013 GC 04	28.4	14.05	89.4	1.66	428	1.69	0.061	0.103	88.9	0.038	2.69	<0.001	0.002
KDI-16-013 GC 05	40.1	11.55	54.5	1.05	284	1.32	0.072	0.125	56.5	0.08	5.85	<0.001	<0.002
KDI-16-013 GC 06	51.5	9.84	90.8	1.72	448	3.11	0.071	0.098	85.5	0.042	4.79	0.002	<0.002
KDI-16-013 GC 07	58.2	14.25	66.5	1.59	434	1.54	0.074	0.125	78.4	0.041	2.72	0.001	<0.002
KDI-16-013 GC 08	70.1	12.7	89.6	1.68	430	1.61	0.066	0.09	84.5	0.021	2.96	0.002	<0.002
KDI-16-013 GC 09	80.1	9.46	59.4	1.04	299	1.31	0.068	0.097	54	0.075	2.4	<0.001	<0.002
KDI-16-013 GC 10	87.8	24.3	71.6	1.18	363	1.31	0.067	0.126	65.6	0.133	6.73	<0.001	<0.002
KDI-16-013 GC 12	110.7	9.58	99.3	1.77	485	1.39	0.075	0.119	89.6	0.053	2.11	<0.001	<0.002
KDI-16-013 GC 13	123.0	8.6	50.6	0.84	259	1.13	0.09	0.103	43	0.074	2.39	<0.001	<0.002
KDI-16-013 GC 14	130.0	13.55	76.3	2	436	3.53	0.081	0.116	114	0.041	4.13	0.001	<0.002
KDI-16-013 GC 15	143.2	12.5	64.7	1.42	319	1.49	0.077	0.097	64.8	0.05	3.42	0.002	<0.002
KDI-16-013 GC 16	150.6	9.22	85.3	1.45	416	1.67	0.076	0.127	70.3	0.046	2.84	<0.001	<0.002
KDI-16-013 GC 17	160.8	15.55	100.5	1.98	470	1.96	0.074	0.117	103	0.05	5.11	0.001	<0.002
KDI-16-013 GC 18	168.9	18.2	93.5	1.53	427	1.47	0.065	0.068	58.8	0.054	2.15	<0.001	<0.002
KDI-15-048a GC 01	202.5	13.45	61.7	1.25	366	1.74	0.097	0.102	65.8	0.11	4.22	<0.001	<0.002
KDI-15-048a GC 02	211.3	12.25	70.6	1.4	399	1.57	0.095	0.124	67.9	0.084	2.61	<0.001	<0.002
KDI-15-048a GC 03	221.8	11.75	76.7	1.48	331	1.43	0.094	0.1	73.6	0.038	2.06	<0.001	<0.002
KDI-15-048a GC 04	233.0	8.49	49.3	0.8	244	0.9	0.108	0.072	42.4	0.049	1.98	<0.001	<0.002
KDI-15-048a GC 05	240.0	14.15	74.4	1.48	419	1.45	0.113	0.118	72.8	0.04	3.02	0.001	<0.002
KDI-15-048a GC 06	254.5	18.65	89.1	1.71	439	3.4	0.107	0.149	84	0.042	4.79	0.001	<0.002
KDI-15-048a GC 07	259.3	13.5	85.6	2	526	1.78	0.101	0.133	93.5	0.027	2.88	0.001	<0.002
KDI-15-048a GC 08	269.1	10.95	70.6	1.53	409	1.8	0.093	0.152	84.1	0.122	2.68	0.001	<0.002
KDI-15-048a GC 09	280.4	14.35	65.2	1.42	367	1.62	0.081	0.136	81.6	0.033	2.71	0.001	<0.002
KDI-15-048a GC 10	291.1	9.43	51.6	0.99	302	1.16	0.09	0.11	44.2	0.026	2.03	0.001	<0.002
KDI-15-048a GC 11	300.8	14.3	80.2	1.87	508	2.32	0.082	0.147	105	0.015	5.27	0.002	<0.002
KDI-15-048a GC 12	308.5	15.05	66.7	1.47	383	1.77	0.092	0.112	68.5	0.044	3.78	0.002	<0.002
KDI-15-048a GC 13	320.2	9.5	54.4	1.28	353	1.49	0.083	0.12	68.5	0.11	5.21	0.002	<0.002

Drill Core Aqua Regia ICP-MS Results

Sample ID	Depth m	La ppm	Li ppm	Mg %	Mn ppm	Mo ppm	Na %	Nb ppm	Ni ppm	SiO2 %	Pb ppm	Pd ppm	Pt ppm
KDI-15-048a GC 14	322.9	11.55	54.5	1.25	344	1.42	0.096	0.096	59.8	0.073	2.89	<0.001	<0.002
KDI-15-048a GC 15	340.1	12.75	75.8	1.84	500	2.43	0.098	0.119	92.6	0.036	2.86	0.002	<0.002
KDI-15-048a GC 16	350.6	14.15	75.7	2.01	420	1.78	0.095	0.1	96	0.043	3.24	0.001	<0.002
KDI-15-048a GC 17	360.7	14.55	63.9	1.5	423	1.81	0.087	0.101	89	0.035	3.09	0.002	<0.002
KDI-15-048a GC 18	370.7	8.44	31.2	0.59	213	0.79	0.119	0.059	24.7	0.083	3.66	<0.001	<0.002
KDI-15-048a GC 19	377.8	10.1	57.8	1.35	359	1.55	0.085	0.096	67.3	0.052	2.84	<0.001	<0.002
KDI-15-048a GC 20	388.8	14.3	67.3	1.59	364	1.59	0.091	0.086	76.5	0.038	3.36	0.001	<0.002
KDI-15-048a GC 21	400.8	12.55	60.5	1.18	344	1.43	0.079	0.121	72.8	0.128	4.54	0.001	<0.002
KDI-15-048b GC 01	70.7	11.1	107	2.03	431	2.32	0.084	0.106	101.5	0.055	2.35	0.002	<0.002
KDI-15-048b GC 02	80.1	9.87	74.3	1.13	342	1.66	0.074	0.096	49.5	0.033	2.14	0.001	<0.002
KDI-15-048b GC 03	89.8	14.4	80.2	1.32	309	1.84	0.093	0.121	66	0.038	2.28	0.001	<0.002
KDI-15-048b GC 04	100.5	13.1	66.4	1.25	333	1.58	0.103	0.111	64.2	0.036	2.34	<0.001	<0.002
KDI-15-048b GC 05	109.0	14.25	99.5	1.8	414	1.69	0.096	0.12	86.3	0.021	2.84	0.001	<0.002
KDI-15-048b GC 06	121.0	14.7	97.3	1.69	422	1.69	0.087	0.139	84.7	0.016	2.51	0.001	<0.002
KDI-15-048b GC 07	130.0	19.8	89.8	1.67	376	2.49	0.085	0.182	102.5	0.028	7.56	0.002	<0.002
KDI-15-0069b GC 01	302.5	12.95	53.1	0.92	257	1.26	0.108	0.102	52.6	0.055	3.15	<0.001	<0.002
KDI-15-0069b GC 02	310.2	15.3	85.9	1.69	399	2.47	0.095	0.148	93.3	0.049	2.83	0.002	<0.002
KDI-15-0069b GC 03	322.6	13.05	89.5	1.63	380	1.55	0.1	0.126	75.3	0.022	2.88	0.001	<0.002
KDI-15-0069b GC 04	329.0	11.7	83.4	1.74	411	1.93	0.105	0.136	95	0.042	2.71	0.001	<0.002
KDI-15-0069b GC 05	341.3	10.1	69.9	1.63	437	2.08	0.084	0.149	83.3	0.068	2.81	0.001	<0.002
KDI-15-0069b GC 06	352.7	9.3	95.1	1.64	395	1.16	0.088	0.138	88.7	0.01	2.69	0.002	<0.002
KDI-15-0069b GC 07	363.8	11.4	76.8	1.46	402	1.44	0.1	0.104	69.2	0.019	2.71	0.002	<0.002
KDI-15-0069b GC 08	371.2	14.75	113	2.23	578	2.32	0.099	0.117	106.5	0.028	3.88	0.002	<0.002
KDI-15-0069b GC 09	381.0	11.75	68.3	1.42	370	1.45	0.097	0.135	77.9	0.074	2.54	0.001	<0.002
KDI-15-0069b GC 10	392.9	12.85	59	1.21	312	1.55	0.105	0.111	66.3	0.022	2.23	0.001	<0.002
KDI-15-0069b GC 11	400.9	12.2	67.4	1.24	283	1.59	0.09	0.087	66.5	0.029	2.74	0.002	<0.002
KDI-15-0069b GC 12	409.9	12.95	51.7	1.12	301	1.35	0.098	0.127	58	0.013	2.73	0.001	<0.002
KDI-15-0069b GC 13	421.2	11.3	53.7	1.13	295	1.42	0.097	0.11	51.3	0.019	2.94	0.001	<0.002
KDI-15-0069b GC 14	431.7	16.45	48.3	1.28	286	1.8	0.093	0.158	75.1	0.041	2.88	<0.001	<0.002

Drill Core Aqua Regia ICP-MS Results

Sample ID	Depth m	La ppm	Li ppm	Mg %	Mn ppm	Mo ppm	Na %	Nb ppm	Ni ppm	SiO2 %	Pb ppm	Pd ppm	Pt ppm
KDI-15-0069b GC 15	441.1	10.8	69.6	1.53	373	1.4	0.105	0.101	77.7	0.041	2.58	0.001	<0.002
KDI-15-0069b GC 16	450.8	12.55	46	1.11	233	1.56	0.106	0.128	63.2	0.033	2.61	0.001	<0.002
KDI-15-0069b GC 17	460.3	11.6	78.3	1.79	450	1.76	0.103	0.114	91.5	0.026	2.72	0.001	<0.002
KDI-15-0069b GC 18	470.9	10.8	52.4	1.08	260	1.35	0.099	0.116	60.3	0.037	2.14	0.001	<0.002
KDI-15-0069b GC 19	478.7	10.4	95.7	1.94	504	2.78	0.1	0.122	91.1	0.016	2.82	0.001	<0.002
KDI-15-0069b GC 20	488.9	11.3	64.1	1.58	390	1.67	0.089	0.121	75	0.013	2.47	0.001	<0.002
KDI-15-0069b GC 21	500.3	13.05	39.6	1.03	345	1.51	0.107	0.124	56.2	0.037	2.32	0.002	<0.002
KDI-15-0069b GC 22	510.4	10.05	61.7	1.39	359	1.59	0.091	0.119	74	0.012	2.29	<0.001	<0.002
KDI-15-0069b GC 25	542.5	11.65	82.9	2.1	569	1.57	0.098	0.155	94.4	0.041	4.02	0.001	<0.002
KDI-15-0069b GC 26	553.3	13.35	59.2	1.64	469	1.88	0.099	0.129	83.7	0.025	3.22	0.001	<0.002
KDI-15-0069b GC 27	562.8	15.5	60.6	1.62	439	2.01	0.089	0.156	78.7	0.046	3.6	0.001	<0.002
KDI-15-0069b GC 28	569.6	14.45	75.2	2.06	531	1.63	0.105	0.148	98.9	0.032	3.24	0.002	<0.002
KDI-15-0069b GC 29	579.0	13.6	76.2	2.02	565	2.07	0.107	0.12	105.5	0.024	3.84	0.002	<0.002
KDI-15-0069b GC 30	591.6	16.15	62	1.8	507	1.9	0.089	0.152	94.8	0.013	3.6	<0.001	<0.002

Drill Core Aqua Regia ICP-MS Results

Sample ID	Depth m	Rb ppm	Re ppm	S %	Sb ppm	Sc ppm	Se ppm	Sn ppm	Sr ppm	Ta ppm	Te ppm	Th ppm	Ti %
KDI-16-013 GC 02	9.9	58.3	0.001	0.39	0.065	11.4	0.4	1.14	9.94	<0.005	0.05	4.09	0.22
KDI-16-013 GC 03	21.8	39	0.001	0.1	0.011	5.41	0.2	0.6	11.65	<0.005	0.01	1.945	0.101
KDI-16-013 GC 04	28.4	104.5	0.001	0.14	<0.005	17.55	0.3	1.71	7.42	<0.005	0.03	2.84	0.316
KDI-16-013 GC 05	40.1	66.1	0.001	0.12	0.037	11.55	0.2	1.17	10.6	<0.005	0.03	2.68	0.228
KDI-16-013 GC 06	51.5	107.5	0.001	0.24	0.017	16.25	0.4	2.21	6.23	<0.005	0.04	2.28	0.319
KDI-16-013 GC 07	58.2	91.1	0.001	0.4	<0.005	13.6	0.4	1.23	8.71	<0.005	0.04	3.83	0.306
KDI-16-013 GC 08	70.1	79.5	0.001	0.14	0.012	13.15	0.2	1.22	8.36	<0.005	0.03	2.87	0.257
KDI-16-013 GC 09	80.1	61.2	0.001	0.1	0.009	10.55	0.2	1.04	10.95	<0.005	0.02	1.905	0.201
KDI-16-013 GC 10	87.8	55.1	0.001	0.15	0.007	10.9	0.3	0.99	11.7	<0.005	0.04	6.81	0.198
KDI-16-013 GC 12	110.7	103	0.001	0.17	0.005	17.65	0.3	1.77	8.01	0.007	0.04	2.04	0.318
KDI-16-013 GC 13	123.0	51.1	<0.001	0.11	0.017	8.71	0.2	1.2	13.1	0.006	0.03	1.83	0.163
KDI-16-013 GC 14	130.0	108.5	0.002	0.25	0.025	20.6	0.4	2.01	8.09	<0.005	0.06	2.93	0.354
KDI-16-013 GC 15	143.2	45.6	0.001	0.22	0.009	8.93	0.2	0.91	10.45	<0.005	0.03	3.72	0.166
KDI-16-013 GC 16	150.6	72.8	0.001	0.17	0.011	13.6	0.3	1.24	15	0.008	0.05	2.47	0.234
KDI-16-013 GC 17	160.8	99.2	0.001	0.15	0.023	18.05	0.2	1.56	10.55	0.006	0.03	3.57	0.304
KDI-16-013 GC 18	168.9	40.5	0.001	0.07	0.034	8.93	0.2	1.05	10.15	<0.005	0.02	4.86	0.143
KDI-15-048a GC 01	202.5	68.6	0.001	0.14	0.007	9.09	0.2	1.49	14.3	0.007	0.03	2.81	0.201
KDI-15-048a GC 02	211.3	81.3	0.001	0.15	0.01	13.45	0.2	1.91	10.55	0.006	0.04	2.6	0.261
KDI-15-048a GC 03	221.8	71.9	<0.001	0.15	0.008	11	0.2	1.29	12.9	<0.005	0.02	2.61	0.256
KDI-15-048a GC 04	233.0	32.6	<0.001	0.11	0.009	6.16	0.2	0.63	15.8	<0.005	0.01	1.815	0.118
KDI-15-048a GC 05	240.0	71.6	0.001	0.18	0.013	12.5	0.2	1.78	12.3	0.007	0.03	3.31	0.241
KDI-15-048a GC 06	254.5	89.6	0.002	0.14	0.007	18.4	0.2	1.54	14.85	0.011	0.03	3.6	0.298
KDI-15-048a GC 07	259.3	110.5	0.001	0.21	0.007	17.15	0.3	2.92	8.13	0.009	0.04	2.82	0.354
KDI-15-048a GC 08	269.1	78.3	0.001	0.21	0.009	14.65	0.3	1.74	13.15	0.011	0.04	2.26	0.263
KDI-15-048a GC 09	280.4	70.8	0.001	0.21	0.008	13.15	0.3	1.4	9.3	0.009	0.01	3.13	0.253
KDI-15-048a GC 10	291.1	49	0.001	0.1	0.013	8.84	0.2	0.99	10.05	0.008	0.02	2.1	0.173
KDI-15-048a GC 11	300.8	86.4	0.001	0.45	0.01	14.8	0.4	1.86	7.82	0.012	0.04	3.13	0.283
KDI-15-048a GC 12	308.5	61.4	0.001	0.23	0.018	11.6	0.3	1.29	11.4	0.006	0.02	3.08	0.204
KDI-15-048a GC 13	320.2	68.5	0.001	0.16	0.01	11.85	0.3	1.31	10.55	0.006	0.03	1.94	0.229

Drill Core Aqua Regia ICP-MS Results

Sample ID	Depth m	Rb ppm	Re ppm	S %	Sb ppm	Sc ppm	Se ppm	Sn ppm	Sr ppm	Ta ppm	Te ppm	Th ppm	Ti %
KDI-15-048a GC 14	322.9	69.2	<0.001	0.15	0.011	11.75	0.2	1.21	12.9	<0.005	0.03	2.51	0.225
KDI-15-048a GC 15	340.1	108	0.001	0.2	0.005	15.9	0.3	1.9	10.7	0.006	0.03	2.67	0.302
KDI-15-048a GC 16	350.6	119	0.001	0.14	<0.005	19.4	0.2	1.89	9.25	<0.005	0.02	3.03	0.339
KDI-15-048a GC 17	360.7	82	0.001	0.22	0.008	13.3	0.3	1.76	9.79	<0.005	0.05	3.22	0.25
KDI-15-048a GC 18	370.7	29.1	<0.001	0.1	0.019	4.04	0.2	0.75	18.05	<0.005	0.02	1.845	0.082
KDI-15-048a GC 19	377.8	79.7	<0.001	0.12	0.021	12.65	0.2	1.6	9.48	<0.005	0.03	2.53	0.241
KDI-15-048a GC 20	388.8	78.7	0.001	0.13	0.016	12.65	0.2	1.76	10.4	<0.005	0.03	3.78	0.236
KDI-15-048a GC 21	400.8	68.5	0.001	0.23	0.011	9.44	0.2	1.61	11.35	0.005	0.06	3.16	0.197
KDI-15-048b GC 01	70.7	118	0.001	0.15	0.008	22.1	0.2	1.75	11	<0.005	0.05	2.48	0.358
KDI-15-048b GC 02	80.1	62.2	0.001	0.1	0.014	9.45	0.3	1.3	9.32	0.008	0.02	2.09	0.192
KDI-15-048b GC 03	89.8	77.7	0.001	0.32	0.011	10.65	0.3	0.98	13.15	<0.005	0.05	3.6	0.267
KDI-15-048b GC 04	100.5	78.7	0.001	0.23	<0.005	10.85	0.3	0.98	11.6	<0.005	0.03	2.79	0.262
KDI-15-048b GC 05	109.0	109.5	0.001	0.23	0.01	16.3	0.3	1.92	10.1	0.006	0.03	3.07	0.329
KDI-15-048b GC 06	121.0	97.2	0.001	0.21	0.007	15.6	0.3	1.42	10.7	0.008	0.03	2.97	0.293
KDI-15-048b GC 07	130.0	98.3	0.001	0.79	0.005	15.8	0.8	1.43	7.94	0.012	0.11	5.56	0.322
KDI-15-0069b GC 01	302.5	54.2	0.001	0.2	0.007	9.22	0.2	1.5	14.4	0.006	0.04	2.86	0.187
KDI-15-0069b GC 02	310.2	97.7	0.001	0.15	0.011	18.5	0.2	1.53	13.4	0.017	0.04	2.89	0.319
KDI-15-0069b GC 03	322.6	88.2	<0.001	0.1	0.005	15.75	0.2	1.19	17.7	0.015	0.02	3.04	0.284
KDI-15-0069b GC 04	329.0	92.7	0.001	0.12	0.007	19.15	0.2	1.06	13.9	0.016	0.03	2.57	0.32
KDI-15-0069b GC 05	341.3	93.6	0.001	0.15	0.012	15.05	0.2	1.78	11.4	0.019	0.04	2.41	0.289
KDI-15-0069b GC 06	352.7	86.9	0.001	0.18	0.008	15.05	0.2	1.03	11.7	0.015	0.04	2.6	0.277
KDI-15-0069b GC 07	363.8	83.4	<0.001	0.14	0.01	13.75	0.2	1.27	12.1	0.011	0.03	2.59	0.262
KDI-15-0069b GC 08	371.2	129.5	0.001	0.14	0.042	21.8	0.2	2.03	9.47	0.011	0.04	3.04	0.405
KDI-15-0069b GC 09	381.0	80.2	0.001	0.18	0.008	15	0.2	1.02	13.45	0.017	0.02	2.52	0.269
KDI-15-0069b GC 10	392.9	72.6	<0.001	0.16	0.011	11.8	0.2	0.73	13.8	<0.005	0.03	2.69	0.262
KDI-15-0069b GC 11	400.9	70.3	0.001	0.31	0.017	10.2	0.3	0.7	17.05	<0.005	0.05	2.76	0.247
KDI-15-0069b GC 12	409.9	68.3	0.001	0.21	0.01	11.2	0.2	1.11	12.95	0.018	0.04	3.28	0.236
KDI-15-0069b GC 13	421.2	65.1	<0.001	0.17	0.011	10.35	0.2	0.85	14.25	0.012	0.05	2.49	0.201
KDI-15-0069b GC 14	431.7	82.3	0.001	0.45	0.007	12.5	0.4	0.91	11.6	0.008	0.05	4.59	0.288

Drill Core Aqua Regia ICP-MS Results

Sample ID	Depth m	Rb ppm	Re ppm	S %	Sb ppm	Sc ppm	Se ppm	Sn ppm	Sr ppm	Ta ppm	Te ppm	Th ppm	Ti %
KDI-15-0069b GC 15	441.1	87.8	0.001	0.11	0.007	15.2	0.2	0.87	14.4	0.01	0.03	2.29	0.269
KDI-15-0069b GC 16	450.8	67.2	0.001	0.28	0.007	11.3	0.3	0.8	13.55	0.005	0.06	2.97	0.259
KDI-15-0069b GC 17	460.3	108.5	0.001	0.19	0.005	17.7	0.2	1.17	11.6	0.007	0.03	2.69	0.325
KDI-15-0069b GC 18	470.9	69.1	<0.001	0.21	0.018	10.5	0.2	0.59	15.9	0.008	0.04	2.59	0.23
KDI-15-0069b GC 19	478.7	110.5	0.001	0.18	0.005	18.15	0.2	1.07	12.9	0.009	0.04	2.56	0.299
KDI-15-0069b GC 20	488.9	95	0.001	0.15	0.007	16	0.2	1.09	9.55	0.012	0.03	2.45	0.283
KDI-15-0069b GC 21	500.3	70.5	0.001	0.23	0.01	10.6	0.2	0.72	14.45	0.005	0.05	3.39	0.25
KDI-15-0069b GC 22	510.4	78.6	0.001	0.19	0.017	13.95	0.3	0.9	11.6	0.012	0.04	2.05	0.258
KDI-15-0069b GC 25	542.5	101.5	0.001	0.16	<0.005	18.45	0.2	1.24	10.95	0.013	0.04	3.49	0.301
KDI-15-0069b GC 26	553.3	87.1	0.001	0.24	0.006	15.4	0.2	1.19	10.55	0.01	0.04	3.49	0.302
KDI-15-0069b GC 27	562.8	81.2	0.001	0.23	0.01	13.7	0.3	1.09	10.55	0.012	0.04	3.89	0.261
KDI-15-0069b GC 28	569.6	106	0.001	0.14	0.007	18.75	0.2	1.11	12.35	0.012	0.03	3.65	0.333
KDI-15-0069b GC 29	579.0	100	0.001	0.2	0.005	18.3	0.3	1.16	13.2	0.012	0.05	4.53	0.316
KDI-15-0069b GC 30	591.6	94.5	0.001	0.19	<0.005	17.1	0.2	1.19	8.87	0.012	0.03	4.65	0.302

Drill Core Aqua Regia ICP-MS Results

Sample ID	Depth m	Tl ppm	U ppm	V ppm	W ppm	Y ppm	Zn ppm	Zr ppm
KDI-16-013 GC 02	9.9	0.333	1.045	95.9	0.265	4.36	86.5	11.05
KDI-16-013 GC 03	21.8	0.241	1.21	43.7	0.2	9.53	73.2	6.39
KDI-16-013 GC 04	28.4	0.582	1.11	119	0.462	4.86	91.7	7.72
KDI-16-013 GC 05	40.1	0.372	1.05	82.3	0.308	7.33	69.3	9.48
KDI-16-013 GC 06	51.5	0.61	0.81	115	0.424	4.04	101	8.35
KDI-16-013 GC 07	58.2	0.493	1.11	108.5	0.246	4.19	92.4	7.7
KDI-16-013 GC 08	70.1	0.465	0.696	108.5	0.187	2.89	99.6	4.96
KDI-16-013 GC 09	80.1	0.345	0.779	65.3	0.218	5.87	78.2	7.93
KDI-16-013 GC 10	87.8	0.332	1.66	81.9	0.254	11.25	90.9	8.94
KDI-16-013 GC 12	110.7	0.569	0.82	110.5	0.377	5.07	100.5	8.71
KDI-16-013 GC 13	123.0	0.285	1.055	54.3	0.318	6.73	51.7	6.14
KDI-16-013 GC 14	130.0	0.624	0.874	142.5	0.627	4.4	109.5	6.53
KDI-16-013 GC 15	143.2	0.273	1.03	82.4	0.183	4.9	88.8	11.65
KDI-16-013 GC 16	150.6	0.431	0.895	95.8	0.363	4.89	83.5	3.04
KDI-16-013 GC 17	160.8	0.591	0.887	126.5	0.288	4.67	83.7	9.95
KDI-16-013 GC 18	168.9	0.241	1.13	80.5	0.191	5.55	57.7	9.93
KDI-15-048a GC 01	202.5	0.403	1.65	75.5	0.533	10.5	74.3	6.15
KDI-15-048a GC 02	211.3	0.456	1.22	91.1	0.42	8.34	80.2	2.63
KDI-15-048a GC 03	221.8	0.424	0.722	94.6	0.347	4.09	78.8	6.32
KDI-15-048a GC 04	233.0	0.198	0.741	47.6	0.261	4.52	42.2	2.78
KDI-15-048a GC 05	240.0	0.425	1.245	94.2	0.391	5.05	81.4	4.08
KDI-15-048a GC 06	254.5	0.515	1.34	127.5	0.407	5.34	116	7.34
KDI-15-048a GC 07	259.3	0.632	0.976	127	0.484	3.85	108.5	2.59
KDI-15-048a GC 08	269.1	0.45	1.175	103	0.411	10.25	85.8	3.42
KDI-15-048a GC 09	280.4	0.436	1.165	93.9	0.319	4.13	79.7	3.98
KDI-15-048a GC 10	291.1	0.289	0.833	62.8	0.356	2.98	52.6	1.98
KDI-15-048a GC 11	300.8	0.536	1.045	113.5	0.4	2.9	101.5	8.15
KDI-15-048a GC 12	308.5	0.371	1.03	90.2	0.295	4.74	66.5	6.48
KDI-15-048a GC 13	320.2	0.389	0.995	80.3	0.364	9.87	83.5	5.1

Drill Core Aqua Regia ICP-MS Results

Sample ID	Depth m	Tl ppm	U ppm	V ppm	W ppm	Y ppm	Zn ppm	Zr ppm
KDI-15-048a GC 14	322.9	0.409	1.035	82.7	0.387	6.54	70.3	4.56
KDI-15-048a GC 15	340.1	0.607	1.025	120.5	0.531	4.32	102	2.98
KDI-15-048a GC 16	350.6	0.676	0.986	140	0.507	4.68	97.9	4.23
KDI-15-048a GC 17	360.7	0.48	1.135	99.5	0.452	4.53	86.8	3.84
KDI-15-048a GC 18	370.7	0.173	1.155	29.7	0.418	7.49	35.6	5.08
KDI-15-048a GC 19	377.8	0.455	1.015	91.7	0.397	5.19	75.1	4.87
KDI-15-048a GC 20	388.8	0.456	1.41	96.5	0.38	4.62	77.8	5.98
KDI-15-048a GC 21	400.8	0.411	1.54	79.8	0.396	12.2	76.3	6.57
KDI-15-048b GC 01	70.7	0.661	0.615	143	0.44	4.49	101	1.72
KDI-15-048b GC 02	80.1	0.368	1.08	66.6	0.303	3.63	61.3	4.78
KDI-15-048b GC 03	89.8	0.453	0.986	89.8	0.168	4.13	81.5	14.3
KDI-15-048b GC 04	100.5	0.463	0.723	88.4	0.149	3.71	78.7	10.7
KDI-15-048b GC 05	109.0	0.637	0.971	124.5	0.406	3.56	103.5	8.59
KDI-15-048b GC 06	121.0	0.56	1.125	113.5	0.36	3.34	96.2	6.07
KDI-15-048b GC 07	130.0	0.659	1.49	109.5	0.318	4.2	92.1	19.55
KDI-15-0069b GC 01	302.5	0.339	1.17	67.6	0.368	6.05	58.4	7.14
KDI-15-0069b GC 02	310.2	0.57	1.24	125	0.449	5.8	94.1	2.47
KDI-15-0069b GC 03	322.6	0.516	0.946	116.5	0.387	3.28	90.3	2.29
KDI-15-0069b GC 04	329.0	0.54	0.88	132.5	0.388	4.55	92.4	1.15
KDI-15-0069b GC 05	341.3	0.536	1.085	108	0.497	5.59	93.7	4.08
KDI-15-0069b GC 06	352.7	0.51	0.78	119.5	0.403	2.43	88.4	1.19
KDI-15-0069b GC 07	363.8	0.478	0.993	99.3	0.415	3.05	83.7	1.98
KDI-15-0069b GC 08	371.2	0.742	1.15	156	0.61	3.87	127	2.78
KDI-15-0069b GC 09	381.0	0.461	1.015	104.5	0.414	7.15	81.6	1.28
KDI-15-0069b GC 10	392.9	0.432	0.655	92.1	0.241	3.04	68.6	3.53
KDI-15-0069b GC 11	400.9	0.418	0.683	87.1	0.156	3.26	74	4.39
KDI-15-0069b GC 12	409.9	0.394	1.15	79.6	0.416	3.28	69	1.73
KDI-15-0069b GC 13	421.2	0.387	1.055	70.5	0.406	2.94	65.9	2.13
KDI-15-0069b GC 14	431.7	0.49	1.195	101.5	0.353	4.65	82.7	7.04

Drill Core Aqua Regia ICP-MS Results

Sample ID	Depth m	Tl ppm	U ppm	V ppm	W ppm	Y ppm	Zn ppm	Zr ppm
KDI-15-0069b GC 15	441.1	0.541	0.712	113	0.316	4.2	84.5	2.29
KDI-15-0069b GC 16	450.8	0.406	0.794	89.5	0.242	3.82	69.6	3.87
KDI-15-0069b GC 17	460.3	0.644	0.759	130.5	0.382	3.48	101	1.11
KDI-15-0069b GC 18	470.9	0.429	0.677	82.9	0.204	4.08	64.3	1.76
KDI-15-0069b GC 19	478.7	0.674	0.836	141	0.405	2.94	104.5	2.46
KDI-15-0069b GC 20	488.9	0.551	0.857	108.5	0.386	2.7	91	1.39
KDI-15-0069b GC 21	500.3	0.423	0.852	83.3	0.978	4.69	68.9	3.32
KDI-15-0069b GC 22	510.4	0.448	0.595	99.9	0.295	2.28	77.1	1.22
KDI-15-0069b GC 25	542.5	0.601	1.335	132.5	0.389	5.2	113.5	1.46
KDI-15-0069b GC 26	553.3	0.522	1.075	119.5	0.388	3.72	96.4	1.42
KDI-15-0069b GC 27	562.8	0.489	1.66	107.5	0.425	6.03	92.2	1.53
KDI-15-0069b GC 28	569.6	0.611	1.015	136	0.379	4.42	115.5	1.17
KDI-15-0069b GC 29	579.0	0.595	1.415	136.5	0.382	4.39	107.5	1.37
KDI-15-0069b GC 30	591.6	0.561	1.66	134	0.427	4.1	105	1.35

D.12 Drill Core Pb Isotope Ratio Q-ICP-MS Results

Lead isotope ratio results are presented for the Q-ICP-MS analysis of the drill core samples.

Drill Core Pb Isotope Ratio Q-ICP-MS Results

Sample ID	Depth m	Pb^{206}/Pb^{204}	Pb^{207}/Pb^{204}	Pb^{208}/Pb^{204}	Pb^{208}/Pb^{206}	Pb^{208}/Pb^{207}	Pb^{206}/Pb^{207}
KDI-16-013 GC 02	9.9	17.91	15.67	37.83	2.113	2.414	1.142
KDI-16-013 GC 09	80.1	17.56	15.49	36.70	2.09	2.369	1.134
KDI-16-013 GC 17	160.8	22.15	16.12	41.93	1.893	2.6	1.372
KDI-15-048a GC 07	259.3	20.11	15.85	39.35	1.957	2.483	1.267
KDI-15-048a GC 15	340.1	19.27	15.71	37.68	1.955	2.398	1.226
KDI-15-048b GC 01	70.7	19.22	15.72	39.62	2.061	2.521	1.222
KDI-15-048b GC 07	130.0	24.32	16.62	43.19	1.776	2.598	1.464
KDI-15-0069b GC 06	352.7	18.63	15.55	37.69	2.023	2.423	1.195
KDI-15-0069b GC 17	460.3	18.24	15.44	37.46	2.053	2.426	1.177
KDI-15-0069b GC 28	569.6	19.88	15.79	39.09	1.967	2.475	1.257

D.13 Country Rock Thin Section Descriptions

Petrographic descriptions and representative photomicrograph images are presented for the thin section of metaturbidite country rock.

KDI-15-048a GC09 280.4m

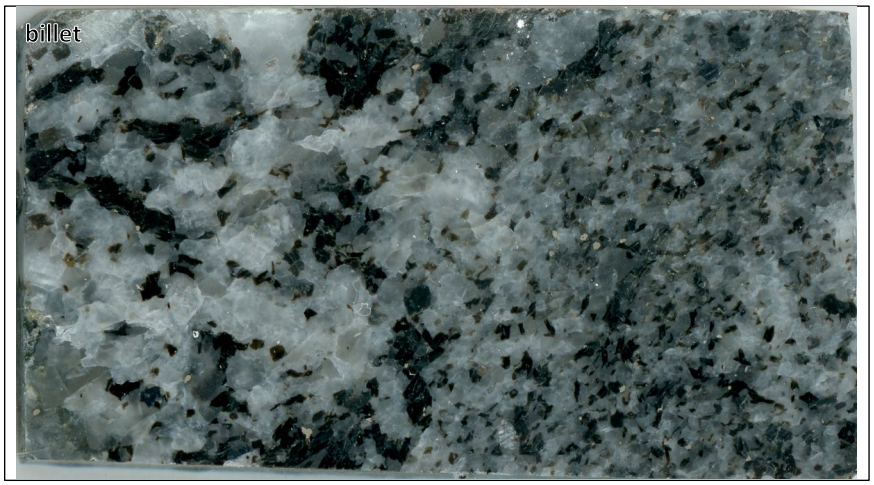

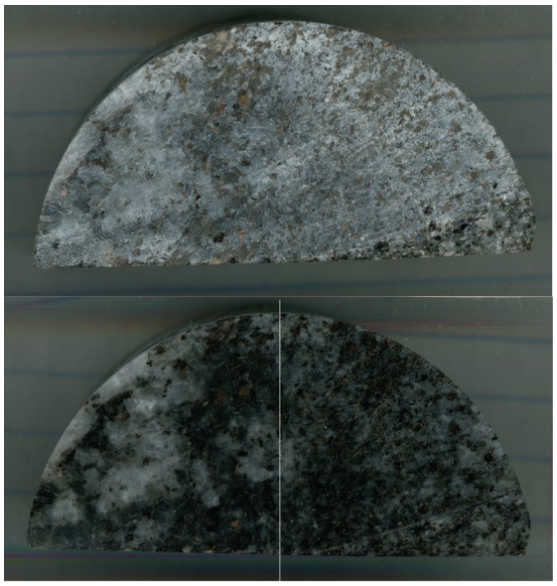

Rock Description:
50% qtz, 10% plag, wavy grain boundaries (not perfect triple). 15% elongate bt, variably chloritized, additional 5% chloritized biotite. 5% chl xls(?). 5-7% elongate muscovite. Musc is partially poikilitic partially forming irregular with qtz-plag poikoblasts [pic].
Sil: 5% acicular but mostly fibrous, or in fibrous fairly radial patches. Partially replacing (?) bt & chl-bit
Possibly <1% rare cordierite round nodules

Alteration Evidence:
None
Greywacke, gneiss

Fractures/Fabrics:
Spaced foliation defined by bt-musc.

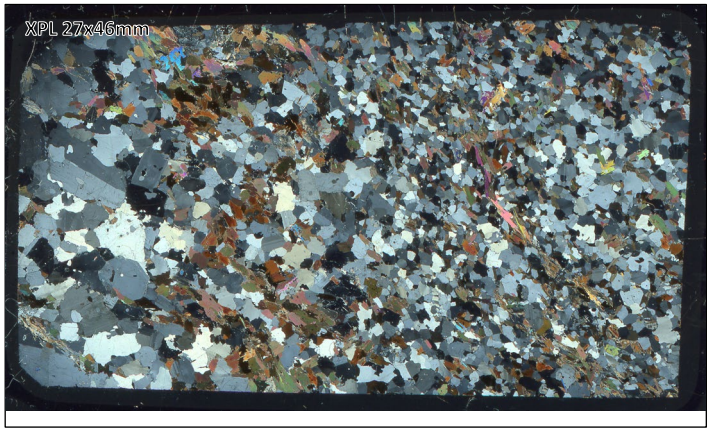

KDI-15-048a GC19 337.8m

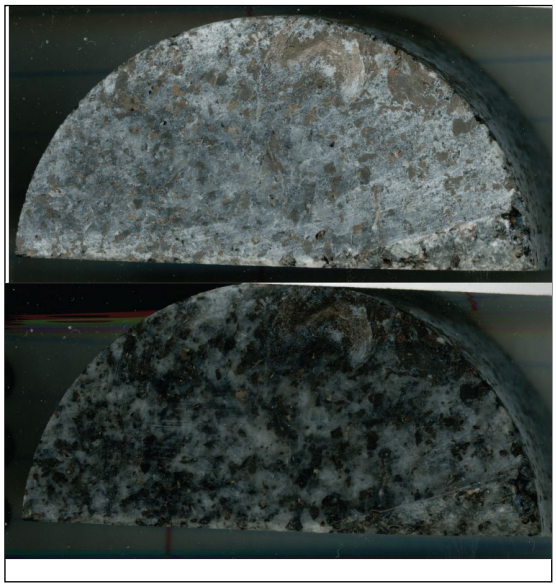

Rock Description:
40% qtz, 20% plag, 1-3mm across.
15% elongate bt, variably chloritized, additional 5% chloritized biotite. 5% chl xls(?). 5% muscovite. Musc is partially poikilitic partially forming irregular with qtz-plag poikoblasts.
Sil: 10% fibrous forming lenses and radial patches [pics] Partially replacing (?) bt & chl-bit
Perthitic orthoclase (?) 2% [pic]

Alteration Evidence:
None
Greywacke, arkose ss – migmatite?, gneiss?

Fractures/Fabrics:
Spaced and pretty weak foliation defined by bt-musc-sil

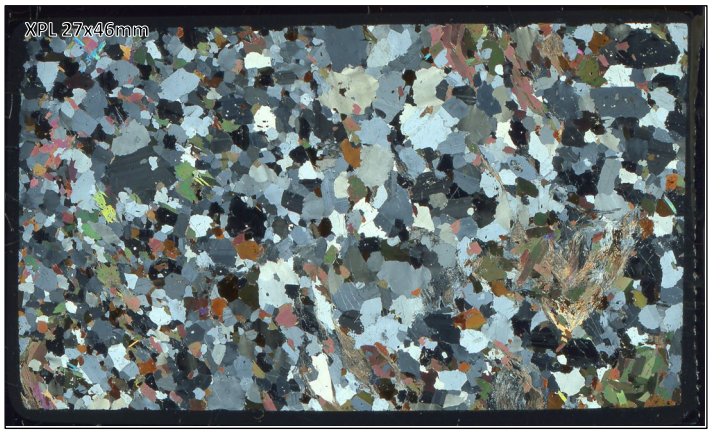

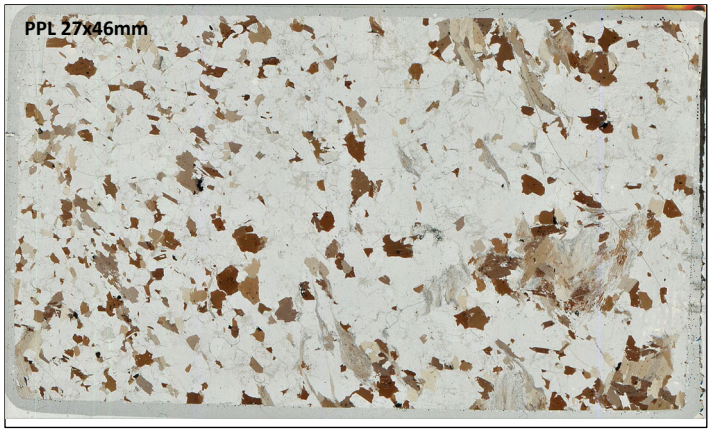

KDI-15-048b GC03 89.8m

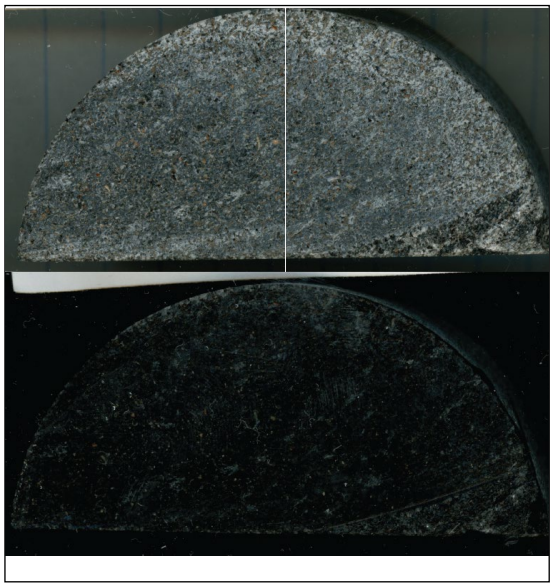

Rock Description:
40% qtz, 20% plag orthoclase.
5% elongate fresh bt, is slightly lighter color and preserves lineations. Strongly chloritized though (75% of all bt is chloritized), about 10% modal of chloritized biotite.
5% elongate muscovite. Musc is partially poikilitic partially forming irregular with qtz-plag poikoblasts [pic].
Sil: fibrous 2% minor replacement of bt-musc
3%: ameboid med-high relief poikilitic fractured isotropic mineral [pic], garnet or staurolite? Poiks of bt-qtz

Alteration Evidence:
None
Schist, semipelite/mudstone

Fractures/Fabrics:
Spaced foliation defined by bt-musc.

Qtz-plag grains sizes are ~1mm. Elongate mins (bt-musc) are ~1mm

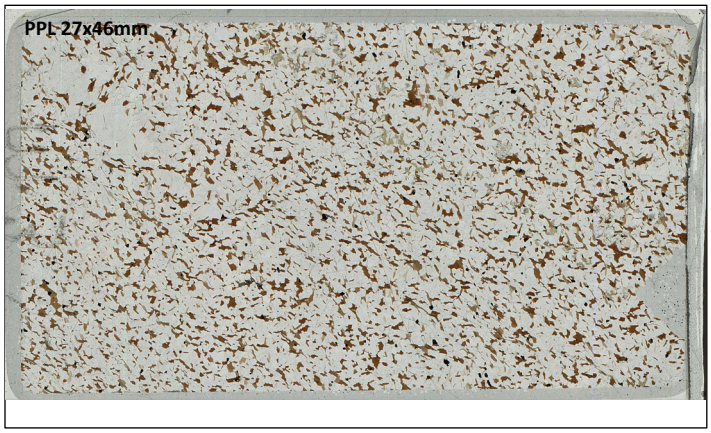

KDI-15-048b GC06 121.0m

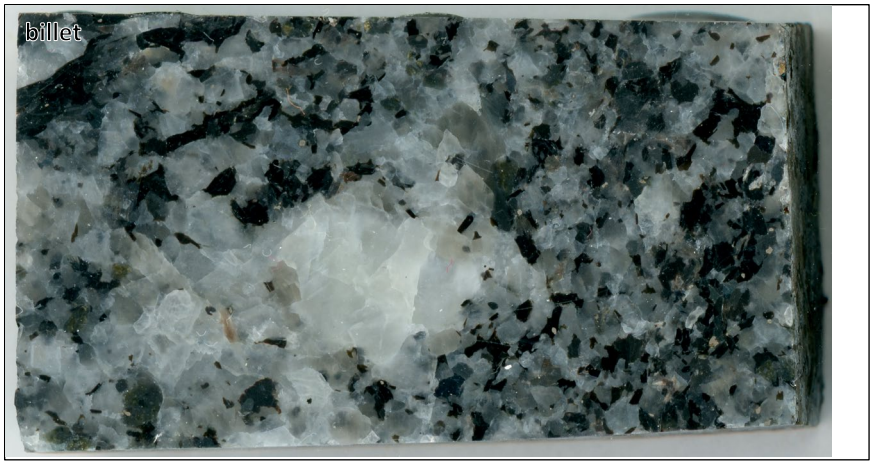

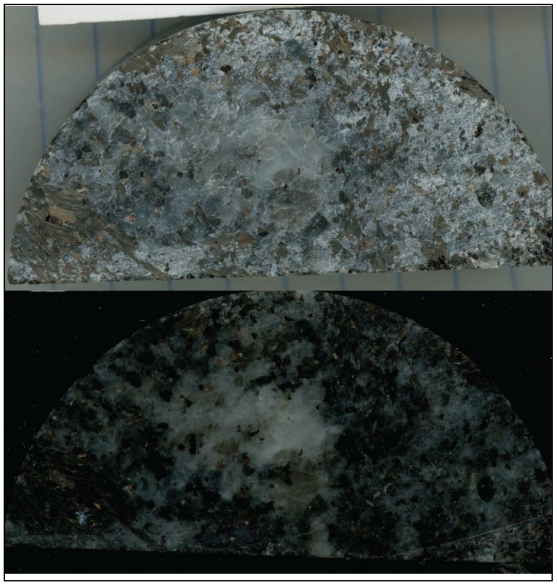

Rock Description:
30% qtz, 30% plag&ortho. 15% elongate total bt, variably (50%) chloritized. 5% primary chl xls(? – not bt pseudomorphs).
5% elongate muscovite. Not poikilitic
Sil: 7% acicular but mostly fibrous, or in fibrous fairly radial patches. Partially replacing (?) bt & chl-bit
3%: ameboid med-high relief fractured isotropic mineral [pic], garnet or staurolite? Altered on fractures by high bf mineral [pic]

Alteration Evidence:
Little clay alteration.

Gneiss, greywacke

Fractures/Fabrics:
Spaced foliation defined by bt-musc.
Central third is coarse felsic segregation (leucosome or just gneissose?). Coarse 2-10mm qtz-plag-ortho w/ 5% chl-bt [pics]. Otherwise qtz-feld are 1-2mm.
Diffuse boundary around felsic seg. No rimming restite.

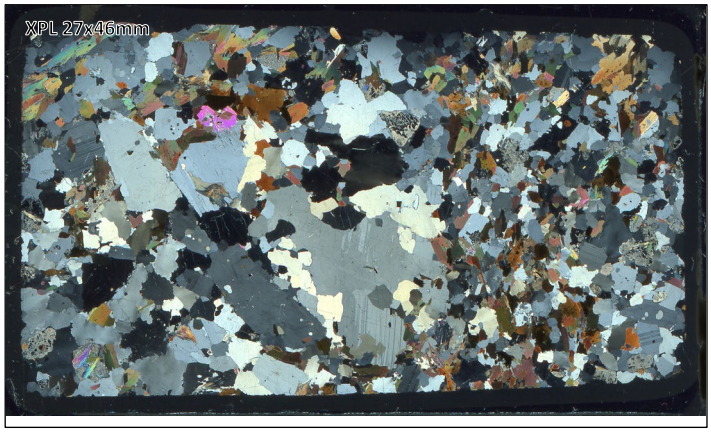

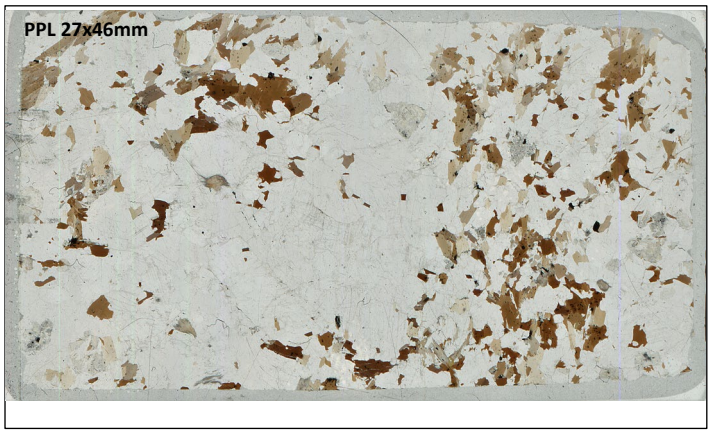

KDI-15-069b GC06 352.7m

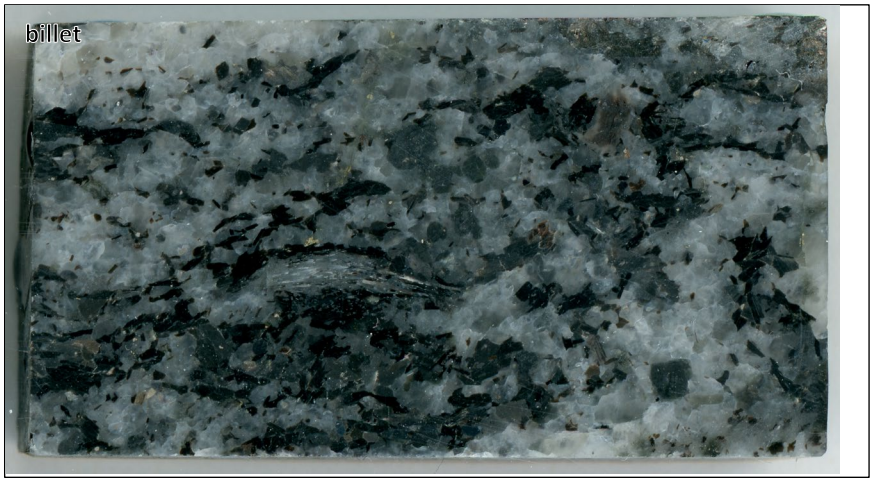

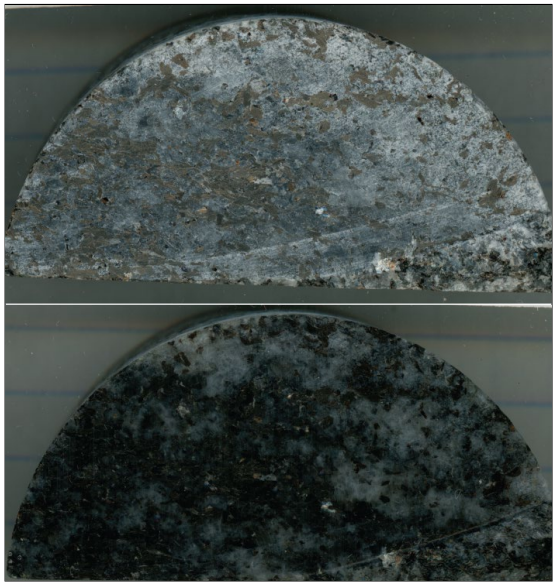

Rock Description:
20% qtz, 30% plag&ortho. 25% elongate total bt, variably (50+%) chloritized.
5% elongate muscovite. Not poikilitic
Sil: 5% acicular but mostly fibrous, or in fibrous fairly radial patches.
5%: ameboid med-high relief fractured isotropic mineral [pic], garnet? Altered on fractures by high bf mineral [pic]

Alteration Evidence:
Some sort of clay alteration of garnet/staur porphyroblasts and maybe qtz-feld grains?

Gneiss, greywacke

Fractures/Fabrics:
Spaced foliation defined by bt-musc.

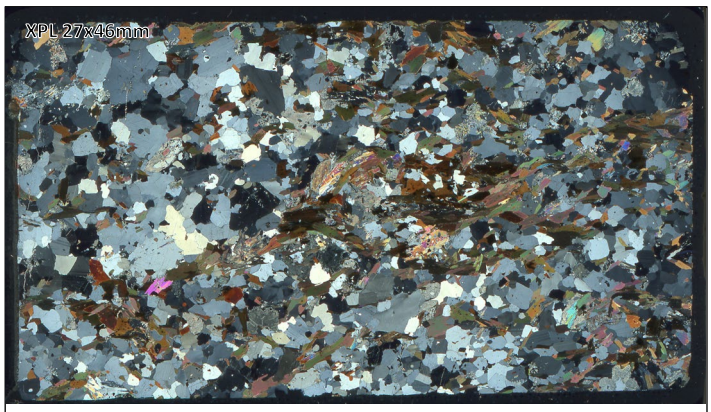

KDI-15-069b GC14 431.7m

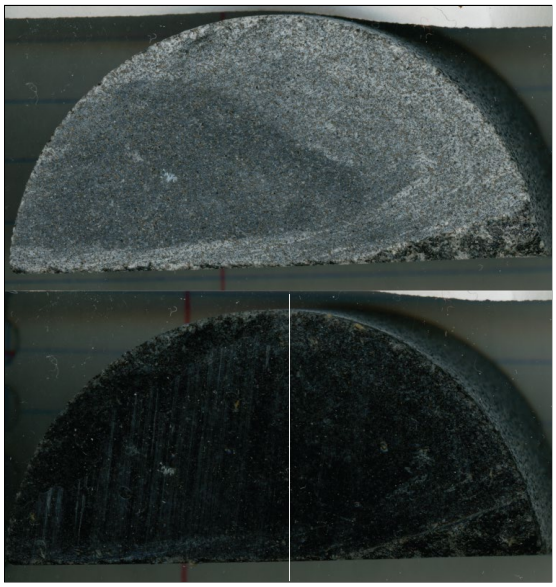

Rock Description:
50% qtz, 20% plag&ortho. 15% elongate total bt, variably (50%) chloritized.
5% elongate muscovite. <3mm long – longer than bt. Poikilitic musc containing felsic qtz-feld mins
Sil: 1% acicular but mostly fibrous, or in fibrous fairly radial patches. Partially replacing (?) bt & chl-bit

Alteration Evidence:
None

Schist, metapelite/mudstone

Fractures/Fabrics:
Spaced foliation defined by bt-musc. Qtz-plag are undeformed, just bound by elongate bt.

Qtz-feld <0.5mm

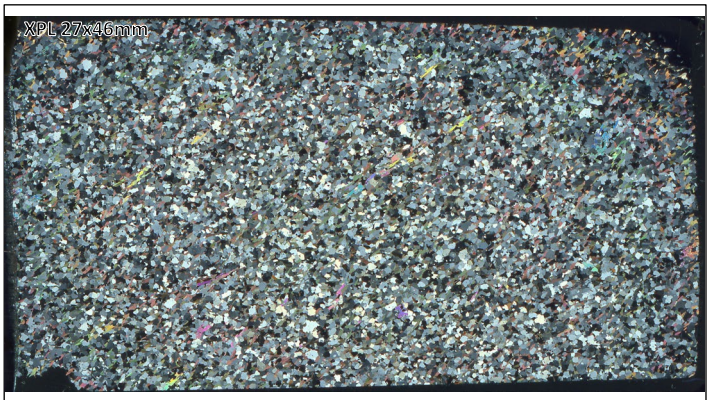

KDI-15-069b GC27 562.8m

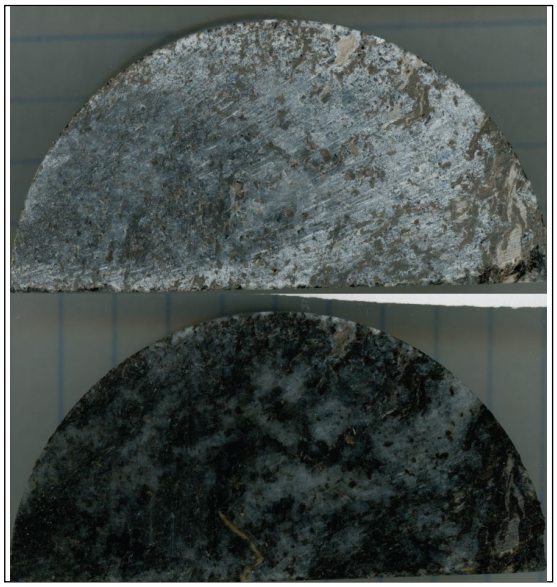

Rock Description:
30% qtz, 20% plag&ortho. 20% elongate total bt, variably (40%) chloritized. More chloritized in the coarser section
5% elongate muscovite.
Sil: 7% acicular but mostly fibrous, or in fibrous fairly radial patches and lenses. Partially replacing (?) bt & chl-bit
3%: ameboid med-high relief fractured isotropic mineral [pic], garnet? Altered on fractures by high bf mineral [pic]

Alteration Evidence:
None

Gneiss, greywacke

Fractures/Fabrics:
Spaced foliation defined by bt-musc.

Middle ¼ qtz-feld coarsen from <1-2 to >2mm wide, bt % decreases as well. Gneissose segregation, diffuse boundary and not rimmed by restite

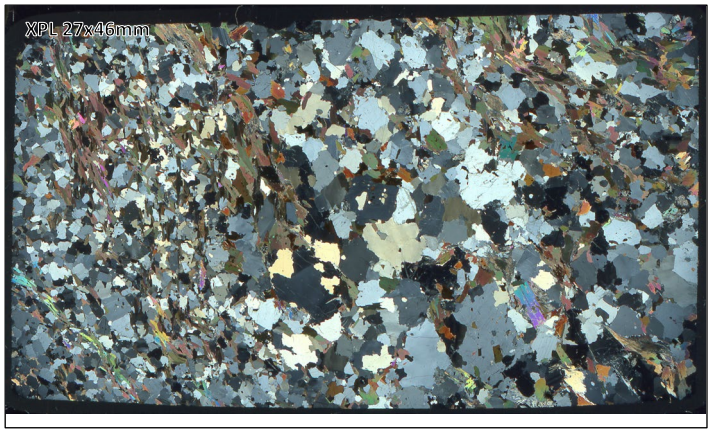

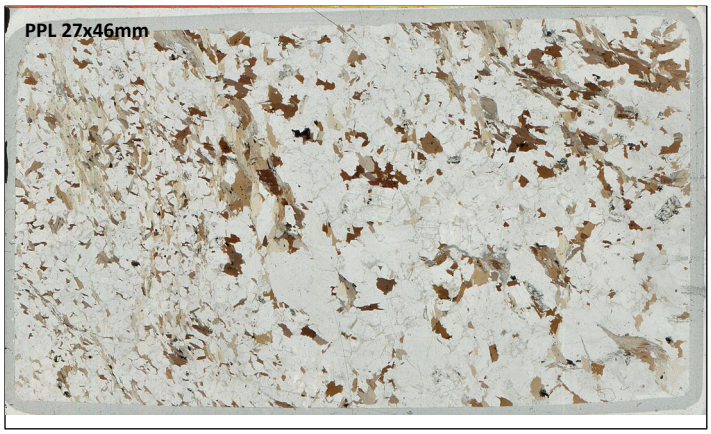

KDI-16-013 GC05 40.1m

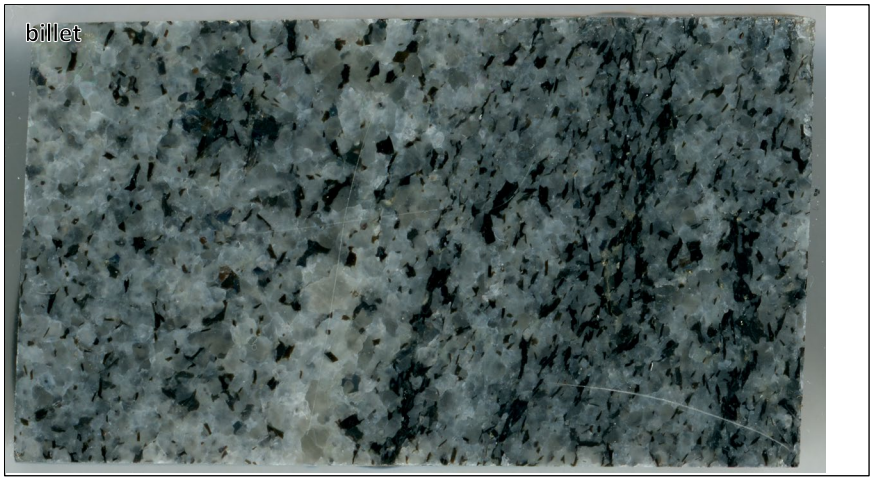

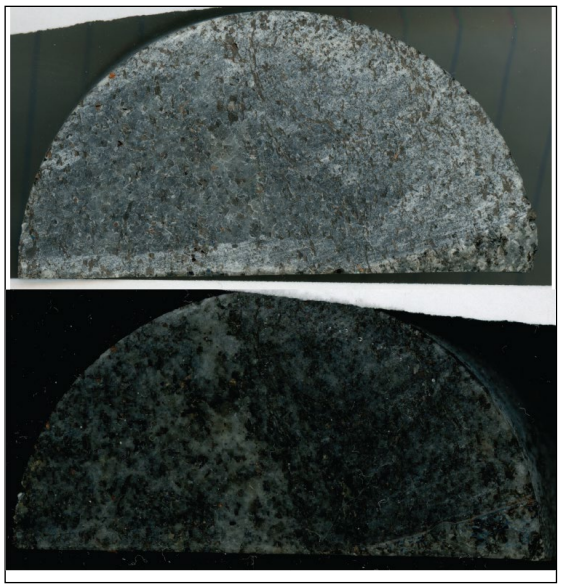

Rock Description:
Semipelitic on one half grading into coarser more felsic half.
30% qtz, 30% plag&ortho. 15% elongate total bt, variably (50%) chloritized. Bt is slightly more chloritized on felsic half.
5% elongate muscovite.
Sil: 3% acicular but mostly fibrous, or in fibrous fairly radial patches. Partially replacing (?) bt & chl-bit

Alteration Evidence:
Sulfide vein that follows grain boundaries and bt rich foliated lense. No associated qtz in it. [pic]

schist +- gneiss, semipelite

Fractures/Fabrics:
Spaced foliation defined by bt-musc. Well defined in semipelitic half, poorly developed in coarser half.

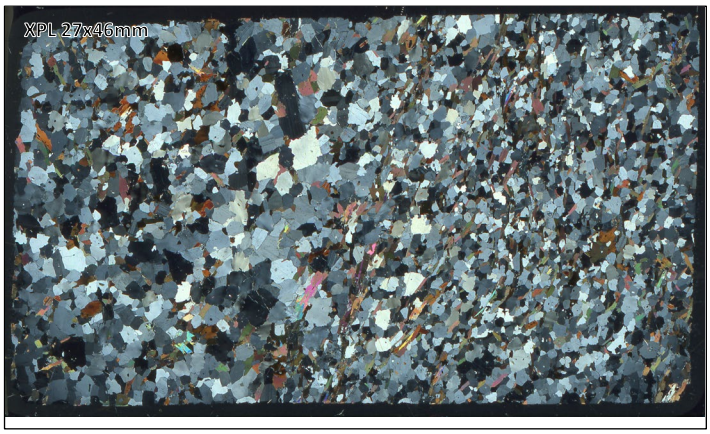

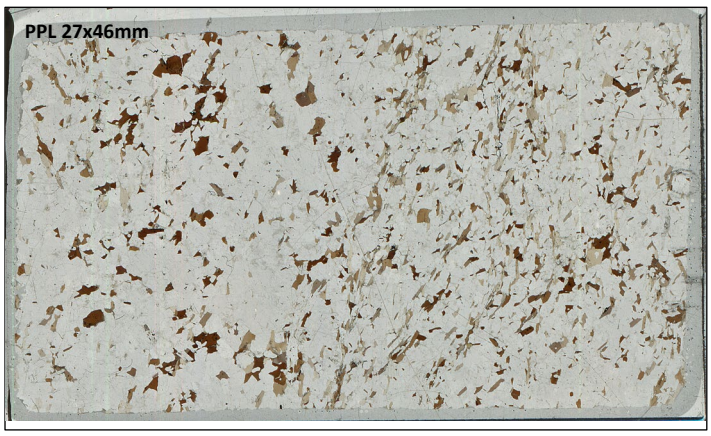

KDI-16-013 GC12 110.7m

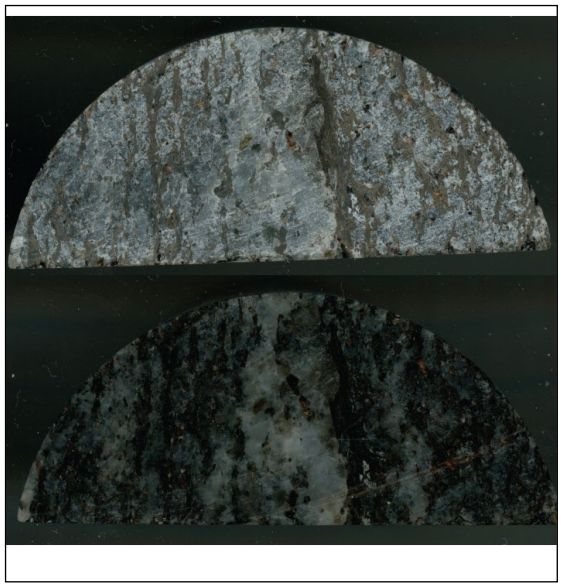

Rock Description:
30% qtz, 30% plag&ortho. 15% elongate total bt, variably (50%) chloritized.
7% elongate muscovite. Not poikilitic
Sil: 5% acicular but mostly fibrous, or in fibrous fairly radial patches. Partially replacing (?) bt & chl-bit
3%: ameboid poik med-high relief fractured isotropic mineral [pic], garnet/staur?

Alteration Evidence:
Some clay alteration as seen before [pic]. No evidence that these crystals were staur or garnet, but do contain unaffected qtz/plag poiks, so likely were porphyroblasts of those two minerals since replaced by some clay. Not high enough relief or green enough to be sil.
Gneiss, greywacke

Fractures/Fabrics:
Spaced foliation defined by bt-musc. Well defined in greywacke.

Central third is coarse felsic segregation (leucosome or just gneissose?). Coarse 2-5mm qtz-plag-ortho w/ <5% chl-bt [pics]. Otherwise qtz-feld are <1mm. Rimmed by 2-3mm thick bt rich well foliated restite?

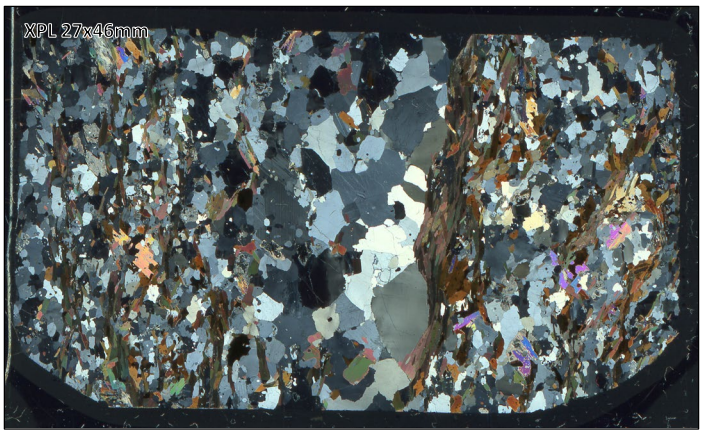

KDI-16-013 GC17 160.8m

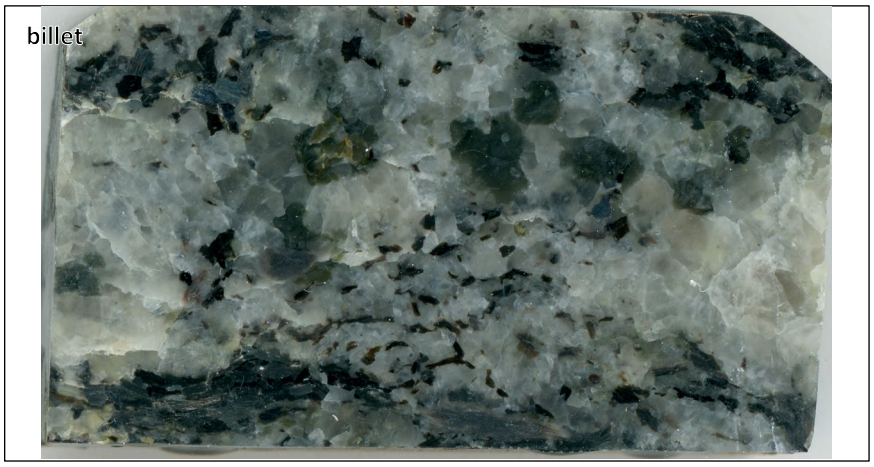

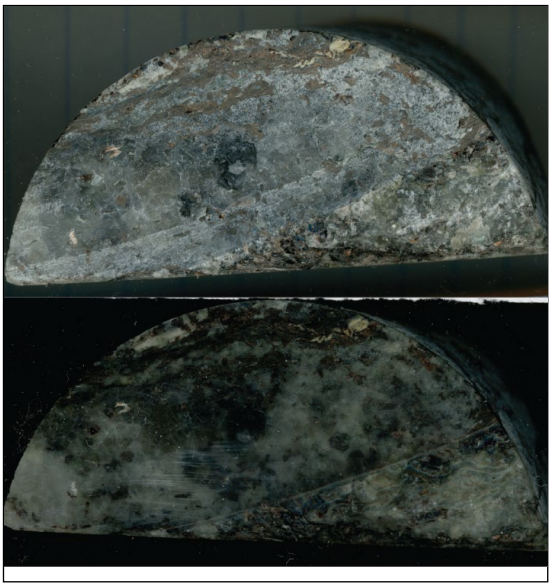

Rock Description:
30% qtz, 30% plag&ortho. 15% elongate total bt, variably (50+%) chloritized.
5% elongate muscovite.
Sil: 7% acicular but mostly fibrous, or in fibrous fairly radial patches. Partially replacing bt & chl-bit

Alteration Evidence:
Amorphous clay alteration by clay mineral, but texturally different from fibrous sil [pics].
Mostly replacing plag preserving remnant polysynthetic twinning.,

Gneiss, greywacke

Fractures/Fabrics:
Spaced foliation defined by bt-musc. Parallel to TS long axis. Middle half of coarse 1-5mm qtz-plag-ortho leucosome segregation. Somewhat gradational contact, not rimmed by bt-rich restite. Possibly just gneissose texture.

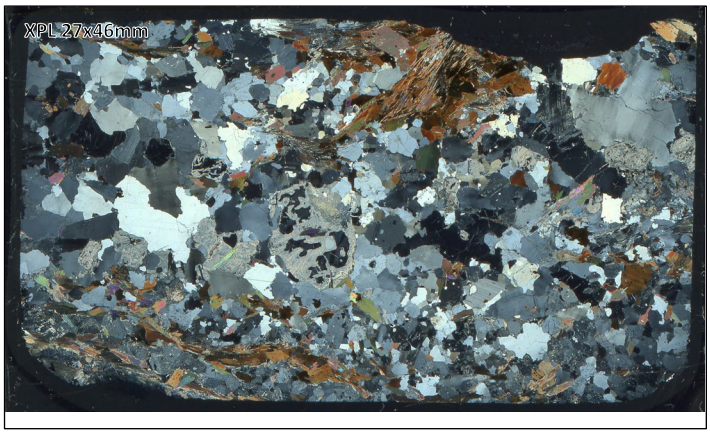

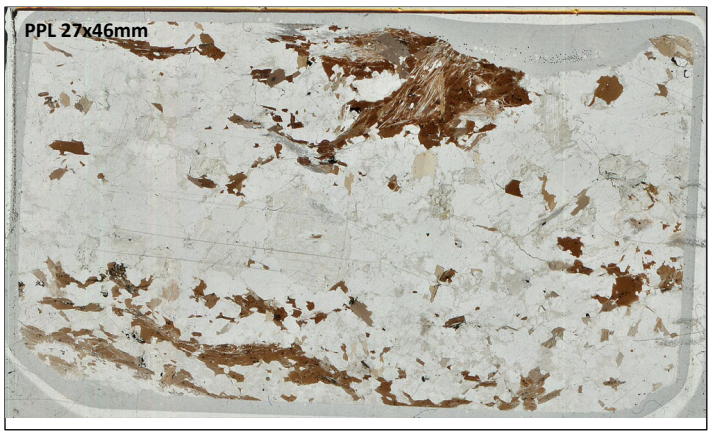

D.14 Kelvin Kimberlite Thin Section Descriptions (SRK Consulting)

Petrographic descriptions and representative photomicrograph images are presented for the series of thin sections of the Kelvin kimberlite provided by SRK consulting.

SRK HQ14-024b 54.14-0.24 A

Alteration: abundant crosscutting carbonate veining. <0.1mm up to 5mm thick. 70% is carb with some minor amounts of associated fibrous talc.
Structure: --
Texture:

Compound Clasts:
- **Magmaclasts**: few thin-skinned melt bearing magmaclasts (evidence of KPK texture)
- **Xenoliths**: Country rock clasts present as relict patch of unaltered euhedral biotite and secondary chlorite replacing coarse-grained feldspar (some preserved twinned microcline)
- **Autoliths**: --
- **Accretionary Clasts**: --

Crystals:
- **Macrocrysts**: evidence is preserved of olivine macrocrysts, phenocrysts, and magmaclasts (xenocryst with magmaclast). Mostly just the phl and spn remnant halos are preserved since the carbonate veining.
- **Phenocrysts**: --

Interstitial Matrix: serpentine
Defining feature: Late stage stockwork carbonate veining.

Mineralogical Classification + Parental Magma Type: --
Textural Classification: PK
Textural-Genetic Classification: Country Rock Breccia
Intrusive/Extrusive Spatial Context:
Genetic/Process Interpretation: --
Kelvin Model Phase: At one point, was a KPK unit before veined. Probably vein/fracture related as one of the first emplacement phases.

Kimberley type pyroclastic phlogopite kimberlite country rock breccia prior to overprint by stockwork carbonate-talc veins likely associated with later kimberlite phase.

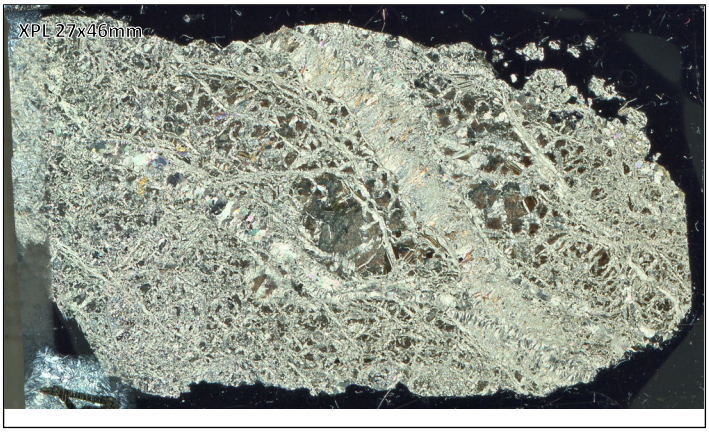

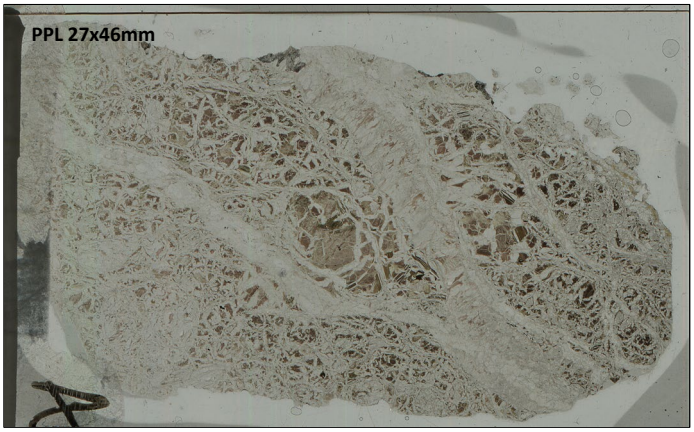

SRK HQ14-16b 37.16 A

Alteration: pervasive serpentine replacement of olivine, variably moderate to strong country rock alteration.
Structure: massive, uniform,
Texture: matrix supported

Compound Clasts:

Magmaclasts: common around angular or elongate CRX. Thin selvages on most olvph. Groundmass of serp, phl, spl, per.

Xenoliths: 15% mod-strong altered. Biotite xenocrysts common. Low abundance and increased alteration of xenoliths suggests transitional textures.

Autoliths: --

Accretionary Clasts: --

Crystals:

Macrocrysts: 10%, mostly >3mm

Phenocrysts: 20% with common thin selvages.

Interstitial Matrix: well defined ser-chl microlites. >50%

Mineralogical Classification + Parental Magma Type: phl kimberlite
Textural Classification: *(CK/HK) PK*
Textural-Genetic Classification: KPKt
Intrusive/Extrusive Spatial Context: --
Genetic/Process Interpretation: olivine macrocryst poor phl kpk-kpkt
Kelvin Model Phase: KIMB1

Olivine macrocryst poor Kimberley-type pyroclastic kimberlite to transitional texture phlogopite kimberlite.

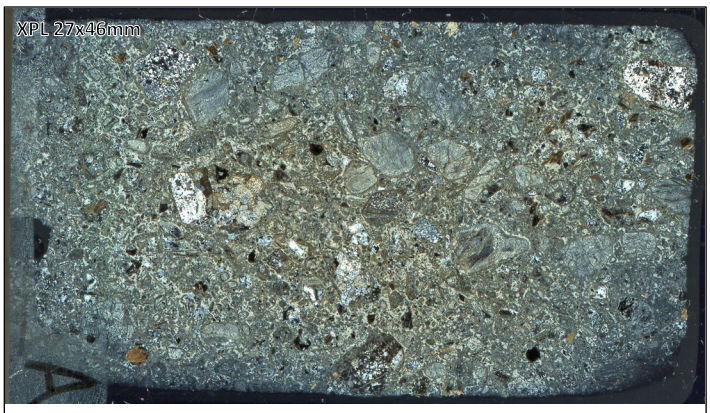

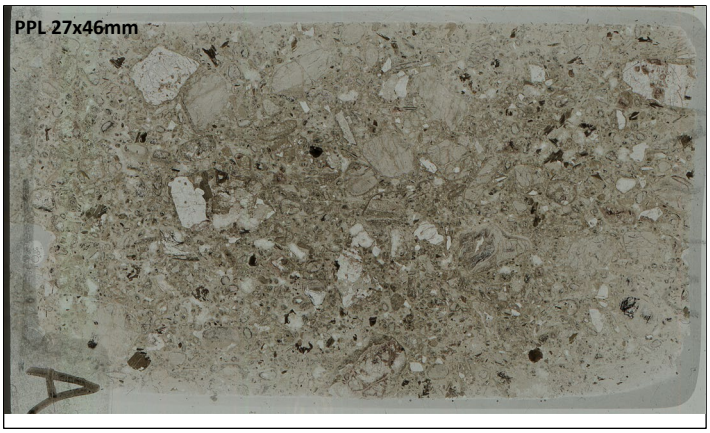

SRK HQ14-024b 59.67-0.27 A

Alteration: pervasive deuteric replacement of olivine with serpentine – chlorite. No fresh olivine.
Late-stage carbonate recrystallization (subparallel <1mm thick), possibly associated with interstitial groundmass carbonate and olv macrocryst patchy carb coring.
Structure: massive
Texture: clast supported, well sorted.

Compound Clasts:
Magmaclasts: Melt-bearing pyroclasts are abundant always focused around a kernel of country rock xenolith, macrocryst or phenocryst. These melt selvages are <0.25mm thick consisting of often serp, phl, spinel, perovskite.
Xenoliths: 5-7%, mostly xenoliths (rather than xenocrysts). Strongly digested and replaced by very fine-grain serp, chlorite.
Autoliths: --
Accretionary Clasts: --
Crystals:
Macrocrysts: 10-15% >1mm anhedral, smooth surfaced. Uniform distribution. No fresh olivine present, completely pseudomorphed by serp-chl. Often cored by carbonate (possibly related to late stage veining).
Phenocrysts: 20% <1mm, fully pseudomorphed – no fresh olivine.
Interstitial Matrix: 60% consisting of cryptocrystalline serp.

Mineralogical Classification + Parental Magma Type: cpx phl kimberlite
Textural Classification: HKt
Textural-Genetic Classification: HKt
Intrusive/Extrusive Spatial Context: Intrusive. Transitional zone within HK-KPK system.
Genetic/Process Interpretation: --
Kelvin Model Phase: KIMB2B

Olivine macrocrystic, xenolith rich hypabyssal to transitional-textured phlogopite kimberlite

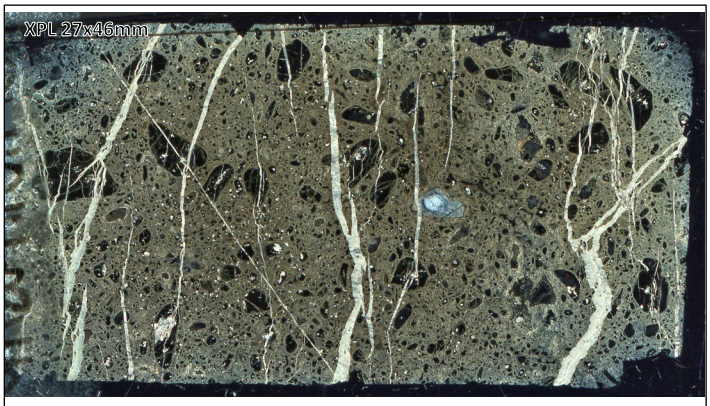

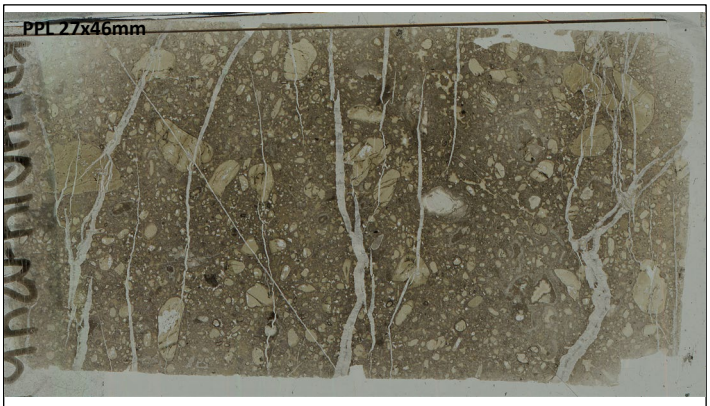

SRK HQ14-024b 66.21-0.31 A

Alteration: pervasive replacement of olivine macrocrysts/phenocrysts by serpentine and chlorite.
Structure: Massive
Texture: inequigranular, clast supported

Compound Clasts:

Magmaclasts: ubiquitous subrounded magmaclasts cored by olv macrocrysts or phenocryst or CR xenocryst. These thin selvages (<0.1mm) are composed of serp, phl, and cpx with spinel, perovskite. Diffuse contacts/boundaries that grade out into microlitic groundmass.

Xenoliths: 25%. Overall moderate-strong alteration of xenoliths. Serpentine selectively pseudomorphing quartz and feldspars, biotite altered to chlorite. Rare <1mm biotite xenocryst, altered to chlorite and weakly digested.

Autoliths: --

Accretionary Clasts: --

Crystals:

Macrocrysts: 15% no fresh olivine – completely pseudomorphed by serp±chlor. Typical macrocryst characteristics: smooth surface, anhedral. Uniform distribution.

Phenocrysts: 25% <1mm, fully pseudomorphed – no fresh olivine.

Interstitial Matrix: exemplary microlites of phl and unknown high-relief fibrous mineral. Slightly coarser IMM than 59.67m t/s. Well defined microlites.

Mineralogical Classification + Parental Magma Type: phlogopite kimberlite
Textural Classification: *(CK/HK)*
Textural-Genetic Classification: HKt
Intrusive/Extrusive Spatial Context: --
Genetic/Process Interpretation: --
Kelvin Model Phase: KIMB2B/KIMB3A

Macrocrystic, xenolith poor hypabyssal to transitional textures phlogopite kimberlite.

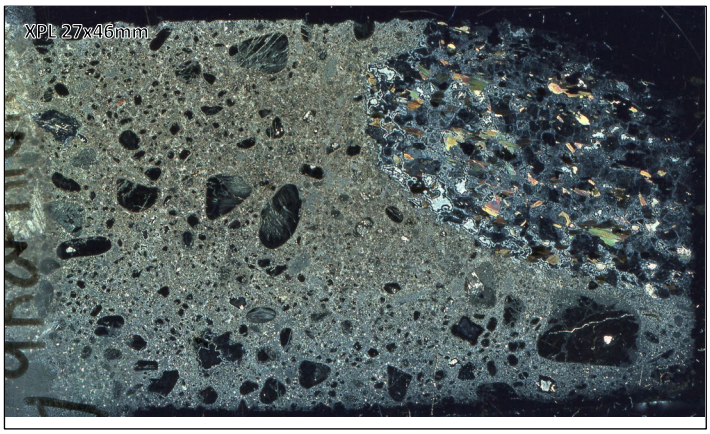

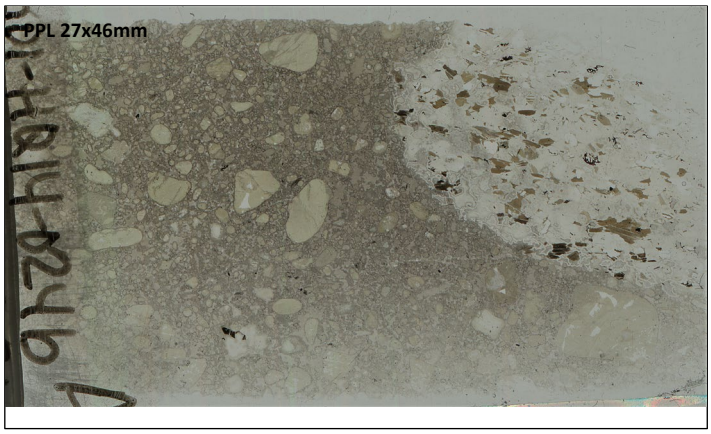

SRK HQ14-024b 77.37-0.28 A

Alteration: pervasive deuteric replacement of all olivine by serpentine. Country rock xenoliths often moderately-weakly altered by serpentine and chlorite. Limited to contacts with magma and grain boundaries. Preferential replacement of qtz & feldspars before biotite.
Structure: uniform olivine distribution
Texture: matrix supported

Compound Clasts:

Magmaclasts: Ubiquitous and well defined. Melt selvages on elongate or angular shard xenoliths & xenocrysts often have thicker selvages up to 0.5mm thick. Magmaclasts are always cored by an olvma, olvph, or cxr, and occasionally two CR xenocrysts. Selvages are thinner on olivine phenocrysts, and thinnest on macrocrysts. Groundmass is dominated by serp-spinel.

Xenoliths: 50% fresh-weak alteration by serpentine and antigorite (replacing phl). CR xenocrysts (angular or elongate) often preserve primary mineralogy, and when fragment is partially pseudomorphed grain boundaries remain sharp and well defined.

Autoliths: --

Accretionary Clasts: --

Crystals:

Macrocrysts: No fresh olivine, all pseudomorphed by serp. Olv macrocryst poor. 7%. <3mm. Anhedral and smooth surfaced. Often very thin selvages and subtle grain boundaries and difficult to distinguish in ppl.

Phenocrysts: subhedral-euhedral, 15%. Often encased in thin melt selvage.

Interstitial Matrix: consists of serp, phl, some cpx, & <0.1mm CR microxenocrysts/fragments (dominantly biotite & quartz). Weakly defined phl microlites.

Mineralogical Classification + Parental Magma Type: phlogopite kimberlite
Textural Classification: PK
Textural-Genetic Classification: KPK
Intrusive/Extrusive Spatial Context:
Genetic/Process Interpretation: macrocryst poor, crx rich KPK.
Kelvin Model Phase: ashy matrix, likely KIMB3A/B

Macrocryst poot country, country rock xenolith rich Kimberley-type pyroclastic phlogopite kimberlite.

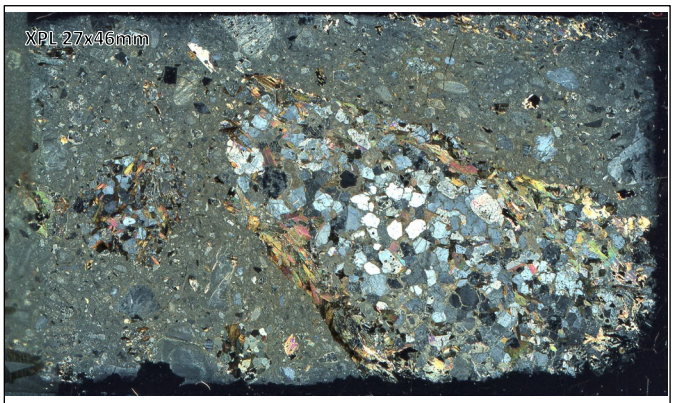

SRK HQ14-024b 91.16-0.32 A

Alteration: pervasive deuteric replacement of all olivine by serpentine. Country rock xenoliths often moderately-weakly altered by serpentine and chlorite. Limited to contacts with magma and grain boundaries. Preferential replacement of qtz & feldspars before biotite.
Structure: uniform olivine distribution
Texture: clast supported

Compound Clasts:

Magmaclasts: Magmaclasts are common. melt selvages on elongate or angular shard xenoliths & xenocrysts often have thicker selvages up to 0.5mm thick. Magmaclasts are always cored by an olvma, olvph, or cxr. Selvages are thinner on olivine phenocrysts, and thinnest and often absent on macrocrysts. Groundmass is dominated by serp, phl, spinel.

Xenoliths: 65% fresh-weak alteration. Abundant <1mm shard elongate angular xenocrysts and >5mm xenoliths.

Autoliths: --

Accretionary Clasts: --

Crystals:

Macrocrysts: No fresh olivine, all pseudomorphed by serp. olv macrocryst poor. 7%. <3mm. anhedral and smooth surfaced. Often very thin to no melt selvage and subtle grain boundaries and difficult to distinguish in ppl.

Phenocrysts: subhedral-euhedral, 10%. Often encased in thin melt selvage.

Interstitial Matrix: consists of serp, phl, some cpx, & <0.1mm CR microxenocrysts/fragments (dominantly biotite & quartz). Poorly developed phl microlites. Very rare interstitial pools of carbonate – aren't pools in the groundmass, crosscut everything, and indicate they are late stage indiscriminate and vein related.

Mineralogical Classification + Parental Magma Type: phlogopite kimberlite
Textural Classification: PK
Textural-Genetic Classification: KPK
Intrusive/Extrusive Spatial Context: macrocryst poor, crx rich KPK.
Genetic/Process Interpretation: --
Kelvin Model Phase: KIMB5

Macrocryst poor, country rock xenolith rich Kimberley-type pyroclastic phlogopite kimberlite.

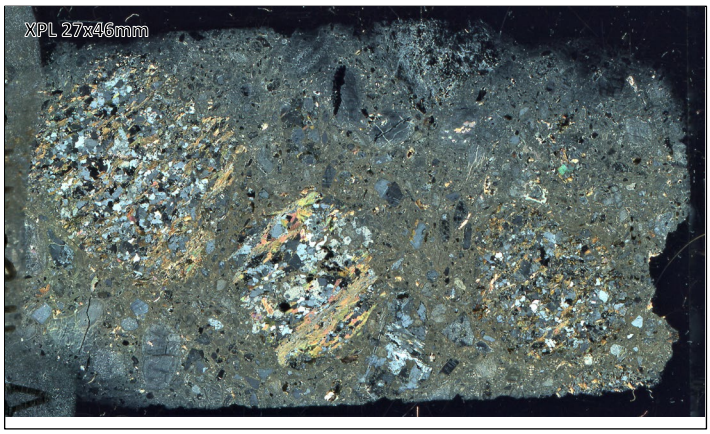

SRK HQ14-024b 100.15-0.31 B

Alteration: pervasive deuteric replacement of all olivine by serpentine. Country rock xenoliths often moderately-weakly altered by serpentine and chlorite. Limited to contacts with magma and grain boundaries. Preferential replacement of qtz & feldspars before biotite.
Structure: uniform olivine distribution
Texture: matrix-clast supported

Compound Clasts:

Magmaclasts: Magmaclasts are common. melt selvages on elongate or angular shard xenoliths & xenocrysts often have thicker selvages up to 0.5mm thick. Magmaclasts are always cored by an olvma, olvph, or cxr. Selvages are thinner on olivine phenocrysts, and thinnest and often absent on macrocrysts. Groundmass is dominated by serp, spinel, per.

Xenoliths: 30% moderately altered. Abundant <1mm shard elongate angular xenocrysts and >5mm xenoliths. Preferential alteration of quartz and plagioclase to serpentine. Biotite, muscovite, and microcline are less altered. Increased CRX digestion spatially correlated with more serp microlite development.

Autoliths: --

Accretionary Clasts: --

Crystals:

Macrocrysts: 7%. <3mm. anhedral and smooth surfaced. No fresh olivine, all pseudomorphed by serp. olv macrocryst poor. Often very thin to no melt selvage and subtle grain boundaries and difficult to distinguish in ppl.

Phenocrysts: subhedral-euhedral, 20%. Often encased in thin melt selvage.

Interstitial Matrix: consists of serp, phl. Poorly developed phl microlites. 2% carbonate as groundmass patched. Noticeably more phl in IMM around CRX and on half of the thin section. The other half, serpentine is the dominant matrix mineral.

Mineralogical Classification + Parental Magma Type: phlogopite kimberlite
Textural Classification: PK
Textural-Genetic Classification: KPK-t
Intrusive/Extrusive Spatial Context: macrocryst poor, crx rich KPK.
Genetic/Process Interpretation: --
Kelvin Model Phase: KIMB3B

Macrocryst poor, country rock xenolith rich Kimberley-type Pyroclastic to transitional-textured phlogopite kimberlite.

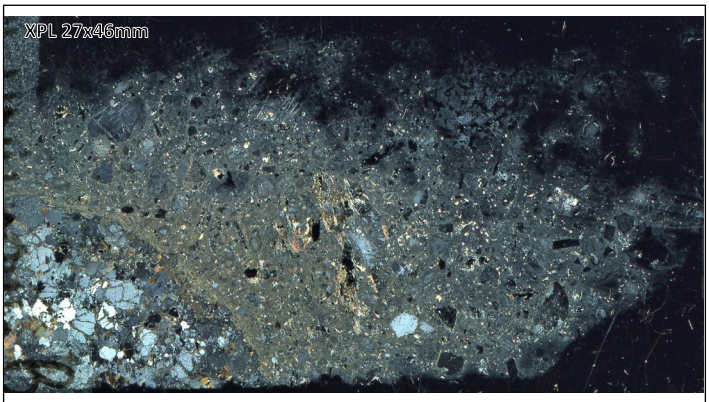

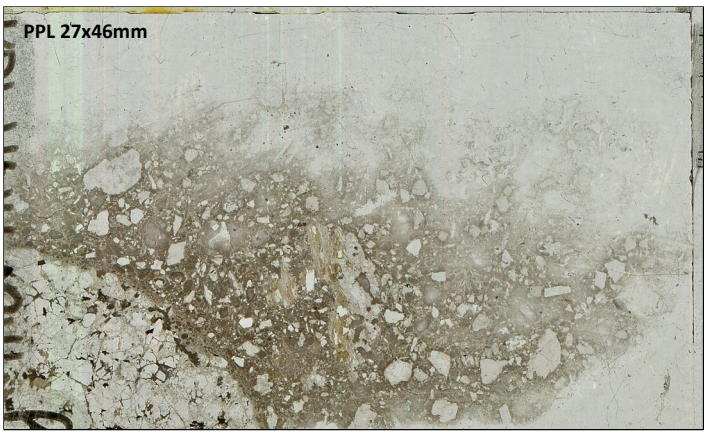

SRK HQ14-024b 118.53-0.31 A

Alteration: Variable intensities of country rock alteration. Fresh to strong alteration: often strongest on single xenocrysts. As seen in other phases, biotite is only altered to chlorite and often forms elongate xenocrysts sitting in magmaclasts/with thicker melt selvages.
Structure: uniform
Texture: clast supported, tightly packed, xenolith rich

Compound Clasts:
Magmaclasts: Melt depleted. Rare magmaclasts, composed of serp. Xenoliths and xenocrysts rarely have melt selvage. Common only on angular CR shards. Occasionally on olivine phenocrysts, but rare on olivine macrocrysts (or at least very thin).
Xenoliths: 55% contains more xenocrysts compared to xenoliths. Variable amount of alteration. Fresh-mod/strong. Includes lots of very fine lithic xenocrysts mixed in with matrix.
Autoliths: --
Accretionary Clasts: --
Crystals:
Macrocrysts: macrocryst poor. 5%
Phenocrysts: No fresh olivine. Mostly replaced by serp, possibly some chlorite (less that previous phases). Phenocrysts commonly have thin melt selvage. Macrocrysts rarely do (discrete grains).
Interstitial Matrix: IMM dominated by very-fine grained serp-phl-carb and fine grained lithic fragments.

Mineralogical Classification + Parental Magma Type: --
Textural Classification: VK
Textural-Genetic Classification: KPK
Intrusive/Extrusive Spatial Context: --
Genetic/Process Interpretation: --
Kelvin Model Phase: KIMB3C

Macrocryst-poor xenolith rich Kimberley-type pyroclastic kimberlite

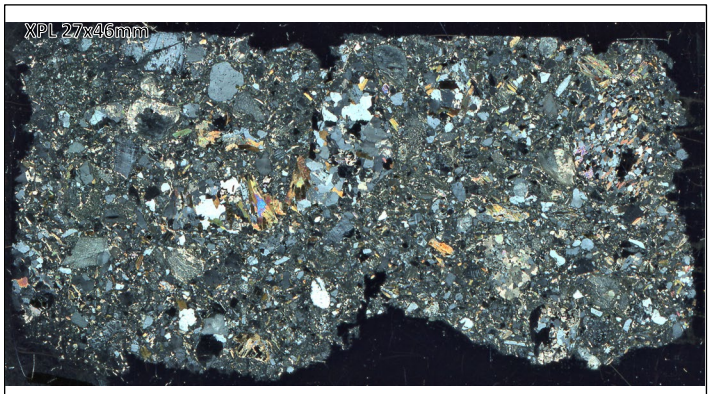

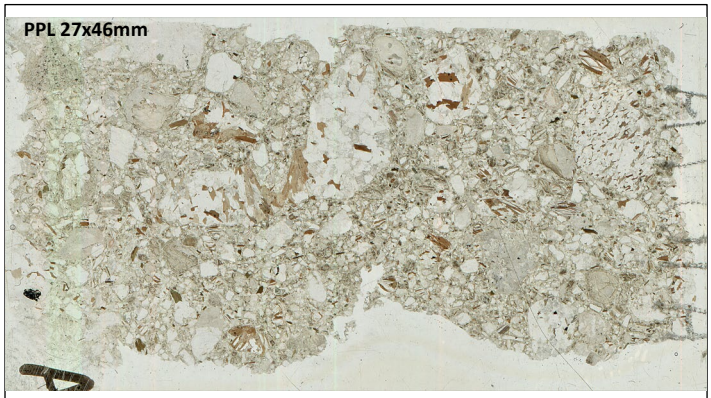

SRK HQ14-024b 124.40-0.27 A

Alteration: No fresh olivine, completely pseudomorphed by serp and chl. Sample is partially carbonatized by late-stage carbonate veining relating to deuteric replacement. Carbonate veins crosscut xenoliths and macrocrytss.
Structure: uniform
Texture: matrix-clast supported

Compound Clasts:

Magmaclasts: melt depleted. Rare magmaclasts. Xenoliths and xenocrysts rarely have metl selvage. Common only on angular CR shards. Occasionally melt selvages on olivine phenocrysts, but rare on olivine macrocrysts (or at least very thin).

Xenoliths: 40%. Contains more xenocrysts compared to xenoliths. Variable amount of alteration. Fresh-mod/strong. Includes lots of very fine lithic xenocrysts mixed in with matrix (20% of IM matix).

Autoliths: a few. Diagnostic of this phase.

Accretionary Clasts: --

Crystals:

Macrocrysts: macrocryst poor. 10%. Completely pseudomorph by serpentine-chl.

Phenocrysts: 15%. No fresh olivine. Mostly replaced by serp, & chlorite. Phenocrysts commonly have thin melt selvage. Macrocrysts rarely have thin melt selvages (discrete grains).

Interstitial Matrix: More by volume (matrix supported) Appears to be two different IMMs. (1) is serpentine serp-phl dominated, similar as the magmaclast groundmass. (2) Deuteric carbonatization. Contacts between two appear as both diffuse or slightly sharp.

Mineralogical Classification + Parental Magma Type: carb-phl kimberlite
Textural Classification: VK
Textural-Genetic Classification: KPK-t
Intrusive/Extrusive Spatial Context: --
Genetic/Process Interpretation: --
Kelvin Model Phase: KIMB6

Macrocryst poor, xenolith rich Kimberley-type pyroclastic to transitional phlogopite kimberlite with late-stage deuteric carbonatization.

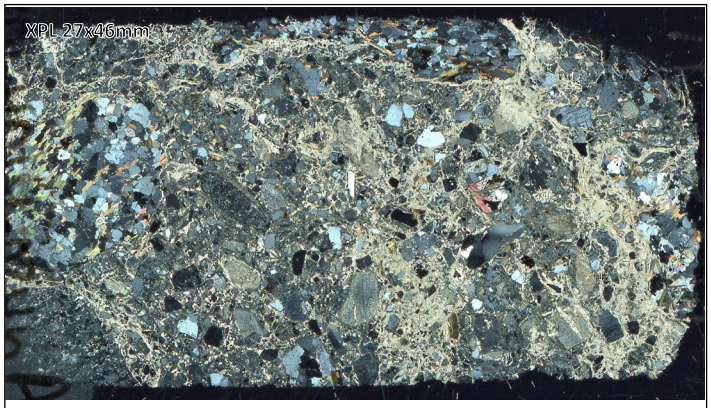

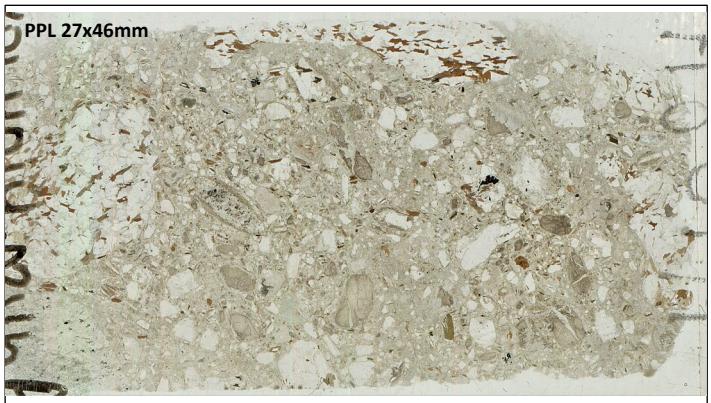

SRK HQ14-024b 135.57-0.29 A

Alteration: pervasive serpentine has pseudomorphed all olivine and country rock xenoliths or xenocrysts. Alteration is strong to intense, with a few surviving xenocrysts of Kspar (microcline). Late stage (<0.5mm thick) carbonate veins are occasionally crosscutting.
Structure: massive uniform
Texture: *matrix supported*

Compound Clasts:
Magmaclasts: Rare. Composed of serp-phl-spl. Only thin melt selvages on few olvph and thicker selvages (<0.25mm) on elongate CRX shards.
Xenoliths: 12% strong to intense alteration by serpentine. Rare fresh xenocryst of kspar. Even biotite is being altered.
Autoliths: --
Accretionary Clasts: --
Crystals:
Macrocrysts: 12%. Anhedral and smooth surface. Completely replaced by serp.
Phenocrysts: 20%. HK-like olivine distribution. Subhedral to euhedral. Completely replaced by serp. Thin melt selvages (discrete phenocrysts).
Interstitial Matrix: >50% dominantly serpentine-phl (little to no spl), increased phl microlite composition in selvages around CR xenoliths. Very fine grained, not well crystallized.

Mineralogical Classification + Parental Magma Type: --
Textural Classification: PK
Textural-Genetic Classification: KPK
Intrusive/Extrusive Spatial Context: --
Genetic/Process Interpretation: --
Kelvin Model Phase: KIMB7
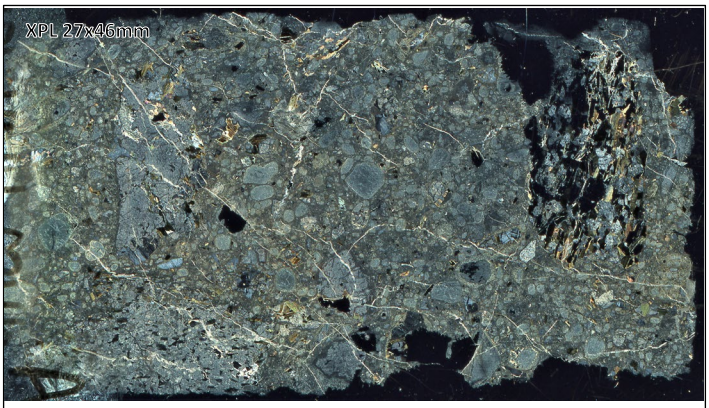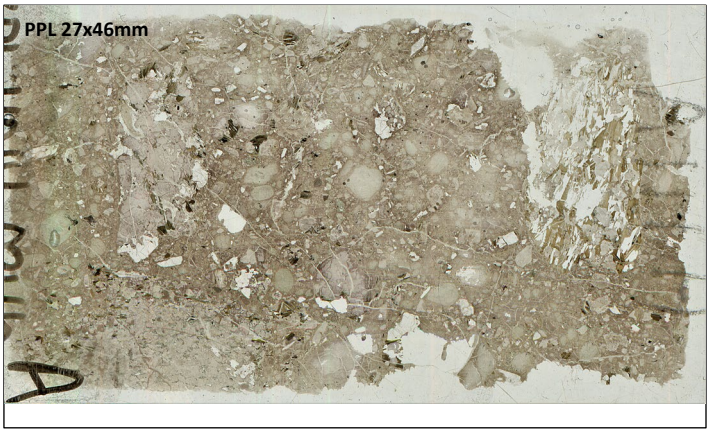
Macrocryst poor, xenolith poor Kimberley-type pyroclastic phlogopite kimberlite